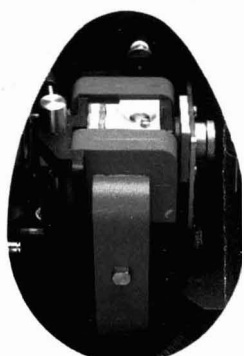
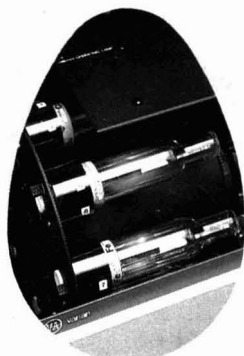
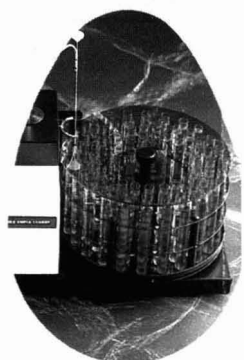
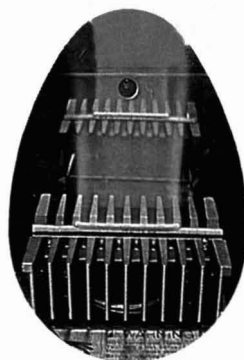
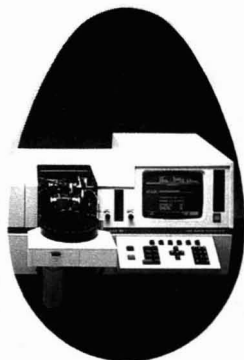


JANUARY 1991
ENVIRONMENTAL SCIENCE & TECHNOLOGY

ES&T

Alaska oil spill: Lessons learned
page 14



A DOZEN GOOD REASONS TO CHOOSE VARIAN AA.

With the powerful SpectrAA series of atomic absorption spectrometers, you can select from dozens of state of the art components such as the innovative VGA-76 for fully automated hydride and cold vapor analyses and the GTA-96 with HOT INJECTION to enhance graphite furnace productivity.

Choose the spectrometer that suits your needs, from the moderately-priced SpectrAA-10/20 to the top of the line SpectrAA-300/400. Central control from an IBM PS/2 Model 30-286™ ensures simple operation, extensive method and data storage, and access to dozens of software packages.

Take advantage of SpectrAA's features for fully automatic multi-element analyses, advanced sample handling, and powerful reporting capabilities. Varian's patented Zeeman Background Correction technology ensures fast, accurate correction of spectral interferences and structured background for every sample.

Varian's extensive Quality Control Protocols (QCP) software meets more US EPA CLP requirements than any other AA package, with automatic overrange

volume reduction, check standards, spikes, duplicates, time and date stamping, precision testing and more.

Add high performance accessories to your AA toolkit such as the Mark-V1 spray chamber and burner, the ACT-80 Atom Concentrator Tube, and productivity tools such as bar code readers for rapid entry of sample labels.

For consistent, quality results by the dozen, choose Varian AA. For more information, call 1-800-926-3000. In Canada, call 416-457-4130.

AA WITH A FUTURE

varian 

Editor: William H. Glaze
Associate Editors: Walter Giger, Ronald A. Hites,
Jerald L. Schnoor, John H. Seinfeld, Joseph
Suflita

ADVISORY BOARD

Roger Atkinson, Joan M. Daisey, Fritz H.
Frimmel, George R. Helz, Ralph Mitchell, Joseph
M. Norbeck, Walter J. Weber, Jr., Alexander J. B.
Zehnder, Richard G. Zepp

WASHINGTON EDITORIAL STAFF

Managing Editor: Stanton S. Miller
Associate Editor: Julian Josephson

MANUSCRIPT REVIEWING

Manager: Yvonne D. Curry
Associate Editors: Diane Scott,
Marie C. Wiggins

Editorial Assistant: Bryan D. Tweedy

MANUSCRIPT EDITING

Journals Editing Manager: Mary E. Scanlan
Associate Editor: Lorraine Gibb

Director, Operational Support:

C. Michael Phillippe

GRAPHICS AND PRODUCTION

Head, Production Department: Leroy L. Corcoran
Art Director: Alan Kahan

Designer: Neal Clodfelter

Production Editor: Jennie Reinhardt

PUBLICATIONS DIVISION

Director: Robert H. Marks
Head, Special Publications Department:
Randall E. Wedin

Head, Journals Department: Charles R. Bertsch

ADVERTISING MANAGEMENT

Centcom, Ltd.

For officers and advertisers, see page 54.

Please send *research* manuscripts to Manuscript Reviewing, *feature* manuscripts to Managing Editor. For editorial policy, author's guide, and peer review policy, see the January 1991 issue, page 45, or write Yvonne D. Curry, Manuscript Reviewing Office, ES&T: A sample copyright transfer form, which may be copied, appears on the inside back cover of the January 1991 issue.

Environmental Science & Technology, ES&T (ISSN 0013-936X), is published monthly by the American Chemical Society at 1155 16th Street, N.W., Washington, D.C. 20036. Second-class postage paid at Washington, D.C., and at additional mailing offices. POSTMASTER: Send address changes to *Environmental Science & Technology*, Membership & Subscription Services, P.O. Box 3337, Columbus, Ohio 43210.

SUBSCRIPTION PRICES 1991: Members, \$39 per year; nonmembers (for personal use), \$73 per year; institutions, \$329 per year. Foreign postage, \$16 additional for Canada and Mexico, \$36 additional for Europe including air service, and \$45 additional for all other countries including air service. Single issues, \$25 for current year; \$31 for prior years. Back volumes, \$367 each. For foreign rates add \$4 for single issues and \$16 for back volumes. Rates above do not apply to nonmember subscribers in Japan, who must enter subscription orders with Maruzen Company Ltd., 3-10 Nihon bashi 2 chome, Chuo-ku, Tokyo 103, Japan. Tel: (03) 272-7211.

COPYRIGHT PERMISSION: An individual may make a single reprographic copy of an article in this publication for personal use. Reprographic copying beyond that permitted by Section 107 or 108 of the U.S. Copyright Law is allowed, provided that the appropriate per-copy fee is paid through the Copyright Clearance Center, Inc., 27 Congress St., Salem, Mass. 01970. For reprint permission, write Copyright Administrator, Publications Division, ACS, 1155 16th St., N.W., Washington, D.C. 20036.

REGISTERED NAMES AND TRADEMARKS, etc., used in this publication, even without specific indication thereof, are not to be considered unprotected by law.

SUBSCRIPTION SERVICE: Orders for new subscriptions, single issues, back volumes, and microform editions should be sent with payment to American Chemical Society, Dept L-0011, Columbus, OH 43268-0011. Phone orders may be placed, using VISA, MasterCard, or American Express, by calling the ACS Sales Office at (614) 447-3776 or toll free (800) 333-9511 from anywhere in the continental U.S. (For general information, in the Washington, D.C., area call 872-4363 or toll free 800-227-5558). Changes of address, subscription renewals, claims for missing issues, and inquiries concerning records and accounts should be directed to Manager, Membership and Subscription Services, ACS, P.O. Box 3337, Columbus, Ohio 43210. Changes of address should allow six weeks and be accompanied by old and new addresses and a recent mailing label. Claims for missing issues will not be allowed if loss was due to insufficient notice of change of address, if claim is dated more than 90 days after the issue date for North American subscribers or more than one year for foreign subscribers, or if the reason given is "missing from files."

The American Chemical Society assumes no responsibility for statements and opinions advanced by contributors to the publication. Views expressed in editorials are those of the author and do not necessarily represent an official position of the society.

SERIES

- 14
The Alaska oil spill: Its effects and lessons. Introduction to a five-part series on the *Exxon Valdez* oil spill of March 1989. Jerald L. Schnoor, University of Iowa, Iowa City, IA.



- 16
Alaska's response to the Exxon Valdez oil spill. Part 1 of a five-part series. Dennis D. Kelso and Marshal Kendziorrek, Alaska Department of Environmental Conservation, Juneau, AK.



- 24
The Exxon Valdez oil spill: Initial environmental impact assessment. Part 2 of a five-part series. Alan W. Maki, Exxon Company U.S.A., Anchorage, AK.

FEATURE

- 30
Dynamic modeling of wastewater treatment processes. Its current status. Paul Lessard, Université Laval, Québec, PQ, Canada; and M. B. Beck, Imperial College, London, England, U.K.

REGULATORY FOCUS

- 40
The momentary politics of the environment. Alvin L. Alm examines recent defeats of environmental referenda and does not see them as a permanent public rejection.

DEPARTMENTS

- 3 Editorial
6 Letters
6 New associate editor appointment
9 Currents
41 Books
43 Products
44 Advisory Board
45 Editorial policy

UPCOMING

Oil spill response, and fate and transport of the Alaska spill. Parts 3 and 4, respectively, of a five-part series

RESEARCH

- 55
Removal of NO_x and SO₂ from flue gas using aqueous emulsions of yellow phosphorus and alkali. David K. Liu, Di-Xin Shen, and Shih-Ger Chang*
Aqueous emulsions containing yellow phosphorus and an alkali are shown to be effective in the removal of NO and SO₂ from simulated flue gas.

- 61
Analysis of alkyl nitrates and selected halocarbons in the ambient atmosphere using a charcoal preconcentration technique. Elliot Atlas* and Sue Schaffler

A method is developed to measure organic nitrates and halocarbons at pptv levels in ambient air.

- 68
Biodegradation of aromatic hydrocarbons by aquifer microorganisms under denitrifying conditions. Stephen R. Hutchins,* Guy W. Sewell, David A. Kovacs, and Garmon A. Smith

A series of laboratory tests is conducted to evaluate whether denitrification would be a suitable alternative for bioremediation of an aquifer contaminated with JP-4 jet fuel.

ESTHAG 25(1)1-186 (1991)
ISSN 0013 936X

Cover: ©1990 Ken Graham Photography
Credits: p. 9, Carol T. Powers, The White House; p. 16, Vanessa Vick/Alaska Department of Environmental Conservation; pp. 24, 25, Gary Lok/Exxon Co., U.S.A.; p. 26, Exxon Co., U.S.A.; p. 30, Neal Clodfelter

ห้องสมุดจุฬาลงกรณ์มหาวิทยาลัย
28 มิ.ย. 2534

- 76
Mechanism of pentachloroethane dehydrochlorination to tetrachloroethylene. A. Lynn Roberts and Philip M. Gschwend*
The dehydrochlorination of pentachloroethane to tetrachloroethylene is investigated to gain insight into mechanisms of hexachloroethane reduction and structure-reactivity relationships for polyhalogenated alkanes.
- 87
Characterization of the H4IIE rat hepatoma cell bioassay as a tool for assessing toxic potency of planar halogenated hydrocarbons in environmental samples. Donald E. Tillitt,* John P. Giesy, and Gerald T. Ankley
This *in vitro* bioassay is identified as an accurate, precise, and potentially useful tool to assess the overall potency of complex mixtures of planar halogenated hydrocarbons.
- 93
Subchronic toxicity study of ozonated and ozonated/chlorinated humic acids in Sprague-Dawley rats: A model system for drinking water disinfection. F. Bernard Daniel,* Merrel Robinson, H. Paul Ringhand, Judy A. Stober, Norbert P. Page, and Greg R. Olson
The administration of ozonated and ozonated/chlorinated humic acids in drinking water to Sprague-Dawley rats for 90 days produces essentially no evidence of subchronic toxicity.
- 99
Identification of oxidized and reduced forms of the strong bacterial mutagen (Z)-2-chloro-3-(dichloromethyl)-4-oxobutenoic acid (MX) in extracts of chlorine-treated water. Leif Kronberg, Russell F. Christman,* Ravinder Singh, and Louise M. Ball
The quantitative determination in chlorinated solutions and the mutagenic potency by the Ames assay of (Z)-2-chloro-3-(dichloromethyl)-4-oxobutenoic acid is performed.
- 104
Study of adsorption-desorption of contaminants on single soil particles using the electrodynamic thermogravimetric analyzer. Leonardo Tognotti, Maria Flytzani-Stephanopoulos, Adel Fares Sarofim, Harris Kopsinis, and Michael Stoukides*
Results of the use of the electrodynamic thermogravimetric analyzer in the study of adsorption and desorption of organic vapors on single particles of several porous soils are reported.
- 110
Environmental applications for the analysis of chlorinated dibenzo-*p*-dioxins and dibenzofurans using mass spectrometry/mass spectrometry. Eric J. Reiner,* David H. Schellenberg, and Vince Y. Taguchi
The optimization of the instrumental parameters and the analysis of polychlorinated dibenzo-*p*-dioxins and dibenzofurans using MS/MS is described.
- 117
Comparative response of reconstituted wood products to European and North American test methods for determining formaldehyde emissions. William J. Groah, John Bradfield,* Gary Gramp, Rob Rudzinski, and Gary Heroux
European and North American test protocols for formaldehyde emissions from wood products are compared.
- 123
Technique for removing water from moist headspace and purge gases containing volatile organic compounds. Application in the purge with whole-column cryotrapping (P/WCC) method. James F. Pankow
A water trap technique that reduces the amount of water in volatile organic compounds containing gas streams is described.
- 127
Solubilization of polycyclic aromatic hydrocarbons in micellar nonionic surfactant solutions. David A. Edwards, Richard G. Luthy,* and Zhongbao Liu
Mole fraction partition coefficients between surfactant micelles and the aqueous pseudophase for three PAH compounds and four nonionic surfactants are evaluated.
- 134
Nonequilibrium sorption of organic chemicals: elucidation of rate-limiting processes. Mark L. Brusseau,* Ron E. Jessup, and P. Suresh C. Rao
The results of experiments designed to identify the process(es) responsible for nonequilibrium sorption of hydrophobic organic chemicals by natural sorbents are reported.
- 143
Hydrolysis of phenyl picolinate at the mineral/water interface. Alba Torrents and Alan T. Stone*
A catalytic effect, analogous to metal ion catalysis observed in solution, is shown to accelerate the hydrolysis of picolinate esters at FeOOH and TiO₂ surfaces.
- 150
Application of the Master Analytical Scheme to the determination of volatile organics in wastewater influents and effluents. Larry C. Michael,* Edo D. Pellizzari, and Daniel L. Norwood
Isolation, identification, and quantitation of 50 target and 55 nontarget volatile organic compounds in wastewater influents and effluents demonstrate the application of the U.S. EPA Master Analytical Scheme.
- 155
Pesticide occurrence and distribution in fog collected near Monterey, California. Charlotte J. Schomburg,* Dwight E. Glotfelty, and James N. Seiber
Evidence supporting the hypothesis that enhanced pesticide concentration in fogwater is caused by sorptive nonfilterable particles and colloids in the fog liquid is presented.
- 161
Detection of poly(ethylene glycol) residues from nonionic surfactants in surface water by ¹H and ¹³C nuclear magnetic resonance spectrometry. J. A. Leenheer,* R. L. Wershaw, P. A. Brown, and T. I. Noyes
The NMR and colorimetric assays of organic solutes isolated from Clear Creek, CO, and from the lower Mississippi River indicate that poly(ethylene glycol) residues are ubiquitous contaminants during both summer and winter.
- 169
Sorption and microbial degradation of naphthalene in soil-water suspensions under denitrification conditions. James R. Mihelcic* and Richard G. Luthy
A coupled solute desorption-degradation model for microbial degradation of hydrophobic organic compounds that are desorbed from porous soil aggregates is presented.
- 178
Use of colloid filtration theory in modeling movement of bacteria through a contaminated sandy aquifer. Ronald W. Harvey,* and Stephen P. Garabedian
This study evaluates the advantages and limitations of using filtration theory in mathematical descriptions of bacterial transport through sandy aquifer sediments.

*To whom correspondence should be addressed.

This issue contains no papers for which there is supplementary material in microform.

Regulation of disinfection by-products

At the Water Quality Technology Conference of the American Water Works Association in San Diego in mid-November, an EPA official announced a new time track for regulation of disinfection by-products (DBPs). DBPs are compounds such as trihalomethanes and haloacetic acids that are formed during the treatment of drinking water with chlorine, ozone, and other disinfectants. The announcement followed a period of several years in which the agency gave signals to the drinking-water industry that the maximum contaminant level (MCL) for trihalomethanes would probably be lowered from its present value of 0.10 mg/L and that other MCLs for DBPs would be promulgated. As a result, many utilities either have converted their treatment plants or are in the process of studies to do so. The most popular option that seemed to be emerging was the combination of preozonation and postchlorination or postchloramination.

The new position of the agency is apparently based on pressure from various quarters to balance the risk of chemical contamination of water (by potentially carcinogenic DBPs) with the risks of microbial contamination caused by inadequate disinfection. What the agency now is saying is that it needs more time to evaluate these chemical and microbiological risks so that it can propose regulations that will ensure safe drinking water from both perspectives.

No one can seriously question this strategy on scientific grounds. If the agency feels that it does not have the information available to propose rational and effective regulations, it should not propose them. What informed people are asking is, What does the agency plan in the way of research to improve the science on which new regulations are based? In San Diego there were questions about the use of models to compare microbiological and chemical risks: Are these models now available, or must they be developed? What data will be used to validate these models? Hardly any detailed microbiological data on water distribution systems are available because of the reliance of the agency on the coliform surrogate in the past. Moreover, few new data are available to show how alternative disinfectants will affect distribution system quality. Will EPA sponsor basic research to develop more meaningful microbiological indicators

and to utilize these in studies of distribution systems using alternative disinfectants, or will the agency simply pick another surrogate such as *Giardia* and use pilot scale data to compare treatment regimes?

In evaluating chemical risks, will the agency include mechanistic considerations in its models for cancer, or will it continue to use the linear extrapolation, no-threshold effect models? What new data does the agency plan to obtain in its health effects research program to address the lack of detailed study of most DBPs? Will chemical exposure studies be expanded to include distribution systems that use alternative disinfectant regimes? How will such studies be controlled?

Another issue that was raised has to do with the impact of the new regulations on small distribution systems. EPA is apparently concerned that there will be an impact on small water supplies if they are brought under the new regulations. Is this concern based on water quality considerations, economics, or politics? Indeed, one wonders to what extent all of the new interest in microbiological risks reflects new approaches within a reorganized Office of Water. One also wonders whether the approach will change again if the faces change in a future administration.

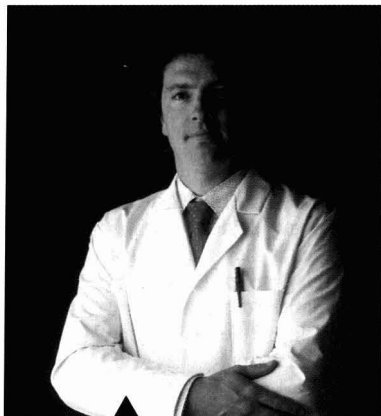
Most of all, given that EPA has slashed the budget for drinking-water research and dismantled a part of its program in Cincinnati, how does the agency plan to carry out all of this research, which is needed to rationally compare microbiological and chemical risks? Will the new models be mere exercises in hand waving?

Since 1974, the American people and the American water industry have looked to EPA for leadership in developing new standards for drinking-water quality, and countries around the world have followed our lead. If we are to reevaluate our position on disinfection by-products, let it be based on sound science, thorough research, and meaningful, verified models.



The Last Three Generations Your Lab Has Three Weeks

"OUR TESTING HAS TO BE DONE QUICKLY. AND ACCURATELY. AND IT HAS TO BE RIGHT THE FIRST TIME." — Dan Vollmer



Dan Vollmer is the lab director for Waste Stream Technology in Buffalo, New York.

Vollmer and his team support Waste Stream's remediation operation by performing critical point-in-time analysis on soil samples from prospective remediation projects. Old industrial sites and landfills contaminated by crude oil, coal tar, benzene, and other volatile aromatics. Waste that has been buried — and often reburied — for decades.

"When we remediate a site, we don't just haul it away," Vollmer says. "We eliminate it. And the method we

use means that we just can't afford downtime. Ever."

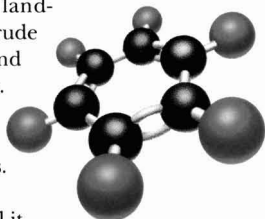
Testing is done with Perkin-Elmer gas chromatographs.

Waste Stream performs the remediation by spraying the site with bacteria which use the contaminant as their carbon source. The bacteria "eat" the contaminant.

"But some 'bugs' work better than others," Vollmer explains. "So first, we do a treatability study. We introduce different bacteria to soil samples, and test the samples at seven-day intervals for three weeks. Then we compare those data to see what kind of degradation rates we're getting. Data handling is the crux of the matter."

Data handling is done with a PE Nelson data station.

In a sample treated with bacteria, the contaminant concentration changes constantly.



Testing complex soil samples for aromatic hydrocarbons contributes to a heavy sample schedule.

Timing is critical. You can't stop the bugs.



Have Buried The Problem. To Uncover The Solution.



Reliable, accurate instruments; complete data handling integration; unparalleled service and support; Perkin-Elmer supplies environmental labs with everything they need for everything they do.

"Our test results not only have to be right," Vollmer says. "They have to be right — right *now*. So it's important that our instruments are up and running. And that we have a quick response to any problems."

The lab relies on Perkin-Elmer service.

Chromatography, spectroscopy, elemental analysis. Instruments, data handling, service. Perkin-Elmer and PE Nelson supply environmental chemists around the world with everything they need for everything they do.

Like the affordable and versatile Model 3100 Atomic Absorption Spectrometer equipped with flow injection; the fast and flexible ELAN 5000 Inductively Coupled Plasma-Mass Spectroscopy system; the ruggedly dependable, totally integrated AutoSystem Gas Chromatograph; the revolutionary Model 1020 Personal Integrator. Or uniquely convenient PE XPRESS, ready to ship in-stock consumables in 24 hrs.*

Whatever the application, whatever the problem. From



Efficient and reliable chromatographic data handling enhances laboratory productivity.

methodologies required by the EPA to deadlines imposed by hungry bacteria. Perkin-Elmer provides solutions to environmental problems through total integration.

*U.S. only

**FOR LITERATURE CALL:
1-800-762-4000***



PERKIN ELMER

Perkin-Elmer Corporation, 761 Main Avenue, Norwalk, CT 06859 U.S.A.
Bodenseewerk Perkin-Elmer GmbH, Postfach 10 11 64, D-7770 Ueberlingen, Federal Republic of Germany
Perkin-Elmer Ltd., Maxwell Road, Beaconsfield, Bucks HP9 1QA, England

See us at the Pittsburgh Conference—Booth #4162.

Circle reader service numbers for:

#15 General Information
#16 AutoSystem GC

#17 AA 3100
#18 1020 Integrator

A protective suit is needed when collecting potentially toxic soil samples.

ES&T LETTERS

Bioconcentration

Dear Sir: We read with great interest Mace Barron's comprehensive discussion on factors influencing bioconcentration (*ES&T*, November 1990, p. 1612). Predicting accumulation of contaminants in aquatic organisms is not only of scientific concern, but plays a vital role in the development of environmental regulations as well. Barron's article is especially timely in light of EPA's soon-to-be-released guidance document on bioconcentratable substances.

The current EPA risk assessment formula for establishing water quality criteria uses a bioconcentration factor to predict aquatic organism accumulation of contaminants and subsequently, human exposure to contaminants. Implicit in this methodology is the assumption that aquatic organisms accumulate contaminants only via bioconcentration (diffu-

sion across the gill membrane). However, as Barron mentioned, strong hydrophobes (like dioxin and certain PCBs) are not bioavailable to aquatic organisms via bioconcentration. Rather, the important uptake route for these substances is ingestion of contaminated food and sediment. In order to correctly predict aquatic organisms contaminant levels of hydrophobic compounds, the ingestion uptake pathway cannot be ignored.

Continued focus on the bioconcentration of strongly hydrophobic substances points to a significant gap in the melding of scientific research and regulatory needs. In order to develop scientifically sound water quality criteria for these pollutants, any risk assessment formula (which functions as a predictor of fish tissue contaminant levels) must consider the ingestion uptake route. For this to

occur: (1) greater emphasis must be placed on development of accumulation factors which predict aquatic organism accumulation of contaminants via the ingestion route; and (2) regulators must begin to focus on effluent solids when regulating strongly hydrophobic compounds.

We have proposed an alternative to the standard water quality criterion risk assessment formula, which considers aquatic organism ingestion of hydrophobic contaminants (1). We hope that this serves to stimulate further research and discussion in this area.

Reference

- (1) Rifkin, E.; LaKind, J. J. *Toxicol. Environ. Health*, in press.

Judy LaKind
Rifkin & Associates
Columbia, MD 21044

Schnoor named associate editor

Continuing the overall high quality of *ES&T*, Editor William Glaze has appointed Jerald L. Schnoor as associate editor to replace Philip C. Singer, who will continue his teaching and research assignments at the University of North Carolina-Chapel Hill.

Schnoor is professor in the Department of Civil and Environmental Engineering at the University of Iowa in Iowa City. He was chair of the department for five years and chose to continue research and teaching in environmental engineering.

He received his Ph.D. from the University of Texas at Austin in 1975. His research specialty is inorganics of aquatic systems.

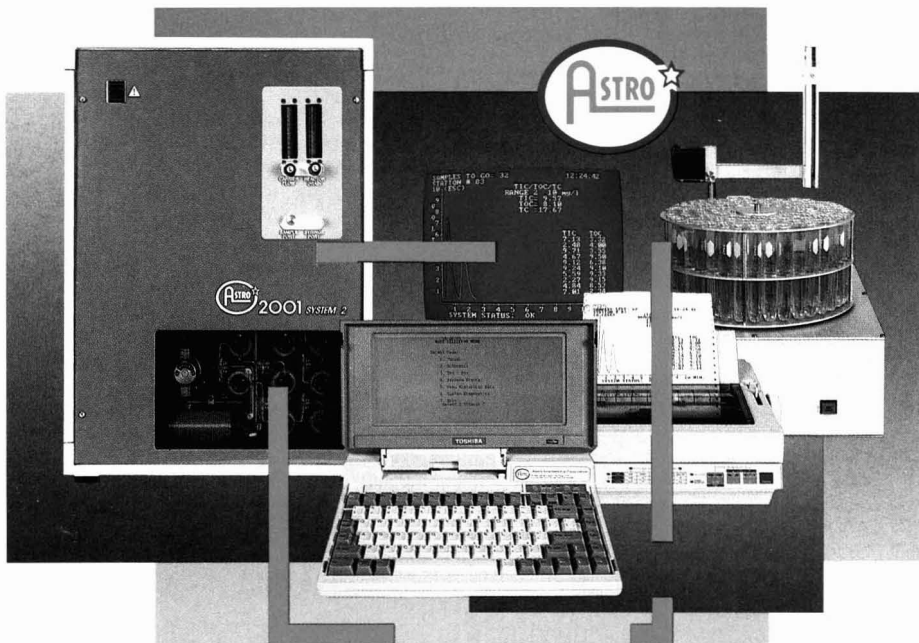
Schnoor teaches graduate courses in environmental systems modeling, environmental chemistry, and water quality. A major focus of his research is water quality modeling and aquatic chemistry, especially the effects of acid deposition, ground water toxics and pesticides, and global climate change.

Schnoor is a traveler who keeps in contact with the environmental community. He visited Alaska and invited experts to contribute to *ES&T*'s oil spill series; he visited Hungary recently to participate in environmental cleanup; he visits EAWAG and maintains associations with researchers there; and he will chair the Gordon Research conference on water in June 1992.



Schnoor: Liaison with water reviewers

AUTOMATED. AFFORDABLE. TOC ANALYSIS.



The complete ASTRO SYSTEM 2 price includes:

System 2 is actually two laboratory analyzers in one, with the ability to handle both low temperature uv oxidation and optional high temperature combustion analysis. It performs TOC, TIC, and TC analysis on the same sample and includes a dual wavelength NDIR detector designed for corrosive gases. A remarkable sensitivity range insures accurate results from parts per billion to 20,000 parts per million. The System 2 complies with EPA 415.1 and standard methods 505A and 505B.

System 2 stores months of raw data—

- ASTRO Model 2001 TIC/TOC/TC Analyzer
- 120 Station Autosampler
- Toshiba T1000 Laptop Computer with 1Mb RAM
- Real-Time Graphics with Statistical and Reporting Software
- Full-Sized Printer
- All Cables and Operating Software

up to 10,000 analyses per disk — for easy retrieval and evaluation. Statistical and reporting software uses real-time graphics and data displays.

Options include a VOA vial autosampler upgrade and a high temperature module for volatile samples, solids, and sludges.

For complete product information, including the surprisingly low System 2 price, contact Astro International Corporation, 100 Park Avenue, League City, Texas 77573. Phone: (713) 332-2484 FAX: (713) 554-6795

Emerging Developments in Environmental Science

Emerging Developments in Environmental Science

ENVIRONMENTAL SCIENCE & TECHNOLOGY

Enter your own monthly subscription to ES&T and receive the most authoritative technical and scientific information on environmental issues today.

YES! I want my own one-year subscription to ENVIRONMENTAL SCIENCE & TECHNOLOGY at the rate checked below:

1991 Published Monthly	U.S.	Canada & Mexico	Europe	All Other Countries
ACS Members:	\$ 39	\$ 55	\$ 75	\$ 84
Nonmembers-Personal	\$ 73	\$ 89	\$109	\$118
Nonmembers-Institutional	\$329	\$345	\$365	\$374

In a hurry? Call Toll FREE 800/227-5558 (U.S. and Canada) or 202/872-4363 (in D.C. and outside the U.S. and Canada). To FAX your order call: 202/872-4615.

Payment Enclosed (Payable to American Chemical Society)
 Bill Me Bill Company Charge my VISA/MasterCard

Card No. _____

Expires _____ Signature _____

Name _____

Title _____ Employer _____

Address Home Business _____

City, State, ZIP _____

Employer's Business:
 Manufacturing Academic Government Other _____

Member rates are for personal use only. Subscriptions outside the U.S., Canada, and Mexico are delivered via air service. For a calendar year subscription, notify ACS when order is placed. Foreign payment must be made in U.S. currency by international money order, UNESCO coupons, or U.S. bank draft. Orders accepted through your subscription agency. For nonmember rates in Japan, contact Maruzen Co. Ltd. Please allow 45 days for delivery of your first issue. Redeem until December 31, 1991.

580 **MAIL THIS POSTAGE-PAID CARD TODAY** 6031P

ENVIRONMENTAL SCIENCE & TECHNOLOGY

Enter your own monthly subscription to ES&T and receive the most authoritative technical and scientific information on environmental issues today.

YES! I want my own one-year subscription to ENVIRONMENTAL SCIENCE & TECHNOLOGY at the rate checked below:

1991 Published Monthly	U.S.	Canada & Mexico	Europe	All Other Countries
ACS Members:	\$ 39	\$ 55	\$ 75	\$ 84
Nonmembers-Personal	\$ 73	\$ 89	\$109	\$118
Nonmembers-Institutional	\$329	\$345	\$365	\$374

In a hurry? Call Toll FREE 800/227-5558 (U.S. and Canada) or 202/872-4363 (in D.C. and outside the U.S. and Canada). To FAX your order call: 202/872-4615.

Payment Enclosed (Payable to American Chemical Society)
 Bill Me Bill Company Charge my VISA/MasterCard

Card No. _____

Expires _____ Signature _____

Name _____

Title _____ Employer _____

Address Home Business _____

City, State, ZIP _____

Employer's Business:
 Manufacturing Academic Government Other _____

Member rates are for personal use only. Subscriptions outside the U.S., Canada, and Mexico are delivered via air service. For a calendar year subscription, notify ACS when order is placed. Foreign payment must be made in U.S. currency by international money order, UNESCO coupons, or U.S. bank draft. Orders accepted through your subscription agency. For nonmember rates in Japan, contact Maruzen Co. Ltd. Please allow 45 days for delivery of your first issue. Redeem until December 31, 1991.

580 **MAIL THIS POSTAGE-PAID CARD TODAY** 6031P



(800)227-5558 (U.S. and Canada)



BUSINESS REPLY MAIL

FIRST CLASS PERMIT NO. 10094 WASHINGTON, D.C.

POSTAGE WILL BE PAID BY ADDRESSEE

American Chemical Society
Marketing Communications Department
1155 Sixteenth Street, N.W.
Washington, D.C. 20077-5768



(800)227-5558 (U.S. and Canada)

BUSINESS REPLY MAIL

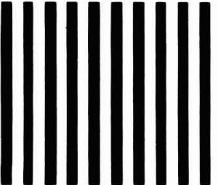
FIRST CLASS PERMIT NO. 10094 WASHINGTON, D.C.

POSTAGE WILL BE PAID BY ADDRESSEE

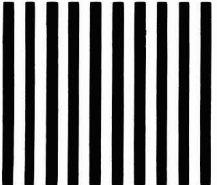
American Chemical Society
Marketing Communications Department
1155 Sixteenth Street, N.W.
Washington, D.C. 20077-5768



NO POSTAGE
NECESSARY
IF MAILED
IN THE
UNITED STATES



NO POSTAGE
NECESSARY
IF MAILED
IN THE
UNITED STATES



ES&T CURRENTS

INTERNATIONAL

The British government has published its first comprehensive survey of all aspects of environmental concern in a White Paper issued Sept. 25. After discussing general principles and objectives, the White Paper deals with the U.K.'s approach to domestic and international problems such as global climate change, stratospheric ozone depletion, acid rain, pollution control, and land use planning and conservation. The document also stresses the need "to find the right balance between regulation and market mechanisms" and maintains that "responsibility for the environment is not a duty for government alone." *ES&T's* U.S. readers who desire more information on the White Paper, entitled "This Common Inheritance," should contact Roger D. Jennings, First Secretary (Science and Technology), British Embassy, 3100 Massachusetts Ave., N.W., Washington, DC 20008.

The United States refused to join other industrialized nations in making a commitment to limit emissions of so-called greenhouse gases. Representing the United States at a United Nations conference in Geneva, John Knauss, administrator of the National Oceanic and Atmospheric Administration, acknowledged the need to develop a program to reduce greenhouse gases. He added, however, "We just don't believe in targets . . . we are not prepared to guarantee our projections." Currently, the United States generates 22% of the world's carbon dioxide emissions. Germany has committed itself to a 30% reduction of its CO₂ emissions by 2005. Other European countries, Australia, and Japan have pledged to stabilize or reduce emissions of greenhouse gases by 2000. Negotiations on a worldwide treaty to control greenhouse gas emissions are scheduled to begin in Washington in February.

FEDERAL

Attorney General Dick Thornburgh announced Nov. 5 the first-ever federal indictment against a company for violations of the Safe Drinking

Water Act (SWDA). Weatherbee Supply Inc. (Bowling Green, KY) and its president, Glenn Weatherbee, are charged with 10 counts of willfully constructing and operating five underground injection wells to inject fluids into a source of drinking water without first obtaining an EPA permit. They also are accused of falsifying an application for an injection permit by understating the number of wells they intended to construct and operate. Each violation of the SDWA carries a maximum penalty of three years' imprisonment and a \$250,000 fine for an individual and a maximum fine of \$500,000 for the corporation.

EPA administrator William Reilly signed regulations Oct. 31 that cover permits for stormwater discharge. He signed them under a court order (*Williams v. EPA*). The new rules require more than 100,000 industrial plants, 173 cities, and 47 counties to obtain permits designed to limit discharges of storm water runoff that contains pollutants such as oil, grease, pesticides, and debris. James Elder, director of EPA's enforcement and permit operations, says that these regulations, actually released Nov. 5, represent a first phase and that more nonpoint source rules will be issued in a few months.



Bush signs Clean Air Act

On Nov. 15, President Bush signed the Clean Air Act of 1990. Among the new law's provisions are limits on automotive emissions of 0.25 g/mi for hydrocarbons (HC) and 0.4 g/mi for NO_x. Limits under the old law were 0.41 g/mi for HC and 1 g/mi for NO_x. Moreover, gasoline sold in the "dirti-

est" cities must be reformulated to reduce toxic emissions by 15% by 1995 and by at least 20% by 2000. The new law also mandates maximum achievable control technology (MACT) for emitters of 189 airborne toxics by 2003. Emissions of SO₂ must be reduced to 8.9 million tons per year by 2000, a 10 million-ton reduction from 1980 levels. Carbon tetrachloride and methyl chloroform essentially become forbidden solvents by 2000 and 2002, respectively, and recycling of chlorofluorocarbons in air conditioners and refrigerators must begin in 1992.

EPA announced Nov. 13 that it has revised the Superfund Hazard Ranking System (HRS) to improve accuracy in assigning priorities to hazardous waste sites for placement on the National Priorities List (NPL). The revised HRS addresses surface water contamination that may affect the human food chain, *potential* as well as ambient air contamination, and possible threats to drinking-water wells. Other revisions include the consideration of soil, as well as other media, as a path of exposure; the consideration of chronic and carcinogenic threats as well as acute toxicity; and improved precision in considering the migration of certain contaminants through groundwater and air. Sites currently on the NPL need not be reassessed. The revised HRS will affect new sites, most likely beginning in early 1991. Hazard evaluation for the NPL also is addressed in *ES&T* 1990, 24(12), 1778.

The National Library of Medicine (NLM) has placed the Chemical Identification File (ChemID) on line; it's a "directory assistance" program for users who need to retrieve biomedical and toxicological information about chemicals from NLM data bases. ChemID also provides information from other selected resources. The computer data base contains records on more than 180,000 chemicals—according to an NLM spokesperson, a small fraction of the 10 million substances cited in the literature, but one that "encompasses the core set of chemicals of biomedical and toxicological

interest." Online charges for ChemID average \$30 per connect hour. For more information telephone (301) 496-6193 or (800) 638-8480.

EPA has issued the first emissions certificate for a vehicle designed to run on M85, a blend of 85% methanol and 15% unleaded gasoline. The vehicle is a Chevrolet Lumina which also can use unleaded gasoline. According to EPA studies, the use of M85 will reduce emissions of toxic pollutants and smog precursors by 30-40%. These studies, however, still engender controversy among scientists and engineers in the field of automotive emissions.

An EPA survey of the nation's community drinking-water wells indicates that 10% of them are contaminated with pesticides. In addition, 4% of rural domestic drinking-water wells may contain detectable residues of at least one pesticide. Nevertheless, fewer than 1% have pesticide levels above which human health is considered threatened. More than 50% of the nation's wells, however, contain nitrates, with about 1.2% of the community wells and 2.4% of rural wells showing levels above the 10-ppm level established to protect human health. To conduct the survey, EPA sampled 1347 wells nationwide and included wells in each state.

STATES

Carlsbad, NM, will be the site of limited experimental disposal of mixed low-level radioactive and hazardous wastes. Under the terms of a permit EPA issued to the Department of Energy Nov. 1, a maximum of 8500 drums of mixed waste may be placed in DOE's Waste Isolation Pilot Plant (WIPP), located in Carlsbad. That number represents 1% of WIPP's total capacity. Also, the waste must be readily retrievable in case WIPP proves unsuitable for permanent disposal of wastes. Moreover, DOE must monitor the air within WIPP and test wastes for hazardous compounds and flammable gases before their placement in the plant. If DOE ultimately decides that WIPP is a suitable facility, it must get a new permit from EPA to continue using the site. For more on mixed waste disposal, see *ES&T* 1990, 24(8), 1140.

Kentucky Gov. Wallace Wilkinson signed an order that forbids creating new landfills or expanding existing ones in the state. Issued Oct. 19,

the order remains in effect at least until a special session of the legislature is convened to consider stricter solid waste rules, including limits on wastes imported from out of state. In addition, existing landfills may accept no more than 5% by weight or volume of the amount of wastes they accepted between July 1989 and June 1990, unless they have contracts dated before Oct. 19 that require a greater amount, or unless cognizant officials find that more capacity is needed to take wastes generated in Kentucky. Gov. Wilkinson wants the legislature to mandate a comprehensive program for managing solid wastes. "I don't want Kentucky to be a dumping ground for out-of-state wastes," he added.

Solid waste management facility operators in Minnesota must develop plans for handling household hazardous wastes, under rules proposed Oct. 8 by the Minnesota Pollution Control Agency (MPCA). By June 30, 1992, facility operators must show how they will handle wastes such as antifreeze, oils, paints, and solvents. They also must explain how they will take part in county management programs and provide the public with information that is consistent with county household hazardous waste education programs. In addition, MPCA proposed rules Nov. 1 that would regulate the disposal of used batteries, thus bringing the rules into conformity with federal regulations.



Response training at CHMR site

The University of Pittsburgh now has a 10-acre training complex for chemical emergency responses. Located in Harmarville, PA, the facility provides response training for situations such as railroad car derailments, chemical spills, abandoned waste sites, tanker truck rollovers, and decontamination processes. Major course categories include hazardous waste operation, emergency response, occupational health and safety, and environmental compliance. The site is managed by the university's Center

for Hazardous Materials Research (CHMR) and was dedicated Sept. 21.

The Zimmer Generating Station (Moscow, OH) will be the first nuclear plant to be converted to a coal-fired power plant. The 1300-MW plant is scheduled to go on stream in June 1991 at a budgeted cost of \$3.6 billion. Spokespersons for American Electric Power Service (AEPS), the project manager, say the plant will remove a minimum of 91% of the SO₂ produced during coal combustion and 99.8% of fly ash or particulate matter. The air pollution control system will produce a granular material "suitable for placement in Zimmer's landfill." But why convert the plant at all? Because of fierce local opposition to a nuclear plant, uncertainty of the technology involved, and management's desire not to abandon more than \$1.7 billion already invested in the plant whose construction had been stopped back in 1982.

AWARDS

The 1991 Innovative Radon Mitigation Design Competition is under way. It is open to any individual or group of individuals who have developed a practical or theoretical innovative design for radon mitigation. Deadline for submission of entries is Jan. 31, 1991. The grand prize is \$4000; second prize is \$3000; third prize is \$1500. There also are prizes for a theoretical design and a student's design. For more information and an entry form, contact Ruth Bennett, Innovative Radon Mitigation Design Competition, Association of Energy Engineers, 4025 Pleasantdale Road, Suite 420, Atlanta, GA 30340; phone (404) 447-5083.

SCIENCE

How do acid rain, ozone, and other air pollutants damage pine forests? To answer this question, a team of scientists from the Lawrence Livermore National Laboratory and other organizations are using a portion of the U.S. Forest Service facility near Chico, CA, as the world's largest outdoor laboratory for controlled studies of air pollution effects. The object of the study is all parts of ponderosa pine trees and seedlings; this species covers more than 4.5 million acres (1.8 million ha) in California. The scientists are using various types of apparatus, including a specially developed branch exposure chamber to measure effects of specific amounts

of chemicals on trees. The equipment and methods include gas exchange, radioactive isotopes, enzymatic assays, and electron microscopy.

There is no evidence of excess occurrence of cancer among persons living near nuclear power facilities, according to results of a two-year study by the National Cancer Institute. The study, *Cancer In Populations Living Near Nuclear Facilities*, assessed mortality from 16 types of cancer in people living in 107 counties in 34 states, near 62 nuclear facilities. Cancer mortality was found to be no higher in those counties than in 292 counties without nuclear facilities. In fact, the risk of death from leukemia actually was found to be lower. Leukemia was emphasized because of its short latency period, which averages about five years. Moreover, no adverse health effects were demonstrated for exposures below 10 rem, a level thousands of times higher than that permitted by the Nuclear Regulatory Commission for a hypothetical person standing at the fencepost of a nuclear plant 24 h/day for one year.

Why haven't contaminants from a uranium mill tailings pile migrated to groundwater? Doctoral candidate Patrick Longmire believes that a unique interaction among groundwater, contaminants, and the surrounding soil at a site outside Maybell, CO, is forming a natural geochemical barrier. He hopes that what he learns may lead to the design of a cost-effective geochemical that can prevent chemical and radioactive wastes from migrating to groundwater. Longmire presented his findings at the annual meeting of the Geological Society of America in Dallas, TX, in late October. He has been conducting his research for the Los Alamos National Laboratory (Los Alamos, NM).

If the world's climate warms as much as some fear, world food supplies could be substantially reduced, according to a report, *Climate Change and World Agriculture*, released by the United Nations Environment Programme and the International Institute for Applied Systems Analysis (Laxenburg, Austria). The report projects increases in global mean temperatures by 1.1 °C by 2030 and by 4 °C by 2090. Because of warmer, dryer conditions, losses in agricultural production could run as high as 10–30% in "breadbasket" regions such as the American Midwest, the Soviet Ukraine, the Argentine pampas, and

the Australian wheat belt. These losses would not be offset by gains in other areas, according to the report.

TECHNOLOGY



Warsawsky (l) and Gressel show weed killer's action

It may become possible to reduce herbicide use substantially because of a new weed-fighting strategy developed at the Weizmann Institute of Science (WIS, Rehovot, Israel). Scientists Jonathan Gressel, Yosef Shaaltiel, and Abraham Warsawsky devised a chemical agent that breaks down a weed's natural defenses against herbicides. These defenses usually consist of enzymes that act as shields against the herbicides' hydroxyl radicals that kill the weeds. The weeds' enzymes must work in the presence of certain trace metals. The WIS researchers use a chelator to remove the trace metals, thereby rendering the weeds' defensive enzymes inoperative. Moreover, they found a way to make their chemical work synchronously with the herbicide. The scientists estimate that with their chemical, herbicide applications may be reduced by 50–75%.

Methane can be converted to other valuable hydrocarbons without the production of unwanted carbon dioxide, thanks to a catalyst that consists of a ternary mixture of calcium, nickel, and potassium oxide. When methane and oxygen are passed over the catalyst at 600 °C, about 10–12% is converted to higher paraffins and olefins that, in turn, can be used to make gasoline or chemical feedstocks. Methane is the principal component of natural gas, which the United States has in relative abundance. Researchers at the Lawrence Berkeley Laboratory, where the work is being done, add that they operate their process with steam "which no one else has done," and that conventional processes that produce by-product CO₂ work at 750–850 °C. Moreover, unconverted methane can be recycled with no need for expensive CO₂ scrubbing steps.

BUSINESS

Environmental performance certification of companies could be the wave of the future, says Gilbert Hedstrom of Arthur D. Little (Cambridge, MA). Certification could be a way to assure stockholders, customers, the government, and the public that a firm is environmentally responsible. Hedstrom points out, however, that standards used for certification need to be defined. Also, he asks, "Should certification cover the audit process only, the environmental, health, and safety (EHS) management systems, or the company's overall EHS performance?" Hedstrom adds that although certification handled internally rather than by an outsider would be less costly, "the down side would be the likely perception that the certification lacks objectivity." A final issue involves the kind of information to be released for certification, he notes.

Merck & Co. (Rahway, NJ), a major chemical manufacturer, announced Nov. 1 a set of ambitious emission control goals. Among these goals is a 90% reduction of emissions of suspected carcinogens in Merck's worldwide operations by the end of 1991; a total elimination of those emissions or the application of best available technology by the end of 1993; and a 90% worldwide reduction of all environmental releases of toxic chemicals by the end of 1995. Merck spokesman John Doorley says that his company is undertaking these tasks "even though our emissions are well below permitted limits." He adds that Merck will increase efforts to conserve energy, recycle renewable resources, and find ways to prevent generating waste.

U.S. companies wanting to do environmental business with Southeast Asian countries and firms would do best to initially concentrate on wastewater and solid waste management, hazardous waste control, air pollution, and environmental assessments and modeling, according to the U.S.–ASEAN Council for Business and Technology. The countries involved are Brunei Darussalam, Indonesia, Malaysia, the Philippines, Singapore, and Thailand. For more information on Southeast Asian markets and seminars on this topic, contact Ernest Bower at U.S.–ASEAN Council, Suite 650, 1400 L St., N.W., Washington, DC 20005; (202) 289-1911; Fax: (202) 289-0519.



sartorius

0 100 %
+ 00.00 g
R1 $\Delta\Delta$



T



With 1 mg readability, this is how your balance perceives a casual draft

Perception is a matter of perspective. To an ordinary balance with 1 mg readability, the draft in a fume hood is a hurricane. The slam of a cabinet door is a clap of close thunder.

Given this perspective, it's easy to understand how a digital readout may have difficulty maintaining its accuracy. But when digits begin racing, you are the one left waiting for stabilization.

Scientists commonly call these normal laboratory disturbances "ambient conditions." The performance of your balance at any readability is crucial. Uncertainty about your readout, or having to wait for the storm to blow over are the last things you want.

What you do want is for the precise readout to appear and stabilize, regardless of ambient conditions.

And that's what Sartorius MC 1 balance technology gives you. These are the only balances with a microcomputer—a functioning intelligence beyond microprocessors—programmed to filter out noise, vibrations, and other disturbances. The result? The display stabilizes in *half the time* of the competition.

With MC 1 technology, your balance will keep its balance, and your results will be true to your world.

For more information on this breakthrough in balance technology, call, write, or circle the number below. Sartorius Instruments, 1430 Waukegan Rd., McGaw Park, IL 60085. Phone: 800-544-3409 FAX: 708-689-2038.

sartorius

Stable. Smart. Sartorius.

CIRCLE 14 ON READER SERVICE CARD

The Alaska oil spill: Its effects and lessons

On March 24, 1989, a serious environmental accident occurred. It was not a human tragedy of the magnitude of the methyl isocyanate leak at Bhopal, India, or of the Chernobyl nuclear disaster in the Soviet Union. However, the oil spill in Prince William Sound, Alaska, soaked and killed plants and animals over 2,000 miles of shoreline and 500 miles away. Some 30,000 dead birds of 90 species were retrieved within the first four months following the spill. Scientists continue to research the long-term effects on bird hatching success, fish spawning, and mammal bioaccumulation of hydrophobic organics. Reasonable people differ in their interpretation of these results, the magnitude of the long-term damage, and estimates of recovery time. In the series of articles beginning in this issue, the leading authorities who were involved with the cleanup effort and scientific studies will report their results for the first time.

When the *Exxon Valdez* broke open on Bligh Reef and spilled 11.2 million gallons of crude oil, a unique environmental insult occurred. It was the largest oil spill ever recorded in the United States and one of the largest in the world. Prince William Sound is in a cold-water region where reproduction rates for animal and plant life are slow—an ecologically sensitive area as well as an area of renowned scenic beauty, national parks, and national forests. Fifteen-foot tides made control of the spill difficult. The spill presented logistical, technical, and scientific challenges never before encountered.

Legal and jurisdictional duties were complicated—the U.S. Coast Guard was in charge of overseeing spill cleanup; the Alyeska Pipeline Service Company was responsible for immediate spill response under the Oil Spill Emergency Response Plan; Exxon was in charge of directing and paying for the cleanup;

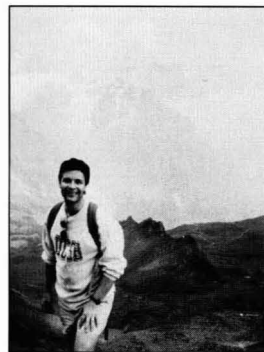
and the Alaska Department of Environmental Conservation (ADEC), in conformance with state law, had jurisdiction over water quality and fisheries. The spill tested the ability of government and industry to cooperate on a scale rarely encountered in the United States and required a tremendous amount of resources. Exxon has spent some 2 billion dollars to date; more than 100 lawsuits are outstanding. Damage assessments have not been completed and will remain in the courts for several years.

In this series, the following five articles will be presented in the January–March issues.

- “Alaska’s Response to the *Exxon Valdez* Spill” by Dennis Kelso and Marshall Kendziorek, Alaska Department of Environmental Conservation. Kelso is the Commissioner of Alaska’s Department of Environmental Conservation and was in charge of the state’s efforts, especially shoreline cleanup and surveys.
- “The *Exxon Valdez* Oil Spill: Initial Environmental Impact Assessment” by A. K. Maki, Exxon Company. Alan Maki led Exxon’s cleanup response and scientific studies.
- “Oil Spill Response Capabilities in the U.S.” by William Westermeyer, U.S. Congress, Office of Technology Assessment (OTA). Westermeyer wrote the 1989 OTA “Report on Oil Spill Response Technology.”
- “Fate and Transport of the *Exxon Valdez* Oil Spill” by J. A. Galt, W. J. Lehr, and D. L. Payton, National Oceanic and Atmospheric Administration (NOAA). Jerry Galt, of NOAA’s Seattle Hazardous Materials Section, directed mathematical modeling of the fate and transport of the oil and its constituents.
- “Bioremediation of the Alaska Oil Spill” by P. H. Pritchard, EPA, Gulf Breeze Environmental Research Labo-

ratory. ‘‘Hap’’ Pritchard headed EPA’s bioremediation efforts and related research studies.

The oil spill at Prince William Sound was caused by human error and was largely preventable. We hope to learn from these disasters so we do not have to relive them. This series in *ES&T* reports the first comprehensive technical data on the *Exxon Valdez* oil spill, its impacts, and some lessons learned.



Jerald Schnoor

The outline of this series was written by Jerald L. Schnoor, who suggested and coordinated the articles and encouraged officials and scientists to contribute to the series. Schnoor is on the ES&T advisory board and is codirector of the Center for Global and Regional Environmental Research at the University of Iowa Department of Civil and Environmental Engineering. After visiting Alaska last May, Schnoor was in the enviable position of inviting the most appropriate, credible, and reliable officials to share their information in this series.

Attention
ACS Members

Support the
American
Chemical
Society's
**CAMPAIGN
FOR
CHEMISTRY**

- ◆ to promote scientific literacy.
- ◆ to ensure a future generation of scientists and researchers.
- ◆ to meet the long-term technical demands of our society.

When it's your turn to give...
remember your investment
in the Campaign for Chem-
istry is an investment in
everyone's future.

For details:
Phone 202/872-4094



**CAMPAIGN
FOR
CHEMISTRY**

**WATER
TESTING
REAGENTS
AND
SOLUTIONS**



From Ferrous Ammonium Sulfate to Densotrophic Solvent, Anderson Laboratories can supply the water testing reagent to fit your particular need, no matter how common or how rare.

Anderson Laboratories has a large selection of water testing reagents in stock with many more available. Reagents and solutions are available for: EPA (Clean Water Act); ASTM; AOAC; APHA; and USGS recommended tests.

WE SHIP WITHIN 48 HOURS:

Because of our large network of dealers throughout the U.S. we can fill and ship your order within 48 hours. We have dealers in every major metropolitan area in the U.S. Your BANCO® dealer is listed in the yellow pages under *Laboratory Equipment and Supplies* or call to find the dealer nearest you.

BANCO®
• STANDARDIZED •

Anderson Laboratories, Inc.
5901 Fitzhugh Avenue
Fort Worth, Texas 76119
Telephone: (817) 457-4474

CIRCLE 1 ON READER SERVICE CARD

**One trapping
system for
air, water
and solids!**

CDS Concentrators meet
the tough demands of
environmental
analysis...



Easily interchangeable modules—
sparger, impinger, thermal desorber—
permit use of the same trapping
system for wastewater, drinking water,
air, soil and sludge for volatiles and
foods. Plus, CDS 300/330 concen-
trators interface easily to any GC and
meet or exceed all EPA requirements.

**Complete versatility to meet your
demanding specifications.**

- Purge and trap, headspace, air monitoring, pyrolysis and reactant gas analyses.
- 9 method storage (most available anywhere).
- 1°C temperature control.
- Trap dry and bake functions standard.
- Cryogenic trapping and refocusing.

Call toll free in USA
(800) 541-6593

Free technical support from our applications lab.

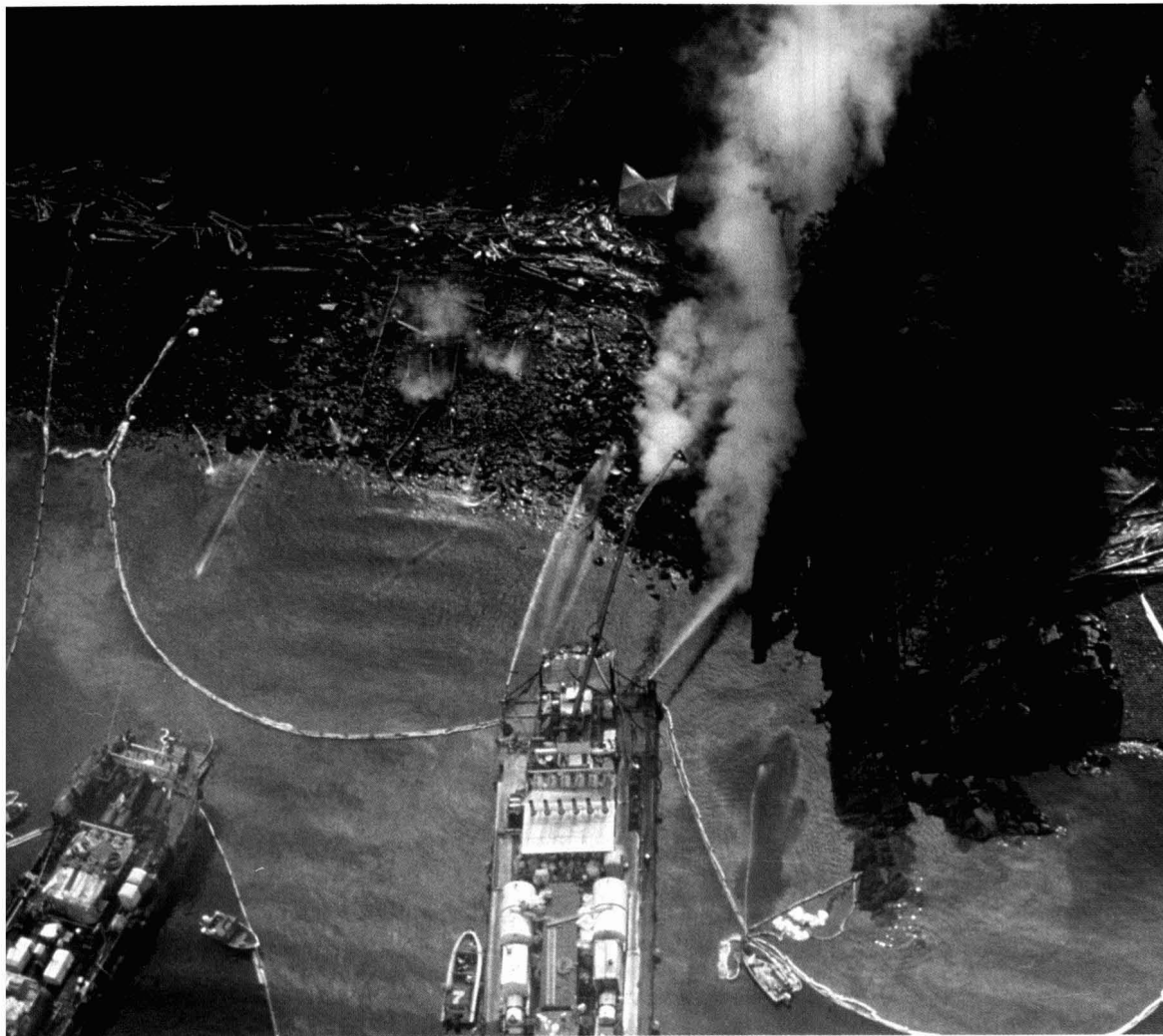
CDS™
INSTRUMENTS

Autoclave Engineers—Oxford
7000 Limestone Road, Oxford, PA 19363
Phone: 215-932-3636 FAX: 215-932-4158
Telex: 83-5308

CIRCLE 2 ON READER SERVICE CARD

Alaska's response to the *Exxon Valdez* oil spill

Part 1 of a five-part series



Dennis D. Kelso
Marshal Kendziorek
*Alaska Department of
Environmental Conservation
Juneau, AK 99811*

When the tanker *Exxon Valdez* ripped its hull on Bligh Reef in Alaska's Prince William Sound, spilling nearly 11 million gallons of crude oil, it also shattered

the confidence of many Americans in the technology and management systems used to prevent and respond to spills. The March 1989 oil spill killed more wildlife than any spill in history: an estimated 100,000–300,000 sea birds, thousands of marine mammals, and hundreds of bald eagles (1). The spill disrupted the herring and salmon harvests of commercial and subsistence fisheries that had consistently supported commu-

nities in the spill area. In villages scattered along more than a thousand miles of the affected coastlines, the spill devastated subsistence fishing, hunting, and gathering—essential parts of the rural economy and Native American culture.

Oil on the beaches also impaired recreation and local tourism businesses. The immediate impacts were magnified by uncertainties about the future: What would be the long-range effects of the

spill on the health and productivity of the damaged ecosystems? Would the shorelines return to their original condition? How long would it take? No one really knew the answers. And people throughout the country were asking another hard question: What can we do to make sure this never happens again?

The sense of national urgency increased as a swarm of smaller spills followed the *Exxon Valdez* disaster: The *World Prodigy* ran aground off Providence, Rhode Island; an Exxon pipeline spilled oil into Arthur Kill between New York and New Jersey; the *American Trader* punctured its hull near Huntington Beach, California; the *Mega Borg* caught fire and spilled oil in the Gulf of Mexico; and vessel collisions in the Houston ship channel produced multiple spills. Even worse, this series of spills was not an anomaly. According to the Alaska Oil Spill Commission, oil discharges the size of the *Exxon Valdez* spill occur somewhere in the world every year (2); on average, a spill of a million gallons happens every month (2).

Anatomy of the response

This spill response had three phases: immediate containment and recovery of oil from the water; emergency removal of oil from the shoreline; and long-term shoreline treatment to remove oil. In addition to the direct spill response, state and federal agencies also initiated natural resource damage assessment and restoration efforts.

Phase 1: Containment and recovery of oil from the water. Effective response requires immediate action to contain and recover as much oil as possible before the oil spreads and becomes even more difficult to collect. Rapid removal of oil helps limit damage to wildlife and other natural resources by minimizing contact with the oil and by reducing the amount that reaches shore or other sensitive areas. In addition to protecting natural resources by removing oil from the environment, defensive measures—booms, skimmers, and other equipment—can be used to exclude the oil from the most sensitive areas.

One of the technologies that had been identified in the oil spill contingency plan for Prince William Sound was use of chemical dispersants. This technique also had been preapproved by the state of Alaska for use in a large section of Prince William Sound bordering the tanker lanes (Figure 1). Several conditions must exist for a dispersant application to be effective:

- Weather and sea conditions must be energetic enough for mixing to take place but not so rough as to preclude use of the application equipment.

- Adequate equipment must be in place to apply the dispersant.
- Enough dispersant must be readily available for application. Based on a commonly used chemical:surface area ratio of 1:20, it would have been necessary to apply more than 500,000 gallons of dispersant.
- The oil must be relatively unweathered.

In the first days, weather and sea conditions were not favorable for dispersant use. Initial trial applications of dispersants were unsuccessful either because of misapplication or because of the lack of wave action to help mix and distribute the dispersant. A successful application occurred on the evening of the third day as the weather began to change. Nonetheless, dispersants did not make a

“

By the fourth day [after the spill], the state had developed a geographic information system on site for mapping the movement of the slick.

”

substantial contribution to the response, largely because Exxon and Alyeska lacked adequate quantities of dispersant and application equipment to cover the more than 90 square miles the spill then covered.

The same weather changes that contributed to the successful dispersant application on Day 3 also were the beginning of a wind storm that continued for 10 to 12 hours, lasting into the morning of the fourth day. These winds grounded aircraft, delaying further dispersant application for several hours. By the time the wind subsided, the oil covered more than 175 square miles, extending southwest almost 40 miles from the grounded *Exxon Valdez*. Heavy seas began the process of converting the fresh crude oil into an emulsion referred to as mousse (Figure 2). Once this emulsion has formed, dispersants are not effective

even if other conditions are suitable.

Exxon's request to burn a portion of the oil slick was approved immediately by the state of Alaska. An Exxon contractor ignited oil that had been gathered in a curve of fire-resistant boom. Between 15,000 and 30,000 gallons of oil burned, less than 0.27% of the spilled cargo. Subsequent efforts to ignite the oil were unsuccessful, apparently because of the evaporation of many of the volatile fractions of the crude oil. Because of the safety risks and the possibility of releasing the one million barrels of crude oil still on board the tanker, no attempt was made to ignite the oil in the vicinity of the tanker.

Difficulties

The immediate containment and recovery phase of this spill response revealed several problems: the approved spill response plan was not followed; the available technology proved insufficient for the task; there was a severe lack of equipment available in time to do the job; and even the best technology could not perform without effective logistics and management.

Effective spill response requires rapidly deploying considerable amounts of equipment, personnel, and other resources. Although Exxon eventually brought in large quantities of equipment, precious time was lost because these resources were not available in the region. For nearly three days after the grounding, calm seas and low winds were ideal for mechanical recovery, but the lack of response resources seriously hampered the containment and recovery; while the oil was pooled and drifting slowly away from the ship, recovery totaled only 3000 barrels of oil mixed with substantial quantities of water (3).

The adequacy of mechanical recovery technology was also a problem. The efficiency of the oil removal equipment was substantially below its "nameplate" rating. Some difference had been anticipated, but the efficiency was dramatically lower than what had been promised in the oil spill contingency plan. It quickly became apparent that the technology available for removal of oil from the water was being overwhelmed by the magnitude of the spill. Some of the technology—certain skimmers, for example—did perform as predicted, but much of the equipment simply could not handle the oil.

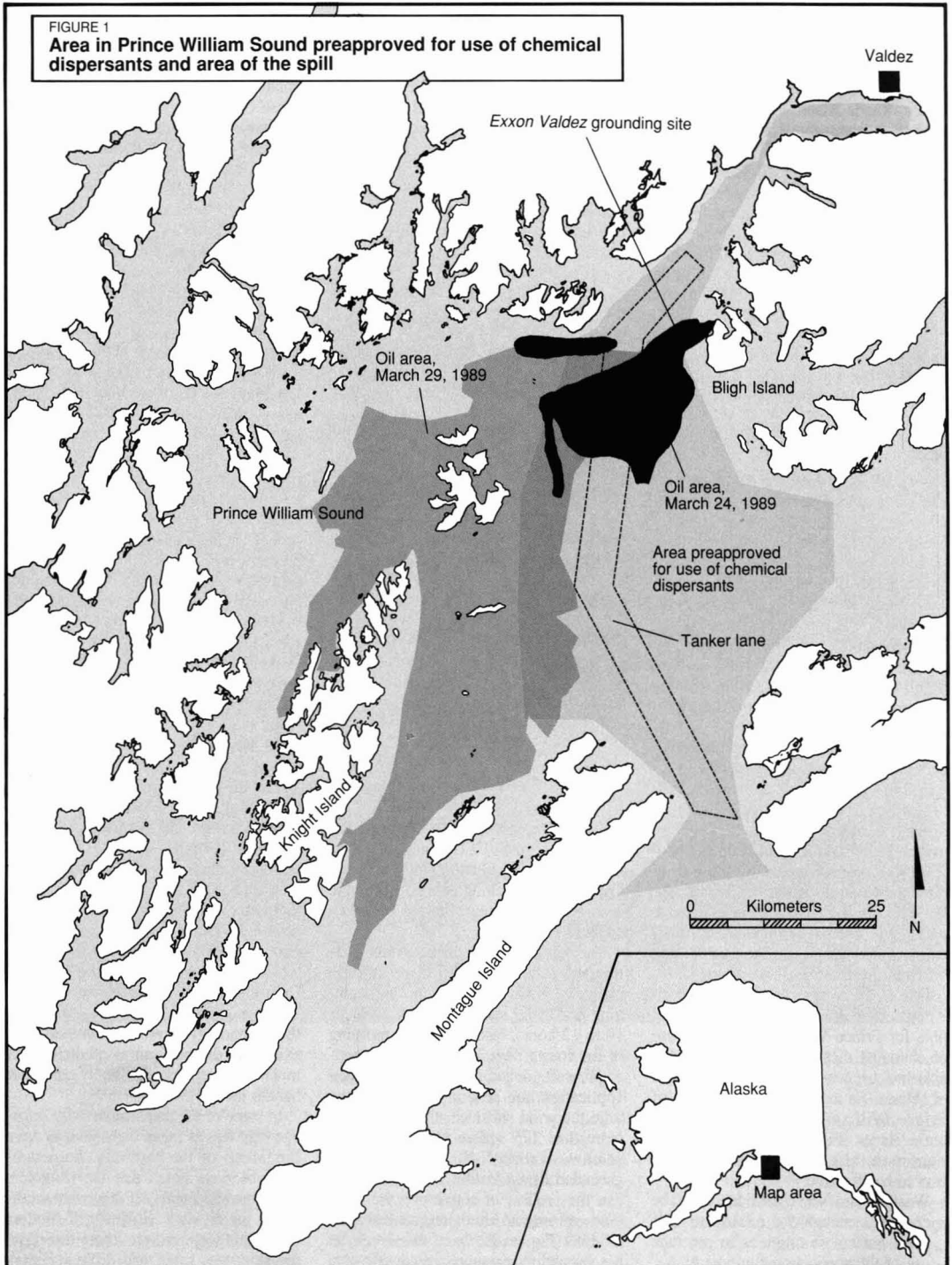
In some of the response activity, management was as much a problem as were limitations of the hardware. For example, observers noted that the skimmers performed acceptably if they were working in the oil slick. However, if spotters in aircraft were not providing direction, the skimmers often had difficulty stay-

ing in the heavy oil. Skimmers operating on the edge of or outside the slick were much less efficient than if they had been properly directed.

Observers also reported that some equipment collected oil effectively but

became temporarily useless once filled. Skimmers that traveled three hours to offload accumulated oil and another three hours back to the skimming site were essentially out of service for six hours. Barges and pumps were often un-

available for offloading collected oil. Virtually none of the equipment could operate at night. These and many other examples demonstrated that technology and response capacity are only part of the picture. Logistics and management



problems hampered the performance of well-established technologies.

The early days of the response were plagued by more oil than the equipment on site could handle and persistent problems with deployment and operation of the equipment that was available. However, during this particularly difficult time, some notably effective tools were developed. One was the successful spill-tracking technology that was put together and adapted on site. Beginning virtually at dawn of the first day, the state's oil spill overflight team mapped the spill from the air. When personnel arrived from Exxon and the National Oceanic and Atmospheric Administration (NOAA), they also began tracking operations. In the first few days, new maps were drawn several times a day. As the spill spread out and drifted to the south, more time was required to complete an overflight, but mapping continued throughout the daylight hours as long as oil was observed in the water.

Maps were then digitized and entered into a small, flexible network of microcomputers. By the end of the fourth day, the state had developed a geographic information system (GIS) on site for mapping the movement of the slick. This GIS provided "real time" maps to response managers and the public. The mapped data showed hourly changes in the spill and provided a reference point for subsequent stages of the response. The maps supplied not only graphic representation but also precise data on distance, extent, and trajectory. Figures 1 and 2 were taken directly from this GIS data base. Mapping data were shared with Exxon, other state and federal agencies, and the public. These maps provided much of the information on which early response decisions were based.

Once the winds had blown the oil toward Knight Island, three to four days after the initial grounding of the *Exxon Valdez*, the priority changed from containment and recovery in the vicinity of the tanker to removing as much oil as possible from the moving slick before it hit shore. Exxon mobilized large amounts of equipment and personnel at very substantial cost, but there was little to show for the effort.

As the oil began coming ashore, state officials and local people stepped outside their normal roles to respond. The objective was to protect three salmon hatcheries and a bay particularly important for commercial fisheries. Although these areas were designated for action to exclude oil in the site-specific oil spill contingency plan, the work had not yet been done. Consequently, the state and local people put in place their own defensive measures for these sensitive lo-

cations. The Department of Environmental Conservation scraped together skirted booms, borrowed a "skycrane" helicopter from the Alaska National Guard, and sent staff to join Prince William Sound fishermen who brought fishing vessels, crews, and local knowledge. Exxon agreed to support the effort. The resulting boom deployment—and constant vigilance and maintenance—kept oil out of these critical areas.

Within a few days, the state teamed up with local residents again. This time they pushed low-tech oil spill response equipment to the limit and pioneered some adaptations. First, they borrowed a ferry from the Alaska Marine Highway, converted it to a floating oil spill operations base, and staffed it with fishermen and other volunteers. Using the most basic equipment—skiffs, sorbent booms and pads, hand-thrown oil snares, and buckets—they picked up oil and oily debris. Because no skimmers were reliably available, they came up with a "new" technology. The state's contractor obtained a vacuum truck normally used to pump drilling muds and other heavy fluids in Alaska's North Slope oil fields. The cleanup crew mounted the truck on a barge, dropped the big vacuum hose over the side, and sucked up the oil corralled by the skiff crews. The idea worked, and "Miss Piggy," as the first of these units was dubbed, soon proved herself among the most productive of the spill response technologies.

The inadequacy of available technologies to deal with a spill of this magnitude has been documented by the Congressional Office of Technology Assessment (OTA), which observed "historically, it has been unusual for more than 10–15% of oil to be recovered from a large spill . . ." (4). OTA predicts that improvements in technology and response capability should make it "feasible to do much better, but it is unlikely that the technical improvements will result in recovery of even half the oil from a typical large spill" (emphasis in original) (4). In the *Exxon Valdez* spill, the combination of technology limitations and management problems made the outlook for removal of oil from the shoreline seem bleak.

Phase 2: Emergency removal of oil from the shoreline. Once oil began hitting the beach, trouble was everywhere. Still containing relatively high concentrations of aromatics, the crude oil moved onto the beach with waves and tides. The oil slipped between the rocks deep into the beach matrix and drifted back into the water and onto other beaches. The impacts on organisms stemmed not only from crude oil's toxic components but also its mechanical ef-

fects: it simply smothered animals or destroyed the thermal-regulating capability of fur and feathers. Intertidal organisms that had escaped the impacts of the oil while it was floating on the water now faced serious threats. Even forest-dwelling animals that frequented the beach were at risk. People who used the beaches—village subsistence shellfish harvesters, for example—worried about the oil's effects on their foods and the impairment of recreational uses of the beaches.

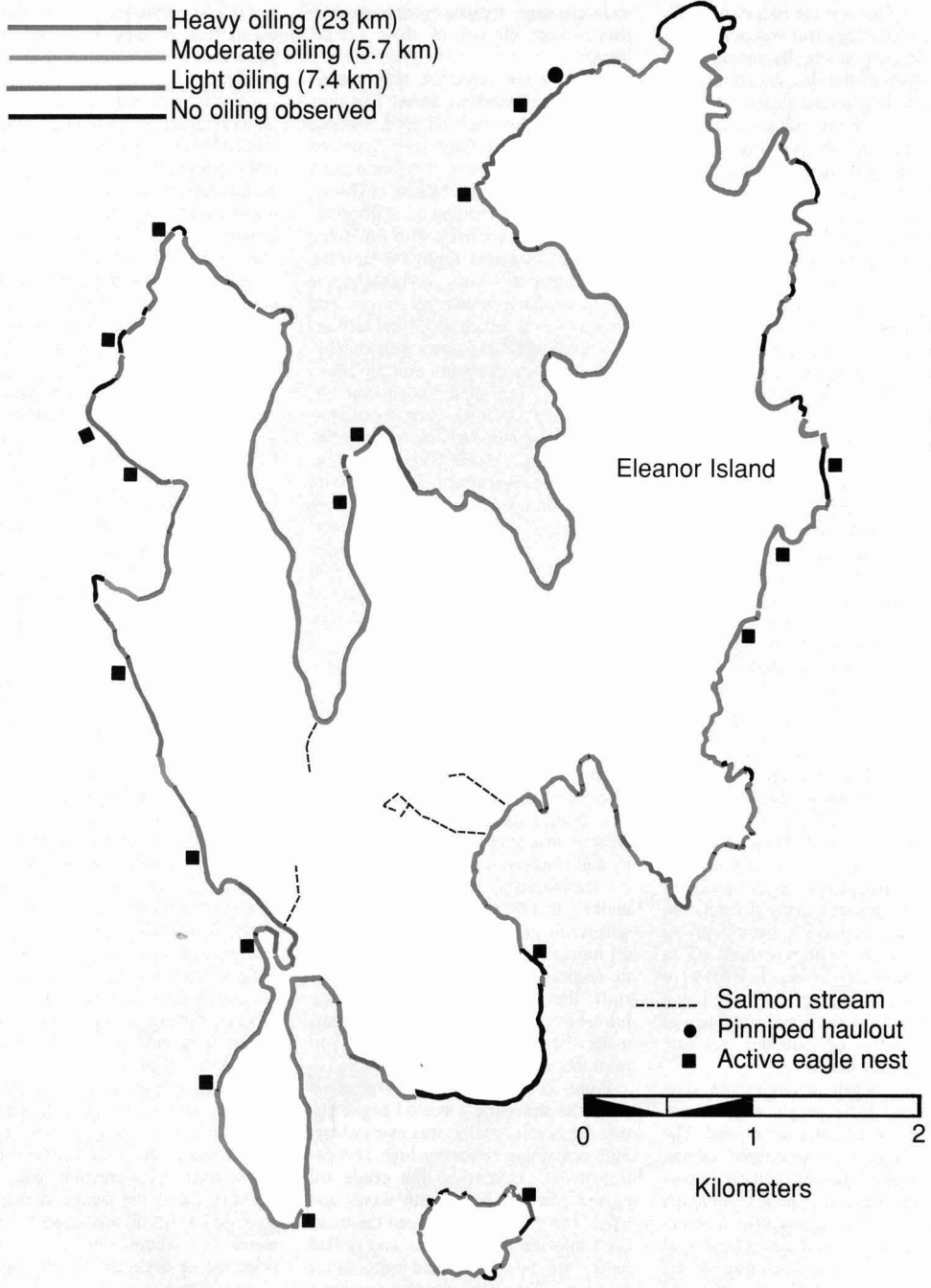
To determine where and how much oil was impacting the shoreline, the state sent field teams, led by a coastal geologist experienced in oil spill response, to evaluate the places where oil was coming ashore. Using low-level, slow-flying helicopters, the teams surveyed shorelines to determine the extent and degree of oiling. Where oil appeared to be present, the crews landed to take samples and compile detailed profiles of beach geomorphology, oiling, and other physical observations. The information was then added to the GIS data base, and real-time maps were generated (Figure 3). This information was provided to Exxon, the Coast Guard, NOAA, and state and local officials for use in making spill response decisions. The shoreline survey data continue to provide a baseline for shoreline treatment activities, additional survey efforts, damage assessment studies, restoration planning, and day-to-day natural resource management decisions.

By the time the oil had contacted shoreline beyond Prince William Sound, Exxon had acquired a large workforce and a formidable array of equipment. But the task had become even more complicated. The spill had impacted more than a thousand miles of coastline by the end of the summer of 1989. Shoreline characteristics varied markedly over that distance, as did the consistency and behavior of the oil. Shoreline treatment became a difficult, labor-intensive operation.

A variety of techniques were tried. Manual removal—using shovels, buckets, and absorbent materials—was useful in some situations, despite the enormity of the task and the slow pace of the technique. High-pressure hot water spray was used on some shorelines, despite fears that oil might be driven deeper into gravel or cobble beaches or that the hot water itself would cause substantial damage. Low-pressure, cold water flushing, called the deluge system, was also used to lift oil and move it into the water near shore where it could be skimmed or collected by absorbent or oleophilic materials. Various water temperatures were tried as well in an attempt to find the most effective cleanup

FIGURE 2

Geographic information system map showing degree of oiling, representative area



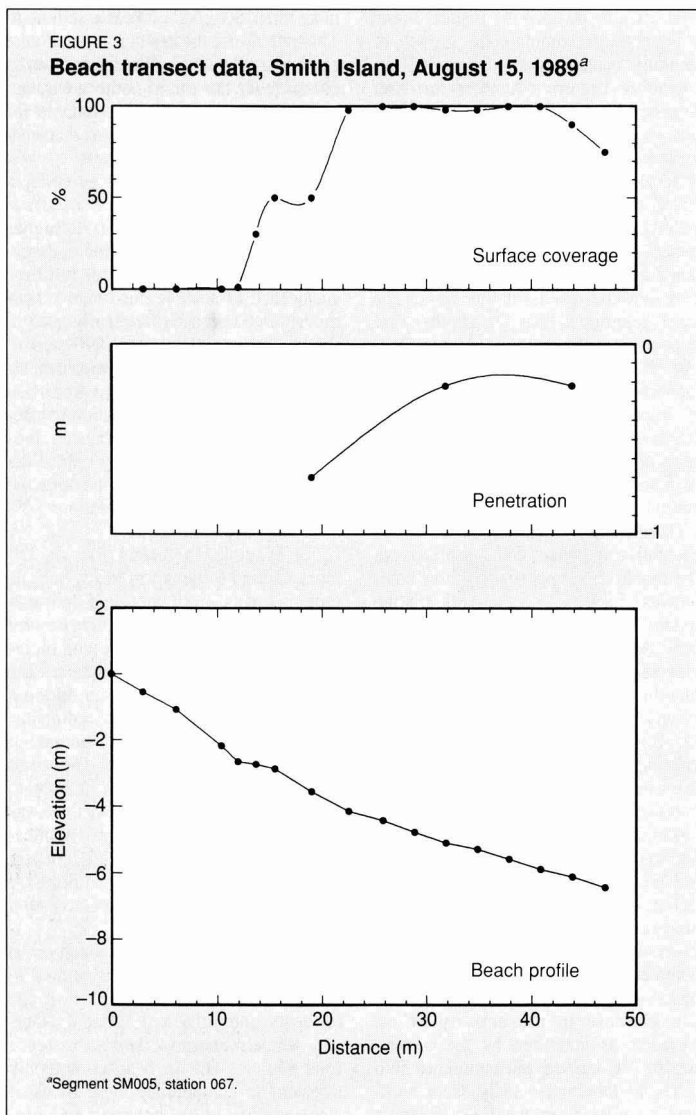
method. In short, the technology was largely invented and fabricated as the shoreline effort proceeded.

The oil soaked deep into the interstitial spaces of loosely aggregated beaches, in some instances as deep as 70 cm (5) (Figure 4). Although the oil was still moving with the waves and tides, sometimes oiling new areas or reoiling others, over time the mobility of the oil changed along with its chemical characteristics. As weeks passed, the lighter components of the crude oil continued to evaporate. Mousse patties, tarballs, and tarry clumps of debris became familiar features from Prince William Sound to the Kodiak archipelago and the Alaska Peninsula, nearly 500 miles from the grounding site. At the surface of the oiled beaches throughout the entire spill area, stiff asphalt patches and mats developed, while oil buried beneath the beach surface remained relatively fluid. Slicks formed in the water, and sheens drifted with each tide. Although animals were dying from the effects of the oil well into the summer of 1989 (1), the acute injury stage was passing into the chronic exposure stage. The response moved from the emergency removal phase into long-term treatment, although no clear line marked the transition.

Phase 3: Long-term treatment of oiled shorelines. Long-term treatment began during the summer of 1989, continued throughout the 1990 summer field season, and is expected to carry into 1991 or beyond. As the oil became more viscous in Prince William Sound and the other areas affected by the spill, untested technologies were proposed by Exxon. The U.S. Coast Guard, the state of Alaska, and Exxon expressed sharply different perspectives regarding both the overall goal and the levels of acceptable risk to the oiled habitats.

For example, Exxon requested approval in 1989 to use Corexit 9580 M2, a kerosene-based solvent that the company hoped would lift oil from rock surfaces. For Exxon, the risks of toxic side effects were fully justified by the possibility of faster, more effective removal. In 1989, the toxicity data on Corexit 9580 M2 were sketchy. Exxon proposed to apply the compound to low-lying, cobble beaches by spraying the rocks with Corexit, flushing the beach with water, and recovering the Corexit-oil mixture in the near-shore marine environment. When Exxon attempted to use Corexit, however, observers reported that an unrecoverable plume was visible beyond the containment area (6).

Although Corexit appeared to cut the oil, problems with application of the chemical and recovery of the resulting oil-Corexit mixture prompted state and federal agencies evaluating its perfor-



mance to decide that Corexit 9580 M2 should not be approved for general use. Under federal law, use of chemicals in oil spill response must be approved by the Regional Response Team (RRT), a technical group that includes staff from the state of Alaska as well as federal agencies (7). Decisions of the RRT are made by consensus and can be overridden only by the commandant of the U.S. Coast Guard.

In 1990, Exxon proposed a different approach for the use of Corexit 9580 M2. The company requested approval for a site-specific, "spot washing" approach, in which a limited amount of the solvent would be used to treat high-angle rock faces. The RRT approved a series of tests and two were conducted.

The first Corexit application showed some oil-dissolving capabilities. However, containment was inadequate, and water temperatures were not properly regulated to allow meaningful comparison between the use of Corexit with warm water and the use of hot water alone. The second trial was more effective than the first at dissolving oil but the oil freed by the solvent action was not recovered from the environment to the extent required by the RRT's approval criteria. Consequently, the RRT denied the general use of Corexit 9580 M2.

During the 1989 field season EPA began field tests of Inipol EAP-22, an oleophilic liquid fertilizer developed by a French firm subsequent to the 1978

Amoco Cadiz oil spill off France. Inipol is intended to stimulate the growth of naturally occurring populations of oil-degrading bacteria. Another fertilizer proposed was Customblen, a granular slow-release product. EPA designed experiments to evaluate the effectiveness of fertilizer addition in Prince William Sound conditions. In addition, studies of toxicity and eutrophication were conducted. The state of Alaska also convened an independent panel of scientists to review the results of this work. The panel determined that the results were inconclusive. However, in order to facilitate the 1989 cleanup effort, ADEC approved the conditional application of Inipol and the granular fertilizer Customblen. The state stipulated that application of the fertilizer must be accompanied by a scientific monitoring program designed to answer unresolved questions.

Three study sites were selected as representative of surface and subsurface oil. The monitoring program had three components. EPA conducted work on the toxicity of the two fertilizers at the study sites. ADEC, in conjunction with the University of Alaska at Fairbanks, did microbiological work to determine the activity rates of the oil-degrading bacteria. Exxon was responsible for the chemistry to quantify the amount and characteristics of the oil.

Results to date from the bioremediation monitoring program have shown that toxicity does not appear to be a problem in the water column. However, higher concentrations resulting from increased application amounts would approach potentially toxic levels of ammonia and butoxyethanol (8). Microbiological results (9) reveal a two- to three-fold increase in the activity of oil degraders as measured by the conversion of ^{14}C -labeled phenanthrenes into C^{14}O_2 in laboratory analyses of sediment samples from the field. Exxon's chemistry data are available only from samples taken prior to application of the fertilizers. Results of the other analyses have not been released as of this writing.

Fertilizer application appears to enhance biodegradation of hydrocarbons on the sites monitored. With proper application of fertilizers, a pulse of increased biological activity has been observed (9). Periodic reapplication of fertilizers can sustain this elevated degradation rate, but the upper limit remains at two to five times (9, 10) the natural rate. Extrapolations based on the monitoring data indicate that the bacteria can degrade 5–10 g of hydrocarbons per kilogram of beach sediment over the course of a year. This rate of biodegradation must be considered in light of the amounts of oil present on different beaches, which range from near zero to

more than 50 g/kg of beach sediment. This rate also indicates that it could take as long as 10 years for biodegradation to break down the oil in some areas, assuming that the oil remains suitable for biodegradation, an assumption that may not be warranted.

Bioremediation can serve as either a primary removal method or as a secondary "polishing" technique. At higher concentrations, additional time and sustained periodic applications of fertilizer are needed to achieve maximum oil removal. One approach frequently used in Prince William Sound in 1990 was to pretreat heavily oiled areas mechanically and manually to reduce hydrocarbon concentrations. The combination of adequate pretreatment and enhanced biodegradation can significantly reduce the amount of time required to achieve the lowest hydrocarbon concentrations possible with this technology.

For example, in Sleepy Bay on Lattouche Island a "lens" of heavy subsurface oil was first removed using a tracked backhoe. Then fertilizers were applied to complete the work with bioremediation. A second technique, tilling the beach sediments, was used during a rising tide to flush oil from sediments. In some areas "oil snare" booms of oleophilic material were anchored downslope on the site in an attempt to collect the freed oil. A third method was combined tilling and fertilizer application. This combination mixed fertilizer with beach material and helped bring oil nearer the surface where bioremediation could be more effective.

The timely removal of as much oil as is technologically possible is critical to users of coastal resources. For village residents, intertidal and subtidal plants and animals are important subsistence food sources. Oil on beaches not only threatens to contaminate these foods, it also interferes with gathering and processing the resources. The removal of oil is also crucial for commercial and recreational users.

Impacts on natural resources are not always obvious. Acute mortality or other gross impacts are only part of the picture. For example, the 1990 run of pink salmon to Prince William Sound spawning streams was strong. This suggests that massive mortality of salmon fry did not occur in the 1989 brood year. This encouraging salmon return is consistent with the brief exposure of these anadromous fish to the oil. The majority of wild (nonhatchery) salmon fry were hatched and reared in the stream beds upriver from the oiled marine environment. The salmon fry's outmigrating behavior moved them through the oiled intertidal areas, exposing them to the contamination for relatively short peri-

ods. Hatchery fish were kept penned in areas protected by booms and released at times that would minimize their exposure to oil contamination. In order to protect the subsequent spawning of wild stocks, a high priority was given to the cleanup of contaminated anadromous fish streams during the 1989 and 1990 field seasons.

Unlike the migratory salmon, resident species may face a different risk from chronic low-level exposure. Observations following the 1989 field season showed that although some oil may remain in surface material or be buried in subsurface sediments, much of it ultimately is transported into subtidal sediments by storm tides, high-energy waves, and other erosive forces. Current research indicates that chronic exposure to these hydrocarbons may harm the health and reproduction of intertidal and subtidal fishes (11). Samples of pink salmon fry (*Oncorhynchus gorbuscha*), halibut (*Hippoglossus stenolepis*), kelp greenling (*Hexagrammus decagrammus*), and three species of intertidal fishes (*Anoplarchus purpureus*, *Xiphister atropurpureus*, and *Pholis laeta*) taken from Prince William Sound were analyzed for the induction of cytochrome P-450E. Cytochrome P-450 dependent monooxygenases are enzymes that perform a significant role in the metabolism of several organic compounds. Cytochrome P-450E is induced by hydrocarbons, including many of those found in oil. P-450E is an enzyme that catalyzes the reactions induced by these hydrocarbons.

Studies have shown that elevated levels of P-450E correspond to long-term chronic effects in fish (12). Metabolism of organic compounds may, in some cases, form active carcinogenic derivatives and may interfere with reproductive success (13). The samples exposed experimentally to oiled sites showed significantly higher levels of cytochrome P-450E than the samples from unoiled sites. This experiment indicates that induction of P-450E is taking place in areas oiled by the *Exxon Valdez* spill (14). Although the fraction of oil now present may no longer be acutely toxic, this study suggests a significant biochemical consequence that may adversely affect the organisms exposed to the inducing agents.

More work remains to be done to evaluate the long-term impacts of the spill, particularly chronic sublethal effects. As the experiments with nonmigratory fish have shown, there is the potential for such effects on some populations. However, effects on individual species lead to larger questions about the long-term effects of the oil spill on the ecosystems. Until these ef-

fects are more fully understood, the prudent course is to remove oil using combinations of the available technologies with appropriate safeguards and scientific monitoring. In light of shoreline conditions observed in beach surveys following the 1990 summer field season, additional treatment to remove oil may be needed in 1991.

Natural resource damage assessment studies are now being conducted under the direction of state and federal agency heads designated as Natural Resources Trustees in accordance with federal law (15, 16). The Trustees guide the Natural Resources Damage Assessment (NRDA), under which 72 state and federal studies were initiated to assess injuries and quantify spill damages. Ultimately, a damage claim will be presented to Exxon and other responsible parties, which will include "lost-use" and restoration costs.

Recovered funds must be used to restore, replace, or acquire the equivalent of the injured resource. A state-federal interagency planning team is developing a restoration program concurrently with the damage assessment process (17). Once the oil removal work has ended and restoration funds are available, either as a result of an NRDA claim or settlement that avoids extended litigation, the restoration program can be implemented.

Restoration can include direct measures such as enhancing the productivity of anadromous fish streams through the placement of egg boxes or construction of spawning channels. Changes in management practices, such as adjustments to fishing and hunting seasons, can help restore injured resources. Restoration can also occur indirectly, through, for example, protection of upland habitats adjacent to injured coastal habitats. Prevention of further degradation to the resources injured by the spill is essential to long-term recovery of the area environment.

Conclusion

The primary lesson of the *Exxon Valdez* spill is that oil spill prevention and response technologies need substantial, sustained research and development. There must be adequate amounts of equipment in place in time to properly respond to an oil spill. Management systems need to be improved so they effectively use these technologies. The combination of inadequate technology, insufficient amounts of response equipment, and ineffective management of the available resources produced serious problems in the initial response. Exxon eventually deployed large amounts of equipment and personnel. By the time the long-term shoreline treatment phase

began, Exxon had also improved the management of its operations. However, at that point, much of the damage had already occurred. The extent of injury to natural resources is now being assessed through scientific studies. Based on the results of these studies, the final step in the response will be restoration projects which are now in the planning stage.

In light of the experience with the *Exxon Valdez* spill, state and federal laws have been strengthened to provide better prevention measures, response planning, and in-region cleanup capacity. As with most pollution problems, prevention—through both management and technology—should be the first line of defense.

Acknowledgments

The authors would like to thank the thousands of workers who contributed their efforts to cleaning up this oil spill, in particular the many state employees who worked tirelessly. We also thank Michele Brown, Larry Dietrick, Richard Fineberg, JoEllen Hanrahan, and Stanley Senner for comments on drafts of this article.

References

- 1) Piatt, J. F. et al. *The Auk* 1990, 107, 2.
- 2) *SPILL: The Wreck of the Exxon Valdez*; Executive Summary, Report of the Alaska Oil Spill Commission: Juneau, AK, January 1990, p. 11.
- 3) Dietrick, L., director of Alaska Department of Environmental Conservation, Division of Environmental Quality; field notes, summer 1989.
- 4) "Coping with an Oiled Sea—An Analysis of Oil Spill Response Technologies"; U.S. Congress, Office of Technology Assessment. U.S. Government Printing Office: Washington, DC, 1990.
- 5) Alaska Department of Environmental Conservation beach profile data from Smith Island, Prince William Sound, AK, August 15, 1989.
- 6) Kitagawa, J. Field notes from the August 9–14, 1989, test on Smith Island, AK.
- 7) National Oil and Hazardous Substance Pollution Contingency Plan (NCP), 40 C.F.R. sect. 300.81–86; *Fed. Reg.* 1990, 55, 8666, 8861–64.
- 8) Clarke, J. R. Notes on toxicological work from the 1989 and 1990 bioremediation monitoring program; coordinators, Alaska Department of Environmental Conservation, Exxon, and U.S. Environmental Protection Agency.
- 9) Preliminary report on bioremediation monitoring. Alaska Department of Environmental Conservation, Exxon, U.S. Environmental Protection Agency, July 1990.
- 10) Second preliminary report on bioremediation. Alaska Department of Environmental Conservation, Exxon, U.S. Environmental Protection Agency, August 1990.
- 11) Lech, J. J.; Bend, J. R. *Environ. Health Perspect.* 1980, 34, 115–31.
- 12) Stegeman, J. J.; Skopek, T. R.; Thilly, W. G. In *Carcinogenic Polynuclear Aromatic Hydrocarbons in the Marine Environment*; Richards, N., Ed.; EPA conference, Pensacola, FL; U.S. Environmental Protection Agency: Washington, DC, 1981.
- 13) Stegeman, J. J. In *Pollutant Studies in Marine Fish*; Giam, C. S.; Ray, L., Eds.; CRC Press: Pensacola, FL, 1987.

- 14) "Effects of the *Exxon Valdez* Oil Spill: Enzyme Induction in Fish"; Alaska Department of Environmental Conservation, Juneau, AK, September 1990.
- 15) Comprehensive Environmental Response, Compensation, and Liability Act; 43 U.S.C. sect. 9607 (f) (2).
- 16) Federal Water Pollution Control Act; 33 U.S.C. sect. 1321 (f) (5).
- 17) Restoration Planning Work Group. "Restoration Planning Following the *Exxon Valdez* Oil Spill"; August 1990 Progress Report.



Dennis D. Kelso was commissioner of the Alaska Department of Environmental Conservation between 1987 and 1990. He boarded the *Exxon Valdez* within hours of the spill on March 12, 1989, and remained in the spill area for five weeks. He supervised state oversight of the spill response between March 1989 and December 1990. Kelso received his B.S. degree from Iowa State University and his J.D. degree from Harvard University. Prior to his appointment as commissioner of ADEC, he served as deputy commissioner of the Alaska Department of Fish and Game.



Marshal Kendziorek has worked with the Alaska Department of Environmental Conservation since 1984. He is currently section chief of the statewide Data Management group. He has worked extensively on the *Exxon Valdez* oil spill since March 26, 1989. Kendziorek's background is in marine community ecology; he has a B.S. degree in zoology from the University of Washington. He did graduate work in fisheries at the University of Alaska, working in the intertidal area of Bristol Bay.

The *Exxon Valdez* oil spill: Initial environmental impact assessment

Part 2 of a five-part series



FIGURE 1

(a) Smith Island, Prince William Sound, April 1989

Alan W. Maki

Exxon Company, U.S.A.
Anchorage, AK 99519-0409

The March 24, 1989, grounding of the *Exxon Valdez* on Bligh Reef in Prince William Sound, Alaska, was unprecedented in scale. So too was Exxon's response to the oil spill and the subsequent shoreline cleaning program, including the employment of more than 11,000 people, utilization of essentially the entire world supply of containment booms and skimmers, and an expenditure of more than two billion dollars. In the days immediately following the *Valdez* spill, Exxon mobilized a massive environmental assessment program. A large field and laboratory staff of experienced environmental professionals and in-

ternationally recognized experts was assembled that included intertidal ecologists, fishery biologists, marine and hydrocarbon chemists. This field program to measure spill impacts and recovery rates was initiated with the cooperation of state and federal agencies. Although the agencies subsequently foreclosed cooperation in most of these studies because of litigation concerns, this comprehensive assessment program continues today. Through the end of 1989, this program has resulted in well over 45,000 separate samples of water, sediment, and biota used to assess spill impacts.

It is the intent of this paper to provide initial observations and preliminary conclusions from several of the 1989 studies. These conclusions are based on factual, scientific data from studies designed to objectively measure the extent of the impacts

from the spill. Data from these studies indicate that wildlife and habitats are recovering from the impacts of the spill and that commercial catches of herring and salmon in Prince William Sound are at record high levels. Ecosystem recovery from spill impacts is due to the combined efforts of the cleanup program as well as natural physical, chemical, and biological processes. From all indications this recovery process can be expected to continue.

Design of the assessment program

In early 1990 *Environmental Science & Technology* completed a four-part series on the state of the science of ecotoxicology and ecological risk assessment (1-4). This series reviewed the development and current regulatory applications of the ecological risk assess-



FIGURE 1

(b) Smith Island, June 1990

ment paradigm based on sequential comparisons of environmental fate (chemistry) data and biological effects data. Much of this literature is the basis for the Technical Information Documents (5, 6) being used by the regulatory agencies and supports the "Type B" natural resource damage assessment rules promulgated under Section 301 (C) of the Comprehensive Environmental Response, Compensation, and Liability Act (CERCLA).

The environmental fate-and-effects approach also forms the backbone of the *Exxon Valdez* environmental impact assessment program as discussed in these pages. Each of the studies was carefully designed to accurately measure hydrocarbon concentrations in the environment and within specific biological components as well as measure observed biological effects at individual trophic levels. For each program, environmental fate data complemented effects data to ensure that a fate-and-effects correlation could be developed to assess the likelihood of impacts.

Shoreline habitat

As a result of the grounding of the *Exxon Valdez*, some 258,000 barrels of crude oil were released into the water. Winds of more than 70 mph on the third day after the grounding rendered con-

tainment of oil on the water impossible, with the result that shoreline habitat in the southwestern segment of Prince William Sound was impacted. During the next few weeks more than 1100 miles of shoreline in south-central Alaska were impacted by oil to varying degrees (Table 1). These shoreline areas represented the habitat most obviously impacted by the spill where floating oil and mousse (oil-water emulsion) were washed ashore and deposited in intertidal areas. Indeed, it was these areas that were the focus of the two-billion-dollar cleanup program during 1989 and 1990.

It is important to point out that, at the very worst, slightly more than 10% of the shoreline habitat in Prince William Sound and the Gulf of Alaska was impacted by oil, thus leaving 85–90% of the regional shoreline untouched by oil (Table 1). Predictably, the percentage of impacted areas dropped significantly to approximately 1% of the shoreline areas in 1990 as a result of both the cleaning program and natural weathering. This effect can be seen most dramatically in the accompanying photographs of heavily impacted shoreline in 1989 and the comparatively clean state in the spring of 1990 (Figure 1).

Shoreline oiling data are the results of the 1990 spring shoreline assessment wherein 20 separate teams, each consist-

ing of state of Alaska, federal agency, and Exxon representatives, surveyed more than 1200 miles of shoreline in Prince William Sound and the Gulf of Alaska. A total of 822 miles of shoreline assessed had no oil; 115.6 miles contained oiling in <3–6 m or wider bands. In addition, 5071 pits were dug to determine the extent of subsurface oiling. Subsurface oil (oil deeper than 10 cm) was found in 733 (14%) of the pits dug. The locations recommended for 1990 summer cleaning were widely scattered and generally confined to short lengths of shoreline; all identified areas received attention during the summer.

Biota. The shorelines of southern Alaska are predominantly large rocks, boulders, and cobbles with less than 10% of the area characterized as soft substrate. This rocky intertidal zone is an extremely harsh habitat. Plants and animals living there have evolved to cope with a highly unstable substrate, extremely forceful breaking waves, and wide seasonal and diurnal ranges in photoperiod and temperature. As a result, many of these areas have naturally low species density and diversity.

Barnacles, mussels, and rockweed (*Fucus*) are the best indicator species for visually estimating the biological condition of these intertidal habitats. They are good indicators of trends in recruitment

and loss caused by oil or other natural phenomena. In order to assess spill impacts on shorelines, these species and the intertidal communities in Prince William Sound and the Gulf of Alaska have been sampled via counts of species density, percent cover, species diversity, and photographic surveys of intertidal biota.

Results from the shoreline surveillance program indicate that although species densities were lower on heavily oiled shorelines, and high local mortalities occurred where oil coverage exceeded 90%, the species compositions of communities are similar to those that would be expected on comparable shorelines in the absence of oil. Even where oiling remains in sheltered, soft substrate areas, the spring and summer growing season of 1990 confirmed that continued recovery was under way (Figure 2). Thus, intertidal invertebrates and plants do survive on oiled shorelines, a point that supported spill researchers' conclusions that further extensive, intrusive shoreline cleaning efforts were unwarranted (7).

This recruitment trend also has been observed in several studies of other spills worldwide that showed that shoreline biota recovered in impacted areas within a few years after the spill (8).

Shoreline field-monitoring data support the following conclusions:

- The amount of oil remaining on the shoreline has continued to decrease since the summer of 1989. There are few oiled shores remaining.
- The major impact to intertidal communities was a decrease in the numbers of individuals of each species and not a decrease in the species composition of the communities. The intertidal communities are intact.
- Intertidal plants and animals were found settling and surviving on shorelines throughout Prince William Sound and the Gulf of Alaska throughout the 1989 and 1990 growing seasons.
- Even where residual oil remains on a few shorelines, biological recovery is taking place.

Water quality

Within six days of the spill, Exxon initiated an extensive water quality sampling program in Prince William Sound to help assess possible impacts on the marine biological community by measuring hydrocarbon concentrations in the waters of the Sound. Water samples were collected from March through October 1989 at 35 offshore locations.

More than 2300 water quality samples have been analyzed to date. Figure 3 is a plot of the average polycyclic aromatic hydrocarbon (PAH) concentrations through-

TABLE 1
Alaskan coast impacted by Exxon Valdez oil

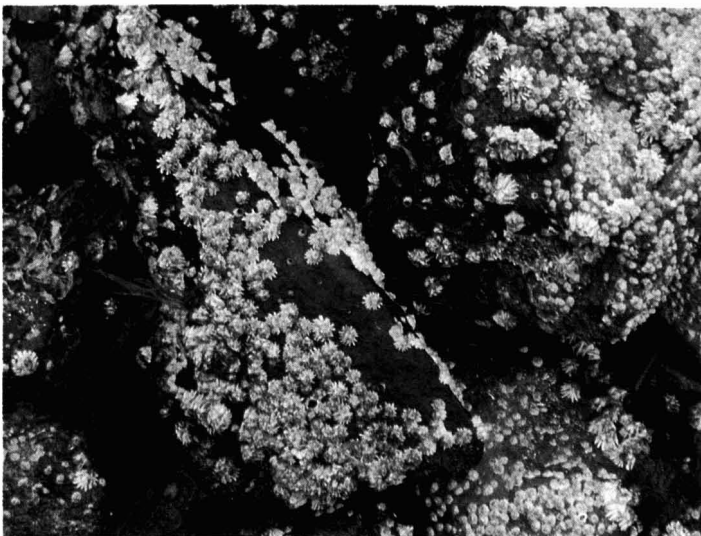
Area	Total coast (miles)	Oil-impacted coast, May 1989 (miles)	Total coast impacted, May 1989 (%)	July 1990 oil-impacted coast (miles) ^a	Total coast with oil, July 1990 (%)
Prince William Sound	3061	357	11.6	91.5	3.0
Gulf of Alaska	6345	732	11.5	24.1	0.4
Total (miles)	9406	1089		115.6	

^aJoint Exxon/Agency Spring Shoreline Assessment Teams (SSAT) report. Wide (>6 m), moderate (3-6 m), and narrow (<3 m) oiling widths combined.

FIGURE 2
Biological growth in Prince William Sound, spring and summer 1990



Grass sprouting from sediment containing residual oil



Barnacle growth on oil-stained rock

out the year. The three curves represent the averages of different sites. The solid line represents the three sites with the highest concentrations. These are three bays that were heavily oiled. Note that the average of these three worst bays peaked at only 7% of the Alaska state water quality standard. The average of all primary sites has a maximum value of about 1/50th of the state allowable limit for aromatics in water (9).

These data all confirm that average hydrocarbon concentrations measured in the water column for the more toxic components have consistently been well below state of Alaska standards and are 10–1000 times lower than levels lethal to plants and animals living in the water column, including commercially important fish species.

Fisheries

Pacific herring. Annually, millions of herring enter Prince William Sound to spawn in early April. This spawning period determines the commercial herring fishing season which had a 1988 value of \$12 million. The *Valdez* spill occurred approximately three weeks prior to the peak of the Pacific herring spawn. Concern regarding potential impacts to the herring resulted from the fact that herring deposit their eggs on kelp in the intertidal and shallow subtidal zones in Prince William Sound.

Results of aerial surveys flown by Alaska Department of Fish and Game field biologists confirm that both 1989 and 1990 spawning activity was comparable to historical averages for the years immediately preceding the spill (Figure 4). These data provide convincing evidence that herring spawning activity has been neither impaired nor delayed during the period when highest potential existed for exposure to spilled oil.

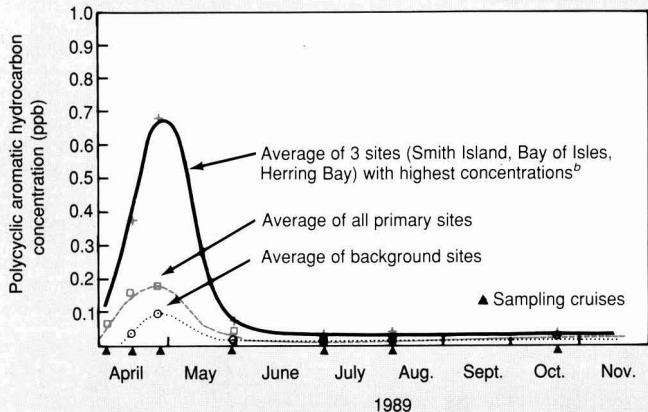
These conclusions were further substantiated by the results of the 1990 commercial herring fishing season wherein 8300 tons of herring were harvested during the 20-minute season opening on April 12th—an all-time record catch for the sac roe fishery. Record harvests were also achieved in the gill net and wild roe-on-kelp fishery seasons, thus minimizing concerns over long-term impacts on this important commercial fish species.

Pink salmon. The Prince William Sound salmon harvest is dominated by pink salmon and was worth approximately \$63 million in 1988. Data collected during the critical life stages of the pink salmon population show no significant oil-related effects.

An extremely healthy and vigorous zooplankton bloom supported the spring 1989 release of more than 600 million fry from the commercial fish hatcheries of Prince William Sound. Outmigrating

FIGURE 3

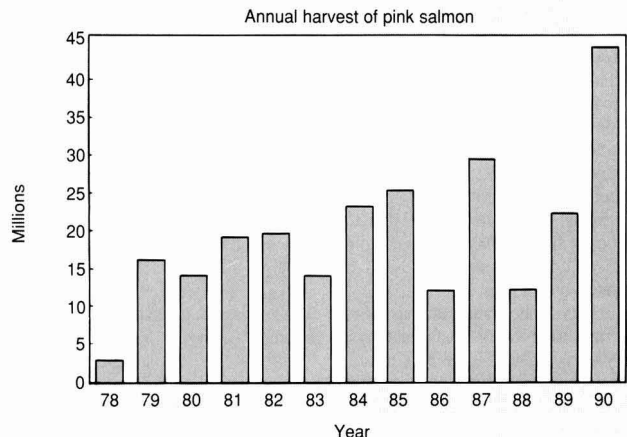
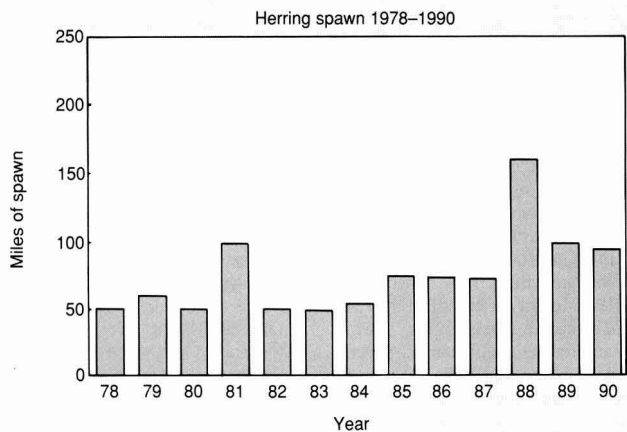
Average polycyclic aromatic hydrocarbon concentrations for Prince William Sound water^a



^aState of Alaska criterion for petroleum aromatics in water is 10 ppb.
^b Peak is 7% of state allowable limit.

FIGURE 4

Prince William Sound fish production



fry and juveniles in 1989 were apparently not impacted, and many juvenile salmon were observed in both oiled and unoiled nearshore areas. Similarly, field experiments with caged juveniles noted no differences in survival between oiled and unoiled sites. When the 1989 adults returned to spawn in the streams flowing into Prince William Sound, several streams had abnormally large numbers of returning fish. Also, no differences were evident in the spawning utilization of streams in oiled areas versus unoiled areas. Subsequent experiments in the fall with the incubation of eggs buried in gravel at several oiled and unoiled sites demonstrated similar survival and hatching rates between these sites, thus minimizing concerns over oil effects on this sensitive life stage.

Pink salmon have a short two-year life cycle. In the summer of 1990, those young salmon that left their native streams in April 1989, just after the spill, returned to spawn. The reported harvest through September 12, 1990, was 35.1 million fish taken, with an additional 8.9 million taken from hatchery stocks. This makes the 1990 commercial catch an all-time record, ahead of the 1987 record level by about 14 million fish and 163% ahead of the pre-season forecast for cumulative harvest. This strong run consists of both hatchery and wild-stock production (Figure 4).

In summary, there have been no indications of any significant pink salmon kills or effects on spawning activity related to oil exposure.

Shellfish and subsistence fisheries. Shellfish and crustaceans constitute a much less significant but still important part of Alaskan commercial, subsistence, and recreational fisheries. Several species of clams, mussels, crabs, and shrimp occupy the spill-impacted areas. Following the spill, a cooperative program was initiated between the Alaska Department of Fish and Game, the National Oceanic and Atmospheric Administration (NOAA), Exxon, and the subsistence communities to examine subsistence food safety in the spill-impacted areas. As of July 1990, more than 1300 samples of fish and shellfish have been collected in seven sampling cycles representing 23 species of fish and shellfish from 13 subsistence resource areas. They are being tested for aromatic hydrocarbons, the toxic components of crude oil most likely to be assimilated by shellfish.

The results of the chemical analyses received from the NOAA Seattle laboratory are very encouraging (Figure 5). Contaminant levels in all the fish and most shellfish were extremely low compared to data for fish and shellfish from a control site at the village of Angoon, outside the spill-impact-

ed area. Except for shellfish taken from Windy Bay and from Kodiak Harbor, all food resources sampled showed safe hydrocarbon levels.

A Toxicological Expert Committee consisting of representatives of the Food and Drug Administration, the National Institute of Environmental Health Sciences, NOAA, the National Marine Fisheries Service, the Alaska Department of Public Health, and various university and industry toxicologists reviewed the data and filed a consensus report. The committee concluded that finfish from anywhere in the study area are safe to eat in unlimited quantities, and except for those taken from obviously oiled shores, shellfish are also safe to eat (10).

Wildlife: Initial impacts

Some 36,000 bird mortalities were documented between March and September 1989. Although some of these were natural mortalities, no doubt exists that a significant number were caused by the spill. More than 1000 sea otter and 153 bald eagle mortalities were initially attributed to the spill. Although there was an extensive effort to recover dead birds and animals, actual mortalities were likely higher. When the above mortality figures are compared with total populations in the spill-impacted area—more than 10,000,000 sea birds; more than 30,000 sea otters; and 5000 eagles—indications are that recolonization has been rapid and robust, as it has been following other spills throughout the world (8).

Furthermore, extraordinary measures were taken to rescue and care for birds and otters that were impacted. From the period of March through September 1989, Exxon organized the largest and most comprehensive bird and sea otter rescue and rehabilitation programs ever attempted. Facilities for the holding, cleaning, and care of oiled birds and otters were built at Valdez, Seward, Homer, Kodiak, and Anchorage. During the program, more than 140 boats and 5 aircraft were used to retrieve oiled birds and otters from remote locations throughout Prince William Sound and the Gulf of Alaska.

Some 71 species of birds were handled during the six-month program. More than 1600 birds were brought in live for treatment with a release rate for the sea birds of 50%. Given the time of year of the spill, the climate, the remoteness of the site, and the logistics, this survival and release rate compares favorably with the 30–60% range of release rates seen in other spills. At its maximum, the bird program employed some 400 bird rescue personnel; this effort cost more than \$25 million.

Teams were hired to work in Prince

William Sound and Kodiak to collect eagles from heavily impacted areas to determine the need for potential rehabilitation. These capture teams caught 114 eagles; only 16 required treatment. (An additional 23 eagles caught by others not associated with the capture teams were also treated).

The staff of the otter centers grew to more than 320 specialists and volunteers at all three locations. From March 30 until September 15, 357 sea otters were treated and held at the centers; 223 (62%) were rehabilitated and released or placed in aquariums. Expenditures for this effort exceeded \$18 million.

Wildlife monitoring program

As noted, in spite of the best efforts by all parties, many birds died. To assess overall population-level impacts, comprehensive wildlife monitoring programs were initiated after the spill and are ongoing.

Bird monitoring. Results of Exxon and agency winter, spring, and summer wildlife monitoring programs are very encouraging. There have been no documented reports of oil or sheens affecting populations of birds or marine mammals, and there have been no confirmed mortalities attributable to oil since September 1989. Additionally, wildlife observations in Prince William Sound indicate that significant numbers of birds from 45 different species occupy previously heavily oiled areas and appear to be unaffected by existing conditions. Species diversity and density are similar for both oiled and unoiled areas.

The findings of the winter wildlife population surveys are most encouraging. These surveys of oiled areas in Prince William Sound show that bald eagle sightings have consistently increased since the summer of 1989. Data from cooperative U.S. Fish and Wildlife Service eagle surveys throughout the summer of 1990 indicate that 1031 of 2030 nests (51%) in the spill area were active and that 61 of 75 previously active nests (81%) in Prince William Sound cleanup sites produced an average of 1.4 eaglets per nest, thus matching historical productivity statistics for this area. It is recognized these data do not allow definitive statements of eagle population dynamics, but they do provide conclusive evidence that animal life is present in habitats previously impacted by the oil spill.

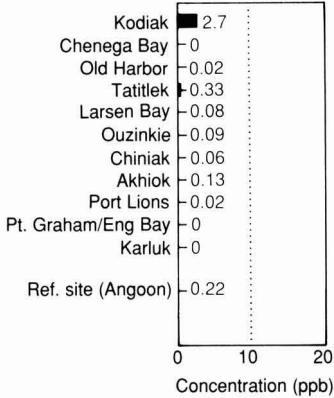
Mammal monitoring. Results of the winter mammal monitoring program indicate the presence and successful reproduction of mink and river otters in both oiled and unoiled bays of Prince William Sound. Sea otters are present in all areas in apparently equal numbers in oiled and unoiled bays.

FIGURE 5

Concentrations of aromatic hydrocarbons^a

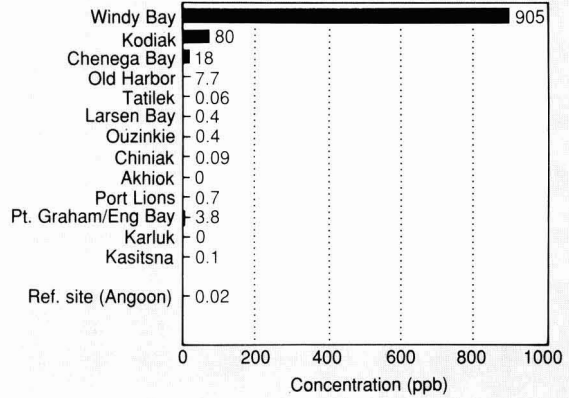
In salmon

Village site



In mussels and clams

Village site



^aPrince William Sound, lower Cook Inlet, Kodiak.

Although census results of sea otters often vary widely, the Prince William Sound population has been generally estimated at 5000 to 6000 (11), with some recent estimates being as high as 9000. The Prince William Sound population was believed to be less than 50 individuals when commercial harvesting of this species ended in 1911. The population has increased very rapidly in recent years, and field surveys of 550 miles of oiled shorelines counted more than 350 sea otters. This survey covered about one-sixth of the total Prince William Sound shoreline. It indicates that otter populations are approaching pre-spill densities (11) and provides convincing evidence of sea otter recolonization of previously heavily oiled areas.

In summary, the monitoring data for mammals indicate that environmental conditions have improved enough that the spill should have no further substantive impacts on wildlife. Recovery is well under way.

Conclusions

A recently published Congressional Research Service report (12) carefully reviews the extent of environmental impacts from several previous oil spills worldwide and concludes that "To date, pollution from offshore petroleum activities has not appeared to be a significant threat to the survival of various species... Despite short-term media attention to the catastrophic nature of major spill events, the chemicals contained in petroleum have long been part of the marine environment and physical impacts are likely to be temporary in the dynamic natural flux of the coastal environment."

Available data to date for the Valdez spill are consistent with the observations made in this report. Samplings of petroleum aromatic hydrocarbon concentrations in the waters of Prince William Sound clearly demonstrate that average levels have remained well below exposure levels known to cause acute and chronic effects to sensitive aquatic life. Field counts of plants, fish, and mammals from throughout the spill area provide convincing data that wildlife species are surviving and reproducing, thus confirming that biological recovery is rapidly taking place.

References

- (1) Bascietto, J. et al. *Environ. Sci. Technol.* **1990**, *1*, 10-14.
- (2) Cairns, J.; Mount, D. *Environ. Sci. Technol.* **1990**, *2*, 154-61.
- (3) Hoffman, D.; Rattner, B.; Hall, R. *Environ. Sci. Technol.* **1990**, *3*, 276-83.
- (4) Harris, H. et al. *Environ. Sci. Technol.* **1990**, *5*, 598-603.
- (5) "Injury to Fish and Wildlife Species"; Type B Technical Information Document, CERCLA 301 Project; U.S. Department of the Interior: Washington, DC, June 1987.
- (6) "Guidance on Use of Habitat Evaluation Procedures and Suitability Index Models for CERCLA Application"; Type B Technical Information Document, CERCLA 301 Project; U.S. Department of the Interior: Washington, DC, June 1987.
- (7) "Excavation and Rock Washing Treatment Technology—Net Environmental Benefit Analysis"; compiled by Hazardous Materials Response Branch, National Oceanic and Atmospheric Administration: Seattle, WA, July 1990.
- (8) Baker, J.; Clark, R.; Kingston, P. *Natural Recovery of Cold Water Marine Environments After an Oil Spill: Environmental Recovery in Prince William Sound and the Gulf of Alaska*; 13th annual Arctic and Marine Oil Spill Program; Edmonton, AB, Canada, June 1990.

- (9) Neff, J. "Water Quality in Prince William Sound"; Special Report of Battelle Ocean Sciences Laboratory: Duxbury, MA, April 1990.
- (10) "Summary of Findings of Toxicological Expert Committee for Evaluating Data Related to the Consumption of Marine Subsistence Foods (*Exxon Valdez Oil Spill*)"; National Oceanic and Atmospheric Administration: Seattle, WA, Feb. 21-22, 1990.
- (11) Irons, D.; Nysewander, D.; Trapp, J. *Prince William Sound Sea Otter Distribution in Relation to Population Growth and Habitat Type*; Alaska Investigations Field Office. U.S. Fish and Wildlife Service: Anchorage, AK, April 1988.
- (12) Mielke, J. *Oil in the Ocean: The Short and Long-Term Impacts of a Spill*; Congressional Research Service; Library of Congress: Washington, DC, July 24, 1990.



Alan W. Maki is currently senior science advisor to Exxon Company, U.S.A., in Anchorage, AK. He received a B.S. degree from the University of Massachusetts, an M.S. degree from the University of North Texas, and his Ph.D. in fisheries and wildlife management from Michigan State University. His research interests have focused on the development of applied ecotoxicology and ecological risk assessment. He has served on numerous EPA and National Academy of Sciences advisory panels and is a former president of the Society of Environmental Toxicology and Chemistry. He has been stationed in Alaska for the past five years.

Dynamic modeling of wastewater treatment processes

Its current status

Paul Lessard

Department of Civil Engineering
 Université Laval
 Québec, PQ G1K 7P4
 Canada

M. B. Beck

Department of Civil Engineering
 Imperial College
 London SW7 2BU U.K.

Until recently, the main task for river pollution control in populous industrialized regions has been to mitigate the effects of gross pollution, usually as measured in terms of biochemical oxygen demand (BOD) and suspended solids (SS). What has become of increasing concern, however, is not only the mean fixed level of water quality to be achieved in the future, but also the operational problem of maintaining, or improving upon, this baseline condition in the face of a more readily apparent temporal variability of types and levels of pollution (1). The latter can be achieved only through effective control of all elements of the urban river system (Figure 1) and, in particular, of the wastewater treatment plant.

Effective control of the dynamic behavior of a unit process, or of the entire treatment plant, depends on three factors: the ability to observe the state of the process and its response to various perturbations (i.e., monitoring); the ability to relate unambiguously causes (inputs, controls) to effects (outputs, responses); and the capacity to act, that is, to manipulate the causes (control inputs) to correct undesirable effects or to bring about more desirable effects. The focus of this review is on the second of the above three factors—the ability to relate causes to effects, or the acquisition and assembly of process knowledge. For this, a dynamic, unsteady-state model is the most natural form of representation.

The primary purpose of this review is to evaluate the current status of model-

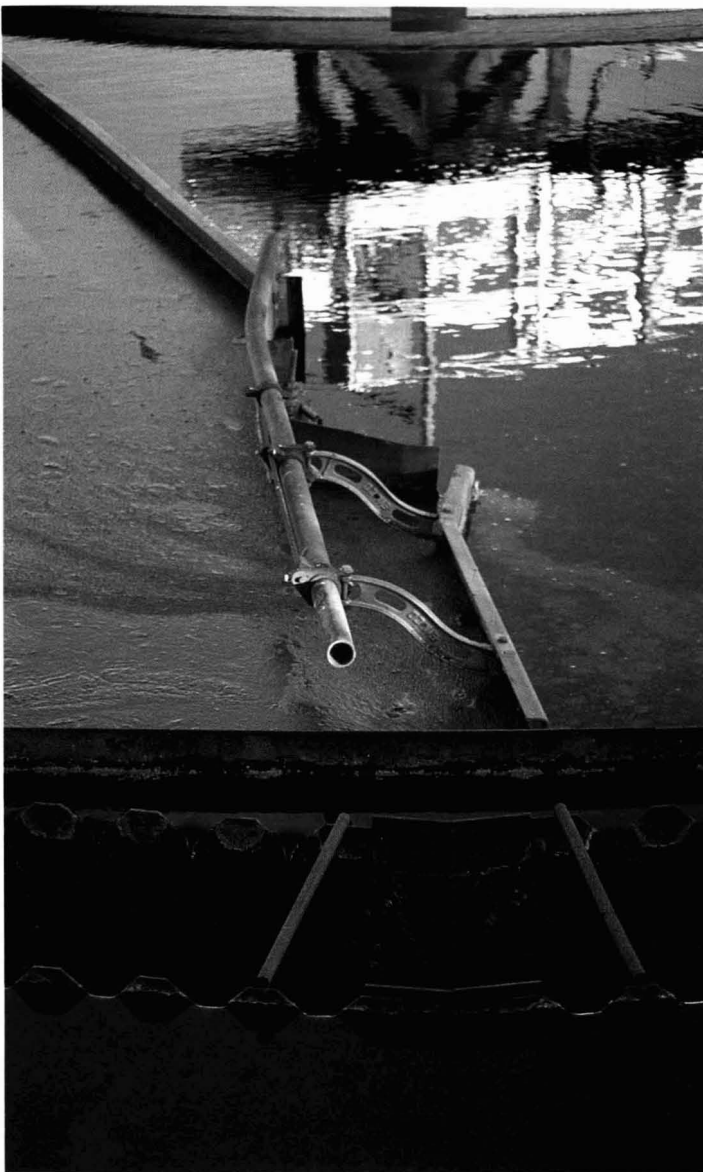
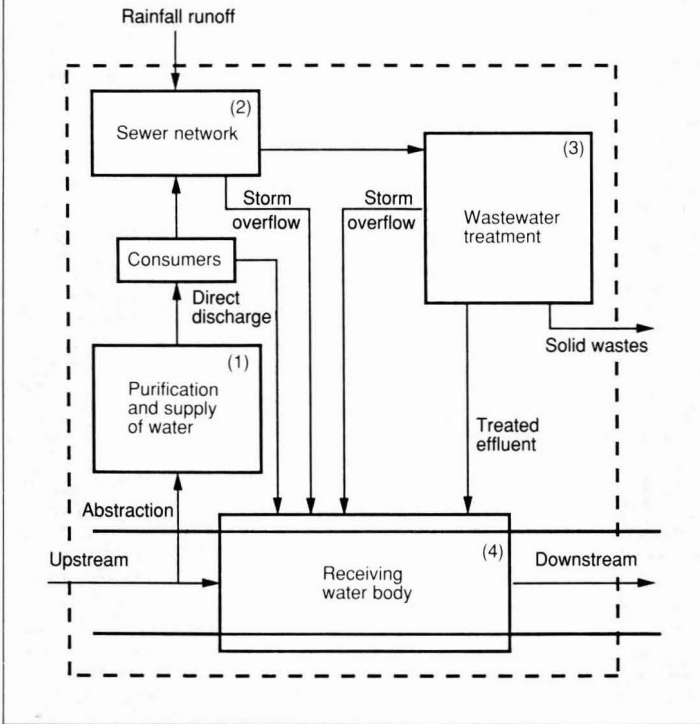


FIGURE 1

The water quality system



ing wastewater treatment units and to identify those models that would be of most use in studying and advancing the operation of these units in the wider context of river quality management (1-5). We summarize the principal contributions to this field for the most commonly encountered unit processes of treatment (Figure 2) and outline the avenues for further research.

For each of the unit processes shown in Figure 2, there may be different objectives for the development of a dynamic model, different ways of depicting the model, and a variety of means for testing its adequacy. For example, design, operation, and real-time control are three different objectives that will require different ways of expressing the dynamics of a process. In any of these applications, there are bound to be tradeoffs among the needs for accuracy, simplicity, and expediency (6, 7). In broad terms, we can distinguish four types of models for the description of process dynamics (8): linguistic models (i.e., models based typically on the "IF-THEN" rules of mental reasoning), time-series or black-box models, lumped-parameter models (i.e., ordinary differential equations), and distributed-parameter models (i.e., partial differential equations). Although each has a par-

ticular advantage for a specific purpose, the majority of the models developed for wastewater treatment systems have been of the lumped-parameter form.

Research into the development of dynamic models of wastewater treatment processes has a history of some 20 years; nevertheless, no comprehensive surveys have appeared in the open literature since the tutorial paper of Andrews (9) and the review paper by Olsson (10) were published. There have been, however, papers of a more specific review nature; for example, on the modeling of biological unit processes (11, 12) and on the identification, estimation, and control of these processes (13-16). The collection of papers in the recently edited volume by Patry and Chapman (17) also provides an overview, with special reference to the application of expert systems.

Storm sewage retention

The retention of storm sewage is important not only for the control of combined sewer overflows to receiving waters but also for the manipulation of the influent flow to the treatment plant. Although storm tanks are widely used (at least in Europe) and always are cited as one of the most immediate means of solving the problem of combined sewer

overflows, few dynamic models have been proposed for simulating their detailed behavior on an event basis. Studies have tended to examine the long-term performance of stormwater retention basins in preliminary assessments of urban runoff impacts (18). The few dynamic models proposed until now have dealt almost exclusively with the description of the dynamic sedimentation mechanism alone. These models usually consist of a set of two ordinary differential equations: one for volume variation within the tank and one for the balance of SS (19, 20). More sophisticated models (two and three dimensions) have also been proposed (21).

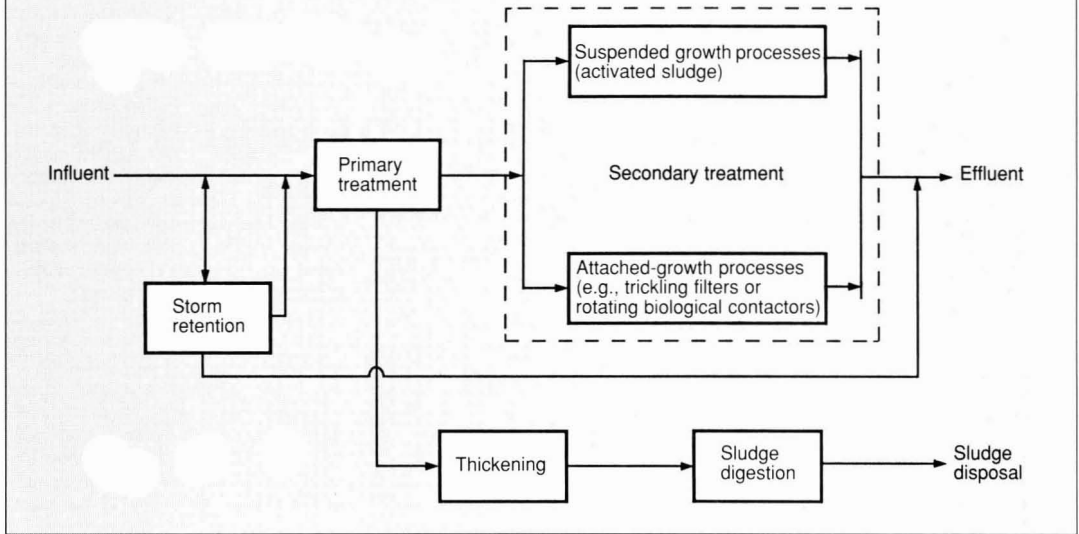
Interest in the dynamic behavior of storm tanks is also derived from the opportunities for controlled pumping of the stored storm sewage back to the treatment works after an event, both quickly enough to avoid overlap with the following event and smoothly enough to avoid impairment of the normal treatment efficiency of the plant. Lessard and Beck (22) have proposed a model to describe the four modes of behavior identified for these tanks (filling, dynamic sedimentation, quiescent settling, and drawing) and to examine the impacts on the plant of returning the stored storm sewage.

Primary sedimentation

Many scientists believe that the dynamic behavior of primary sedimentation processes is too complex to be modeled properly; the characteristics of the influent are highly variable; particle sizes and corresponding settling velocities are varied; there are subtle flow and density currents in the tank; and scouring phenomena and the effects of temperature cannot necessarily be neglected. Nevertheless, many models have been proposed, ranging from simple time-series models (23-25) to lumped-parameter models (26-28) and distributed-parameter models (29-32). Not surprisingly, the simpler lumped-parameter models have been criticized on the grounds that they do not satisfactorily represent behavior (33), and the distributed-parameter models have been criticized for their excessive complexity (34).

There is no doubt that the fundamental nature of particle settling may be considered to be extremely complex and essentially probabilistic, according to the theoretical studies of Lordache and Corbu (35) on the effects of particle interaction during settling. However, as Alarie et al. (36) have indicated in response to criticisms of their paper, if the prediction capabilities of a relatively simple mechanistic model applied to real-world problems are fairly good, why make the model more complicated

FIGURE 2

Unit processes of wastewater treatment

just for the sake of sophistication? In fact, simple lumped-parameter models have proven to be reliable (26, 28).

Secondary treatment

Suspended-growth processes. The activated sludge process forms the heart of many wastewater treatment plants. It consists of a biological reactor and a solid-liquid separator. The objectives of the performance of these two units are diametrically opposed: the aerator's is to bring the biomass (sludge) into as intimate a contact as possible with its substrate (sewage); the clarifier's is to separate the sludge from the treated sewage and to thicken the sludge before it is recycled to the aerator. The presence of this recycle loop emphasizes the need for a good understanding of the interaction between the aerator and the clarifier if process control is to be successful. A vast volume of research has been conducted on the dynamics of the activated sludge unit, dominated by work on the biological behavior of the aeration basin.

The biological reactor. During the last 20 years, attention has been focused on the modeling of carbonaceous oxidation and the processes of nitrification and denitrification. Notable contributions include those of Busby and Andrews (37), Poduska and Andrews (38), Ekama and Marais (39), Dold et al. (40), Clift and Andrews, (41) and van Haandel et al. (42). They have proposed a wide range of models for these aspects of behavior during treatment, culminating in the publication of the International Association on Water Pollution Re-

search and Control (IAWPRC) Task Group model (43). This latter represents the state of the art in modeling the activated sludge process; it subsumes much of the earlier work.

Other mechanisms also have been addressed through the development of dynamic models:

The behavior of dissolved oxygen (DO). Predominant interests have been not so much fundamental knowledge (44, 45), but rather control system design and on-line estimation and forecasting in association with the aeration-DO control loop (46-48). It is significant that the IAWPRC Task Group report, which is so concerned with basic understanding, reveals little new thinking on the behavior of the DO profile. In general, the tendency has been to assume that changes in DO concentration are the net result of almost every other reaction taking place in the aerator; therefore, these other reactions have been the subjects of primary research activities. For the same reason, it is not surprising that the dynamics of DO have become the best-studied subject of on-line estimation and control applications. Many of these applications have been reviewed elsewhere (15, 16).

Sludge bulking. This is a common operational problem in many activated sludge plants. Its consequences are a significant loss of sludge biomass through the clarifier effluent, and it is now widely agreed that the growth of filamentous species of microorganisms is a primary cause of sludge bulking. For modeling, it is necessary to assume that at least two species of organisms

are present: one floc-forming and one filamentous, to simulate the subtle types of interactions that may lead to sludge bulking (49-55). Factoring in these organisms amounts merely to an extension of the system's description and can be accommodated without difficulty into the general form of the activated sludge model.

Nevertheless, model representations of the formation (and consequences) of sludge bulking are still in their infancy. The diversity of its causes, as well as the number of microorganisms known to be associated with its occurrence, is likely to make progress slow. The wealth of qualitative empirical knowledge of the associated phenomena, however, predisposes the subject to the fruitful application of less conventional approaches, which are being explored for the purposes of the design (56) and operational management of activated sludge units (57).

Biological removal of phosphorus. This has also attracted interest, and Bundgaard et al. (58) have proposed an appropriate extension of the IAWPRC model. Adding this additional feature to the model results in an increase in the number of processes simulated from 8 to 17, and almost certainly will lead to practical difficulties in the calibration of the extended model and the estimation of its many parameters. Early work has been completed on the use of a linguistic model for assessing biological phosphorus removal (59).

The primary thrust of the research on modeling the activated sludge process has been directed toward the develop-

Please circle appropriate numbers to receive additional information

READER SERVICE

1	2	3	4	5	6	7	8	9	10	11	12	13	14
16	17	18	19	20	21	22	23	24	25	26	27	28	29
31	32	33	34	35	36	37	38	39	40	41	42	43	44
46	47	48	49	50	51	52	53	54	55	56	57	58	59
61	62	63	64	65	66	67	68	69	70	71	72	73	74
76	77	78	79	80	81	82	83	84	85	86	87	88	89
91	92	93	94	95	96	97	98	99	100	101	102	103	104
106	107	108	109	110	111	112	113	114	115	116	117	118	119
121	122	123	124	125	126	127	128	129	130	131	132	133	134
136	137	138	139	140	141	142	143	144	145	146	147	148	149

**CIRCLE
NUMBERS
FOR FREE
INQUIRY
SERVICE**

Principal product to which my work relates:

- | | |
|--|--|
| <input type="checkbox"/> A. Oil/Gas/Petroleum | <input type="checkbox"/> M. Machinery |
| <input type="checkbox"/> B. Plastics/Resins | <input type="checkbox"/> N. Auto/Aircraft |
| <input type="checkbox"/> C. Rubber | <input type="checkbox"/> O. Instrument/Controls |
| <input type="checkbox"/> D. Drugs/Cosmetics | <input type="checkbox"/> P. Inorganic Chemicals |
| <input type="checkbox"/> E. Food/Beverages | <input type="checkbox"/> Q. Organic Chemicals |
| <input type="checkbox"/> F. Textile/Fiber | <input type="checkbox"/> R. Other Manufacturing |
| <input type="checkbox"/> G. Pulp/Paper/Wood | <input type="checkbox"/> S. Design/Construction |
| <input type="checkbox"/> H. Soaps/Cleaners | <input type="checkbox"/> T. Utilities |
| <input type="checkbox"/> I. Paint/Coating/Ink | <input type="checkbox"/> U. Consulting Services |
| <input type="checkbox"/> J. Agrichemicals | <input type="checkbox"/> V. Federal Government |
| <input type="checkbox"/> K. Stone/Glass/Cement | <input type="checkbox"/> W. State Government |
| <input type="checkbox"/> L. Metals/Mining | <input type="checkbox"/> X. Municipal Government |
| | <input type="checkbox"/> Y. Education |

NAME: _____

POSITION: _____

ORGANIZATION: _____

STREET: _____

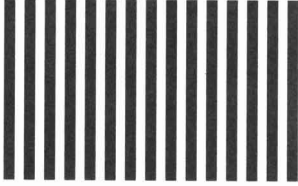
CITY: _____

STATE: _____ ZIP: _____

TELEPHONE: (____) - _____



NO POSTAGE
NECESSARY
IF MAILED
IN THE
UNITED STATES



BUSINESS REPLY MAIL

FIRST CLASS PERMIT NO. 516 RIVERTON, NJ

POSTAGE WILL BE PAID BY ADDRESSEE

Environmental
Science & Technology

GENTCOM, LTD.

P.O. BOX 1834

RIVERTON, NJ 08077-9434



ES&T
**Reader
Service
Reply Card**

**It's computer
processed
for fast
response
to your
inquiries
AND, IT'S
FREE**

ment of lumped-parameter models. Most of this research has treated the particulate microbial floc and the liquid as a single-phase system, although in reality the two phases are separate. This largely reflects the dominance of an interest in the microbial nature of the process, with a concern for detailed mass transfer considerations (necessitating distributed-parameter models) developing only relatively recently (60, 61). At the other end of the spectrum, however, input-output time-series models of the activated sludge process have been the subjects of steady, but modest, interest over the years (62-68).

The detail, completeness, and synthesis of the IAWPRC model have undeniably been significant contributions. Nevertheless, it is surely not appropriate for every purpose of model application—no model is uniquely and universally best—and in a number of practical respects, the development of the IAWPRC model thus far has certain shortcomings (69). Larger models, such as the IAWPRC model, contain many parameters that are unknown and must be evaluated with reference to field data. In terms of control theory, the IAWPRC model suffers from a lack of identifiability; that is, many combinations of parameter estimates will fit the data equally well and considerable uncertainty will attach to these estimates (8-15). More basic research will be required before the successful development of models that can portray accurately the biogenic and inhibitory interactions among the various organic substrates (70). In this respect, the dynamic modeling of the removal of heavy metals in the activated sludge process is yet another possible area for expanded research.

Above all, we now need to confront most of the lumped-parameter models of the activated sludge process with rigorous tests of their identifiability against comprehensive sets of field data from full-scale plant installations. There is a danger of a widening gap between theory and practice in the modeling of wastewater treatment plant processes—a gap that sooner or later becomes apparent (and unacceptable) in almost all areas of mathematical modeling (71).

The secondary clarifiers. Although the literature on the dynamics of secondary sedimentation is not comparable in quantity with that on the activated sludge aerator, it is nevertheless abundant. Much research has been carried out on the many aspects of sedimentation in the activated sludge process; yet there is no coherent theory to describe the dynamics of particle settling, despite advances in understanding at a basic level (72).

The behavior of the secondary settler generally is viewed in terms of two independent functions—clarification and

thickening; the term “independent” means here that no obvious relation exists between the two. The sludge blanket level can be viewed as an element that links these two component mechanisms, some studies having demonstrated the importance of the sludge blanket to clarification (72, 73). Other studies, however, flatly refute this (74, 75).

Most models of the clarification processes are empirical and are based on statistical relationships identified from field data or bench-scale experiments (76). Having reviewed all the major models, Hill (75) has found that the most important variables are flow-related variables and the concentration of SS in the mixed liquor. Although such empirical models may be used to predict gross changes in clarification behavior, they are not adequate for describing performance accurately at low concentrations of effluent suspended solids (77). Using time-series analysis of continuously monitored effluent data, Olsson and Chapman (78) have identified some simple input-output models whose parameter estimates illuminate the time-varying character of sludge settling, indicating significant differences of behavior between decreases and increases in flow rate. The model parameters varied gradually as a function of changing floc properties and instrument drift. Although the parameters of such models do not have any strict physical interpretation, they nevertheless can be used for on-line monitoring and fault detection.

On balance, the thickening function of the secondary clarifier has received more attention than clarification. The first major contribution to the description of continuous thickening was made by Bryant (79), whose model divided the sludge blanket into a series of 20 constant-volume continuously stirred tank reactor (CSTR) elements. Most subsequent models have been based on Bryant's model and have simulated the blanket as a series of n layers with variable or fixed volumes (44, 75, 77, 80). Other work has concentrated on achieving a more accurate representation of the theoretical behavior of an ideal slurry (81, 82). It has given rise to complex models with relatively complicated boundary constraints, whose computation requires the manipulation of multiple layers of varying thickness and concentration (83). Such models certainly would not be appropriate for the design of control systems, as observed by Stehfest (84), who has developed a lumped-parameter model consisting of two variable-volume CSTRs. The three state variables of his model are sludge blanket height, mean solids concentration above the blanket, and mean solids concentration below the blanket.

More complex models using finite-difference solutions of a partial-differential equation representation have been proposed (85-87). Arguably, the advantage of such schemes is that they do not require the imposition of artificial constraints for agreement with a steady-state analysis.

It is difficult to say which models of clarification and thickening would constitute the state of the art in the dynamic simulation of the secondary clarifier tank. Some observations, however, are that:

- Settlers are usually conceptualized as two different and independent processes (clarifier and thickener), an assumption that has yet to be unequivocally supported.
- The models generally have not been evaluated with reference to sound experimental work at plant scale; this is especially true for the thickener models.
- Clarification models are based mostly on empirical relationships, are therefore strongly site specific, and are unable to characterize sludge blanket entrainment into the clarifier overflow.
- There has been some debate as to whether solids flux theory, which is known to provide a reasonable description of thickening, albeit qualitatively (88), can predict the sludge blanket level (86). However, recent analysis of a first-order, partial differential equation representation—solved by the method of characteristics—has demonstrated that solids flux theory can describe the dynamics of the sludge blanket (89).

That no simple and reliable model has yet emerged is probably a reflection of the nature of the process itself. So many factors such as side water depth, inlet position, and sludge removal mechanism can influence a model, including fundamentally the behavior of the biological reactor, which affects sludge settling characteristics. Also, there is a lack of experimental data on the dynamic perturbation of the process that would allow one to uncouple the behavior of the clarifier from that of the aerator and identify each as a separate unit.

Because the biological reactor plays such an important role in the clarification-thickening process, one could argue that as long as the aerator model does not incorporate items to differentiate between floc-forming and bulking sludges, attempts to elaborate more sophisticated models of the clarifier are doomed to failure. Moreover, once the flocs have been formed in the aeration unit, it is not apparent how, or whether, the approximation of a simple settling velocity could be used to characterize the retention or separation of entrapped

microparticles in the settling floc mesh. According to Sheintuch (90), the construction of a quantitative model for this purpose would appear to require, among other components, the determination of the boundaries of microbial population shift and an accurate description of polymer production. A more appropriate objective might be to develop a simplified model based on solids flux theory and to establish its limitations with respect to its departure from the ideal and its applicability to real activated sludge (83).

Attached-growth processes. Trickling filters and rotating biological contactors are among the processes of attached-growth, or biofilms, most commonly found in wastewater treatment plants. Until now, most research on them has been focused on modeling detailed features of the growth of the biofilm rather than on attempting to describe the process as a whole.

In an earlier review of the state of the art in the modeling of biological fixed films, Grady (91) drew this conclusion: "It is clear that a complete and general mechanistic model for biofilms, which can be used to simulate the performance of a broad range of fixed film processes, has not yet been developed." Since Grady's review, however, the results from substantial research into the modeling of fixed film processes have been published, and many simulation models have been proposed (92-95). Such publications accurately reflect the revival of interest in attached-growth processes, at least in the case of trickling filters, although the models are not nearly as authoritative as the IAWPRC model of suspended-growth processes.

The inherent two-phase nature of fixed-film processes and the complexity of the mechanisms of film loss (sloughing) present difficulties of mathematical expression that will not be easily overcome. When contrasted with the virtual absence of any corresponding process field data, models of the daunting complexity of 19 ordinary and 10 partial differential equations, for example (92), can be regarded as merely hypothetical explorations intended to generate preliminary insights. Although they are able to quantify in greater detail the transformation of soluble organic matter, ammonia, and nitrate by multiple species of bacteria, these models remain largely speculative (96).

Few, if any, dynamic models have been developed for the purposes of operational control of attached-growth processes, although that presented recently by Gujer and Boller (97) for rotating biological contactors and, to a lesser extent, those by James (98, 99) for trickling filters, look promising. Gu-

jer and Boller's work is especially notable because it incorporates both the microscopic features of substrate transport and reaction within the biofilm and the macroscopic features of bulk liquid flow past the film. The vast majority of models, however, are not dynamic, and it is important to reflect on why this should be so. For example, there are the difficulties of modeling the biofilm, the widespread belief in the relative stability and good performance of these unit processes, and the lack of opportunity for process control. This latter is perhaps the most important; the control of biofilm processes has been regarded primarily as a matter of handling contingencies (100).

The plant operator has relatively little direct control over any of the internal process-state variables, either singly or collectively; other than the output effluent quality, there are no easily accessible indicators comparable with, for instance, the mixed liquor suspended solids (MLSS), DO, and sludge blanket height of an activated sludge unit. The operator is therefore constrained to the exercise of less direct (external) forms of control, such as altering the angular velocity of a contactor unit; changing the hydraulic loading of the contactor or filter unit; providing forced-draft ventilation of a filter or in-channel aeration of a contactor; or recycling effluent to decrease the influent soluble BOD concentration, if not the mass loading of organic material (101). It is hardly surprising, therefore, that studies oriented toward process control are entirely absent from the literature.

The curiosity, then, is that these processes, such as the trickling filter, which have long epitomized the view that treatment plants achieve steady, acceptable performance without active operational intervention, have yet attracted much detailed attention with respect to their microscopic biofilm dynamics. Indeed, the curiosity is sharpened by the fact that published time series of hourly, day-to-day performance in the field, which might reveal the practical problems of process control, if any, are virtually nonexistent (those of Cazelles and Bacquet [102] are the only exception). The same is true of the humus tanks that provide separation and settling of the detached biofilm flocs: Examination of their dynamic behavior appears to have attracted no attention whatsoever.

Sludge treatment

The treatment of the sludges separated from the liquid wastes, that is, from the primary and secondary clarifiers (or humus tanks), is normally carried out using the processes of thickening (grav-

ity and/or flotation), digestion (aerobic or anaerobic), and dewatering. Much less research has been devoted to the dynamic behavior of sludge treatment processes than to the processes of the liquid train of treatment. Interest has been largely restricted to the process of anaerobic digestion alone, despite its reputation of being difficult to operate, and prone to failure.

The biological stabilization of sludges can be achieved through either aerobic or anaerobic processes. The former was more popular during the 1960s when the requisite energy input was inexpensive and readily available. The popularity of aerobic processes declined throughout the 1970s to the extent that anaerobic digestion began to dominate as the preferred method of solids destruction. Currently, aerobic digestion is used primarily in small plants where its disadvantage of higher energy consumption is offset by simplicity of operation and lower capital cost. This waning of interest in the process itself is doubtless the reason for few publications on models of its dynamic behavior (103-105). Nevertheless, increasingly stringent restrictions on the options for sludge disposal may signal a renewed enthusiasm for applications of the process, at least in its thermophilic form (106), and operation at a higher temperature in turn generally implies a greater requirement for careful process control.

In contrast, justification for the use of anaerobic digestion is usually based on the benefit of energy production, in the form of methane gas, which outweighs the process's disadvantages of presumed difficulties of operation. Frostell (107) has defined the desirable performance of anaerobic digestion in the following terms: a consistent achievement of a high degree of waste stabilization, a maximal conversion of waste to methane, and a minimal production of excess solids at the highest possible concentration.

Practical control of the anaerobic process is directed at detection and preemptive suppression of instabilities (107). For this reason, the dynamic modeling of the process clearly should be of considerable assistance in predicting short-term failure with a view to implementing corrective control actions. Almost all of the pioneering work on the dynamic modeling of anaerobic digestion has been done by Andrews and his co-workers (108-113). Their model consists of three phases (biological, liquid, and gas), and assumes that the feed sludge has been solubilized and converted to volatile acids before its entry into the digester, so that only the methanogenic stage of the process is simulated. This simplification may not be appropri-

ate in all cases, however, and multiple-species models, comprising acid-forming (facultative heterotrophs) and methane-forming (obligate anaerobes) bacterial cultures have since been developed (114–117).

Many authors have used the Andrews model and its derivatives to evaluate the performance and control of anaerobic digesters (118–121). Further refinements of description have been proposed by Torre and Stephanopoulos (122) whose model has the following features: All three basic steps of anaerobic digestion—hydrolysis, acidogenesis, and methanogenesis—are accounted for; relationships between acid-forming bacteria (lumped into a single species) and methane formers are identified, together with some basic properties of commensalism (i.e., living with, or in, another organism, but not to the detriment of the two participating bacterial species); and three distinct groups of methanogenic bacteria are considered, each acting on a different substrate, such as acetic, propionic, and butyric acids.

For the most part these models have only been evaluated against data from bench-scale digesters. There has been little work with data from full-scale plants and consequently few studies in time-series analysis. One notable exception consists of results for the gas production dynamics of the digesters at Norwich Sewage Works (15). For the lumped-parameter conceptual models, the same problems of a lack of model identifiability, as noted for the activated sludge process, can be expected.

The plant as a whole

The extent of this review furnishes evidence of the substantial interest in describing the dynamic behavior of the unit processes of wastewater treatment. The activated sludge process alone has attracted most of this attention in terms of model development (123–126). In contrast there have been few studies on the integration of the constituent unit process models into a description of the plant as whole. This is understandable because such a task is considerably more challenging. Other reasons, however, account for this absence of sustained investigation. Primary treatment has generally been considered to have little significance for the exercise of process control; operation of the activated sludge aerators incurs the greatest cost, and is therefore the prime target for efficient process control; and the treatment and disposal of sludge have not been viewed as matters of urgent concern until very recently (127).

In retrospect, then, the work of Andrews and his colleagues has been of a pioneering character because it seeks to

achieve the goal of a dynamic model for the plant as a whole. In practice, however, as with the few other studies, it has been restricted largely to the liquid treatment train alone (37, 44, 79, 128–131).

In addition, software packages for simulating the dynamic behavior of wastewater treatment plants have only recently become available (7, 43, 132). Not surprisingly, their scope and capabilities are hardly comparable with the much more mature software market that already exists for contaminant fate and transport models, as discussed, for example, by Ambrose et al. (133).

Likely paths of innovation

Many forces will shape the nature of innovation in the design and operation of municipal wastewater treatment plants in the near future. For the time being, with environmental issues high on the political agenda, the pressure for innovation will doubtless be increased. In Europe, for example, nutrient removal, disinfection (in association with pollution of bathing waters), and sludge treatment and disposal are some of the areas in which progress must be expected. These may not require an understanding of dynamic behavior for the purposes of process control, but there are clear indications that they will. Subjecting the liquid waste stream to alternating aerobic, anoxic, and anaerobic conditions for the biological removal of nutrients is likely to be facilitated by a good understanding and control of aeration rates (105, 134, 135). A final stage of disinfection of the clarified effluent may perform optimally only if the prior removal of suspended solid matter—especially sensitive to the transient, dynamic perturbations of storm events—has been successful. The increasing difficulties of sludge disposal are likely to sharpen the desirability of operating policies for primary and secondary treatment that minimize their production of sludge. In short, the assumption of a steady state in the behavior of wastewater treatment processes is, strictly speaking, a fiction. Any novelty associated with the subject of dynamic modeling of these processes is derived from the fact that steady-state models have simply become the norm in the classical problem of process design.

Innovation is therefore needed to help us escape the confines of steady-state design analyses. Specifically, within the context of river basin management, control of the effects of stormwater surges and seasonal policies for the removal of ammonium are likely to be among the primary agents of change (3, 4). For each of the groups of unit processes reviewed herein, further developments in dynamic modeling can be expected to be

stimulated along the following lines:

Storm retention and primary sedimentation. Filling and withdrawal strategies for storm sewage retention tanks, and the rates and timing of flows between storm and primary settling tanks, are matters that are central to stormwater management and amenable to greater variety and flexibility than hitherto assumed. The increasing popularity of chemical flocculant addition for the purposes of advanced single-stage treatment and disinfection (136) will open up an alternative means of control and expose a possible sensitivity of such treatment to the dynamic perturbations of storm events.

Suspended growth processes. The abilities to vary the location at which the settled sewage is fed to the aerator basin (step-feed), and likewise to vary the point of return of the recycled sludge (step-sludge); to exercise intermittent storage of the sludge (137); to alter the volumetric capacity of the aerator and its aerobic and anoxic subunits; and to vary the spatial distribution of aeration rates (135) collectively create a substantial capacity for effective real-time control of these processes. This has immediate implications in several directions: protecting the sludge mass from wash-out during the transient increase in hydraulic loading from storm sewage (step-feed); altering the sludge loading pattern in the suppression of a bulking sludge (step-sludge); and, as already noted, tailoring aeration patterns to the needs of biological nutrient removal. The sensitivity of nitrification of ammonium to elevated hydraulic loadings may well lead to a separation of the nitrifying and non-nitrifying functions required of the several aeration channels that usually constitute an activated sludge system. Extensions of the multiple-species models, necessary for the study of a bulking sludge, are under consideration from the point of view of degradation of wastes previously thought to be resistant to biological treatment.

Attached-growth processes. The current revival of interest in the trickling filter (138), the association of attached-growth processes with the biological restoration of contaminated soils, and the fact that so little work on the dynamics of these systems has been undertaken in the past lead one to expect considerable advance into this largely uncharted territory.

Secondary clarification. The inevitable consequence of any strategy of suppressing stormwater overflows is the greater retention of sewage within the sewer network and its subsequent channeling to the treatment plant. This will increasingly impose greater average hydraulic and suspended solids loadings

on the secondary clarifier, and require a better understanding of the nature of clarification and its interaction with the sludge blanket.

Sludge treatment. The dynamics of sludge treatment are naturally slower than those of the unit processes for treating the liquid stream, and accordingly of less obvious relevance. However, any strategic shift of interest to the greater use of elevated operating temperatures for the destruction of solids by thermophilic digestion is likely to enhance the concern for process stability and reliable process control. Moreover, interactions between the sludge and liquid treatment lines are already known to be significant and highly dynamic. Torpey et al. (139) have reported an improved destruction of solids from the recycling of thermophilically digested sludge through an aerobic activated sludge unit, and Lessard and Beck's (28) study of primary clarifier dynamics shows clearly the highly transient input perturbations resulting from the recycling of sludge liquors. More systematic examination and exploitation of these interactions will probably be accelerated in the near future; the tendencies of liquid treatment units to generate sludge, and of the disposal costs of this sludge to increase relatively rapidly, lend strong support to such speculation.

The dynamic modeling of wastewater treatment process remains in good health. When it has suffered in the past, it has been the result of a widely held belief that operational control is rendered redundant by a good process design and that good process design can be based solely on the analysis of steady states. We now have a better appreciation of the fact that neither of these premises is strictly true, and this must be a liberating influence.

A balance must be struck, however. It would be easy to make the prognosis that today's models will become tomorrow's ever more complex models. We expect that as more constituent hypotheses are incorporated into models, the less fallible will be their predictions. After all, if everything of conceivable relevance has been included in the model, how could its results possibly be wrong? With respect to the activated sludge process, the problem is that these results can indeed be wrong—or at least uncertain and ambiguous—precisely because of the inclusion of too many constituent hypotheses. What has been true in the study of the activated sludge process may well be reflected in future studies of the dynamics of attached-growth processes. It is vital that the tendency towards model complexity be tempered by a more exhaustive examination of the extent to which such models can be

identified against field data from intensive, specialized monitoring exercises.

Acknowledgments

This work was carried out in part through a contract with the Water Research Centre (Stevenage, U.K.), whose permission to publish this paper is gratefully acknowledged. Paul Lessard also wishes to acknowledge the financial support of the Overseas Research Student award scheme.

This article was reviewed by John Andrews, Rice University, Houston, TX, and for suitability as an *ES&T* feature by Gustav Olsson, Lund Institute of Technology, S-22100 Lund, Sweden.



Paul Lessard (l) is an assistant professor in the Department of Civil Engineering at Université Laval (Québec, Canada). He holds a bachelor's degree in civil engineering from Université Laval, a master's degree in environmental engineering from Ecole Polytechnique de Montréal, and a Ph.D. in civil engineering from the Imperial College of Science, Technology, and Medicine in London. His principal areas of research are modeling of wastewater processes and operational water quality management.

M. B. Beck (r) is a Reader in applied systems analysis in the Department of Civil Engineering at the Imperial College, London. Formerly, he was task leader, Environmental Quality Control and Management, at the International Institute for Applied Systems Analysis (Laxenburg, Austria) and Ernest Cook Trust Research Fellow in environmental sciences at Cambridge University. His research interests include modeling and forecasting the behavior of environmental systems, and the application of control theory to the automatic operation of wastewater treatment processes.

References

- (1) Beck, M. B.; Finney, B. A. *Water Resour. Res.* **1987**, *23*, 2030–42.
- (2) Beck, M. B. "Operational Water Quality Management: Beyond Planning and Design"; Executive Report 7, IIASA: A-2361 Laxenburg, Austria, 1981.
- (3) Beck, M. B. et al. In *Systems Analysis in Water Quality Management*; Beck, M. B., Ed.; Pergamon Press: Oxford, U.K., 1987; pp. 357–68.
- (4) Beck, M. B. et al. In *Urban Discharges and Receiving Water Quality Impacts*, Ellis, J. B., Ed.; Pergamon Press, London, 1989; pp. 87–105.
- (5) Lessard, P.; Beck, M. B. *Res. J. Water Pollut. Control Fed.* **1990**, *62*(6), 810–19.
- (6) Sheffer, M. S. et al. *Water Sci. Technol.* **1984**, *17*, 247–58.
- (7) Olsson, G. et al. In *Instrumentation and Control of Water and Wastewater Treat-*

- ment and Transport Systems*; Drake, R.A.R., Ed.; Pergamon Press: Oxford, U.K., 1985; pp. 721–28.
- (8) Beck, M. B., In *Dynamic Modeling and Expert Systems in Wastewater Engineering*; Patry, G. G.; Chapman, D., Eds.; Lewis Publishers: Chelsea, MI, 1989; pp. 261–315.
- (9) Andrews, J. F. *Water Res.* **1974**, *8*, 261–89.
- (10) Olsson, G. *AIChE Symposium Series* **1977**, *72*, 52–76.
- (11) James, A. *Water Sci. Technol.* **1982**, *14*, 227–40.
- (12) Olsson, G. In *Comprehensive Biotechnology*; Young, M. M., Ed.; Pergamon Press: London, 1986; pp. 1107–19.
- (13) Olsson, G. In *Real Time Forecasting/Control of Water Resources Systems*; Wood, E. F., Ed.; Pergamon Press: London, 1980; pp. 93–108.
- (14) Olsson, G. In *Dynamic Modeling and Expert Systems in Wastewater Engineering*; Patry, G. G.; Chapman, D., Eds.; Lewis Publishers: Chelsea, MI, 1989; pp. 325–44.
- (15) Beck, M. B. *IEE Proceedings* **1986**, *133*, 254–64.
- (16) Marsili-Libelli, S. *Adv. Biochem. Eng. Biotechnol.* **1989**, *38*, 90–148.
- (17) Patry, G. G.; Chapman, D. *Dynamic Modeling and Expert Systems in Wastewater Engineering*; Lewis Publishers: Chelsea, MI, 1989.
- (18) Nix, S. J. et al. *J. Environ. Eng. Div. Proc. Am. Soc. Civ. Eng.* **1988**, *114*, 1331–43.
- (19) Amandes, C. B.; Bedient, P. B. *J. Environ. Eng. Div. Proc. Am. Soc. Civ. Eng.* **1980**, *106*, 403–19.
- (20) Ferrara, R. A.; Hildick-Smith, A. *Water Resour. Bull.* **1982**, *18*, 975–81.
- (21) Alhert, R. C.; Wu, J. S. In *Proceedings of the International Symposium on Urban Hydrology, Hydraulics and Sediment Control*; University of Kentucky: Lexington, KY, 1984; pp. 255–59.
- (22) Lessard, P.; Beck, M. B. *Water Res.* **1990**, in press.
- (23) Crowther, J. M. et al. *Prog. Water Technol.* **1977**, *9*, 579–86.
- (24) Crowther, J. M.; Al-Ani, S. *Water Sci. Technol.* **1981**, *13*, 247–54.
- (25) Dalrymple, J. F.; Crowther, J. M. In *Mathematics in Microbiology*, Bazin, M., Ed.; Academic Press: London, 1983; pp. 235–85.
- (26) Alarie, R. L. et al. *J. Environ. Eng. Div. Proc. Am. Soc. Civ. Eng.* **1980**, *106*, 293–309.
- (27) Shiba, S. et al. *J. Environ. Eng. Div. Proc. Am. Soc. Civ. Eng.* **1979**, *105*, 1113–29.
- (28) Lessard, P.; Beck, M. B. *J. Environ. Eng. Div. Proc. Am. Soc. Civ. Eng.* **1988**, *114*, 753–69.
- (29) Schramber, D. R.; Larock, B. E. *J. Environ. Eng. Div. Proc. Am. Soc. Civ. Eng.* **1983**, *109*, 753–862.
- (30) Tay, J. H.; Heinke, G. W. *J. Water Pollut. Control Fed.* **1983**, *55*, 261–69.
- (31) Valioulis, I. A.; List, E. J. *J. Environ. Sci. Technol.* **1984**, *18*, 242–47.
- (32) Abdel-Gawad, S.; McCorquodale, J. A. *Can. J. Civ. Eng.* **1985**, *12*, 454–63.
- (33) Barror, R. F.; Schroeder, E. D. *J. Environ. Eng. Div. Proc. Am. Soc. Civ. Eng.* **1980**, *106*, 1209–11.
- (34) Hudgins, R. R.; Silveston, P. L. *J. Environ. Eng. Div. Proc. Am. Soc. Civ. Eng.* **1984**, *110*, 862–63.
- (35) Iordache, O.; Corbu, S. *Chem. Eng. Sci.* **1986**, *41*, 2589–93.
- (36) Alarie, R. L. et al. *J. Environ. Eng. Div. Proc. Am. Soc. Civ. Eng.* **1982**, *108*, 427–28.
- (37) Busby, J. B.; Andrews, J. F. *J. Water Pollut. Control Fed.* **1975**, *47*, 1055–80.
- (38) Poduska, R. A.; Andrews, J. F. *J. Water Pollut. Control Fed.* **1975**, *47*, 2599–2619.
- (39) Ekama, G. A.; Marais, G.V.R. *J. Water Pollut. Control Fed.* **1979**, *51*, 534–56.

- (40) Dold, P. L. et al. *Prog. Water Technol.* **1980**, 12, 47-77.
- (41) Clifft, R. C.; Andrews, J. F. *J. Water Pollut. Control Fed.* **1981**, 53, 1219-32.
- (42) van Haandel, A. C. et al. *Water Res.* **1981**, 15, 1135-52.
- (43) Henze, M. et al. *IAWPRC Report No. 1*; IAWPRC: London, 1987.
- (44) Stenstrom, M. K. Ph.D. Dissertation, Clemson University, Clemson, SC, 1975.
- (45) Olsson, G.; Andrews, J. *Water Res.* **1978**, 12, 985-1004.
- (46) Howell, J. A.; Sodipo, B. O. In *Modeling and Control of Biotechnological Processes*, Preprints 1st IFAC Symposium; Johnson, A., Ed.; Pergamon Press: Oxford, U.K., 1985; pp. 191-98.
- (47) Holmberg, U.; Olsson, G. In *Modeling and Control of Biotechnological Processes*, Preprints 1st IFAC Symposium; Johnson, A., Ed.; Pergamon Press: Oxford, U.K., 1985; pp. 185-89.
- (48) Olsson, G. et al. In *Instrumentation and Control of Water and Wastewater Treatment and Transport Systems*; Drake, R.A.R., Ed.; Pergamon Press: Oxford, U.K., 1985; pp. 473-80.
- (49) Curds, C. R. *Water Res.* **1973**, 7, 1269-84.
- (50) Curds, C. R. *Water Res.* **1973**, 7, 1439-52.
- (51) Beck, M. B. *Trans. Inst. Meas. Control* **1984**, 6, 117-31.
- (52) Takamatsu, T. et al. *AIChE J.* **1984**, 30, 368-76.
- (53) Lau, A. O. et al. *J. Water Pollut. Control Fed.* **1984**, 56, 52-61.
- (54) Hermanowicz, S. W. *Water Sci. Technol.* **1987**, 19, 889-95.
- (55) van Niekerk, A. M. et al. *J. Water Pollut. Control Fed.* **1988**, 60, 100-06.
- (56) Geselbracht, J. J. et al. *J. Environ. Eng. Proc. Am. Soc. Civ. Eng.* **1988**, 114, 54-73.
- (57) Beck, M. B. et al. *Sciences Techniques Eau* **1990**, 23, 157-61.
- (58) Bundgaard, E. et al. In *Proceedings of the 11th Symposium on Wastewater Treatment*; Ministère Approvisionnement et Services: Montreal, 1988; pp. 49-56.
- (59) Pinheiro, M.; Camara, A. In *Management Strategies for Phosphorus in the Environment*. Lisbon, Portugal; Lester, J.; Kirk, P., Eds.; Selper: London, 1985; pp. 394-98.
- (60) Benefield, L. D.; Molz, F. *Biotechnol. Bioeng.* **1983**, 25, 2591-2615.
- (61) Benefield, L. D.; Molz, F. *Biotechnol. Bioeng.* **1984**, 26, 352-61.
- (62) Murphy, K. L. et al. *Prog. Water Technol.* **1977**, 9, 279-90.
- (63) Berthouex, P. M. et al. *Water Res.* **1978**, 12, 957-72.
- (64) Hansen, J. L. et al. *J. Water Pollut. Control Fed.* **1980**, 52, 1966-75.
- (65) Debelak, K. A.; Sims, C. A. *Water Res.* **1981**, 15, 1173-83.
- (66) Corder, G. D.; Lee, P. L. *Water Res.* **1986**, 20, 301-09.
- (67) Booman, K. A. et al. In *Systems Analysis in Water Quality Management*; Beck, M. B., Ed.; Pergamon Press: Oxford, U.K., 1987; pp. 289-96.
- (68) Melcer, H. et al. *Water Sci. Technol.* **1989**, 21, 351-62.
- (69) Ekama, G. A.; Marais, G.v.R. *Water Sci. Technol.* **1986**, 18, 11-19.
- (70) Grady, C.P.L. In *Dynamic Modeling and Expert Systems in Wastewater Engineering*; Patry, G. G.; Chapman, D., Eds.; Lewis Publishers: Chelsea, MI, 1989; pp. 1-39.
- (71) Beck, M. B. *Water Resour. Res.* **1987**, 23, 1393-1442.
- (72) Lumley, D. G. *Publikation 6:85*; Chalmers University of Technology: Göteborg, Sweden, 1985.
- (73) Ghoibrial, F. H. *Water Res.* **1978**, 12, 1009-16.
- (74) "Hydraulic Characteristics of Activated Sludge Secondary Clarifiers"; Crosby, R. M.; Bender, J. H. U.S. Environmental Protection Agency: Washington, DC, 1984; EPA-600/2-84-131.
- (75) Hill, R. D. Ph.D. Dissertation; Rice University: Houston, TX, 1985.
- (76) Pflanz, P. In *Advances in Water Pollution Research*; Jenkins, S. H., Ed.; Pergamon Press: London, 1969; pp. 569-81.
- (77) Vitasovic, Z. In *Dynamic Modeling and Expert Systems in Wastewater Engineering*; Patry, G. G.; Chapman, D., Eds.; Lewis Publishers: Chelsea, MI, 1989; pp. 423-32.
- (78) Olsson, G.; Chapman, D. In *Instrumentation and Control of Water and Wastewater Treatment and Transport Systems*; Drake, R.A.R., Ed.; Pergamon Press: Oxford, U.K., 1985; pp. 405-12.
- (79) Bryant, J. O. Ph.D. Dissertation; Clemson University: Clemson, SC, 1972.
- (80) Tracy, K. D.; Keinath, T. M. *AIChE Symposium Series* **1974**, 70, 291-308.
- (81) Attir, U. et al. *AIChE Symposium Series* **1976**, 73, 49-54.
- (82) George, D. B.; Keinath, T. M. *J. Water Pollut. Control Fed.* **1978**, 50, 2560-72.
- (83) Forster, D. M. Master of Science Report; Imperial College of Science, Technology and Medicine, London, 1985.
- (84) Stehfest, H. *Trans. Inst. Meas. Control* **1984**, 6, 160-64.
- (85) Anderson, H. M.; Edwards, R.V. *AIChE Symposium Series* **1981**, 77, 227-38.
- (86) Olsson, G. In *Systems Analysis in Water Quality Management*; Beck, M. B., Ed.; Pergamon Press: Oxford, U.K., 1987; pp. 349-56.
- (87) Lev, O. et al. *AIChE J.* **1986**, 32, 1516-25.
- (88) Ekama, G. A.; Marais, G.v.R. *Water Pollut. Control* **1986**, 85, 101-13.
- (89) Diehl, et al. Paper presented at the 5th IAWPRC Workshop on Instrumentation, Control and Automation of Water and Wastewater Treatment Transport Systems; Kyoto, Japan, 1990.
- (90) Sheintuch, M. *Water Res.* **1987**, 21, 1463-72.
- (91) Grady, C.P.L. In *Fixed-Film Biological Processes for Wastewater Treatment*; Wu, Y. C.; Smith, E. D., Eds.; Noyes Data Corporation: Park Ridge, NJ, 1983; pp. 75-134.
- (92) Kissel, J. C. et al. *J. Environ. Eng. Div. Proc. Am. Soc. Civ. Eng.* **1984**, 110, 393-411.
- (93) Benefield, L. D.; Molz, F. *Biotechnol. Bioeng.* **1985**, 27, 921-31.
- (94) Wanner, O.; Gujer, W. *Biotechnol. Bioeng.* **1986**, 28, 314-28.
- (95) Rittmann, B. E. In *Dynamic Modeling and Expert Systems in Wastewater Engineering*; Patry, G. G.; Chapman, D., Eds.; Lewis Publishers, Chelsea, MI, 1989; pp. 39-59.
- (96) Arvin, E.; Harremoës, P. *Water Sci. Technol.* **1990**, 22 (1, 2), 171-92.
- (97) Gujer, W.; Bollner, M. *Water Sci. Technol.* **1990**, 22(1, 2), 53-73.
- (98) James, A. In *Mathematical Models in Water Pollution Control*; James, A., Ed.; John Wiley & Sons: Chichester, U.K., 1978; pp. 303-18.
- (99) James, A. *An Introduction to Water Quality Modeling*; John Wiley & Sons: Chichester, U.K., 1984.
- (100) Wang, K. et al. *Eff. Water Treatment J.* **1984**, 24, 93-97.
- (101) Ball, R. O. In *Fixed-Film Biological Processes for Wastewater Treatment*; Wu, Y. C.; Smith, E. D., Eds.; Noyes Data Corporation: Park Ridge, NJ, 1983; pp. 174-205.
- (102) Cazelles, B.; Bacquet, G. In *Proceedings of Technical Advances in Biofilm Reactors*, Nice, France, 1989; pp. 515-17.
- (103) Kambhu, K.; Andrews, J. F. *J. Water Pollut. Control Fed.* **1969**, 41, r127-r141.
- (104) Dold, P.L. et al. In *Instrumentation and Control of Water and Wastewater Treatment and Transport Systems*; Drake, R.A.R., Ed.; Pergamon Press: Oxford, U.K., 1985; pp. 375-81.
- (105) Warner, A.P.C. et al. *Water Res.* **1986**, 20, 943-58.
- (106) Noone, G. P. *J. ChemE Symposium Series (UK)* **1986**, 96, 101-17.
- (107) Frostell, B. *Water Sci. Technol.* **1985**, 17, 173-89.
- (108) Andrews, J. F. *J. Sanit. Eng. Div. Proc. Am. Soc. Civ. Eng.* **1969**, 95, 245-60.
- (109) Andrews, J. F. In *Mathematical Models in Water Pollution Control*; James, A., Ed.; John Wiley & Sons: Chichester, U.K., 1978; pp. 281-302.
- (110) Graef, S. P.; Andrews, J. F. *AIChE Symposium Series* **1974**, 70, 101-31.
- (111) Graef, S. P.; Andrews, J. F. *J. Water Pollut. Control Fed.* **1974**, 46, 666-83.
- (112) Bühr, H. O.; Andrews, J. F. *Water Res.* **1977**, 11, 129-43.
- (113) Andrews, J. F. In *Dynamic Modeling and Expert Systems in Wastewater Engineering*; Patry, G. G.; Chapman, D., Eds.; Lewis Publishers: Chelsea, MI, 1989; pp. 83-129.
- (114) Hill, D. T.; Barth, C. L. *J. Water Pollut. Control Fed.* **1977**, 49, 2129-43.
- (115) Kleinstreuer, C.; Poweigha, T. *Biotechnol. Bioeng.* **1982**, 24, 1941-51.
- (116) Hirotsuji, J. et al. In *Instrumentation and Control of Water and Wastewater Treatment and Transport Systems*; Drake, R.A.R., Ed.; Pergamon Press: Oxford, U.K., 1985; pp. 637-40.
- (117) Moletta, R. et al. *Water Res.* **1986**, 20, 427-34.
- (118) Collins, A. S.; Gilliland, B. E. *J. Environ. Eng. Div. Proc. Am. Soc. Civ. Eng.* **1974**, 100, 487-506.
- (119) Carr, A. D.; O'Donnell, R. C. *Prog. Water Technol.* **1977**, 9, 727-38.
- (120) Rozzi, A. *Trans. Inst. Meas. Control* **1984**, 6, 153-59.
- (121) Renard, P. et al. *Biotechnol. Bioeng.* **1988**, 31, 287-94.
- (122) Torre, A. D.; Stephanopoulos, G. *Biotechnol. Bioeng.* **1986**, 28, 1138-53.
- (123) Attir, U.; Denn, M. M. *AIChE Journal* **1978**, 24, 693-98.
- (124) Cashion, B. S. et al. *J. Water Pollut. Control Fed.* **1979**, 51, 815-33.
- (125) Holmberg, A. *Water Res.* **1982**, 16, 1233-46.
- (126) Stehfest, H. *Environ. Technol. Lett.* **1985**, 6, 556-65.
- (127) Bruce, A. M.; Davis, R. D. *Water Sci. Technol.* **1989**, 21, 1113-28.
- (128) Lech, R. F. et al. *Water Res.* **1978**, 12, 811-90.
- (129) Tanthapanichakoon, W.; Himmelbau, D.M. *Water Res.* **1981**, 15, 1185-95.
- (130) Vitasovic, Z.; Andrews, J. A. In *Systems Analysis in Water Quality Management*; Beck, M. B., Ed.; Pergamon Press: Oxford, U.K., 1987; pp. 357-68.
- (131) Lessard, P.; Beck, M. B. In *Proceedings of the 12 Symposium on Wastewater Treatment*; Ministère Approvisionnement et Services: Montreal, 1989; pp. 205-25.
- (132) Patry, G. G.; Takacs, I. Report, Environmental Systems Engineering, McMaster University: Hamilton, ON, Canada, 1989.
- (133) Ambrose, R. B., et al. *Environ. Software* **1989**, 4(2), 76-93.
- (134) Harremoës, P. *J. Inst. Water Environ. Manag.* **1988**, 2(2), 191-99.
- (135) Aspegren et al. Paper presented at the 5th IAWPRC Workshop on Instrumentation, Control and Automation of Water and Wastewater Treatment Transport Systems; Kyoto, Japan, 1990.
- (136) Ødegaard, H. In *Pre-treatment in Chemical Water and Wastewater Treatment*; Hahn, H. H.; Klute, R., Eds.; Springer-Verlag: Berlin, 1988; pp. 249-60.
- (137) Gonzalez-Martinez, S. et al. *J. Water Pollut. Control Fed.* **1987**, 59(2), 65-71.
- (138) *Water Quality International* **1990**, 3, 16-17.
- (139) Torpey et al. *J. Water Pollut. Control Fed.* **1984**, 56, 62-68.

The momentary politics of the environment



Alvin L. Alm

Voter unwillingness to pass a substantial number of environmental initiatives or bond issues in the last election has raised questions about the depth of public support for environmental programs. Most notably, voters turned thumbs down on initiatives in the two largest, and generally pro-environment, states of California and New York. With the economy weakening, some fear (or hope) that the steam has gone out of the environmental juggernaut.

The most prominent environmental loss occurred in California, where the so-called "Big Green" initiative was soundly rejected by 63% of the voters. The Big Green initiative was an extremely complex proposal, covering every issue from banning certain pesticides to precluding the cutting of mature forests.

Actually, there are some explanations. Complex initiatives all did poorly in California. The Big Green initiative was radical by any standard and lost the support of moderates. It promised more government intervention at a time when voters were cynical about government's role. It promised higher costs as the economy was deteriorating. Moreover, the campaign against the initiative was well-heeled and skillful, featuring former U.S. Surgeon General Koop who, in fatherly tones, said the initiative was unnecessary. The opponents were able to tie the Big Green initiative to Tom Hayden, an extremely liberal state representative from Santa Monica, thereby lessening its appeal to moderates. In essence, Big Green was probably the wrong initiative, with the wrong sponsor, at the wrong time.

The New York initiative was a better test of voter sentiment. Although a *New York Times* poll indicated that 80% of the voters were willing to pay almost any price for environmental improvement, the \$2 billion New York bond issue to fund a host of environmental improvements was narrowly defeated. This result seemingly indicates that the polls do not reflect voter sentiment or that voter sentiment has changed. The New York vote, however, must be viewed in context. The failure of the New York bond proposal was tied strongly to anti-tax sentiment. Governor Cuomo, whose own plurality fell from 65% of the vote in 1986 to 53% in 1990, has raised New York taxes by a billion dollars in each of the last two years. The state's serious economic deterioration, coupled with recent tax increases, helped kill the bond issue. Even with such a negative backdrop, the vote was close: 51 to 49%.

The failure of environmental proposals in California, New York, and in other states does not necessarily represent a long-term rejection of environmental initiatives. The 1990 election is something of an anomaly in every respect. The president's acquiescence to tax increases created a firestorm. Congressional difficulties in reaching agreement on the budget compounded the cynicism over government, and a declining economy added to voter frustration. Voters were in an ugly mood and did not favor proposals that would have resulted in greater taxes or more government.

The real issue is whether public support for environmental initiatives will be rekindled in the future. Environmental expenditures and restrictions are rapidly increasing. During the next decade, total environmental expenditures by the public and private sectors will increase dramatically. By the next century, according to EPA Administrator Bill Reilly, the United States will spend 2.7% of its GNP on restoring and maintaining environmental quality. If the New York vote were considered the basis for a mandate, the public would not tolerate expenditures of this magnitude.

In my opinion, the commitment to en-

vironmental programs will be forthcoming. First, one must remember that support for any policy issue will wax and wane. But public support of environmental issues has been extremely strong, eclipsed only by concern over drugs and, recently, the economy. Second, support for national legislation is stronger than state bond issues or complex referenda, which are not subject to the give and take of the legislative process. Because the costs and local economic effects of national legislation are more obscure, it is easier to pass. Even as voters are pondering state initiatives, the highly controversial Clean Air Act was finally enacted. Finally, if history is a guide, even an economic downturn will not greatly affect national environment support. During the last recession in 1981-1983, the public and the Congress demanded bigger environmental budgets and stronger enforcement.

Even if general support for environmental programs is sustained, there is a lesson to be learned from the 1990 election. First, the electorate cannot be taken for granted. Second, initiatives must be sensible and must be capable of garnering the support of moderates. Environmental proponents are unwise to support radical, overly complex proposals. Third, they must gauge other sweeping voter sentiments, such as hostility to taxes or government. Although one can argue that the failed initiatives in 1990 do not constitute a rejection of environmental values, that argument will wear thin if environmental proposals fare poorly in 1992. The lesson of 1990 is clear. Environmental proponents must develop proposals that appeal to a broad range of voters and they must work hard to get them passed.

Alvin L. Alm is director and senior vice-president for energy and the environment for Science Applications International Corp., a supplier of high-technology products and services related to the environment, energy, health, and national security.

ES&T BOOKS

Bioenergy and the Environment.

Janos Pasztor and Lars A. Kristoferson, Eds. Westview Press, 5500 Central Ave., Boulder, CO 80301. 1990. 409 pages. \$39.95.

Biomass fuels are the second largest sources of energy worldwide (fossil fuels are the largest). They include wood, animal and crop wastes, and alcohol. What is their effect on the environment? This book suggests that bioenergy systems are less damaging than fossil fuels because their impacts are many, but small. Fossil fuels have fewer impacts but they affect much larger areas. *Bioenergy and the Environment* presents several papers that examine specific biomass fuels and their effects on the environment.

Wastewater Biology: The Microlife.

Water Pollution Control Federation, 601 Wythe St., Alexandria, VA 22314-1994. 1990. \$40 (\$30 for WPCF members).

Wastewater Biology describes the ecology and the beneficial and detrimental roles of microorganisms in wastewater treatment. The book reviews life forms, including coliform, filamentous microorganisms, free-living nematodes, wastewater parasites, rotifers, protozoa, and pathogens. Aids to identification and procedures for examining these life forms also are presented.

Pesticides in the Soil Environment: Processes, Impacts, and Modeling.

H. H. Cheng, Ed. Soil Science Society of America, Book Order Dept., 677 S. Segoe Rd., Madison, WI 53711-1086. 1990. 554 pages. \$36.

Pesticides in the Soil Environment explores the pathways of pesticides from their entry through retention, transport, and transformation processes. The impact of pesticides also is discussed.

Total Exposure Assessment Methodology.

Order Code VIP-16. Air & Waste

Management Association, P.O. Box 2861, Pittsburgh, PA 15230. 1990. 682 pages. \$70 (\$45 for association members).

Topics include human activity patterns and exposure pathways, microenvironmental field studies, implications of dose in health effects studies, biological monitoring, human exposure assessment, and research needs and policy implications.

Upgrading of Wastewater Treatment

Plants. W. Hegemann, W. Bischofsberger, and E. Engelmann, Eds. Pergamon Press, Maxwell House, Fairview Park, Elmsford, NY 10523. 1990. ix + 324 pages. \$113, paper.

Although a number of topics are considered, the emphasis is on nutrient removal, especially nitrogen and phosphorus, and on oxygen transfer and aeration. Papers and posters presented include nitrification and denitrification in combined activated sludge systems; upgrading oxygen transfer in the activated sludge process; and facilitating nitrogen removal without tank expansion. The book results from the International Association on Water Pollution Research and Control's symposium of the same name held in Munich, Germany, in September 1989. The editors say that because many problems need to be solved, another symposium will be organized, probably to be held in 1992.

Agricultural Chemical News. W. T. Thomson, Ed. Thomson Publications, P.O. Box 9335, Fresno, CA 93791. Periodical. \$80/year; \$100/year, foreign.

Agricultural Chemical News is designed to keep the reader up to date on matters such as new registrations of agricultural chemicals, including biocides, new regulations, and new use patterns.

NEW MICROWAVE DIGESTION BOMBS



PAT. PENDING

Now in two sizes, 23 ml and 45 ml.

The speed and convenience of microwave heating can now be applied to the digestion of inorganic, organic, or biological materials in a Teflon Lined Bomb. The new Parr Microwave Digestion Bombs have been designed to combine the advantages of closed high-pressure and high temperature digestion with the requirements of microwave heating. Many samples can be dissolved or digested with less than one minute heating times. As with all Parr Digestion Vessels, careful design and testing effort have gone into the safety and sealing aspects of this unique vessel and operating environment.

Call or write for Bulletin 4781 with complete technical details.



**PARR
INSTRUMENT
COMPANY**

211 Fifty-third Street
Moline, IL 61265
Phone: (309) 762-7716
Telex: 270226

CIRCLE 12 ON READER SERVICE CARD

In 1890, industrial testing was simple —
If the canary lived, air quality was acceptable.

Modern industrial
air emissions testing is complex.
Today you need ENTROPY.

PROVIDING INDUSTRY WITH STATE-OF-THE-ART TESTING SERVICES SINCE 1972

ENTROPY

COMPREHENSIVE AIR EMISSIONS TESTING

Call Pete Watson, Director of Sales 1-800-486-3550

ENTROPY ENVIRONMENTALISTS, INC.
P.O. BOX 12291 • RESEARCH TRIANGLE PARK, NC 27709-2291

CIRCLE 3 ON READER SERVICE CARD

INTERNATIONAL SYMPOSIUM ON CALCIUM MAGNESIUM ACETATE: ("CMA")

An Emerging Bulk Chemical for Environmental Applications

May 14-16, 1991

Center for Biotechnology Engineering
Northeastern University
342 Snell Engineering Center
Boston, MA 02115

"CMA" or Calcium Magnesium Acetate is a new bulk chemical emerging on the world market. Two major uses for this chemical identify it as being used in multimillion ton quantities in the near future. One use is as an organic biodegradable noncorrosive deicing salt, already established by the U.S. Federal Highway Administration as the road salt selected to replace sodium chloride. The second major use for CMA is as an additive to coal-fired combustion units such as those used by electrical utilities in order to bind sulfur.

Co-sponsors include:

- Chevron Chemical Company
- Federal Highway Administration
- Electric Power Research Institute
- Massachusetts Audubon Society
- Environmental Protection Agency
- Massachusetts Dept. of Public Works

CALL FOR ABSTRACTS: 1 PAGE
DUE: February 1, 1991

Presented papers will be published in a special topical issue of *Resources, Conservation and Recycling*, an International Journal published jointly by Elsevier Science Publishers, B.V., Amsterdam, The Netherlands and Pergamon Journals Ltd., Oxford, Great Britain.

WRITE: Donald L. Wise, Ph.D.
Cabot Professor of Chemical Engineering
Director, Center for Biotechnology Engineering
617-437-2992 (TEL); 617-437-2501 (FAX)

CIRCLE 8 ON READER SERVICE CARD

Radon in the Environment. M. Wilkening. Elsevier Science Publishing, P.O. Box 882, Madison Square Station, New York, NY 10159. 1990. 138 pages \$69.25.

Topics include radioactivity, radon and its decay products in the atmosphere, sources of radon, radon in water, indoor and outdoor radon, and health effects.

Biological Markers of Environmental Contamination. John F. McCarthy and Lee R. Shugart, Eds. Lewis Publishers, 2000 Corporate Blvd., Boca Raton, FL 33431. 1990. 600 pages. \$69.95, U.S.; \$83, foreign.

Biological Markers reviews the use of biological markers in animals and plants to evaluate ecological and health effects of contamination. Topics include testing for genotoxicity, disease biomarkers, oncogenes, and sentinel species (species that suffer effects first, thus giving early warning of contamination).

The Changing Atmosphere: The Global Challenge. John Firor. Yale University Press, 92A Yale Station, New Haven, CT 06520. 1990.

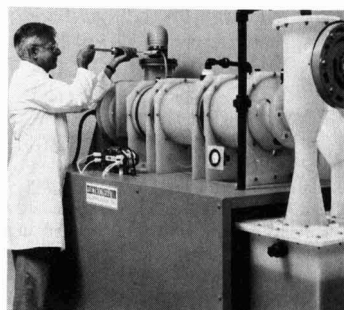
Will nature eventually cleanse the atmosphere of pollutants put there by humans? Is the greenhouse effect the invention of doomsayers? Emphatically not, according to the author, who believes that experts' warnings should be taken very seriously. He adds, however, that although it would be nearly impossible to halt the spread of chemicals into the air, steps to slow pollution are feasible and often economically beneficial (cutting use of fossil fuels, for example).

CRC Handbook of Chemistry and Physics, 71st ed. David R. Lide, Ed. CRC Press, 2000 Corporate Blvd., Boca Raton, FL 33431. 1990. 2384 pages. \$99.50; \$117, foreign.

The *CRC Handbook* is the well-known compendium of properties of many inorganic and organic chemicals. Environmental material has been added to this edition of the handbook. This includes threshold limit values for airborne contaminants (in the workplace), properties of priority organic pollutants, permissible quarterly intake of radionuclides, chemical carcinogens, and handling and disposal of chemicals in laboratories.

ES&T PRODUCTS

AIR POLLUTION



Toxic pollutant destruction. The Electroincinerator system is designed to destroy most airborne toxic chemicals, odors, bacteria, and viruses at ambient temperatures in a single pass. Electroincinerator Technologies **99**

Diesel exhaust purifier. PTX-Ultra is designed to purify exhaust from diesel-powered equipment in mines and indoor construction and to reduce gas odor and levels of CO and sulfate responsible for eye, nose, and lung irritations. Engelhard **102**

HAZARDOUS MATERIALS

Plastics recycling. System is designed to recycle used plastics such as high-density polyethylene (HDPE) and polyethylene terephthalate (PET). One was installed in Southern California in December, with provision for expansion to other plastics and to increased HDPE/PET recycling. John Brown **105**

Inhibiting groundwater contamination. "Modular Flooring Systems" are

Need more information about any items? If so, just circle the appropriate numbers on one of the reader service cards bound into this issue and mail in the card. No stamp is necessary.

Companies interested in a listing in this department should send their release directly to Environmental Science and Technology, Attn: Products, 1155 16th St., N.W., Washington, DC 20036.

designed to provide positive secondary containment for storing, transporting, and dispensing hazardous materials and to prevent their reaching groundwater. Cost is said to be a fraction of conventional "dike" systems. P&D System-technic **107**

INSTRUMENTS

UST monitoring. TLS-350 underground storage tank (UST) monitor is designed to provide in-tank leak detection and interstitial, vapor, and groundwater monitoring in accordance with applicable EPA regulations. System is computer-compatible. Veeder-Root **108**

Carbamate analysis. Carbamate Analysis system is designed to analyze *N*-methylcarbamate pesticides in raw source water and drinking water according to EPA Method 531.1, Revision 3.0, by high-performance liquid chromatography. Millipore/Waters **109**

Personal CO detection. DEAD/STOP indicator badge warns when the level of carbon monoxide in a breathing area approaches or exceeds the maximum allowable under federal regulations. Tracor Atlas **110**

Sulfur and chlorine analysis. MCTS-130/120 automated sulfur and chlorine analyzer also analyzes for nitrogen in aqueous, hydrocarbon, and solid samples. Rosemount Analytical **112**

Benchtop quadrupole GC/MS/DS. The TRIO-1 S is a benchtop instrument designed to produce library-searchable EI+ spectra with samples as small as 10 µg. VG Instruments **118**

VOC analysis. Model 2000 concentrator with Model 2010 canister manifold measures volatile organic carbons in a fully automated manner. System supports PCs. Entech **120**

Environmental analyses. Systems are available for organic and inorganic analysis by ion, high-performance liquid,

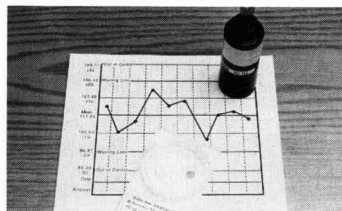
and supercritical fluid chromatography. They can be configured for current and future needs. Dionex **124**

SERVICES

Guide to service firms. 1991 *EI Environmental Services Directory* provides information about ~4500 environmental service firms in the United States. Headings include asbestos, laboratories, consultants, and emergency response. Environmental Information **131**

Biological pest control. Company has expanded its production of the insect-killing microbe *Bacillus thuringiensis*. Sandoz Crop Protection **136**

STANDARDS



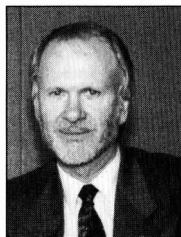
Asbestos references. Two new asbestos analytical reference materials help fulfill NIOSH requirements for daily analyses of reference materials and blanks and help monitor laboratory proficiency. Ask about TechChek and LabTrack. Forensic Analytical Specialties **141**

WATER TREATMENT

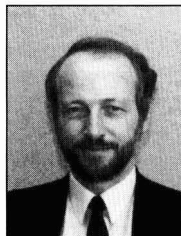
Wastewater treatment controls. DCI system is designed to provide advanced computer graphic control for wastewater treatment systems. Fischer & Porter **143**

Lead removal. LeadOUT-10 filter uses a proprietary alumina-based filter medium to reduce lead levels in drinking water to ≤ 4 ppb; EPA's maximum contaminant level, now 50 ppb, is expected to be lowered to 5 ppb. Filter is designed to remove other heavy metals as well. Selecto **148**

ES&T's 1991 Advisory Board



Dr. William H. Glaze
Editor
University of
North Carolina



Dr. Walter Giger
Associate Editor
(Europe)
EAWAG



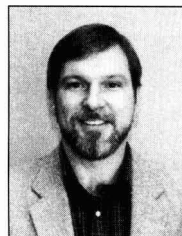
Dr. Ronald A. Hites
Associate Editor
Indiana University



Dr. Jerald L. Schnoor
Associate Editor (water)
University of Iowa



Dr. John H. Seinfeld
Associate Editor (air)
California Institute of
Technology



Dr. Joe Sufita
Associate Editor
University of Oklahoma

ES&T Editor William H. Glaze has appointed Jerald L. Schnoor associate editor (water). Schnoor replaces Philip C. Singer, who has served with distinction as associate editor since July 1983. Schnoor, who is well known in the water quality field, will be in charge of manuscripts concerning water. He also will act as liai-

son with reviewers in this field. For more information about Schnoor, see page 6 of this issue. Otherwise, the editorial and advisory boards remain the same for 1991 as they were in 1990. Board members serve three-year terms. The last year of each member's term is noted in parentheses.



Dr. Roger Atkinson
University of
California, Riverside
(1993)



Dr. Joan M. Daisey
Lawrence Berkeley
Laboratory
(1991)



Dr. Fritz H. Frimmel
Technical University
of Munich
(1992)



Dr. George Helz
University of
Maryland
(1992)



Dr. Ralph Mitchell
Harvard University
(1991)



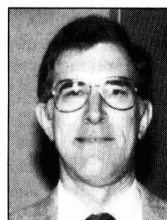
Dr. Joseph M. Norbeck
Ford Motor Company
(1992)



Dr. Walter J. Weber, Jr.
University of
Michigan
(1991)



**Dr. Alexander J. B.
Zehnder**
Agricultural
University
of Wageningen
(1991)



Dr. Richard G. Zepp
EPA
(1991)

Editorial Policy

Environmental Science & Technology reports on aspects of the environment and its control by scientific, engineering, and political means. Contributed materials may appear as feature articles, critical reviews, current research papers, research communications, and correspondence. Central to the evaluation of all contributions is a commitment to provide the readers of *ES&T* with scientific information and critical judgments of the highest quality. For the convenience of authors, the specific nature of each type of contribution is outlined below.

Feature articles. A manuscript submitted for publication as a feature article should present useful discussion and opinion on important research directions in environmental science; developing technology; environmental processes; and social, political, or economic aspects of environmental issues. Each manuscript undergoes review by qualified peers as well as by the editors for the purpose of balance and elimination of inappropriate bias. Review criteria include significance of the scientific issue or process described, quality and succinctness of the text, and identification of potential research needs. Strict requirements for documentation of results, completeness of data, and originality, such as those applicable to research manuscripts, are not included in the review criteria for feature articles. Four copies are required.

Views. A manuscript submitted for publication as a view should be objective, not an advertisement for a product or method, and should comment on a timely event or development. Views are *not* news items, but insightful commentaries on timely environmental topics. The manuscript should be about 1000 words long. The manuscript will be reviewed by members of the *ES&T* advisory board or reviewers to judge the suitability of its publication in *ES&T*.

Critical reviews. Critical reviews are thoroughly documented, peer-reviewed assessments of selected areas of the environmental science research literature for the purpose of identifying critical research needs. Criteria for acceptability include current importance of the field under review, thoroughness of the literature coverage, clarity of text, and adequacy of research need identification.

Current research papers. The research pages of *ES&T* are devoted to the publication of critically reviewed papers concerned with the fields of water, air, and waste chemistry, and with other scientific and technical fields that are relevant to the understanding and management of the water, air, and land environments. Contributed research papers, in general, describe complete and fully interpreted results of original research.

Environmental Science & Technology seeks to publish papers of an original and significant nature. Originality should be evidenced by new experimental data, new interpretations of existing data, or new theoretical analysis of environmental phenomena. Significance will be interpreted with respect to the breadth of impact of the reported findings. Manuscripts reporting data of a rou-

tine nature that do not offer heretofore unavailable important information or do not substantially augment already available data will be declined publication in *ES&T*. The scope of the reported data in ambient monitoring studies should be such that broad conclusions applicable to more than the particular local scale are possible.

All research articles emphasizing analytical methodology for air or water analysis must include substantial application to environmental samples. *ES&T* faces some overlap with other journals in this area, and articles that do not contain, in the editors' judgment, a significant emphasis on environmental analysis will be returned to the authors for submission elsewhere.

Manuscripts should be prepared with strict attention to brevity. The vast majority of articles are expected to be fewer than four published pages. Processing time will be shortened if the editors do not have to return manuscripts to be condensed.

Research Communications. Research Communications are short research reports describing results of unusual significance. The subject of the communication should be of such importance and the report of such quality that rapid publication is warranted. Communications are expected to be preliminary reports that will be followed by a more detailed publication. The communication should be no longer than two printed pages including figures, tables, and references. Every effort should be made to keep the length substantially below this maximum, such as by avoiding a lengthy introductory section. The Experimental Section should be as brief as possible, giving only essential details. An abstract should be sent with the communication for publication in *Chemical Abstracts* but it will not be published in *ES&T*. See Current Research Author's Guide for directions for preparation of Abstract. Communications will be reviewed expeditiously and published as rapidly as possible. To ensure prompt attention to their manuscript, authors should consider sending Communications by FAX to the ACS manuscript office (FAX# 202-872-6325) or sending it by express courier. A FAX number for return communications should be included, if available. If minor revisions are required, manuscripts will be returned to authors as expeditiously as possible and should be returned to ACS headquarters within two weeks. The need for major revision is just cause for rejection of the Communication.

Correspondence is a significant comment on work published in the research section of *ES&T*. Comments should be received within six months of date of publication of the original article. The authors of the original article ordinarily will be allowed to reply.

Send manuscripts to: *Environmental Science & Technology*, 1155 16th St., N.W., Washington, DC 20036. Address feature manuscripts to: Managing Editor; research manuscripts to Manager, Manuscript Office. Include a signed copyright transfer form; a copy appears on the inside back cover of the January issue.

Peer review in *ES&T*

Characteristics of *ES&T*

ES&T stands out among American Chemical Society journals in that it combines both a magazine and a journal. Only one other ACS publication contains this combination—our sister publication, *Analytical Chemistry*. Because of the hybrid nature of our publication, it serves a large and diverse audience.

Central to the evaluation of all contributions to *ES&T* is a commitment to provide our readers with scientific information of the highest quality. The publication seeks the most significant, original, and broadly applicable types of articles for its current research section. A vast number of persons review original manuscript contributions and indicate in their evaluations the originality and scientific validity of the work, as well as the appropriateness of the material for our publication.

The Editor and Associate Editors, who are located at the University of North Carolina, the California Institute of Technology, EAWAG, Indiana University, the University of Iowa, and the University of Oklahoma are fully responsible for all material published in *ES&T*. This policy is a general one applicable to all editors of American Chemical Society publications. The 10 members of the Advisory Board are chosen by the editor to provide input to *ES&T*'s operation. The members are chosen to represent various constituent groups in the research and reader communities and serve three-year terms. Although the editors seek advice and help from individuals in the scientific community and from advisory groups, it is ultimately the editors' responsibility to provide editorial direction, set editorial policies, and make individual publication decisions.

The Washington editorial staff handling the current research section is responsible for the day-to-day operation of the peer review system. All editorial staff members have chemistry or related science degrees.

General guidelines and overall editorial policies set by the editor form the basis for evaluating reviewers' comments on research articles submitted for the current research section.

A look at peer review

Each manuscript submitted to the current research section is reviewed by a staff editor and, on the basis of its content, assigned to one of the associate editors or to the editor (hereafter called technical editor). The subject matter of the manuscript determines which editor will receive the file. The technical editor is responsible for the manuscript—including choosing reviewers; evaluating the content of the paper; taking into account the comments of reviewers; and communicating ultimate acceptance or rejection to the corresponding author. The staff editor in Washington assists in this process by screening papers initially to determine whether papers may fall outside of *ES&T*'s scope, by monitoring the progress of the review process, and by carrying out a final check of accepted manuscripts for appropriate format and style.

Beginning in January 1990, reviewers are picked by the technical editors. Three reviewers are carefully selected for each paper, based on the subject matter of the paper, the experts available in a given area, and the editorial staff member's knowledge of the habits of proposed reviewers. Thus, known slow reviewers are avoided when possible. Potential reviewers for each paper are identified through various means, one of which involves a computer search of subjects that reviewers have indicated are their

areas of expertise. Reviewers are normally asked to respond within three weeks, and if they are late, reminders are sent. Late review notifications are generated and dispatched as mailgrams on a weekly basis.

Also beginning in January 1990, reviews will be sent directly to the technical editor to whom the paper has been assigned. If the reviewers do not agree on the disposition of the paper, or if the technical and scientific strengths or shortcomings of the work have not been adequately addressed, an additional reviewer may be selected. The reviews (usually at least two) are used by the technical editor in making the final decision about the disposition of the manuscript. Letters communicating the decision proceed directly from the office of the technical editor to the corresponding author.

If the technical editor has recommended revision of the manuscript, the staff editor goes over the paper carefully in a "pre-edited" check to aid the author in revising the manuscript.

Tips for authors of papers submitted to *ES&T*

- Prepare your paper with the audience of the publication in mind. Papers prepared for other journals are likely to need some revision to make them suitable for *ES&T*.
- Clearly state in the introduction the purpose of the work and put the work in perspective with earlier work in the area. This may appear obvious, but authors often fail to clearly state the purpose and significance of their work.
- Write concisely. The vast majority of articles are expected to be fewer than five published pages. Long manuscripts are looked at much more closely and critically both by reviewers and editors. Do not repeat information or figures or tables that have appeared elsewhere. Use illustrative data rather than complete data where appropriate.
- Suggest names of possible reviewers for your paper. You may also suggest the names of persons whom you do not want to review the paper. The editors try to use at least one reviewer who has been suggested by authors. This cannot be assured, however, since specific reviewers may not be available for reviewing or may already be overloaded.
- Follow the Current research author's guide, published in every January issue.

If your manuscript is rejected

- Read the reviews carefully. If the reviewers have "missed the point," as authors often claim, consider how the presentation can be clarified and improved to make the point clear. If reviewers have not understood, it is unlikely that readers will understand.
- Is the manuscript, after all, more suitable for another journal?
- Is the work sufficiently complete, or do you need to do more work before seeking publication?
- If you feel strongly that the paper has not been judged fairly, then carefully revise the manuscript taking into account the reviewers' criticisms and send the manuscript to the office of the technical editor with a rebuttal letter asking that the manuscript be reconsidered. Provide an itemized list of changes made in the manuscript in response to reviewer comments, as well as objective rebuttals to the criticisms with which you do not agree.

Current research author's guide

This manuscript preparation guide is published to aid authors in writing, and editors and reviewers in expediting the review and publication of research manuscripts in *Environmental Science & Technology*, including full research articles and communications. For a detailed discussion with examples of the major aspects of manuscript preparation, please refer to *The ACS Style Guide* (1986).

Title

Use specific and informative titles. They should be as brief as possible, consistent with the need for defining the subject of the paper. If trade names are used, give generic names in parentheses. Key words in titles assist in effective literature retrieval.

Authorship

List the first name, middle initial, and last name of each author. Omit professional and official titles. Give the complete mailing address where work was performed. If present address of author is different, include the new information in a footnote. In each paper with more than one author, the name of the author to whom inquiries should be addressed carries an asterisk. The explanation appears on the contents page.

Abstracts

An abstract, which will appear at the beginning of each paper, must accompany each manuscript. Authors' abstracts frequently are used directly for *Chemical Abstracts*. Use between 100 and 150 words to give purpose, methods or procedures, significant new results, and conclusions. Write for literature searchers as well as journal readers.

Text

Consult a current issue for general style. Assume your readers to be professionals not necessarily expert in your particular field. Historical summaries are seldom warranted. However, documentation and summary material should be sufficient to establish an adequate background. Divide the article into sections, each with an appropriate heading, but do not oversectionalize. The text should have only enough divisions to make organization effective and comprehensible without destroying the continuity of the text. Keep all information pertinent to a particular section within that section. Avoid repetition. Do not use footnotes; include the information in the text.

Introduction. Discuss relationship of your work to previously published work, but do not repeat. If a recent article has summarized work on the subject, cite the summarizing article without repeating its individual citations.

Experimental. Apparatus: List devices only if of specialized nature. Reagents: List and describe preparation of special reagents only. Procedure: Omit details of procedures that are common knowledge to those in the field. Brief highlights of published procedures may be included, but details must be left to literature cited. Describe pertinent and critical factors involved in reactions so that the method can be reproduced, but avoid excessive description.

Results and discussion. Be complete but concise. Avoid non-pertinent comparisons or contrasts.

Manuscript requirements

Five complete legible copies of the manuscript are required. They should be typed double or triple spaced on 22 × 28 cm paper, with text, tables, and illustrations of a size that can be mailed to reviewers under one cover. Duplicated copies will be accepted only if very clear.

If pertinent references are unpublished, furnish copies of the work or sufficient information to enable reviewers to evaluate the manuscript.

In general, graphs are preferable to tables if precise data are not required. When tables are submitted, however, they should be furnished with appropriate titles and should be numbered consecutively in Roman numeral style in order of reference in the text. Double space with wide margins, and prepare tables in a consistent form, each on a separate 22 × 28 cm sheet.

Submit original drawings (or sharp glossy prints) of graphs, charts, and diagrams prepared on high-quality inking paper. All lines, lettering, and numbering should be sharp and unbroken. If coordinate paper is used, use blue cross-hatch lines because no other color will "screen out."

Typed lettering does not reproduce well: Use black India ink and a lettering set for all letters, numbers, and symbols. On 20 × 25 cm copy, lettering should be at least 0.32 cm high. Lettering on copy of other sizes should be in proportion. Label ordinates and abscissas of graphs along the axes and outside the graph proper. Do not use pressed wax for numbering or lettering.

Photographs should be supplied in glossy print form, as large as possible, but preferably within the frame of 20 × 25 cm. Sharp contrast is essential.

Number all illustrations consecutively using Arabic numerals in the order of reference in the text. Include a typed list of captions and legends for all illustrations on a separate sheet. If drawings are mailed under separate cover, identify by name of author and title of manuscript. Advise editor if drawings or photographs should be returned to the author. Color reproduction is possible provided the author bear all incremental charges. An estimate of these charges will be given upon request. A letter acknowledging the author's willingness to defray the cost of color reproduction should accompany.

Nomenclature

Nomenclature should conform with current American usage. Insofar as possible, authors should use systematic names similar to those used by Chemical Abstracts Service or IUPAC. *Chemical Abstracts* nomenclature rules are contained in Appendix IV of the current *Chemical Abstracts Index Guide*. A list of ring systems, including names and numbering systems, is found in the *Ring Systems Handbook*, American Chemical Society, Columbus, OH, 1988.

Use consistent units of measure (preferably SI).

If nomenclature is specialized, include a "Nomenclature" section at the end of the paper, giving definitions and dimensions for all terms. Write out names of Greek letters and special symbols in margin of manuscript at point of first use. If subscripts and superscripts are necessary, place them accurately. Avoid trivial names. Trade names should be defined at point of first use (registered trade names should begin with a capital letter). Identify typed letters and numbers that could be misinterpreted, for example, one and the letter "1," zero and the letter "O."

Formulas and equations

Chemical formulas should correspond to the style of ACS publications. Chemical equations should be balanced and numbered consecutively along with mathematical equations. The mathematical portions of the paper should be as brief as possible, particularly where standard derivations and techniques are commonly available in standard works.

Safety

Authors are requested to call special attention—both in their manuscripts and in their correspondence with the editors—to safety considerations such as explosive tendencies, precautionary handling procedures, and toxicity.

Acknowledgment

Include essential credits in an "Acknowledgment" section at the end of the text, but hold to an absolute minimum. Give meeting presentation data or other information regarding the work reported (for example, financial support) in a note following Literature Cited.

References

Literature references should be numbered and listed in order of reference in text. They should be listed by author, patentee, or equivalent. In the text, just the number should be used, or the name should be followed by the number. "Anonymous" is not acceptable for authorship. If the author is unknown, list the reference by company, agency, or journal source. Do not list references as "in press" unless they have been formally accepted for publication. Give complete information, using abbreviations for titles of periodicals as in the *Chemical Abstracts Service Source Index, 1907-84*.

For periodical references to be considered complete, they must contain authors' surnames with initials, journal source, year of is-

sue, volume number, and the first and last page numbers of the article. Consult *The ACS Style Guide* for reference style.

Supplementary material

Extensive tables, graphs, spectra, calculations, or other material auxiliary to the printed article will be included in the microfilm edition of the journal. Identify supplementary material as to content, manuscript title, and authors. Three copies of the supplementary material, one in a form suitable for photoreproduction, should accompany the manuscript for consideration by the editor and reviewers. The material should be typed on white paper with black typewriter ribbon or printed on high quality (300 dpi) laser printer. If individual characters for any of the material, computer or otherwise, are broken or disconnected, the material is definitely unacceptable.

Figures and illustrative material should preferably be original high-contrast drawings or good prints of originals. Optimum size is 22 × 28 cm. Minimum acceptable character size is 1.5 mm. The caption for each figure should appear on the same piece of copy with the figure. Be sure to refer to supplementary material in text where appropriate.

Supplementary material may be obtained in photocopy or microfiche form at nominal cost. Material of more than 20 pages is available in microfiche only. Photocopy or microfiche must be stated clearly in the order. Prepayment is required. See instructions at the end of individual papers.

The supplementary material is abstracted and indexed by Chemical Abstracts Service.

Subscribers to microfilm editions receive, free, the supplementary material in microfiche form from individual papers in any particular issue. For information, contact Microforms Program at the ACS in Washington, DC, or call (202) 872-4554.

Research Communications. Please refer to Editorial Policy for guidelines on research communications.

TESTING

Chemical testing is our business.

That's why, for more than 20 years, customers in both industry and government have depended on TEI[®] for quality and service in chemical testing.

TEI Analytical, Inc. is accredited by the American Association for Laboratory Accreditation in the field of Environmental Chemical Analysis.

Call, FAX, or use the Reader Services Card to receive more information on our capabilities.

TEI Analytical, Inc.
7177 N. Austin
Niles, IL 60648
TEL: (708) 647-1345
FAX: (708) 647-0844

CIRCLE 13 ON READER SERVICE CARD

CLASSIFIED SECTION

BROWARD COUNTY FLORIDA EXEMPT SERVICE OPPORTUNITY DIRECTOR, OFFICE OF NATURAL RESOURCE PROTECTION \$59,598 - \$88,801

Broward County, Florida (population 1.3M—County Seat Fort Lauderdale) has a beautiful environment and wants it protected and enhanced. To help bring that about, the Broward County Board of County Commissioners has approved a strengthened Office of Natural Resource Protection reporting directly to the County Administrator. The County is seeking a very experienced, innovative, and dedicated director to lead a staff of 130 in enforcing environmental protection regulations and in developing pro-active policies for the future.

The director will be a seasoned professional with at least seven years of recent experience in the field, at least four years of which will be responsible management and administrative experience. The new director will have at least a four-year college degree with a major in engineering, chemistry, environmental science or a related field, although a graduate degree and other examples of leadership in the profession will be very desirable.

Resumes are subject to public disclosure in accordance with Florida's Public Records Act. Resumes and a salary history must arrive not later than 5:00 p.m., Friday, January 11, 1991.

**Broward County Personnel
Governmental Center
Room 508
115 S. Andrews Avenue
Fort Lauderdale, FL 33301**

EQUAL EMPLOYMENT OPPORTUNITY M/F/H/V

Leadership Excellence Innovation

Environmental Scientist/Analyst

SERI is the nation's leading laboratory for the research and development of renewable and alternative energy sources. The Energy and Environmental Analysis Division is seeking qualified applicants for the position of Environmental Scientist/Analyst to perform scientific analysis of environmental factors, regulations, and policies affecting the development and use of renewable energy conversion and energy-efficient technologies. Examples include studies on full-fuel cycle analysis of conventional, renewable, and demand-side energy technologies and the role of renewable energy technologies in reducing greenhouse gas emissions. Applicants must have undergraduate or graduate degrees in physical or biological science and experience working on environmental assessment and/or policy analyses related to energy/environment issues.

We offer an excellent compensation and benefit program. For immediate consideration, please send resume to: **Human Resources Office, E2600-EEA, 1617 Cole Blvd., Golden, CO 80401.** Women and minorities are encouraged to apply. We are an equal opportunity employer.

SERI 
Solar Energy Research Institute



ENVIRONMENTAL ENGINEERING FACULTY

New Mexico Institute of Mining and Technology is seeking qualified applicants for a tenure-track assistant or associate professor level faculty position in Environmental Engineering. The position is open January 1991 but will remain open until filled. Strong qualifications in air quality and hazardous waste management and computer applications are desired. The successful candidate will teach undergraduate courses in Environmental Engineering including air pollution engineering and will be expected to initiate research programs. A Ph.D. in Civil Engineering, Environmental Engineering or related discipline is required. Good communication skills, both oral and written, are essential. Experience in Environmental Engineering is desirable. Send resume to **New Mexico Institute of Mining & Technology, Human Resources Box C-046, Socorro, New Mexico 87801.**

AAEEOE

CAREER OPPORTUNITIES NATIONWIDE

At Ansara, Bickford & Fiske, we have the finest positions available with operating & consulting clients. Experienced engineers & scientists are sought with the following disciplines: Water/Waste water * Hydrogeology * Solid Waste * Health & Safety * Geotech * Air Quality * Chemistry * Industrial Hygiene * Many Others positions. Contact Peter Ansara for confidential consideration: 413-733-0791 Fax 413-731-1486 or send resume to: A.B.F., P.O. Box 239, West Springfield, MA 01090. All fees employer paid.

COLORADO SCHOOL OF MINES Golden, Colorado FACULTY POSITIONS IN ENVIRONMENTAL ENGINEERING

Colorado School of Mines Department of Environmental Sciences and Engineering invites applications for tenure track positions at the Assistant Professor rank with an anticipated start date of August 1991. Areas of specialization are open but individuals whose research interests are in hazardous/industrial waste treatment or in the transport and fate of contaminants are especially encouraged to apply.

Successful applicants must possess a Ph.D. in environmental engineering or a related engineering field and a commitment to graduate level teaching and research. Professional registration and academic or industrial experience are desirable.

The selection process will continue until such time as positions are filled. Applicants should submit a resume, academic transcripts, examples of research output, and the names and addresses of three references to:

**COLORADO SCHOOL OF MINES
Environmental Sciences Search Committee
P.O. Box 69, Golden, CO 80402**

AN EQUAL OPPORTUNITY/AFFIRMATIVE ACTION EMPLOYER
Minorities and Females Encouraged To Apply

SUBSURFACE CONTAMINANT TRANSPORT

The Department of Civil Engineering at the University of Washington seeks candidates for a tenure-track faculty position beginning Autumn, 1991, in the general area of subsurface contaminant fate and transport. Some capability in both experimental investigation and modeling of such processes is desirable, although strong candidates with experience in only one of these areas are also encouraged to apply. The appointment will be at the Assistant Professor level. In addition to conducting and directing research in the specified areas, the successful candidate will have teaching responsibilities in undergraduate and graduate engineering courses.

Those interested in applying should send a resume and the names of three references to the Chair of the search committee, Mark Benjamin, at the following address:

**Dr. Mark Benjamin
Department of Civil Engineering FX-10
University of Washington
Seattle, WA 98195**

Consideration of applications will begin on March 1, 1991.

The University of Washington is an equal opportunity, affirmative action employer. Applications from women and underrepresented minority groups are encouraged.

ENVIRONMENTAL PROFESSIONALS

Our Growth is Your Opportunity

NUS Corporation, one of the nation's leading consulting firms specializing in environmental, safety, and nuclear safety services, has immediate openings in its Aiken, SC office. These opportunities call for experienced professionals with the ability to provide responsive and innovative solutions for our clients. Positions include:

- **Regulatory Compliance Supervisor**
- **Environmental Scientists/Engineers**
- **NEPA Specialists**
- **Waste Management Specialists**
- **Environmental Health Physicists**
- **Socioeconomic/Cultural Resources Specialist**
- **Risk Assessment Specialist**

These environmental professionals will review and evaluate regulatory compliance; assess impacts; perform appraisals; and plan, prepare, and review program documentation.

You need a BS or MS in science or

engineering and a minimum of 3-8 years experience. Knowledge of regulatory requirements and excellent communication skills are essential, as are skills in planning, impact assessment, and project management. You must be a U.S. citizen.

We offer competitive salaries, generous benefits, and excellent growth opportunities. If you are interested in working with a team of professionals, send resume in confidence to:

NUS Corporation
Savannah River Center
Dept. ES-15SH
900 Trail Ridge Road
Aiken, SC 29803



U A Halliburton Company

An equal opportunity/affirmative action employer.

U.S. ENVIRONMENTAL PROTECTION AGENCY RESEARCH GRANTS

The U.S. Environmental Protection Agency (EPA) is accepting proposals to conduct basic investigative research in the general areas of biology, health, chemistry, physics, engineering or socioeconomics. The Agency is interested in proposals focusing on any aspect of pollution identification, characterization, abatement or control, or which address the effects of pollutants on human health or the environment. Proposals will also be accepted which investigate the social or economic consequences of environmental policy. Applicants successfully passing competitive peer review will receive a research grant for up to three years. Non-profit institutions and state or local governments are encouraged to apply.

For more information, write to:

**Research Grants Program
Office of Research and
Development, RD-675
U.S. Environmental Protection Agency
401 M Street, S.W.
Washington, D.C. 20460
Or call: 202-382-7445**

HEAD OF DIVISION OF ENVIRONMENTAL SCIENCES: School of Public Health, Columbia University. The Division offers a Masters and a Doctorate of Public Health. The position requires a productive researcher and administrator, as well as someone with a strong concern for teaching. The Division has major teaching and research programs in (1) cellular and molecular mechanisms of carcinogenesis, mutagenesis and tumor promotion, (2) molecular epidemiology, (3) occupational health (with an AMA-accredited residency), and (4) risk assessment-communication and environmental policy. Send curriculum vitae to **Dr. Eugene Litwak, Division of Sociomedical Sciences, Columbia University School of Public Health, 600 W. 168th Street, New York, NY 10032.** Columbia University takes affirmative action towards equal opportunity.

GRADUATE STUDY in ENVIRONMENTAL SCIENCE AND ENGINEERING at the Oregon Graduate Institute. Highly qualified, strongly motivated students sought for exciting research programs in transport and fate of organic and inorganic contaminants, atmospheric chemistry and physics, aquifer remediation, microbial ecology and physiology, biodegradation, biogeochemistry, analytical environmental chemistry, numerical modeling, estuarine and coastal studies, elemental cycling in terrestrial ecosystems. Intensive research experience, state-of-the-art instrumentation, maximum faculty-student interaction. Research assistantships with tuition remission available to qualified Ph.D. applicants. Write: **Carl D. Palmer, Department of Environmental Science and Engineering, 19600 N.W. Von Neumann Dr., Beaverton, OR 97006, (503) 690-1196.** (Closing date 4/1/91). Affirmative Action/Equal Opportunity Employer.

SCIENTIFIC/TECHNICAL SENIOR RESEARCH POSITIONS

The U. S. Environmental Protection Agency (EPA) is seeking highly qualified candidates for senior research positions at our environmental research laboratories in the following locations: Narragansett, Rhode Island; Research Triangle Park, North Carolina; Athens, Georgia; Gulf Breeze, Florida; Cincinnati, Ohio; Duluth, Minnesota; Las Vegas, Nevada and Corvallis, Oregon. The person filling one of these positions will report directly to the Laboratory Director.

Depending on the specific position, applicants should have an advanced degree (doctorate preferable) in one of the following areas: ecological sciences, health sciences, environmental sciences, physical sciences, engineering or mathematical sciences; and several (at least seven) years experience as a principal investigator and direct experience with scientific assessments for environmental issues. Applicants must also meet the technical qualifications described in the Vacancy Announcement.

To obtain a copy of the Vacancy Announcement for the position in which you are interested, a copy of the Federal Application Form (SF-171), and a description of each laboratory, call or write **Ms. Chaunta Gladney, U.S. EPA, Executive Resources and Special Programs Division, PM-224, Room 3910, 401 M Street S.W., Washington, D.C. 20460, (202/382-3328).**

APPLICATIONS MUST BE POSTMARKED BY: February 28, 1991.
EPA IS AN EQUAL EMPLOYMENT OPPORTUNITY EMPLOYER

ENVIRONMENTAL/CHEMICAL ENGINEERS

NATIONWIDE opportunities with consulting and operating companies in Environmental Engineering, Hazardous Waste, Remediation, Air Quality, Landfill Design, Hydrogeology, Wastewater Treatment. Fees are company paid. Send resume to: **JAMES E. IANNONI & ASSOC. P.O. Box 66, Hampton, CT 06247 203-455-0151**

CLASSIFIED ADVERTISING RATES

Unit	1-T	3-T	6-T	12-T	24-T
1 inch	\$130	\$125	\$120	\$115	\$110

(Check Classified Advertising Department for rates if advertisement is larger than 10".)

SHIPPING INSTRUCTIONS:
Send all material to

**Environmental Science & Technology
Classified Advertising Department
500 Post Road East
P.O. Box 231
Westport, CT 06881
(203) 226-7131/Fax (203) 454-9939**

We Create An Environment For Growth.



Is restoring the planet vital to you? Are you anxious to find real-life solutions to real-life problems — affordable and effective ways we can preserve our environment and keep America technologically competitive?

If so, you can make a major impact as a member of our team at Battelle, Pacific Northwest Laboratories. Our staff includes 3,500 scientists, engineers and specialists with widely diverse capabilities and internationally recognized expertise. They work individually and in multidisciplinary teams to attack problems affecting waste disposal, environmental restoration, global change, human health and energy resources. And their efforts make Battelle a leader in technical innovation and a steward of the environment.

We currently offer research opportunities in the following areas:

- Regulatory Analysis
- Global Climate Change
- Site Characterization
- Health Physics
- Oceanography
- Geochemistry
- Microbiology
- Ecophysiology
- Environmental Economics
- Energy Planning
- Risk and Safety Assessment
- Organic Chemistry
- Aquatic Toxicology
- Technological Assessment
- Hydrology

Working at our Laboratories in Richland, Washington, you can enjoy big-city amenities and a small-town lifestyle. The community offers affordable housing, quality education, pleasant climate and year-round recreational opportunities.

Help us in deploying strategies that will protect the earth's resources. Fax/send your resume to: **Battelle, Pacific Northwest Laboratories, Staffing Center, Dept. RZ40, PO Box 1406, Richland, Washington 99352. FAX # (509) 376-9099.** We are an Equal Opportunity Employer. U.S. Citizenship Required.

 **Battelle**
...Putting Technology To Work

UNIVERSITY OF CALIFORNIA AT BERKELEY DEPARTMENT OF CIVIL ENGINEERING

The University of California at Berkeley, Department of Civil Engineering, invites applicants for a tenure-track assistant professor position in **Environmental Engineering** in the area of contaminant transformations and transport in environmental systems. This position requires an engineer familiar with the fundamentals of thermodynamics, chemical and biological kinetics and fluid mechanics to address pollutant fate in air, water, or soil systems. Desirable areas of expertise include, but are not limited to the following: adsorption from gas and aqueous phases onto solids, photochemistry in gas and aqueous phases, aerosol or hydrosol dynamics, contaminant partitioning in multimedia systems, and advanced oxidation procedures for contaminant destruction. The successful candidate will be responsible for teaching undergraduate and graduate courses in environmental engineering and must show potential for high quality research in this field. An engineering background and a doctoral degree in an appropriate field are required. Pending budgetary approval.

The position will be available July 1, 1991.

Interested persons should apply in writing by submitting a resume, statement of interests, list of publications, and names and addresses of references. Applications must be submitted by March 1, 1991. Apply to:

**Search Committee for faculty position
in Environmental Engineering
c/o Professor Keith C. Crandall, Chair
Department of Civil Engineering
Room 760 Davis Hall
University of California
Berkeley, CA 94720**

The University of California is an Equal Opportunity, Affirmative Action Employer.

FACULTY POSITION IN ENVIRONMENTAL ENGINEERING CLARKSON UNIVERSITY

The Department of Civil and Environmental Engineering at Clarkson University invites applications for a tenure-track position in Environmental Engineering to begin July 1991. Duties of the position include teaching at the graduate and undergraduate level and continued active participation in research and cognate scholarly activities. The rank of the position is open, and outstanding recent Ph.D. recipients will be considered. Preference, however, will be given to applicants with a proven record of accomplishment in their research area, which should relate directly to environmental engineering: environmental chemistry, water or wastewater treatment processes, bioengineering, hazardous waste management, air quality engineering, and mathematical modeling of aquatic systems in surface and subsurface environments. Review of applications will begin January 1, 1991 and will continue until the position is filled. Send a current resume plus the names of at least three references to **Dr. Norbert L. Ackermann, Department of Civil and Environmental Engineering, Clarkson University, Potsdam, NY 13699-5710.** Clarkson University is an Affirmative Action/Equal Opportunity Employer. POS. #233.

POSTDOCTORAL RESEARCH ASSOCIATE ENVIRONMENTAL ENGINEERING/CHEMISTRY

Postdoctoral research associate in environmental engineering or chemistry. One position is available immediately. The work is focussed on the determination of toxic organic contaminants, e.g. PCBs, PAHs, and mirex in bottom sediments from the Milwaukee Harbor Estuary. Analysis for radionuclides such as Pb-210 and Cs-137 will also be carried out. New analytical instrumentation (GC/MSD and GC/MS) and excellent facilities are available for this project. Candidates should have a Ph.D. in an appropriate discipline and be experienced in the chemical analysis for environmental contaminants. Competitive salary. Send letter of application and names of three references to: **Dr. Erik R. Christensen, Department of Civil Engineering and Mechanics, University of Wisconsin-Milwaukee, Milwaukee, WI 53201.**

UWM is an equal opportunity/affirmative action employer.

TOXIKON ENVIRONMENTAL SCIENCES 106 Coastal Way, Jupiter, FL 33477 (407) 575-2477

Toxikon Environmental Sciences is one of the nation's leading contract facilities which conducts laboratory and field ecotoxicity studies and provides counsel to the chemical industry. We presently have immediate openings in our Florida facility. Positions include:

Environmental Toxicologist—Education and experience in freshwater ecology conducting aquatic field studies and preparing ecological risk assessments.

Fate Chemist—Education and experience in conducting chemical fate tests in the laboratory and field.

Aquatic Toxicologist—Education and experience in conducting aquatic toxicity studies with freshwater and saltwater algae, fish and invertebrates.

Salaries will be commensurate with education and experience. Submit resume to address listed above. EOE.

DEAN School of Natural Resources The University of Michigan

Applications and nominations are invited for the position of Dean of the School of Natural Resources at the University of Michigan. The Dean is the chief academic and administrative officer of the School and reports directly to the Academic Vice President. The School of Natural Resources is an interdisciplinary, research-oriented, professional school, focusing on research and the development of policies and management programs that promote the conservation, protection, and sustainable use of natural resources. In addition, the School educates practitioners and researchers who will seek these ends. The School's activities include instruction at the undergraduate, master's, and doctoral levels and an active research program. Faculty interests are diverse: Resource Ecology and Management, Resource Policy and Behavior, and Landscape Architecture. The School is committed to an integrative, interdisciplinary, problem-solving approach in collaboration with related disciplinary departments and professional schools.

The Dean provides leadership in program planning, development, and evaluation. Qualifications should include an earned doctorate, a distinguished record appropriate for a tenure appointment in the School, and the ability to generate funds for programs at the local, state, national, and international levels. The committee will begin reviewing candidate files on February 4, 1991. Applications and nominations should be sent to: **Professor Burton Barnes, Chair, School of Natural Resources, Dean Search Advisory Committee, The University of Michigan, 520 E. Liberty, Ann Arbor, MI 48104-2210.** A non-discriminatory, affirmative action employer.

CLASSIFIED ADVERTISING RATES

Unit	1-T	3-T	6-T	12-T	24-T
1 inch	\$130	\$125	\$120	\$115	\$110

(Check Classified Advertising Department for rates if advertisement is larger than 10".)

SHIPPING INSTRUCTIONS:
Send all material to

**Environmental Science & Technology
Classified Advertising Department
500 Post Road East
P.O. Box 231
Westport, CT 06881
(203) 226-7131
FAX: (203) 454-9939**

GROWTH POSITIONS \$30,000-\$70,000+

Nationwide environmental openings for Engineers, Scientists, Chemists, Geologists, Ind. Hygienists in operating and A&E companies. All fees company paid. Contact: **Gordon Hassell, V.P., Longberry Employment Service, Inc., 850 Main Place, P.O. Box 471, Niles, OH 44446, (216) 652-5871 — Fax (216) 652-3683.**

ENVIRONMENTAL PROFESSIONALS

ICF Kaiser Engineers, Inc., widely recognized for our excellence in the investigation, management, and minimization of hazardous and radioactive wastes, has opportunities available for qualified professionals interested in applying their expertise to a variety of challenging public and private sector projects. Our rapidly expanding practices offer unique domestic and international assignments, talented and knowledgeable professionals, and unlimited advancement potential. Current opportunities include:

PROJECT MANAGER — Requires 5-10 years of environmental experience in such areas as property transfer and compliance audits, industrial waste management, RI/FS, and remedial design. Must also have thorough knowledge of RCRA and CERCLA, excellent communication skills, and business development capabilities.

AIR SPECIALIST — Requires 3-7 years of experience in air permitting, testing, exposure assessments, data analyses, audits, control design, and modeling. Positions available in Chicago, Denver, and Fairfax, Virginia.

ENVIRONMENTAL CHEMISTS — Requires 1-5 years of environmental lab experience, including multimedia sample analysis, data review and validation, and QA/QC procedures. Familiarity with CLP a plus.

Various junior-, mid-, and senior-level positions are also available for experienced Environmental Geologists, Hydrogeologists, and Environmental and Chemical Engineers. All interested candidates should possess a Bachelor's or advanced degree in a relevant field, environmental experience or training, and strong oral and written communication skills. Enjoy excellent salary and benefits. Qualified candidates should send their resume with geographical preference to:

ICF KAISER ENGINEERS

Personnel - CHES
P.O. Box 2606
Fairfax, VA 22031-1207

Fairfax, VA Pittsburgh, PA Chicago, IL
Edison, NJ Ft. Lauderdale, FL

Equal Opportunity Employer

PROVIDE ENVIRONMENTAL RESEARCH EXPERTISE FOR PHARMACEUTICAL RESEARCH AND DEVELOPMENT.

The Environmental Research Laboratory at SmithKline Beecham, one of the world's largest pharmaceutical research and development companies, is responsible for insuring that chemicals and processes used in or produced by drug development and manufacturing do not endanger the environment. We currently have two positions available in this critically important group.

ASSOCIATE SENIOR INVESTIGATOR

You will plan and initiate projects to meet the environmental analysis requirements of R&D projects and IND/NDA submissions; create models for predicting the environmental behavior of chemicals; develop and test waste treatment/minimization strategies for specific, problematic chemicals; and create reports related to IND/NDA submission.

Requirements include a Ph.D. in analytical, physical or environmental chemistry with 1-3 years' experience, or M.S. degree with 5 years; excellent planning and communication skills; facility with computers and office automation systems. We prefer supervisory and environmental fate and effects testing experience.

MANAGER, ENVIRONMENTAL ANALYTICAL LABORATORY

You will manage the environmental analytical laboratory to provide full environmental analytical support for new product development, including design of sampling and assay protocols; coordination of in-house and contract analyses; and development of new analytical methods. You will also provide analytical support for Environmental/Assessment documentation for IND/NDA submissions by developing physical/chemical property and environmental fate and effects assays.

Requirements include a Ph.D. in Chemistry with 1-3 years' experience or an M.S. in Analytical Chemistry with 5 years; experience in environmental analytical chemistry; proven statistical skills; knowledge of FDA and EPA GLP guidelines; facility with computers and lab automation systems; the ability to critically read and interpret scientific literature; and excellent interpersonal skills and the ability to work well with all levels of personnel.

SmithKline Beecham offers highly competitive salaries and an excellent benefits package. To apply, please send your resume to: Central Employment, SmithKline Beecham, 1510 Spring Garden St., Philadelphia, PA 19101. We are an Equal Opportunity Employer, M/F/H/V.



SmithKline Beecham
Pharmaceuticals

professional consulting services directory



"TREATMENT BY DESIGN"

WE FOCUS ON SOIL & GROUNDWATER CLEAN-UP ON-SITE

Services including:

- Bioremediation (BIOTA Division)
- Chemical Fixation (TOXCO Division)
- Vapor Extraction
- UV Ozonation
- Remedial Investigations
- Underground Tank Removals

1-800-753-1818

CHEMPET RESEARCH CORPORATION

FORENSIC GEOCHEMISTRY

- Stable Isotope Tracers (C, H, O, N, S, Sr, Pb, Nd) Environmental, Hydrologic, Toxicologic Applications.
- Major & Trace Element Chemistry
- Radiochemistry
- Fate/Transport Analyses

For Pricing & Information
330 N. Zachary Ave., Suite 107
Moorpark, CA 93021
Phone or Fax (805) 529-0814

Staff Recruiters, Inc.

PROFESSIONAL RECRUITING SERVICES

Staffing Problems?

Finding the solution is our specialty.

- Recruiting to specifications
- Cost effective retained and contingency search programs
- All disciplines
 - All geographies
 - Time responsive
 - 250 affiliate firms nationwide

Professional candidates seeking opportunity are invited to respond to **Keith O. Nyman, CPC**; Ph: (206) 695-3221, FAX: (206) 693-2450; Suite M, 415 E. Mill Plain Blvd., Vancouver, WA 98660

EXCLUSIVELY EMPLOYER PAID



Search Northwest

Search Northwest specializes in NATIONWIDE recruitment and placement of professionals in the following disciplines:

- Environmental
- Risk Assessment
- Toxicology
- Chemical Engr.
- Safety Engineers
- Permitting Specialist
- Hazardous Waste Mgmt.
- Incineration
- Hydrogeology
- Water/Waste Water
- Chemistry
- Industrial Hygienists
- Regulatory Compliance
- Civil Engineering

Contact Hank Scrivines, (503) 285-6560/FAX (503) 285-6150 or send resume to: 4055 N. Channel, Portland, OR 97217.

ALL FEES EMPLOYER PAID

Experts in the Environment

Roy F. Weston, Inc.,
West Chester, PA
215-692-3030

WESTON
ENVIRONMENTAL

40 Offices Nationwide • 4 Analytical Laboratories

ROUX

GROUND-WATER CONSULTANTS

- SARA RI/FS
- RCRA Compliance
- Property Transfers
- UST Management
- Pesticide Monitoring
- Remediation

ROUX ASSOCIATES INC.

Offices in Atlanta, Chicago, Danbury, Denver, Hartford, Philadelphia, New York, Princeton, San Francisco.

Call 1 - (800) 322-ROUX



GERAGHTY & MILLER, INC.
Environmental Services

125 East Bethpage Road
Plainview, New York 11803
(516) 249-7600

Offices Located Nationwide

USE THE CONSULTANTS' DIRECTORY

INDEX TO THE ADVERTISERS IN THIS ISSUE

ADVERTISERS	PAGE NO.
*Anderson Laboratories, Inc.	15
Crocker Associates	
*Astro International Corporation	8
Cunningham/Smith	
*J.T. Baker, Inc.	7
Stiegler, Wells & Brunswick, Inc.	
CDS Instruments	15
Powerline, Inc.	
*Entropy Environmentalists, Inc.	42
Pendragon	
International Symposium on CMA/ Northeastern University	42
Millipore Corporation	OB
Mintz & Hoke, Inc.	
Parr Instrument Company	41
FBA Marketing/Communications	
*Perkin-Elmer Corporation	4-5
Keiler Advertising	
Sartorius Instruments	12-13
Dunlap, Schulze Associates	
*TEI Analytical, Inc.	48
DesignMarks Corporation	
Varian	IFC
Lang Associates	

* See ad in Environmental Buyers' Guide.

Advertising Management for the
American Chemical Society Publications

CENTCOM, LTD.

President

James A. Byrne

Executive Vice President

Benjamin W. Jones

Robert L. Voepel, Vice President

Joseph P. Stenza, Production Director

500 Post Road East

P.O. Box 231

Westport, Connecticut 06880

(Area Code 203) 226-7131

Telex No. 643310

Fax No. (203) 454-9939

ADVERTISING SALES MANAGER

Bruce E. Poorman

ADVERTISING PRODUCTION MANAGER

Jane F. Gatenby

SALES REPRESENTATIVES

Philadelphia, PA. . . . CENTCOM, LTD. GSB Building, Suite 405, 1 Belmont Ave., Bala Cynwyd, PA. 19004 (Area Code 215) 667-9666, FAX: (215) 667-9353

New York/New Jersey . . . John F. Raftery, CENTCOM, LTD., Schoolhouse Plaza, 270 King Georges Post Road, Forde, NJ 08863 (Area Code 908) 738-8200

Westport, CT. . . . Edward M. Black, CENTCOM, LTD., 500 Post Road East, P.O. Box 231, Westport, CT 06880 (Area Code 203) 226-7131, FAX: (203) 454-9939

Cleveland, OH. . . . Bruce E. Poorman, CENTCOM, LTD., 325 Front St., Berea, OH 44017 (Area Code 216) 234-1333, FAX: (216) 234-3425

Chicago, IL. . . . Michael J. Pak, CENTCOM, LTD., 540 Frontage Rd., Northfield, Ill. 60093 (Area Code 708) 441-6383, FAX: (708) 441-6382

Houston, TX. . . . Michael J. Pak, CENTCOM, LTD., (Area Code 708) 441-6383

San Francisco, CA. . . . Paul M. Butts, CENTCOM, LTD., Suite 1070, 2672 Bayshore Frontage Road, Mountainview, CA 94043 (Area Code 415) 969-4604

Los Angeles, CA. . . . Paul M. Butts, CENTCOM, LTD., (Area Code 415) 969-4604

Boston, MA. . . . Edward M. Black, CENTCOM, LTD., (Area Code 203) 226-7131

Atlanta, GA. . . . CENTCOM, LTD., (Area Code 216) 234-1333

Denver, CO. . . . Paul M. Butts, CENTCOM, LTD., (Area Code 415) 969-4604

Removal of NO_x and SO₂ from Flue Gas Using Aqueous Emulsions of Yellow Phosphorus and Alkali

David K. Liu, Di-Xin Shen, and Shih-Ger Chang*

Applied Science Division, Lawrence Berkeley Laboratory, University of California, Berkeley, California 94720

■ Aqueous emulsions of yellow phosphorus (P₄) have been shown to be effective in removing NO from flue gas in a simple wet scrubber. Factors influencing NO removal efficiencies include the concentration of P₄ used, the temperature and pH of the aqueous emulsion, and the concentration of O₂ in flue gas. When limestone was added to the phosphorus emulsions, up to 100% removal efficiencies of both NO and SO₂ could be achieved. The NO absorbed can be converted to ammonium, nitrite, and nitrate ions, whereas the P₄ consumed can be recovered as a mixture of hypophosphite, phosphite, and phosphate. The stoichiometric ratios for NO removal by P₄ (i.e., moles of P consumed per mole of NO removed) were measured to be 0.5 when bisulfite was absent and 0.8 when bisulfite was also present in the scrubbing liquor.

Introduction

The combustion of fossil fuels in power plants generates flue gas containing SO₂ and NO_x. These sulfur and nitrogen oxides can be oxidized in the atmosphere to form sulfuric and nitric acids, respectively, resulting in the production of acid rain. Currently, only a small fraction of all power plants in the world has installed flue gas desulfurization (FGD) scrubbers (1). The majority of these scrubbers involves wet limestone (CaCO₃) processes, which utilize aqueous slurries of limestone to neutralize the sulfurous and/or sulfuric acids produced from the dissolution and oxidation of flue gas SO₂ in scrubbing liquors. The resulting solid slurries containing CaSO₃·1/2H₂O and gypsum (CaSO₄·2H₂O) can then be hauled away for disposal.

The wet FGD scrubbers described above are very efficient in the removal of SO₂ from flue gas. However, they are incapable of removing NO because of its low solubility in aqueous solutions. Research efforts to modify existing wet FGD processes for the simultaneous control of SO₂ and NO_x emissions have led to several new approaches to enhance NO_x absorption in scrubbing liquors. These include the oxidation of NO to the more soluble NO₂ using oxidants such as O₃ and ClO₂ (2) and the addition of various iron(II) chelates to the scrubbing liquors to bind and activate NO (2-9). Despite high removal efficiencies of both SO₂ and NO_x, none of these methods has been demonstrated to be cost effective to date.

We report herein a new approach for the simultaneous removal of NO_x and SO₂ from flue gas. This process, which utilizes aqueous emulsions of yellow phosphorus (P₄) and an alkali in a simple wet scrubber, is capable of efficiently scrubbing both NO_x and SO₂ from flue gas and converting

them to potentially valuable fertilizer chemicals including phosphate, nitrate, and sulfate, thus avoiding the need for disposal of solid and/or liquid wastes. A preliminary cost analysis (10, 20) of this phosphorus-based process showed that it may provide a cost-effective alternative to a conventional FGD system used in conjunction with selective catalytic reduction (SCR) for simultaneous SO₂ and NO_x control.

Experimental Section

The removal efficiency of NO from flue gas by aqueous yellow phosphorus emulsions was studied by using a bench-scale gas scrubber. In a typical experiment, 1.0 g of yellow phosphorus (mp = 44.1 °C) was melted in 0.2 L of water at 60 °C in a Pyrex reaction column (50 mm i.d. × 210 mm). The pH of the aqueous emulsion was generally between 3 and 4. Yellow phosphorus globules were dispersed in water upon the bubbling of a gaseous mixture containing ~550 ppm NO, 4% O₂, and the balance N₂ through the fritted disk at the bottom of the reaction column at a flow rate of 0.8-1.0 L min⁻¹. The gas mixture was passed through a condenser (length 390 mm), a gas washing bottle containing 0.2 L of a 0.2 M NaOH solution, a second condenser (length 200 mm), and finally a liquid nitrogen/ethyl acetate cold trap. The NO and NO₂ concentrations in the outlet gas were measured by a Thermolectron Model 14A chemiluminescent NO_x analyzer. The pH of the scrubbing liquor and the NaOH absorber solution after the experiment were generally about 1.5 and 12.5, respectively. The NO- and P₄-derived products in the spent solution in the scrubber as well as the NaOH absorber were determined by ion chromatography (IC). A Dionex 2101i ion chromatograph equipped with a conductivity detector and Dionex AS3 and AS4 anion separation columns was used for such analyses. The eluant used was either Na₂CO₃ (3.5 or 5.3 mM) or a mixture containing 4.0 mM Na₂CO₃, 2.0 mM NaOH, and 0.5% v/v CH₃CN.

The simultaneous removal of NO and SO₂ using yellow phosphorus and limestone (CaCO₃) was studied with a reactor different from the one described above, as shown in Figure 1. This jacketed reactor has a volume of ~1.2 L (110 mm i.d. × 130 mm) and has adaptors for a thermometer, a pH electrode, and an addition funnel. A 0.3% w/w phosphorus/5.0% w/w CaCO₃ slurry with a total volume of ~0.9 L was dispersed by a magnetic stir bar, and the flue gas mixture containing 560 ppm NO, 2900 ppm SO₂, 10% O₂, and balance N₂ was bubbled into the slurry by using a fritted gas disperser. The reaction tem-

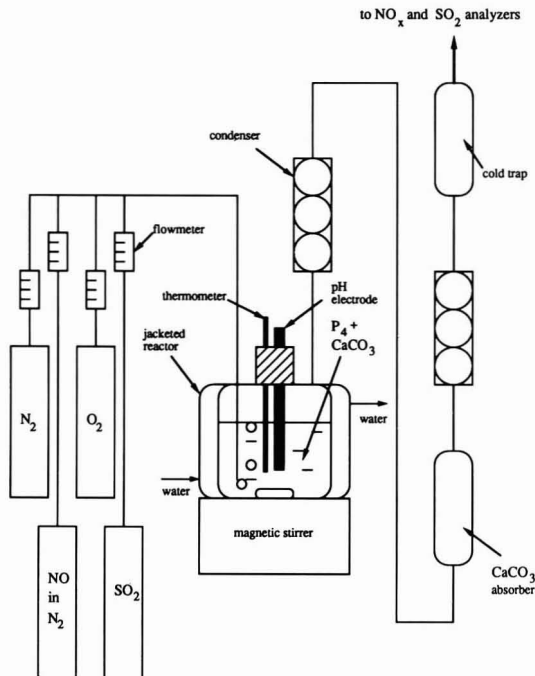


Figure 1. Laboratory-scale apparatus for the simultaneous removal of nitrogen and sulfur oxides from flue gas using yellow phosphorus and limestone.

perature was maintained at 55 °C, whereas the pH of the slurry dropped from 7.5 at the beginning of the experiment to 4.2 after 3 h. The solid and liquid phases in the scrubber and absorber were separated after the experiment by suction filtration. The dried solids were analyzed by laser Raman spectroscopy using a Coherent Innova argon ion laser, a Spex 1403 double spectrometer, and a Spex Datamate computer. The liquid phases were analyzed for various oxy acid salts of N, S, and P by IC as described above. In addition, the analyses of nitrogen-sulfur compounds were carried out using a Dionex AG4 guard column with 12.0 mM Na₂CO₃ eluant or a Dionex AS4 anion separation column with 1.5 mM NaHCO₃ eluant (11). The analysis of ammonium ion was carried out by the phenate method (12).

The stoichiometric ratios for NO removal by phosphorus were measured in a closed reaction system. A 1.0-L round-bottom flask containing 0.25 mg of P₄, 0.1 g of CaCO₃, and 60 mL of deionized H₂O was evacuated and refilled with 1 atm of a gas mixture consisting of 500 ppm NO, 10% O₂, and the balance N₂. The reaction mixture was stirred magnetically at 50 °C until all phosphorus had been consumed (~4 h). The composition of the reaction mixture was analyzed at regular time intervals by IC to determine the concentrations of various NO- and P₄-derived anions. Control experiments were carried out without the added P₄ in order to determine the extent of NO oxidation by O₂ under similar experimental conditions.

Results and Discussion

Removal of NO by Phosphorus Emulsions in a Wet Scrubber. The passage of the simulated flue gas mixture through the scrubbing column containing molten phosphorus creates a fine yellow phosphorus dispersion in water. When O₂ is present in the flue gas, a dense white fume is produced, which could lead to a significant re-

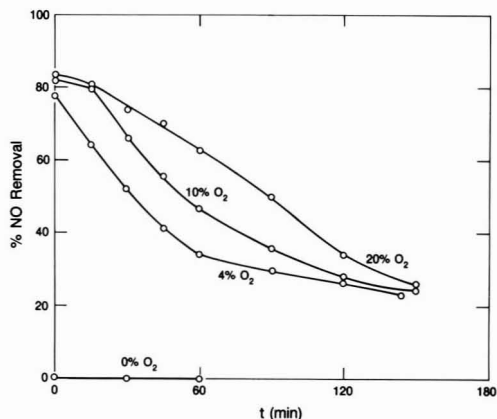


Figure 2. NO removal efficiency of P₄ emulsions as a function of O₂ concentration in flue gas. Reaction conditions were as follows: T = 60 °C; pH(initial) = 3.0; P_{NO} = 550 ppm; 0.5% w/w P₄.

sponse from the chemiluminescent NO_x analyzer if left unchecked. This is believed to result from the chemiluminescence produced by the incomplete oxidation of P₄ (13). This interference decreased substantially when the concentration of O₂ in the flue gas was increased, consistent with the more complete oxidation of P₄ to P₄O₁₀ under those conditions. The use of a NaOH absorber and a liquid nitrogen/ethyl acetate cold trap coupled with monitoring of the scrubbed flue gas in the NO_x mode on the chemiluminescent analyzer (which involves passage of the gas mixture through a stainless steel column at 650 °C half of the time) can totally eliminate such interference. In industrial applications where the scrubbing liquor is recycled, the capture of phosphorus oxide vapor as well as NO₂/N₂O₃/N₂O₄ from NO oxidation (see below) would be much more efficient than our laboratory scrubbing column and the use of an absorber downstream may be unnecessary.

With proper precautions taken to suppress the phosphorus oxide interference with the chemiluminescent NO_x analyzer, the removal of NO from a simulated flue gas stream upon bubbling through an aqueous phosphorus emulsion can be observed. We found that the NO removal efficiency (i.e., percent of flue gas NO removed) is affected by such factors as the O₂ concentration in the flue gas, the amount of P₄ used, and the temperature and pH of the aqueous emulsion.

The influence of the O₂ content of flue gas on NO removal efficiency of a yellow phosphorus emulsion is shown in Figure 2. We found that the presence of O₂ is essential for the removal of NO by yellow phosphorus emulsions, and that the NO removal efficiency of a phosphorus emulsion increases as the O₂ content of the simulated flue gas mixture increases from 0% to 20% by volume. It is therefore apparent that the removal of NO by P₄ proceeds via an oxidative pathway (see section on mechanistic aspects below), as opposed to the reductive mechanisms generally found with metal chelate additives (3-6).

The effect of the amount of added P₄ on NO removal efficiency has been studied, and the results are shown in Figure 3. The initial NO removal efficiencies reached ~90% when 2.0% w/w P₄ was used. When the same experiment was performed using only 0.25% w/w P₄, the initial NO removal efficiency decreased to ~50%. Our results indicate that more added P₄ ensures better mixing with flue gas, resulting in higher P₄ vaporization rates and increased NO removal efficiencies.

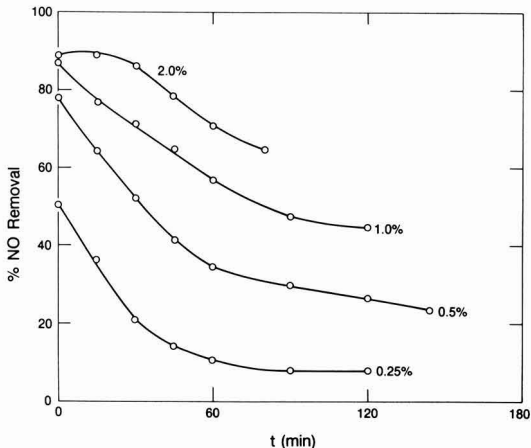


Figure 3. NO removal efficiency of P₄ emulsions as a function of yellow phosphorus added. Reaction conditions were as follows: T = 60 °C; pH(initial) = 3.0; P_{NO} = 550 ppm; P_{O₂} = 4%.

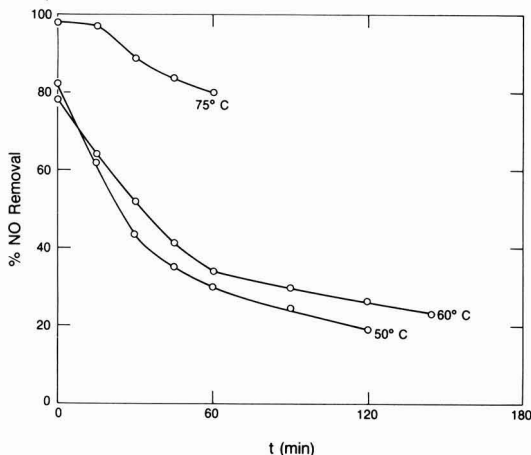


Figure 4. NO removal efficiency of P₄ emulsions as a function of temperature of the scrubbing liquor. Reaction conditions were as follows: pH(initial) = 3.0; P_{NO} = 550 ppm; P_{O₂} = 4%; 0.5% w/w P₄.

The removal of NO by yellow phosphorus is also dependent upon the temperature of the emulsion, as shown in Figure 4. The initial NO removal efficiencies were found to be higher at higher temperatures. For instance, the initial NO removal percentage was increased from 78% to 98% when the temperature of the emulsion was raised from 50 to 75 °C. The increase in NO removal efficiencies at higher emulsion temperatures can be attributed to the increase in P₄ vapor concentration in the absorber under such conditions.

The influence of pH on the effectiveness for NO removal of a yellow phosphorus emulsion has been examined for the pH range of 3.0–9.0, and the results are shown in Figure 5. Whereas the initial NO removal efficiency appears to be higher at lower pH, the efficiency decreases much more sharply for the lower pH emulsion until after ~2 h, the original higher pH emulsion would absorb more NO. On the basis of these results, it may be concluded the general decline of NO removal efficiency at longer reaction times shown in Figures 2–5 is due to the increasing acidity, which favors the formation of HNO₂ and hence NO and NO₂ (see eqs 6 and 8 below) from the dissolved

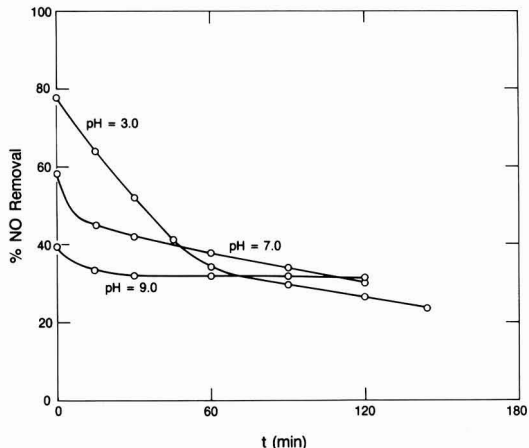


Figure 5. NO removal efficiency of P₄ emulsions as a function of the initial pH of the scrubbing liquor. Reaction conditions were as follows: T = 60 °C; P_{NO} = 550 ppm; P_{O₂} = 4%; 0.5% w/w P₄.

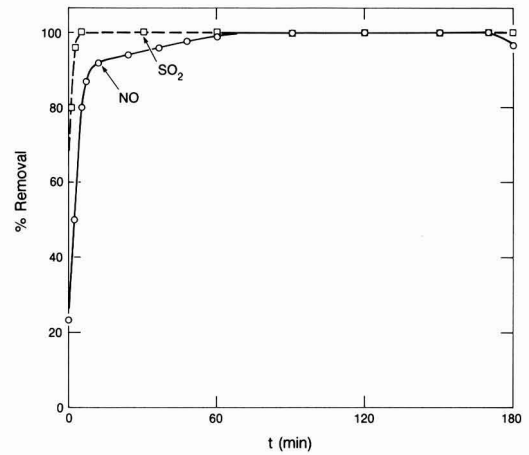


Figure 6. Simultaneous NO and SO₂ removal from flue gas by using an aqueous P₄ emulsion also containing CaCO₃. Reaction conditions were as follows: T = 55 °C; pH(initial) = 7.5; P_{NO} = 560 ppm; P_{SO₂} = 2900 ppm; P_{O₂} = 10%; 0.3% w/w P₄; 5.0% w/w CaCO₃.

Table I. Removal Efficiencies of NO and P/NO Stoichiometric Ratios as a Function of NO Concentration^a

NO, ppm	P ₄ added, g	max % NO removal	av % NO removal	P/NO ratio ^b
60	0.31	100	100	4.5
430	0.40	100	76	2.6
720	0.56	93	84	2.7
1700	0.32	61	40	1.2
2000	0.60	47	29	1.5

^aThese experiments were carried out at 50 °C with 11–12% O₂ in the simulated flue gas. The reaction times were 2 h, and the initial and final pH values were ~7.0 and ~4.0, respectively.

^bThe P/NO ratios were determined by IC according to eq 1.

NO₂⁻ in the scrubbing liquor. However, high NO removal efficiency may be sustained for a long period of time with the addition of an alkali to the scrubbing liquor (Figure 6).

To explore the possible application of this P₄-based approach to the treatment of NO emission from other sources, such as smelters, nitric acid plants, and municipal

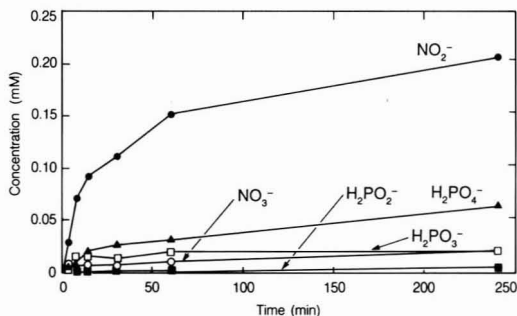


Figure 7. Concentrations of NO- and P₄-derived anions in a closed P₄/NO reaction system as a function of time. Reaction conditions were as follows: *T* = 50 °C; *P*_{NO} = 500 ppm; *P*_{O₂} = 10%; 0.04% w/w P₄; 0.17% w/w CaCO₃.

incinerators, we have studied the NO removal efficiency of phosphorus emulsions at various concentrations of NO. The reaction conditions and results of such experiments are listed in Table I. Our results indicate that in addition to flue gas clean-up, aqueous yellow phosphorus emulsions can also be employed for the control of low-level NO emissions (<100 ppm) such as those from natural gas boilers and high-level NO emissions (>2000 ppm) such as those from nitric acid plants.

Simultaneous NO/SO₂ Removal by the P₄/CaCO₃ System. We found that yellow phosphorus emulsions do not react with HSO₃⁻ at any appreciable rate under the reaction conditions used in our NO removal experiments. The simultaneous removal of NO_x and SO₂ from a simulated flue gas mixture can be achieved by the inclusion of an alkali such as limestone in the scrubber. Also, limestone can be used in the place of NaOH in the absorber downstream. For instance, when 0.95 L of a 0.3% w/w P₄ and 5.0% w/w CaCO₃ slurry at 55 °C and pH 7.5 was used as the scrubbing liquor and 0.2 L of a 5.0% w/w CaCO₃ suspension was used in the absorber, ~95% of the 560 ppm NO and ~100% of the 2900 ppm SO₂ introduced can be removed for at least 3 h (Figure 6).

Determination of Reaction Products and P/NO Stoichiometric Ratios. The contents of the spent solutions in the scrubbing column and the NaOH absorber after NO absorption experiments were analyzed by IC. It was determined that all the NO removed from the simulated flue gas can be recovered as a mixture of nitrite (NO₂⁻) and nitrate (NO₃⁻), whereas all the yellow phosphorus consumed was converted to a combination of hypophosphite (H₂PO₂⁻), phosphite (H₂PO₃⁻), and phosphate (H₂PO₄⁻). The mass balance of N and P was studied in a closed reaction system, and the effectiveness of NO removal of a phosphorus emulsion can be expressed as a P/NO ratio where

$$P/NO = \frac{[H_2PO_2^-] + [H_2PO_3^-] + [H_2PO_4^-]}{[NO_2^-] + [NO_3^-]} \quad (1)$$

The results of such a typical measurement (see Experimental Section for detailed conditions) involving 0.25 mg of P₄ and 500 ppm NO are shown in Figures 7 and 8. In this experiment, ~9 times more NO₂⁻ than NO₃⁻ was found, and most of the P₄ was recovered as H₂PO₄⁻, along with some H₂PO₃⁻ and H₂PO₂⁻ (Figure 7). A P/NO ratio of 0.5 ± 0.1 can be calculated from eq 1, meaning that 1 mol of P₄ can remove 8 mol of NO. Control experiments without yellow phosphorus indicated that NO removal via oxidation by O₂ to form NO₂ accounted for <10% of the total NO removed when yellow phosphorus was present.

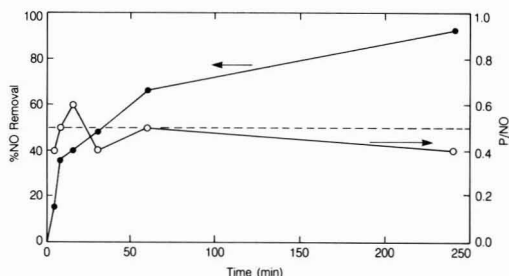


Figure 8. Percentage NO removal and P/NO ratio in a closed P₄/NO reaction system as a function of time. Reaction conditions were as follows: *T* = 50 °C; *P*_{NO} = 500 ppm; *P*_{O₂} = 10%; 0.04% w/w P₄; 0.17% w/w CaCO₃.

The effect of flue gas SO₂ on the P/NO ratio has been studied. When 0.92 mM HSO₃⁻ (corresponding to ~3000 ppm flue gas SO₂) was added to the above closed reaction flask containing 0.25 mg of P₄ and 500 ppm NO, a P/NO ratio of 0.8 was obtained, compared to 0.5 in the absence of HSO₃⁻. Also, ~75% of the HSO₃⁻ was oxidized to SO₄²⁻ during the course of the reaction.

Other factors influencing the P/NO ratio were found to be the same as those affecting NO removal efficiency, i.e., O₂ concentration in the flue gas, concentration of P₄ used, and temperature of the scrubbing liquor. We have studied each of these factors qualitatively under flow conditions identical with those used to study NO removal efficiencies. In these experiments, the unspent P₄ was recovered from the scrubber and weighed while the amount of NO removed was determined from the flue gas NO concentration, average percent NO removal and the reaction time. These experiments were only qualitative because of the difficulty associated with recovering all the unspent P₄ and consequently the P/NO ratios found were generally much higher than those from closed experiments using IC to determine P/NO. The results showed that low P/NO ratios were obtained at high O₂ concentration, low P₄ concentration, and low emulsion temperature. Under such conditions, O₂ is present in excess of P₄ and complete oxidation and utilization of P₄ can occur, resulting in lower P/NO ratios. It is interesting to note that the experimental parameters we have examined, i.e., O₂ and P₄ concentrations and emulsion temperature, affect the P/NO ratio and NO removal efficiency in exactly opposite manners. Therefore, actual reaction conditions can be chosen depending on whether high NO removal efficiency or low P/NO ratio is desired. In reality, the scrubber operating conditions are likely to be chosen as a compromise between reasonably high NO removal efficiencies and reasonably low P/NO ratios.

An interesting finding concerns the distribution of NO- and P₄-derived products as a function of the relative amounts of NO and P₄ present in the closed reaction systems described above. If an excess of P₄ is used, NO₃⁻ is the primary NO-derived product. For example, when 3.7 mg of P₄ and 500 ppm NO ([P]:[NO] = 8) were used in the above closed experiment, the NO₃⁻/NO₂⁻ ratio obtained was ~5:1. However, if the amount of P₄ used is roughly equal to or less than the amount of NO present, NO₂⁻ becomes the dominant product. As shown in Figure 7, when 0.25 mg of P₄ and 500 ppm NO ([P]:[NO] = 0.5) were used, the NO₃⁻/NO₂⁻ ratio became ~1:9. Interestingly, the trend H₂PO₄⁻ > H₂PO₃⁻ > H₂PO₂⁻ remained the same, despite the difference in the amount of P₄ used.

The reaction products from the NO/SO₂ removal experiment using P₄/CaCO₃ (Figure 6) were also examined.

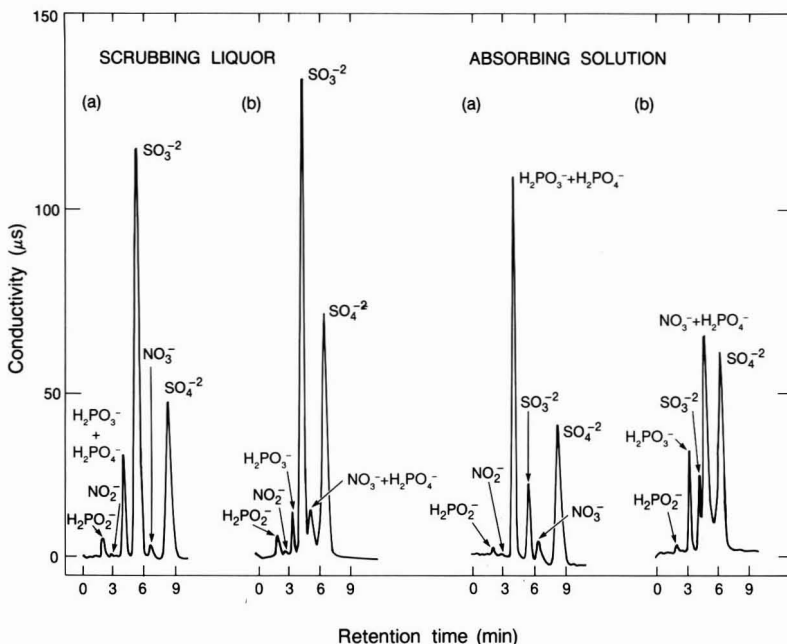
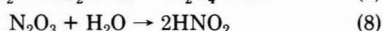
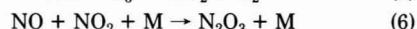
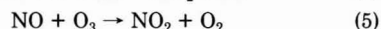
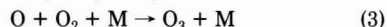
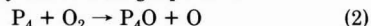


Figure 9. Ion chromatograms of 25X diluted spent scrubber and absorber solutions from the simultaneous NO and SO₂ removal experiment with P₄/CaCO₃ using (a) 5.3 mM Na₂CO₃ eluant and (b) 4.0 mM Na₂CO₃/2.0 mM NaOH/0.5% v/v CH₃CN eluant.

The solid collected from the scrubber after the reaction was analyzed by laser Raman spectroscopy and was shown to contain CaSO₄·2H₂O, in addition to unused CaCO₃ and yellow phosphorus. In the absorber downstream, only unused CaCO₃ was detected. No CaSO₃·1/2H₂O precipitate was detected in the solid collected from either the scrubber or the absorber. The liquid phase in both the scrubber and the absorber were analyzed by IC, and the results are shown in Figure 9. It was found that both the scrubbing liquor and the absorbing solution contain NO₂⁻, NO₃⁻, HSO₃⁻, SO₄²⁻, H₂PO₂⁻, H₂PO₃⁻, and H₂PO₄⁻. Since the amount of NO₂⁻ and NO₃⁻ recovered could only account for ~50% of the NO absorbed and a substantial amount of HSO₃⁻ was present in the scrubbing liquor, a search for nitrogen-sulfur compounds was conducted. Indeed, we found that ~40% of the NO absorbed could be accounted for by the formation of the nitrogen-sulfur compounds hydroxyimidodisulfate (HIDS) and imidodisulfate (IDS) in the slightly acidic (pH ~4) scrubbing liquor. We also found that both HIDS and IDS could subsequently be hydrolyzed to NH₄⁺ when the pH of the scrubbing liquor was decreased to 1.5 or below. The formation of nitrogen-sulfur compounds via the reaction of NO₂⁻ and HSO₃⁻ in scrubbing liquor and their hydrolysis reactions have been well studied (14). Therefore, the use of yellow phosphorus emulsions for combined NO_x and SO₂ removal results in the conversion of undesirable NO to NH₄⁺, NO₃⁻, and NO₂⁻, all of which are desirable chemicals for the manufacture of fertilizers (15).

Mechanistic Aspects of the NO Absorption Reaction. The mechanism of NO removal by yellow phosphorus is presently under investigation. It appears that the reaction between P₄ and O₂ can take place in both the aqueous phase and the gas phase. The reaction in the aqueous phase would involve the oxidation of P₄ by O₂, which occurs on the surface of the phosphorus globules. Therefore, parameters that control the dispersion of molten phosphorus in water such as liquid to gas ratio,

reactor design, temperature, and additives that change the dielectric constant of the aqueous phase would affect the P₄ oxidation and hence the NO removal rate. In the gaseous phase, O₂ would react with P₄ vapor evolved from the aqueous emulsion of yellow phosphorus at elevated temperature. Under thermal equilibrium conditions, the concentration of P₄ is ~420 ppm at 55 °C and 1 atm (16). Therefore, the concentration of P₄ at the temperature of wet FGD scrubbing liquors is approximately the same as that of NO (~500 ppm) in flue gas. The reaction of O₂ and P₄ results in the production of O and O₃ (eqs 2 and 3). Given that the reaction rates for P₄ + O₂ and P₄ + O are about the same order of magnitude (17) and the concentration of O₂ in flue gas (~5%) is substantially higher than that of O, it is likely that most of the P₄ is oxidized by O₂ (18). On the other hand, the oxidation of NO to NO₂ (eqs 4 and 5) may be effected by either O or O₃. The NO₂ thus produced can either react with another molecule of NO to form N₂O₃ (eq 6) or dimerize to form N₂O₄ (eq 7). Both N₂O₃ and N₂O₄ are much more soluble in water compared to NO, and their dissolution in water leads to the formation of nitrous and nitric acids (eqs 8 and 9). Therefore, the removal of NO by P₄ in the gas phase may be summarized by the following equations:



where M is a another molecule, which remains unchanged after the reaction. The proposed mechanism is consistent with the finding that O₂ is required for the NO absorption

reaction and can account for the findings that NO removal efficiency is higher with increased O₂ concentration in flue gas, larger amount of P₄ used, and increased temperature of the scrubbing liquor. Also, both NO₂⁻ and NO₃⁻ production in the spent scrubbing liquor and absorbing solution can be explained by this reaction scheme. The mechanism for the oxidation of phosphorus to various phosphorus oxy acids appears to be rather complicated, and intermediates such as PO, PO₂, P₂O, and P₄O are believed to be present in the oxidation of P₄ by O₂ (18, 19). The kinetic and mechanistic studies of phosphorus oxidation under our reaction conditions are currently under way.

Conclusions

We have discovered that both NO_x and SO₂ in flue gas can be removed by use of an aqueous emulsion containing yellow phosphorus and an alkali such as limestone in a simple wet scrubber. The factors affecting NO removal efficiency of this system include the concentration of P₄ used, the temperature and the pH of the aqueous emulsion, and the O₂ concentration in the flue gas. Furthermore, we found that emissions containing NO at either very low (<100 ppm) and very high (>2000 ppm) levels can also be treated efficiently with yellow phosphorus emulsions. Finally, when CaCO₃ was used in conjunction with yellow phosphorus in the wet scrubber, up to 100% NO and SO₂ removal efficiencies can be accomplished.

The reaction products in the removal of NO by phosphorus emulsions were determined to consist of NO₂⁻, NO₃⁻, H₂PO₂⁻, H₂PO₃⁻, and H₂PO₄⁻. Therefore, the spent scrubbing liquor would be useful in the formulation of fertilizers. The stoichiometric ratios for NO removal by phosphorus were measured by closed experiments to be as low as 0.5 when HSO₃⁻ is absent and 0.8 when HSO₃⁻ is also present in the scrubbing liquor. Based on the facts that no expensive equipment or chemical engineering processes are involved, and that the spent scrubber liquor contains valuable fertilizer chemicals and thus does not require waste disposal, this yellow phosphorus approach presents a potentially cost-effective method for the simultaneous removal of NO_x and SO₂ from flue gas (10).

Literature Cited

- (1) Rubin, E. S.; et al. *Environ. Sci. Technol.* **1986**, *20*, 960, and references therein.
- (2) Yaverbaum, L. H. *Nitrogen Oxides Control and Removal*; Noyes Data Corp.: Park Ridge, NJ, 1979.
- (3) Chang, S. G. In *Fossil Fuels Utilization: Environmental Concerns*; Markuszewski, R., Blaustein, B. D., Eds.; ACS Symposium Series 319; American Chemical Society: Washington, DC, 1986; pp 159-75, and references therein.
- (4) Liu, D. K.; Frick, L. P.; Chang, S. G. *Environ. Sci. Technol.* **1988**, *22*, 219.
- (5) Liu, D. K.; Chang, S. G. *Environ. Sci. Technol.* **1988**, *22*, 1196.
- (6) Chang, S. G.; Littlejohn, D.; Liu, D. K. *Ind. Eng. Chem. Res.* **1988**, *27*, 2156.
- (7) Zhuang, Y.; Deng, Y. *Acta Sci. Circumstantiae* **1985**, *5*, 347.
- (8) Harkness, J. B. L.; Doctor, R. D. Presented at the AIChE Spring National Meeting, New Orleans, LA, April 1986; Paper 2e.
- (9) Bedell, S. A.; Tsai, S. S.; Grinstead, R. R. *Ind. Eng. Chem. Res.* **1988**, *27*, 2092.
- (10) Chang, S. G.; Liu, D. K. *Nature* **1990**, *343*, 151.
- (11) Littlejohn, D.; Chang, S. G. *Anal. Chem.* **1986**, *58*, 158.
- (12) Greenberg, A. E., et al., Eds. *Standard Methods for the Examination of Water and Wastewater*, 16th ed.; APHA: Washington, DC, 1985; pp 382-3.
- (13) Van Wazer, J. R. *Phosphorus and Its Compounds*; Interscience Publishers: New York, 1958; Vol. I, pp 109-12.
- (14) Chang, S. G.; Littlejohn, D.; Lin, N. H. In *Flue Gas Desulfurization*; Hudson, J. L., Rochelle, G. T., Eds.; ACS Symposium Series 188; American Chemical Society: Washington, DC, 1982; pp 127-52.
- (15) Huffman, E. O. In *Kirk-Othmer Encyclopedia of Chemical Technology*, 3rd ed.; Bushey, G. J., et al., Eds.; John Wiley & Sons: New York, 1980; Vol. 10, pp 31-125.
- (16) Bailer, J. C., Jr., et al., Eds. *Comprehensive Inorganic Chemistry*; Pergamon Press: Oxford, 1973; Vol. 2, p 398.
- (17) Davies, P. B.; Thrush, B. A. *Proc. Roy. Soc. A* **1968**, *302*, 243.
- (18) Cordes, H.; Witschel, W. *Z. Phys. Chem.* **1965**, *46*, 35.
- (19) Andrews, L.; Withnall, R. *J. Am. Chem. Soc.* **1988**, *110*, 5605.
- (20) Lee, G. C.; Shen, D. X.; Littlejohn, D.; Chang, S. G. Presented at the 1990 SO₂ Control Symposium, sponsored by EPRI and U.S. EPA, New Orleans, LA, May 8-11, 1990; Session 6B.

Received for review January 25, 1990. Revised manuscript received August 27, 1990. Accepted August 29, 1990. This work was supported by the Assistant Secretary for Fossil Energy, U.S. Department of Energy under Contract DE-AC03-76SF00098 through the Pittsburgh Energy Technology Center, Pittsburgh, PA.

Analysis of Alkyl Nitrates and Selected Halocarbons in the Ambient Atmosphere Using a Charcoal Preconcentration Technique

Elliot Atlas*[†] and Sue Schauffler[†]

Department of Oceanography, Texas A&M University, College Station, Texas 77843

■ A method has been developed to measure $\geq C_3$ alkyl nitrates and C_1 - C_2 halocarbons, such as perchloroethylene and bromoform, in ambient air. The method preconcentrates analytes on a 5-mg charcoal trap from multiliter volumes of air. Analytes are desorbed from the charcoal with a small volume of solvent and are analyzed by high-resolution gas chromatography with electron capture detection. Laboratory and field tests have been performed to evaluate method precision, analyte breakthrough, and compound recovery from the charcoal. Tests verified that the sampling/analytical system is free from artifact formation under clean to moderately polluted conditions, but further tests are required for areas of high concentrations of hydrocarbons, NO_x , and oxidants. The method allows measurement of halocarbons and $\geq C_3$ alkyl nitrates at concentrations in the pptv range.

Introduction

Hydrocarbon and nitrogen oxide (NO_x) emissions are known to have a significant impact on the chemistry of urban atmospheres (1, 2). Photochemical reactions of hydrocarbons and NO_x contribute to the formation of ozone, peroxyacetyl nitrate (PAN), and other reactive chemical species in the urban atmosphere. Transport of reactive hydrocarbons and NO_x combined with emission of natural hydrocarbons in rural and remote areas also can produce a significant impact on the chemistry of the clean troposphere (3-7). To fully understand the chemical interactions and transformations of carbon species and NO_x , it is necessary to measure the full range of reactants and products. One of the potentially important products that form from the interaction of hydrocarbons and NO_x are alkyl nitrates ($RONO_2$) (8, 9).

Alkyl nitrates are formed in the atmosphere during the OH-radical-initiated oxidation of alkanes in the presence of NO_x ($NO + NO_2$). The mechanism proposed for the formation of alkyl nitrates involves the reaction of an alkylperoxy radical with NO to form an alkyl nitrate (10, 11). The reaction mechanism favors the formation of secondary alkyl nitrate species over primary and tertiary alkyl nitrates of a given carbon chain length. Also, the yield of alkyl nitrates from the oxidation of alkanes increases with carbon chain length. For typical atmospheric conditions, the yield of alkyl nitrates increases from <1.4% for ethane to 33% for octane (12). More complex multifunctional nitrates also may form during the oxidation of unsaturated hydrocarbons (13-16).

Even though alkyl nitrates have been observed in smog chamber studies (17), there have been few actual measurements of these compounds in the ambient atmosphere (18) and different techniques have been utilized. A few reports identified alkyl nitrates in air samples from different locations (19-21), but only recently have there been more systematic studies of alkyl nitrates in the atmosphere. Buhr et al. (22) reported the concentrations of alkyl nitrates in rural Pennsylvania using whole air samples and

packed column gas chromatography with electron capture detection. Flocke et al. (23) used a cryogenic concentration technique to measure alkyl nitrates in ambient air in Germany. In their technique, samples are separated by capillary gas chromatography; selective detection of nitrogen compounds is obtained with a chemiluminescence detector. Techniques to measure different organic nitrates in the workplace atmosphere also have been reported (24-26). The technique we describe here has been successfully applied in different environments, ranging from the Arctic to the tropics, and has been shown to be useful, with some limitations, to measure $\geq C_3$ alkyl nitrates and selected halocarbons at concentrations in the pptv to sub-pptv range (27, 28). Our procedure is based on preconcentration of alkyl nitrates on charcoal, solvent extraction, and quantitation by capillary gas chromatography with electron capture detection. Also, the method can be used to measure several halocarbons, such as perchloroethylene and bromoform, in ambient air, but this report will emphasize the measurement of alkyl nitrates.

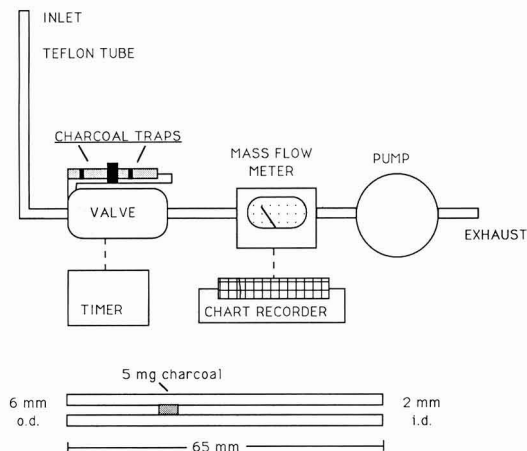
Experimental Section

Sampling and Preconcentration. The charcoal adsorbent tubes contain a nominal 5 mg of charcoal in a glass tube (65 mm \times 6 mm o.d. \times 2 mm i.d.). The charcoal bed itself is typically 2-3 mm long. For these studies, the tubes were obtained from Tekmar Co. (Cincinnati, OH). The normal configuration for air sampling is as follows. Two charcoal tubes are connected in series by a Cajon Ultra-Torr (or equivalent) connector. For automatic sample collection, the tubes are connected to an electrically actuated Valco eight-port valve (Valco Inc., Houston, TX). The flow path of the valve isolates and seals the ends of each set of charcoal tubes when they are not in the sample line. This configuration prevents contamination of the adsorbent tubes before and after the sample collection period. The valve is actuated at preselected times with an automatic timer. A Teflon-coated diaphragm pump (KNF Neuberger Inc., Princeton, NJ) or a metal bellows pump (Metal Bellows Co., Sharon, MA) draws air through the charcoal tubes and through a mass-flow meter. The output of the mass-flow meter is recorded on a strip-chart recorder to obtain an integrated flow measurement during the sample period. Typical flow rates through the system described here are in the range of 125-250 mL/min, depending on the pump and length and diameter of tubing used to connect the system. For samples in the clean troposphere, sample sizes ranging from 1 to 100 L have been used. A schematic of the sampling system is shown in Figure 1.

Extraction. Prior to sampling, adsorbent tubes are precleaned with methanol, followed by repeated rinsing with benzene. No heat treatment of the charcoal is necessary. Adsorbent tubes are stored with a small volume of benzene covering the charcoal bed. Immediately after sampling, the adsorbent tubes are extracted with 30-50 μ L of redistilled benzene. It has been found that most commercial brands of high-purity benzene contain traces of trichloroethylene and tetrachloroethylene, which can be removed by distillation. Best results are obtained when

[†]Current address: National Center for Atmospheric Research, P.O. Box 3000, Boulder, CO 80307.

SAMPLING SYSTEM



CHARCOAL TRAP

Figure 1. Schematic of air sampling system and charcoal trap.

the still is protected from contamination by room air with a charcoal or other filter. Prior to extraction of the sample, an internal standard containing 30 ng of 1,2-dichlorobenzene is added to the charcoal bed in 3 μ L of a benzene solution. Next, 10–15 μ L of benzene is used to extract the charcoal bed. This is accomplished by placing a rubber or Teflon bulb at the end of the glass sample tube and gently squeezing and releasing the bulb to move the solvent plug back and forth a minimum of 20 times through the charcoal bed. The solvent is removed by using a 10- μ L syringe and the extraction is repeated a total of three to five times. We have found it convenient to store the extract in glass capillary tubes, which can be heat sealed if

the sample is not to be analyzed immediately. Before the capillary tube is sealed, it is necessary to freeze the solvent. We have found that failure to freeze the solvent prior to sealing the tube may add artifacts to the sample extract.

Gas Chromatography/Quantitation. Sample extracts are analyzed by high-resolution, fused-silica capillary gas chromatography with electron capture detection. A Varian 3500 capillary gas chromatograph with splitless injector and ^{63}Ni electron capture detector was used for most analyses. Injector temperature was 125 $^{\circ}\text{C}$ and the detector was 275–325 $^{\circ}\text{C}$. The oven temperature program was 40 $^{\circ}\text{C}$ (3 min), 3 $^{\circ}\text{C}/\text{min}$ to 120 $^{\circ}\text{C}$, and then 10 $^{\circ}\text{C}/\text{min}$ to 175 (or 225) $^{\circ}\text{C}$. A 50-m, 310- μm -i.d., 1- μm film thickness nonpolar column (Hewlett-Packard, HP-1) was used for separation. Helium was used for carrier gas at 16 psi (~ 30 cm/s), and nitrogen was the detector make-up gas at 20 mL/min. These conditions allowed separation of alkyl nitrates from C_3 to C_7 . A chromatogram of an air sample extract from the Canadian Arctic is shown in Figure 2.

Quantitative standards of alkyl nitrates were prepared from compounds synthesized in the laboratory (29) or from compounds commercially available. Standards for all possible C_3 – C_7 alkyl nitrates have not yet been prepared, but qualitative standards of a number of nitrates were synthesized in a laboratory test chamber described below. Analyte quantitation in the samples was achieved by using an internal standard method. Chromatographic data were stored and analyzed by a Varian DS654 data system, which allowed interactive, graphical reintegration and baseline modifications.

Laboratory Test Flow System. The effect of alkanes, nitrogen oxides, and other reactive compounds on the analysis of alkyl nitrates was tested in a flow system shown in Figure 3. The system was constructed of glass and stainless steel. For our experiments, we added potentially reactive compounds to an air stream of either purified cylinder air or outside ambient air. Total flow rate of air

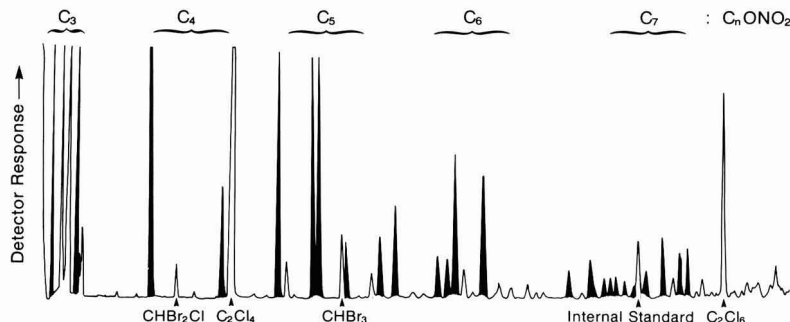


Figure 2. High-resolution electron capture gas chromatogram of air sample from the Canadian Arctic. Note that most peaks with electron capture response are alkyl nitrates. Chromatographic conditions are given in the text.

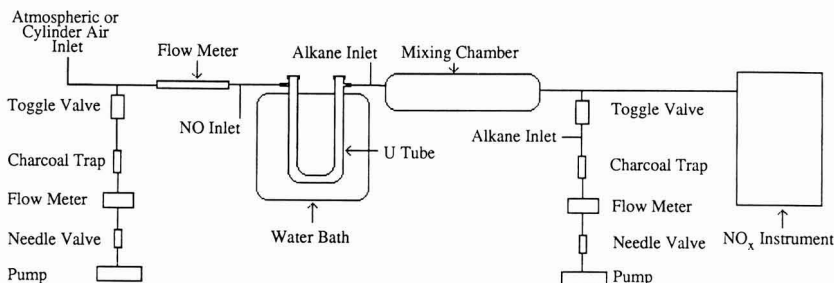


Figure 3. Schematic of laboratory system for testing artifact formation.

Table I. Percent Recovery of Alkyl Nitrates and Selected Halocarbons from Microcharcoal Adsorbent Tubes

							av	±SD
amt added, pg	200	400	600	1000	600	600		
<i>n</i>	3	3	3	2	1	1		
nitrates								
isopropyl				83	107	96	95	12
<i>n</i> -propyl	92	94	95	86	97	82	91	6
2-butyl	110	116	114	98	105	102	108	7
<i>n</i> -butyl	89	91	94	87	99	88	91	5
3-pentyl	105	104	108	97	107	98	103	5
2-pentyl	104	101	104	96	105	100	102	3
<i>n</i> -pentyl	86	88	90	84	98	84	88	5
halocarbons								
CHBr ₂ Cl	98	97	98	91	102	107	99	5
C ₂ H ₄ Br ₂	88	90	92	80	101	64	86	13
CHBr ₃	101	99	100	92	104	105	100	5
C ₂ Cl ₄				97	106		102	6
C ₂ Cl ₆				97	106		102	6
1,1,1,2-Cl ₄ C ₂ H ₂					103	110	107	5
1,1,2,2-Cl ₄ C ₂ H ₂	80	81	82		99	85	85	8
C ₂ HCl ₅					99	31	65	48
C ₂ Cl ₆					101	91	96	7

through the system was ~2 L/min. Hydrocarbons were added to the system from a 1000 ppm gas mixture of C₁-C₆ alkanes (Scott Specialty Gases, Plumsteadville, PA) or from pure liquid alkane (C₅ and C₆) in glass diffusion tubes. NO was added from a standard mixture of 9.33 ppm NO in N₂ (Scott Specialty Gases). The source of NO₂ was a permeation tube with a release rate of 1715 ng/min (VICI Metronics, Santa Clara, CA). The concentrations of NO and NO₂ were measured with a ThermoElectron NO_x detector (Waltham, MA). Hydrogen peroxide was added to the system from an aliquot of 37% H₂O₂ placed in a test tube in the flow stream. The concentration of H₂O₂ in the gas phase was not measured. Gas flows were controlled by needle valves and were monitored with mass-flow meters.

Recovery Experiments. To evaluate recovery of analytes from charcoal traps, 1-4 μL solutions of alkyl nitrates and halocarbons dissolved in benzene were added to a flowing gas stream. The compounds were allowed to evaporate at room temperature, and the gas stream was passed through a charcoal cartridge to collect the volatilized compounds. Charcoal cartridges were extracted and analyzed as previously described. Total amounts of analyte spiked into the gas stream ranged from 200 to 1000 pg per compound. The presence of microliter amounts of solvent in the gas stream did not appear to affect the collection of analytes by the charcoal.

Results and Discussion

Recovery Tests. Recovery of alkyl nitrates and selected halocarbons from charcoal tubes is given in Table I. Several sets of experiments were conducted using different amounts of analyte and different charcoal tubes. Average recovery of all nitrates was 97%, with a range from 88 to 108%. Similarly, most halocarbons tested showed excellent recovery from the charcoal tubes. Ethylene dibromide had somewhat lower and more variable recovery compared to other organobromine compounds. Pentachloroethane also had anomalously low and variable recovery compared to other chloroethanes. The level of analyte spike used in our tests was comparable to amounts found during "normal" sampling. A 600-pg spike corresponds to atmospheric concentrations of ~3-6 pptv (depending on the compound) in a 20-L sample.

The recovery of analytes reported here is based on the recovery of analyte relative to the internal standard added

prior to extraction. Because of the small volumes of solvent used in the extraction and the potential for errors due to volume measurement, use of the internal standard method is required to obtain the most consistent results. The excellent and nearly uniform recovery of a range of analytes at low concentrations suggests that the internal standard used here (1,2-dichlorobenzene) serves as an appropriate monitor of compound desorption from the charcoal. Absolute recovery of analyte and internal standard depends primarily on the amount of solvent and number of extractions of the charcoal bed. Desorption of the charcoal trap with 3 × 10 μL of benzene yields typical (absolute) recoveries of from 70 to 85%. Increasing the total extraction to 5 × 10 μL improves absolute recovery to 80-95%. However, marginal improvements in recovery with increasing volumes of solvent will dilute the concentration of analytes in the final extract and decrease the overall analytical sensitivity.

Our normal procedure is to extract the charcoal trap as soon as possible after sampling. However, circumstances may occur that make it necessary to store the traps prior to extraction. A set of experiments was conducted to determine the effect of storage on recovery of analytes. A series of sample tubes was spiked with alkyl nitrates and halocarbons as described above and the tubes were sealed with Swagelok fittings containing Viton O-rings. Sample tubes were covered with aluminum foil and stored either in a freezer or at room temperature. The results of these experiments are given in Table II. These experiments indicate loss of 30-40% of most analytes over a 48-h period at room temperature. In these experiments, ethylene dibromide and pentachloroethane showed greater loss than the other test compounds. With the exception of these latter compounds, it appears that alkyl nitrates and halocarbons collected on charcoal traps may be stored at room temperature for approximately 6 h with no noticeable effects. Freezing the sample tube improved recovery of analytes. Though some initial recoveries seemed low, the samples stored frozen remained reasonably intact for at least 1 month.

Breakthrough/Trapping Studies. Factors that can affect the retention of organic compounds on the charcoal trap include temperature, humidity, flow rate, sample volume, other organics in the air, and the physical condition of the charcoal in the trap (30, 31). Since all ambient sampling utilizes two traps in series, we evaluated break-

Table II. Effect of Storage Time and Temperature on Percent Recovery of Alkyl Nitrates and Selected Halocarbons from Microcharcoal Adsorbent Tubes

storage time, h <i>n</i>	room temp				frozen					
	2	6	26	48	48	144	288	720		
	2	2	1	2	2	2	1	3		
nitrates										
isopropyl	91	103	83	63	73	77	89	85		
<i>n</i> -propyl	91	100	77	65	71	86	91	89		
2-butyl	104	110	86	73	81	94	93	102		
<i>n</i> -butyl	96	105	30	69	77	93	86	93		
3-pentyl	102	104	82	72	79	95	94	99		
2-pentyl	101	102	81	73	80	96	93	105		
<i>n</i> -pentyl	91	90	75	70	70	91	84	93		
halocarbons										
CHBr ₂ Cl	103	111	88	75	82	95	96	108		
C ₂ H ₄ Br ₂	72	73	48	30	61	78	67	82		
CHBr ₃	105	108	88	74	80	98	93	105		
C ₂ Cl ₄					123					
1,1,1,2-Cl ₄ C ₂ H ₂	108	108	85	73	83	96	95			
1,1,2,2-Cl ₄ C ₂ H ₂	88	90	73	47	70	88	77	85		
C ₂ HCl ₅	14	9	1	1	26	25	13	24		
C ₂ Cl ₆	93	84	69	69	77	92	80	99		

through of test compounds through the first trap under a variety of actual sampling conditions and for a large number of different traps. In Table III we compare the amount of analyte collected on the first trap to the total amount of analyte collected in the first and second traps. Despite the small quantity of charcoal used in the trap, the retention of alkyl nitrates and halocarbons from multiliter volumes of air was generally excellent. Breakthrough of isopropyl nitrate was observed in samples collected in St. Petersburg, FL, and in many samples collected in the Shenandoah Mountains. At both these sites, ambient humidity was high and/or air temperatures were also relatively high (~28–30 °C). Other alkyl nitrates were effectively retained during sampling. Of the halocarbons, dibromochloromethane was observed most often in the back-up traps. The presence of small quantities of perchloroethylene in the back-up traps was usually comparable to amounts seen in blank traps. In addition to breakthrough experiments using normal sample volumes and several liters to several tens of liters of air, we also tested breakthrough of compounds for sample sizes of several hundred liters. For example, at Mauna Loa, HI, less than 5% breakthrough of isopropyl nitrate was observed in a sample containing 244 L of air. All other measured compounds showed less breakthrough.

Because of potential breakthrough of analytes through the charcoal trap, we recommend that at least two traps be used in series for normal ambient air sampling. This allows one to make a reasonable estimation of collection efficiency for actual sampling conditions. There are three reasons analytes may be found in the back-up collection trap. Breakthrough of compounds from the first trap into the second trap due to desorption or incomplete adsorption is the first reason. As noted, a number of factors can influence this process, and not all factors can be measured or evaluated for every sample and every individual trap. We are still in the process of defining the effect of water vapor and temperature on the collection (and extraction) efficiency of the microcharcoal trap. Also, as traps are repeatedly used and reused, collection efficiency may be lost (though we have not yet observed this "aging" effect). The second reason analytes may be found on a back-up trap is carryover from prior sampling. Carryover from prior samples is a possibility since it is our normal procedure to alternate front and back traps for sampling. Such carryover might be recognized by appearance of all

Table III. Average Collection Efficiency (%) of Alkyl Nitrates and Selected Halocarbons on 5-mg Microcharcoal Adsorbent Traps under Normal Field Collection Conditions^a

<i>n</i> vol, L	Mauna Loa	Shenandoah Mts		St. Pete.	Arctic
		19	6	36	3
	67	19	6	36	3
	25	34	19	18	50
nitrates					
isopropyl	86 (10)	60 (24)	85 (6)	55 (20)	99 (0)
<i>n</i> -propyl	96 (8)	77 (15)	79 (5)	74 (19)	98 (0)
2-butyl	89 (10)	97 (2)	97 (4)	91 (10)	99 (1)
<i>n</i> -butyl		97 (4)	98 (3)	97 (8)	98 (3)
3-pentyl	98 (12)	98 (4)	99 (2)	93 (7)	97 (3)
2-pentyl	92 (17)	99 (2)	99 (1)	96 (4)	98 (2)
<i>n</i> -pentyl		100 (0)	100 (0)	93 (7)	97 (4)
halocarbons					
CHBr ₂ Cl	80 (16)	83 (18)	95 (7)	67 (13)	98 (2)
C ₂ H ₄ Br ₂	97 (10)			82 (19)	100 (0)
CHBr ₃	99 (4)	99 (3)	100 (0)	94 (4)	98 (2)
C ₂ Cl ₄	>88 (8)	95 (6)	98 (1)	>87 (4)	99 (1)
1,1,1,2-Cl ₄ C ₂ H ₂	91 (16)	100 (0)	100 (0)	84 (14)	98 (3)
1,1,2,2-Cl ₄ C ₂ H ₂	99 (6)			83 (20)	100 (0)
C ₂ Cl ₆	100 (0)	100 (0)	100 (0)	96 (6)	96 (4)

^a Collection efficiency is calculated from the amount of analyte collected on the front trap divided by the total analyte concentration in the top + bottom trap. Standard deviation is given in parentheses.

analytes at reduced concentration in the back-up trap. This effect is rarely observed since sufficient clean-up of traps is obtained between sample collections. Alternately, a full range of compounds in the back-up trap may result from channeling of air through a poorly packed or damaged front trap. Our experience thus far indicates that a trap must be visibly damaged before noticeable channeling will occur. The third reason is related to artifacts or contaminants introduced during sample processing. The most common contaminants observed in our studies are perchloroethylene and trichloroethylene. These are most often associated with contamination of the extraction solvent or contamination by the laboratory atmosphere. Rarely do we note background contamination from alkyl nitrates.

Reproducibility. Sampling and analytical precision

Table IV. Comparison of Replicate Samples Collected at Different Locations on the Island of Hawaii^a

location	analyte concn, pptv										
	C _n -alkyl nitrates						halogenated compounds				
	i-C ₃	n-C ₃	2-C ₄	n-C ₄	3-C ₅	2-C ₅	CHBr ₂ Cl	C ₂ H ₄ Br ₂	CHBr ₃	C ₂ Cl ₄	C ₂ Cl ₆
sea level	3.2	1.1	2.5	0.15	0.37	0.48	0.41	0.27	4.5	9.1	0.30
	3.0	1.1	2.5	0.17	0.36	0.60	0.41	0.27	4.1	9.0	0.30
sea level	3.2	1.0	2.3	0.11	0.41	0.53	0.30	0.19	2.5	8.6	0.21
	3.1	1.0	2.3	0.15	0.35	0.41	0.32	0.20	2.6	9.2	0.30
sea level	3.3	1.1	2.5	0.21	0.49	0.62	0.46	0.28	3.3	10.2	0.30
	3.8	1.2	2.7	0.27	0.30	0.42	0.49	0.32	3.5	16.3	0.30
sea level	4.0	1.3	3.2	0.20	0.49	0.64	1.0	0.36	8.9	11.0	0.34
	4.3	1.3	3.5	0.20	0.44	0.51	1.1	0.41	10.3	12.0	0.38
coast											
150 m	4.6	1.3	2.9	0.16	0.43	0.45	0.14	0.08	0.68	9.8	0.26
	3.9	1.2	3.1	0.19	0.53	0.58	0.15	0.12	0.72	9.5	0.33
1500 m	4.2	1.3	3.2	0.22	0.55	0.59	0.13	0.10	0.44	10.8	0.36
	4.1	1.3	3.2	0.20	0.43	0.56	0.13	0.10	0.41	10.6	0.32
MLO											
168 L	1.7	0.54	1.2	0.09	0.17	0.36	0.12	0.06	0.22	5.4	0.23
25 L av	1.6	0.52	1.2	0.06	0.18	0.33	0.12	0.05	0.22	3.9	0.28
MLO											
80 L	3.5	0.98	3.4	0.20	0.47	0.77	0.12	0.08	0.32	9.1	0.18
25 L av	3.6	0.99	3.5	0.15	0.50	0.72	0.16	0.07	0.33	7.2	0.21
MLO											
25 L av	1.5	0.53	1.3	0.07	0.22	0.42	0.11	0.06	0.21	4.5	0.27
MLO											
151 L	1.1	0.41	0.88	0.08	0.16	0.28	0.08	0.05	0.17	4.6	0.22
25 L av	1.3	0.47	0.99	0.05	0.12	0.28	0.11	0.06	0.19	3.7	0.26
MLO											
80 L	2.1	0.60	1.8	0.14	0.44	0.72	0.12	0.07	0.23	6.0	0.13
25 L av	1.5	0.52	1.6	0.09	0.38	0.65	0.11	0.07	0.21	4.0	0.25
MLO											
244 L	0.93	0.33	0.53	0.05	0.07	0.23	0.07	0.05	0.13	4.5	0.20
25 L av	0.78	0.38	0.53	0.02	0.05	0.14	0.11	0.05	0.14	3.0	0.25

^aThe first six sample pairs were collected simultaneously and were approximately equal volumes (~12 L). The sample replicates at MLO were collected over the same time interval at locations approximately 15 m apart and by using different sample intervals. The larger volume samples were collected with no inlet line prior to the adsorbent. The results of the long sample are compared to the average of three to eight shorter samples taken over the same time interval.

was tested by replicate analysis of standard solutions and by the analysis of paired samples. During the month-long field experiment at Mauna Loa, standards were run routinely along with samples during the experiment. A suitable calibration was obtained to account for changes in sensitivity during the time of the experiment. With the appropriate standardization, standards were recalculated to determine variability associated with quantitation. Over a range of concentration from ~0.05 to 10 pptv, the average error of alkyl nitrate measurement was estimated at $\pm(0.1 \pm 8\%)$ pptv. For the halocarbons the error was estimated at $\pm(0.1 \pm 5\%)$ pptv. Replicate analyses of air samples, even at low or sub-pptv concentrations, indicates that these are reasonable estimations of the overall precision of the sampling and analytical technique (Table IV). These data also show that the materials used in the inlet system (glass, Teflon, stainless steel) have no measurable effect on the analysis of simple alkyl nitrates and halocarbons.

Artifact Formation. One of the problems often encountered in the analysis of atmospheric constituents is artifact formation due to reaction between the analyte and other chemical constituents normally present in the air. Artifact formation may be a particular problem for secondary species, such as alkyl nitrates, formed from interactions of reactive chemicals in the atmosphere. A number of tests were performed in the laboratory and in the field to evaluate artifact formation, which might occur when the charcoal preconcentration technique described here was used. Tests involved addition of possible reactive chemical species in different combinations and concentrations into a flow stream, and subsequent measurement

of alkyl nitrate formation. These tests are summarized below:

Addition of up to 500 ppb NO₂ and 100 ppb NO to ambient air in College Station, TX, or to purified cylinder air with added hydrocarbon produced no measurable alkyl nitrate artifacts.

Similar tests of NO addition were conducted in the clean air conditions of Mauna Loa, HI. Addition of NO from a standard cylinder into a glass sample manifold increased ambient NO from ~15 to 1000 pptv. No increase in alkyl nitrate concentration was found to occur with the increased NO.

Alkyl nitrates *could be* produced when an oxidant (hydrogen peroxide) was added to the air stream containing either NO or NO₂ and hydrocarbons. Presumably the reaction forming alkyl nitrates may proceed via OH radical production from H₂O₂ on glass surfaces (32).

Passing the reactive air stream (NO, NO₂, H₂O₂) through a glass-wool filter coated with sodium thiosulfate removed oxidants from the airstream and eliminated the formation of alkyl nitrates.

In tests on the campus of Texas A&M University, ambient air spiked with hydrocarbon (C₅ or C₆), and no additional oxidant, was capable of forming measurable quantities of alkyl nitrates. Hexyl nitrates appeared to be more easily formed than pentyl nitrates in these tests. Interestingly, alkyl nitrate formation was measured during both daylight and nighttime hours at this location. Alkyl nitrate formation was eliminated by passing the airstream through thiosulfate-coated filters prior to the addition of hydrocarbon. The hydrocarbon concentration in the spiked airstream was not measured, but it is estimated at

ppm or higher concentrations. The process of nitrate formation also may be related to the surface-catalyzed OH radical production from ambient H₂O₂.

Similar tests adding pentane and hexane to ambient air at alternate sites in College Station, TX (away from Campus traffic), as well as at sites in St. Petersburg, FL, and Mauna Loa, HI, gave no measurable production of pentyl or hexyl nitrates.

Ambient air sampled at the Texas A&M University campus with and without a thiosulfate filter had equal concentrations of alkyl nitrates. Hydrocarbon addition to the same airstream showed alkyl nitrate "artifacts" could be formed. This experiment indicates that under "normal" conditions, artifact formation is not a significant problem. Typical ambient conditions were NO_x ~50 ppb and O₃ ~20-40 ppb. Hydrocarbon concentrations were not measured in these experiments, but they are expected to be in the ppb range (33).

In summary, our experiments indicate that in moderately polluted and clean air conditions the collection of alkyl nitrates on charcoal produces no measurable artifacts due to interactions of reactive precursors. This collection technique has not been applied to highly reactive atmospheres such as heavily polluted urban atmospheres. Further tests are required to evaluate artifact formation under these conditions.

Gas Chromatography. One of the advantages of the charcoal preconcentration technique is that volatile analytes are easily preconcentrated into a small volume of solvent for analysis by conventional gas chromatography. No gas sampling valve or cryogenic enrichment apparatus is required for the analyses described here. Excessive temperatures in the chromatographic system, though, can have an effect on the analysis of alkyl nitrates. We found, for example, that increasing the injector temperature decreased the system sensitivity to alkyl nitrates (presumably because of thermal decomposition of nitrates in the injection port), but detector temperature had little effect on the analytical sensitivity. Presumably, on-column injection may provide a better method for sample introduction to the GC system.

Since no chemical separation techniques are applied to the extract to isolate alkyl nitrates, separation of analytes from potential interferences must be accomplished with high-resolution chromatography. Using a nonpolar column, we have found that C₃-C₆ alkyl nitrates are well separated from most common halogenated compounds found in ambient air. Indeed, with the exception of a few common halocarbons, most of the compounds found to have electron capture response in our samples are alkyl or multifunctional nitrates. Because of the large number of isomers of ≥C₇ alkyl nitrates, identification and separation of all ≥C₇ RONO₂ species becomes difficult with GC/ECD. However, positive identification of alkyl nitrates is possible with negative ion chemical ionization (NICI) GC/MS (27), and this technique may be the method of choice for sensitive and specific detection of RONO₂. Table V lists the elution order and retention times of alkyl nitrates and halogenated compounds under typical conditions described above. (See also Figure 1.) Because both alkyl nitrates and halogenated compounds have excellent electron capture response, the method described here is useful for simultaneous monitoring of both classes of compounds. Though responses of individual compounds are different, our system is capable of detecting a minimum of 0.2 pg of most of the alkyl nitrates and halocarbons discussed in this report. If this amount represents 5% of the total sample collected on the charcoal trap, the limit

Table V. Elution Order and Relative Retention Time of Alkyl Nitrates and Halocarbons on Nonpolar (HP-1) Capillary Column^a

compound	retentn time, min	RRT (C ₂ Cl ₄)
isopropyl nitrate	8.71	0.653
methylene bromide	8.94	0.670
dichlorobromomethane	9.07	0.680
trichloroethylene	9.11	0.683
<i>n</i> -propyl nitrate	9.30	0.697
2-butyl + isobutyl nitrate	11.26	0.844
dibromochloromethane	11.96	0.897
ethylene dibromide	12.42	0.931
<i>n</i> -butyl nitrate	13.11	0.983
perchloroethylene	13.34	1.000
2-isopentyl nitrate (?)	14.52	1.088
1,1,1,2-tetrachloroethane	14.72	1.103
3-pentyl nitrate	15.40	1.154
2-pentyl nitrate	15.57	1.167
hydroxypropyl nitrate (isomer)	16.10	1.207
bromoform	16.17	1.212
<i>n</i> -isopentyl nitrate	16.29	1.221
1,1,2,2-tetrachloroethane	17.27	1.295
hydroxypropyl nitrate (isomer)	17.64	1.322
<i>n</i> -pentyl nitrate + 2-methylpentyl nitrate isomer	18.32	1.373
2-methylpentyl nitrate isomer	18.74	1.405
3-methylpentyl nitrate isomer	19.80	1.484
3-methylpentyl nitrate isomer	20.02	1.501
hexyl nitrate (3-hexyl?)	20.23	1.516
hexyl nitrate (2-hexyl?)	20.93	1.569
pentachloroethane	21.53	1.614
2-methylhexyl nitrate isomer	23.58	1.768
2-methylhexyl nitrate isomer	24.06	1.804
3-methylhexyl nitrate isomer	24.22	1.816
2-methylhexyl nitrate isomer	24.42	1.831
2-methylhexyl nitrate isomer	24.66	1.849
3-methylhexyl nitrate isomer	24.87	1.864
heptyl nitrate isomer	24.96	1.871
heptyl nitrate isomer	25.36	1.901
cyclohexyl nitrate isomer	25.77	1.932
heptyl nitrate isomer	25.96	1.946
hexachloroethane	26.86	2.019

^aRelative retention time is computed with perchlorethylene as reference peak; chromatographic conditions given in text.

of detection is approximately 4 pg/compound. In a 10-L air sample, this amount corresponds to <0.1 pptv for all the analytes discussed here.

Additional Comments on Organic Nitrate Measurement. The method described here has proven to be a useful technique for analysis of a variety of compounds at trace levels in the atmosphere. However, there are some limitations to the method that should be mentioned and some different approaches that are being evaluated. The first obvious limitation to the technique is that it cannot be used to measure methyl and ethyl nitrate. Because the technique uses benzene as the extraction solvent, the more volatile methyl and ethyl nitrates cannot be separated and detected by the chromatographic system described above. Different solvents (e.g. higher boiling) may allow separation of C₁ and C₂ nitrates, but the retention of methyl and ethyl nitrate on charcoal has not been tested, and under certain conditions even C₃ nitrates are not well retained by charcoal. Both methyl and ethyl nitrates have been identified in ambient samples, so it may be important to determine their concentration in addition to the higher molecular weight ≥C₃ alkyl nitrates. Several alternate methods may be used to measure C₁ + C₂ nitrates. One method utilizes cryogenic preconcentration of whole air samples and separation on a chromatographic column of suitable polarity (18, 22, 23). A second method currently under evaluation in our laboratory utilizes a solid adsor-

bent (Tenax or Carbotrap) and thermal desorption. In spite of potential problems of thermal degradation of nitrates, the method appears promising for C₁-C₅ nitrates. At this time, though, not all nitrates are unambiguously separated from halocarbons by using a variety of GC columns or combinations of columns.

A second aspect to the analysis of organic nitrates in the ambient atmosphere is related to the measurement of multifunctional nitrate compounds. Peroxyacyl nitrates (PAN and others) are an important class of organic nitrates that requires special protocols because of its thermal lability (34); they will not be considered here. However, a variety of other nitrates with polar substituents (alcohols, ketones, carboxylic acids) of increasing complexity are predicted to form during the oxidation of unsaturated hydrocarbons (8, 34, 35). The behavior of these compounds in any normal sampling system has not yet been fully tested. Our samples from the Shenandoah Mountains revealed the presence of several hydroxypropyl nitrates, and possibly other polar nitrates. These compounds were not well extracted from the charcoal by using benzene. A more polar mixture (10% methanol-benzene) improved extraction of these (and possibly other) nitrate species. Anderson et al. (24) also reported poor recovery of other organic nitrate compounds including nitroglycerin and ethylene glycol dinitrate from charcoal using carbon disulfide. Increased recoveries of these compounds were obtained from XAD-2 resin. Further studies on polar nitrate compounds are necessary to determine the significance of atmospheric transformations and products of hydrocarbon oxidation. For polar and multifunctional nitrate species, a suitable solid adsorbent/solvent system may have advantage over a gas-phase concentration system since polar organic may suffer adsorption losses in a gas-phase system.

Acknowledgments

We thank B. Ridley for coordinating the Mauna Loa experiment and helpful discussions, E. Robinson and co-workers for support at the GMCC site at Mauna Loa, J. Greenberg for providing portable sampling equipment, and others at the Mauna Loa site for technical assistance. We thank G. Patton for collecting air samples from the Canadian Arctic.

Registry No. CHBr₂Cl, 106-93-4; C₂H₄Br₂, 124-48-1; CHBr₃, 75-25-2; C₂Cl₄, 127-18-4; 1,1,1,2-C₂H₂Cl₄, 630-20-6; 1,1,2,2-C₂H₂Cl₄, 79-34-5; C₂HCl₅, 76-01-7; C₂Cl₆, 67-72-1; isopropyl nitrate, 1712-64-7; *n*-propyl nitrate, 627-13-4; 2-butyl nitrate, 924-52-7; *n*-butyl nitrate, 928-45-0; 3-pentyl nitrate, 82944-59-0; 2-pentyl nitrate, 21981-48-6; *n*-pentyl nitrate, 1002-16-0.

Literature Cited

- Leighton, P. A. *Photochemistry of Air Pollution*; Academic Press: New York, 1961.
- Finlayson-Pitts, B. J.; Pitts, J. N. *Atmospheric Chemistry*; John Wiley and Sons: New York, 1986.
- Crutzen, P. J. *Annu. Rev. Earth Planet. Sci.* **1979**, *7*, 443-472.
- Logan, J. A.; Prather, M. J.; Wofsy, S. C.; McElroy, M. B. *J. Geophys. Res. D* **1981**, *86*, 7210-7254.
- Logan, J. A. *J. Geophys. Res. D* **1983**, *88*, 10785-10807.
- Altshuller, A. P. *Atmos. Environ.* **1986**, *20*, 245-268.
- Singh, H. B. *Environ. Sci. Technol.* **1987**, *21*, 320-327.
- Calvert, J.; Madronich, S. *J. Geophys. Res. D* **1987**, *92*, 2211-2220.
- Atherton, C. S.; Penner, J. E. *Tellus* **1988**, *40B*, 380-392.
- Darnall, K. R.; Carter, W. P. L.; Winer, A. M.; Lloyd, A. C.; Pitts, J. N., Jr. *J. Phys. Chem.* **1976**, *80*, 1948-1050.
- Atkinson, R. *Chem. Rev.* **1985**, *85*, 69-201.
- Atkinson, R.; Aschmann, S. M.; Carter, W. P. L.; Winer, A. M.; Pitts, J. N., Jr. *J. Phys. Chem.* **1982**, *86*, 4563-4569.
- Brewer, D. A.; Ogliaruso, M. A.; Augustsson, T. R.; Levine, J. S. *Atmos. Environ.* **1984**, *18*, 2723-2744.
- Shepson, P. B.; Edney, E. O.; Kleindienst, T. E.; Pittman, G. H.; Namie, G. R.; Cupitt, L. T. *Environ. Sci. Technol.* **1985**, *19*, 849-854.
- Gu, C.; Rynard, C. M.; Hendry, D. G.; Mill, T. *Environ. Sci. Technol.* **1985**, *19*, 151-155.
- Killus, J. P.; Whitten, G. Z. *Environ. Sci. Technol.* **1984**, *18*, 142-148.
- Carter, W. P. L.; Lloyd, A. C.; Sprung, J. L.; Pitts, J. N., Jr. *Int. J. Chem. Kinet.* **1979**, *11*, 45-101.
- Roberts, J. M. *Atmos. Environ.* **1989**, *23A*, 243-247.
- Grosjean, D. *Environ. Sci. Technol.* **1983**, *17*, 13-17.
- Williams, I. H. *Anal. Chem.* **1965**, *37*, 1723-1732.
- Juttner, F. *J. Chromatogr.* **1988**, *442*, 157-163.
- Buhr, M.; Fehsenfeld, F. C.; Parrish, D. D.; Sievers, R.; Roberts, J. Contribution of organic nitrates to the total odd-nitrogen budget at a rural Eastern U.S. site. Presented at the American Geophysical Union Meeting, San Francisco, CA, December 6-11, 1988.
- Flocke, F.; Volz, A.; Kley, D. Kopplung eines Chemolumineszenz-detektors mit einem Gaschromatographen zur selektiven Messung oxidierter Stickstoffverbindungen in der Atmosphäre. Technical Report. KFA-Julich, July 1988.
- Andersson, K.; Levin, J.-O.; Nilsson, C.-A. *Chemosphere* **1983**, *12*, 821-826.
- Mottram, D. S. *J. Agric. Food Chem.* **1984**, *32*, 343-345.
- Tomkins, B. A.; Manning, D. L.; Griest, W. H.; Jones, A. R. *Anal. Chim. Acta* **1985**, *169*, 69-78.
- Atlas, E. *Nature* **1988**, *331*, 426-428.
- Atlas, E.; Schauffler, S. Organic nitrates and selected halocarbons in the Pacific atmosphere. Presented at American Geophysical Union meeting, San Francisco, CA, December 6-11, 1988.
- Boschan, R.; Merrow, R. T.; Van Dolah, R. W. *Chem. Rev.* **1955**, *55*, 485-510.
- Melcher, R. G.; Langner, R. R.; Kagel, R. O. *Am. Ind. Hyg. Assoc. J.* **1978**, *39*, 349-361.
- Saalwaechter, A. T.; McCammon, C. S., Jr.; Roper, C. P.; Carlberg, K. S. *Am. Ind. Hyg. Assoc. J.* **1977**, *38*, 476-486.
- Audley, G. J.; Baulch, D. L.; Campbell, I. M. *J. Chem. Soc., Chem. Commun.* **1982**, 1053-1055.
- Sexton, K.; Westberg, H. *Atmos. Environ.* **1984**, *18*, 1125-1132.
- Singh, H. B.; Salas, L. J. *Atmos. Environ.* **1983**, *17*, 1507-1516.
- Madronich, S.; Calvert, J. *J. Geophys. Res. D* **1990**, *95*, 5697-5716.
- Lloyd, A. C.; Atkinson, R.; Lurmann, F. W.; Nitta, B. *Atmos. Environ.* **1983**, *17*, 1931-1950.

Received for review April 6, 1990. Revised manuscript received August 2, 1990. Accepted August 6, 1990. This work was supported by NSF Grants ATM-8717002 and OCE 84157216. The National Center for Atmospheric Research and the NOAA Aeronomy Laboratory provided additional funding for the Mauna Loa Experiment.

Biodegradation of Aromatic Hydrocarbons by Aquifer Microorganisms under Denitrifying Conditions

Stephen R. Hutchins,* Guy W. Sewell, David A. Kovacs, and Garmon A. Smith

U.S. Environmental Protection Agency and NSI Technology Services, Robert S. Kerr Environmental Research Laboratory, P.O. Box 1198, Ada, Oklahoma 74820

■ A series of laboratory tests were conducted to evaluate whether denitrification would be a suitable alternative for bioremediation of an aquifer contaminated with JP-4 jet fuel. Microcosms were prepared from both uncontaminated and contaminated aquifer material from the site, in an anaerobic glovebox, amended with nitrate, nutrients, and aromatic hydrocarbons, and incubated under a nitrogen atmosphere at 12 °C. With uncontaminated core material, there was no observable lag period prior to removal of toluene whereas 30 days was required before biodegradation commenced for xylenes, ethylbenzene, and 1,2,4-trimethylbenzene. An identical test with contaminated aquifer material exhibited not only much longer lag periods but decreased rates of biodegradation; benzene, ethylbenzene, and *o*-xylene were not significantly degraded within the 6-month time period even though active denitrification occurred at this time. First-order biodegradation rate constants ranged from 0.016 to 0.38 day⁻¹ for uncontaminated core material and from 0.022 to 0.067 day⁻¹ for contaminated core material. Tests with individual compounds in uncontaminated core indicated that benzene and *m*-xylene inhibited the basal rate of denitrification. These data demonstrate that several aromatic compounds can be degraded under denitrifying conditions, but rates of biodegradation may be lower in material contaminated with JP-4 jet fuel.

Introduction

Leaking underground storage tanks are a major source of groundwater contamination by petroleum hydrocarbons. There are approximately 1.4 million underground tanks storing gasoline in the United States, and some petroleum experts estimate that 75 000-100 000 of these tanks are leaking (1). Gasoline and other fuels contain benzene, toluene, and xylenes (collectively known as BTX), which are hazardous compounds regulated by the U.S. Environmental Protection Agency (2). Although these aromatic hydrocarbons are relatively water-soluble, they are contained in the immiscible bulk fuel phase, which serves as a slow-release mechanism for sustained groundwater contamination. Pump-and-treat technology alone is economically impractical for renovating aquifers contaminated with bulk fuel, because the dynamics of immiscible fluid flow result in prohibitively long time periods for complete removal of the organic phase (3, 4). Bioremediation, in conjunction with free product recovery, has been recommended as a viable treatment alternative and involves enhancing the activity of the native subsurface bacteria to degrade fuel hydrocarbons through addition of nutrients and other compounds. Aerobic bioremediation has been shown to be effective for many fuel spills (5, 6). However, success is often limited by the inability to provide sufficient oxygen to the contaminated intervals due to the low solubility of oxygen (7, 8). This problem can be partially

overcome by using hydrogen peroxide to provide greater quantities of oxygen to the active zone, but this also has disadvantages, including the toxicity of hydrogen peroxide to subsurface microorganisms and its reactivity with inorganic species such as ferric iron (5, 6, 9). Anaerobic processes, once thought to be ineffective for biodegradation of aromatic compounds, have now been clearly established in the fate of these contaminants (10, 11). However, it is still not clear to what extent anaerobic processes can be successfully used in bioremediation of contaminated aquifers.

Nitrate can also serve as an electron acceptor; this results in anaerobic biodegradation of organic compounds associated with the processes of nitrate reduction and denitrification (12). Because nitrate is much more soluble than oxygen, it may require less time and hence be more economical to restore fuel-contaminated aquifers under denitrifying rather than aerobic conditions. This is especially true when one considers that much of the oxygen that is supplied to the subsurface, whether as gaseous oxygen or hydrogen peroxide, can be lost prior to being transported to the contaminated zone of interest through degassing and reaction with inorganic species.

Several oxygenated hydrocarbons, typical of intermediates of metabolism of fuel hydrocarbons, can be degraded under denitrifying conditions. These include cyclohexanol and cyclohexanone (13), phenol and cresols (14-16), and benzoic and hydroxybenzoic acids (17-19). Less established is the biodegradation of reduced aromatic fuel hydrocarbons under denitrifying conditions, and reports are often conflicting. Bower and McCarty found no utilization of ethylbenzene and naphthalene by sewage microorganisms incubated under anoxic conditions with nitrate (20), and Tschek and Fuchs demonstrated that pure cultures of denitrifying pseudomonads that degraded phenol could not degrade toluene (16). In contrast, Zeyer et al. showed that toluene and *m*-xylene could be mineralized under denitrifying conditions in laboratory aquifer columns (21). The *m*-xylene-adapted microorganisms could also degrade several oxygenated intermediates but were unable to utilize benzene, ethylbenzene, *o*- and *p*-xylene, or naphthalene (22). Mihelcic and Luthy, however, were able to demonstrate naphthalene biodegradation under denitrifying conditions (23, 24). Major et al., using aquifer material, observed biodegradation of benzene, toluene, and all three xylene isomers under denitrifying conditions (25). It therefore appears that BTX biodegradation under denitrifying conditions can be influenced by several undefined factors, and that site-specific studies are required prior to implementing a nitrate-based remediation for fuel-contaminated aquifers.

This report describes a series of laboratory tests that were conducted to evaluate whether denitrification would be a suitable alternative for bioremediation of a shallow water table aquifer contaminated with JP-4 jet fuel at Traverse City, MI. The use of nitrate to promote biological removal of fuel aromatic hydrocarbons is being investigated for the jet fuel spill through an on-going field demon-

U.S. Environmental Protection Agency,
NSI Technology Services.

stration project in cooperation with the U.S. Coast Guard and the U.S. Air Force.

Experimental Section

Field Site and Sampling. The aquifer is composed of thick glacial deposits with the upper portions containing an upper sand and gravel unit and an underlying clay unit (26). The water table varies seasonally and ranges from 3.7 to 5.5 m below the land surface with a seepage velocity of 1.5 m day⁻¹. Extensive subsurface coring was carried out by EPA personnel to better define the horizontal and vertical extent of contamination and to provide samples for chemical analyses and laboratory microcosms. Core samples were obtained by aseptic sampling techniques under nonoxidizing conditions to prevent oxygen intrusion and thus better maintain the microbial community structure and chemical integrity of the cores (27). The cores were collected in sterile Mason jars with the field anaerobic glovebox described by Leach et al. (27) and were sealed to prevent aeration upon removal from the glovebox. The core samples were placed on ice and transported to the laboratory for storage at 12 °C. Subsamples were aseptically obtained from the cores in an anaerobic glovebox and were analyzed for fuel carbon and JP-4 content according to the method developed by Vandegrift et al. (28).

Microcosm Preparation. Two composite core samples were used to prepare microcosms for denitrification studies. Uncontaminated core was obtained downgradient from the fuel spill and had no detectable JP-4 (50 mg/kg detection limit). Uncontaminated core was used for most of the microcosm tests because it represented the primary treatment zone in the field demonstration project. In addition, contaminated core was obtained adjacent to the source area of the original spill. A previous test had shown that replicate microcosms could not be consistently prepared from highly contaminated core because of the loss of volatile hydrocarbons during sample preparation. Therefore, the most contaminated core, which contained 1000 mg/kg JP-4, was degassed in the airlock of the anaerobic glovebox to draw off the more volatile compounds. This core was then mixed with the other contaminated cores and the composite sample was again degassed as above.

Microcosms were prepared aseptically in an anaerobic glovebox to preclude intrusion of oxygen. All preparations were made when the atmospheric oxygen concentration in the glovebox was less than 10 ppm (v/v) as measured by an oxygen monitor. Test chemicals were reagent-grade and all glassware and preparation supplies were sterilized. Dilution water, used to prepare stock solutions and to transfer core material, consisted of distilled water which was then sterilized and aseptically purged with nitrogen gas.

Specific preparation methods varied for the individual tests. In the initial tests, replicate samples contained 17.0 g of uncontaminated core material in 12-mL serum bottles. Core material was rinsed into the serum bottles with a small quantity of water and each sample was amended with nutrients to provide solution concentrations of 100 mg/L NH₄ N and 20 mg/L PO₄ P. These small microcosms were further amended with potassium nitrate to yield 30 or 75 mg/L NO₃ N; controls contained 250 mg/L mercuric chloride and 500 mg/L sodium azide as biocides to inhibit microbial growth. Each microcosm was then spiked with an aqueous stock containing benzene, toluene, ethylbenzene, *m*-xylene, *p*-xylene, *o*-xylene, and 1,2,4-trimethylbenzene to yield final solution concentrations of 2–7 mg/L for each compound. Immediately after spiking,

the microcosms were filled and sealed without headspace by using Teflon-lined butyl rubber septa. The samples were then placed in an anaerobic pressure chamber prior to removal from the glovebox and the chamber was subsequently pressurized to 10 psi with nitrogen; this was done to further reduce the possibility of oxygen leakage and subsequent aerobic reactions. Microcosms were incubated anaerobically in the dark at 12 °C, the temperature of the groundwater at Traverse City. This test was set up with the contaminated core as well. In addition, one set of samples received the nitrate and nutrient amendments but no combination BTX spike. This was done to evaluate background nitrate removal.

For the next test, individual hydrocarbons were evaluated in microcosms prepared with uncontaminated core. These microcosms were constructed to be repeatedly sampled and were prepared by adding 25.0 g of core material to 60-mL serum bottles equipped with Teflon Mininert valves. Each set consisted of duplicate samples with a single control containing 250 mg/L mercuric chloride. Nutrients were added as before and nitrate concentrations were adjusted to 50 mg/L NO₃ N. Benzene, toluene, ethylbenzene, *m*-xylene, and *o*-xylene were added as individual compounds in aqueous solution to the respective sets; final concentrations ranged from 16 to 22 mg/L for the separate analytes. Volumes were adjusted to allow a minimum headspace, and the samples were incubated in the dark at room temperature in the anaerobic glovebox.

The final test was conducted with toluene to better define the role of the denitrifying bacteria in aromatic hydrocarbon degradation. Replicate microcosms were constructed with 75.0 g of uncontaminated core material in 160-mL serum bottles and were amended with 10 mg/L NH₄ N and 10 mg/L PO₄ P. These were then separated into four treatment groups: (1) nitrate only, (2) toluene only, (3) nitrate and toluene, and (4) controls. Microcosms within each group were amended with 30 mg/L NO₃ N and/or 25 mg/L toluene; controls received both nitrate and toluene, 250 mg/L mercuric chloride, and 500 mg/L sodium azide. These microcosms were filled without headspace, sealed with Teflon-lined butyl rubber septa, and incubated in the dark at room temperature in the glovebox.

Sampling and Analysis. Three replicates from each set were sacrificed at designated time intervals. Each microcosm was mixed and centrifuged at 1500 rpm for 30 min to clarify the supernatant. For those tests requiring repeated sampling, the microcosms were mixed and allowed to settle overnight. The sample volume was not replaced for the microcosms equipped with Mininert valves. To prevent accumulation of headspace in the final test, the septum was removed and the sample amount was replaced with sterile 2-cm³ Pyrex glass rods prior to re-sealing with the unpunctured septum.

The volatile aromatic hydrocarbons were analyzed by purge-and-trap gas chromatography using an OI 4460 sample concentrator and an HP 5890 GC with cryogenic cooling and a photoionization detector. Hydrocarbons were purged onto a Tenax trap for 12 min at 30 °C followed by a 4-min dry purge and desorbed for 4 min at 180 °C. Samples were chromatographed on a 30 m × 0.25 mm megabore DB-1301 capillary column with a 1.0- μ m film thickness. The injector temperature was 200 °C and the oven temperature was programmed from -80 (4 min) to 30 °C (0.05 min) at 50 °C/min and then to 150 °C at 8 °C/min with a flow rate of 10 mL/min. The PID detector was set at 230 °C with medium lamp intensity. For BTX analysis, this technique does not distinguish between

Table I. Kinetic Parameters for Biodegradation of Monoaromatic Hydrocarbons in Microcosms with Uncontaminated and Contaminated Core at 12 °C Using Low (30 mg/L NO₃ N) and High (75 mg/L NO₃ N) Doses of Nitrate

compound	aquifer material	nitrate treatment dose	C ₀ ^a mg/L	t ₀ ^b day	rate constant, day ⁻¹	±95% confidence interval
toluene	uncontaminated	low	5.35	0	-0.163	-0.190, -0.137
		high	5.29	0	-0.151	-0.167, -0.135
		control	5.58	0	-0.00182	-0.00635, +0.00271
	contaminated	low	5.15	49	-0.0224	-0.0265, -0.0183
		high	5.90	49	-0.0350	-0.0389, -0.0312
		control	5.18	49	0.000246	-0.00208, +0.00257
ethylbenzene	uncontaminated	low	3.34	28	-0.0158	-0.0241, -0.00749
		high	3.24	28	-0.0652	-0.0948, -0.03566
		control	3.19	28	-0.00157	-0.0112, +0.00807
	contaminated	low	4.53	0	-0.00174	-0.00288, -0.00060
		high	4.20	0	-0.00229	-0.00324, -0.00133
		control	4.42	0	-0.00213	-0.00309, -0.00118
<i>m,p</i> -xylene	uncontaminated	low	5.63	28	-0.178	-0.216, -0.140
		high	5.20	28	-0.381	-0.408, -0.354
		control	5.95	28	-0.00353	-0.0211, +0.0141
	contaminated	low	6.46	62	0.000429	-0.00163, +0.00249
		high	7.26	62	-0.0665	-0.0695, -0.0636
		control	6.95	62	0.00103	-0.00028, +0.00234
<i>o</i> -xylene	uncontaminated	low	2.99	28	-0.0184	-0.0295, -0.00723
		high	2.77	28	-0.0164	-0.0275, -0.00524
		control	2.79	28	-0.000523	-0.0121, +0.0110
	contaminated	low	4.88	0	-0.00166	-0.00274, -0.00058
		high	4.55	0	-0.00234	-0.00324, -0.00142
		control	4.75	0	-0.000954	-0.00186, -0.00005
1,2,4-trimethylbenzene	uncontaminated	low	1.20	28	-0.148	-0.178, -0.118
		high	1.11	28	-0.270	-0.295, -0.245
		control	1.41	28	-0.000843	-0.0152, +0.136
	contaminated	low	2.79	62	0.00315	-0.00520, +0.0115
		high	3.06	62	-0.0422	-0.0515, -0.0328
		control	3.18	62	0.000478	-0.00443, +0.00538

^aInitial concentration at t₀. ^bTime used for beginning acquisition of rate data.

m- and *p*-xylene; these are therefore reported collectively as *m,p*-xylene. The quantitation limit for these compounds was 1–25 µg/L based on the sample amount available.

Samples were also analyzed for aqueous nitrate, nitrite, and ammonia concentrations by standard EPA methods (29). Selected microcosms were examined for microbial counts by using a direct counting method with acridine orange as described by Ghiorse and Balkwill (30). For the final test, microcosms from each treatment group were sacrificed on days 0, 3, 5, and 7 for analysis of intermediates of aromatic hydrocarbon metabolism. The contents were acidified to pH < 2 with sulfuric acid and extracted for 18 h with methylene chloride in a Soxhlet extractor. The solvent was dried with sodium sulfate and concentrated to 100 µL by using a Kuderna–Danish evaporator and nitrogen. The extracts were analyzed with a Finnigan 4615 gas chromatograph/mass spectrometer with separation done with a 29 m × 0.32 mm i.d. DB-5 fused-silica column. The GC oven was programmed from 40 (2 min) to 205 °C at 8 °C/min using a helium flow of 40 cm/s. External standards were prepared from hypothesized intermediates, including benzoic acid, phenol, cresols, hydroxybenzoic acids, and catechol, and quantitation was by internal standard addition. Detection limits were approximately 0.1 mg/L for the phenols, 1.0 mg/L for catechol and benzoic acid, and 75 mg/L for hydroxybenzoic acids.

Results

In the first tests, microcosms were prepared with both uncontaminated and contaminated core material, spiked with a combination of selected monoaromatic hydrocarbons, and incubated under denitrifying conditions. For the uncontaminated core, biodegradation and nitrate re-

moval were observed for each of the compounds with the exception of benzene (Figure 1). However, some of the labile compounds were removed more quickly than others, and different degradation profiles were observed. There appeared to be no observable lag period prior to the removal of toluene, whereas approximately 30 days was required before active biodegradation commenced on the xylenes, ethylbenzene, and 1,2,4-trimethylbenzene. The test period was 56 days; by this time, toluene, *m,p*-xylene, and 1,2,4-trimethylbenzene were degraded to below 25 µg/L. With one exception from among the three replicates, ethylbenzene was also completely degraded under the high-nitrate dose. Biodegradation occurred but was especially slow for *o*-xylene; the other two isomers were much more susceptible to microbial attack under denitrifying conditions.

Biodegradation of the substituted benzenes varied for the individual compounds and was not clearly zero or first order (Figure 1). For purposes of comparison, reaction rates were assumed to be first order and the reaction was considered to commence after the observed lag period. Kinetic data for this and the subsequent test using contaminated core were derived for the labile compounds (Table I). First-order rate constants ranged from a low of 0.016–0.018 day⁻¹ for *o*-xylene to a high of 0.18–0.38 day⁻¹ for *m,p*-xylene and were not significant in the corresponding controls. Rates of removal were significantly greater with the high-nitrate dose for ethylbenzene, *m,p*-xylene, and 1,2,4-trimethylbenzene. Nitrate removal was evident in both cases as was nitrite accumulation toward the end of the test (Figure 2). The rate constant for nitrate removal ranged from 0.016 to 0.033 day⁻¹ for the first 45 days; afterwards, nitrate was undetectable in the low-dose samples and did not appreciably decline in the

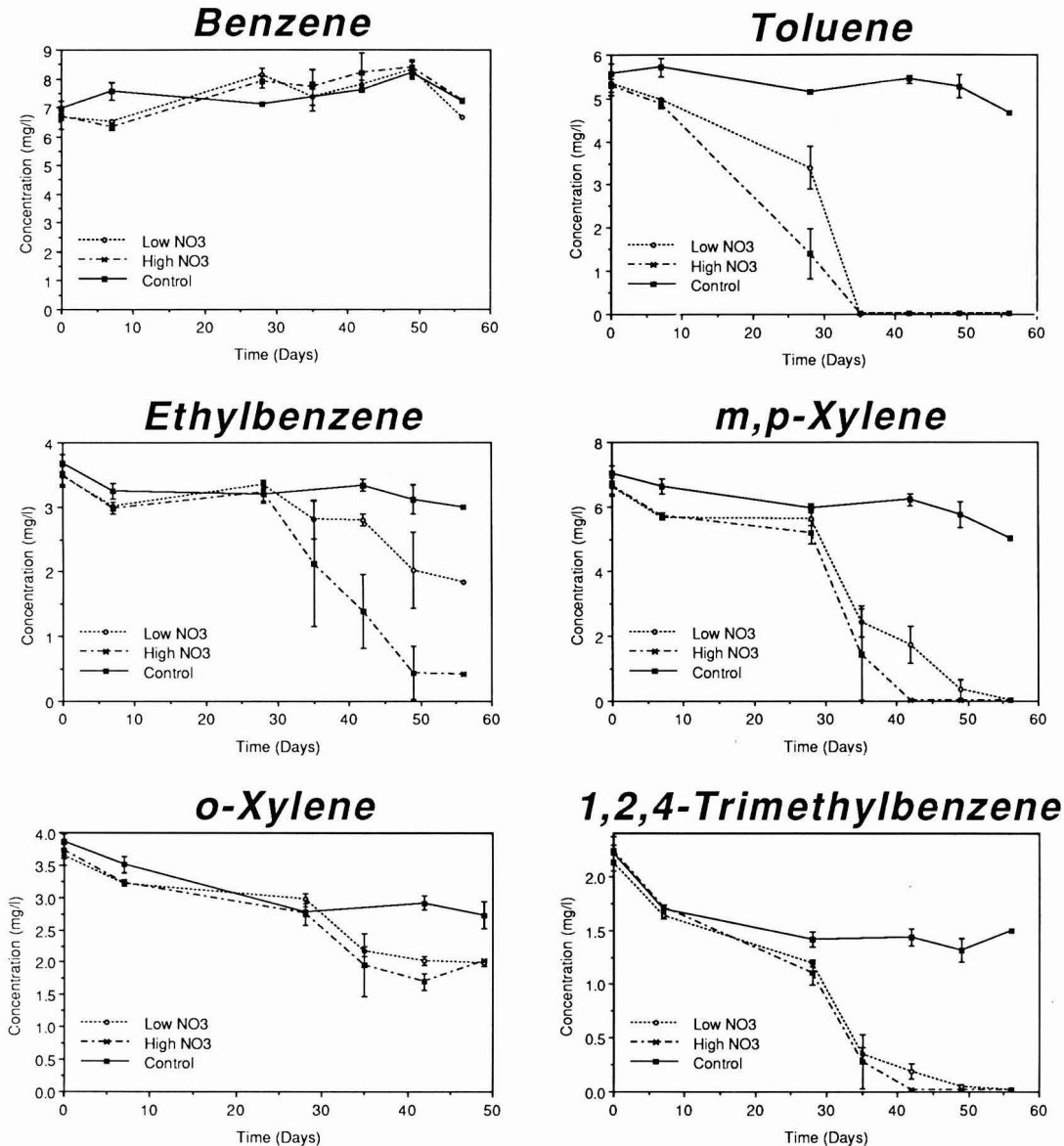


Figure 1. Removal of aromatic hydrocarbons in microcosms with uncontaminated cores at 12 °C using 30 (low), 75 (high), and 30 mg/L NO₃ N with biocides (control). Mean of three replicates with standard error.

high-dose samples. Total microbial numbers by direct count increased only slightly from 9.8×10^7 to 1.4×10^8 cells/g.

This test was repeated using contaminated instead of uncontaminated aquifer material. In contrast to the previous test, there was no significant removal of most of the aromatic hydrocarbons during the first 60 days (Figure 3). Only after an extended lag period was there a decline in total solution concentrations of toluene, *m,p*-xylene, and 1,2,4-trimethylbenzene. There was a significant decrease in toluene concentrations in the low and high nitrate dose samples after 50 days and in *m,p*-xylene and 1,2,4-trimethylbenzene in the high nitrate dose samples after 60 days.

First-order rate constants were calculated for those compounds that were degraded and revealed that, in ad-

dition to the extended lag period, biodegradation rates were 3–7 times lower in the contaminated core than in the uncontaminated core (Table I). There was a gradual increase in concentrations of the less soluble aromatic hydrocarbons in the microcosms that had not been spiked with BTX; aqueous concentrations of 1,2,4-trimethylbenzene, *m,p*-xylene, and *o*-xylene rose from approximately 10 µg/L to 100, 70, and 60 µg/L, respectively, in 160 days. This is probably a result of slow release of BTX from the residual hydrocarbon phase. Benzene, toluene, and ethylbenzene concentrations remained below 20 µg/L throughout the test.

Although total BTX removal was inhibited in this test compared to that observed with uncontaminated aquifer material, nitrate removal was enhanced relative to the previous test (Figure 4). Nitrate was rapidly removed

Table II. Removal of Aromatic Hydrocarbons and Nitrite Accumulation in Denitrifying Microcosms Spiked with the Individual Compounds^a

microcosm test, compd added	time, days	aromatic substrate		nitrite (NO ₂ N)	
		inocultd	control	inocultd	control
benzene microcosms	0	19.8 ± 1.2	20.5	0.1 ± 0.0	<0.05
	7	18.2 ± 0.1	<i>b</i>	0.1 ± 0.0	0.6
	14	17.9 ± 0.3	20.8	0.1 ± 0.0	0.9
	28	17.6 ± 0.2	<i>b</i>	0.4 ± 0.4	1.5
	37	19.2 ± 0.5	21.3	0.3 ± 0.2	1.9
	63	17.9 ± 0.3	19.4	0.2 ± 0.2	2.7
toluene microcosms	0	22.7 ± 0.1	22.1	0.3 ± 0.2	<0.05
	7	0.00 ± 0.00	18.3	8.0 ± 5.8	0.1
	14	0.00 ± 0.00	19.0	7.4 ± 4.3	0.2
	28	0.00 ± 0.00	16.1	2.9 ± 3.7	0.2
	37	0.01 ± 0.01	15.4	2.0 ± 2.7	0.3
	63	0.02 ± 0.01	11.0	0.5 ± 0.6	1.5
ethylbenzene microcosms	0	22.7 ± 0.3	21.6	<0.05	<0.05
	7	13.7 ± 0.4	19.6	1.3 ± 0.7	0.2
	14	0.00	18.7	6.9 ± 8.2	0.6
	28	0.07 ± 0.02	17.5	<0.05	1.4
	37	0.10 ± 0.01	18.8	<0.05	2.2
	63	0.15 ± 0.1	11.0	<0.05	5.7
<i>m</i> -xylene microcosms	0	<i>b</i>	<i>b</i>	<0.05	<0.05
	7	15.7 ± 0.1	15.9	0.1 ± 0.0	0.1
	14	15.3 ± 0.6	16.7	0.1 ± 0.0	0.1
	28	14.6 ± 0.2	16.6	0.3 ± 0.2	0.3
	37	17.2 ± 0.2	16.7	0.4 ± 0.1	0.3
	63	14.2 ± 0.4	<i>b</i>	<0.05	0.7
<i>o</i> -xylene microcosms	0	24.1 ± 1.4	21.4	0.1 ± 0.0	<0.05
	7	19.1 ± 3.0	18.9	0.2 ± 0.1	<0.05
	14	16.3 ± 3.6	20.0	0.1 ± 0.0	0.1
	28	14.2 ± 2.5	19.1	0.1 ± 0.1	0.2
	37	15.9 ± 2.9	21.4	<0.05	0.3
	63	13.2 ± 2.7	19.8	<0.05	0.8

^aData are mean of two replicates with standard error for the inoculated samples and single samples for the controls. All concentration units are milligrams per liter aqueous concentrations. ^bNo data available.

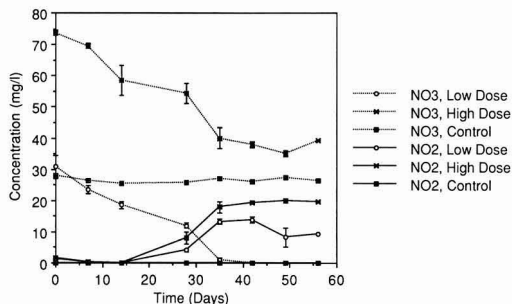


Figure 2. Nitrate removal and nitrite accumulation in microcosms using uncontaminated core amended with BTX and 30 (low), 75 (high), and 30 mg/L NO₃ N with biocides (control). Mean of three replicates with standard error.

from solution in samples containing the low-nitrate dose, requiring that these microcosms be periodically respiked to maintain appreciable concentrations of the electron acceptor in solution. To maintain equivalent conditions among the four sets, all of the microcosms were respiked at these times as well. Nitrate removal was similar in the low-dose samples with and without the BTX spike, indicating that the added aromatic compounds were not increasing the nitrate demand significantly.

Nitrite concentrations initially ranged from 8.2 ± 1.9 to 8.9 ± 0.5 mg/L NO₂ N in all of the inoculated samples, indicating that denitrification occurred during the first sampling period. However, nitrite concentrations rapidly dropped and remained below 0.5 mg/L NO₂ N throughout the test. The only exception occurred for the high nitrate dose samples at the end of the test; nitrite concentrations

rose to 8.9 ± 5.7 mg/L NO₂ N and then to 13.4 ± 4.3 mg/L NO₂ N after 84 and 161 days, respectively. Microscopic examination revealed numerous bacteria present as rods either singly or in aggregates. Small oil droplets were also visible in the stained smears prepared for direct microscopic counts. Direct counts remained relatively constant in the range from 5.2×10^8 to 2.1×10^9 cells/g before and after the test, with no significant differences based on the various treatment levels.

Five aromatic compounds were selected for further evaluation and added individually to microcosms prepared from uncontaminated core material. Initial concentrations ranged from 16 to 22 mg/L in solution. These microcosms were incubated at room temperature and were periodically sampled rather than sacrificed. Rapid biodegradation of toluene and ethylbenzene occurred under these conditions, although significant concentrations of ethylbenzene remained throughout the 63-day study (Table II). Toluene was removed to below detection limits within 7 days; this corresponds to a first-order rate constant of >1.1 day⁻¹. Similarly, ethylbenzene was degraded at a rate significantly higher than that observed previously, with a first-order rate constant of 0.55 day⁻¹. As observed in the previous test with uncontaminated core, *o*-xylene was only slowly degraded and benzene was recalcitrant (Table II). In contrast to the previous test, *m*-xylene was recalcitrant when added as a single compound at an initial concentration of 16 mg/L.

The uncontaminated core material exhibited a basal rate of denitrification even without the presence of added hydrocarbons (Figure 5). Addition of toluene or ethylbenzene resulted in removal of the substrate aromatic compound, and this accelerated the consumption of nitrate. Although a low rate of biodegradation of *o*-xylene

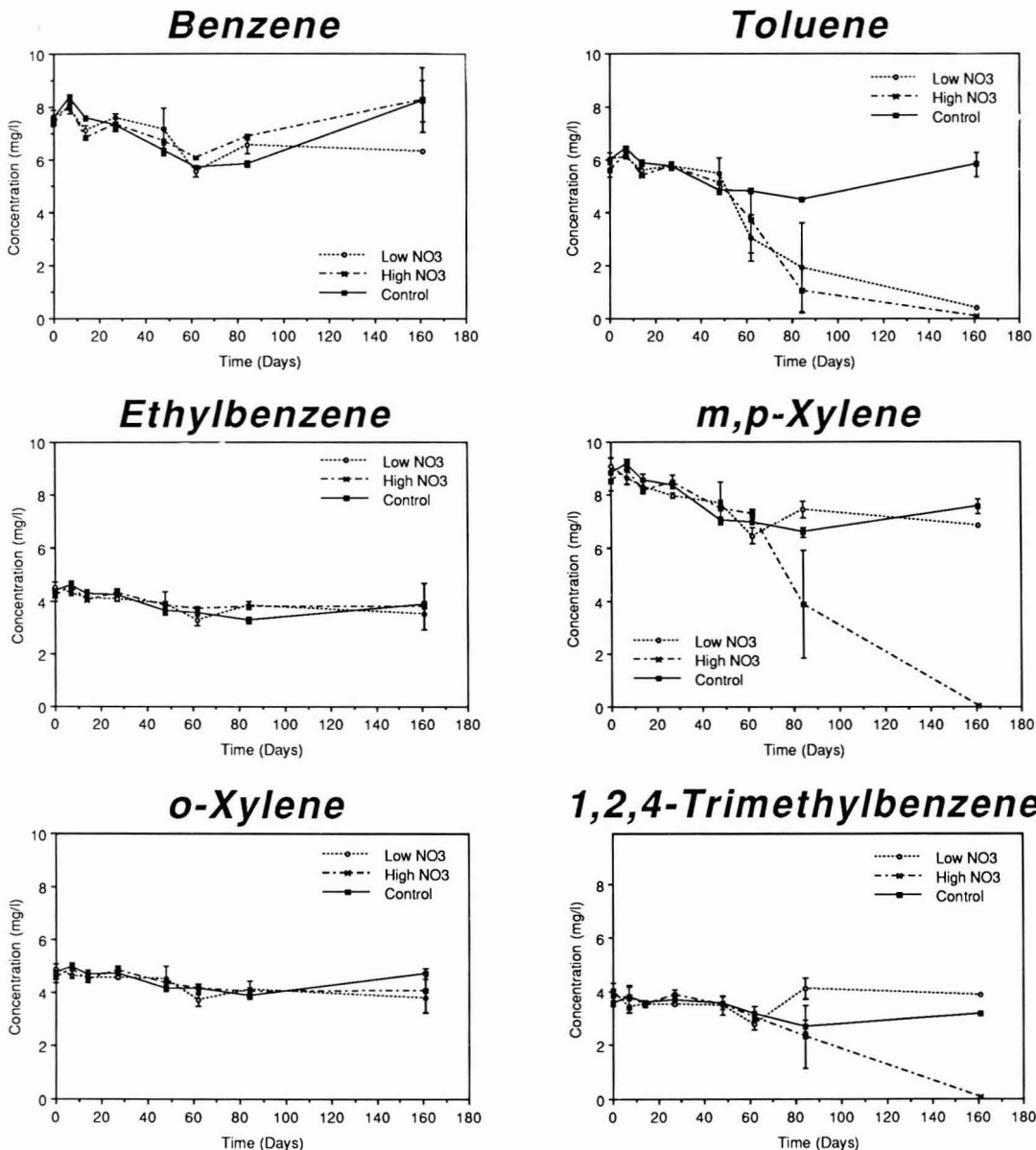
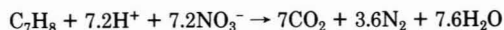


Figure 3. Removal of aromatic hydrocarbons in microcosms with contaminated core at 12 °C using 30 (low), 75 (high), and 30 mg/L NO₃ N with biocides (control). Mean of three replicates with standard error.

was also observed, this had no significant effect on denitrification. Surprisingly, *m*-xylene was not only recalcitrant but also appeared to inhibit the basal rate of denitrification. This was observed with benzene as well, although the effect on nitrate removal was not as pronounced (Figure 5). For the inoculated samples, nitrite accumulation was transitory and only appeared at the beginning of the test (Table II).

In the final test, there was no toluene removal from any of the viable microcosms unless nitrate was present (Figure 6). Similarly, there was little nitrate removal or nitrite accumulation in the viable microcosms unless toluene was present (Figure 6). Ammonia nitrogen levels also dropped by 1.6–2.3 mg/L NH₄ N in the toluene plus nitrate-

amended samples relative to the other treatment groups. The following stoichiometric relationships were used to calculate how much of the toluene removal could be attributed to mineralization:



Nitrate removal and nitrite accumulation were corrected for those samples not receiving toluene, and it was assumed that the nitrate that did not account for nitrite production was completely denitrified. Based on these calculations, the additional nitrate removal in the toluene-amended microcosms was sufficient to account for 72% of the tol-

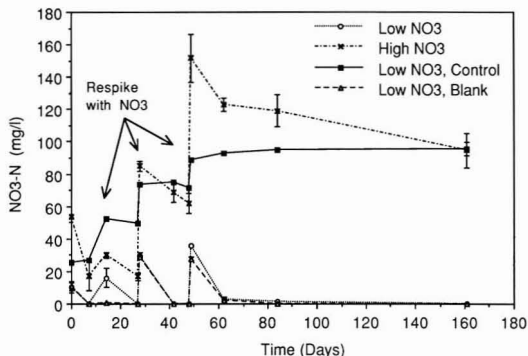


Figure 4. Nitrate removal in microcosms using contaminated core amended with BTX and 30 (low), 75 (high), and 30 mg/L $\text{NO}_3\text{-N}$ with biocides (control). Blank samples received 30 mg/L $\text{NO}_3\text{-N}$ but no BTX spike. Samples were respiked on days 14, 27, and 48 with nitrate. Mean of three replicates with standard error.

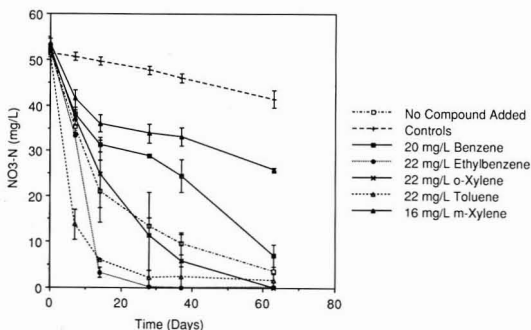


Figure 5. Nitrate removal in microcosms using uncontaminated core material and respiked with either no compound, benzene, toluene, ethylbenzene, *m*-xylene, or *o*-xylene. Mean of six samples with standard error for controls; mean of two replicates with standard error for inoculated samples.

uene being mineralized. No intermediates of toluene metabolism were detected. Phenol, cresols, and benzoic acid were present in the original microcosm supernatants at concentrations corresponding to less than 20, 2, and 200 $\mu\text{g/L}$, respectively, in all samples including controls. Hydroxybenzoic acids and catechol were not detected; the detection limit corresponded to 1 $\mu\text{g/L}$ for catechol and

75 $\mu\text{g/L}$ for the hydroxybenzoic acids. There were no other compounds detected in the toluene plus nitrate treatment group that were not also present in the other treatment groups.

Discussion

Data from the initial tests indicate that indigenous microorganisms in uncontaminated aquifer material at Traverse City are capable of degrading monoaromatic hydrocarbons, with the possible exception of benzene, under denitrifying conditions. Biodegradation of toluene did not occur without the presence of nitrate and nitrate removal was minimal without the presence of toluene over a 10-day incubation period. Assuming that the nitrogen demand for cell synthesis is being met by the ammonia nitrogen that was consumed, stoichiometric relationships indicate that 72% of the toluene removal can be attributed to mineralization on a theoretical basis. This agrees with other estimates that 25–30% of the amount of organic carbon required for energy can be required for cell synthesis by denitrifying bacteria (31). Although this does not prove that denitrifying bacteria are responsible for toluene biodegradation, it is strong presumptive evidence. It is also likely that the other aromatic hydrocarbons are also being degraded by denitrifying bacteria.

The initial tests were conducted at a relatively low in situ temperature of 12 °C, and in most cases, a significant lag period occurred prior to the onset of active biodegradation for those aromatic compounds that were degraded. Hence it is possible that the more recalcitrant compounds may have required an extended adaptation period. Adaptation can be defined as a change in the microbial community that is brought about by exposure to a selected substrate and results in more rapid utilization of that substrate. One explanation for the observed adaptation period is that addition of nitrate stimulated oxidation of organic substrates other than the fuel hydrocarbons in the initial phase of the test. Denitrifying bacteria are diverse and hence can exhibit a widespread metabolic potential. Even deep subsurface sediments can contain enough organic carbon for denitrification to proceed, and in some cases, exogenous carbon sources have no stimulatory effect (32). Both the uncontaminated and contaminated core materials used in these tests supported basal rates of denitrification without the addition of carbon sources. However, it is not known whether the microorganisms that were responsible for BTX biodegradation were actively metabolizing the indigenous carbon sources at this time.

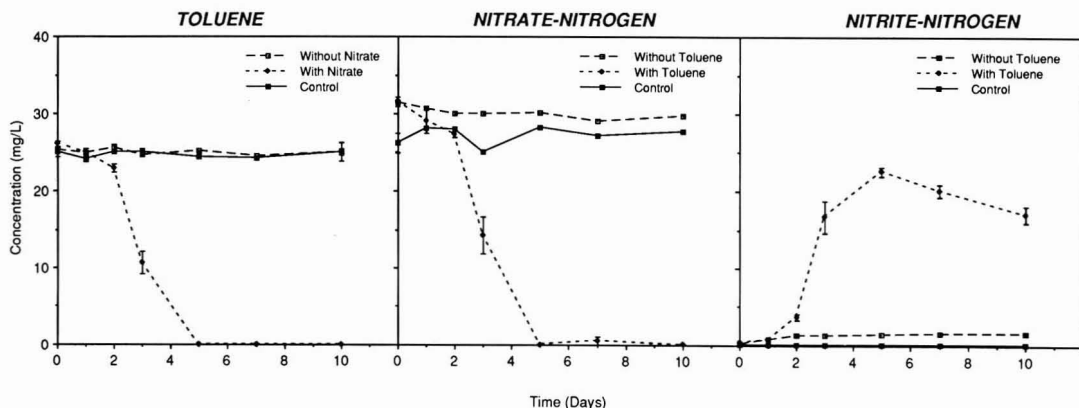


Figure 6. Toluene removal, nitrate removal, and nitrite accumulation in microcosms using uncontaminated core with various amendments. Mean of three replicates with standard error.

The longer lag period observed with the contaminated core material is consistent with the hypothesis of metabolism of indigenous organic carbon, but the effects of toxicity of the components of JP-4 or metabolic byproducts should also be considered. Evidence for this is given by the decreased basal rate of denitrification in uncontaminated core microcosms upon exposure to either benzene or *m*-xylene. These compounds were present at concentrations similar to those that would be found in fuel-contaminated aquifers at equilibrium. It should be noted, however, that the inhibition of denitrification observed in this particular test results from an effect on the general denitrifying population and may not be specific to those microorganisms responsible for BTX biodegradation.

Kinetic data on BTX biodegradation by denitrifying bacteria is scarce in the literature. Zeyer et al. (21) reported a pseudo-first-order rate constant of $>0.45 \text{ h}^{-1}$ for mineralization of *m*-xylene in a column containing aquifer material at 30 °C. Other studies generally report the disappearance of the parent compound, which ranges from several days to several months, depending upon the compound under study and the environmental conditions (20, 23–24). Biodegradation of the aromatic hydrocarbons in these microcosm tests, using both uncontaminated and contaminated aquifer material, was not clearly zero or first order based on the resolution of the available data. This is not unexpected considering the potential diversity of the active microflora and the potential presence of alternate substrates. In the uncontaminated core, first-order reaction rates ranged from 0.016 to 0.38 day⁻¹ and were generally enhanced under conditions of greater nitrate availability. The corresponding rates appeared to be 3–7 times lower in microcosms prepared with contaminated core material. In the next test, toluene and ethylbenzene were degraded at much higher rates than those observed previously. There are several possible reasons to account for this, including the use of higher concentrations, incubation at a higher temperature, and more efficient utilization of a single versus multiple substrates. But it is surprising that *m*-xylene was much more recalcitrant in this test compared to the previous experiments. This reaffirms that caution should be applied when the results based on sole substrate studies are extrapolated to situations where multiple substrates prevail.

Benzene biodegradation under denitrifying conditions is enigmatic; some studies report benzene to be recalcitrant (20–22) whereas other studies indicate that benzene is rapidly degraded (25, 33, 34). In some of these latter systems, the possibility of oxygen intrusion into microcosms cannot be discounted based on available information concerning the experimental design, but it is also possible that subsurface microbial populations and previous exposure differ sufficiently to account for the discrepancy. Benzene is a major problem from a regulatory standpoint and therefore its fate under denitrifying conditions requires more evaluation. However, it should be noted that the problem of benzene recalcitrance may be overestimated for field situations that will be undergoing bioremediation. The laboratory study was conducted under strictly anaerobic conditions, and it is doubtful that oxygen penetration will be prohibited to the same extent under field conditions. Because benzene is rapidly oxidized under aerobic conditions, there may be sufficient oxygen available to initiate the degradative sequence and result in complete mineralization as oxygen becomes depleted and denitrification begins. Further work is needed in this area to better assess the potential for nitrate-based bioremediation of fuel-contaminated aquifers.

Acknowledgments

We would like to thank Lynda Pennington and Mark White of NSI Technology Services for conducting the inorganic analytical work and Jim Cloud of CSC Inc. for help in statistical analysis. We also thank John Wilson for review and comments on the manuscript. Total microbial counts were performed by Bob Smith.

Registry No. toluene, 108-88-3; ethylbenzene, 100-41-4; *m*-xylene, 108-38-3; *p*-xylene, 106-42-3; *o*-xylene, 95-47-6; 1,2,4-trimethylbenzene, 95-63-6; benzene, 71-43-2.

Literature Cited

- (1) Feliciano, D. Congressional Research Service Report. U.S. Library of Congress, Washington, DC, January 1984.
- (2) Serial No. 95-12. U.S. Government Printing Office, Washington, DC, 1977.
- (3) Wilson, J. L.; Conrad, S. H. In *Proceedings, Conference on Petroleum Hydrocarbons and Organic Chemicals in Ground Water: Prevention, Detection, and Restoration*; NWWA/API: Houston, TX, 1984; pp 274–298.
- (4) Bouchard, D. C.; Enfield, C. G.; Pivoni, M. D. In *Reactions and Movement of Organic Chemicals in Soil*; Sawhney, B. L., Brown, K., Eds.; SSSA Special Publication 22; Soil Science Society of America and American Society of Agronomy: Madison, WI, 1989; pp 349–371.
- (5) Thomas, J. M.; Lee, M. D.; Bedient, P. B.; Borden, R. C.; Canter, L. W.; Ward, C. H. RSKERL Publication. EPA 600/2-87/008; 1987.
- (6) Lee, M. D.; Thomas, J. M.; Borden, R. C.; Bedient, P. B.; Wilson, J. T.; Ward, C. H. *Crit. Rev. Environ. Control* 1988, 18, 29–89.
- (7) Wilson, J. T.; Leach, L. E.; Henson, M.; Jones, J. N. *Ground Water Monit. Rev.* 1986, 6, 56–64.
- (8) Barker, J. F.; Patrick, G. C.; Major, D. *Ground Water Monit. Rev.* 1987, 7, 64–71.
- (9) Thomas, J. M.; Ward, C. H. *Environ. Sci. Technol.* 1989, 23, 760–766.
- (10) Evans, W. C. *Nature* 1977, 270, 17–22.
- (11) Schink, B. In *Biology of Anaerobic Microorganisms*; Zehnder, A. J. B., Ed.; John Wiley & Sons: New York, 1988; pp 771–846.
- (12) Tiedje, J. M. In *Biology of Anaerobic Microorganisms*; Zehnder, A. J. B., Ed.; John Wiley and Sons: New York, 1988; pp 179–244.
- (13) Dangel, W.; Tschech, A.; Fuchs, G. *Arch. Microbiol.* 1988, 150, 358–362.
- (14) Bakker, G. *FEMS Lett.* 1977, 1, 103–108.
- (15) Bossert, I. D.; Rivera, M. D.; Young, L. Y. *FEMS Microbiol. Ecol.* 1986, 38, 313–319.
- (16) Tschech, A.; Fuchs, G. *Arch. Microbiol.* 1987, 148, 213–217.
- (17) Taylor, B. F.; Campbell, W. L.; Chinoy, I. J. *Bacteriol.* 1970, 102, 430–437.
- (18) Ziegler, K.; Braun, K.; Bockler, A.; Fuchs, G. *Arch. Microbiol.* 1987, 149, 62–69.
- (19) Kuhn, E. P.; Sufita, J. M.; Rivera, M. D.; Young, L. Y. *Appl. Environ. Microbiol.* 1989, 55, 590–598.
- (20) Bouwer, E. J.; McCarty, P. L. *Appl. Environ. Microbiol.* 1983, 45, 1295–1299.
- (21) Zeyer, J.; Kuhn, E. P.; Schwarzenbach, R. P. *Appl. Environ. Microbiol.* 1986, 52, 944–947.
- (22) Kuhn, E. P.; Zeyer, J.; Eicher, P.; Schwarzenbach, R. P. *Appl. Environ. Microbiol.* 1988, 54, 490–496.
- (23) Mihelcic, J. R.; Luthy, R. G. *Appl. Environ. Microbiol.* 1988, 54, 1182–1187.
- (24) Mihelcic, J. R.; Luthy, R. G. *Appl. Environ. Microbiol.* 1988, 54, 1188–1198.
- (25) Major, D. W.; Mayfield, C. I.; Barker, J. F. *Ground Water* 1988, 26, 8–14.
- (26) Twenter, F. R.; Cummings, T. R.; Grannemann, N. G. *Water-Resour. Invest. Rep. (U.S. Geol. Surv.)* 1985, No. 85-4064.
- (27) Leach, L. E.; Beck, F. P.; Wilson, J. T.; Kampbell, D. H. In *Proceedings, Second National Outdoor Action Conference on Aquifer Restoration, Ground Water Monitoring*

and Geophysical Methods; NWWA: Dublin, OH, 1989; Vol. 1, pp 31-51.

(28) Vandegrift, S. A.; Kampbell, D. H. *J. Chromatogr. Sci.* 1988, 26, 566-569.

(29) Kopp, J. F.; McKee, G. D. *Manual—Methods for Chemical Analysis of Water and Wastes*; EPA-600/4-79-020; 1979.

(30) Ghiorse, W. C.; Balkwill, D. L. *Dev. Ind. Microbiol.* 1983, 24, 213-224.

(31) Metcalf & Eddy, Inc. *Wastewater Engineering: Collection, Treatment, Disposal*; McGraw-Hill: New York, 1972; p 664.

(32) Francis, A. J.; Slater, J. M.; Dodge, C. J. *Geomicrobiol. J.* 1989, 7, 103-116.

(33) Batterman, G. In *1985 TNO Conference on Contaminated Soil*; Assink, J. W., van den Brink, W. J., Eds.; Nijhoff:

Dordrecht, The Netherlands, 1986; pp 711-722.

(34) Berry-Spark, K.; Barker, J. F.; Major, D.; Mayfield, C. I. In *Proceedings, Petroleum Hydrocarbons and Organic Chemicals in Ground Water: Prevention, Detection and Bioremediation*; NWWA/API: Houston, TX, 1986; pp 613-623.

Received for review December 5, 1989. Revised manuscript received May 3, 1990. Accepted July 19, 1990. Although the research described in this paper has been funded by the U.S. Environmental Protection Agency through an in-house research program, it has not been subjected to Agency review and therefore does not necessarily reflect the views of the Agency, and no official endorsement should be inferred.

Mechanism of Pentachloroethane Dehydrochlorination to Tetrachloroethylene

A. Lynn Roberts and Philip M. Gschwend*

Ralph M. Parsons Laboratory, Department of Civil Engineering, Massachusetts Institute of Technology, Cambridge, Massachusetts 02139

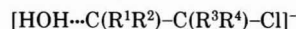
■ The dehydrochlorination of pentachloroethane to tetrachloroethylene was investigated to gain insight into mechanisms of hexachloroethane reduction as well as structure-reactivity relationships for polyhalogenated alkanes. Although the absence of deuterium exchange excludes the possibility of an $(E_{1CB})_R$ mechanism, several factors suggest the transition state possesses considerable carbanion character: the reaction is insensitive to buffer catalysis, exhibits a moderately large solvent kinetic isotope effect, and only displays a neutral mechanism at low pH. Though our results cannot rule out a stepwise $(E_{1CB})_I$ or $(E_{1CB})_{IP}$ sequence, we believe $CHCl_2CCl_3$ reacts via a concerted mechanism based on a comparison of its dehydrohalogenation kinetics with proton-exchange rates for $CHCl_3$ and $CHCl_2CF_3$. Pentachloroethane reported in the reduction of hexachloroethane to tetrachloroethylene is unlikely to result from carbanion protonation. Rather, it may be diagnostic of free-radical reduction mechanisms. Because pentachloroethane reacts relatively rapidly, future studies of hexachloroethane reduction should consider whether pentachloroethane represents a reaction intermediate instead of dismissing it as a minor side product.

Introduction

Reductive dehalogenation and dehydrohalogenation reactions dominate the transformation of many polyhalogenated alkanes in aqueous systems. Of the two classes, reductive dehalogenation is the less well studied, and its mechanisms in complex environmental samples are poorly understood. Recent studies have attempted to amend this by investigating biologically mediated and abiotic reductive transformations; several have emphasized the reduction of hexachloroethane to tetrachloroethylene (1-5), although little progress has been made in elucidating the actual reaction pathway(s). Investigations of hexachloroethane reduction by Fe(II) porphyrins (6), rat liver microsomal preparations (7), or microorganisms in groundwater samples (8) have noted pentachloroethane as a minor product. This could conceivably be generated either via hydrogen atom abstraction by a pentachloroethyl radical (formed by a one-electron reduction of hexachloroethane) or via protonation of a pentachloroethyl carbanion (resulting from a net two-electron reduction), as shown in Figure 1. Pentachloroethane can itself react to tetrachloroethylene, albeit via dehydrochlorination; several possible mechanisms could involve a pentachloro-

ethyl carbanion intermediate. Understanding the details through which this elimination reaction proceeds should provide some basis for weighing the relative likelihood of the potential hexachloroethane reduction pathways. In addition, knowing the rate at which pentachloroethane reacts should prove useful in assessing whether it represents a side product or a reaction intermediate. Finally, comparing the kinetics of pentachloroethane elimination to rates for other polychlorinated ethanes should provide substantial insight into the influence of structural factors on reactivity in this class of important environmental contaminants.

Dehydrohalogenation mechanisms for pentachloroethane such as the E_1 and the $(E_{1CB})_{anion}$ mechanisms can be ruled out by the observed dependence of reaction rate on pH (among other factors). Reactions exhibiting second-order kinetics can occur by two different classes of mechanism (9), referred to as E_2 and E_{1CB} (Figure 2); the latter path is frequently ignored by introductory organic chemistry textbooks. In the E_2 mechanism (Figure 2a), proton loss and halide ion elimination occur in a concerted fashion, whereas E_{1CB} reactions (Figure 2b) are characterized by the initial formation of a carbanion intermediate. Depending on the relative rates of reprotonation and elimination steps, this carbanion can either revert to starting material via a reversible proton-transfer step [$(E_{1CB})_R$ mechanism] or proceed to form the olefin with little reprotonation [$(E_{1CB})_I$ mechanism]. Closely related to the $(E_{1CB})_R$ mechanism is the $(E_{1CB})_{IP}$ mechanism, the difference being that in the latter case, the free carbanion is not formed, but remains intimately associated as an ion pair or hydrogen-bonded pair with the conjugate acid of the former base, as designated by the intermediate



in Figure 2b. These mechanisms are kinetically indistinguishable: all are characterized by a first-order dependence on the concentration of the effective base, as indicated in Figure 2.

A key question is whether pentachloroethane reacts via an $(E_{1CB})_R$ or an $(E_{1CB})_{IP}$ mechanism. If so, any pentachloroethyl carbanion formed during the reduction of hexachloroethane would be expected to undergo proton transfer to form pentachloroethane. Conversely, if pentachloroethane were to react via an E_2 or an $(E_{1CB})_I$ mechanism, this implies a pentachloroethyl carbanion is

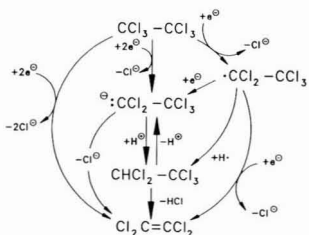


Figure 1. Potential pathways for the reduction of hexachloroethane to pentachloroethane and tetrachloroethylene, and for the dehydrochlorination of pentachloroethane to tetrachloroethylene.

so unstable under ambient conditions that either it is unlikely ever to be formed (whether from hexachloroethane or pentachloroethane) or at least it should decompose to tetrachloroethylene rather than persist long enough to become protonated. In this case, any pentachloroethane produced from hexachloroethane might be diagnostic of a free-radical reduction pathway.

Most simple alkyl halides are believed to react via concerted E_2 mechanisms, although many exceptions exist. A number of compounds have been shown to undergo proton-exchange reactions, indicative of $(E_{1CB})_R$ -like mechanisms. These include di- and trihaloethylenes (10-12), haloforms (13-18), and several pentahaloethanes (all 1,1,1-trifluoro-2,2-dihaloethanes; ref 19). These substrates are all characterized by acidic hydrogens and unfavorable leaving groups. Pentachloroethane also has an acidic hydrogen (in terms of the inductive effects of the five chlorine atoms at the α - and β -carbons), but any of the chlorines bonded to the sp^3 -hybridized C_α constitute a much better leaving group than the halogens in the above examples. Whether the latter factor is sufficient to favor the E_2 mechanism over an E_{1CB} mechanism is difficult to predict

a priori. Several chlorinated and brominated substrates with similar inductive effects at C_β may react via E_{1CB} pathways. An $(E_{1CB})_I$ mechanism has been claimed for DDT (1,1,1-trichloro-2,2-bis(*p*-chlorophenyl)ethane) and some of its analogues (20, 21), although this has been contested by other researchers for reactions under somewhat different conditions (22). Other evidence indicates several substituted polyhaloethanes, including $C_6H_5CHClCF_2Cl$, $C_6H_5CHBrCF_2Br$, and $C_6H_5CHBrCH_2Br$, react via an $(E_{1CB})_{IP}$ mechanism even in protic solvents (23, 24). These substrates all contain phenyl substituents capable of stabilizing a carbanion, but some stabilization might also be expected from the chlorines in pentachloroethane. One researcher (25) has even gone so far as to question the prevalence of E_2 reactions, suggesting that E_{1CB} reactions may be much more common than previously recognized.

Walraevens et al. (26) studied the reaction of pentachloroethane in water at high pH via conductivity measurements. They suggested the absence of significant buffer catalysis and the negative value computed for the activation entropy might reflect an E_{1CB} mechanism, without conducting further tests to support this hypothesis. Although Walraevens et al. were not specific, in all probability they envisioned an $(E_{1CB})_R$ mechanism; other E_{1CB} mechanisms, which had only very rarely been described at the time their study was conducted, are more likely to be subject to buffer catalysis.

In the present study, we have measured parameters required to model the transformation of pentachloroethane under environmental conditions (near-ambient temperatures and low to moderate pH). Very recently, Jeffers et al. (27) and Cooper et al. (28) published results of similar kinetic experiments without, however, proposing any mechanistic interpretation. These two studies confirm our measured activation parameters, and the study of Jeffers et al. (27) provides evidence of a neutral dehydrochloro-

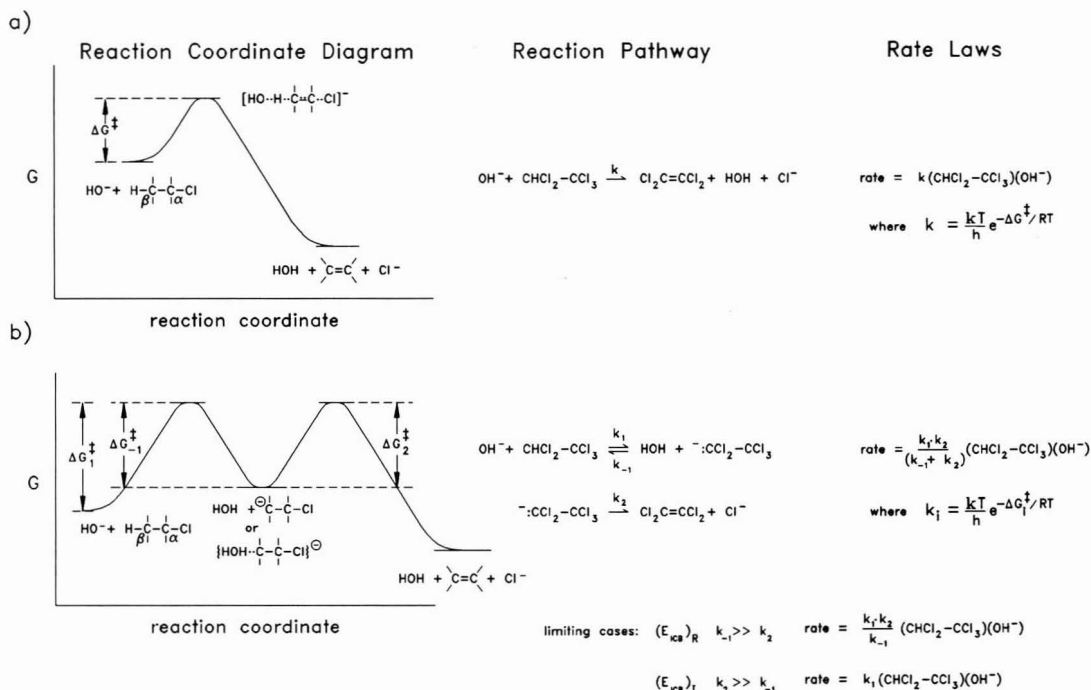


Figure 2. Potential mechanisms of HCl elimination from pentachloroethane. (a) E_2 mechanism: concerted elimination of HCl. (b) E_{1CB} mechanisms: initial formation of a carbanion intermediate.

mination reaction not observed in our experiments. The primary objective of the present study was to obtain evidence concerning the mechanism by which pentachloroethane reacts to permit us to evaluate its significance when observed during hexachloroethane reduction. This study complements our continuing investigations of polyhalogenated alkane reduction mechanisms, both by microorganisms in anoxic groundwater and by reduced sulfur species under clean chemical conditions and in sulfide-rich natural waters (8).

Materials and Methods

Reagents. Dehydrochlorination rates were measured in buffered systems containing one or more of the following reagent-grade salts: sodium benzoate, sodium acetate, sodium dihydrogen phosphate, disodium hydrogen phosphate, sodium sulfide, and sodium tetraborate decahydrate. Buffer solutions were prepared with the appropriate salt or salts plus sufficient HCl to bring the pH approximately to the pK_a of the buffer acid. Although the buffers used are generally fairly dilute, concentrations are high enough relative to initial pentachloroethane levels that we expect at most a 3% change in the hydroxyl ion concentration during the course of the reaction (<0.2% for the most of the buffers used). Ionic strength was adjusted as required with NaCl. Mercuric chloride (10 mg/L) was added to inhibit microbial activity for all but the hydrogen sulfide buffer and the D_2O buffer used for the isotope-exchange experiment. For the latter experiment, D_2O (99.9%) was obtained from Cambridge Isotope Laboratory, Woburn, MA. Otherwise, aqueous solutions were prepared with high-purity (>15 M Ω /cm) deionized distilled water prepared with a Milli-Q water system (Millipore Corp., Bedford, MA).

Determinations of pH were performed at the appropriate temperature with an Orion Model SA 720 pH/ISE meter and an Orion Ross combination pH electrode. For the experiment in D_2O , the pH meter was calibrated against buffers in normal water, and the meter reading converted to pD as described by Perrin and Dempsey (29). Hydroxyl ion activities were computed from pH measurements by using pK_w values of 13.9965 at 25 °C and 13.6801 at 35 °C. The OD^- ion activity was obtained by using a pK of 14.869 at 25 °C (30). For determining second-order rate constants, OH^- or OD^- concentrations were calculated from ion activities by using activity coefficients estimated from the extended Debye-Hückel relationship for solutions with $I \leq 0.05$ and from the Davies equation for solutions with $I = 0.1$ equiv/L.

Stock solutions of $CHCl_2CCl_3$ (96%) (Aldrich) and $Cl_2C=CCl_2$ (98%) (MCB) were dissolved in methanol for spiking experimental flasks and preparing aqueous standard solutions. For most experiments, either CCl_3F (99+%) or $Cl_2C=CHCl$ was included to establish the integrity of our glass reaction vessels against losses of volatile compounds. For the isotope-exchange experiment, a stock solution of $CHCl_2CCl_3$ was prepared in CH_3OD (99.5+%) immediately prior to use. All halogenated compounds were used as received without further purification. Gas chromatography (GC) and combined gas chromatography/mass spectrometry (GC/MS) analyses of the $CHCl_2CCl_3$ indicated it contained low levels (~2%) of $Cl_2C=CCl_2$; corrections were generally not required for this contamination.

For most experiments, samples were analyzed via cold on-column direct aqueous injection electron capture detection gas chromatography (31), using external aqueous standards prepared freshly each day from methanol stock solutions. For the isotope-exchange experiment and the

buffer catalysis experiment conducted at pH 4.6, in which analyses were conducted of hexane extracts, standards were prepared by diluting alkyl halides directly into hexane.

Glassware. Most experiments were performed in three-necked round-bottom flasks (250-mL nominal volume) fitted with ground-glass stopcock adapters or stoppers. Aqueous standards were prepared by spiking stock solutions into 20- or 50-mL glass syringes filled with water. A 50-mL glass syringe was also used as a reaction vessel for the isotope-exchange experiment instead of a three-necked flask to permit removal of relatively large aliquots for solvent extraction without creating headspace.

Kinetic Experiments. After reaction vessels were filled with buffer solutions, leaving minimal headspace to prevent volatilization (generally <1-mL headspace to 300-mL total volume), they were transferred to water baths to reach thermal equilibrium (either at 24.9 ± 0.09 °C or 35.0 ± 0.18 °C). Reaction vessels were then spiked with 7–100- μ L aliquots of CCl_3F or $Cl_2C=CHCl$ plus $CHCl_2CCl_3$ in methanol (or 7.5 μ L of $CHCl_2CCl_3$ in CH_3OD) to give initial pentachloroethane concentrations of 0.5–50 μ M. The resulting methanol concentration (less than 1.5×10^{-4} mol fraction) is too small to influence reaction rates. After an initial mixing period and sampling, reaction vessels were returned to the water baths for incubation in the dark.

Aliquots were periodically removed for analysis. In most cases, only a few microliters of solution were removed for injection directly onto the GC column. For some experiments, however, a preliminary dilution step was required. To quench reactions that proceeded rapidly at high pH (>8), 100- μ L samples were diluted into 2-mL samples of dilute HCl to lower the pH below pH 6. Samples were then stored on ice for a few hours until analyses could be completed. Experiments conducted at pH 8 with and without a dilution step showed no significant differences. For the experiment conducted with the H_2S buffer, 100- μ L sample aliquots were diluted into 2 mL of deoxygenated deionized water prior to direct aqueous injection analysis. This enabled us to avoid the electron capture detector quenching we have observed at high $(H_2S)_T$ concentrations. For the buffer catalysis experiments conducted at pH 4.6, which required relatively concentrated buffers, direct aqueous injection GC was not used to avoid baseline problems we have encountered with such solutions. Rather, 100- μ L aliquots were periodically removed from the reaction vessels and extracted with 1 mL of hexane. One-milliliter samples were also extracted with 0.5 mL of hexane (containing 1,1,1,2-tetrachloroethane as an internal standard) for GC/MS analysis in the isotope-exchange experiment.

For most experiments, efforts were made to monitor the reaction over at least 2–3 half-lives to ensure tetrachloroethylene was in fact the sole product. At pH <5, however, where half-lives were very long (>100–1900 days), incubations were only monitored for 9 or 10 weeks.

Data Analysis. For each experiment, monitoring $CHCl_2CCl_3$ disappearance and $Cl_2C=CCl_2$ appearance permitted independent estimates of pseudo-first-order rate constants. These were generally obtained by fitting the $CHCl_2CCl_3$ data via a regression of the form $\ln(CHCl_2CCl_3) = \ln(CHCl_2CCl_3)_0 - k_{obs}t$ or via a nonlinear fit of the $Cl_2C=CCl_2$ data to an equation of the form $(Cl_2C=CCl_2) = (CHCl_2CCl_3)_0[1 - \exp(-k_{obs}t)]$. At low pH (<5), $Cl_2C=CCl_2$ data were fit to $(Cl_2C=CCl_2) = (CHCl_2CCl_3)_0[1 - \exp(-k_{obs}t)] + (Cl_2C=CCl_2)_0$ to incorporate the small amount of $Cl_2C=CCl_2$ present as a contaminant in the $CHCl_2CCl_3$. For the $Cl_2C=CCl_2$ regressions at low pH, the

Table I. Results of Dehydrochlorination Experiments Conducted at Low Ionic Strength (0.005 equiv/L) in H₂O

pH	mM buffer	N ^a	from CHCl ₂ CCl ₃		from Cl ₂ C=CCl ₂		predicted k, b s ⁻¹
			k _{obs} , s ⁻¹	R ²	k _{obs} , s ⁻¹	R ²	
25 °C Results							
4.15	2.5 (benzoate) _T	10	1.41 × 10 ⁻⁸	0.5386	4.19 × 10 ⁻⁹	0.9612	4.20 × 10 ⁻⁹
4.71	2.5 (acetate) _T	10	3.35 × 10 ⁻⁸	0.8849	1.14 × 10 ⁻⁸	0.9865	1.53 × 10 ⁻⁸
7.09	2.5 (PO ₄) _T	10	3.28 × 10 ⁻⁶	0.9996	3.59 × 10 ⁻⁶	0.9806	3.66 × 10 ⁻⁶
7.94	1.25 (PO ₄) _T + 1.25 (BO ₃) _T	11	2.90 × 10 ⁻⁵	0.9845	3.75 × 10 ⁻⁵	0.9772	2.59 × 10 ⁻⁵
7.98	1.67 (PO ₄) _T + 1.67 (BO ₃) _T	11	3.02 × 10 ⁻⁵	0.9975	4.07 × 10 ⁻⁵	0.9923	2.84 × 10 ⁻⁵
9.10	2.5 (BO ₃) _T	17	4.39 × 10 ⁻⁴	0.9991	4.60 × 10 ⁻⁴	0.9982	3.75 × 10 ⁻⁴
35 °C Results							
4.14	2.5 (benzoate) _T	10	3.70 × 10 ⁻⁸	0.9016	2.20 × 10 ⁻⁸	0.9865	2.48 × 10 ⁻⁸
4.68	2.5 (acetate) _T	10	9.83 × 10 ⁻⁸	0.9666	7.74 × 10 ⁻⁸	0.9906	8.62 × 10 ⁻⁸
7.06	2.5 (PO ₄) _T	7	2.03 × 10 ⁻⁵	0.9937	2.53 × 10 ⁻⁵	0.9939	2.07 × 10 ⁻⁵
7.90	1.25 (PO ₄) _T + 1.25 (BO ₃) _T	15	1.44 × 10 ⁻⁴	0.9988	1.53 × 10 ⁻⁴	0.9949	1.43 × 10 ⁻⁴

^aN, number of samples. ^b See text.

(CHCl₂CCl₃)₀ value used was constrained to equal the value determined from the regression to the CHCl₂CCl₃ data. In all other cases, parameters were independently obtained to avoid assumptions concerning product distribution.

Gas Chromatography. GC analyses were performed with a Carlo-Erba Fractovap Series 2150 or a Carlo-Erba HRGC 5160 unit equipped with a cold on-column injector, a 30 m × 0.32 mm i.d. thick film (5-μm cross-linked SE-30 equivalent) fused-silica capillary column (Restek Corp., Bellefonte, PA), and a ⁶³Ni electron capture detector. Concentrations were determined by comparing peak areas for samples to those measured for external standards. Because the detector response was nonlinear, standards were analyzed each day generally at five or more concentrations spanning the ranges measured in the samples, and a calibration curve was obtained by fitting the responses to a curve of the form (area) = a(picomoles)^b.

GC/MS Analyses. GC/MS measurements of hexane extracts were conducted with a Hewlett-Packard Model 5995 gas chromatograph/mass spectrometer. The column used was a 30-m, thin-film (0.25 μm) fused-silica capillary column with a nonpolar DB-5 (cross-linked SE-54 equivalent) phase (J&W Scientific, Folsom, CA). The mass spectra were recorded under electron impact ionization at 70 eV. For most analyses, only the following ions were monitored to maximize sensitivity: m/e 116–119, 133, and 164–172. Complete scans (m/e 59–210) were, however, performed on selected samples to confirm the identity of the transformation product.

Results

Reaction Rate vs pH. Example results of our experiments conducted with dilute buffers are shown in Figure 3. Pentachloroethane transformation under the conditions studied is relatively rapid, in many cases occurring over a period of hours to weeks. As shown in Figure 3a, concentrations of the CCl₃F tracer used to validate our reaction vessel subsampling technique displayed no tendency to decrease even over as long a period of 63 days. This compound is much more volatile (*H* = 3.65 mol L_(air)⁻¹ mol L_(water)⁻¹; ref 32) than either Cl₂C=CCl₂ (*H* ≈ 0.5–0.7; refs 33 and 34) or CHCl₂CCl₃ (*H* ≈ 0.09; ref 33). The disappearance of CHCl₂CCl₃ can thus be attributed solely to chemical transformation, rather than volatilization. Rate constants obtained at low buffer concentrations are summarized in Table I, along with information concerning buffer compositions. As demonstrated by the data in this table, transformation rates are strongly dependent on pH.

At pH < 5, *k*_{obs} values obtained from the pentachloroethane data appear somewhat larger than those obtained from the tetrachloroethylene data. One explanation for

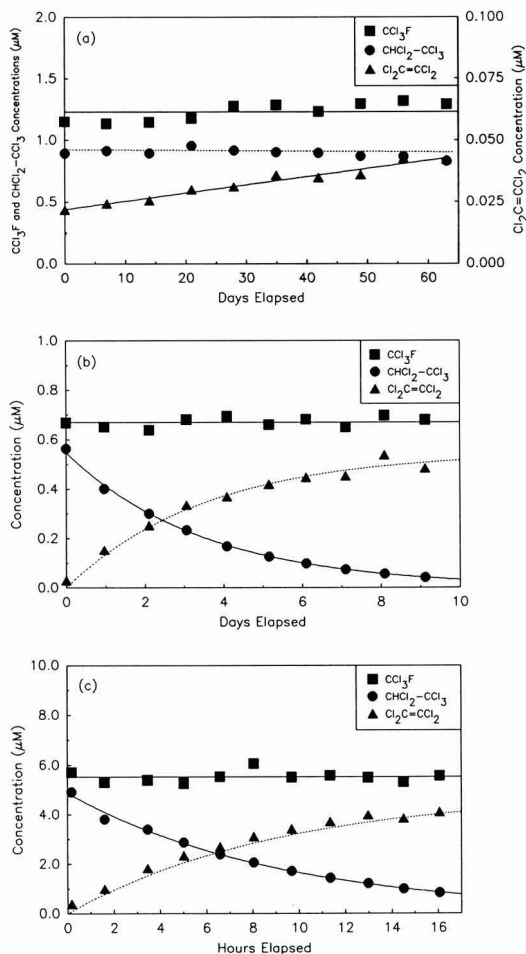


Figure 3. Example time courses showing transformation of pentachloroethane to tetrachloroethylene at 25 °C at (a) pH 4.15, (b) pH 7.09, and (c) pH 7.98. Note variations in scales. Symbols represent measured concentrations. Solid lines represent model fits or (in the case of CCl₃F data) mean concentration. Dashed lines represent predicted values.

this apparent discrepancy might simply lie in difficulties associated with making precise estimates of reaction rates from parent compound disappearance at relatively early times. Because pentachloroethane reacts very slowly at

low pH and 25–35 °C, it is difficult to obtain a very accurate estimate of its reaction rate from the pentachloroethane data, which display relatively small changes. For these experiments, the tetrachloroethylene data (which exhibit much larger changes) provide a more precise estimate. Despite the apparent discrepancy in observed rates at low pH, rate constants obtained from model fits to the tetrachloroethylene data still predict pentachloroethane concentrations quite well, as indicated on Figure 3a.

An alternative explanation for the apparent discrepancy in k_{obs} values might be that at low pH, pentachloroethane is reacting via some mechanism in addition to dehydrochlorination, such as perhaps a nucleophilic substitution reaction. In such a case, the integrated rate expression for pentachloroethane can be written as

$$(\text{CHCl}_2\text{CCl}_3) = (\text{CHCl}_2\text{CCl}_3)_0 \exp[-(k_E + k_N)t] \quad (1)$$

where k_E refers to the pseudo-first-order rate constant for dehydrochlorination to tetrachloroethylene and k_N to the corresponding rate constant for the hypothetical substitution reaction. In this case, the observed rate constant k_{obs} would correspond to the sum of $k_E + k_N$. Similarly, the expression for tetrachloroethylene would be given as

$$(\text{Cl}_2\text{C}=\text{CCl}_2) = (\text{CHCl}_2\text{CCl}_3)_0 [k_E / (k_E + k_N)] [1 - \exp[-(k_E + k_N)t]] \quad (2)$$

At relatively small time, however, $\exp[-(k_E + k_N)t]$ approaches $1 - (k_E + k_N)t$, and the expression simplifies to

$$(\text{Cl}_2\text{C}=\text{CCl}_2) \approx (\text{CHCl}_2\text{CCl}_3)_0 k_E t \quad (3)$$

i.e., the observed rate constant k_{obs} corresponds to k_E when product accumulation is monitored at early time. Although the results of Jeffers et al. (27) indicated quantitative conversion to tetrachloroethylene under all conditions investigated, their experiments at low pH were conducted at substantially higher temperatures than our experiments; elimination reactions, which frequently exhibit larger activation energies than other potential mechanisms such as substitution reactions, could contribute to a greater extent at higher temperatures than at lower temperatures. A polar product might well have been missed by our analytical technique.

For the experiments conducted at $\text{pH} \geq 7$, there is rarely any significant difference (at the 95% confidence level) between k_{obs} [or $(\text{CHCl}_2\text{CCl}_3)_0$] values obtained from the pentachloroethane data vs those obtained from the tetrachloroethylene data. For these experiments, the pentachloroethane data generally provide more precise estimates of rate constants than the tetrachloroethylene data, as indicated by the R^2 values in Table I. Rate constants obtained from model fits to the pentachloroethane data successfully predict tetrachloroethylene concentrations, as shown in Figure 3b and c. The close correspondence at higher pH between predicted and observed concentrations indicates that tetrachloroethylene represents the predominant if not the sole product of pentachloroethane transformation.

Figure 4 summarizes the relationship between rates shown in Table I and the pH at which the measurements were made. A regression on $\log k_{\text{obs}}$ vs $\log(\text{OH}^-)$ at 25 °C yielded a model fit of the form $\log k_{\text{obs}} = 1.05 (\pm 0.02) \log(\text{OH}^-) + 1.76 (\pm 0.06)$, with $R^2 = 0.9996$ (values in parentheses reflect 95% confidence intervals); similarly, at 35 °C the fit is of the form $\log k_{\text{obs}} = 1.01 (\pm 0.02) \log(\text{OH}^-) + 1.97 (\pm 0.06)$, with $R^2 = 0.9997$. In performing the regressions, the values of k_{obs} were weighted according to their estimated standard error as described by Bevington (ref 35, p 182). Because regressions performed independently on k_{obs} values obtained from the pentachloro-

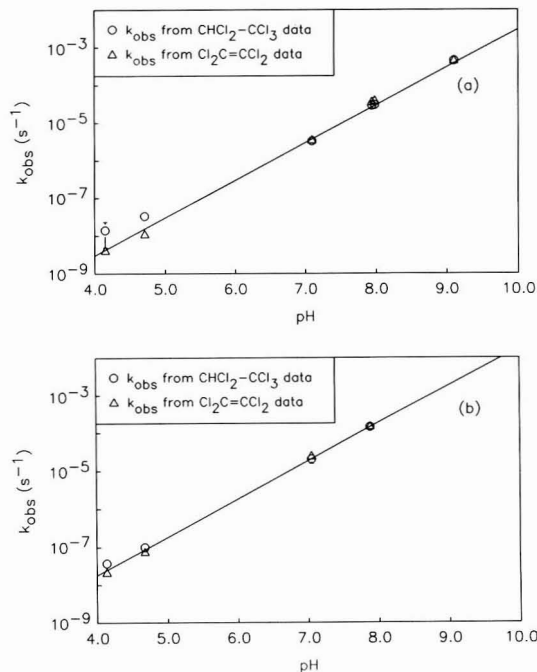


Figure 4. Observed rate constants for low ionic strength experiments as a function of pH. Solid lines indicate rates predicted from calculated second-order rate constants; (a) 25 °C results; (b) 35 °C results.

ethane data and those obtained from the tetrachloroethylene data gave results that were not significantly different at the 95% confidence level, rate constants at each temperature were pooled to yield an improved estimate.

The slopes of the model fits are very close to 1, indicating the reaction of pentachloroethane is first order in OH^- at both temperatures throughout the pH range investigated; our results do not provide any evidence for a neutral mechanism involving H_2O as a base. Analysis of our data assuming the reaction is truly first order in OH^- (again weighting k_{obs} values according to their estimated standard error) provides estimates for the second-order rate constant k_{OH^-} of $27.3 (\pm 0.3) \text{ M}^{-1} \text{ s}^{-1}$ at 25 °C and $79.7 (\pm 1.6) \text{ M}^{-1} \text{ s}^{-1}$ at 35 °C. Pseudo-first-order rate constants predicted from this k_{OH^-} value are shown in Figure 4 and also in Table I. Omitting the k_{obs} values determined at pH 4.1–4.2 does not significantly affect the magnitudes of k_{OH^-} estimates at either temperature. Our results correspond to a half-life for pentachloroethane of approximately 2.9 days at pH 7, 25 °C. This is somewhat less than the half-life of 3.5 days calculated from the results of Walraevens et al. (26) or the value of 3.7 days given by Jeffers et al. (27) and greater than the value of 1.7 days given by Cooper et al. (28), yet still within the 95% confidence limits reported by each of these investigators or computed from their data.

Isotope-Exchange Experiment. To investigate the possibility of an $(\text{E}_{1\text{CB}})_\text{R}$ mechanism, we conducted an isotope-exchange experiment in D_2O . The buffer used in this experiment contained 10 mM $(\text{PO}_4)_\text{T}$ plus 10 mM $(\text{BO}_3)_\text{T}$, with an ionic strength of approximately 0.025 equiv/L and pD 8.69. This buffer was spiked to give an initial pentachloroethane-*h* concentration of 50 μM . Under the chromatographic conditions used in GC/MS analyses of hexane extracts of this buffer, tetrachloroethylene,

Table II. Results of Dehydrochlorination Experiments Conducted at 25 °C in H₂O To Investigate General-Base (Buffer) Catalysis^a

pH	mM buffer	N ^b	from CHCl ₂ CCl ₃		from Cl ₂ C=CCl ₂		predicted <i>k</i> , ^c s ⁻¹
			<i>k</i> _{obs} , s ⁻¹	R ²	<i>k</i> _{obs} , s ⁻¹	R ²	
6.95	15.3 (H ₂ S) _T + 0.5 (PO ₄) _T	11	2.79 × 10 ⁻⁶	0.9989	3.75 × 10 ⁻⁶	0.9930	3.04 × 10 ⁻⁶
4.61	5 (acetate) _T	11	5.32 × 10 ⁻⁸	0.8443	7.60 × 10 ⁻⁹	0.9715	1.45 × 10 ⁻⁸
4.62	25 (acetate) _T	11	1.30 × 10 ⁻⁸	0.1226	1.07 × 10 ⁻⁸	0.9811	1.48 × 10 ⁻⁸
4.62	50 (acetate) _T	11	2.67 × 10 ⁻⁸	0.5068	9.71 × 10 ⁻⁹	0.9810	1.50 × 10 ⁻⁸
4.63	75 (acetate) _T	11	3.25 × 10 ⁻⁸	0.7373	8.40 × 10 ⁻⁹	0.9742	1.51 × 10 ⁻⁸
4.63	100 (acetate) _T	11	3.44 × 10 ⁻⁸	0.8276	8.86 × 10 ⁻⁹	0.9728	1.53 × 10 ⁻⁸

^a Ionic strength 0.05 equiv/L for H₂S/HS⁻ buffer and 0.1 equiv/L for acetic acid/acetate buffers. ^b N, number of samples. ^c Predicted pseudo-first-order rate in absence of buffer catalysis.

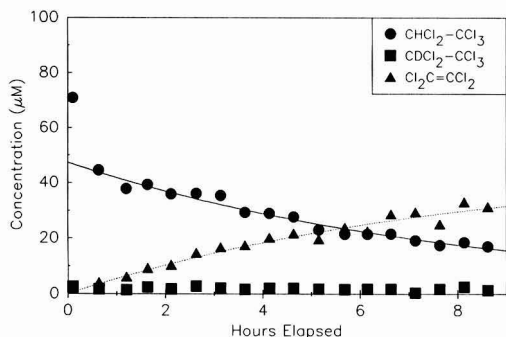


Figure 5. Results of isotope-exchange experiment conducted in D₂O at 25 °C. Solid line through CHCl₂CCl₃ data represents exponential fit; dashed line through Cl₂C=CCl₂ data shows predicted values assuming all CHCl₂CCl₃ is converted to Cl₂C=CCl₂.

1,1,1,2-tetrachloroethane, and pentachloroethane were all fully resolved. Lacking a deuterated pentachloroethane standard, however, we could not be certain that this would also be the case for pentachloroethane-*d* and pentachloroethane-*h*; our method of data analysis assumed the labeled and unlabeled pentachloroethane would coelute. In analyzing each sample, the ion *m/e* 166 (corresponding to ³⁵Cl₃³⁷Cl¹²C₂) was used to calculate tetrachloroethylene concentrations. The ion *m/e* 117 (³⁵Cl₃¹²C) was used to monitor total pentachloroethane. Because pentachloroethane lacks a parent ion, pentachloroethane-*h* concentrations were computed from *m/e* 165 (³⁵Cl₄¹²C₂H) [after correcting for ³⁵Cl₄¹³C¹²C based on ¹³C abundances reported by McLafferty (36)]. The ion *m/e* 168 (³⁵Cl₃³⁷Cl¹²C₂D) proved useful for calculating pentachloroethane-*d* concentrations (after similar corrections for ³⁵Cl₃³⁷Cl¹³C¹²CH and ³⁵Cl₂³⁷Cl₂¹²C₂).

The results are shown in Figure 5. After an initial mixing period, pentachloroethane concentrations exhibited first-order decay; pentachloroethane-*h* concentrations computed from *m/e* 165 were essentially equal to total pentachloroethane calculated from *m/e* 117. No trend was detected in the results for pentachloroethane-*d*, which remained at our detection limit. Pentachloroethane-*h* disappearance was accompanied by the production of tetrachloroethylene. The pseudo-first-order rate constant calculated from pentachloroethane disappearance (3.4 × 10⁻⁵ s⁻¹) is not significantly different from the rate constant calculated from tetrachloroethylene appearance (3.6 × 10⁻⁵ s⁻¹). As in previous graphs, the dashed line through the tetrachloroethylene data represents a prediction based on the fit to the pentachloroethane-*h* data, assuming tetrachloroethylene is the sole product of pentachloroethane transformation. The second-order rate constant *k*_{OD} that can be estimated from the pentachloroethane data (44.2 M⁻¹ s⁻¹) is 1.6 times that determined for *k*_{OH} at 25 °C,

within the range of solvent isotope effects measured for E₂ reactions (37, 38) and slightly larger than reported *k*_{OD}/*k*_{OH}⁻ ratios of ~1.5 for (E₁CB)₁ reactions (39). Substantially larger solvent isotope effects as great as 7.7 have been reported for (E₁CB)_R reactions (40).

Buffer Catalysis. Two buffer systems were used to investigate general-base (buffer) catalysis at 25 °C, H₂S/HS⁻ and acetic acid/acetate. Buffer compositions used and experimental results are summarized in Table II, along with rates predicted (in the absence of buffer catalysis) from *k*_{OH}⁻ and the measured pH.

Initial experiments (using H₂S/HS⁻ as a buffer) failed to display any buffer catalysis, in agreement with the observations of Walraevens et al. (26) with phenolate buffers. The second-order rate constant computed by using the measured OH⁻ concentration (25 M⁻¹ s⁻¹) is 8% less than our estimate of *k*_{OH}⁻ from the studies conducted in the absence of bisulfide ion. This discrepancy is within our estimates of experimental error at this pH, based on duplicate measurements at pH 8, 25 °C (Table I), as well as on the results of preliminary replicate experiments that were carried out at pH 4–7 (data not included).

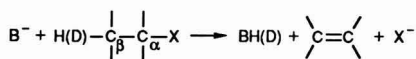
Experiments conducted with varying concentrations of total acetate at pH 4.6 also failed to reveal buffer catalysis. As with other experiments at this pH, the extent of pentachloroethane transformation during the course of these incubations was so slight that the tetrachloroethylene data are considered to provide a better estimate of the dehydrochlorination rate. Subtracting the contribution of *k*_{OH}⁻(OH⁻) from the observed rates should yield the acetate-promoted rate; no significant trend was discernable in a regression of these rates vs acetate concentration (R² = 0.07). This indicates differences in observed rates are dominated by experimental error rather than by buffer catalysis. Neglecting any potential contribution from an acetate-promoted reaction, the *k*_{OH}⁻ values calculated in these experiments exhibited a relative standard deviation of 13%, an estimate of experimental error that can be used in establishing a lower limit on the Brønsted coefficient β.

Discussion

Mechanism of Pentachloroethane Dehydrochlorination. Available Tests of Mechanism. Several tests have been proposed (9, 41, 42) for differentiating between E₂ and E₁CB reactions: those pertinent are summarized in Table III. For purposes of the present study, the isotope-exchange experiment provides the most definitive test. The lack of any detectable conversion of pentachloroethane-*h* to pentachloroethane-*d* through observations over more than 1 half-life proves that proton transfer is not faster than chloride ion elimination, decisively ruling out an (E₁CB)_R mechanism.

Many of the remaining tests in Table III can also be used to distinguish between the various possibilities, yet une-

Table III. Tests Useful in Differentiating between E₂ and E_{1CB} Mechanisms of Base-Promoted Dehydrohalogenation Reactions^a



test	mechanism			
	E ₂ ^b	(E _{1CB}) ₁	(E _{1CB}) _{ip}	(E _{1CB}) _R
β-protium exchange faster than elimination?	no	no	no ^c	yes
ΔV [‡] value ^d	negative	positive ^e	positive	positive
k _H /k _D	2-8	2-8	1-1.2 ^f	1.0 ^g
leaving group element or isotope effect	small	small to negligible	substantial	substantial
ΔS [‡] value ^h		more negative for E ₂ or (E _{1CB}) ₁	than for (E _{1CB}) _R	
susceptible to buffer catalysis?	yes	yes	yes ⁱ	no

^a Primarily adapted from ref 42. ^b Assuming an E₂ transition state with considerable carbanion character. ^c An example of an (E_{1CB})_{ip} reaction accompanied by protium exchange has, however, been described by Koch et al. (24). ^d Results predicted by Brower et al. (41). ^e Note, however, that Brower et al. (41) measured a negative value for 2-chloroethyl phenyl sulfone, a substrate that appears to react via an (E_{1CB})₁ mechanism. ^f Substantially larger values have been reported for some substrates which nonetheless appear to react via an (E_{1CB})_{ip} mechanism [e.g., k_H/k_D = 4.34 for C₆H₅CLBrCH₂Br (23)]. ^g Somewhat larger values have, however, been reported for (E_{1CB})_R-like reactions [e.g., 1.42 for chloroform (43)]. ^h Results predicted by Saunders and Cockerill (9); by analogy, results for (E_{1CB})_{ip} reactions might be assumed to resemble (E_{1CB})_R results. ⁱ Only when ion pair assists in removal of leaving group or when first step is rate-limiting.

quovocally identifying the correct mechanism in the absence of β-hydrogen exchange still represents a challenging problem in physical organic chemistry. Although measuring the volume of activation ΔV[‡], primary kinetic isotope effect k_H/k_D, and leaving group isotope or element effects might help pinpoint the mechanism, such experiments are difficult to conduct, requiring measurement of rates as a function of pressure or synthesis of isotopically labeled substrates. Moreover, several recent studies indicate the results of such tests can prove ambiguous, as suggested by the footnotes in Table III. We therefore restrict our discussion primarily to the significance of ΔS[‡] values and buffer catalysis, since these formed the basis for the suggestion of an E_{1CB} mechanism by Walraevens et al. (26).

Significance of Activation Entropy. Saunders and Cockerill (9) suggested that activation entropy ΔS[‡] might be used to distinguish between E₂ and E_{1CB} mechanisms. The slow step in (E_{1CB})_R and (E_{1CB})_{ip} reactions involves halide ion elimination from a carbanion, a unimolecular process; in gas-phase reactions, such processes are frequently characterized by positive ΔS[‡] values. Conversely, the slow step in E₂ and (E_{1CB})₁ reactions involves a collision and formation of an activated complex between the base and the substrate, a bimolecular process that (again ignoring solvation effects) might be expected to give rise to negative ΔS[‡] values. Saunders and Cockerill (9) suggested that ΔS[‡] should be more negative for E₂ or (E_{1CB})₁ reactions in solution than for (E_{1CB})_R reactions, but cautioned that this criterion's reliability had not been tested. Data for dehydrofluorination of pentahaloethanes (44) [(E_{1CB})_R reaction] and C₆H₅CHClCF₃ (24) [(E_{1CB})_{ip} mechanism] exhibit positive ΔS[‡] values of 50–100 J mol⁻¹ K⁻¹ in methanol solution, which might appear consistent with the predictions of Saunders and Cockerill (9). Other halo-genated ethanes believed to react via (E_{1CB})_{ip} mechanisms, such as C₆H₅CHBrCF₂Br, C₆H₅CHClCF₂Cl, *p*-ClC₆H₄CHClCF₂Cl, and C₆H₅CHBrCH₂Br, however, reveal smaller ΔS[‡] values in ethanol or methanol of -8 to 20 J mol⁻¹ K⁻¹ (23).

Activation parameters for base-promoted elimination reactions of chlorinated ethanes are summarized in Table IV. ΔH[‡] values for a given substrate generally agree closely; this rarely is the case with ΔS[‡] values, however, which display considerable scatter, reflecting their relatively small contribution to ΔG[‡]. Precise measurements of ΔS[‡] are notoriously difficult to obtain. Although error

Table IV. Activation Parameters for Base-Promoted Dehydrochlorination Reactions of Chlorinated Ethanes in Aqueous Solution^a

substrate	ΔH [‡] , kJ mol ⁻¹	ΔS [‡] , J mol ⁻¹ K ⁻¹	N ^b	ref
CH ₂ CCH ₂ Cl	82.4	-70 (120 °C)	2	45
CH ₂ CCH ₂ Cl ^c	93.8 ± 0.2	-40	5	26
CH ₂ CCH ₂ Cl ^c	95.0	-30	d	46
H ₃ CCHCl ₂ ^c	110 ± 4	-20	5	27
Cl ₂ HCCH ₂ Cl ^e	91.3 ± 0.2	10	5	26
Cl ₂ HCCH ₂ Cl ^e	88 ± 17	-10	4	27
CH ₂ CCCl ₃ ^c	105 ± 1	40	6	26
CH ₂ CCCl ₃ ^c	98 ± 3	20	4	27
Cl ₂ HCCHCl ₂ ^c	91.9 ± 0.3	60	4	26
Cl ₂ HCCHCl ₂ ^c	89 ± 3	50	11	47
Cl ₂ HCCHCl ₂ ^c	76 ± 2	3	4	27
Cl ₂ HCCCl ₃ ^c	61.1 ± 0.4	-10	5	26
Cl ₂ HCCCl ₃ ^c	79 ± 21 ^{c,d}	40	5	27
Cl ₂ HCCCl ₃ ^c	75 ± 2	40	6	28
Cl ₂ HCCCl ₃ ^c	78 ± 2 ^e	50	2	this study

^a Estimated error limits correspond to twice the estimated standard deviation unless otherwise noted. ^b Number of different temperatures at which reaction rates were measured. ^c Complete product information not provided; calculated activation parameters assume Arrhenius parameters correspond entirely to a single dehydrochlorination reaction. ^d Information not provided. ^e For reaction to 1,1-dichloroethylene. ^f One standard deviation. ^g Estimated error limits based on calculated uncertainty in second-order rate constants at each temperature.

limits on ΔS[‡] could be estimated from uncertainties in the intercepts of the Arrhenius plots, a more meaningful estimate of the uncertainty in ΔS[‡] can be approximated as σ_{ΔS[‡]} ≈ σ_{ΔH[‡]}/T (48). For the substrates in Table IV, such an estimation indicates relative errors in ΔS[‡] are often large, limiting the usefulness of ΔS[‡] as a diagnostic test of reaction mechanism.

The negative ΔS[‡] value computed for pentachloroethane by Walraevens et al. (26) stood out in contrast to the positive values they obtained for most other chlorinated ethanes, forming part of the reason why these researchers hypothesized (without further justification of their logic) that it might react via an E_{1CB} mechanism. Although our results, being based on measurements at only two temperatures, undoubtedly contain significant uncertainty, our estimated ΔS[‡] value of 50 J mol⁻¹ K⁻¹ is still substantially

different from the value of $-10 \text{ J mol}^{-1} \text{ K}^{-1}$ determined by Walraevens et al. (26). Moreover, it is virtually identical with ΔS^\ddagger values calculated from the results of Jeffers et al. (27) and Cooper et al. (28).

With the exception of the ΔS^\ddagger value reported for pentachloroethane by Walraevens et al. (26), the ΔS^\ddagger values in Table IV generally increase with increasing substrate chlorination. Of these substrates, pentachloroethane (which has the most acidic hydrogen) is the most likely to react via an $(E_{1CB})_R$ pathway, yet our isotope-exchange results prove otherwise. The majority of the ΔS^\ddagger values in Table IV are positive even though negative ΔS^\ddagger values might be expected for bimolecular reactions.

Most published studies of elimination mechanisms have been conducted with charged substrates in aqueous solution or neutral substrates in organic solvents. Solvation of neutral molecules by water is sufficiently different that the results of such experiments should be extrapolated with care to hydrophobic compounds in aqueous solution. We do not believe that positive ΔS^\ddagger values are inconsistent with an E_2 mechanism; both the apparent discrepancy between the positive ΔS^\ddagger measurements and anticipated values and the general increase in ΔS^\ddagger with chlorination can be explained as resulting from solvation. Smaller ions being more highly solvated in water than larger ions, there should be a greater increase in entropy in the activated complex $[\text{HO}\cdots\text{H}\cdots\text{C}(\text{R}^1\text{R}^2)\cdots\text{C}(\text{R}^3\text{R}^4)\cdots\text{Cl}]^-$ as chlorine is successively substituted for hydrogen in $\text{R}^1\text{-R}^4$, either for the transition state for an E_2 reaction or for the corresponding transition state for the first step of an $(E_{1CB})_I$ reaction. At the same time, S° values for the solvated ground-state substrate $\text{H-C}(\text{R}^1\text{R}^2)\text{-C}(\text{R}^3\text{R}^4)\text{Cl}$ should decrease with increasing substitution as more water molecules become organized around progressively larger solution cavities (49). The value of ΔS^\ddagger , which reflects the difference $S^\circ_{\text{transition state}} - (S^\circ_{\text{OH}^-} + S^\circ_{\text{substrate}})_{\text{ground state}}$, should thus increase with increasing chlorination, as observed. Although loss of translational and vibrational energy as two species interact to form an activated complex might tend to decrease entropy, inclusion of solvation effects can still result in positive ΔS^\ddagger values for bimolecular reactions. All of this suggests that the sign of the ΔS^\ddagger value may not reliably indicate whether reactions in aqueous solution occur via E_{1CB} mechanisms: citing a negative ΔS^\ddagger value in support of an E_{1CB} pathway appears tenuous.

Buffer Catalysis in Pentachloroethane Dehydrochlorination. The other factor leading Walraevens et al. (26) to suggest an E_{1CB} mechanism for pentachloroethane was the lack of observed general-base (buffer) catalysis in the presence of a phenolate buffer. With PhO^-/OH^- ratios from 10^3 to 10^4 , rates measured at 25°C were only 1–2 times the rate in the absence of phenolate (interpolated from measurements conducted at other temperatures). We have also observed a negligible effect with an even higher ratio of HS^-/OH^- (10^5) in our experiments with hydrogen sulfide/bisulfide buffers. This encouraged us to search for buffer catalysis in acid–base systems with lower pK_a values.

Brønsted and Pedersen (50) noted that the kinetic reactivity of an acid or base buffer species could be related to its thermodynamic strength as an acid or base. For base-promoted processes such as bimolecular elimination mechanisms, the relationship takes the form

$$k_B = G(K_{\text{HB}})^{-\beta} \quad (4)$$

where k_B is the second-order rate constant for general-base catalysis by the base B^- , G is a constant for a given substrate, K_{HB} is the ionization constant for the acid HB , and the Brønsted coefficient β reflects the susceptibility of a given substrate to general-base catalysis. The parameter

β is often interpreted as indicating the extent of proton transfer between the substrate and the base in the transition state; its value should therefore lie between 0 and 1 (barring complications such as quantum-mechanical tunneling). Thus, for $(E_{1CB})_R$ and presumably for most $(E_{1CB})_{\text{ip}}$ reactions (assuming formation of ion pairs generally proceeds as a rapidly reversible preliminary equilibrium step), β should equal 1, whereas for $(E_{1CB})_I$ and E_2 mechanisms, β should be somewhat less than 1.

It can be difficult to observe buffer catalysis for substrates with high (or low) values of β . If the enhancement by a buffer constituent B^- of a base-promoted reaction is given by the ratio $(k_B)(\text{B}^-)/(k_{\text{OH}^-})(\text{OH}^-)$ [ignoring any contribution from $k_{\text{H}_2\text{O}}(\text{H}_2\text{O})$], it can be shown (43) that this ratio is equal to

$$\frac{(k_B)(\text{B}^-)}{(k_{\text{OH}^-})(\text{OH}^-)} = (\text{HB}) \left[\frac{K_{\text{HB}}}{K_{\text{W}}} \right]^{1-\beta} \quad (5)$$

For $(E_{1CB})_R$ or $(E_{1CB})_{\text{ip}}$ reactions with $\beta = 1$, concentrations of the acidic form of the buffer (HB) as high as 0.1 M would only produce a 10% rate enhancement. For smaller values of β , greater enhancement is predicted for higher ratios of $K_{\text{HB}}/K_{\text{W}}$. Although weaker bases are less effective than OH^- at removing protons, their greater abundance at low pH can more than compensate for their lesser reactivity. The lack of substantial catalysis by HS^- or PhO^- thus signifies a high value of β , but should not be taken to indicate an $(E_{1CB})_R$ or $(E_{1CB})_{\text{ip}}$ mechanism. Unfortunately, eq 5 cannot readily be applied to the buffer system studied by Walraevens et al. (26) to obtain an estimate for β , because the high buffer concentrations used by these investigators (0.9 M total phenol) violate the dilute solution approximations implicit in this expression.

Our studies with acetate buffers were designed to take advantage of eq 5; the ratio of ionization constants $K_{\text{HB}}/K_{\text{W}}$ is as large as possible while still permitting reaction at a rate sufficiently rapid to measure. Our observations (Table II) do not allow us to determine a precise β value for this reaction, although we can set reasonable lower limits on β . If we assume that the true experimental error at this pH is equal to the 13% relative standard deviation we observed in second-order rate constants, then at the highest acetate concentration, a β value of 0.88 should produce a rate increase equivalent to 5 times our experimental error, while a β value of 0.85 should lead to a 10-fold increase in rate, relative to experimental error. Thus, the small or negligible effect of added acetate implies a high β value (>0.85).

An estimate for β can also be obtained from the experiments conducted in D_2O , based on knowledge of the relative acidities of HOD and DOD. For E_2 reactions at 25°C , $k_{\text{OD}^-}/k_{\text{OH}^-}$ values can be related (37) to β via the expression

$$k_{\text{OD}^-}/k_{\text{OH}^-} = 2.12^\beta \quad (6)$$

When our measurements in D_2O are used, this expression results in a β value of approximately 0.64; the accuracy of this estimate is very sensitive to errors in k_{OD^-} or k_{OH^-} .

Finally, estimates of β can also be obtained by comparing the rates of OH^- -promoted and neutral elimination reactions. In this case, applying eq 4 results in the expression

$$k_{\text{H}_2\text{O}}/k_{\text{OH}^-} = 10^{-15.74\beta} \quad (7)$$

In addition, the pH below which the neutral reaction predominates can be related to β by the expression

$$\text{pH}^* = 15.74(1 - \beta) \quad (8)$$

where pH^* is the pH at which $k_{\text{H}_2\text{O}}(\text{H}_2\text{O}) = k_{\text{OH}^-}(\text{OH}^-)$.

Table V. Calculated pH* and β Values for Polychlorinated Ethanes^a

substrate	pH*	β
H ₃ C _{β} C _{α} HCl ₂	12.48	0.21
ClH ₂ C _{β} C _{α} H ₂ Cl	<10.08	>0.36
ClH ₂ C _{β} C _{α} Cl ₃	8.08	0.49
Cl ₂ HC _{β} C _{α} H ₂ Cl	4.74	0.70
Cl ₂ HC _{β} C _{α} HCl ₂	4.51	0.71
Cl ₂ HC _{β} C _{α} Cl ₃	3.58	0.77

^aEstimates obtained from rates reported by Jeffers and co-workers (27, 46).

Extrapolating measurements of the rates of the neutral and base-promoted dehydrochlorination reaction of pentachloroethane reported by Jeffers et al. (27) to 25 °C, we can estimate values of β and pH* of 0.77 and 3.58, respectively.

Bronsted Coefficients for Other Polychlorinated Ethanes: Structure-Reactivity Implications. In addition to pentachloroethane, the results of Jeffers et al. (27) can be used to estimate β for other polychlorinated ethanes. Some caveats should however be noted in applying eq 7 or 8 to this data set. Complete product information was not generally provided (with the exception of pentachloroethane); other pathways such as substitution reactions may have contributed to observed rates. In most cases, substrate inertness required extrapolating results from higher temperatures to 25 °C. Nevertheless, this expression is relatively insensitive to errors in either second-order rate constant. Calculated values of β and pH*, summarized in Table V, reveal interesting trends. Increasing halogenation clearly produces increasing values of β , associated with lower pH* values below which the neutral reaction predominates. Chlorine substituents on C _{β} have a markedly greater impact on β than substituents on C _{α} . We can test whether the inductive effects of chlorine atoms as given by these β values contribute in an additive manner to the "acidity" of the hydrogen via a linear free-energy relationship. If we ignore steric effects, such a relationship might be given by the expression

$$\log_{10} (k_{\text{OH}^-} / k_{\text{H}_2\text{O}}) = 15.74\beta = \rho(n\sigma_{\beta\text{Cl}} + m\sigma_{\alpha\text{Cl}}) \quad (9)$$

where ρ represents the sensitivity of β values to inductive effects, n the number of chlorine atoms on C _{β} , and m the number of chlorine atoms on C _{α} . The parameters $\sigma_{\beta\text{Cl}}$ and $\sigma_{\alpha\text{Cl}}$ represent the inductive effects of a chlorine substituent on C _{β} and C _{α} , respectively. Applying a multiple regression to the limited set of data provided by 1,1-dichloroethane, 1,1,1,2-tetrachloroethane, 1,1,2-trichloroethane, 1,1,2,2-tetrachloroethane, and pentachloroethane results in estimated values of $\rho\sigma_{\beta\text{Cl}} = 4.54$ and $\rho\sigma_{\alpha\text{Cl}} = 1.16$ ($R^2 = 0.995$). That is, the inductive effect of a chlorine atom on C _{β} is nearly 4 times as great as that of a chlorine atom on C _{α} . This relative effect accords reasonably well with inductive constants obtained from the study of other systems. For example, for the polar substituent constant σ_1 (with σ_1 for H defined as 0), values are ~ 0 for CH₃, 0.17 for CH₂Cl, and 0.46 for Cl (51). For the polychlorinated ethanes in Table V, these inductive effects are primarily expressed through k_{OH^-} values, which tend to increase dramatically with increasing halogenation.

Implications for Experimental Determination of Dehydrohalogenation Kinetics. Recent investigations (e.g., ref 47) have conducted dehydrohalogenation experiments at high (0.1 M) buffer concentrations. Such systems certainly present advantages in terms of ease of obtaining stable pH measurements, but they raise the question of whether the results are subject to error because

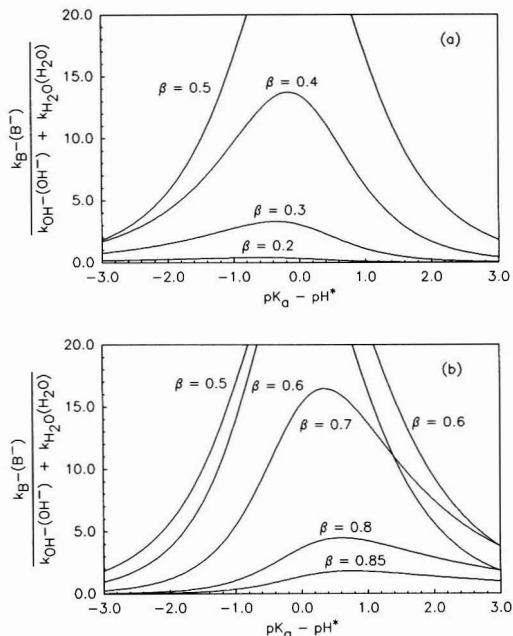


Figure 6. Theoretical contribution of buffer catalysis to dehydrohalogenation rates measured in buffer systems of varying pK_a as a function of substrate pH^* and β . Calculations assume pH of experimental system equals buffer pK_a , with total buffer concentration of 0.10 M; (a) $\beta \leq 0.5$; (b) $\beta \geq 0.5$.

of unrecognized buffer catalysis. For any dehydrohalogenation experiment, the total rate will be the sum of the contributions from the OH⁻-promoted, the buffer-promoted, and the neutral reaction, i.e.:

$$\text{observed rate} = k_{\text{OH}^-}(\text{OH}^-) + k_{\text{B}^-}(\text{B}^-) + k_{\text{H}_2\text{O}}(\text{H}_2\text{O}) \quad (10)$$

The relative magnitudes of these terms can be estimated for any system for a given pH and buffer concentration from the Bronsted relationship. If we assume experiments are conducted at a pH equal to the pK_a of the buffer acid-base system, we can plot the contribution of the $k_{\text{B}^-}(\text{B}^-)$ term for various values of β as a function of the difference between the pH of the experiment (the pK_a of the buffer) and the pH^* value of the substrate, as shown in Figure 6. Our calculations indicate that buffer catalysis is most likely to be important in an experiment at pH values near the pH^* value, especially for substrates with intermediate values of β . At higher pH, the greater ratio of OH⁻ to the conjugate base of the buffer salt makes significant buffer catalysis less likely, especially as β increases, while at lower pH, the much greater abundance of H₂O will cause the $k_{\text{H}_2\text{O}}(\text{H}_2\text{O})$ term to dominate the rate expression, particularly for substrates with small values of β .

Such an analysis may explain the results of Burlinson et al. (52), who noted that different buffers varied in their ability to catalyze the dehydrohalogenation of 1,2-dibromo-3-chloropropane. For this substrate, we can estimate β and pH^* values at 25 °C of 0.6 and 6.9 from their data obtained at other temperatures. With this β value, 1,2-dibromo-3-chloropropane should be more susceptible to general-base catalysis by buffers with a pK_a near 6.9 than by buffers with substantially higher or lower pK_a values. Observations of catalysis in experiments conducted at pH 6.8–6.9 with H₂PO₄⁻/HPO₄²⁻ buffers ($pK_a \approx 7$), but not with H₃BO₃/H₂BO₃⁻ buffers ($pK_a \approx 9$) at pH 8.9, or

with phthalate buffers ($pK_{a1} \approx 3$, $pK_{a2} \approx 5$) at pH 4, agree qualitatively with these predictions.

Conclusions with Respect to Pentachloroethane Reaction Mechanism. In terms of understanding the mechanism of pentachloroethane dehydrochlorination, the values estimated for the Brønsted coefficient β indicate a high degree of proton transfer in the transition state. Although we cannot rule out an $(E_{1CB})_I$ or an $(E_{1CB})_{IP}$ pathway from the available data, we still believe the most likely mechanism is the concerted E_2 reaction, albeit via a transition state with considerable E_{1CB} character in the context of a variable transition-state model. If any substrate reacts via a concerted mechanism, then the simple chlorinated alkanes of Table IV certainly represent likely candidates. The absence of any abrupt change in activation parameters for pentachloroethane (Table IV) might indicate a common reaction mechanism, although uncertainties in many of the available measurements somewhat weaken this argument.

Additional evidence in favor of an E_2 mechanism is provided by comparing the kinetics of pentachloroethane dehydrochlorination with rates of proton exchange for chloroform and 1,1,1-trifluoro-2,2-dichloroethane. In the case of an E_{1CB} mechanism for pentachloroethane, the rate of proton removal (k_1 in Figure 2b) ought to be similar for all three substrates, under the reasonable assumption that these are dominated by inductive effects. Using a deprotonation rate extrapolated from $CDCl_3$ reaction with OH^- in H_2O of $0.202 M^{-1} s^{-1}$ (14), and applying the primary hydrogen isotope effect of 1.42 (43), we can estimate a rate for the deprotonation of $CHCl_3$ by OH^- in H_2O of $0.29 M^{-1} s^{-1}$ at 25 °C. Available data are insufficient to provide as precise an estimate of the rate of $CHCl_2CF_3$ deprotonation in H_2O , but an approximate rate of $\sim 0.2 M^{-1} s^{-1}$ for this reaction can be obtained from data for $CDCl_2CF_3$ in methanol (19), noting that $CHCl_2CF_3$ proton transfer in D_2O at 0 °C is 10 times faster than $CDCl_2CF_3$ deuterium exchange in methanol at the same temperature. If pentachloroethane were to react via any E_{1CB} mechanism, then the overall rate of dehydrochlorination could not be any faster than the rate of this first step in the reaction sequence. That pentachloroethane's reaction is 2 orders of magnitude faster than the rates of proton exchange for chloroform and 1,1,1-trifluoro-2,2-dichloroethane suggests that some other factor, such as partial double-bond formation accompanied by partial carbon-chlorine bond breakage, is stabilizing the transition state.

Implications for Hexachloroethane Transformation. Our results indicate that pentachloroethane undergoes dehydrochlorination via a bimolecular, pH-dependent reaction at a rate that is rapid relative to other polychlorinated ethanes. Although we cannot prove this transformation occurs via a concerted E_2 mechanism, we can rule out a stepwise $(E_{1CB})_R$ mechanism and can discount an $(E_{1CB})_{IP}$ mechanism in which reprotonation to revert to the starting material is much more rapid than halide ion elimination to yield tetrachloroethylene. Thus, pentachloroethane occasionally reported from the reduction of hexachloroethane is not likely to result from protonation of a free pentachloroethyl carbanion, but rather is almost certainly produced by hydrogen atom abstraction by a pentachloroethyl radical. This may be true even for intermediates stabilized as organometallic complexes in the active sites of enzymes. On the basis of electron donor mass balances, Nastainczyk et al. (7) concluded that all of the pentachloroethane they observed during the reduction of hexachloroethane by cytochrome P-450 in rat liver microsomal preparations resulted from H^\bullet abstraction

by a pentachloroethyl radical rather than via carbanion protonation. Production of pentachloroethane thus might prove useful as a diagnostic feature for free radical as opposed to two-electron mechanisms for hexachloroethane reduction.

Because pentachloroethane dehydrochlorination to tetrachloroethylene may be rapid, any study of hexachloroethane reduction mechanisms needs to address the possibility that pentachloroethane might represent a reaction intermediate. This is particularly true for experiments conducted at high pH or for experiments conducted at neutral pH if hexachloroethane reduction is relatively slow. Depending on the relative rates of hexachloroethane and pentachloroethane transformation to tetrachloroethylene, even minor amounts of pentachloroethane may signify a role as a reaction intermediate rather than a side product. In such a case, the reduction of hexachloroethane to tetrachloroethylene (rapidly becoming entrenched in the environmental chemistry literature as an example of reductive elimination) might even prove to occur to a significant extent via the entirely incidental dehydrochlorination reaction of pentachloroethane. Studies we have conducted investigating the reduction of hexachloroethane by microorganisms under reducing conditions in groundwater (8) revealed traces of pentachloroethane, absent in poisoned controls. Consideration of the relative rates of hexachloroethane and pentachloroethane transformation indicates that even though measured concentrations of pentachloroethane were very low, a significant fraction of the transformation pathway—on the order of 20–30% or more—could still be proceeding via a pentachloroethane intermediate. Our results should provide parameters needed by future studies to further address this issue.

Acknowledgments

We gratefully acknowledge the helpful comments provided by Dr. F. D. Greene, Dr. O. C. Zafiriou, Dr. F. M. Morel, Dr. P. M. Jeffers, and Dr. W. J. Cooper. AUTOCAD figures were generated through J. MacFarlane's wizardry.

Registry No. Cl_2CHCCl_3 , 76-01-7; $Cl_2C=CCl_2$, 127-18-4.

Literature Cited

- (1) Criddle, C. S.; McCarty, P. L.; Elliott, M. C.; Barker, J. F. *J. Contam. Hydrol.* **1986**, *1*, 133–142.
- (2) Jafvert, C. T.; Wolfe, N. L. *Environ. Toxicol. Chem.* **1987**, *6*, 827–837.
- (3) Reinhard, M.; Curtis, G. P.; Buehler, C. Abiotic reductive dehalogenation of perhaloalkanes in clay and sediment slurries. *EOS, Trans. Am. Geophys. Union* **1988**, *69*, 1201 (Abstr.).
- (4) Curtis, G. P.; Reinhard, M. Reductive dehalogenation of hexachloroethane by aquifer materials. *Natl. Meet.—Am. Chem. Soc., Div. Environ. Chem.* **1989**, *29*, 85–86 (Abstr.).
- (5) Peijnenburg, W.; den Hollander, H.; Verboom, H.; van de Meent, D.; Wolfe, N. L. Transformations of halogenated hydrocarbons in anoxic heterolytic systems: rates, mechanisms and products. *Natl. Meet.—Am. Chem. Soc., Div. Environ. Chem.* **1989**, *29*, 87–89 (Abstr.).
- (6) Mansuy, D.; Fontecave, M. *Biochem. Biophys. Res. Commun.* **1982**, *104*, 1651–1657.
- (7) Nastainczyk, W.; Ahr, H. J.; Ullrich, V. *Biochem. Pharmacol.* **1982**, *31*, 391–396.
- (8) Roberts, A. L. Ph.D. Thesis, Massachusetts Institute of Technology, in preparation.
- (9) Saunders, W. H., Jr.; Cockerill, A. F. *Mechanisms of Elimination Reactions*; John Wiley and Sons: New York, 1973.
- (10) Leitch, L. C.; Bernstein, H. J. *Can. J. Res.* **1950**, *28B*, 35–36.
- (11) Houser, T. J.; Bernstein, R. B.; Miekka, R. G.; Angus, J. C. *J. Am. Chem. Soc.* **1955**, *77*, 6201–6203.

- (12) Miller, S. I.; Lee, W. G. *J. Am. Chem. Soc.* **1959**, *81*, 6313-6319.
- (13) Horiuti, J.; Sakamoto, Y. *Bull. Chem. Soc. Jpn.* **1936**, *11*, 627-628.
- (14) Hine, J.; Peek, R. C., Jr.; Oakes, B. D. *J. Am. Chem. Soc.* **1954**, *76*, 827-829.
- (15) Hine, J.; Burske, N. W.; Hine, M.; Langford, P. B. *J. Am. Chem. Soc.* **1957**, *79*, 1406-1412.
- (16) Hine, J.; Butterworth, R.; Langford, P. B. *J. Am. Chem. Soc.* **1958**, *80*, 819-824.
- (17) Hine, J.; Burske, N. W. *J. Am. Chem. Soc.* **1956**, *78*, 3337-3339.
- (18) Andreades, S. *J. Am. Chem. Soc.* **1964**, *86*, 2003-2010.
- (19) Hine, J.; Wiesboeck, R.; Ghirardelli, R. *J. Am. Chem. Soc.* **1961**, *83*, 1219-1222.
- (20) McLennan, D. J.; Wong, R. J. *J. Chem. Soc., Perkin Trans. 2* **1974**, 526-532.
- (21) McLennan, D. J.; Wong, R. J. *J. Chem. Soc., Perkin Trans. 2* **1974**, 1373-1377.
- (22) MacLaury, M. R.; Saracino, A. *J. Org. Chem.* **1979**, *44*, 3344-3347.
- (23) Koch, H. F.; Dahlberg, D. B.; McEntee, M. F.; Klecha, C. *J. Am. Chem. Soc.* **1976**, *98*, 1060-1061.
- (24) Koch, H. F.; Dahlberg, D. B.; Lodder, G.; Root, K. S.; Touchette, N. A.; Solsky, R. L.; Zuck, R. M.; Wagner, L. J.; Koch, N. H.; Kuzemko, M. A. *J. Am. Chem. Soc.* **1983**, *105*, 2394-2398.
- (25) Bordwell, F. G. *Acc. Chem. Res.* **1972**, *5*, 374-381.
- (26) Walraevens, R.; Trouillet, P.; Devos, A. *Int. J. Chem. Kinet.* **1974**, *41*, 777-786.
- (27) Jeffers, P. M.; Ward, L. M.; Woytowich, L. M.; Wolfe, N. L. *Environ. Sci. Technol.* **1989**, *23*, 965-969.
- (28) Cooper, W. J.; Slifker, R. A.; Joens, J. A.; El-Shazly, O. A. In *Biohazards of Drinking Water Treatment*; Larson, R. A., Ed.; Lewis: Chelsea, MI, 1989; Chapter 3, pp 37-46.
- (29) Perrin, D. D.; Dempsey, B. *Buffers for pH and Metal Ion Control*; Chapman and Hall: London: 1974.
- (30) Weast, R. C.; Astle, M. J.; Beyer, W. H., Eds. *CRC Handbook of Chemistry and Physics*, 64th ed.; CRC Press, Inc.: Boca Raton, FL, 1983.
- (31) Grob, K.; Habich, A. *J. High Resolut. Chromatogr. Chromatogr. Commun.* **1983**, *6*, 11-15.
- (32) Hunter-Smith, R. J.; Balls, P. W.; Liss, P. S. *Tellus* **1983**, *35B*, 170-176.
- (33) Mackay, D.; Shiu, W. Y. *J. Phys. Chem. Ref. Data* **1981**, *10*, 1175-1199.
- (34) Howe, G. B.; Mullins, M. E.; Rogers, T. N. Evaluation and Prediction of Henry's Law Constants and Aqueous Solubilities for Solvents and Hydrocarbon Fuel Components: Vol. I: Technical Discussion. Air Force Engineering and Services Center Report ESL-TR-86-66, Tyndall Air Force Base, FL, 1987.
- (35) Bevington, P. R. *Data Reduction and Error Analysis for the Physical Sciences*; McGraw-Hill: New York, 1969.
- (36) McLafferty, F. W. *Interpretation of Mass Spectra*, 3rd ed.; University Science Books: Mill Valley, CA, 1980.
- (37) Steffa, L. J.; Thornton, E. R. *J. Am. Chem. Soc.* **1967**, *89*, 6149-6156.
- (38) Thornton, E. K.; Thornton, E. R. In *Isotope Effects in Chemical Reactions*; Collins, C. J., Bowman, N. S., Eds.; Van Nostrand Reinhold: New York, 1970; pp 213-285.
- (39) Keefe, J. R.; Jencks, W. P. *J. Am. Chem. Soc.* **1983**, *105*, 265-279.
- (40) Keefe, J. R.; Jencks, W. P. *J. Am. Chem. Soc.* **1981**, *103*, 2457-2459.
- (41) Brower, K. R.; Muhsin, M.; Brower, H. E. *J. Am. Chem. Soc.* **1976**, *98*, 779-782.
- (42) Cockerill, A. F.; Harrison, R. G. In *The Chemistry of Double-Bonded Functional Groups*; Patai, S., Ed.; John Wiley and Sons: New York 1977; Part 1, Supplement A, pp 149-329.
- (43) Margolin, Z.; Long, F. A. *J. Am. Chem. Soc.* **1973**, *95*, 2757-2762.
- (44) Hine, J.; Wiesboeck, R.; Ramsay, O. B. *J. Am. Chem. Soc.* **1961**, *83*, 1222-1226.
- (45) Okamoto, K.; Matsuda, H.; Kawasaki, H.; Shingu, H. *Bull. Chem. Soc. Jpn.* **1967**, *40*, 1917-1920.
- (46) Jeffers, P. M. State University of New York, Cortland, NY, personal communication, 1990.
- (47) Cooper, W. J.; Mehran, M.; Riusech, D.; Joens, J. A. *Environ. Sci. Technol.* **1987**, *21*, 1112-1114.
- (48) Petersen, R. C.; Markgraf, J. H.; Ross, S. D. *J. Am. Chem. Soc.* **1961**, *83*, 3819-3823.
- (49) Tanford, C. *The Hydrophobic Effect: Formation of Micelles and Biological Membranes*; John Wiley and Sons: New York, 1984.
- (50) Bronsted, J. N.; Pedersen, K. *Z. Phys. Chem.* **1924**, *108*, 185-235.
- (51) Hine, J. *Structural Effects on Equilibria in Organic Chemistry*; John Wiley and Sons: New York, 1975.
- (52) Burlinson, N. E.; Lee, L. A.; Rosenblatt, D. H. *Environ. Sci. Technol.* **1982**, *16*, 627-632.

Received for review April 30, 1990. Revised manuscript received July 16, 1990. Accepted July 19, 1990. Partial funding for this research was provided by a grant from the National Institute of Environmental Health Studies (Grant 2 P30 ESO 2109-11).

Characterization of the H4IIE Rat Hepatoma Cell Bioassay as a Tool for Assessing Toxic Potency of Planar Halogenated Hydrocarbons in Environmental Samples

Donald E. Tillitt* and John P. Giesy

201 Pesticide Research Center, Department of Fisheries and Wildlife, Center for Environmental Toxicology, Michigan State University, East Lansing, Michigan 48824

Gerald T. Ankley

U.S. Environmental Protection Agency, Environmental Research Laboratory, 6201 Congdon Boulevard, Duluth, Minnesota 55804

■ An *in vitro* system, the H4IIE rat hepatoma cell bioassay, was characterized for use in assessing the overall toxic potency of PCBs, PCDDs, and PCDFs in extracts from environmental samples. This *in vitro* bioassay of cytochrome P450IA1 catalytic activity in the H4IIE cells in response to planar halogenated hydrocarbons (PHHs) was repeatable over time and standards were reproducible among laboratories when dosing conditions were similar. Three common extraction/cleanup procedures tested had no adverse effect on the response of the cells and biogenic interferences were not encountered. Comparison of the response of the H4IIE cells to extracts was calibrated against their response to the standard, 2,3,7,8-tetrachlorodibenzo-*p*-dioxin (TCDD). This method of calibration proved to be effective for quantitation of known amounts of PHHs spiked into a sample matrix. The potential utility of this bioassay is as an integrative tool to assess the toxic potency of complex mixtures of PHHs. The results of this bioassay can complement chemical residue analysis and direct the need for such analysis, as well as aid in the interpretation of biological effects data from environmental studies.

Introduction

Planar halogenated hydrocarbons (PHHs) are a group of chemicals with isosteric configurations or structures and include, among other environmental contaminants, polychlorinated biphenyls (PCBs), polychlorinated dibenzo-*p*-dioxins (PCDDs), and polychlorinated dibenzofurans (PCDFs). PHHs were used industrially for decades or were contaminants of chemical synthesis and entered the environment by both intentional and inadvertent release. The recalcitrant nature of PHHs, along with their inherent toxic properties and a propensity to bioaccumulate, has caused concern that these environmental contaminants may reach concentrations in organisms at the top of the food chain great enough to elicit toxic effects (1-4). The problem that scientists face in this respect is the evaluation of PHH residues that occur in the environment. Currently, there are analytical techniques to extract, concentrate, isolate, separate, and quantitate PHHs from environmental samples (5-9). However, concentrations of PHHs provide only part of the information necessary to evaluate their potential for adverse effects on fish, wildlife, and humans. This is because PHH congeners each have different toxic potencies (10-13) and the complex interactions of synergism, antagonism, and additivity, which are known to occur

within mixtures of PHHs (14-24), are not understood completely at this time. These interactions are not considered when attempts are made to predict biological effects from concentrations of PHHs alone.

PHHs are proximate isostereomers, which exert their toxic effects through the same biological receptor (10-12). Although differing in potency, PHHs elicit the same suite of toxicological effects across many phylogenetic lines (12). The characteristic symptoms of PHH poisoning include weight loss (wasting syndrome), thymic atrophy, subcutaneous edema, immune suppression, hormonal alterations, P450IA1-associated enzyme induction, and the reproductive effects of fetotoxicity and teratogenesis (see reviews, refs 25 and 26). Additionally, there are strong correlations between the enzyme induction potency of individual congeners and their potency for causing effects such as weight loss and thymic atrophy (27-30). These correlations are significant ($r > 0.90$) for both *in vivo* enzyme induction potency versus the toxic potency *in vivo* with rats, and for *in vitro* enzyme induction potency in H4IIE rat hepatoma cells versus the toxic potency *in vivo* in rats (31). In other words, the response of the H4IIE cells to the individual congeners was predictive of the toxic responses of whole organisms to these PHH congeners. Therein lies the potential utility of this *in vitro* bioassay as an integrative bioanalytical tool for screening PHH extracts of environmental samples.

The H4IIE cells were derived from the Reuber hepatoma H-35 (32) by Pitot and co-workers (33). It is a continuous cell line and was characterized with regard to aryl hydrocarbon hydroxylase (AHH) activity by Nebert and co-workers (34). Besides excellent growth characteristics and low basal cytochrome P450IA1 activity, they found the H4IIE cells to have inducible AHH enzyme activities. These researchers went on to characterize the AHH induction response of the H4IIE cells to 2,3,7,8-tetrachlorodibenzo-*p*-dioxin (TCDD), the prototypic PHH, and suggested that the H4IIE rat hepatoma cell culture bioassay might be useful in detecting TCDD (35). They found that the H4IIE cells are exquisite in their response to TCDD with a detection limit of 10 fmol.

Simultaneous to the developments of the H4IIE bioassay, structure-activity relationships of PHHs indicated that halogen substitution in the lateral positions of the dioxin, furan, or biphenyl molecules imparted a greater receptor affinity, AHH induction potency, and toxicity to these compounds (10-13). In particular, a strong correlation between AHH or ethoxyresorufin-*O*-deethylase (EROD) induction potency *in vitro* in the H4IIE cells and the toxic potency *in vivo* of individual biphenyl (29, 36), dioxin (37), and furan (28, 30) congeners was observed. These reports were summarized by Safe (31). The corre-

*Current address: National Fisheries Contaminant Research Center, U.S. Fish and Wildlife Service, Route 2, 4200 New Haven Road, Columbia, MO 65201.

lations of $-\log ED_{50}$ (effective dose for half-maximal induction) for weight loss in rats versus $-\log EC_{50}$ for AHH induction in H4IIE cells and $-\log ED_{50}$ for thymic atrophy in rats versus $-\log EC_{50}$ for AHH induction in H4IIE cells had correlation coefficients of 0.93 and 0.92, respectively (31). These strong correlations between *in vitro* induction potency and *in vivo* toxic potency were critical validations for the use of this bioassay for prediction of potential toxicity of PHHs.

The first use of the H4IIE bioassay as a tool for assessing complex mixtures of PHHs in extracts was by the U.S. Food and Drug Administration. They performed the initial analytical characterization of the H4IIE bioassay as an environmental extract assay (37–40). Isooctane (ISO) as the solvent carrier for extracts or pure compounds optimally enhanced bioassay sensitivity (39). A detection limit of 10 pg of TCDD was reported with the isooctane solvent carrier system, with an ED_{50} of 45 pg of TCDD/plate (0.14 pmol/plate, 28 pM). A quantitation limit for this solvent system was not reported; however, in subsequent publications the limit of quantitation was 25 pg of TCDD and the linear response range was 25–500 pg of TCDD/plate (38, 40). Thus, the sensitivity of this bioassay system for detection of PHHs had been established.

The H4IIE bioassay has been shown to be a sensitive tool for detection of PHHs in extracts of environmental samples (38–40) and much of the initial analytical characterization was performed by these scientists. However, due to improvements in PHH extractions, cleanup, and quantitation techniques in the past 10 years, studies to confirm and expand on the work already done are necessary if this bioassay technique is to be adapted as a bioanalytical tool. In this study we reexamine the isooctane carrier solvent system, detection and quantitation limits, and some reference toxicants. Additionally, we investigate potential endogenous and exogenous interferences of matrices or extraction protocols. We also investigate the quantitative ability of the H4IIE bioassay with spike/bioanalysis experiments. These studies are important because to date investigations of this bioassay have been fragmented and performed in different laboratories. This is the first study to systematically investigate the H4IIE bioassay as a quantitative bioassessment tool for PHHs.

Experimental Section

Extractions and Spike/Bioanalysis Protocols. Three extraction and cleanup protocols were investigated: the method used by FDA scientists in the original bioassay reports (41); an improved method used for PCB analysis, which utilizes column extractions with dichloromethane (6); and a modification of this latter method, which results in extracts that contain PCBs, PCDDs, and PCDFs in one fraction (42). The PAM procedure (41), which results in a fraction that contains PCBs without PCDDs or PCDFs, was used in PCB spike/recovery bioanalysis experiments with chicken eggs and with environmental waterbird egg samples. We found extraction efficiencies of the PAM procedure for [^{14}C]-2,2',4,4',5,5'-hexachlorobiphenyl (PCB 153) were 57–61% from fortified chicken eggs. A second, more contemporary extraction/cleanup method with dichloromethane (DCM), which also results in a fraction that contains PCBs without PCDDs or PCDFs, was used in PCB spike/recovery bioanalysis experiments with chicken eggs and fish samples (6). This method is routinely used to extract environmental samples for PCB-congener-specific analysis. The DCM method results in a fraction that contains PCBs (90–98% recovery efficiency) without PCDDs, PCDFs, polar pesticides, or most organochlorine

pesticides (6). A series of TCDD spike/recovery bioassay experiments were conducted to ensure that PCDDs and PCDFs were not cocontaminants in the resultant PCB fraction of the PAM or DCM methods. We were unable to detect any activity when the TCDD-fortified chicken egg extracts of either the DCM or PAM procedures were tested in the H4IIE bioassay (spike concentrations up to 1000 pg of TCDD/g; data not presented). Last, we assessed a modified version of the DCM procedure in which an acidic silica gel (AS) column cleanup was used after GPC. This AS procedure was previously described (42). The resultant fraction contains PCBs with recovery efficiencies of 90–100% for all quantifiable PCBs. External standardization of the AS procedure for PCDD/PCDF recovery efficiency had not been described previously. Therefore, duplicate 10-g portions of chicken egg homogenates were spiked with 7×10^3 , 21×10^3 , 70×10^3 , 210×10^3 , or 700×10^3 DPM [3H]TCDD (specific activity approximately 45 Ci/mmol). The resultant recovery efficiencies (\pm SD) were 95.4 ± 4.0 , 93.2 ± 1.0 , 96.3 ± 0.7 , 97.7 ± 3.3 , and $103.5 \pm 3.5\%$, respectively, with an average of $97.2 \pm 4.2\%$. It should be noted that none of the bioassay results were corrected on the basis of external standard recovery efficiencies.

A series of experiments were performed in which "clean" samples were spiked with a PCB (3,3',4,4'-tetrachlorobiphenyl, congener 77) or TCDD, extracted, and then analyzed with the H4IIE bioassay. The sample matrix used in these studies consisted of chicken eggs from a retail store because many of the samples we are currently analyzing are bird eggs. The first spike/bioanalysis experiment was PCB 77 spiked into chicken eggs at 0.1, 0.5, 1.0, 5.0, 10, 50, and 100 μ g/g, extraction with either the PAM (41) or DCM (6) procedure, followed by bioanalysis of the extracts. A second spike/bioanalysis experiment consisted of a TCDD spike of 0.01, 0.1, 0.5, 1.0, or 10 ng/g into chicken eggs. These eggs were then extracted with the AS protocol (42), and extracts were subjected to bioanalysis.

PHH standards tested in this study consisted of TCDD, 2,3,7,8-tetrachlorodibenzofuran (TCDF, Ultra Scientific, Hope, RI) and four PCB congeners (3,3',4,4'-tetrachlorobiphenyl, PCB 77; 3,3',4,4',5-pentachlorobiphenyl, PCB 126; 2,3,3',4,4'-pentachlorobiphenyl, PCB 105; and 2,3,3',4,4',5'-hexachlorobiphenyl, PCB 156, Ultra Scientific). Purity of all PHH congeners was confirmed by mass spectral analysis by Jay W. Gooch, Chesapeake Biological Laboratory, University of Maryland, Solomons, MD. All PCB congeners and TCDD were >99% pure. 2,3,7,8-TCDF contained an impurity, 1,2,7,8-TCDF, at 0.84–1.59%, which was not considered to be significant based on the relatively low potency of 1,2,7,8-TCDF as compared to 2,3,7,8-TCDF.

Cell Culture and Bioassay Procedure. The H4IIE rat hepatoma cells were obtained from the American Type Culture Collection (ATCC No. CRL 1548). Cells were cultured in Dulbecco's modified Eagle's medium (D-MEM) base (Sigma, D5030) supplemented with $1 \times$ glutamine, $1.5 \times$ vitamins (Sigma, M6895), $2 \times$ nonessential amino acids, $1.5 \times$ essential amino acids, 1 mM pyruvate, 1000 mg/L D-glucose, 2200 mg/L sodium bicarbonate, 15% fetal bovine serum (Gibco, 200-6140AJ), and 50 mg/L gentamicin. These conditions provided optimal growth and EROD induction potential of the H4IIE cells. Stock cultures were grown in 75-cm² flasks at 37 °C in a humidified 95:5 air-CO₂ atmosphere. New cultures were started from frozen cells after nine or less passages.

The bioassay conditions were slight modifications of previous reports (36–40). Cells, trypsinized from stock

flasks at confluency, were seeded in Petri dishes (15 × 100 mm) at 0.8×10^6 /plate in 10 mL of D-MEM. After a 24-h incubation, the cells were dosed with extract, an appropriate control, or reference compound in 100 μ L of iso-octane. There was no effect of dosing volume between 10 and 150 μ L of iso-octane when either an extract or standard (TCDD) was tested. Dosed cells were incubated for 72 h, rinsed with phosphate-buffered saline (PBS), and then harvested with cell scrapers (Gibco) into Tris-sucrose (0.05–0.2 M) buffer, pH 8.0 (37). Cells were then centrifuged for 10 min at 5000g and resuspended in Tris-sucrose buffer, and protein was determined in duplicate (43). Duplicate EROD determinations, by a modification of the spectrofluorometric method of Pohl and Fouts (44), were made with 100- μ L aliquots of the standardized (1 mg of protein/mL) cell suspensions. Briefly, this method has a final reaction volume of 1.25 mL consisting of 1.0 mL of NADPH generator system (5 mM glucose 6-phosphate, 5 mM MgSO₄, 3.5 mM NADP, and 1.6 mg of bovine serum albumin/mL in 0.1 M HEPES buffer, pH 7.8), 0.1 mL of 25 units/mL glucose-6-phosphate dehydrogenase (G6PDH), 0.1 mL of cell suspension (100 μ g of protein), and 0.05 mL of 15 μ M ethoxyresorufin (ER) in methanol. The reaction mixtures (less the ER) were preincubated 10 min at 37 °C, after which reactions were initiated by the addition of the ER at 10-s intervals. After 10 min, the reactions were stopped by the addition of 2.5 mL of cold methanol, again at 10-s intervals. Proteins were allowed to flocculate for 5 min at 37 °C and then the samples were centrifuged at 5000g, 4 °C, for 10 min. Resorufin in the supernatant was determined spectrofluorometrically (550-nm excitation, 585-nm emission) against a standard curve, which was calibrated with a resorufin standard each bioassay. EROD specific activity was calculated as picomoles of resorufin formed per milligram of protein per minute.

Along with each set of extracts, appropriate standards were analyzed on the same day. All environmental extracts were calibrated against a TCDD standard curve for calculation of "TCDD equivalents" (TCDD-EQ) in the extract. The effective doses for half-maximal EROD induction (ED₅₀) were calculated by probit analysis (45). Calculations of extract potency for each sample were made according to eq 1 as reported by Sawyer et al. (46), where

$$\text{extract potency} = \text{TCDD ED}_{50} / \text{extract ED}_{50} \quad (1)$$

TCDD ED₅₀ is in picograms per plate, extract ED₅₀ is in microliters per plate, and extract potency is in picograms of TCDD-EQ per microliter. The calculations to TCDD-EQ in an environmental sample were not corrected for extraction efficiencies of the various extraction methods. Variance estimates were calculated according to eq 2 and

$$CV_T = [(CV_E)^2 + (CV_S)^2]^{1/2} \quad (2)$$

an additive model of variance (47), where CV_T is the coefficient of variation for TCDD-EQ, CV_E the coefficient of variation for extract ED₅₀, and CV_S the coefficient of variation for standard ED₅₀. Standard deviations (SD) were obtained by multiplying the fractional CV_T by the estimated TCDD-EQ of the sample or extract. Goodness of fit test of a normal distribution for TCDD ED₅₀ values was according to Kolmogorov-Smirnov (47).

Results and Discussion

The H4IIE bioassay has traits that make it a particularly useful technique for the determination of PHHs in environmental extracts. The basal EROD activity of the H4IIE cells ranges from 0.5 to 5.0 pmol/mg-min. Iso-octane, which

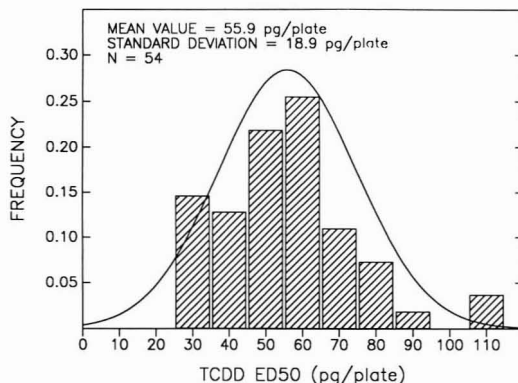


Figure 1. Frequency distribution of TCDD ED₅₀ values in the H4IIE bioassay.

gave optimal response and sensitivity in previous reports (37–39), was also an ideal carrier in our studies. Solvent controls had no induction over basal EROD in the H4IIE cells, nor was there any apparent toxicity as determined by cell viability or cellular protein. The dosing volume of extracts or standards was constant at 100 μ L (1% media volume). However, there was no effect of dosing volume on the inductive response of the H4IIE cell cultures when volumes between 10 and 100 μ L of extracts or standards were tested. The use of iso-octane as a carrier is also compatible with most chemical residue analysis techniques for PHHs.

Sensitivity of the H4IIE bioassay is quite exquisite for PHHs and TCDD in particular. The limit of detection was 10 pg of TCDD (31 fmol) per plate in our studies, which is the same as that reported by others (35, 37–39). The coefficients of variation for within bioassay variance of TCDD ED₅₀ estimates were generally small with an average of 3.70%. The coefficients of variation associated with extract ED₅₀ estimates are generally in the range of 5–15%. Precision of this bioassay, therefore, is fairly high with the final estimates of TCDD-EQ in environmental samples having coefficients of variation between 10 and 20%. However, this type of precision is only observed when a TCDD standard curve is run with each set of environmental samples. Our average ED₅₀ for TCDD over a 2-year period and 54 standard curves was 55.9 pg/plate (0.17 pmol/plate), also very similar to the 45 pg/plate (0.14 pmol/plate) ED₅₀ reported previously with a similar solvent system (39). This demonstrates the reproducibility of the H4IIE bioassay, even among different laboratories. The ED₅₀ values for TCDD in this system followed a normal distribution ($p = 0.80$, coefficient of skewness = 0.0, coefficient of kurtosis = 3.0) with a range of 30–115 pg/plate and standard deviation of 18.9 pg/plate (Figure 1). This corresponds to a coefficient of variation among bioassays of 33.8%. If the average TCDD ED₅₀ value with its 34% CV were used, resultant estimates of TCDD-EQ would have CV = 40–50%. Therefore, in bioanalytical applications of the H4IIE bioassay, it is important to run a TCDD standard with each set of environmental extracts.

Another test of reproducibility with this bioassay is interlaboratory comparisons of other PHH standards. For this purpose we tested TCDF, PCB 77, PCB 126, PCB 105, and PCB 156, in addition to TCDD (Table I). A comparison of PHH ED₅₀ values from different laboratories is given (Table II). ED₅₀ values from this study were very close to those reported by others (39) when iso-octane was used as a carrier solvent (Table II), even when different

Table I. ED₅₀ Values and Relative Potencies of Selected PHHs for EROD Induction in the H4IIE Bioassay^a

compd	ED ₅₀ , pg/plate ± SD	ED ₅₀ , pmol/plate ± SD	relative potency
TCDD	5.59 ± 1.89 × 10 ¹	0.17 ± 0.06	1.0
TCDF	8.08 ± 0.16 × 10 ³	26.4 ± 0.52	6.4 × 10 ⁻³
PCB 126	2.48 ± 0.02 × 10 ³	7.59 ± 0.07	2.2 × 10 ⁻²
PCB 156	1.13 ± 0.03 × 10 ⁶	3120 ± 89.9	5.5 × 10 ⁻⁵
PCB 77	2.74 ± 0.10 × 10 ⁶	9370 ± 341	1.8 × 10 ⁻⁵
PCB 105	7.34 ± 0.81 × 10 ⁶	22500 ± 2480	7.6 × 10 ⁻⁶

^aAll bioassays carried out in duplicate except TCDD where *n* = 54, *r* = 2-3. ED₅₀, effective dose for half-maximal EROD induction; potencies are calculated relative to TCDD as (TCDD ED₅₀, pmol/plate)/(compound ED₅₀, pmol/plate).

substrates were used to monitor P450IA1 catalytic activity of the cells. A large part of this stability is attributable to the fact that a standardized stock of H4IIE cells is available at ATCC. Discrepancies begin to appear among ED₅₀ values when comparisons are made among solvent carrier systems (39, 48, 49). Isooctane increases the sensitivity of the H4IIE bioassay toward TCDD as compared to dimethyl sulfoxide (DMSO) (39). ED₅₀ values for TCDD are 4-10 times less when isooctane was the carrier as compared to when DMSO was used (Table II). However, greater sensitivity was not seen with the isooctane carrier solvent system for all PHHs. There appears to be little effect of carrier solvent on TCDF or PCB 156 potency and DMSO seems to result in greater bioassay sensitivity for PCB 126, PCB 105, and PCB 77 as compared to isooctane (Table II). This phenomenon of apparent differential sensitivity caused by the carrier solvent system may be due to PHH solubility differences. It should also be mentioned at this point that the similarities in potency noted above are based on ED₅₀ values. If effective concentration values (EC₅₀) are compared, there is not a good agreement between values from different laboratories. The effective concentration for half-maximal induction, EC₅₀, is calculated by normalizing the dose per plate to the volume of media in the plate (ED₅₀/media volume) and has been used by some researchers (36, 48). The size of Petri dish and volume of media used varied among all laboratories, but the cell densities were fairly constant between 0.8 × 10⁶ and 1.0 × 10⁶ cell/plate. The fact that ED₅₀s and not EC₅₀s are similar among laboratories, along with the similarity in cell seeding rates, suggests that most of the PHH dose is effectively reaching the cells. However, radiotracer studies are required to understand if differential solubilities can explain this phenomenon of differential PHH potencies in the H4IIE bioassay. This also has implications on calculations of relative potency factors of PHHs based on their H4IIE cell induction potency. If ED₅₀ values are more reliable and consistent estimates of PHH induction potency, as they appear to be, perhaps

ED₅₀ values instead of EC₅₀ values should be used in calculation of H4IIE-derived potency factors of individual PHH congeners relative to TCDD. These potency factors are being used with increasing frequency (50), in particular to calculate TCDD-EQ from chemical residue analysis (51, 52).

Use of the H4IIE bioassay for the determination of TCDD-EQ in environmental samples requires a knowledge of potential endogenous and exogenous interferences caused by the matrix or extraction protocols. To address these issues we examined matrix and procedural blanks and performed spike/bioanalysis studies. Characterization of extraction protocols was done to ensure that the fractions known to contain PHHs induced EROD in the H4IIE cells and fractions containing pesticides did not contain measurable amounts of inducible materials. The three extraction procedures tested, PAM (41), DCM (6), and AS (42), showed no induction with procedural blanks or pesticide fractions and significant induction with PHH fractions from these methods (data not presented). The PAM characterization was similar to results reported by previous authors using this method (38). Matrix blanks (unfertilized chicken eggs, fertilized 10-day-old chicken eggs, salmon eggs, and rainbow trout flesh), with ≤0.01 μg of total PCBs/g, caused no EROD induction in the H4IIE cells at 1-3 g-equiv of sample/plate. This indicated that endogenous substances in these matrices did not cause false positive responses in the H4IIE bioassay. Because *p,p'*-DDE is a major cocontaminant of PCBs in these extraction procedures, we exposed the H4IIE cells to 10, 100, 1000, or 10000 ng of *p,p'*-DDE/plate. There was no EROD induction or cytotoxicity, as measured by cell growth, at any dose of *p,p'*-DDE.

To assess the ability of the H4IIE bioassay to quantitate PHHs in biological samples, PHH spike/bioanalysis studies were conducted. The information to be gained by these experiments is 3-fold. First, the actual induction magnitude and dose-response of the extract may be compared with that of the pure congener. Second, the slopes of the extracted and pure congener dose-response curves may be compared in a situation where only a single compound is present. Third, a threshold for detection inclusive of both extraction and bioassay efficiency may be estimated. PAM (41) and DCM (6) extraction methods were used in combination with the H4IIE bioassay to assess quantitation of PCB 77 and AS (42) extraction methods were used to assess quantitation of TCDD.

Extracts of PCB 77 spiked chicken eggs produced a dose-response curve that was in good concordance with that seen when PCB 77 was added directly to the cell cultures (Figure 2). There were similar slopes in all three cases, indicating no extraction or matrix effects on the dose-response curves. ED₅₀ values calculated for the extracts varied less than 25% compared to the standard. Correction for the extraction efficiency of each method

Table II. Comparison of Reported ED₅₀ Values (pmol/Plate) in the H4IIE Bioassay for Selected PHHs

ref	system	assay	PHH					
			TCDD	TCDF	PCB 77	PCB126	PCB156	PCB105
Bradlaw and Casterline (39)	ISO	AHH	0.14	13.0	10250	6.00		
	DMSO	AHH	1.54					
Sawyer and Safe (36)	DMSO	AHH	0.77		281	1.92	16600	700
	DMSO	EROD	0.64		708	1.98	7170	960
Sawyer and Safe (48)	DMSO	AHH		15.6			3540	
	DMSO	EROD		8.1			4000	
Zacharewski et al. (49)	DMSO	AHH	0.73					
	DMSO	EROD	0.51					
this study	ISO	EROD	0.17	26.4	9370	7.60	3120	22500

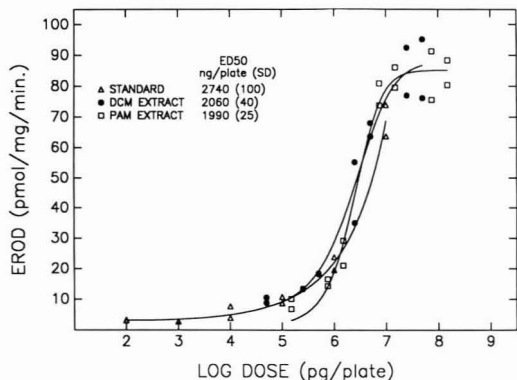


Figure 2. Dose-response relationship of pure and extracted PCB 77 in the H4IIE bioassay. DCM (6) and PAM (41) extraction protocols were tested with clean chicken eggs fortified with PCB 77 at seven concentrations. Dose to the cells was calculated based on 50 μ L (5%) of a 1-mL extract/plate, spike concentration in chicken eggs, and 100% extraction efficiency.

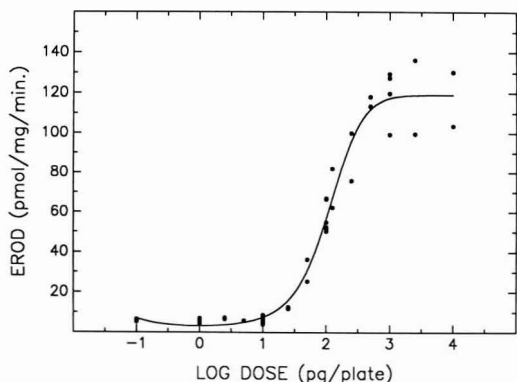


Figure 3. Dose-response relationship of pure and extracted TCDD in the H4IIE bioassay. The AS (42) extraction protocol was tested with clean chicken eggs fortified with TCDD. Dose to the cells was calculated based on a dosing volume (1, 10, 25, or 100 μ L) of a 1-mL extract/plate, spike concentration in chicken eggs, and 100% extraction efficiency.

could reduce these differences among ED₅₀ values.

Spike/bioanalysis experiments with TCDD and the AS extraction procedure indicated that the H4IIE bioassay could accurately predict extract potency. Extracted TCDD produced a similar dose-response curve in the H4IIE cells compared to that of the standard (Figure 3). Slopes of the curves were not significantly different, indicating no extraction or matrix effect on the response of the bioassay. Extract potency was calculated from observed ED₅₀ values for each spike concentration, as would be done with environmental extracts, and these were compared with the known concentration of TCDD in the extract (Figure 4). The nominal concentrations of the extracts were 0.1, 1.0, 5.0, 10, and 100 pg of TCDD/ μ L. The extract at 0.1 pg of TCDD/ μ L was below the limit of quantitation, however, the bioassay predicted extract potency within a factor of 2 for the other concentrations. Predictions of extract potency by the ED₅₀ method were linear between 1.0 and 100 pg of TCDD/ μ L and the regression slope of observed versus expected was not different from 1.0, the ideal. It is clear from this set of experiments that the H4IIE bioassay can accurately and precisely determine the potency of PHH extracts. Comparison of extract and

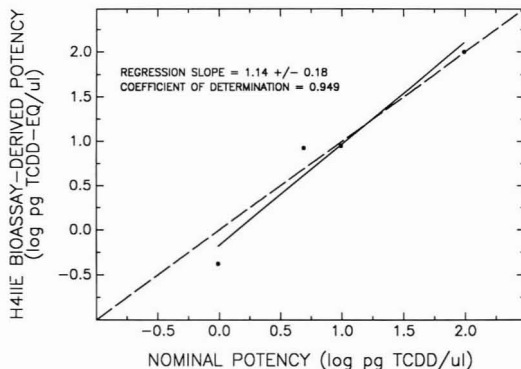


Figure 4. Observed versus expected potency of TCDD in spike/bioanalysis experiments. The nominal potency (pg of TCDD/ μ L) of extracts was based on the TCDD spike to the chicken egg sample and an assumption of 100% extraction efficiency. H4IIE bioassay derived potency (pg of TCDD-EQ/ μ L) based on eq 1 for each of four extracts.

Table III. H4IIE Bioassay-Derived TCDD-EQ in Environmental Samples from the Great Lakes^a

sample/site	TCDD-EQ, pg/g \pm SD
chinook salmon, Lake Michigan	
dorsal muscle	26.7 (2.9)
eggs	115.8 (5.8)
double-crested cormorant eggs	
Green Bay, Lake Michigan	344.1 (25.6)
Beaver Is., Lake Michigan	94.0 (7.9)
Caspian tern eggs	
Green Bay, Lake Michigan	281.2 (23.8)
Saginaw Bay, Lake Huron	415.7 (48.1)
Beaver Is., Lake Michigan	49.7 (2.2)
black-crowned night heron eggs,	
Saginaw Bay, Lake Huron	221.8 (19.7)

^a All samples collected 1986-1987, composited, and extracted according to ref 41, except chinook salmon, which were extracted according to ref 6.

standard ED₅₀s from the H4IIE bioassay is a simple and accurate method of calculating potencies and associated error estimates for PHH extracts.

H4IIE bioassay derived TCDD-EQ were determined for some fish and wildlife samples taken from the Great Lakes (Table III). The samples were extracted and extracts subjected to H4IIE bioanalysis. The range of TCDD-EQ found in these samples is reflective of the values we have observed in environmental samples in this region. The precision of these measurements is also typical of the analytical precision of this bioassay when environmental samples are tested ($CV_T = 5-15\%$). The H4IIE-derived TCDD-EQ calculations for environmental samples may be compared with biological effects data and chemical residue analysis from the samples to help interpret these data. The utility of this bioassay system is to aid chemical residue analysis and act as a data reduction tool to help understand the complex interactions of PHHs. Studies are currently underway to determine the validity of using this mammalian bioassay system to predict the toxic potency of PHH mixtures to avian and fish species.

Summary

Previous studies have used the H4IIE bioassay to estimate the potency of individual PHHs (36, 37), assess environmental extracts of PHHs (37, 46, 48, 49), and address the complex interactions of synergism, antagonism, and additivity (18-21, 24). This is impossible to do by chemical

residue analysis alone. The H4IIE bioassay has been shown to be a sensitive bioanalytical tool (35, 37-40, 48, 49) with potential for predicting the toxic effects of PHHs in whole organisms (31). In this study we demonstrate the reproducibility of the H4IIE bioassay among laboratories and its repeatability over time within a laboratory. We also provide experimental data of its ability to quantitatively predict known concentrations of PHHs in biological extracts. The potential utility of this bioassay is as an integrative tool, which can complement chemical residue analysis and biological effects data from environmental studies. The H4IIE bioassay can also be used to screen or prioritize chemical residue analysis and thereby save valuable time and funds.

Acknowledgments

We thank David Verbrugge for technical assistance and Dr. Jay W. Gooch of the Chesapeake Biological Laboratory, University of Maryland, for mass spectral confirmation of the purity of the PHHs used in these experiments.

Registry No. TCDD, 1746-01-6; PCB 126, 57465-28-8; PCB 156, 69782-90-7; PCB 77, 32598-13-3; PCB 105, 32598-14-4; TCDF, 51207-31-9.

Literature Cited

- (1) Hutzinger, O.; van den Berg, M.; Olie, K.; Opperhuizen, A.; Safe, S. In *Dioxins in the Environment*; Kamrin, M. A., Rodgers, P. W., Eds.; Hemisphere: New York, 1984, pp 9-32.
- (2) Esposito, M. P.; Tiernan, T. O.; Dryden, F. E. *Dioxins*; EPA-600/2-80-197; U.S. Environmental Protection Agency: Cincinnati, OH, 1980.
- (3) Evans, M. S. *Toxic Contaminants and Ecosystem Health: A Great Lakes Focus*; John Wiley and Sons: New York, 1988.
- (4) Travis, C. C.; Hattemer-Frey, H. A.; Silbergeld, E. *Environ. Sci. Technol.* **1989**, *23*, 1061-1063.
- (5) Smith, L. M.; Stalling, D. L.; Johnson, J. L. *Anal. Chem.* **1984**, *56*, 1830-1842.
- (6) Ribick, M. A.; Smith, L. M.; Dubay, G. R.; Stalling, D. L. In *Aquatic Toxicology and Hazard Assessment*; ASTM STP 737; Branson, D. R., Dickson, K. L., Eds.; Philadelphia, PA, 1981; pp 249-269.
- (7) Smith, L. M. *Anal. Chem.* **1981**, *53*, 2152-2154.
- (8) Tiernan, T. O. In *Chlorinated Dioxins in the Total Environment*; Choudhary, G., Keith, L. H., Rappe, C., Eds.; Butterworth: Boston, MA, 1983; pp 211-237.
- (9) Rappe, C. *Environ. Sci. Technol.* **1984**, *18*, 78A-90A.
- (10) Poland, A.; Greenlee, W. F.; Kende, A. S. *Ann. N.Y. Acad. Sci.* **1979**, *320*, 214-230.
- (11) Poland, A.; Knutson, J. C. *Annu. Rev. Pharmacol. Toxicol.* **1982**, *22*, 517-554.
- (12) Goldstein, J. In *Halogenated Biphenyls, Terphenyls, Naphthalenes, Dibenzodioxins and Related Products*; Kimbrough, R., Ed.; Elsevier/North-Holland: New York, 1980; pp 151-190.
- (13) Yoshimura, H.; Yoshihara, S.; Ozawa, N.; Miki, M. *Ann. N.Y. Acad. Sci.* **1979**, *320*, 179-192.
- (14) Birnbaum, L. S.; Weber, H.; Harris, M. W.; Lamb, J. C.; McKinney, J. D. *Toxicol. Appl. Pharmacol.* **1985**, *77*, 292-302.
- (15) Bannister, R.; Safe, S. *Toxicology* **1987**, *44*, 159-169.
- (16) Keys, B.; Piskorska-Pliszczynska, J.; Safe, S. *Toxicol. Lett.* **1986**, *31*, 151-158.
- (17) Weber, H.; Harris, M. W.; Haseman, J. K.; Birnbaum, L. S. *Toxicol. Lett.* **1985**, *26*, 159-167.
- (18) Leece, B.; Denomme, M. A.; Towner, R.; Li, A.; Landers, J.; Safe, S. *Can. J. Physiol. Pharmacol.* **1987**, *65*, 1908-1912.

- (19) Bannister, R.; Davis, D.; Zacharewski, T.; Tizard, I.; Safe, S. *Toxicology* **1987**, *46*, 29-42.
- (20) Haake, J. M.; Safe, S.; Mayura, K.; Phillips, T. D. *Toxicol. Lett.* **1987**, *38*, 299-306.
- (21) Davis, D.; Safe, S. *Toxicol. Appl. Pharmacol.* **1988**, *94*, 141-149.
- (22) Pluess, N.; Poiger, H.; Hohbach, C.; Schlatter, C. *Chemosphere* **1988**, *17*, 973-984.
- (23) Pluess, N.; Poiger, H.; Hohbach, C.; Suter, M.; Schlatter, C. *Chemosphere* **1988**, *17*, 1099-1110.
- (24) Biegel, L.; Harris, M.; Davis, D.; Rosengren, R.; Safe, L.; Safe, S. *Toxicol. Appl. Pharmacol.* **1989**, *97*, 561-571.
- (25) Safe, S. *Annu. Rev. Pharmacol. Toxicol.* **1986**, *26*, 371-399.
- (26) Whitlock, J. P. *Pharmacol. Rev.* **1987**, *39*, 147-161.
- (27) Bandiera, S.; Sawyer, T.; Campbell, M. A.; Robertson, L.; Safe, S. *Life Sci.* **1982**, *31*, 517-525.
- (28) Bandiera, S.; Sawyer, T.; Romkes, M.; Zmudzka, B.; Safe, L.; Mason, G.; Keys, B.; Safe, S. *Toxicology* **1984**, *32*, 131-144.
- (29) Leece, B.; Denomme, M. A.; Towner, R.; Li, S. M. A.; Safe, S. *J. Toxicol. Environ. Health* **1985**, *16*, 379-388.
- (30) Mason, G.; Farrell, K.; Keys, B.; Piskorska-Pliszczynska, J.; Safe, L.; Safe, S. *Toxicology* **1986**, *41*, 21-31.
- (31) Safe, S. *Chemosphere* **1987**, *16*, 791-802.
- (32) Reuber, M. A. *J. Natl. Cancer Inst.* **1961**, *26*, 891-897.
- (33) Pitot, H. C.; Peraino, C.; Morse, P. A., Jr.; Potter, V. R. *Natl. Cancer Inst. Monogr.* **1964**, *No. 13*, 229-245.
- (34) Benedict, W. F.; Gielen, J. E.; Owens, I. S.; Niwa, A.; Nebert, D. W. *Biochem. Pharmacol.* **1973**, *22*, 2766-2769.
- (35) Niwa, A.; Kumaki, K.; Nebert, D. W. *Mol. Pharmacol.* **1975**, *11*, 399-408.
- (36) Sawyer, T.; Safe, S. *Toxicol. Lett.* **1982**, *13*, 87-84.
- (37) Bradlaw, J. A.; Garthoff, L. H.; Hurley, N. E.; Firestone, D. *Food Cosmet. Toxicol.* **1980**, *18*, 627-635.
- (38) Casterline, J. L.; Bradlaw, J. A.; Puma, P. J.; Ku, Y. J. *J. Assoc. Off. Anal. Chem.* **1983**, *66*, 1136-1139.
- (39) Bradlaw, J. A.; Casterline, J. L. *J. Assoc. Off. Anal. Chem.* **1979**, *62*, 904-918.
- (40) Trotter, W. J.; Young, S. J. V.; Casterline, J. L.; Bradlaw, J. A.; Kamps, L. R. *J. Assoc. Off. Anal. Chem.* **1982**, *65*, 838-841.
- (41) *Pesticide Analytical Manual*; Food and Drug Administration: Washington, DC, 1979; Vol. 1, Section 212.13a.
- (42) Schwartz, T. R.; Lehman, R. G. *Bull. Environ. Contam. Toxicol.* **1982**, *28*, 723-727.
- (43) Lowry, O. H.; Rosebrough, N. J.; Farr, A. L.; Randall, R. J. *J. Biol. Chem.* **1951**, *193*, 265.
- (44) Pohl, R. J.; Fouts, J. R. *Anal. Biochem.* **1980**, *107*, 150-158.
- (45) Finney, D. J. *Statistical Methods in Biological Assay*; Charles Griffin: London, U.K., 1980.
- (46) Sawyer, T. W.; Vatcher, A. D.; Safe, S. *Chemosphere* **1984**, *13*, 695-701.
- (47) Zar, J. H. *Biostatistical Analysis*; Prentice Hall: Englewood Cliffs, NJ, 1974.
- (48) Sawyer, T. W.; Safe, S. *Chemosphere* **1985**, *14*, 79-84.
- (49) Zacharewski, T.; Safe, L.; Safe, S.; Chittim, B.; DeVault, D.; Wiberg, K.; Bergquist, P.; Rappe, C. *Environ. Sci. Technol.* **1989**, *23*, 730-735.
- (50) Olson, J. R.; Bellin, J. S.; Barnes, D. G. *Chemosphere* **1989**, *18*, 371-381.
- (51) Niimi, A. J.; Oliver, B. G. *Chemosphere* **1989**, *18*, 1413-1423.
- (52) Kubiak, T. J.; Harris, H. J.; Smith, L. M.; Schwartz, T. R.; Stalling, D. L.; Trick, J. A.; Sileo, L.; Docherty, D.; Erdman, T. C. *Arch. Environ. Contam. Toxicol.* **1989**, *18*, 706-727.

Received for review February 5, 1990. Revised manuscript received July 30, 1990. Accepted August 6, 1990. We thank the Toxic Substance Control Commission of the Michigan Department of Natural Resources, the Michigan Agricultural Experiment Station, Pesticide Research Center, and Department of Fisheries and Wildlife at Michigan State University for financial support of this research.

Subchronic Toxicity Study of Ozonated and Ozonated/Chlorinated Humic Acids in Sprague-Dawley Rats: A Model System for Drinking Water Disinfection

F. Bernard Daniel,* Merrel Robinson, H. Paul Ringhand, Judy A. Stober, Norbert P. Page, and Greg R. Olson

Health Effects Research Laboratory, U.S. Environmental Protection Agency, Cincinnati, Ohio 45268

Male and female Sprague-Dawley rats were administered drinking water containing humic acids either non-disinfected or following ozonation (O_3) or ozonation/chlorination (O_3/Cl_2) for 90 consecutive days. Test animals drank either of two concentrations of humic acids, 0.25 and 1.0 g/L total organic carbon (TOC), while controls received phosphate-buffered, distilled water. No consistent significant treatment-related effects were observed in body weight gain, organ weights, food or water consumption, or hematological and clinical chemistry parameters. No target organs were identified from the histopathological examination of the tissues. The most significant observation, an increase in liver to body weight ratio for the male animals in the 1.0 g/L O_3/Cl_2 humic acid group, was not observed in any other group, nor was it corroborated via any biochemical measurements or histopathological analysis. Kidney lesions, primarily chronic progressive nephropathy, were a common observation in both controls and treated groups with no apparent relationship to either humic acid concentration or the disinfection process.

Introduction

A search for alternative processes to the disinfection of drinking water by chlorination is underway based on the concern over hazardous byproducts formed by chlorination. Ozonation represents an attractive alternative and has been used to disinfect drinking water in France since 1905. It is currently in widespread use there and to a limited extent elsewhere in Europe. In contrast, ozonation has seen only minor usage in the United States, mainly for the disinfection of waste streams and for specialized disinfection of drinking water supplies e.g., bottled water.

As discussed in the reviews by Anderson et al. (1) and Carmichael et al. (2), ozone has several advantages over alternative disinfectants. It is a strong oxidizing agent reacting with a wide variety of organic compounds and it is highly effective in controlling algal growth and in the elimination of microbes, including bacteria, amoebae, and viruses. In addition, ozone is effective in controlling and imparting desirable color, taste, and odor to finished water. It does not produce trihalomethanes (THM) in water as does chlorination and has, in fact, been shown to lower the levels of precursor organics that lead to THM formation.

However, there are at least two characteristics about ozonation that are drawbacks to its use as a nationwide replacement for chlorination as the pre-disinfectant for drinking water: (1) with current technology for application, it is more costly, and (2) ozone has a rather short half-life (usually ~20 min) in water. While this latter feature may

be desirable from the viewpoint of human consumption, it is an undesirable feature, overall, since there is no residual protection of the water supply to prevent microorganism growth in the drinking water distribution system. To compensate for the lack of a residual effect, it has been proposed that small amounts of chlorine or chloramine be added to ozone-purified water as post-disinfectants to provide residual protection for the distribution system.

A major concern of the United States Environmental Protection Agency centers on the relative lack of knowledge regarding the chemical nature of organic reaction products of the ozonation process and the potential toxicity of these reaction byproducts. Still less is known about the health effects associated with byproducts of combined ozonation and chlorination treatments. This toxicity study is intended to be a preliminary evaluation of the toxic effects that might result from a protracted (90-day) ingestion of a very high concentration of disinfectant byproducts generated via the reaction of ozone or ozone followed by chlorine with aqueous humic acids. Thus, these humic acid solutions represent one approach to the generation of drinking water disinfection byproducts (DBP) at levels suitable for toxicological testing.

The rationale for this approach centers about the observation that a majority of soluble organic materials found in surface waters are in the form of humic acid or fulvic acids. These are a heterogeneous and complex group of compounds, primarily organic acids, probably produced by oxidative coupling of phenolic and aliphatic organics.

While there have been no studies comparable to those reported herein, there have been two related studies: one evaluated the toxic properties of organic concentrates extracted from drinking water treated with various disinfectants in a series of bioassays (3), and the other examined the 90-day subchronic toxicity of water containing gram per liter concentrations of humic acids identical with those reported here which had been previously treated with chlorine (4). In like manner, this study evaluates the comparative toxicity of a 90-day exposure to drinking water containing gram per liter levels of either non-disinfected humic acids or humic acids that had been ozonated or ozonated and subsequently chlorinated (ozonated/chlorinated).

Methods

Preparation of Test Materials. Three materials were prepared for administration to the test animals: (a) untreated (control) humic acid solutions of 1.0 g/L total organic carbon (TOC), (b) humic acid solutions of 0.25 and 1.0 g/L TOC that were ozonated, and finally, (c) humic acid solutions of 0.25 and 1.0 g/L TOC that were first ozonated and subsequently chlorinated. Phosphate buffered (0.05 M) distilled water (pH 8.02) was used as the aqueous vehicle and was administered to the control groups. The distilled water (conductivity ≤ 1 ppm, TOC < 150 ppb) was generated via a Barnstead Thermodrive still equipped with stainless steel condensing tubes. Stock

* Address correspondence to: Biochemical and Molecular Toxicology Branch, Genetic Toxicology Division, Health Effects Research Laboratory, U.S. Environmental Protection Agency, Andrew W. Breidenbach Environmental Research Center, 26 West Martin Luther King Drive, Cincinnati, OH 45268.

Page Associates, 17601 Stoneridge Court, Gaithersburg, MD 20878.

Pathology Associates, 6217 Centre Park Drive, West Chester, OH 45069.

solutions of commercial humic acid (Fluka) were prepared monthly according to the method described in earlier studies by Meier et al. (5), who had also shown them to be stable. This stock solution was stored in glass at 4 °C and was used to prepare, on a biweekly basis, the drinking water solutions, i.e., 1.0 g/L TOC of humic acid–distilled water solution, 0.25 or 1.0 g/L TOC of humic acid solutions ozonated or ozonated/chlorinated.

For ozonation of the humic acid solutions, ozone was generated by a Griffin Technics O₃ generator 117V-5A-10-60 HZ (Model GTC 0.25 electric discharge air-cooled type) using aviators grade oxygen (99.5% pure, H₂O <6 ppm, and a dewpoint of -83 to -84 °F). The buffered distilled water and humic acid solutions were maintained at a pH of 7–8 during ozonation by dripping 0.5 M sodium hydroxide into the reaction mixture while continuously monitoring the pH. The ozone was introduced at a gas flow rate of approximately 1.8 L/min, at the bottom of the batch reactor column via a diffusing stone of crystalline alumina grains (pore size 6 µm). The ozone contact time was 25–30 min for the 0.25 g/L mixture and 105–110 min for the 1.0 g/L mixture and provided a 1:1 carbon to ozone ratio by weight. No ozone was detected in the off-gas via titration of the KI trap solution and under these conditions no ozone breakthrough occurred. Thus, the ozone dose is equivalent to the added ozone. Chlorination was accomplished within 24 h after the ozonation by adding a stock chlorine solution (pH 8.0) to the ozonated humic acids solution at a 1.0:0.35 mole ratio of carbon to chlorine. The carbon level was based on the measured total organic carbon.

Animals and Maintenance. Male and female Caesarian-derived Sprague-Dawley rats (Cr1: CD BR), confirmed free of viral antibodies, bacteria, and parasites, were obtained from Charles River Laboratories, Portage, MI. The rats were held in quarantine for approximately 1 week in a temperature- (20–22 °C) and humidity- (40–60%) controlled room on a 12-h dark, 12-h light cycle for acclimation before treatment. The animals were group housed (two per cage) in elevated wire mesh cages. All aspects of the study adhered to the standards and practices endorsed by the American Association of Accreditation for Laboratory Animal Care.

Purina certified Chow 5002 (Ralston-Purina Co., St. Louis, MO) and tap water were supplied ad libitum. Animals were individually identified by ear tags and assigned to vehicle and treatment groups by using a computer-generated set of random numbers. A color-coded identification card on the cages identified each treatment group.

Experimental Design. One hundred and twenty rats were randomly assigned to 12 groups each consisting of 10 animals, either male or female. Each group received one of the nondisinfected, ozonated, or ozonated/chlorinated humic acid solutions. The basic experimental design was to administer the test materials continuously in the drinking water for a 90-day period with subsequent clinical examinations and pathology evaluations. The treatment groups received humic acid solutions via stainless steel, double-balled sipper tubes. The dosing solutions were replaced every other day with new solutions, at which time the volume of water consumed was calculated. Food consumption was measured once per week.

All rats were observed twice daily for physiological and behavioral responses and for mortality. Body weights were recorded prior to randomization, at initiation of dosing, and weekly thereafter. A final body weight was taken at necropsy after the animals had been fasted for approximately 18 h prior to sacrifice.

Prior to sacrifice, the animals were anesthetized with pentobarbital (60 mg/kg, I.P.) and blood samples were collected via cardiac puncture for hematological and serum clinical chemistry evaluations. Hematology samples were evaluated by use of a Coulter counter for white blood cell (WBC) count, red blood cell (RBC) count, hemoglobin, hematocrit, reticulocyte count, and mean corpuscular volume (MCV). A WBC differential analysis was performed for lymphocytes, monocytes, eosinophils, and segmented neutrophils.

Serum clinical chemistry determinations were performed for glucose, blood urea nitrogen (BUN), creatinine, calcium, inorganic phosphate (PO₄), alanine aminotransaminase (ALT), aspartate aminotransaminase (AST), lactate dehydrogenase (LDH), and total cholesterol.

Blood was collected and the animals were necropsied with euthanasia accomplished via exsanguination during anesthesia. The necropsy included gross examination of the external surface, all orifices, external surface of the brain, all organs, and the cranial, thoracic, abdominal, and pelvic cavities. The adrenal glands, brain (including the brain stem), gonads, heart, kidneys, liver, lungs, spleen, and thymus were weighed. Gross lesions; mesenteric lymph nodes, sternbrae, femur (including bone marrow); thymus; lung and bronchi; stomach; jejunum; colon; liver; pancreas; spleen; kidneys; adrenals; urinary bladder; testes, including epididymis; ovaries; uterus; nasal cavity and nasal turbinates; brain; pituitary; thyroid/parathyroids, heart; tongue; and esophagus were preserved in 10% neutral buffered formalin. Subsequently, these tissues were trimmed, processed, embedded in paraffin, and sectioned; slides were prepared and stained with hematoxylin and eosin from 5 males and 5 females of the control group and from all animals (10 males and 10 females) in the high-dose (1 g/L humic acids) groups. All prepared slides were examined by a veterinary pathologist. Lesions were graded according to severity with a scale of 1–4 (minimal, mild, moderate, or marked). Except for gross lesions, tissues from the lower concentration of humic acid (0.25 g/L) groups were not examined. Data were tabulated for individual animals and the descriptive statistics summarized by group. In addition, the gross observations and microscopic diagnoses were correlated for each animal.

Statistical Evaluation. Male and female rats were considered separately in all statistical analyses. A one-factor analysis of variance (ANOVA) procedure was used to test normally distributed measures for a treatment-related effect (6). The parameters analyzed consisted of the following: body weights, organ weights, organ to body (relative organ) weight ratios, water and food consumption, hematology and clinical chemistry measurements. When a significant treatment-related effect was observed ($p \leq 0.05$), the difference between treatment groups was tested by the Tukey's multiple comparison procedure (7). However, due to the high variability of some of the clinical chemistry measures, a nonparametric analysis of variance, i.e., the Kruskal-Wallis test (8) and associated multiple comparisons procedure were employed to determine significant differences among the treatment groups ($p \leq 0.05$). Statistical analyses of the gross and microscopic pathology diagnoses were not performed.

Results

Mortality. All animals survived the 90-day exposure period.

Food and Water Consumption. The average food consumption ranged from 7.2 ± 0.6 to 8.3 ± 1.3 g/100 g body weight per day for the females, and 5.6 ± 0.3 to 5.8 ± 0.4 g/100 g body weight per day for the males. No

Table I. Relative Organ Weights and Final Body Weights for Rats Exposed to Ozonated/Chlorinated Humic Acids in Drinking Water for 90 Days^a

	humic acids dose group, ^b g/L; disinfectant					
	0; none	1.0; none	0.25; O ₃	0.25; O ₃ /Cl ₂	1.0; O ₃	1.0; O ₃ /Cl ₂
Males						
brain	0.43 ± 0.04 ^{ab}	0.42 ± 0.03 ^{ab}	0.40 ± 0.03 ^a	0.45 ± 0.05 ^{ab}	0.46 ± 0.04 ^b	0.43 ± 0.04 ^{ab}
testes	0.74 ± 0.07	0.71 ± 0.05	0.70 ± 0.06	0.75 ± 0.07	0.70 ± 0.18	0.73 ± 0.07
heart	0.31 ± 0.02	0.32 ± 0.01	0.32 ± 0.02	0.32 ± 0.02	0.32 ± 0.04	0.32 ± 0.04
kidneys	0.79 ± 0.05	0.80 ± 0.10	0.77 ± 0.08	0.83 ± 0.09	0.86 ± 0.15	0.88 ± 0.04
liver	2.76 ± 0.18 ^a	2.95 ± 0.34 ^{ab}	2.97 ± 0.25 ^{ab}	2.83 ± 0.24 ^{ab}	2.77 ± 0.20 ^{ab}	3.09 ± 0.21 ^a
lung	0.42 ± 0.05	0.44 ± 0.05	0.42 ± 0.04	0.42 ± 0.05	0.42 ± 0.05	0.41 ± 0.05
spleen	0.17 ± 0.04	0.17 ± 0.02	0.17 ± 0.01	0.17 ± 0.03	0.19 ± 0.03	0.16 ± 0.02
thymus	0.07 ± 0.01	0.08 ± 0.03	0.09 ± 0.01	0.08 ± 0.03	0.09 ± 0.01	0.09 ± 0.03
adrenals	0.02 ± 0.01	0.02 ± 0.01	0.02 ± 0.01	0.02 ± 0.01	0.02 ± 0.01	0.02 ± 0.01
final body wt, g	496.9 ± 51.4	506.7 ± 37.9	522.7 ± 37.4	486.9 ± 45.1	467.3 ± 26.5	493.0 ± 45.2
water consumptn, mL/100 g body wt	9.5 ± 0.87 ^{ab}	8.6 ± 0.57 ^a	9.7 ± 1.06 ^{ab}	10.6 ± 1.16 ^b	9.6 ± 0.82 ^{ab}	10.5 ± 1.02 ^b
Females						
brain	0.76 ± 0.07	0.73 ± 0.07	0.77 ± 0.06	0.79 ± 0.05	0.78 ± 0.07	0.76 ± 0.06
ovaries	0.08 ± 0.02	0.08 ± 0.02	0.07 ± 0.01	0.08 ± 0.03	0.07 ± 0.02	0.06 ± 0.01
heart	0.36 ± 0.05	0.35 ± 0.03	0.36 ± 0.03	0.38 ± 0.03	0.38 ± 0.04	0.38 ± 0.04
kidneys	0.77 ± 0.06	0.89 ± 0.32	0.82 ± 0.06	0.81 ± 0.06	0.82 ± 0.08	0.87 ± 0.10
liver	2.87 ± 0.27	2.95 ± 0.31	3.16 ± 0.50	3.00 ± 0.13	3.10 ± 0.28	3.08 ± 0.31
lung	0.53 ± 0.05	0.52 ± 0.08	0.53 ± 0.05	0.53 ± 0.05	0.53 ± 0.05	0.52 ± 0.05
spleen	0.21 ± 0.03	0.23 ± 0.06	0.22 ± 0.03	0.22 ± 0.03	0.23 ± 0.04	0.21 ± 0.05
thymus	0.12 ± 0.02	0.13 ± 0.03	0.13 ± 0.04	0.13 ± 0.03	0.13 ± 0.02	0.12 ± 0.02
adrenals	0.04 ± 0.01	0.04 ± 0.02	0.04 ± 0.02	0.04 ± 0.02	0.04 ± 0.01	0.04 ± 0.01
final body wt, g	258.9 ± 24.8	256.6 ± 18.7	248.2 ± 16.5	247.1 ± 22.1	253.8 ± 18.0	257.1 ± 23.3
water consumptn, mL/100 g body wt	13.3 ± 1.79	15.9 ± 3.31	13.8 ± 1.23	15.2 ± 1.62	14.4 ± 1.84	15.2 ± 1.49

^a Parameters (mean ± SD); final body weight is the weight at necropsy; N, 10 animals/group. ^b a and b, means with same letter are not significantly different ($\alpha = 0.05$).

statistically significant differences were found for food consumption between the treatment groups. The average water consumption ranged from 17.1 ± 1.6 to 20.2 ± 3.7 mL/rat per day for the females and 21.8 ± 1.7 to 25.6 ± 1.9 mL/rat per day for the males. On a body weight basis, the males receiving 1.0 g/L nondisinfected humic acids drank significantly less water (19%) than the animals receiving 1.0 g/L ozonated or 1.0 g/L ozonated/chlorinated humic acids.

Body and Organ Weights. Initial and final body weights, weight gain, and absolute organ weights were recorded and analyzed. Terminal body weights and organ to body (relative) weight ratios computed on the weight at necropsy are presented in Table I. There were no statistical differences in the initial mean body weights among the various groups of male or female animals. The analysis of the body weight versus time indicates that the growth curves for all groups were not equivalent, but when expressed as weight gain for the duration of the study, male and female rats in all humic acid groups showed an increase in their body weight comparable to those of the distilled water control and no statistically significant differences were observed in the final weights. Except for the liver, no statistically significant treatment-related effects were seen in the absolute organ weight or organ to body weight ratios. For the liver, a modest, albeit significant, increase in organ to body weight relative to the distilled water control group was observed for males drinking 1.0 g/L ozonated/chlorinated humic acids. Such a change was not observed for the 1 g/L ozonated humic acids or in the female rats.

Hematology. In the analysis of the hematological parameters, two significant differences from the control values were observed: (1) a significant ($p \leq 0.01$) increase in segmented neutrophils (not shown) in females for the 1.0 g/L ozonated/chlorinated humic acids (19.5 ± 8.2% neutrophils) as compared to the water-only group (9.9 ±

4.6% neutrophils), and (2) a significant ($p \leq 0.05$) decrease in hemoglobin in males for the 1 g/L nondisinfected humic acids (14.5 ± 0.6 g/dL) and the 1.0 g/L ozonated humic acids (14.6 ± 0.4 g/dL) groups as compared to the water-only group (15.3 ± 0.5 g/dL) (Table II). These changes were probably not of biological significance, and no adverse treatment-related effects were observed in hematological parameters.

Clinical Chemistry. The serum clinical chemistry analyses (Table II) revealed statistically significant differences from distilled water groups in the following clinical endpoint/dose group combinations: (1) increased calcium levels in females drinking 0.25 g/L ozonated humic acids, 1.0 g/L ozonated humic acids, and 1.0 g/L ozonated/chlorinated humic acids; (b) increased PO₄ levels in females for all of the 1.0 g/L humic acid groups (nondisinfected, ozonated, and ozonated/chlorinated); (c) decreased glucose levels in males for several humic acids groups, 0.25 and 1.0 g/L ozonated and 1.0 g/L ozonated/chlorinated; and (d) decreased LDH and creatinine levels in males for the 1.0 g/L nondisinfected group. Significantly higher creatinine levels and significantly lower calcium levels relative to the 1.0 g/L nondisinfected humic acids were observed for males in the two 1.0 g/L disinfected (ozonated and ozonated/chlorinated) humic acid groups; however, the two disinfected groups did not significantly differ from each other. Similarly, in females the 1.0 g/L nondisinfected humic acid group had significantly lower serum cholesterol levels than the two 1.0 g/L disinfected groups, but the latter two groups did not differ from each other. Comparison of the two 0.25 g/L disinfected humic acid groups showed a significant difference only in BUN levels (Table II).

Gross Pathology. The most noteworthy condition observed at necropsy was the enlargement of mandibular lymph nodes. However, this was a consistent finding in all groups with a 78% incidence in treated groups versus

Table II. Selected Clinical and Hematological Values for Rats Exposed to Ozonated/Chlorinated Humic Acids in Drinking Water for 90 Days

parameter ^b	humic acids dose group, ^a g/L; disinfectant					
	0; none	1.0; none	0.25; O ₃	0.25; O ₃ /Cl ₂	1.0; O ₃	1.0; O ₃ /Cl ₂
	Males					
BUN, mg/dL	14.8 ± 2.4 ^{ab}	16.8 ± 2.3 ^{ab}	17.2 ± 2.0 ^b	13.4 ± 2.4 ^a	20.8 ± 12.0 ^b	16.4 ± 2.0 ^a
creatinine, mg/dL	0.62 ± 0.04 ^{ab}	0.42 ± 0.08 ^c	0.46 ± 0.14 ^{bc}	0.56 ± 0.14 ^{abc}	0.70 ± 0.21 ^a	0.64 ± 0.14 ^{ab}
AST, units/L	36.0 ± 10.4	43.3 ± 9.5	41.9 ± 6.8	38.4 ± 10.0	40.1 ± 8.1	38.6 ± 8.3
ALT, units/L	120.9 ± 20.2	103.8 ± 14.9	128.7 ± 20.6	121.3 ± 20.3	100.6 ± 23.5	100.6 ± 20.1
LDH, units/L	1439 ± 798 ^a	523 ± 185 ^b	897 ± 284 ^{ab}	1322 ± 462 ^a	800 ± 342 ^{ab}	1059 ± 599 ^{ab}
calcium, mg/dL	10.5 ± 0.3 ^{ab}	11.0 ± 0.6 ^b	10.8 ± 0.6 ^b	10.4 ± 0.4 ^{ab}	9.8 ± 0.5 ^a	10.0 ± 0.3 ^a
PO ₄ , mg/dL	7.6 ± 0.6	8.3 ± 0.9	8.0 ± 1.0	7.7 ± 0.7	7.8 ± 0.7	8.2 ± 0.9
glucose, mg/dL	184.2 ± 16.9 ^a	156.3 ± 15.5 ^{abc}	54.4 ± 33.9 ^{bc}	171.5 ± 20.8 ^{ab}	129.1 ± 15.6 ^c	138.4 ± 20.0 ^c
RBC, 10 ⁶ /μL	8.0 ± 0.3	7.7 ± 0.4	7.9 ± 0.4	7.7 ± 0.4	7.8 ± 0.3	7.8 ± 0.3
WBC, 10 ³ /μL	6.7 ± 1.0	5.6 ± 0.7	6.9 ± 1.5	6.5 ± 0.7	6.3 ± 3.7	6.0 ± 1.6
hemoglobin, g/L	15.3 ± 0.5 ^a	14.5 ± 0.6 ^b	14.7 ± 0.5 ^{ab}	14.9 ± 0.7 ^{ab}	14.5 ± 0.4 ^b	14.7 ± 0.5 ^{ab}
hematocrit, %	43.7 ± 2.0	41.6 ± 2.6	42.3 ± 3.1	42.1 ± 2.3	42.7 ± 1.6	42.8 ± 1.4
reticulocytes, %	1.4 ± 0.1	1.2 ± 0.1	1.1 ± 0.4	1.4 ± 0.2	1.6 ± 0.1	1.5 ± 0.1
cholesterol, mg/dL	76.2 ± 11.6	87.6 ± 16.3	80.6 ± 21.9	77.6 ± 23.0	64.6 ± 18.8	79.7 ± 19.0
	Females					
BUN, mg/dL	18.4 ± 2.9 ^{ab}	24.3 ± 14.3 ^{ab}	16.3 ± 2.0 ^a	16.2 ± 2.8 ^a	23.1 ± 5.4 ^b	23.9 ± 3.4 ^b
creatinine, mg/dL	0.66 ± 0.08	0.67 ± 0.15	0.66 ± 0.07	0.59 ± 0.11	0.56 ± 0.15	0.49 ± 0.17
AST, units/L	34.5 ± 11.1	31.2 ± 5.4	34.7 ± 6.2	34.2 ± 8.8	55.4 ± 39.6	36.6 ± 10.4
ALT, units/L	83.8 ± 12.4	86.0 ± 18.7	82.2 ± 15.7	84.8 ± 12.6	113.3 ± 50.3	101.2 ± 19.7
LDH, units/L	462 ± 161	463 ± 231	525 ± 324	390 ± 162	532 ± 235	520 ± 318
calcium, mg/dL	10.1 ± 0.5 ^a	11.2 ± 0.7 ^{abc}	11.6 ± 1.6 ^{bc}	10.4 ± 0.4 ^{ab}	11.6 ± 0.5 ^c	12.0 ± 0.5 ^c
PO ₄ , mg/dL	5.6 ± 0.7 ^a	7.6 ± 1.4 ^{bd}	6.8 ± 0.9 ^{abd}	6.1 ± 0.7 ^{ab}	7.4 ± 1.4 ^{bd}	7.9 ± 0.8 ^d
glucose, mg/dL	141.3 ± 25.1	133.6 ± 27.8	148.8 ± 25.2	130.4 ± 18.0	161.8 ± 36.3	160.8 ± 21.2
RBC, 10 ⁶ /μL	7.4 ± 0.3	7.4 ± 0.4	7.2 ± 0.3	7.5 ± 0.3	7.2 ± 0.2	7.2 ± 0.4
WBC, 10 ³ /μL	93.9 ± 1.2	4.1 ± 2.0	3.5 ± 1.5	5.2 ± 1.5	4.6 ± 1.5	3.5 ± 1.1
hemoglobin, g/L	14.6 ± 0.5	14.2 ± 0.8	14.1 ± 0.5	14.6 ± 0.5	14.1 ± 0.5	14.0 ± 0.7
hematocrit, %	41.0 ± 1.7	40.7 ± 2.4	40.1 ± 2.1	40.9 ± 1.4	40.3 ± 1.6	39.9 ± 2.2
reticulocytes, %	1.4 ± 0.2	2.2 ± 0.4	1.9 ± 0.8	1.4 ± 0.3	1.7 ± 1.0	2.4 ± 0.4
cholesterol, mg/dL	102.8 ± 26.7 ^{ab}	79.9 ± 4.9 ^a	80.3 ± 11.2 ^a	99.4 ± 19.2 ^{ab}	122.1 ± 16.8 ^b	112.1 ± 15.3 ^b

^a a-c, means with the same letter are not significantly different ($\alpha = 0.05$). ^b Parameters (mean ± SD). Measurement made on 10 animals. ^c Measurement on two animals.

Table III. Microscopic Lesions Observed in Rats Exposed to Ozonated/Chlorinated Humic Acids in Drinking Water for 90 Days

	humic acids dose group, g/L; disinfectant			
	0; none	1.0; none	1.0; O ₃	1.0; O ₃ /Cl ₂
no. of animals examined/group	5	10	10	10
lesions, males^a				
heart, chronic inflammation/ degeneration	4	6	6	8
kidney lesions	5	8	10	9
nephropathy, chronic	5	8	10	9
inflammation	0	0	2	0
hyperplasia	0	1	1	0
liver, inflammation/ necrosis	5	10	10	10
lungs, inflammation/congestion	1	3	3	2
pancreas, inflammation/degeneration	4	4	1	4
thyroid lesions	0	7	0	2
colloid depletion	0	5	0	2
follicular cysts	0	3	0	0
lesions, females^a				
heart, chronic inflammation/degeneration	1	2	1	3
kidney lesions	3	5	5	5
nephropathy, chronic	0	1	1	3
inflammation	0	2	1	1
mineralization	2	3	2	0
hyperplasia	0	2	2	1
dilatation	0	2	0	2
liver, inflammation/necrosis	5	10	8	9
pancreas, inflammation/degeneration	3	2	4	5
uterus, dilatation	2	3	7	4

^a Number of animals with lesions, except for specific kidney and thyroid lesions, which are specifically enumerated.

80% incidence in the controls. Pelvic dilatation involving the kidneys and congestion of the lungs was sporadically observed with no apparent treatment-related trend.

Histopathology. While a number of microscopic lesions were observed in the tissues examined, there was no apparent treatment-related effect. Based on these findings,

no specific target organs were identified in either sex at any concentration of humic acids either nondisinfected or when ozonated or ozonated/chlorinated (Table III).

All male and all but three female rat livers examined had areas of inflammation and/or necrosis. These lesions were generally graded as minimal in severity and were not considered treatment-related but rather spontaneous background changes of unknown etiology.

Kidney lesions were also a common observation. The lesion of highest incidence was chronic progressive nephropathy, which was noted with minimal severity in 15/30 treated female and 27/30 treated males but also in 3/5 and 5/5 control females and males, respectively. This lesion is a common spontaneous change in Sprague-Dawley rats, especially males, and is not considered treatment related. Two animals (one male and one female) displayed moderate to severe pyelonephritis, both in the 1.0 g/L ozonated humic acid groups. Another sporadic finding in treated female rats (4/30) was pelvic dilatation occurring both with and without compensatory epithelial hyperplasia and chronic inflammation.

Thyroid lesions were observed in seven males in the 1.0 g/L humic acids group compared to none in the controls and the 1.0 g/L ozonated humic acids group and only two in the other 1.0 g/L ozonated/chlorinated group. Most lesions consisted of colloid depletion of minimal severity, although follicular cysts were also observed. Similar lesions were not observed in the female animals.

Discussion

In these studies, rats were administered drinking water containing gram per liter concentrations of humic acids, which was either nondisinfected or had been disinfected by ozonation or ozonation followed by chlorination. The rats were provided these humic acid-disinfectant combinations for 90 days, after which they were euthanized and subjected to detailed pathological examinations and to hematology/clinical chemistry measurements.

All animals survived the 90-day test period and there was little evidence of a treatment-related effect nor could a target organ be identified for the disinfected humic acid groups. The sporadic and inconsistent differences in clinical chemistry parameters observed in some groups were minor changes, and no pattern evolved to indicate an overall adverse treatment relationship.

The histopathological examination demonstrated many spontaneous background lesions commonly noted in Sprague-Dawley rats. The incidence of some of these lesions was mildly increased but in no case were these increases appreciably greater than the control animals. Two exceptions to this generalization were one male and one female with pyelonephritis, pelvic dilation, and pelvic epithelial hyperplasia, both in the 1.0 g/L ozonated humic groups. However, the incidence of these changes is too low to be clearly classified as a treatment-related response. Nevertheless, these results indicate that additional examination of nephrotoxicity might be warranted. There was no indication of a treatment-related effect on the liver based on the microscopic examinations, but the significant increase in liver to body weight ratio for the male 1.0 g/L ozonated/chlorinated humic acids group might be worthy of further consideration. On the other hand, none of the clinical chemistry measurements suggested liver toxicity.

Minor thyroid effects were observed in the majority of male rats in the 1.0 g/L nondisinfected humic acid group and to a much lesser extent in the 1.0 g/L ozonated/chlorinated group but not in the 1.0 g/L ozonated group. These effects would indicate that future studies should include evaluation of thyroid function (e.g., thyroid stim-

ulating hormone, T3, and T4 levels). However, it would appear that the oxidation of humic acids by ozone may destroy the causative agent, as evidenced by the fact that the 1.0 g/L ozonated humic acid group does not show thyroid effects.

Using a nearly identical subchronic protocol, Condie et al. (4) exposed Sprague-Dawley male rats to drinking water solutions of both nondisinfected and chlorinated humic acids of the same concentration (1.0 g/L) and type used in this study. A significant decrease in terminal body weight and average body weight gain was seen only in the animals receiving the 1.0 g/L chlorinated humic acids (apparently due to reduced daily fluid consumption), but not in 1.0 g/L nondisinfected humic acids. The mean absolute kidney weights were significantly higher in these animals, and in addition, there was an increase in the incidence and severity of hematuria in rats in the chlorinated humic acids group. The hematuria was correlated with the presence of crystalline deposits in the renal pelvis, which, in turn, may have resulted from precipitation of the humic acid chlorination byproducts during reabsorption.

In the present study, however, neither hematuria nor changes in body or organ weights were observed in rats drinking similar concentrations of either ozonated humic acids or ozonated/chlorinated humic acids. There is no apparent explanation for these differences at this time. However, it is possible that ozonation is destroying a critical precursor to the responsible toxicant and this observation merits further investigation.

While ozone is an established inhalation toxicant producing a variety of effects, including toxicity of the lung and other organs (9-12), there have been relatively few studies on the toxicity of ozone or its reaction products when administered via aqueous solution. Short-term, *in vitro* bioassays on ozonated drinking water samples and organics isolated from the same have produced mixed results. Even fewer studies have addressed the combined process of ozonation and chlorination.

A commercial grade of soil humics was used in this study. Suitable quantities of aquatic humics are not available, and it is now well established that chlorination of both soil and aquatic humic acid and fulvic acid solutions results in the generation of mutagenic reaction byproducts (5, 13). Further, these byproducts are similar to those found in the organics from concentrates of chlorine-disinfected surface waters (14). Even more significant is the finding that up to 60% of the total mutagenic activity in both of these media (as measured in bacterial bioassays) has been attributed to a single chemical, 3-chloro-4-(dichloromethyl)-5-hydroxy-2(5H)-furanone (15). Thus, the humic acid model used here appears to be a reasonable surrogate for drinking water disinfection byproducts.

However, while chlorination has been invariably shown to increase the mutagenic activity of a variety of humic and fulvic acid solutions as well as drinking water concentrates, ozonation has been varied in its response, showing both enhancement (16-19) and reduction (3, 20-22) of the mutagenic activity of humic acids and drinking water concentrates. Likewise, the ability of ozone to destroy the precursors to chlorination-derived mutagens has been varied and often dependent on the ozone to TOC ratio and the quality of the source water (25, 26).

One study has shown that topical application of organics concentrated by reverse osmosis from ozone-disinfected water produced a level of skin tumors in SENCAR mice comparable to those from chlorine-disinfected or chloramine-disinfected drinking water concentrates (27).

However, in a subsequent study, 4000-fold concentrates of chlorine- or ozone-disinfected water from the Mississippi River did not induce a neoplastic response in either the rat liver enzyme altered focus assay, the strain A mouse lung adenoma assay, or the SENCAR mouse skin initiation assay, three short-term bioassays for carcinogenesis (3). Finally, it must be noted that the administration of 1.0 g/L chlorinated humic acid (as well as nondisinfected humic acid) in drinking water to B6C3F1 mice for 2 years did not result in increased tumor prevalence or tumor multiplicity (28).

In view of the lack of toxicity at 1.0 g/L humic acid solutions, either with or without ozone or ozone/chlorine disinfection, a no observable adverse effect level (NOAEL) of 1.0 g/L TOC could be suggested for nontreated or treated (ozonated or ozonated/chlorinated) humic acids in rats when administered for 90 consecutive days in drinking water. This NOAEL would be qualified in light of the fact that the O₃ to TOC ratio may influence the toxicity and further study is still advisable. On the other hand, the ratio of TOC to O₃ used in this study was 1:1 (by weight) and this is similar to ratios used in many municipal treatment plants (29). This compares with the NOAEL of 0.5 g/L TOC obtained in the study of Condie et al. (4) with chlorinated humic acids drinking water.

The differences in the observed NOAELs between the chlorinated humic acids and the ozonated humic acids are small. Thus, it cannot necessarily be concluded that ozonation byproducts are less toxic than those produced by chlorination. However, these results are consistent with previous studies that suggest that ozonation byproducts might be somewhat less toxic as regards their responses in various short-term in vivo and in vitro bioassays for genotoxicity and/or cancer. Obviously, no definitive statement regarding the relative toxicity of ozonated versus chlorinated humics can be made at this juncture. Clearly, however, this is a topic of considerable importance due to the widespread human exposure to drinking water disinfection byproducts.

Finally, it is well to recognize that some form of drinking water disinfection is obligatory in order to prevent widespread human death from microbiologically transmitted disease. Thus, it is strongly recommended that further research into the chemistry and toxicology of ozone and ozone/chlorine disinfection byproducts be conducted before definitive conclusions about the relative risk imparted by chlorination versus ozonation/chlorination processes be formulated or before one process or the other is rejected as an unacceptable risk to public health.

Literature Cited

- (1) Anderson, A.; Reimers, R.; deKernion, P. *Am. J. Public Health* 1982, 72, 1290-1293.
- (2) Carmichael, N.; Winder, C.; Borges, S.; Backhouse, B.; Lewis, P. *Life Sci.* 1982, 30, 117-129.
- (3) Miller, R.; Kopfler, F.; Condie, L.; Pereira, M.; Meier, J.; Ringhand, H.; Robinson, M.; Casto, B. *Environ. Health Perspect.* 1986, 69, 129-139.
- (4) Condie, L.; Laurie, R.; Bercz, J. *J. Toxicol. Environ. Health* 1985, 15, 305-314.
- (5) Meier, J.; Ringhand, H.; Coleman, W.; et al. *Mutat. Res.* 1985, 157, 111-122.
- (6) Dixon, M.; Massey, F. In *Introduction to Statistical Analysis*; McGraw-Hill Book Co.: New York, 1969; pp 156-167.
- (7) Winer, B. *Statistical Principles in Experimental Design*; McGraw-Hill Book Co.: New York, 1971.
- (8) Hollander, M.; Wolfe, D. In *Nonparametric Statistical Methods*; 1973; pp 114-129.
- (9) Stockinger, H. E. In *Handbook of Physiology*; Williams and Wilkins Co.: Baltimore, MD, 1965; pp 1067-1087.
- (10) Merz, T.; Bender, M. A.; Kerr, H. D.; Kulle, T. *J. Mutat. Res.* 1975, 31, 299-305.
- (11) Gooch, P. C.; Creasia, D. A.; Brewer, J. G. *Environ. Res.* 1976, 12, 188-195.
- (12) Tice, R. R.; Bender, M. A.; Ivett, J. L.; Drew, R. T. *Mutat. Res.* 1978, 58, 293-304.
- (13) Meier, J. R.; Lingg, R. D.; Bull, R. J. *Mutat. Res.* 1983, 118, 25-41.
- (14) Reckhow, D. A.; Singer, P. C. *J.—Am. Water Works Assoc.* 1990, 82, 173-180.
- (15) Meier, J. R.; Knohl, R. B.; Coleman, W. E.; Ringhand, H. P.; Munch, *Mutat. Res.* 1987, 189, 363-373.
- (16) Dolara, P.; Ricci, V.; Burrini, D.; Griffini, O. *Bull. Environ. Contam. Toxicol.* 1981, 27, 1-6.
- (17) Gruener, N. *Bull. Environ. Contam. Toxicol.* 1978, 20, 522-526.
- (18) Carlberg, G. E.; Loras, V.; Moller, M.; Soteland, N.; Treten, G. *Das Papier* 1981, 35, 257-264.
- (19) Zoeteman, B. C. J.; Hrubec, J.; DeGreef, E.; Kool, H. J. *Environ. Health Perspect.* 1982, 46, 197-205.
- (20) Cognet, L.; Courtois, Y.; Mallevalle, J. *Environ. Health Perspect.* 1986, 69, 165-175.
- (21) Denkhans, R.; Grabow, W.; Prozesky, O. *Prog. Water Technol.* 1980, 12, 571-589.
- (22) Kowbel, D. J.; Ramaswamy, S.; Malaiyandi, M.; Nestmann, E. R. *Environ. Mutagen.* 1986, 8, 253-262.
- (23) Backlund, P.; Kronberg, L.; Tikkanen, L. *Chemosphere* 1988, 17, 1329-1336.
- (24) Kool, H. J.; Hrubec, J.; Van Kreijl, C. F.; Piet, G. *J. Sci. Total Environ.* 1985, 47, 229-256.
- (25) Backlund, P.; Kronberg, L.; Pensar, G.; Tikkanen, L. *Science Total Environ.* 1985, 47, 257-264.
- (26) Bourbigot, M. M.; Hascoet, M. C.; Levi, Y.; Erb, F.; Pommeroy, N. *Environ. Health Perspect.* 1986, 69, 159-163.
- (27) Bull, R.; Robinson, M.; Meier, J.; Stober, J. *Environ. Health Perspect.* 1982, 46, 215-227.
- (28) Van Duuren, B. L.; Melchionne, S.; Seidman, I.; Periera, M. A. *Environ. Health Perspect.* 1986, 69, 109-117.
- (29) Glaze, W. H.; Koga, M.; Cancilla, D. *Environ. Sci. Technol.* 1989, 23, 838-847.

Received for review November 3, 1989. Revised manuscript received July 30, 1990. Accepted August 3, 1990. Disclaimer: This document has been reviewed in accordance with U.S. Environmental Protection Agency policy and approved for publication. Approval does not signify that the contents necessarily reflect the views or policies of the Agency nor does mention of trade names or commercial products constitute endorsement or recommendation for use.

Identification of Oxidized and Reduced Forms of the Strong Bacterial Mutagen (*Z*)-2-Chloro-3-(dichloromethyl)-4-oxobutenoic Acid (MX) in Extracts of Chlorine-Treated Water

Lelf Kronberg,[†] Russell F. Christman,*[‡] Ravinder Singh,[‡] and Louise M. Ball[‡]

Department of Organic Chemistry, The University of Åbo Akademi, Akademigatan 1, SF-20500 Åbo, Finland, and Department of Environmental Sciences and Engineering, School of Public Health, University of North Carolina at Chapel Hill, Chapel Hill, North Carolina 27599-7400

■ Oxidized and reduced forms of (*Z*)-2-chloro-3-(dichloromethyl)-4-oxobutenoic acid (MX) and the oxidized form of its geometric isomer (EMX) were synthesized, evaluated for mutagenic potency in the Ames assay, and quantitatively determined in chlorinated aqueous solutions of fulvic acids, in chlorinated natural humic water, and in chlorinated drinking water. The compounds were found in chlorinated drinking waters at concentrations equal to or greater than MX. In the Ames assay the pure oxidized compounds were nonmutagenic at the dose levels tested while the reduced form of MX was weakly mutagenic relative to MX. These findings suggest that the *cis* arrangement of the dichloromethyl and chlorine groups around the carbon-carbon double bond and the presence of the aldehyde function strongly enhance the mutagenic response.

Introduction

Concern for the potential human health hazards associated with chlorinated drinking water has been heightened by the widespread recognition in recent years of mutagenic activity exhibited by the nonvolatile fraction. The subject has been reviewed by Loper and by Meier (1, 2). In addition, epidemiological studies have suggested that an increase in the risk of bladder cancer is correlated with the intake of chlorinated tap water (3). Although a number of mutagenic compounds have been detected in chlorinated drinking and humic water, the only major mutagen actually identified is the compound (*Z*)-2-chloro-3-(dichloromethyl)-4-oxobutenoic acid (MX) (4-7). The concentration of MX in drinking water is usually less than 60 ng/L, but since MX is an extremely potent mutagen in the Ames assay, this compound may account for as much as 50% of the mutagenicity of chlorinated drinking waters (8).

MX has previously been named 3-chloro-4-(dichloromethyl)-5-hydroxy-2(5*H*)-furanone since the compound forms a furanone ring at pH below 5.3. However, at the pH of drinking water and under the neutral conditions of the Ames assay, MX exists in a ring-opened form (9, 10). Thus, when discussing the chemistry in neutral water solutions and the mutagenicity of MX, one should primarily think of MX as an oxobutenoic acid.

MX has never been observed in chlorinated waters in the absence of its geometric isomer (*E*)-2-chloro-3-(dichloromethyl)-4-oxobutenoic acid (EMX) (7, 8, 11). However, the mutagenic potency of EMX is less than 10% of MX and this compound is responsible for no more than a few percent of the observed mutagenicity (5).

In order to gain a more comprehensive understanding of the impact of mutagens in drinking water, the chemical identity of the compounds responsible for major portions

of the residual activity should be determined. Previous studies have indicated that as much as 90% of the mutagenicity is attributable to nonvolatile compounds with acid properties, and that the major mutagens present are susceptible to attack by nucleophiles (9, 12-15).

MX contains structural features rendering it a highly active mutagen in the Ames assay. Acid compounds with structural similarities to MX could be present in chlorinated water and could be responsible for part of the residual mutagenicity. As MX and EMX contain an aldehyde group, we postulated that the oxidizing conditions of chlorination could form the diacid of each molecule, and that if MX represents a fragment of the original humic structure, the reduced form of MX might be a precursor of the compound and also be present in chlorination mixtures.

In this work, the oxidized and reduced forms of the compounds (except the reduced form of EMX) were successfully synthesized and characterized by proton nuclear magnetic resonance (¹H NMR) spectroscopy and mass spectrometry (MS). The mutagenic potency of each pure compound was determined in the Ames histidine reversion assay (with strains TA98, TA102, and TA100); extracts of chlorinated water were analyzed for the presence of these compounds by gas chromatography/mass spectrometry (GC/MS) and for mutagenicity, in order to determine the contribution made by each compound to the total mutagenicity.

Experimental Section

Water Samples and Chlorination Procedure. Fulvic acids, previously extracted by the method of Thurman and Malcolm (16) from a highly colored natural lake (Lake Drummond, VA), were dissolved in 50 mL of distilled water to give a total organic carbon content (TOC) of 2.5 g/L. The water solution was acidified to pH 2 with 4 N HCl, and the solution was treated with chlorine at a Cl₂/TOC weight ratio of 2.0. Natural humic water, with a TOC content of 20 mg/L, was collected from Lake Savojaervi located in a marsh region in the southwest of Finland. The sample was chlorinated at pH 7 at a Cl₂/TOC weight ratio of 1 (5).

During chlorination, the pH of each sample was monitored and readjusted to the desired value as necessary. After a reaction time of 60 h, the total chlorine residuals in the samples were less than 0.1 mg/L; the pH value of the humic water sample was lowered to pH 2 by addition of 4 N HCl.

A 4-L sample of drinking water, derived from surface water with a TOC content of approximately 5 mg/L, was collected from the distribution system of a municipality in North Carolina. The water had been chlorinated at the treatment plant with approximately 5 mg of Cl₂/L. The sample was stored for 24 h in a decanter glass to get rid of most of the residual chlorine and then the pH of the

[†]The University of Åbo Akademi.

[‡]University of North Carolina at Chapel Hill.

sample was adjusted to pH 2 by addition of 4 N HCl.

Isolation and Concentration of Mutagens. Immediately after the pH of the chlorinated humic water and drinking water was lowered the samples were passed through columns of XAD-4 and XAD-8 resins (1:1 mixture by volume). The flow rate was approximately one bed volume/min (20 mL/min). Most of the residual water in the column was then removed by a gentle stream of nitrogen. The adsorbed organics were eluted with three bed volumes of ethyl acetate. The extracts were concentrated and the final volume was adjusted to 1 mL of ethyl acetate/per L of original water. The extract of chlorinated humic water will be referred to as sample HW and the extract of drinking water as sample DW.

An 8-mL aliquot of fulvic acid solution was chlorinated and extracted with three portions of diethyl ether (3 × 20 mL). The combined extract was evaporated to dryness and redissolved in ethyl acetate so that 1 mL of ethyl acetate corresponded to 1 L of water containing 20 mg of C/L. The chlorinated fulvic acid sample will be referred to as sample FA.

Compound Synthesis. (*Z*)-2-Chloro-3-(dichloromethyl)butenedioic acid (ox-MX) was prepared by oxidation of 185 μmol (40 mg) of MX with fuming nitric acid (2 mL) at 70 °C for 24 h. The reaction mixture was cooled in an ice bath, diluted with 20 mL of ice-cold water, and subsequently extracted three times with diethyl ether. The combined ether extract was washed with 0.01 N HCl and then evaporated to dryness. Following recrystallization from CH₂Cl₂, the pure compound (9.1 mg) was obtained as white crystals. The ¹H NMR spectrum of the compound showed the resonance signal of the proton in the dichloromethyl group at δ 6.78. The direct probe EI mass spectrum of the compound in the anhydride form is shown in Figure 1.

(*E*)-2-Chloro-3-(dichloromethyl)butenedioic acid (ox-EMX) was prepared by oxidation at room temperature of 46.3 μmol (10 mg) of EMX with 56 μmol of NaClO₂ and resorcinol as chlorine scavenger in water at pH 3.5 (17). After 2.5 h, the mixture was adjusted to pH 4.5 and washed with diethyl ether. The pH of the water solution was lowered to pH 2, and ether extraction was repeated. This ether extract was washed with 0.01 N HCl, and following evaporation of the ether, the product was recrystallized from CH₂Cl₂. Finally, the crystals were washed with CCl₄. ox-EMX was obtained as white crystals (3.8 mg). The ¹H NMR resonance signal of the proton in the dichloromethyl group was observed at δ 5.55. Figure 1 shows the direct inlet probe EI mass spectrum of ox-EMX.

3-Chloro-4-(dichloromethyl)-2(5*H*)-furanone (red-MX) was obtained by reduction of 93 μmol (20 mg) of MX with 225 μmol of aluminum isopropoxide in 2-propanol (the Meerwein-Ponndorf reduction) at 70 °C for 2 h (18). The reaction was stopped by the addition of ice and 4 N HCl. Following heating of the acidified mixture for a few minutes to 50 °C and recooling, the mixture was extracted three times with diethyl ether. The combined extracts were washed with 0.01 N HCl; following evaporation of the ether, the crude product was obtained. Purification on SiO₂ (6 g) with CH₂Cl₂-hexane (1:1) as eluent gave the pure compound (3.3 mg) as a colorless liquid. The ¹H NMR resonance signal of the proton in the dichloromethyl group was observed at δ 6.74 and of the two protons in the lactone ring at δ 5.15. High-resolution studies showed the signal at δ 6.74 to be a triplet and the signal at δ 5.15 to be a doublet with a coupling constant (*J*) of approximately 0.8 Hz. The direct-probe electron impact mass spectrum of red-MX is shown in Figure 1.

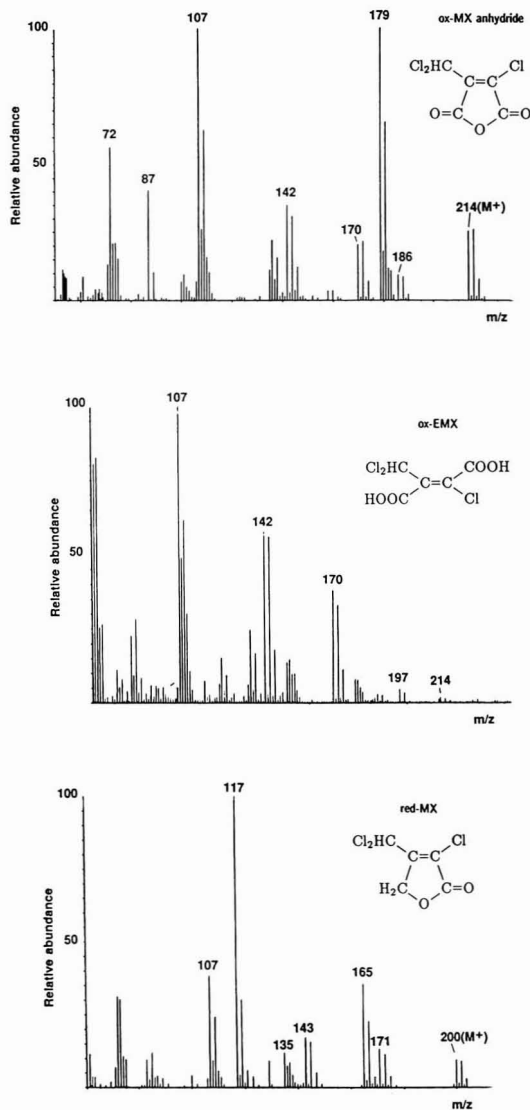


Figure 1. Mass spectra of ox-MX, ox-EMX, and red-MX.

Derivatization and GC/MS Procedures. Prior to derivatization the extracts were evaporated to dryness and the residues methylated with 250 μL of the methylation agent. Extracts for selected ion monitoring (SIM) mode GC/MS analyses of MX and EMX were methylated with 2% (v/v) H₂SO₄ in methanol for 1 h at 70 °C. SIM mode GC/MS determinations of ox-MX and ox-EMX were carried out on extracts methylated with 12% by weight BF₃ in methanol. The methylation was performed at 100 °C for 12 h. The methylated mixtures were neutralized by the addition of 2% aqueous NaHCO₃ and extracted twice with hexane (approximately 2 × 250 μL). The combined hexane extracts were concentrated under nitrogen and injected into the GC apparatus. The mass spectra of methylated ox-MX and ox-EMX are shown in Figure 2.

Quantitative determinations were carried out relative to the standard mucobromic acid (MBA) added in known amounts to the extracts prior to methylation. The analyses of red-MX were carried out on underivatized extracts to

Table I. Ion Peaks Used for SIM Quantification of red-MX, ox-MX, and ox-EMX

compound	fragmentation	m/z	std	relative peak area ratios					
				FA	HW	DW	DW ^a		
							spike level 1	spike level 2	
red-MX	M - Cl	164.951	1.00	1.00	1.00	1.00	1.00	1.00	
		166.948	0.66	0.67	0.62	0.47	0.60	0.55	
	M - CHO	170.917	0.41	0.38	0.42	0.30	0.31	0.31	
		172.914	0.39	0.31	0.36	0.21	0.30	0.28	
ox-MX (anhydride)	M - CO ₂	169.909	0.43	0.40	0.37	0.43	0.39	0.46	
		171.906	0.37	0.34	0.36	0.37	0.36	0.43	
	M - Cl	178.930	1.00	1.00	1.00	1.00	1.00	1.00	
		180.927	0.74	0.62	0.65	0.68	0.70	0.68	
	M ⁺	213.899	0.19	0.22	0.20	0.20	0.21	0.15	
215.896		0.16	0.18	0.16	0.25	0.14	0.19		
ox-MX (methylated)	M - Cl	224.972	0.72	0.42	0.60	1.75 ^b	1.09	0.98	
		226.969	0.58	0.19	0.35	0.46	0.57	0.64	
	M - CH ₃ OH	227.915	0.97	1.03	1.23	1.01	0.95	0.98	
		229.912	1.00	1.00	1.00	1.00	1.00	1.00	
	M - OCH ₃	228.923	1.08	1.41 ^b	0.96	0.69	1.16	1.07	
230.920		1.01	1.57 ^b	1.13	c	0.88	0.86		
ox-EMX	M - COOCH ₃	200.928	0.96	1.03	1.11	1.10			
		202.925	1.00	1.00	1.00	1.00			
	M - OCH ₃	224.972	0.87	0.70	0.71	0.79			
		226.969	0.39	0.43	0.48	0.49			
red-MBA	M - Br	160.924							
MBA	M - OCH ₃	240.832							

^a Spike levels; see Table IV. ^b Interference from ox-EMX ion peak. ^c Interference from background.

which 2,3-dibromo-2(5H)-furanone (red-MBA) was added as standard.

The GC/MS analyses were performed on a Hewlett-Packard 5890 capillary gas chromatograph interfaced to a VG 70-250 SEQ mass spectrometer. The ionization mode was electron impact and the resolving power was 1000. MX, EMX, and red-MX were separated on a DB-1, 30-m-long fused-silica capillary column (temperature program: at 110 °C for 3 min and then at 6 °C/min to 165 °C), while ox-MX and ox-EMX were separated on a DB-5 60-m column (temperature program: at 160 °C for 3 min and then at 6 °C/min to 190 °C). For quantitative and qualitative purposes the mass spectrometer was operated in the SIM mode. The ox-MX, ox-EMX, and red-MX ion peaks monitored are listed in Table I, while the MX and EMX ions selected were those reported previously (5). The standard SIM routine of the VG 11-250J data system was used to record and compute the SIM data. The response factors for the ions of the analytes vs MBA or red-MBA ions were calculated from the analyses of standard mixtures. The identification of the analytes in the extracts was based on positive matching of retention times and relative ratios of ion peak areas.

NMR Spectroscopy. The ¹H NMR spectra were recorded in DMSO with a JEOL GX 400 Fourier transform NMR spectrometer (400 MHz).

Mutagenicity Assay Procedure. The bacterial mutagenicity of red-MX, ox-MX, and ox-EMX was determined in the constructed *Salmonella typhimurium* strains TA100, TA102, and TA98 according to the standard plate incorporation procedure of Maron and Ames (19). The presence of genetic markers as well as spontaneous reversion rates and positive control responses was verified for each master plate before it was used to grow overnight cultures of the strain. The positive control and spontaneous responses were also verified along with every experiment. The positive control chemicals and the amount added per plate were as follows: TA100 (-S9) 1.5 μg of sodium azide (Aldrich, Milwaukee, WI), TA100 (+S9) 0.5 μg of 2-anthramine (Sigma, St. Louis, MO), TA98 (-S9) 3.0 μg of 2-nitrofluorene (Aldrich), TA98 (+S9) 0.5 μg of 2-anthramine, TA102 (-S9) 6.0 μg of daunomycin (Fluka

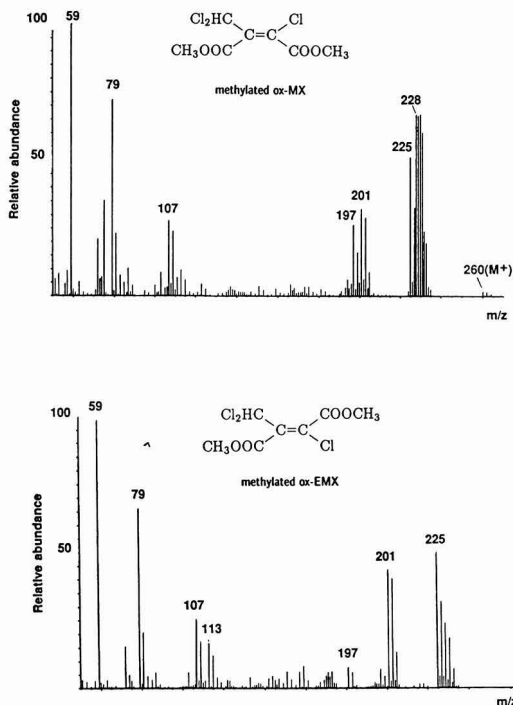


Figure 2. Mass spectra of methylated ox-MX and methylated ox-EMX.

Chemical Corp., Ronkokoma, NY), TA102 (+S9) 30 μg of 1,8-dihydroxyanthraquinone (Sigma). Responses were within historical norms.

The effect of exogenous xenobiotic metabolizing enzymes on the mutagenicity of the MX analogues was tested by adding Aroclor 1254 induced rat liver homogenate fraction, (S9; Molttox, College Park, MD) at 0.6 mg of protein/plate.

The synthesized compounds and the extracts were stored in ethyl acetate which, at the time of testing, was

Table II. Mutagenic Potency of red-MX

tester strain	metabolic activation	no. of revertants found for various doses ^a					revertants/nmol ^b
		0 ng	250 ng	500 ng	1000 ng	2000 ng	
TA98	-S9 mix	15.1 ± 1.2	14.3 ± 4.0	12.7 ± 4.2	19.3 ± 2.1	26.3 ± 5.1	80
TA98	+S9 mix	21.7 ± 5.5	21.7 ± 5.8	23.3 ± 6.8	27.0 ± 7.6	27.7 ± 3.5	
TA100	-S9 mix	138.7 ± 6.0	228.3 ± 10.0	313.7 ± 45.1	570.7 ± 13.2	923.7 ± 10.7	
TA100	+S9 mix	152.7 ± 6.7	131.0 ± 7.9	134.7 ± 6.1	176.0 ± 7.8	215.3 ± 9.6	

^a Mean of three plates ±SD. ^b Calculated by least-squares regression analysis of the dose-response curve.

Table III. Concentration of MX and the MX Analogues in Extracts of Chlorinated Water and the Mutagenicity Contribution of the Active Compounds

sample	mutagenicity, ^a revertants/mL	concn, ng/L					mutagenicity contribn, ^b %		
		MX	EMX	red-MX	ox-MX	ox-EMX	MX	EMX	red-MX
FA	48	675	1204	643	961	26777	36	4	0.5
HW	21	260	526	370	306	5081	32	4	0.7
DW	2.0	13	20	58	53	251	13	2	1.2

^a Determined with strain TA 100 (-S9). ^b Calculated on the basis of 5600, 320, and 80 net revertants/nmol specific MX, EMX, and red-MX TA100 (-S9) mutagenicity, respectively.

evaporated under a stream of nitrogen or helium. The residues were then redissolved in the test solvent, DMSO. All experiments were done at a minimum of four dose levels using duplicate or triplicate plates per dose. Each experiment was repeated at least once on a separate day. A dose-related increase above the background rate of spontaneous reversion indicated mutagenicity. The mutagenic potency was determined from the slope of the line fitted by least-squares linear regression to the data points. The result was accepted only if the correlation factor (*r*) was equal to or greater than 0.90.

Results and Discussion

Compound Potency. red-MX was found to exhibit mutagenicity and to generate 80 revertants/nmol in strain TA100 without S9 mix (Table II). The compound was approximately 70-fold weaker as a mutagen than MX, which produced 5600 revertants/nmol with strain TA100 (5). In the presence of metabolic activation and in strain TA98 red-MX was nonmutagenic even at the highest dose tested (2000 ng). The oxidized compounds (ox-MX and ox-EMX) did not generate reversion in any of the assays and were considered to be nonmutagenic at doses up to 1300 and 3000 ng/plate, respectively.

Ishiguro et al. and Streicher et al. showed that the presence of both dichloromethyl and Cl groups or CHCl₂ throughout on the C=C double bond is of critical importance for the mutagenicity of MX (20, 21). EMX, in which the CHCl₂ and Cl groups are trans to each other, is only one-tenth as mutagenic as MX (5). This indicates that an additional key structural feature for the potency of MX is the cis configuration of the CHCl₂ and Cl groups. The low mutagenicity of red-MX compared to MX and the finding that ox-MX is nonmutagenic suggest that the aldehyde group is also an important structural factor contributing to the potency of MX. Since ox-EMX has neither the favored cis configuration nor the aldehyde group we expected this compound to be nonmutagenic. The data from the Ames assays verified this prediction.

The positive response of red-MX in strain TA100 suggests that like MX, red-MX is a direct-acting mutagen operating primarily through base-pair substitutions at the G-C pairs. red-MX was also active in strain TA102 (23), where mutations occur at A-T base pairs (results not shown). Certain compounds can be procarcinogens that are transformed into electrophiles (which then react with

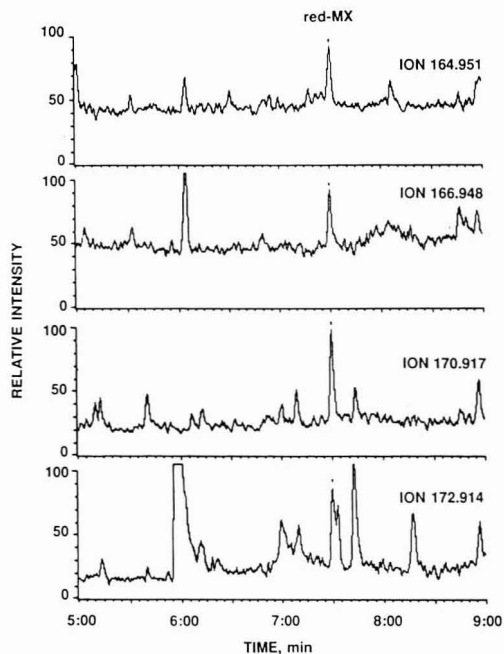


Figure 3. Mass chromatograms of red-MX fragment ions recorded during analysis of an underivatized extract of chlorinated drinking water.

DNA) by the action of the cytochrome P-450 enzyme system within cells and tissues. This makes it necessary to test the compounds for mutagenicity in the presence of the exogenous xenobiotic metabolizing enzyme system, S9. red-MX is a precursor to MX in the sense that it may be oxidized to MX by the P-450 enzyme system, which would lead to a high mutagenic response when red-MX is tested in the presence of S9. However, in the presence of S9, the mutagenicity of red-MX was decreased. It is not known whether oxidation of red-MX actually took place or in that case whether MX immediately upon formation was deactivated by the S9 mix. Several studies have shown that MX itself is deactivated by S9 (21, 22).

Quantitative Analyses. SIM mode GC/MS analyses showed that red-MX, ox-MX, and ox-EMX, in addition

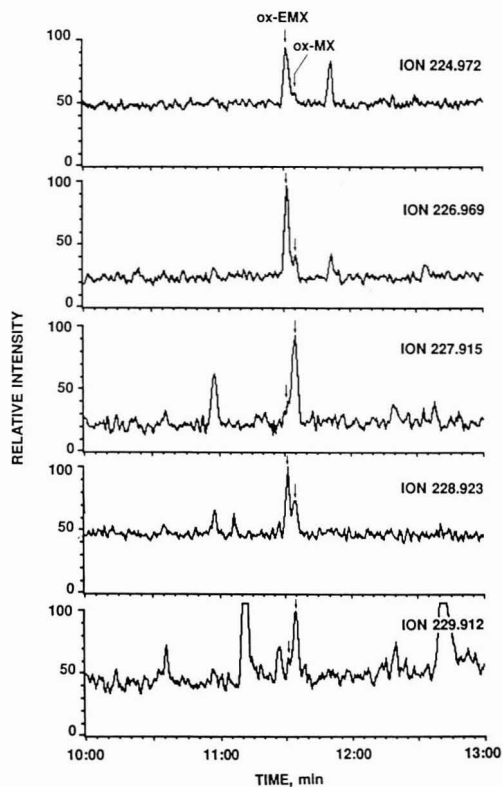


Figure 4. Mass chromatograms of ox-EMX and ox-MX fragment ions recorded during analysis of a methylated extract of chlorinated drinking water.

Table IV. Results of Analyses of ox-MX and red-MX in Unspiked and Spiked Extracts of Chlorinated Drinking Water

compound	spike level, ng/L			
	0	50	100	200
ox-MX (anhydride)	266		403	429
ox-MX (methylated)	53		191	244
red-MX	58	92	164	

to MX and EMX, were in fact present in the extracts of chlorinated water samples (Table I and Figures 3 and 4). The concentration of ox-EMX was 20–40 times higher than the concentration of MX in corresponding samples (Table III). The other MX analogues were present at concentrations slightly higher or equal to the MX concentration. MX was responsible for slightly more than 30% of the observed mutagenicity in the extracts of FA and HW, and for 13% in the extract of DW. EMX accounted for a few percent and red-MX for around 1% of the overall mutagenicity (Table III).

Since ox-MX upon heating in the GC injector forms a volatile anhydride, we initially attempted to quantitate the compound in underivatized extracts. SIM mode GC/MS determinations of ox-MX in nonmethylated samples produced values (6830, 1160, and 266 ng/L in FA, HW, and DW, respectively) much higher than those reported in Table III for analysis of the methylated samples. Analyses of DW extracts spiked with increasing amounts of ox-MX did not yield a linear response (Table IV), and reproducibility was poor.

The higher ox-MX concentrations obtained when underivatized water extracts were analyzed were probably due to interference from ox-EMX, which was present in concentrations several times higher than the concentration of ox-MX, and ox-EMX might upon heating in the GC injector partly isomerize to ox-MX. Indication of isomerization of ox-EMX upon heating is seen in the mass spectra recorded by direct-probe inlet of ox-EMX (Figure 1). The fragment ions at m/z 214 and 216 are most likely due to the formation of the ox-MX anhydride in the heated probe. Analyses of methylated pure ox-MX and ox-EMX showed that isomerization does not occur after methylation (Figure 2).

The results of SIM mode GC/MS analyses of DW extracts spiked with various amount of ox-MX and methylated with BF_3 in methanol showed good reproducibility and a linear increase in detector response with increase in the amount of ox-MX (Table IV). Methylation of pure ox-MX with 2% H_2SO_4 did not seem to go to completion and methylation using diazomethane was not successful. The values reported for ox-MX concentrations in extracts of chlorinated waters (Table III) are therefore those determined in samples methylated with BF_3 in methanol.

Since the fragment ions of methylated ox-MX and ox-EMX useful for qualitative and quantitative analysis are the same, separation of these compounds on the GC column is critical. The DB-5 60-m column was found to give satisfactory, albeit incomplete, separation (Figure 4). Owing to the high concentrations of ox-EMX in the extracts, some of the ion peaks overlap with the ion peaks of ox-MX (Table I and Figure 4), and therefore truly accurate analyses of ox-MX will require the use of a column that provides complete separation. Nevertheless, the quantitative results of the analyses of the DW extract spiked with ox-MX showed that reasonable accuracy for the determination was possible (Table IV).

Conclusions

This work demonstrates that several compounds with structural similarities to the potent mutagen MX are formed in reactions of chlorine with aqueous humic substances. red-MX was the only MX analogue studied that was found to be mutagenic, although the potency of this compound is approximately 70-fold lower than that of MX; red-MX does not, however, make a significant contribution to the total mutagenicity of the extracts of chlorinated water. It is obvious that the aldehyde group of MX is an important structural feature associated with the mutagenic potency of MX.

It is possible that MX and its analogues are formed through sequential oxidations of a common precursor unit in the humic macromolecule. Availability of the oxidized forms of MX and EMX and the reduced form of MX will enable kinetic studies to be undertaken of the formation and isomerization of the compounds in chlorinated water. Such kinetic studies might result in identification of chlorination conditions such that formation of MX is minimized or hindered.

Acknowledgments

We thank Ms. Donna C. Simmons for typing this manuscript.

Literature Cited

- (1) Loper, J. C. *Mutat. Res.* 1980, 76, 241.
- (2) Meier, J. R. *Mutat. Res.* 1988, 196, 211.
- (3) Cantor, K. P.; Hoover, R.; Hartge, P.; Mason, T. J.; Silverman, D. T.; Altman, R.; Austin, D. F.; Child, M. A.; Key, C. R.; Marrett, L. D.; Myers, M. H.; Narayana, A. S.; Levin,

- L. I.; Sullivan, J. W.; Swanson, G. M.; Thomas, D. B.; West, D. W. *J. Natl. Cancer Inst.* 1987, 79, 1269.
- (4) Hemming, J.; Holmbom, B.; Reunanen, M.; Kronberg, L. *Chemosphere* 1986, 15, 549.
 - (5) Kronberg, L.; Holmbom, B.; Reunanen, M.; Tikkanen, L. *Environ. Sci. Technol.* 1988, 22, 1097.
 - (6) Meier, J. R.; Knohl, R. B.; Coleman, W. E.; Ringhand, H. P.; Munch, J. W.; Kaylor, W. H.; Streicher, R. P.; Kopfler, F. C. *Mutat. Res.* 1987, 189, 363.
 - (7) Horth, H.; Fielding, M.; Gibson, T.; James, H. A.; Ross, H. *Identification of Mutagens in Drinking Water*; EC 9105 SLD; PRD 2038-M. Water Research Centre: Medmenham, Bucks, SL7 2HD, Great Britain, 1989.
 - (8) Kronberg, L.; Vartiainen, T. *Mutat. Res.* 1988, 206, 177.
 - (9) Holmbom, B.; Kronberg, L.; Smeds, A. *Chemosphere* 1989, 18, 2237.
 - (10) Meier, J. R.; Blazak, W. F.; Knohl, R. B. *Environ. Mol. Mutagen.* 1987, 10, 411.
 - (11) Backlund, P.; Kronberg, L.; Tikkanen, L. *Chemosphere* 1988, 17, 1329.
 - (12) Kronberg, L.; Holmbom, B.; Tikkanen, L. In *Proceedings of the Fourth European Symposium on Organic Micro-pollutants in the Aquatic Environment*; Bjorseth, A., Angeletti, G., Eds.; Reidel: Dordrecht, Holland, 1986; p 444.
 - (13) Wilcox, P.; Denny, S. In *Water Chlorination: Chemistry, Environmental Impact and Health Effects*; Jolley, R. L., Bull, R. J., Davis, W. P., Katz, S., Roberts, M. H., Jacobs, V. A., Eds.; Lewis: Chelsea, MI, 1985; Vol. 5, p 1341.
 - (14) Cheh, A. M.; Skochdopole, J.; Koski, P.; Cole, L. *Science* 1980, 207, 90.
 - (15) Croue, J.-P.; Reckhow, D.A. *Environ. Sci. Technol.* 1989, 23, 1412.
 - (16) Thurman, E. M.; Malcolm, R. L. *Environ. Sci. Technol.* 1981, 15, 463.
 - (17) Lindgren, B. O.; Nilsson, T. *Acta Chem. Scand.* 1973, 27, 888.
 - (18) Mowry, D. T. *J. Am. Chem. Soc.* 1953, 75, 1909.
 - (19) Maron, D. M.; Ames, B. N. *Mutat. Res.* 1983, 113, 173.
 - (20) Ishiguro, Y.; Santodonato, J.; Neal, M. W. *Environ. Mol. Mutagen.* 1988, 11, 225.
 - (21) Streicher, R. P.; Zimmer, H.; Meier, J. R.; Knohl, R. B.; Kopfler, F. C.; Coleman, W. E.; Munch, J. W.; Schenck, K. M. *Chem. Res. Toxicol.*, in press.
 - (22) Meier, J. R.; Knohl, R. B.; Merrick, B. A.; Smallwood, C. L. Presented at the Sixth Conference on Water Chlorination: Chemistry, Environmental Impact and Health Effects, Oak Ridge, TN, May 3-8, 1987.
 - (23) Levin, D. E.; Holstein, M.; Christman, M. F.; Schwiers, E. A.; Ames, B. D. *Proc. Natl. Acad. Sci. U.S.A.* 1982, 79, 7445.

Received for review March 12, 1990. Revised manuscript received July 17, 1990. Accepted August 2, 1990. This work was supported in part by research grants from the American Water Works Research Foundation, the North Carolina Water Resources Research Institute, and the Academy of Finland, Research Council for the Environmental Sciences.

Study of Adsorption-Desorption of Contaminants on Single Soil Particles Using the Electrodynamic Thermogravimetric Analyzer

Leonardo Tognotti, Marla Flytzani-Stephanopoulos, and Adel Fares Sarofim

Chemical Engineering Department, Massachusetts Institute of Technology, Cambridge, Massachusetts 02139

Harris Kopsinis and Michael Stoukides*

Chemical Engineering Department, Tufts University, Medford, Massachusetts 02155

■ The isothermal adsorption and desorption of organic vapors on a single soil particle was studied with the aid of the electrodynamic thermogravimetric analyzer (EDTGA). Toluene and carbon tetrachloride were tested at room temperature during their adsorption on Spherocarb, montmorillonite, and Carbopack particles. The maximum amount of either organic compound adsorbed was comparable to that required for one monolayer coverage of the particle surface area. Significant differences among various pairs of solid-organic vapor examined were identified and correlated to differences in solid pore structure and chemical affinity between the organic compound and the solid.

Introduction

The increasing public and scientific concern with the problem of hazardous waste disposal has initiated and promoted the study of fundamentals associated with such waste treatment processes (1-3). At present, the dominant way of handling hazardous chemicals is disposal to a landfill site. Nevertheless, studies over the recent years have shown that in many cases such a solution may be detrimental to the environment. Organic compounds, such

as low molecular weight halocarbons, can be released from waste landfills and contaminate groundwater, soil, and air, posing an immediate threat to human health (3-7). The transport of contaminants in the environment is a complex process, and among other factors, it involves the adsorption and desorption of these compounds by soil particles (3).

With landfill costs increasing and regulations on land-filling becoming more strict, a search for alternatives to conventional hazardous waste treatment has become a necessity. Incineration is currently a proven solution for treating most organic contaminants, and well-designed incineration systems provide the highest overall degree of destruction of hazardous waste streams (8). Hence, although a costly treatment, significant growth is anticipated in the use of incineration and other thermal destruction methods (8, 9). In addition to these, the future will see development of several thermal and nonthermal (10-15) soil decontamination techniques including use of microorganisms, electrokinetic methods, vacuum extraction and volatilization, and soil aeration. Most of these treatment methods involve contaminant desorption.

Recent studies have pointed out the importance of adsorption and desorption of contaminants in the soil particles during incineration (1, 2). Pershing and co-workers suggested contaminant desorption as the probable rate-limiting step at long times in the evolution of the contaminant from soil particles, which necessitated heating

*Current address: Chemical Engineering Dept., University of Pisa, Italy.

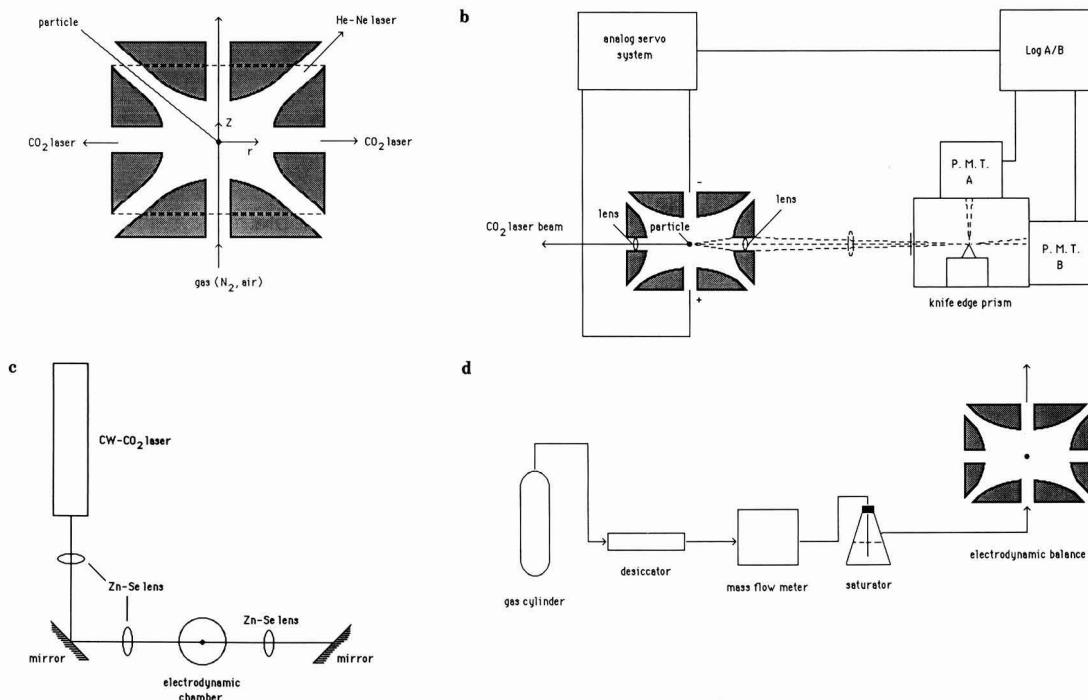


Figure 1. (a) Cross-sectional view of electrodes in electrodynamic balance. (b) Schematic of the position control system. (c) Schematic of the laser heating system. (d) Schematic view of the gas flow system.

well above the boiling point of the organic compound (1). They also suggested that with reactive, porous soils (e.g., clays), the last monolayer of contaminant molecules may be tightly bound to the soil, thus requiring temperatures significantly above the boiling point to ensure adequate cleanup (1).

It is clear that a fundamental study of the adsorption and desorption of contaminant organics on soil particles can contribute considerably to understanding the transport and diffusion of hazardous chemicals in soils and lead to optimization of the operation of incineration systems, such as rotary kilns. Transient phenomena involving rapid waste vapor release, called "puffs", are frequently encountered in rotary kilns and may cause failure of the incineration system (10, 11). Experimental evidence shows that puff magnitude increases with increasing temperature and kiln rotation speed and is also sensitive to the volatility of the waste (12). In the rotary kiln, the solids can be considered as a bed of many layers of particles that are being slowly stirred. Hence, contaminants may exist either adsorbed on the external surface of the particles or adsorbed on the internal pore structure of the particles or as a liquid phase within the bed. Clearly both intraparticle and interparticle effects contribute to the high complexity of the rotary kiln system.

It would be extremely helpful if the characteristics of a single-particle reactor were first investigated. To this end, we have used in our laboratory the electrodynamic thermogravimetric analyzer (EDTGA). The EDTGA is a device that consists of an electrodynamic balance modified to permit single-particle heating by a CO₂ laser, temperature measurement by a two-color infrared-pyrometer system, and continuous weighting by a position control system. The main advantages that the EDTGA has over the conventional TGA can be summarized as follows: (a)

higher accuracy in weight measurement and the fact that the TGA requires a large number of particles, i.e., average values are measured; (b) TGA data are often masked by external diffusion problems.

The fully instrumented EDTGA has been used successfully so far in a number of applications including measurement of temperature and weight of char particles undergoing oxidation (16, 17), measurement of heat capacities, and adsorptivities of single particles (18), calculation of water activities for single electrolyte solutions (19), and photophoretic force measurements on micron-size irradiated particles (20-23). Recently, the same apparatus has been used as a basic tool in developing a novel droplet imaging system that offers unique capabilities for characterizing size, mass, density, and composition of individual droplets (24).

In the present article we report our first results of the use of EDTGA in the study of adsorption and desorption of organic compounds on single particles of several porous soils.

Experimental Methods

Apparatus. The electrodynamic balance (EDB) consists of two endcap electrodes and a ring electrode. The basic characteristics and principles of operation have been described in detail in previous communications (25-28). A schematic of the electrodynamic balance is presented in Figure 1a. The chamber creates a dynamic electric field capable of suspending a single charged particle of sizes varying from 30 to 300 μm . The ac ring electrode provides lateral stability to the particle through an imposed ac field oscillating sinusoidally at 100 Hz and at an amplitude of ± 2000 V. The dc top and bottom electrodes provide vertical stability by cancelling out the gravity force and thus suspending stably the charged particle in the EDB.

A position control system can be used, which automatically adjusts the electric field to keep the particle at the center of the chamber (Figure 1b). An optical microscope (Ealing) is used for viewing the particle and for manual control of the particle position. The microscope allows measurement of the particle size to $\pm 5 \mu\text{m}$.

A 20-W CO_2 laser supplies heat to the suspended particle (Figure 1c) and two-color infrared (2 and $4 \mu\text{m}$) pyrometry is used for temperature measurement. A gas flow system allows exposure of the particle to the desired gaseous environment (Figure 1d). Additional information about the apparatus and its operation can be found elsewhere (25, 28).

Experimental Procedure. In the present study, the EDTGA was used to measure the relative variation of the weight of a suspended particle during adsorption and desorption of organic vapors at room temperature.

A single, dry particle was suspended in the chamber, through which a finite dry nitrogen flow rate was maintained. The particle was degassed before the adsorption runs by heating it with the laser. The voltage was then adjusted in order to balance the particle at its correct position. A nitrogen stream saturated with organic vapor was produced by bubbling the nitrogen through the liquid in a saturator and was then introduced in the balance. The voltage required to keep the particle at the same position was recorded as a function of time.

The desorption experiments followed the adsorption runs and started when the voltage reached a final, stable value. The saturator was switched off and dry nitrogen was introduced again. Saturation was achieved for flow rates of 14.3, 21.4, and $28 \text{ cm}^3/\text{min}$. The introduction of gases flowing upward past the suspended particle produces an aerodynamic drag force F_a , which affects the dc voltage required for balancing the particle. Hence, the force balance on a suspended particle in the EDTGA should be written as

$$mg = qE + F_a \quad (1)$$

where m is the particle mass (kg), g is the gravitational acceleration (m/s^2), q is the excess charge on the particle (C), and E is the electric field strength in the vertical direction (V/m).

The electrical field strength E is given by the equation

$$E = CV/Z_0 \quad (2)$$

where C is the chamber constant, V is the measured balancing voltage across the endcap electrodes and Z_0 is the characteristic length of the EDB chamber (0.004m).

Since low flow rates were used, i.e., the Reynolds numbers were less than 1, the aerodynamic drag on the particle is described by Stokes law:

$$F_a = 3\pi\mu vd \quad (3)$$

where μ is the gas viscosity, v is the gas velocity, and d is the particle diameter.

Combining eqs 1-3, one obtains

$$mg = qCV/Z_0 + 3\pi\mu vd \quad (4)$$

Due to the drag force effect, the voltage required to balance the particle was measured in the absence of gas flow at the beginning of each experiment. As shown in eq 4, the minimum mass variation detectable in the apparatus is given by the minimum voltage difference that can be measured. In the present configuration it was possible to measure $\Delta V/V_0$ as low as 10^{-4} where ΔV is the voltage change and V_0 is the initial voltage required to suspend the particle in the absence of organic vapor. In terms of weight, the above value means that a fractional change of

Table I. Physical Properties of Solid Materials

material	diam, μm	surface area, m^2/g	intrusion vol., cm^3/g	bulk density, g/cm^3	porosity ^a
Spherocharb	125-150	860.0	0.83	0.63	0.525
montmorillonite	90-125	192.3	1.24	0.65	0.802
Carbopack	150-180	10.4	0.64	0.95	0.615

^a Based on mercury porosimetry.

10^{-4} in the particle weight is detectable with typical values of Δm in the range of 10^{-10} - 10^{12} g.

Materials. In order to determine potentially different solid-hydrocarbon affinities, three solids and two hydrocarbons have been examined in this work. Montmorillonite clay and Spherocharb and Carbopack particles were used. The physical properties of these materials are reported in Table I. The surface area was determined by the BET method and all the other properties reported in Table I were obtained by mercury porosimetry. Spherocharb and Carbopack are trade names of chars produced for chromatographic packing by Foxboro Analabs and Aldrich Chemical Co., respectively; they have been selected because of their spherical shape and because their characteristics do not differ significantly from particle to particle. Montmorillonite particles were not uniform in shape and only those with shape close to spherical were used in this study. Two hydrocarbons were examined, toluene and carbon tetrachloride.

Results and Discussion

Typical adsorption-desorption results for toluene are shown in Figure 2a and b. Figure 2a shows the value of V/V_0 vs time for a Spherocharb particle of $170\text{-}\mu\text{m}$ diameter at room temperature. The total volumetric flow rate was maintained at $21.4 \text{ cm}^3/\text{min}$ at all times. At $t = 0$ the voltage required to balance the particle in the presence of the gas flow is recorded as V_0 . The voltage V gradually increases during adsorption to reach a practically constant value recorded as V_a . The voltage required to balance the particle in the absence of gaseous flow (or equivalently in absence of a drag force) is also measured at the beginning of the experiment and recorded as V_{nf} . Using the above values, one can calculate weight changes using the equation

$$\frac{V - V_0}{V_{nf}} = \frac{m - m_0}{m_0} \quad (5)$$

and similarly the maximum amount of contaminant adsorbed per gram of solid particle X_a is given by

$$X_a = \frac{V_a - V_0}{V_{nf}} = \frac{m_a - m_0}{m_0} \quad (6)$$

where m_0 is the mass of dry solid and m_a is m_0 plus the mass of organic adsorbed. Note that the drag force contribution to both V and V_0 is identical since constant flow rate is maintained, and therefore, the difference $V - V_0$ in the numerator gives the net weight gain due to adsorption of the organic.

Figure 2b depicts the desorption profile of toluene at room temperature in dry nitrogen flowing into the EDTGA chamber at constant flow rate. An initial slow decrease in V/V_0 is observed, which probably corresponds to the slowly diminishing vapor pressure of toluene in the chamber. This is followed first by a sharp and then by a slow decrease in V/V_0 .

In order to be able to compare the rates of adsorption and desorption for various experiments the data are re-

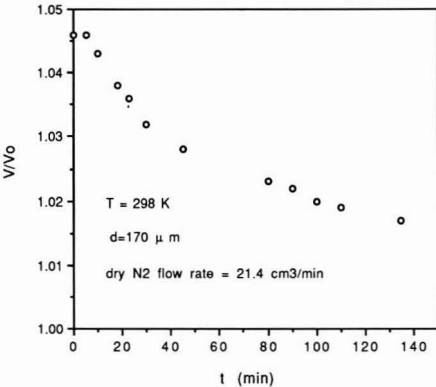
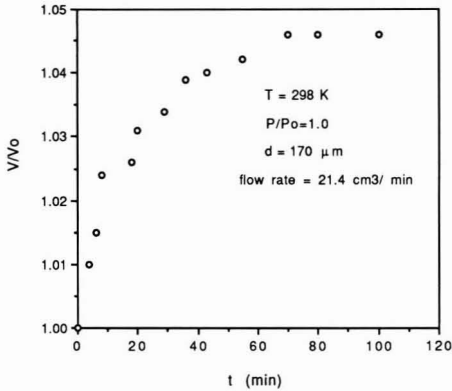


Figure 2. (a) Adsorption of toluene on Sphero carb particle. (b) Desorption of toluene from Sphero carb particle.

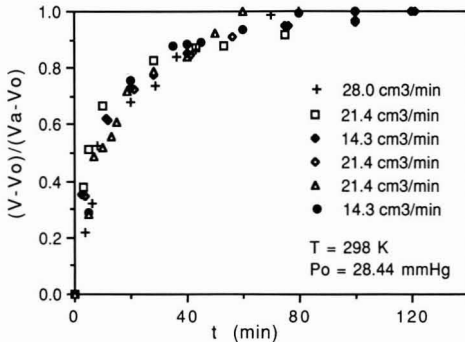


Figure 3. Sphero carb-toluene adsorption runs for different flow rates.

ported as a fractional attainment Y of the maximum adsorption, where

$$Y = \frac{V - V_0}{V_a - V_0} = \frac{m - m_0}{m_a - m_0} \quad (7)$$

Figures 3 and 4 contain normalized data for six Sphero carb particles during adsorption and desorption of toluene. Although the amount of hydrocarbon adsorbed is likely to vary from particle to particle, there is no appreciable variation in the rates of adsorption and desorption. Three different flow rates, 14.3, 21.4, and 28 cm³/min, were used in the experiments shown in Figures 3 and 4. It can be seen that the effect of gas flow rate on the rates of adsorption or desorption is insignificant. Certain scattering

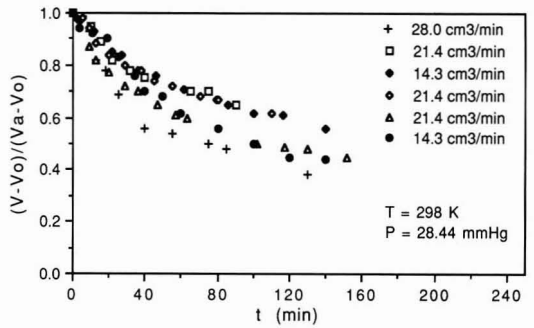


Figure 4. Sphero carb-toluene desorption runs for different flow rates.

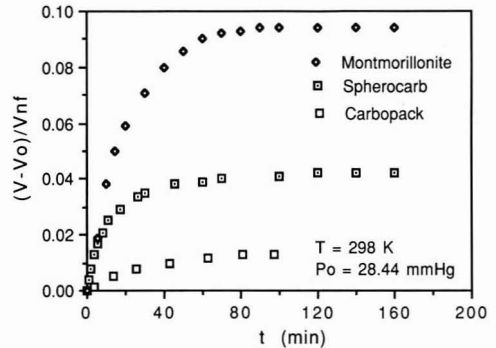


Figure 5. Average adsorption curves of toluene for different materials.

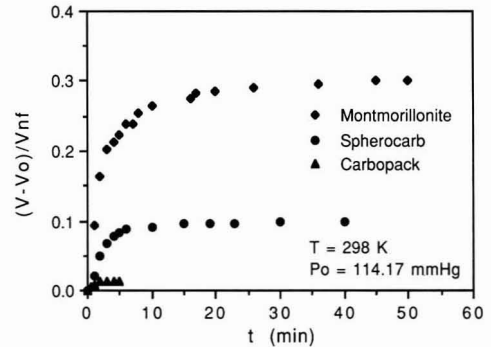


Figure 6. Average adsorption curves of carbon tetrachloride for different materials.

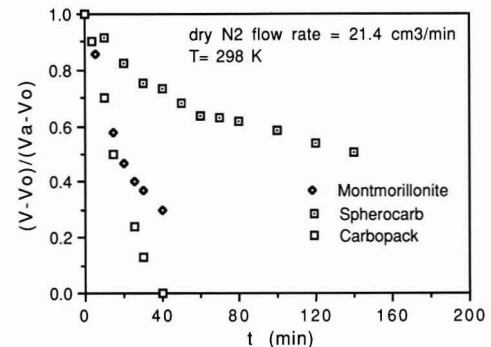


Figure 7. Average desorption curves of toluene for different materials.

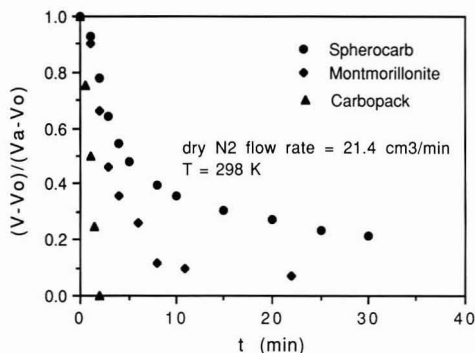


Figure 8. Average desorption curves of carbon tetrachloride for different materials.

Table II. Maximum Amount of Contaminants Adsorbed per Gram of Solid and Corresponding Characteristic Times for Adsorption and Desorption

materials	X_a (g liquid/ g solid)	$\tau_{0.5a}$, min	$\tau_{0.9a}$, min	$\tau_{0.5d}$, min	$\tau_{0.9d}$, min
Sphero carb-C ₇ H ₈	0.029	8	45	140	>200
	0.061				
	0.048				
	0.045				
	0.025				
montmorillonite-C ₇ H ₈	0.045	13	47	17	>40
	0.130				
	0.070				
Carbo pack-C ₇ H ₈	0.100	16	62	15	32
	0.075				
	0.009				
Sphero carb-CCl ₄	0.017	2	7	5	>30
	0.109				
	0.092				
montmorillonite-CCl ₄	0.107	2	17	3	11
	0.087				
	0.292				
	0.290				
	0.272				
	0.347				
Carbo pack-CCl ₄	0.260	1	2	0.5	1.5-2.0
	0.280				
	0.360				
	0.012				
	0.012				
	0.012				

is observed in the desorption curves but there is no systematic trend of dependence of flow rate. This verifies the ability of the EDTGA to study weight changes on a single particle in the absence of external diffusional effects.

The transient adsorption behavior for all pairs of solid-organic vapor investigated is shown in Figures 5 and 6, while the corresponding desorption curves are shown in Figures 7 and 8. Each experimental point in Figures 5-8 corresponds to an average value of at least three particles examined. Each curve shown in Figure 3-8 can provide information about the characteristic time of either the adsorption or the desorption of the organic compound from the particle. The times required for the particles to adsorb 50% and 90% of the maximum amount that can be adsorbed under these conditions was defined as $t_{0.5a}$ and $t_{0.9a}$ respectively. Similarly, the times required to desorb 50% and 90% of the adsorbed compound were defined as $t_{0.5d}$ and $t_{0.9d}$ respectively. Table II contains X_a values for several experiments as well as average values of the above denoted characteristic times.

Table III. Comparison of X_a Values to Those Corresponding to One Monolayer Coverage of the Solid Surface

materials	X_m	X_a
Sphero carb-C ₇ H ₈	0.372	0.042
montmorillonite-C ₇ H ₈	0.081	0.094
Carbo pack-C ₇ H ₈	0.004	0.013
Sphero carb-CCl ₄	0.678	0.098
montmorillonite-CCl ₄	0.148	0.300
Carbo pack-CCl ₄	0.008	0.012

The above experimental results show clearly that considerable differences exist between montmorillonite, Sphero carb, and Carbo pack as well as between toluene and carbon tetrachloride concerning adsorption and desorption characteristics. The amount of contaminant adsorbed can be correlated to certain properties of either the solid or the organic vapors. From the three solids examined, montmorillonite adsorbs the largest amount of C₇H₈ and CCl₄, and as shown in Table I, it has the largest intrusion volume. Sphero carb comes next, although it has the highest surface area. This can be explained by taking into account that Sphero carb consists mainly of micropores (<3 nm). Formation of liquid in pores of that size is highly likely and this could inhibit penetration of the organic compound inside the particle. In other words, the adsorbed compound has access to only a small fraction of the total internal surface area of the Sphero carb particle. Carbo pack adsorbs the least amount of either organic compound and this is in agreement with its low surface area and large pores. In general, larger amounts of CCl₄ than C₇H₈ are adsorbed on all solids examined. This is mainly due to the higher vapor pressure, and consequently greater mole fraction of CCl₄ in the nitrogen stream, given the fact that all experiments were carried out at the same temperature (25 °C) and atmospheric total pressure.

One interesting observation (Figures 7 and 8, Table II) during the desorption experiments is that mainly Sphero carb, and montmorillonite to a lesser extent, seem to retain an appreciable fraction of the adsorbed compound. In certain experiments, e.g., Sphero carb-toluene (Figure 7), the shape of the desorption curve indicates that a finite percentage of the adsorbed organic is irreversibly adsorbed in the porous solid at the temperature studied. A partial explanation of this phenomenon is given in Table III, which contains values determined experimentally for the six solid-vapor pair combinations. Both quantities X_m and X_a presented there are expressed in grams of organic per gram of solid. From mercury porosimetry measurements (29), it is possible to determine an average porosity for each solid. On the other hand, using the average surface area of each solid, which was calculated from N₂ desorption BET measurements (29), one can determine the mass of organic that will be required to cover 1 g of solid with one monolayer. This quantity is denoted as X_m in Table III. Also, an average value of X_a taken from Table II is included in the last column of Table III for comparison. The maximum amount of contaminant adsorbed is of the order of one monolayer for all the materials examined. It can also be seen from the tabulated values that in cases where part of the adsorbed organic is retained by the solid, the remaining quantity corresponds to a coverage of less than a monolayer. It is understood that a monolayer of adsorbate is more strongly bound to the solid surface and its desorption will be a longer process. This is mainly due to the fact that capillary condensation and intercalation of adsorbate molecules in micropores justify the long times that are observed during adsorption and desorption. For

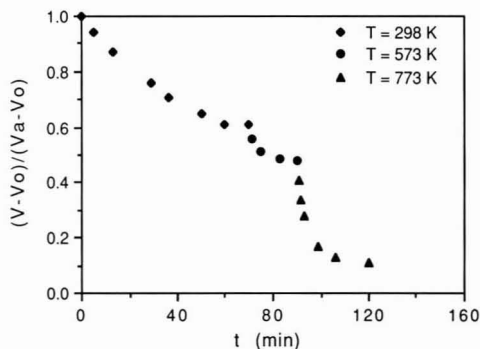


Figure 9. Spherocarb-toluene desorption run for different temperatures.

these times the diffusivity ranges from 10^{-7} to 10^{-9} cm^2/s (30).

As has already been mentioned, all the experiments shown in Figures 3-8 were obtained with both the saturator and the EDB chamber maintained at room temperature. Hence, the vapor-nitrogen stream introduced in the chamber is saturated with the organic vapor. Unsaturated mixtures can be introduced if the saturator temperature is lower. This would also result in a decrease in the partial pressure of the vapor around the soil particle. Experiments done under these conditions showed that complete recovery of the adsorbed compound can be achieved much faster upon decreasing the vapor partial pressure (29). An alternative in accelerating the desorption process is to heat the particle. Figure 9 shows transient desorption of toluene from a Spherocarb particle originally exposed to a nitrogen-toluene stream, saturated in toluene, at 25 °C. After 1-h exposure to a dry nitrogen stream at the same temperature, 60% of the amount originally adsorbed remains trapped in the porous solid. Laser heating of the particle to 300 °C results in a slight decrease of this amount to about 50%, and most of the organic finally desorbs only upon heating to 500 °C.

In summary, EDTGA has been shown to be a useful tool for studying the fundamentals of contamination and decontamination of porous soils. It can also be used for continuously measuring the temperature and weight of a heated particle during small intervals of time, as shown in Figure 9. Significant differences among various solids and contaminant compounds have been identified. The present study focuses primarily on showing the advantages of using EDTGA in related research. A systematic study of the adsorption-desorption characteristics and their dependence on the physical and chemical properties of the soil is necessary. Experimental work toward this goal is currently in progress.

Literature Cited

- (1) Lighty, J. S.; Pershing, D. W.; Cundy, V. A.; Linz, D. G.

- Nucl. Chem. Waste Manage.* **1988**, *8*, 225.
- (2) Lighty, J. S.; Britt, R. M.; Pershing, D. W.; Owens, W. D.; Cundy, V. A. *JAPCA* **1989**, *39*, 187.
- (3) Estes, T. J.; Shah, S. V.; Vilker, V. L. *Environ. Sci. Technol.* **1988**, *22*, 377.
- (4) Evans, R. B.; Schweitzer, G. E. *Environ. Sci. Technol.* **1984**, *18*, 330A.
- (5) McCarty, P. L.; Reinhard, M.; Rittmann, B. E. *Environ. Sci. Technol.* **1981**, *15*, 40.
- (6) Page, G. W. *Environ. Sci. Technol.* **1981**, *15*, 1475.
- (7) Fishbein, L. *EHP, Environ. Health Perspect.* **1976**, *14*, 39.
- (8) Oppelt, E. T. *Environ. Sci. Technol.* **1986**, *20*, 312.
- (9) Oppelt, E. T. *JAPCA* **1987**, *37*, 558.
- (10) Linak, W. P.; McSorley, J. A.; Wendt, J. L.; Dunn, J. E. *JAPCA* **1987**, *37*, 934.
- (11) Linak, W. P.; McSorley, J. A.; Wendt, J. L.; Dunn, J. E. *JAPCA* **1987**, *37*, 54.
- (12) Linak, J. S.; et al. Presented at the AFRC International Symposium on Incineration of Hazardous Municipal and other Wastes, Palm Springs CA, November 2-4, 1987.
- (13) Bury, K. Presented to the Water and Environmental Group of the SCI London, April 5, 1989.
- (14) Bewley, R.; Ellis, B.; Theile, P.; Viney, I.; Rees, J. *Chem. Ind.* December 4, 1989.
- (15) Lageman, R.; Wieberen, P.; Seffinga, G. *Chem. Ind.* September 18, 1989.
- (16) Dudek, D. R. Ph.D. Thesis, Massachusetts Institute of Technology, Cambridge, MA, 1988.
- (17) Bar-Ziv, E.; Jones, D. B.; Spjut, R. E.; Dudek, D. R.; Sarofim, A. F.; Longwell, J. P. *Combust. Flame* **1989**, *75*, 81.
- (18) Manazam, E. R.; Maloney, D. J.; Lawson, L. O. *Rev. Sci. Instrum.* **1989**, *60*, 3460.
- (19) Cohen, M. D.; Flagan, C. F.; Seinfeld, J. H. *J. Phys. Chem.* **1987**, *91*, 4563.
- (20) Greene, W. M.; Spjut, R. E.; Bar-Ziv, E.; Sarofim, A. F.; Longwell, J. P. *J. Opt. Soc. Am. B* **1985**, *2*, 998.
- (21) Greene, W. M.; Spjut, R. E.; Bar-Ziv, E.; Longwell, J. P.; Sarofim, A. F. *Langmuir* **1985**, *1*, 361.
- (22) Spjut, R. E.; Sarofim, A. F.; Longwell, J. P. *Langmuir* **1985**, *1*, 355.
- (23) Spjut, R. E.; Bar-Ziv, E.; Sarofim, A. F.; Longwell, J. P. *Rev. Sci. Instrum.* **1986**, *57*, 1604.
- (24) Maloney, D. J.; Flashing, G. E.; Lawson, L. O.; Spann, J. F. *Rev. Sci. Instrum.* **1989**, *60*, 450.
- (25) Wuerker, R. F.; Shelton, H.; Langmuir, R. V. *J. Appl. Phys.* **1959**, *30*, 342.
- (26) Davis, E. J.; Ray, A. K. *J. Colloid Interface Sci.* **1980**, *75*, 566.
- (27) Philip, M. A. M.S. Thesis, Massachusetts Institute of Technology, Cambridge, MA, 1981.
- (28) Spjut, R. E. Ph.D. Thesis, Massachusetts Institute of Technology, Cambridge, MA, 1985.
- (29) Kopsinis, H. K. M.S. Thesis, Tufts University, 1990.
- (30) Froment, G. F.; Bischoff, K. B. *Chemical Reactor Analysis and Design*; John Wiley & Sons: New York, 1979.

Received for review February 20, 1990. Revised manuscript received July 27, 1990. Accepted August 17, 1990. We gratefully acknowledge the Center for Environmental Management of Tufts University for financial support of this research under Grant CR-813481-02-0. The apparatus utilized had been developed with support from Exxon Research Corp.

Environmental Applications for the Analysis of Chlorinated Dibenzo-*p*-dioxins and Dibenzofurans Using Mass Spectrometry/Mass Spectrometry

Eric J. Reiner,* David H. Schellenberg, and Vince Y. Taguchi

Ontario Ministry of the Environment, P.O. Box 213, Rexdale, Ontario, Canada, M9W 5L1

■ A mass spectrometry/mass spectrometry-multiple reaction monitoring (MS/MS-MRM) technique for the analysis of all tetra- through octachlorinated dibenzo-*p*-dioxins (Cl_xDD, *x* = 4-8) and dibenzofurans (Cl_xDF, *x* = 4-8) has been developed at the Ministry of the Environment (MOE) utilizing a triple quadrupole mass spectrometer. Optimization of instrumental parameters using the analyte of interest in a direct insertion probe (DIP) resulted in sensitivities approaching those obtainable by high-resolution mass spectrometric (HRMS) methods. All congeners of dioxins and furans were detected in the femtogram range. Results on selected samples indicated that for some matrices, fewer chemical interferences were observed by MS/MS than by HRMS. The technique used to optimize the instrument for chlorinated dibenzo-*p*-dioxins (CDDs) and chlorinated dibenzofurans (CDFs) analysis is adaptable to other analytes.

Introduction

The analysis of chlorinated dibenzo-*p*-dioxins (CDDs) and chlorinated dibenzofurans (CDFs) has become one of the major applications of mass spectrometry in the field of organic analysis in recent years (1-17). The presence of chemical interferences in complex matrices, oftentimes at concentrations several orders of magnitude greater than those of the CDDs and CDFs, predicates that efficient sample preparation prior to the instrumental analysis cannot be avoided (12). The difficulties encountered in environmental samples make selectivity and sensitivity important considerations for the method of choice. Capillary column high-resolution gas chromatography/high-resolution mass spectrometry (HRGC/HRMS) has been the standard method for analyzing complex matrices such as sediments, effluents, and biological tissue.

Until recently tandem mass spectrometry (MS/MS) has been able to meet the requirements for selectivity but has been ~1 order of magnitude less sensitive than HRGC/HRMS methods (8, 14). As previously shown (15), when a direct insertion probe equipped with a sample cup containing approximately 1-3 μg of CDD or CDF is used to optimize the instrument, limits of detection (200-600 fg) that begin to approach those of HRGC/HRMS can be obtained.

A number of methods have been reported for the MS/MS analysis of CDD and CDF. Tondeur et al. (13) developed an HRGC/(hybrid)MS/MS method for the analysis of Cl₄DD in environmental samples. They have shown that MS/MS can be more selective than HRMS in some cases. Charles et al. (16) were able to show that HRGC/(hybrid)MS/MS can eliminate the interferences in municipal incinerator ash and pulp and paper effluent extracts that were present in HRGC/HRMS mass chromatograms. Fraisse et al. (17) have shown that in some fly ash extracts, interferences seen in HRGC/(hybrid)MS/MS were not present in HRGC/HRMS, indicating that MS/MS is not always more selective than HRMS. Slayback et al. (14) optimized collision energy and collision

gas pressure for the HRGC/(tandem quadrupole)MS/MS analysis of environmental samples using breakdown graphs (a plot of relative ion abundance vs internal energy) alone. This enhanced sensitivity, but not to the degree that would make it comparable with HRMS.

For the detection of extremely low concentrations of these target compounds, optimization of all instrumental parameters becomes extremely important. Martinez and Cooks reported that there are a number of parameters that affect the signal strength of progeny ions (18). These parameters include the following: the collision gas pressure (the number of collisions the parent ion undergoes within *Q*₂ or target thickness), the collision energy (the duration of the interaction between the parent ion and collision gas), electron energy (proportional to the initial internal energy of the parent ion), the nature of the collision gas (i.e., He, Ar, SF₆, ...), the energy of *Q*₃ relative to *Q*₂, the design of the collision cell (rf voltage and the restrictive interquadrupole aperture of *Q*₂), and the type of detector.

Perfluorotributylamine (PFTBA) is commonly used in the optimization of MS/MS parameters when analyzing for general organic compounds. However, the fragmentation of PFTBA under collision-induced dissociation (CID) conditions does not parallel the behavior of all analytes. According to the quasi-equilibrium theory (QET) (19), the pattern and degree of fragmentation of the parent ion is dependent on its internal energy. Excitation by collision (CID), electron ionization (EI), chemical ionization (CI), fast atom bombardment (FAB), etc., forms a series of parent ions with a distribution of internal energies. Kenttama and Cooks (20) concluded, by using breakdown graphs, that parameters such as collision energy and collision gas pressure have a significant effect on the internal energy of the parent ion and therefore its pattern of dissociation. In principle, parameters that affect the internal energy of the parent ion can be set to direct fragmentation toward the desired fragmentation reaction (loss of COCl in the case of CDD/F). Other parameters such as quadrupole offset voltages and lens voltages must be adjusted so that the desired progeny ions, which have kinetic energies different from those ions formed in the ion source, can be properly mass selected and detected. Catlow et al. (21) have shown that the optimum collision energy and collision gas pressure for one reaction will almost certainly not be the same optimum values for another reaction of that or any other parent ion. This implies that the optimization of a particular fragmentation reaction using the analyte of interest is critical in order to obtain the greatest signal strength possible.

Experimental Section

The Ministry of the Environment (MOE) MS/MS technique can be used to determine CDDs and CDFs in a number of matrices such as soils, sediments, biological tissue, effluents, water, air, chemical reagents, pulp and paper, and petrochemical samples. The sample extract preparation and cleanup procedures have been reported in detail elsewhere (7, 22) and will only be described briefly. Samples were spiked with a 2,3,7,8-substituted ¹³C-containing dioxin for each of the five congener groups mon-

Present address: Research and Productivity Council, P.O. Box 20000, College Hill Rd., Fredericton, NB, Canada, E3B 6C2

itored. The CDD and CDF were extracted by liquid/liquid or Soxhlet extraction. The concentrated extract was then cleaned further by using acidic/basic silica and silver nitrate modified silica/alumina columns. No Carbo-pack C or activated carbon columns were used.

HRGC/MS/MS analysis was accomplished with a Varian 3400 gas chromatograph coupled to a Finnigan MAT TSQ 70 triple-quadrupole mass spectrometer. Data were acquired by using the standard DEC 11/73+ data system.

The Cl₄DD/F to Cl₃DD/F ("congener analysis") congeners were determined by using a WCOT column (SE-52, 30 m × 0.25 mm i.d., 0.25-μm bonded phase). For this analysis, the column was initially set at 120 °C and the temperature was held for 1 min after injection. The temperature was subsequently programmed at 15 °C/min to 250 °C and then at 5 °C/min to 300 °C, where it was held for 5 min. Sample extracts were reconstituted in toluene.

The "isomer-specific" analysis (for the determination of 2,3,7,8-Cl₄DD) was accomplished by using a WCOT column (SP-2331, 60 m × 0.25 mm i.d., 0.2-μm film thickness). The temperature was initially set at 120 °C, held for 1 min, and then programmed at 15 °C/min to 220 °C, followed by 3 °C/min to 250 °C, where it was held for 30 min. These sample extracts were reconstituted in iso-octane.

Samples were injected via a split/splitless injector set at 250 °C in the splitless mode. The column head pressure was 12 psi on the 30-m SE-52 column and 25 psi on the 60-m SP-2331 column. The transfer line from the gas chromatograph to the mass spectrometer was held at 300 °C, and the mass spectrometer ion source was held at 245 °C. The trap current was set at 300 μA, and a Finnigan MAT 4500 ion volume was used instead of a TSQ 70 ion volume. The 4500 ion volume has the electron entrance and exit apertures reversed from the TSQ 70 ion volume. This results in an increased flux of ionizing electrons into the ion source and a higher effective trap current.

The data were collected by monitoring the loss of COCl from the molecular ions of the isotopic cluster that would form the two most abundant daughter ions. For the dioxins, an additional ion formed by the loss of 2COCl was used as a confirmation ion. For the furans, the loss of Cl₂ and HCl from diphenyl oxides (DPO, compounds such as chlorinated diphenyl ethers that can fragment to form furans in the ion source) were monitored to check if any DPO had passed through the cleanup. No other strong daughter ion that could be used for a confirmation ion for the furans was observed.

Each run was split into five groups ranging from Cl₄DD and Cl₄DF in group 1 to Cl₃DD and Cl₃DF in group 5. The corresponding ¹³C-labeled dioxin surrogate standards were also monitored for each group. Table I summarizes the parameters and reactions that were monitored for each group. For the isomer-specific determination of 2,3,7,8-Cl₄DD, only the ions in group 1 were monitored.

The instrument was mass calibrated with PFTBA, first in the Q₁ MS mode, then in the Q₃ MS mode, and finally in the MS/MS mode. Once mass calibration had been accomplished, the dioxin and furan used for tuning were introduced into the ion source by the direct insertion probe. Each of the five groups was optimized by using a separate sample cup containing about 1–3 μg of the dioxin and furan (see Table II for specific congeners). The direct insertion probe was not placed fully into the source so that the probe tip would stay cool, and therefore, only very low amounts of dioxins and furans would enter the ion source. Probe temperatures ranged from 35 °C for Cl₄DD to 80 °C for Cl₃DD. The parent ion signal was first optimized in the Q₁ MS mode in order to maximize the transmission

Table I. Parameters for Selected Reaction Monitoring

compd	mass to charge ratio		reaction
	parent ion	progeny ion	
group 1			
Cl ₄ DD	320	194	M - 2 (COCl)
Cl ₄ DF	304	241	M - COCl
	306	243	M + 2 - COCl
Cl ₄ DD	320	257	M - COCl
	322	259	M + 2 - COCl
[¹³ C]Cl ₄ DD	332	268	M - COCl
	334	270	M + 2 - COCl
Cl ₃ DPO	342	306	M + 2 - HCl
Cl ₃ DPO	376	306	M + 2 - Cl ₂
group 2			
Cl ₃ DD	354	228	M - 2 (COCl)
Cl ₃ DF	338	275	M - COCl
	340	277	M + 2 - COCl
Cl ₃ DD	354	291	M - COCl
	356	293	M + 2 - COCl
[¹³ C]Cl ₃ DD	366	302	M - COCl
	368	304	M + 2 - COCl
Cl ₃ DPO	376	340	M + 2 - HCl
Cl ₃ DPO	410	340	M + 2 - Cl ₂
group 3			
Cl ₃ DD	390	264	M + 2 - 2 (COCl)
Cl ₃ DF	374	311	M + 2 - COCl
	376	313	M + 4 - COCl
[¹³ C]Cl ₃ DF	386	322	M + 2 - COCl
Cl ₃ DD	390	327	M + 2 - COCl
	392	329	M + 4 - COCl
[¹³ C]Cl ₃ DD	402	338	M + 2 - COCl
	404	340	M + 4 - COCl
Cl ₂ DPO	410	374	M + 2 - HCl
Cl ₃ DPO	444	374	M + 2 - Cl ₂
group 4			
Cl ₂ DD	424	298	M + 2 - 2 (COCl)
Cl ₂ DF	408	345	M + 2 - COCl
	410	347	M + 4 - COCl
Cl ₂ DD	424	361	M + 2 - COCl
	426	363	M + 4 - COCl
[¹³ C]Cl ₂ DD	436	372	M + 2 - COCl
	438	374	M + 4 - COCl
Cl ₂ DPO	446	410	M + 4 - HCl
Cl ₃ DPO	480	410	M + 4 - Cl ₂
group 5			
Cl ₃ DD	458	332	M + 2 - 2 (COCl)
Cl ₃ DF	442	379	M + 2 - COCl
	444	382	M + 4 - COCl
Cl ₃ DD	458	395	M + 2 - COCl
	460	397	M + 4 - COCl
[¹³ C]Cl ₃ DD	470	406	M + 2 - COCl
	472	408	M + 4 - COCl

Table II. Congeners Used for Tuning in MS/MS

2,3,7,8-Cl ₄ DD/F	1,2,3,4,6,7,8-Cl ₇ DD/F
1,2,3,7,8-Cl ₅ DD/F	Cl ₈ DD/F
1,2,3,4,7,8-Cl ₆ DD/F	

of the parent ion into the collision quadrupole. The instrument was then switched to the MS/MS mode and the collision gas was allowed to enter the collision quadrupole. Initial values for collision energy and collision gas pressure were set from the breakdown graphs and then iteratively optimized to the point where the relative abundance of the desired daughter ions maximized. These two parameters, as well as the electron energy, were adjusted so that the internal energy distribution of the parent ion and therefore the fragmentation of the parent ion was directed mainly toward the reaction of interest (loss of COCl). The quadrupole offsets, lens voltages, and rf voltages were iteratively set to maximize the desired daughter ion signal. The resolution of both Q₁ and Q₃ were set to unit mass resolution.

Table III. Isotopic Ratios of Daughter Ions

congeners	[M - COCl]:[M + 2 - COCl]
Cl ₄ DD/F	1.00:0.97
Cl ₅ DD/F	0.78:1.00
	[M + 2 - COCl]:[M + 4 - COCl]
Cl ₆ DD/F	1.00:0.65
Cl ₇ DD/F	1.00:0.82
Cl ₈ DD/F	1.00:0.97

The collision gas pressure was set for the optimum value of 2,3,7,8-Cl₄DD (~3 mTorr; which was similar to that of all the dioxins and furans studied) and was not changed throughout the run because the differences in optimum collision gas pressures between the various congeners were minor and because of the difficulties in changing and stabilizing pressures when a fine metering needle valve was used. The collision energies were set to the values that would optimize the signal strength of both the 2,3,7,8-substituted dioxin and furan used to optimize each group. These values ranged between 18 and 27 eV (laboratory energy), while the electron energies maximized signal strengths between 22 and 28 eV.

Once the instrument was optimized, the ion volume used with the direct insertion probe was replaced with a clean EI ion volume. Solvent blanks and internal standards were then injected to ensure that there was no carryover of dioxins or furans from the tuning procedure. Six EI ion volumes giving almost identical signal response were selected and then rotated on a daily basis. A standard (as shown in Figure 6) was injected at least twice daily to ensure good instrument performance.

The criteria for positive CDD/F identification were as follows: correct retention time windows for each group of isomers as determined by a window setting standard that contained the first- and last-eluting dioxin and furan in each group (obtained from the Bremen laboratory at Wright State University; fly ash was used to check the windows), the loss of COCl from the preselected parent ions to the desired daughter ions (forming the two most abundant daughter ions of the isotopic cluster), correct isotopic ratios of the daughter ions (within ±25%; see Table III), and a signal-to-noise (S/N) response greater than 3:1 (the signal must be greater than 3 times the peak-to-peak baseline noise) for both daughter ions. The CDFs must not exhibit the presence of DPO. An additional requirement for the isomer-specific analysis is that the retention time of the congener of interest must elute from the gas chromatograph within ±2 s of its isotopically labeled standard.

Surrogate standards labeled with ¹³C and/or ³⁷Cl were used to determine recoveries by comparison with external standards, and ¹³C₁₂Cl₆DF was used as the internal standard to monitor instrument performance.

Results and Discussion

The limits of detection reported in 1986 by three manufacturers of triple quadrupole mass spectrometers using a calibration compound such as PFTBA or perfluorokerosene (PFK) to optimize the instrument (PFTBA tune) are compared to the limits of detection that were obtained by using dioxins and furans to optimize the instrument (dioxin tune) and to limits of detection that were obtained by HRMS [12000 resolving power (RP)] (1) in Table IV. Detection limits were obtained without using high levels of a ¹³C-labeled carrier. Most of the limits of detection obtained by the MS/MS dioxin tune method are between 1 and 2 orders of magnitude lower than when PFTBA is

Table IV. MOE MS/MS Comparison: Limits of Detection^a

congener	manufacturer			present method	HRMS
	A	B	C		
Cl ₄ DD	2	2	8	0.3	0.2
Cl ₅ DD	5	4	9	0.5	0.2
Cl ₆ DD	10	10	23	0.3	0.2
Cl ₇ DD	15	15	19	0.3	0.2
Cl ₈ DD	20	25	38	0.6	0.4
Cl ₄ DF	4	3	7	0.3	0.2
Cl ₅ DF	5	4	11	0.3	0.2
Cl ₆ DF	10	8	21	0.2	0.2
Cl ₇ DF	15	10	20	0.5	0.2
Cl ₈ DF	20	20	19	0.5	0.4

^a All data in picograms. High levels of ¹³C-labeled CDD/F were not used as carriers.

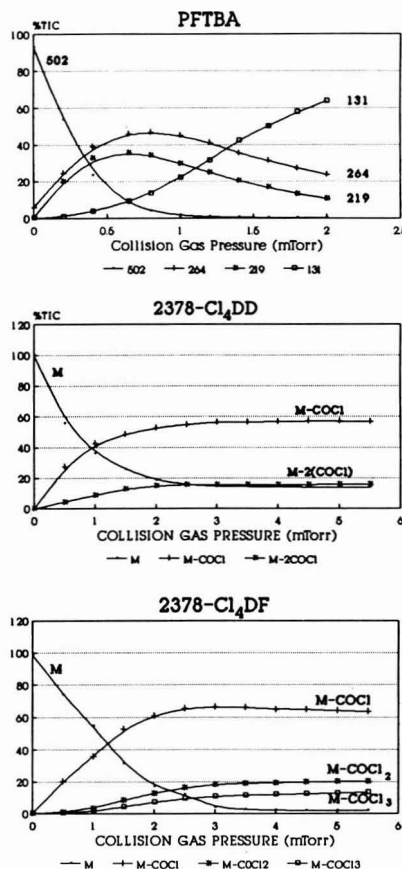


Figure 1. Collision gas pressure breakdown graphs.

used for optimization and begin to approach those obtained by HRMS. The Cl₄DD results in Table IV compare well with those previously reported by Tondeur and co-workers [1.5 pg for MS/MS and 150 fg for HRMS (10000 RP) (calculated at 3:1 S/N) (13)]. HRMS instrument manufacturers have recently reported detection limits for 2,3,7,8-Cl₄DD that are 1 order of magnitude lower. Accurate comparisons are not always possible because some of these results were obtained with high levels of ¹³C-labeled standards as carriers.

The difference in limits of detection obtained by MS/MS is due to the fact that the optimum parameters for the

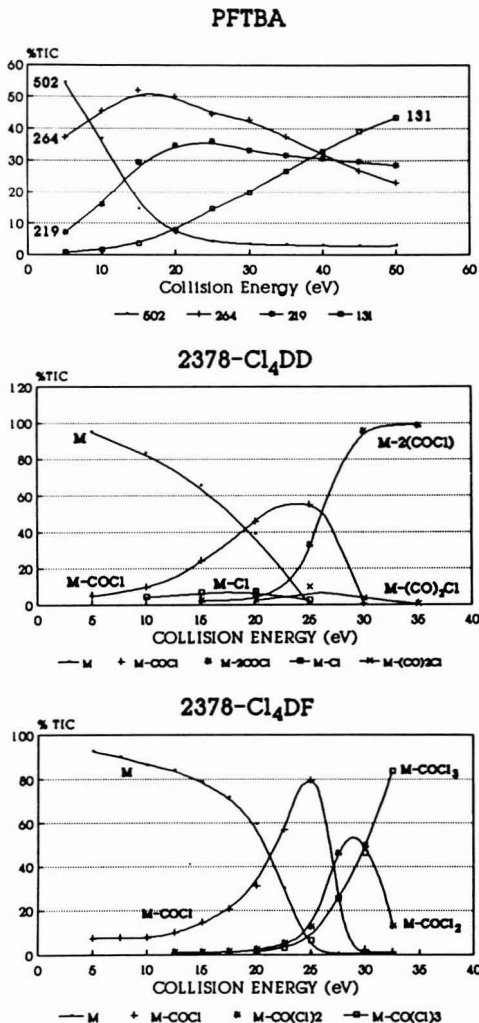


Figure 2. Collision energy breakdown graphs.

fragmentation reaction of PFTBA (usually m/z 502–219) are different from the optimum parameters for the loss of COCl from the molecular ion of the CDDs and CDFs. This can be shown by constructing breakdown graphs for a number of parameters such as collision energy and collision gas pressure.

The breakdown graphs for PFTBA, 2,3,7,8-Cl₄DD, and 2,3,7,8-Cl₄DF plotted against collision gas pressure (collision energy 25 eV laboratory energy) are shown in Figure 1. The optimum collision gas pressure for PFTBA was 0.7 mTorr while that for the dioxin and the furan was 3.3 mTorr. Figure 2 shows the breakdown graphs of PFTBA, 2,3,7,8-Cl₄DD, and 2,3,7,8-Cl₄DF plotted against collision energy (at optimum collision gas pressure). All three have optimum collision energy values of ~25 eV (laboratory energy). Although the optimum collision energies are similar for the latter three compounds, the considerable difference in the optimum collision gas pressure setting and the size of the neutral lost (283 amu for PFTBA and 63 amu for CDD/F) indicates that, for maximum instrument performance in multiple reaction monitoring (MRM), tuning on the analyte of interest is critical. To a first approximation (23), the difference in kinetic energy of the

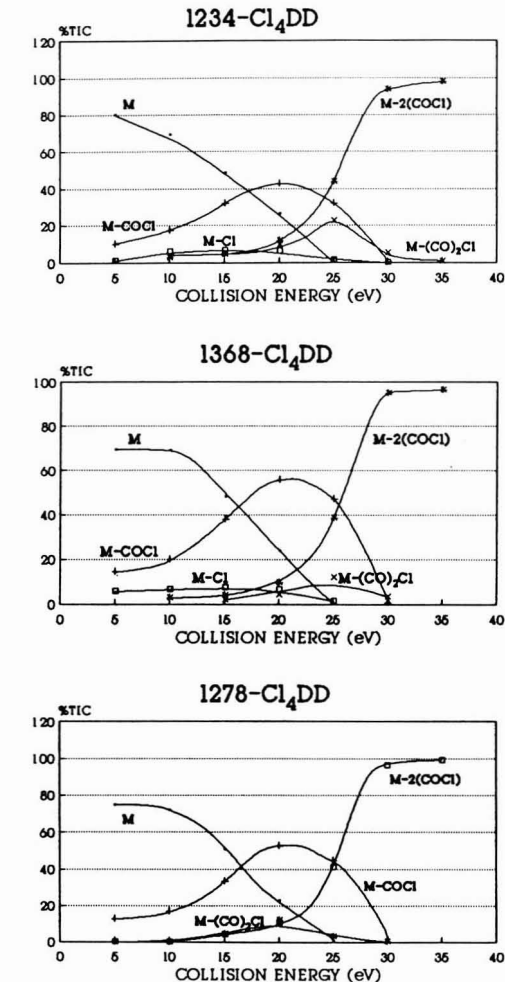


Figure 3. Collision energy breakdown graphs for three tetrachloro-dibenzo-*p*-dioxins.

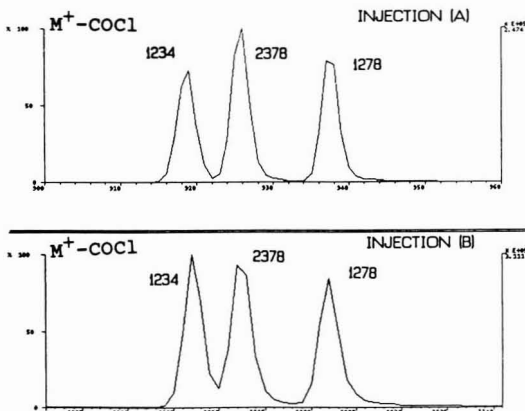


Figure 4. Dependence of relative response factors on collision energy.

daughter ions formed in Q₂ (219/502 or 43.6% of the original KE is carried by m/z 219 of PFTBA compared to 257/320 or 80.5% for m/z 257 of Cl₄DD and 393/456 or 86.2% for m/z 393 of Cl₅DD) with respect to those formed

2378-Cl₄DF

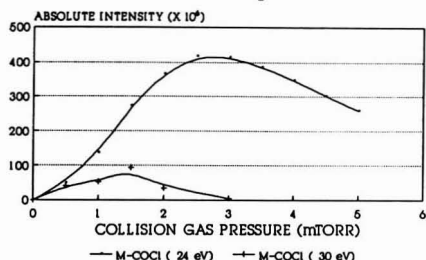


Figure 5. Dependence of absolute signal strength (absolute area) on collision gas pressure and collision energy.

in the ion source predicated that a dioxin or furan must be used to accurately set the energy of Q₃.

Figure 3 shows the collision energy breakdown graphs of three other Cl₄DD isomers. The optimum collision energy for these three isomers is between 18 and 22 eV (laboratory energy). If the collision energy were set to 25 eV (the optimum value for 2,3,7,8-Cl₄DD), the signal strength of the other three Cl₄DD isomers would be between 70% and 80% of their maximum value. This latter result suggests that the relative response factors of the various isomers are dependent on parameters such as collision energy. This is shown in Figure 4. Three Cl₄DD isomers were injected (100 pg of each isomer). Injections A and B were run at collision energies of 27.5 and 22.5 eV (laboratory energy), respectively. As expected from the breakdown graphs, the 2,3,7,8-Cl₄DD signal strength is enhanced in injection A and the 1,2,3,4-Cl₄DD signal

strength is enhanced in injection B.

Figure 5 shows the absolute signal strength of 2,3,7,8-Cl₄DF vs collision gas pressure at two different collision energies. The absolute signal strength of 2,3,7,8-Cl₄DF is lower at 30 eV collision energy than at 24 eV collision energy because at the higher collision energy more energy is imparted into the parent ion. This can cause the daughter ion formed by loss of COCl to fragment further. A change in the collision energy or collision gas pressure causes a corresponding change in the internal energy distribution of the parent ion and the appearance of the daughter ion spectrum. Therefore, in order to obtain standard tuning conditions and instrument-independent relative response factors, a 2,3,7,8-substituted (the most toxic) dioxin and furan congener was chosen for each group. These are listed in Table II.

Figure 6 compares the reconstructed ion chromatogram (RIC) of a series of Cl₄DD/F to Cl₄DD/F standards injected with a PFTBA tune (top) and dioxin tune (bottom). The signal strengths in the dioxin tune are considerably greater than those in the PFTBA tune.

Figure 7 shows the mass chromatogram of a 500-fg standard injected on a 30-m SE-52 capillary column with a split/splitless injector. The signal-to-noise ratio is ~10:1 (peak-to-peak noise definition) for *m/z* 257 and 259.

Figure 8 shows the mass chromatogram for a fish extract that had been cleaned by using a modified Dow dual column method without carbon cleanup (7). This extract was injected 3 weeks after the instrument was last tuned. A value of 2 pg was determined for 2,3,7,8-Cl₄DD.

Figure 9 compares the mass chromatogram for the Cl₄DD region of a fish extract (without carbon cleanup)

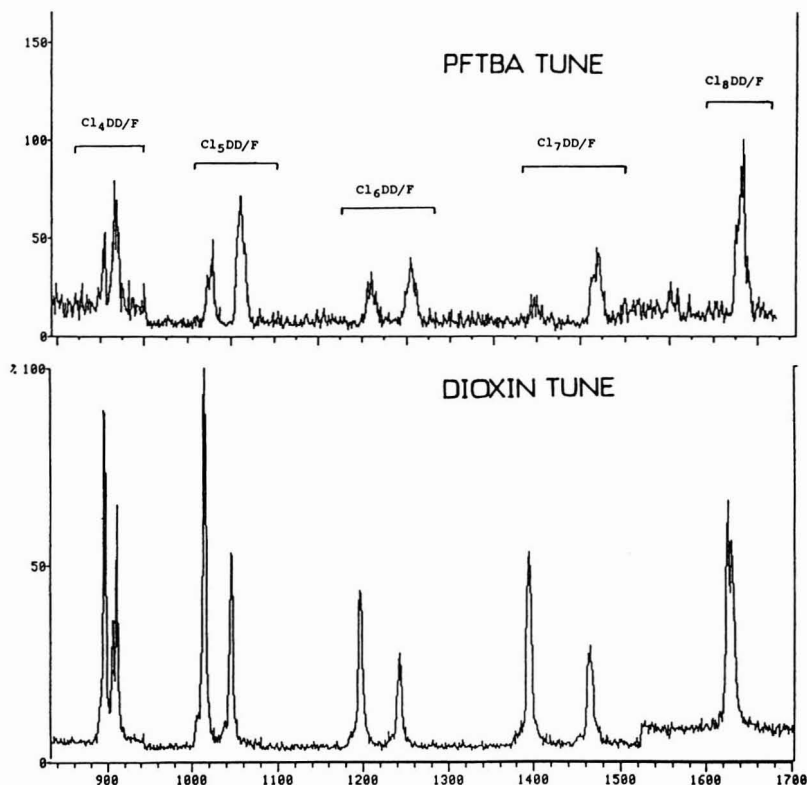


Figure 6. Comparison of standards (RIC) using a PFTBA tune (top) and dioxin tune (bottom). The amounts injected were 10 pg of Cl₄DD/F, 15 pg of Cl₅DD/F and Cl₆DD/F, and 20 pg of Cl₇DD/F and Cl₈DD/F.

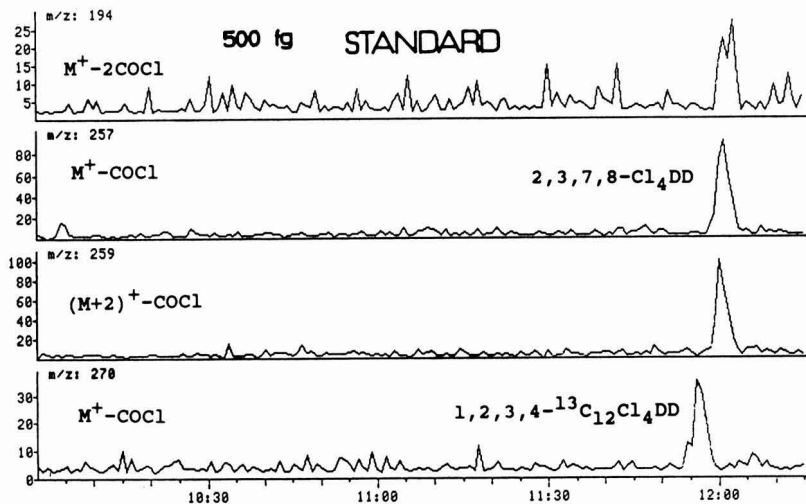


Figure 7. Mass chromatogram of a 500-fg standard injected on a 30-m SE-52 capillary column with a split/splitless injector.

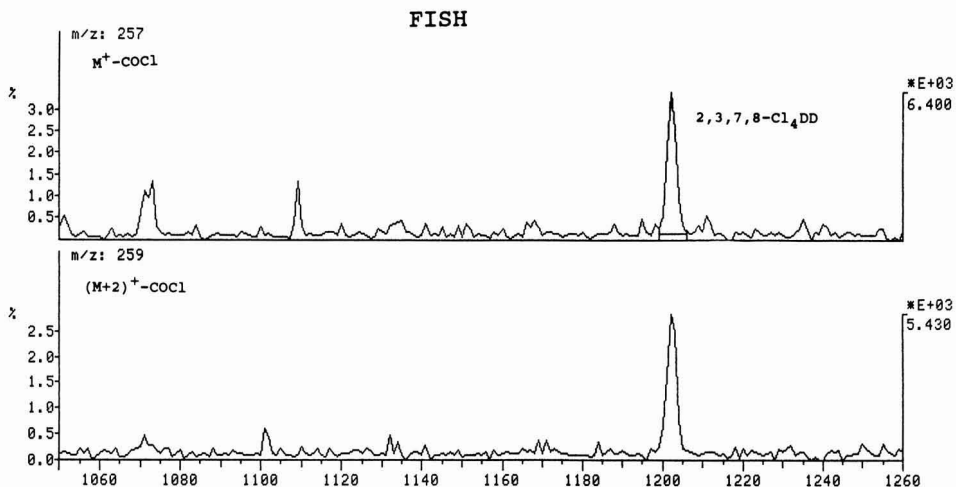


Figure 8. Cl₄DD mass chromatograms for the injection of a fish extract that contained 2 pg of 2,3,7,8-Cl₄DD.

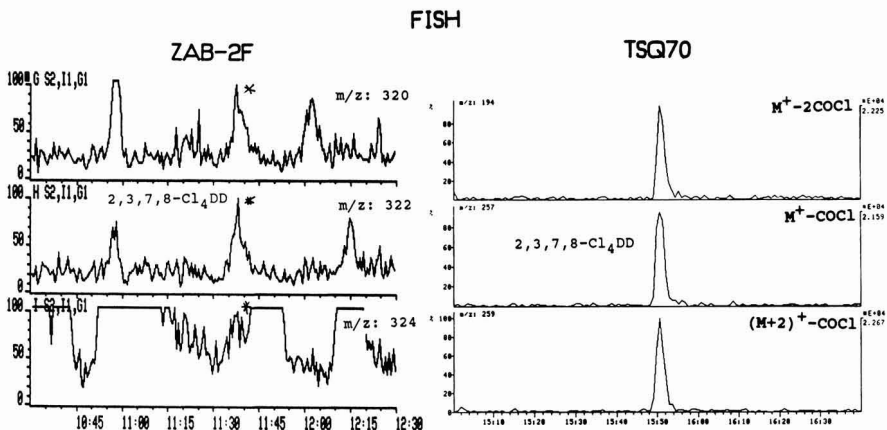


Figure 9. Comparison of the Cl₄DD region of a fish extract run by HRGC/HRMS (left) and HRGC/MS/MS (right).

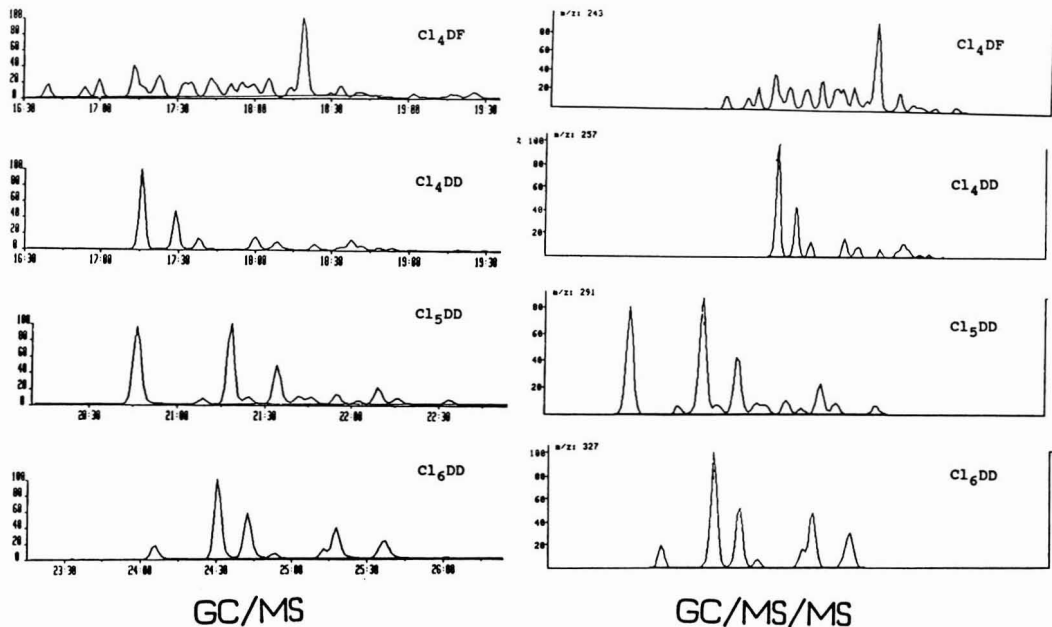


Figure 10. Comparison of the relative response factors obtained in the HRGC/MS mode (left) and HRGC/MS/MS mode (right) for the Cl_4DF , Cl_4DD , Cl_5DD , and Cl_6DD regions.

in the HRMS mode [VG-ZAB-2F (1)] and in the MS/MS mode (TSQ 70). The 2,3,7,8- Cl_4DD isomer is marked with an asterisk. Even at 12000 RP, many of the chemical interferences are still seen in the HRMS mass chromatogram, while in the MS/MS mass chromatogram, none of these interferences are present and 2,3,7,8- Cl_4DD is the only isomer detected. Tondeur et al. (20) have shown that matrix effects are closely related to source instabilities in HRMS when significant amounts of undesirable materials (50 ng/s) reach the ion source. This instability may cause an effective decrease in resolution and change in signal strength, and consequently, quantitation is affected. These results were also obtained on a VG-ZAB-2F mass spectrometer. Newer magnetic sector instruments have their source slits further from the ion source and this design change should help reduce this effect. The stable (flat) baseline and clean mass chromatogram in the MS/MS mode suggest that the concentrations at which this instability occurs in a quadrupole mass spectrometer ion source may be higher than in a magnetic sector instrument. Further experimentation in this area is required.

Figure 10 compares the Cl_4DF , Cl_4DD , Cl_5DD , and Cl_6DD congeners in the MS and MS/MS modes for an effluent sample. The isomer patterns (relative response factors) are similar in both modes when the series of 2,3,7,8-substituted congeners in Table II is used to optimize the instrument in the MS/MS mode. This is an important result, because in order to compare results from all instruments in an analysis of all congeners, reproducible instrument-independent relative response factors are required. Reproducible relative response factors may be obtainable by using a standard set of tuning congeners such as the ones listed in Table II. More study in this area is also needed.

The major disadvantage of using a quadrupole collision cell is that the daughter spectra obtained are strongly dependent on collision cell conditions (25). The nodes and antinodes characteristic of the transmission of ions through an rf-only collision quadrupole dictate that the error in

isotopic ratios in MS/MS is larger than that in HRMS. The range that was used ($\pm 25\%$) is narrower than that used by Slayback et al. (-40% to $+30\%$) (14). This fluctuation begins to appear at lower levels (<5 pg); however, in the majority of cases, ratios fall within $\pm 10\%$ of the ratios listed in Table III. This latter problem has been addressed by using hexapole collision cells (25). Also, at low levels, the signal strength of the confirmation ion for the dioxins (loss of $2COCl$) is very weak because it is generally a factor of 5 lower than the ions formed by loss of $COCl$.

The linear dynamic range is greater than 3 orders of magnitude. The relative standard deviation of the 2,3,7,8- Cl_4DD concentration of five fish extracts rerun after 3 months without optimization (tuning) was less than 10%.

Advantages of the method include the following: selectivity, especially in the Cl_4DD/F region, where for some samples, fewer interferences are observed than in HRMS; infrequent tuning—the instrument is tuned three to four times a year at 200 injections per month (including standards and QA/QC); reduced routine maintenance—the source and rods are cleaned about every 4 to 6 months (the ion volumes are changed daily); and good sensitivity—less than 1 pg of dioxins and furans can be detected for all congeners.

The choices available in the mass spectrometric analysis of CDD and CDF (HRMS vs MS/MS) are dependent on the matrix and the degree of cleanup used. Useful applications of GC/MS/MS appear to be in pulp and paper, petrochemical, and biological samples (16, 25), which have many interfering compounds or a large proportion of aromatic and substituted aromatic components that are not completely removed by the cleanup procedures.

Literature Cited

- Taguchi, V. Y.; Reiner, E. J.; Wang, D. T.; Meresz, O.; Hallas, B. *Anal. Chem.* 1988, 60, 1429.
- Heath, R. G.; Harless, R. L.; Gross, M. L.; Lyon, P. A.; Dupuy, A. E.; McDaniel, D. D. *Anal. Chem.* 1986, 58, 463.

- (3) Harless, R. L.; Dupuy, A. E.; McDaniel, D. D. *Environ. Sci. Res.* 1983, 36, 65.
- (4) Smith, L. M.; Stalling, D. L.; Johnson, J. L. *Anal. Chem.* 1984, 56, 1830.
- (5) Patterson, D. G.; Holler, J. S.; Groce, D. F.; Alexander, L. R.; Lapeza, C. R.; O'Conner, R. C.; Liddle, J. A. *Environ. Toxicol. Chem.* 1986, 5, 355.
- (6) Laycock, D. E. *Can. Chem. News* 1986, 38(8), 7.
- (7) Clement, R. E.; Bobbie, B.; Taguchi, V. *Chemosphere* 1986, 15, 1147.
- (8) Sakuma, T.; Gurprasad, N.; Tanner, S. D.; Ngo, A.; Davidson, W. R.; McLeod, H. A.; Lau, B. P. Y.; Ryan, J. J. In *Chlorinated Dioxins and Dibenzofurans in the Total Environment*; Keith, H., Rappe, C., Choudhary, G., Eds.; Butterworth: Stoneham, MA, 1985; Vol. II, p 139.
- (9) Shushan, B.; Tanner, S. D.; Clement, R. E.; Bobbie, B.; *Chemosphere* 1985, 14, 843.
- (10) Levsen, K. *Org. Mass Spectrom.* 1988, 23, 406.
- (11) Bursey, M. M.; Hass, J. R. In *Tandem Mass Spectrometry*; McLafferty, F. W., Ed.; Wiley: New York, 1983; Chapter 25.
- (12) Tondeur, Y.; Albro, P. W.; Hass, J. R.; Harvan, D. J.; Schroeder, J. L. *Anal. Chem.* 1984, 56, 1344.
- (13) Tondeur, Y.; Niederhut, W. N.; Campana, J. E.; Missler, S. R. *Biomed. Environ. Mass Spectrom.* 1987, 14, 449.
- (14) Slayback, J. R. B.; Taylor, P. A. *Spectra* 1983, 58(4).
- (15) Schellenberg, D. H.; Bobbie, B. A.; Reiner, E. J.; Taguchi, V. Y. *Rapid Commun. Mass Spectrom.* 1987, 1, 111.
- (16) Charles, M. J.; Green, B.; Tondeur, Y.; Hass, J. R. *Chemosphere* 1989, 19, 51.
- (17) Fraisse, D.; Gonnord, M. F.; Becchi, M. *Rapid Commun. Mass Spectrom.* 1989, 3, 79.
- (18) Martinez, R. I.; Cooks, R. G. *Proceedings of the 35th Annual Conference on Mass Spectrometry and Allied Topics*; American Society for Mass Spectrometry, Denver, CO, 1987; p 1175.
- (19) Rosenstock, H. M.; Wallenstein, M. M.; Wahlhaftig, A. L.; Eyring, H. *Proc. Natl. Acad. Sci. U.S.A.* 1952, 38, 667.
- (20) Kenttamma, H. I.; Cooks, R. G. *Int. J. Mass Spectrom. Ion Processes* 1985, 63, 325.
- (21) Catlow, D. A.; Clayton, E.; Monaghan, J. J.; Scrivens, J. H. *Proceedings of the 35th Annual Conference on Mass Spectrometry and Allied Topics*; American Society for Mass Spectrometry, Denver, CO, 1987; p 1036.
- (22) Clement, R. E.; Tosine, H. M.; Osborne, J.; Ozsvacic, V.; Wong, G. In *Chlorinated Dioxins and Dibenzofurans in the Total Environment*; Keith, H., Rappe, C., Choudhary, G., Eds.; Butterworth: Stoneham, MA, 1985; Vol. II, Chapter 34.
- (23) Yost, R. A.; Boyd, R. K. *Tandem Mass Spectrometry: Quadrupole and Hybrid Instruments*. In *Mass Spectrometry: Advances in Enzymology*; McCloskey, J. A., Ed.; Academic Press: New York, Vol. 193, in press.
- (24) Merrin, T. O.; McDowall, M. A.; Hammond, M. *Proceedings of the 37th Annual Conference on Mass Spectrometry and Allied Topics*; American Society for Mass Spectrometry, Miami Beach, FL, 1989, p 1025.
- (25) Reiner, E. J.; Schellenberg, D. H.; Taguchi, V. Y.; Mercer, R. S.; Townsend, J. A.; Thompson, T. S.; Clement, R. E. *Chemosphere* 1990, 20, 1385.

Comparative Response of Reconstituted Wood Products to European and North American Test Methods for Determining Formaldehyde Emissions

William J. Groah, John Bradfield,* Gary Gramp, Rob Rudzinski, and Gary Heroux

National Particleboard Association, 18928 Premiere Court, Gaithersburg, Maryland 20879, and Hardwood Plywood Manufacturers Association, P.O. Box 2789, Reston, Virginia 22090-2789

■ The European large-chamber, the North American large-chamber, the European perforator, and the North American desiccator test protocols for formaldehyde emissions from wood products were compared. Two formaldehyde analytical techniques using chromotropic acid and pararosaniline chemistry were used for the large-chamber testing. Six sample sets, chosen for their range in formaldehyde emissions, provided the experimental data. The sets consisted of five particleboards and one medium-density fiberboard (MDF). The European large-chamber protocol produced values that were 20% lower than the North American large-chamber protocol and both analytical techniques produced similar test results. Linear relationships between all the tests were strong. These relationships should allow manufacturers on both continents a level of confidence in predicting their conformance with formaldehyde emission standards. These tests confirm a similarity seen by others in the emission rates of North American and European products.

Introduction

There has been considerable interest in Europe and North America in quantifying the relationships between various test methods for determining formaldehyde emissions from wood panel products made with formaldehyde-containing adhesives (1-7). This interest is

motivated by a need (1) to better understand the relationships between European and North American test methods, (2) to aid in interpreting progress that has occurred in reducing formaldehyde emissions from wood products, and (3) to determine whether current wood products manufactured in Europe and North America are similar. Another important reason for this interest is to understand data derived from small-scale tests such as the North American 2-h desiccator and the European perforator in the context of large-scale chamber tests. Large-scale chamber tests are designed to simulate actual product loading or usage, typical air-exchange rates, and characteristic temperature and relative humidity conditions in buildings (8).

While these test methods are designed to show relative emission levels between products, care must be exercised in relating formaldehyde emission test measurements to the home. Without rigorous additional study of all applicable parameters, no extrapolation of formaldehyde emission test data to home formaldehyde levels should be attempted. Temperature, humidity, air exchange, and other factors can all affect observed home levels.

The objective of this experiment was to give some insight into the relationships between the principal European and North American methods for determining formaldehyde emissions from reconstituted wood products. There was special focus on large-scale methods since large chambers, capable of testing full size samples, are the basis of European (9) and North American (10) formaldehyde emis-

Hardwood Plywood Manufacturers Association.
National Particleboard Association.

sion guidelines or requirements.

The large-chamber test method developed by the Wilhelm Klauditz Institute (WKI) in the Federal Republic of Germany is the principal European method (9). The WKI chamber value of 0.1 ppm for the West German "E-1" classification is often cited as an important benchmark for low-formaldehyde-emitting building products. The FTM-2 (formaldehyde test method 2) North American large chamber is used for wood panel testing in the United States and Canada (11). FTM-2 is referenced by the U.S. Department of Housing and Urban Development (HUD) for determining formaldehyde emissions from particleboard and plywood used in manufactured (mobile) homes. The HUD emission limit is 0.3 ppm for particleboard and 0.2 ppm for plywood wall paneling.

Large-chamber test methods have been used for some time in both Europe and North America. The complete descriptions of how such chambers should be constructed have yet to be finalized. Formal standardization of chamber operating procedures are now being considered through international organizations on both continents (American Society for Testing and Materials and European Committee for Standardization). The European and North American tests are different in many testing parameters; however, only limited information is available to judge their comparability. In 1986, two sets of E-1 particleboard products were obtained and tested in the United States by three different test laboratories using the FTM-2 protocol (12). The results indicated that the E-1 products were comparable to U.S. products manufactured to the HUD standard.

Materials and Methods

Large-Scale Tests. Significant laboratory variation in results from large-chamber tests has been demonstrated (13). An experiment was designed so that European WKI and North American FTM-2 large-chamber conditions could be evaluated simultaneously in one laboratory to eliminate the effects of laboratory-to-laboratory variation and panel age. WKI and FTM-2 tests were run in two identical chambers within the same laboratory using reconstituted wood panel samples tested in such a way as to reduce the effects of board variation.

Two sets of panels were tested in early 1988 comparing the FTM-2 and the WKI protocols. Four more sets of panels were more extensively tested during 1989. The six reconstituted wood products tested in 1988-1989 exhibited formaldehyde emissions over a broad range. Three of the sets (1-3) were typical of products certified to meet the HUD standard for particleboard. One set (6) was manufactured by using expensive, special techniques designed to lower emission levels to the minimum. The remaining products (4 and 5) were manufactured without the use of scavengers to bring them into HUD compliance. Five of the products were sanded particleboard; product 4 was sanded medium-density fiberboard (MDF).

The principal testing parameters of the WKI and FTM-2 chamber methods are outlined in Table I (9, 11). Each reconstituted wood product was tested simultaneously in two 1080-ft³ (30.6-m³) chambers to WKI and FTM-2 conditions. Air from the heating, ventilating, and air conditioning (HVAC) system passing into the room containing the two chambers was maintained at 65-70% relative humidity (RH) and at ~70 °F. Subsequently the air was dehumidified by air conditioning cooling and then reheated with a resistance heater in a large two-section prechamber. Air was directed through a series of ducts and valves, a totalizing gas meter, and then through a 4-in. (inside diameter) cylinder containing a 6-in. bed of po-

Table I. WKI and FTM-2 Chamber Test Parameters

	loading rate of tested product	minimum size of chamber	temp	relative humidity	air-exchange rate	typical size of individual particleboard samples	conditioning schedule	sampling schedule	preferred analytical method
WKI chamber	0.305 ft ² /ft ³ (1.00 m ² /m ³)	353 ft ^{3a} (10 m ³)	73.4 ± 2 °F (23 ± 1 °C)	45 ± 5%	1 AC/h ±10%	39.4 in. × 78.7 in. (1 m × 2 m)	none	measurement at latest 3 days after samples placed in chamber until equilibrium (≤0.01 ppm day-to-day variation) or to 10 days measurement at 16-20 h after placed in chamber	pararosaniline
FTM-2 chamber (conducted as prescribed by HUD)	0.13 ft ² /ft ³ (0.43 m ² /m ³)	800 ft ^{3a} (22.7 m ³)	77 ± 2 °F (25 ± 1 °C)	50 ± 4%	0.5 AC/h ±10%	35.2 in. × 96 in. ^b (0.89 m × 2.44 m)	7 days ± 3 h, 75 ± 5 °F, 50 ± 5% RH, at ≤0.1 ppm HCHO		chromotropic acid

^a Volume of chambers employed in these comparison tests, 1080 ft³ (30.6 m³). ^b In a chamber of 1080-ft³ volume.

tassium permanganate in alumina (Purafil) so that incoming chamber air could be maintained at or below a formaldehyde level of 0.01 ppm, the level of sensitivity for the chromotropic acid procedure at this laboratory. The air was then heated to test temperatures of 73.4 (23 °C) \pm 1 °F (WKI) or 77 (25 °C) \pm 1 °F (FTM-2) by means of small electric heaters located inside the chambers. Relative humidity conditions of 45% for the WKI simulation tests and 50% for the FTM-2 tests were maintained within a tolerance of \pm 2%. These tolerances are within those allowed (9, 11).

Each chamber has a 10-in.-diameter fan to circulate and mix the air. A hot wire anemometer was used to ensure air flow rates were adequate for the WKI tests (FTM-2 has no specific requirement for air flow). Chamber samples were placed vertically on metal stands with both sides of the samples exposed. The insides of both chambers are lined with polished 3003 alloy aluminum. The dimensions of each chamber are 7.8 ft (2.4 m) wide \times 7.1 ft (2.2 m) high \times 19.5 ft (5.9 m) long for a volume of 1080 ft³ (30.6 m³). Both chambers are operated under positive pressure and the exhaust ducts are located on the opposite end of the chambers from the intake ducts. Exhaust chamber air is ducted out of the building housing the chambers.

All reconstituted wood panel samples were held in polyethylene wrapping until WKI testing or FTM-2 conditioning was to begin. For each set of panels, WKI testing and FTM-2 conditioning were initiated on the same day. For samples tested in accordance with the WKI protocol, polyethylene wrapping was removed and panels were cut into eight samples, each slightly less than 4 m³ in surface area, to achieve a loading rate of 0.305 ft²/ft³ (1 m²/m³). These samples were immediately placed in the chamber and were measured daily for 10 days. The three panels selected for the FTM-2 chamber tests were taken out of the polyethylene wrapping the same day that WKI samples were processed, cut into three 49 in. \times 69 in. samples, and placed for 7 days at a temperature of 75 \pm 5 °F and at 50 \pm 5% relative humidity in a conditioning room where the formaldehyde level was maintained at or below 0.1 ppm. Panels were then placed in the chamber and air samples were taken after 16–20 h.

For both WKI and FTM-2 tests, air samples were collected 54 in. above the floor at two locations, $\frac{1}{3}$ of the distance from each end of the chambers, and at midwidth of the chambers. The air samples for pararosanine analysis were collected in distilled water at a flow rate of 1 L/min for 1 h (9). Air samples for chromotropic analysis were then collected in a solution of 1% sodium bisulfite in water at a flow rate of 1 L/min for 1 h (11).

Chromotropic acid analysis was used in the chamber tests conducted in 1988 on products 1 and 2. More extensive data were collected on the four materials (3–6) tested during 1989:

(1) Pararosanine and chromotropic acid analysis were both performed on air samples for the WKI and FTM-2 chamber tests.

(2) A full array of desiccator and perforator tests was conducted on samples taken from panels used for the chamber test comparison: eight samples for each WKI chamber test and three samples for each FTM-2 chamber test.

Small-Scale Tests. Samples were cut for small-scale, 2-h desiccator (FTM-1) (14) and perforator tests (15) from each panel from products 3–6 used for the WKI and FTM-2 tests. A limited number of small-scale tests were performed on product 2; no small-scale tests were performed on product 1.

Desiccator samples were edge sealed and conditioned for 24 h in the same conditioning area as the FTM-2 samples. Desiccator tests were performed on the following day, the first day that WKI chamber samples were evaluated. The desiccator test is a formaldehyde absorption test where eight 2.75 in. \times 5 in. samples are placed for 2 h in a 10.5 L desiccator with a Petri dish containing 25 mL of distilled water. Formaldehyde emitted from the samples and absorbed in the water is then analyzed by use of chromotropic acid.

Samples cut from products 3–6 were wrapped in polyethylene and transported from the Hardwood Plywood Manufacturers Association (HPMA) laboratory to the National Particleboard Association (NPA) laboratory, a distance of 25 miles. NPA performed perforator tests on specimens of \sim 100 g from each of the 11 large chamber panels (8 specimens for the WKI test and 3 for the FTM-2 test).

The perforator method used in this test series is described in a draft proposed by the European Committee for Standardization (Comite European De Normalisation), CEN/TC 112/WG 5, dated February 1989 (15). This proposed test is derived directly from European standard test, EN 120, dated October 1984 (16).

The perforator is a formaldehyde extraction test method that involves boiling small samples in toluene. The formaldehyde-laden toluene is distilled through distilled/deionized water, which absorbs the formaldehyde. A sample from the water is analyzed photometrically by the pararosanine analysis method. Although the European perforator test primarily references the acetylacetone analytical method, the pararosanine analysis used here is an allowable alternative. The proposed test method provides for two sampling schemes: one for production control and the other for installed product. Since the products were isolated immediately following production, sealed, and sent to the test laboratory, the production control scheme was followed.

Results and Discussion

A brief description of the reconstituted wood panel products and the results of the European and the North American large-chamber and small-scale tests appear in Table II. Formaldehyde emission data for the WKI protocol tests are those observed during the tenth day; data for the FTM-2 tests are 16–20 h after chamber loading following the 7-day conditioning period.

The linear relationship derived from observations from six products using chromotropic acid analysis for both WKI and the FTM-2 samples (regression 4, Table III) had an exceedingly high correlation coefficient (0.99). A correlation coefficient of 0.97 was observed for the more typical analytical methods employed for the chamber tests—pararosanine for the WKI method and chromotropic acid for FTM-2—for products 3–6 (regression 1, Table III). These relationships are plotted in Figure 1.

A difference between the two large-chamber protocols was observed when matched panels were tested. As shown in the last two columns of Table III (regressions 1–4), the WKI chamber test values were \sim 20% lower than FTM-2 at the 0.3 ppm limit established by HUD for particleboard using FTM-2 (10). The slope (0.79) of regression 4, the series having the largest number of observations, indicates that the WKI chamber test would result in values 21% less than the FTM-2 test. A regression analysis of the slope statistic indicates, with greater than 95% probability, that the WKI test gives lower values than the FTM-2 test. Further analysis of variance on this regression equation (*f* test) indicates a strong probability of linearity at 99.9%.

Table II. Results of European and North American Tests on Six Reconstituted Wood Products^a

product no. and description	formaldehyde levels					
	WKI (Para) ^b ppm	WKI (CA) ^b ppm	FTM-2 (Para), ppm	FTM-2 (CA), ppm	FTM-1 Desic, µg/mL	Perf. ^c mg/100 g
1. 1/2 in. particleboard		0.20		0.26		
2. 1/2 in. particleboard		0.11		0.16	0.53	5.23
3. 5/8 in. particleboard	0.19	0.19	0.28	0.27	0.68	9.68
4. 1/2 in. medium-density fiberboard (MDF)	0.32	0.31	0.38	0.41	0.90	14.90
5. 3/8 in. particleboard	0.33	0.30	0.37	0.35	0.86	11.30
6. 5/8 in. particleboard	0.05	0.06	0.06	0.07	0.18	4.44

^aAll products unfinished. Para, pararasaniline; CA, chromotropic acid; Desic, desiccator; Perf, perforator. ^bWKI values are for tenth day. ^cPerforator values average of 11 tests except for board 2 (one test).

Table III. Linear Relationships As Observed in Reconstituted Wood Product Test Series

regression no.	variables ^a		no. of obsns	regression params of Y = a + bx			X value ^b	Y value ^b
	X	Y		a	b	r		
Large-Scale Test Relationships								
1	FTM-2 chamber (CA)	WKI chamber (Para)	4	-0.01	0.86	0.97	0.30	0.24
2	FTM-2 chamber (Para)	WKI chamber (Para)	4	-0.01	0.87	0.98	0.30	0.25
3	FTM-2 chamber (Para)	WKI chamber (CA)	4	0.00	0.77	0.98	0.30	0.24
4	FTM-2 chamber (CA)	WKI chamber (CA)	6	0.01	0.79	0.99	0.30	0.23
Other Test Relationships								
5	WKI chamber (CA)	FTM-1 desiccator (CA)	5	0.15	2.50	0.95	0.10	0.40
6	FTM-2 chamber (CA)	FTM-1 desiccator (CA)	5	0.11	2.06	0.97	0.30	0.73
7	WKI chamber (CA)	perforator	5	1.88	37.27	0.96	0.10	5.61
8	FTM-2 chamber (CA)	perforator	5	1.38	30.68	0.98	0.30	10.58
9	FTM-1 desiccator (CA)	perforator	5	0.63	13.45	0.90	0.73	10.46

^aPara is pararasaniline analysis; CA is chromotropic acid analysis. ^bThe X values in this column are chosen for their correspondence to the formaldehyde limits of the U.S. Department of Housing and Urban Development (10) regulations in regressions 1-4, 6, and 8; for their correspondence with the West German E-1 designation in regressions 5 and 7; and for the correspondence with the Y value from regression 6 in regression 9. Values for X from the column, when used with their corresponding regression parameters on the same line, yield the stated Y values.

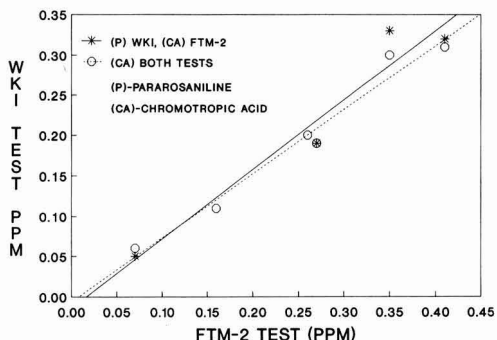


Figure 1. Large-chamber chamber test results. WKI and FTM-2 test results are compared by both the chromotropic acid and pararasaniline analytical techniques.

WKI test conditions tending to reduce observed chamber levels as compared to established FTM-2 conditions—lower chamber temperature (23 vs 25 °C), lower relative humidity (45 vs 50%), and higher air-exchange rate (1.0 vs 0.5 AC/h)—appear to more than offset the lower product loading rate of the FTM-2 procedure (0.43 vs 1.0 m²/m³).

The perforator value of 10 mg/100 g, often associated with the E-1 European board classification and a 0.1 ppm WKI chamber value, is seen in Table III and Figure 2 to more closely approximate the 0.30 ppm HUD chamber limit determined from the FTM-2 test than the 0.1 ppm WKI value. For the panels evaluated in this series, a perforator value of ~6 mg/100 g more closely correlates

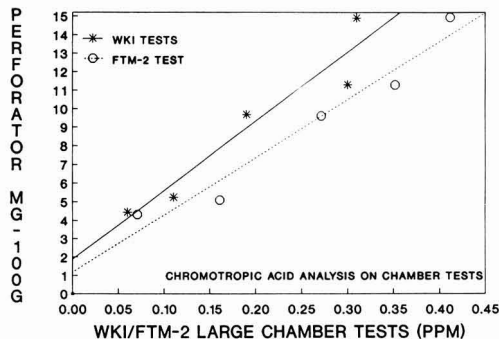


Figure 2. Perforator test results. Comparison of perforator results to the WKI and FTM-2 large-chamber tests where the chromotropic acid analytical technique was performed.

with a WKI chamber value of ~0.1 ppm. Newly proposed West German regulations stipulate an average limit of 6 mg/100 g for particleboard when the perforator test is used instead of the large chamber for certification (9). The observed relationship between the 2-h desiccator (~0.7 µg/mL) and the perforator value of 10 mg/100 g observed in this series of tests is similar to that suggested by Sundin (17).

The linear relationship between the 2-h desiccator test and the WKI and FTM-2 chamber test results with chromotropic acid analysis appears in Figure 3. These data indicate high linear relationship correlation coefficients between the small-scale tests and both large-chamber tests.

Table IV. Desiccator Results from Samples Taken from WKI and FTM-2 Test Panels

product no.	from WKI sample panels				from FTM-2 sample panels			
	no. of obsns	av desic, $\mu\text{g}/\text{mL}$	SD, $\mu\text{g}/\text{mL}$	coeff of var, %	no. of obsns	av desic, $\mu\text{g}/\text{mL}$	SD, $\mu\text{g}/\text{mL}$	coeff of var, %
3	8	0.69	0.036	5.2	3	0.66	0.061	9.2
4	8	0.91	0.033	3.6	3	0.89	0.031	3.5
5	8	0.86	0.041	4.8	3	0.87	0.067	7.7
6	8	0.18	0.011	6.1	3	0.20	0.012	6.0

Table V. Formaldehyde Level Changes (ppm) over 10-Day Duration of WKI Test^a

product no.	day no.									
	1	2	3	4	5	6	7	8	9	10
1	0.253	0.233	0.230	0.225	0.214	0.208	0.202	0.206	0.203	0.204
2	0.122	0.117	0.113	0.112	0.114	0.114	0.109	0.115	0.116	0.113
3	<i>b</i>	0.230	0.218	0.223	0.218	0.223	0.208	0.203	0.189	0.194
4	0.362	0.350	0.344	0.334	0.327	0.329	0.319	0.308	0.308	0.308
5	0.342	0.333	0.332	0.332	0.334	0.323	0.318	0.313	0.308	0.303
6	0.070	0.061	0.061	0.061	0.061	0.061	0.061	0.061	0.061	0.062
av	0.230	0.221	0.216	0.215	0.211	0.210	0.203	0.201	0.198	0.197
av % reductn ^c		4	6	7	8	9	12	13	14	14

^aAll concentrations are calculated to three decimal places from chromotropic acid analysis. Values are adjusted to 73 °F and 45% RH by using temperature and relative humidity effects on formaldehyde levels as reported by Berge et al. (18). ^bAverage assumes value of 0.230 ppm. ^cThe values in each column are reported to three decimal places to facilitate formaldehyde level reduction analysis over the course of the 10-day test.

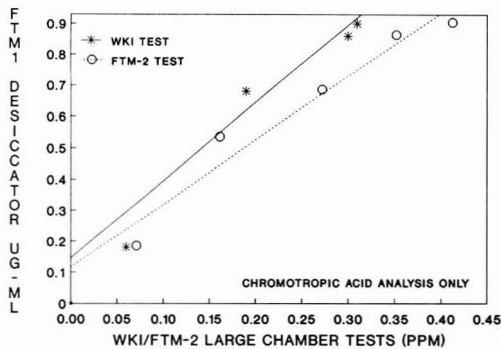


Figure 3. Desiccator test results. Comparison of desiccator results to the WKI and FTM-2 large-chamber tests where the chromotropic acid analytical technique was performed.

Desiccator test data in Table IV (products 3–6) demonstrate that there was little difference in the formaldehyde emission characteristics of panels used for WKI testing as compared with panels used for FTM-2 testing. Average desiccator values from WKI panels were similar to desiccator values from FTM-2 panels and standard deviations calculated from desiccator values for each chamber test are relatively low, with coefficients of variation ranging between 3 and 9%. These data suggest that there was very little variation in samples used in the testing of the four populations (products 3–6) when the European and North American large-chamber methods were compared. Thus, the relationships described here appear to be due to similarities or differences in the large-chamber test methods themselves, with little contribution from within-product variation.

The linear relationship between the perforator and the desiccator tests, displayed in Figure 4, does not appear as strong as the other comparisons. This may reflect a higher degree of variability encountered in the perforator test values within each product set. The perforator test was performed on a relatively small sample taken from each individual board, whereas the eight $2\frac{3}{4}$ in. \times 5 in. samples

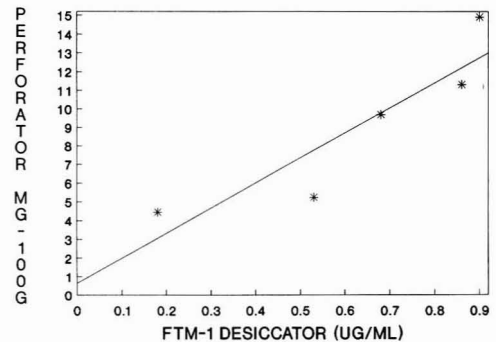


Figure 4. Small-scale test comparison. Comparison of perforator results to desiccator results.

that make up each desiccator test are cut across the width of the board so as to “average out” within board variability.

Eleven individual perforator observations for products 3–6 were used in determining the average value for these four products. For one product (2), only one perforator value was available. If more extensive perforator test information had been available from product 2, it is possible, if not likely, that the linear relationship between the perforator and the 2-h desiccator tests would have been stronger.

The effects of conditions such as ventilation rate, temperature, air-exchange rate, relative humidity, and product decay on formaldehyde levels have been noted by a number of investigators (18–22). The only direct empirical information related to any of these factors from this experiment was short-term product decay observed over the 10-day WKI test sampling period. The data in Table V suggest that a 10–15% decrease in formaldehyde emission potential can occur over the first week or so after the surfaces of products are exposed to the air in the chamber. This also verifies the suggestion that formaldehyde levels from newly manufactured building products change rapidly during the first few days after product surfaces are exposed to air (23).

While this study did not involve the evaluation of any European-made boards, the magnitude of the WKI and FTM-2 chamber values and the relationships between the perforator test and large-chamber levels suggest some similarity between current U.S.- and European-made reconstituted wood product boards produced with urea-formaldehyde adhesives. This finding is consistent with that reported by Grot that "some U.S. manufactured particle boards have characteristics approaching the best European boards" (24).

Conclusions

The information reported in this paper supports the following conclusions:

1. There was a strong linear relationship between the WKI and the FTM-2 large-chamber methods in testing reconstituted wood products. This relationship should allow manufacturers in Europe and North America a measure of confidence in predicting their conformance with formaldehyde emission standards established on both continents.

2. There was a difference between FTM-2 and WKI chamber test values on matched reconstituted wood panel boards described in this study. Linear regression analysis performed on matched sample test observations project WKI values to be ~20% lower than FTM-2 values.

3. Similar formaldehyde levels were observed for the chromotropic acid and the pararosaniline analytical techniques when large-chamber tests were conducted.

4. The small-scale emission tests used in North America and Europe correlate well with their respective chamber measurements. (A knowledge of the relationships between small-scale tests and large-chamber tests is important for routine product acceptance testing and quality control.)

5. These product test results and the relationships between the various small-scale and large-scale formaldehyde tests confirm the similarity between lower formaldehyde emitting North American and European boards reported by other observers.

Registry No. Formaldehyde, 50-00-0.

Literature Cited

- (1) Hanetho, P. *Proc. Wash. State Univ. Int. Symp. Particleboard*, 12th 1978, 275-286.
- (2) Lehmann, W. *Proc. Wash. State Univ. Int. Symp. Particleboard*, 16th 1982, 35-44.
- (3) Marutsky, R.; Mehlhorn, L.; Roffael, E.; Flentge, A. *Holz Roh-Werkst.* 1988, 46, 253-258.
- (4) Myers, G. *For. Prod. J.* 1983, 33(5), 27-37.
- (5) Newton, L. *Proc. Wash. State Univ. Int. Symp. Particleboard*, 16th 1982, 45-61.
- (6) Sundin, B. *Proc. Wash. Univ. Int. Symp. Particleboard*, 12th 1978, 251-273.

- (7) Zinn, T.; Garrison, S. *Proc. Wash. State Univ. Int. Particleboard/Compos. Mater. Ser.*, 17th, 1983, 203-218.
- (8) Singh, J.; Walcott, R.; St. Pierre, C.; Ferrel, T.; Garrison, S.; Gramp, G.; Groah, W. Evaluation of the Relationship Between Formaldehyde Emissions from Particleboard Mobile Home Decking and Hardwood Plywood Wall Paneling in Experimental Mobile Homes. Prepared for the U.S. Dept. of Housing and Urban Development, 1982.
- (9) *Test methods for wood products* (Prüfverfahren für Holzwerkstoffe); Federal Health Agency, Federal Republic of Germany, 1989; Vol. 32, No. 6.
- (10) Manufactured Home Construction and Safety Standards, Final Rule. U.S. Dept. of Housing and Urban Development. *Fed. Regist.* 1984, 49(155), 32011-32013.
- (11) Large Scale Test Method for Determining Formaldehyde Emissions from Wood Products, Large Chamber Method, FTM 2-1985. National Particleboard Association and Hardwood Plywood Manufacturers Association, 1985.
- (12) Zinn, T. National Particleboard Association, personal communication to Greg Schweer of the U.S. Environmental Protection Agency, 1988.
- (13) Report of Preliminary Interlaboratory Formaldehyde Large Chamber Round Robin. Hardwood Plywood Manufacturers Association and National Particleboard Association, 1987.
- (14) Small Scale Test Method for Determining Formaldehyde Emissions from Wood Products, Two Hour Desiccator Test, FTM 1-1983. National Particleboard Association, Hardwood Plywood Manufacturers Association and Formaldehyde Institute, 1983.
- (15) Wood Based Panels—Determination of Formaldehyde Content Extraction Method Called the Perforator Method (draft). CEN/TC 112/WG5; February 20, 1989.
- (16) Particleboard—Determination of Formaldehyde Content—Extraction Method Called the Perforator Method. European standard test EN 120; October 1984.
- (17) Sundin, B. *Proc. Wash. State Univ. Int. Particleboard/Compos. Mater. Symp.*, 19th 1985, 255-275.
- (18) Berge, A.; Mellegard, B.; Hanetho, P.; Ormstad, E. *Holz Roh-Werkst.* 1980, 38, 251-255.
- (19) Groah, W.; Gramp, G.; Garrison, S.; Walcott, R. *For. Prod. J.* 1985, 35(2), 11-18.
- (20) Lehmann, W. *For. Prod. J.* 1987, 37(4), 31-37.
- (21) Myers, G. *For. Prod. J.* 1984, 34(10), 59-68.
- (22) Myers, G. *For. Prod. J.* 1985, 35(9), 20-31.
- (23) Matthews, T.; Hawthorne, A.; Daffron, C.; Reed, T.; Corey, M. *Proc. Wash. State Univ. Int. Particleboard/Compos. Mater. Ser.*, 17th, 1983, 179-202.
- (24) Grot, R.; Habringer, S.; Silberstein, S. Formaldehyde Emissions from Low Emitting Pressed-Wood Products and the Effectiveness of Various Remedial Measures for Reducing Formaldehyde Emissions. National Institute of Standards and Technology, 1988.

Received for review March 13, 1990. Revised manuscript received July 30, 1990. Accepted August 3, 1990. This study was sponsored by the National Particleboard Association Technical Committee.

Technique for Removing Water from Moist Headspace and Purge Gases Containing Volatile Organic Compounds. Application in the Purge with Whole-Column Cryotrapping (P/WCC) Method

James F. Pankow

Department of Environmental Science and Engineering, Oregon Graduate Institute, 19600 N.W. Von Neumann Drive, Beaverton, Oregon 97006

■ Volatile organic compounds (VOCs) are easily removed from water by use of an inert purge gas. VOCs are therefore easily determined by the purge with whole-column cryotrapping (P/WCC) method. In P/WCC, purging takes place directly from a sample to a capillary gas chromatography (GC) column while the latter is maintained at a cryotrapping temperature. Water vapor is purged to the column along with the analytes. The water can cause variability problems with the GC retention times and responses. A water trap technique is described that reduces the amount of water in VOC-containing gas streams. The technique involves passing most of the purge gas stream through a short column of glass beads at -10°C . Analytes collected in the trap are quantitatively transferred to the GC column in a final short purge of the trap carried out at ambient temperature. Desiccation efficiencies of 90% can be obtained without any loss of analytes.

Introduction

When gas chromatography (GC) is used to analyze water, soil, and sediment samples for volatile organic compounds (VOCs), it is common to include a step that separates the analytes from the relatively large amounts of water that are also usually present. Headspace and dynamic purging based methods rely on the volatility of VOCs to create a gas phase in which there is enrichment in the VOC/water ratio relative to the sample. The EPA purge and trap (P&T) method for water samples (1) provides for additional water removal during a selective collection of VOC analytes on a sorbent trap that is later thermally desorbed to the column. A disadvantage of this approach is that portions of very volatile analytes (e.g., methyl chloride) may break through the trap and be lost.

In order to eliminate losses of very volatile analytes, the purge with whole-column cryotrapping (P/WCC) method (2, 3) does not carry out intermediate sorbent trapping, but rather provides for the *direct* passage of purge gas flow onto the column. If the column is maintained at -90°C during the purge step, then compounds even as volatile as methyl chloride can be trapped in a narrow band, and virtually all of the EPA purgeable priority pollutants can be resolved on a 30 m long, 0.32 or 0.53 mm i.d. fused-silica capillary column of the DB-624 type. If the compounds of interest are less volatile than methyl chloride, then WCC temperatures warmer than -90°C can be used. When the volumes of purge gas are low (e.g., 20 mL or less), then when the purge vessel is at 20°C , P/WCC transfers less than 0.4 μL of condensed water to the column (3).

Disadvantages of too much water (e.g., more than 1 μL) on the column include peak splitting as well as variabilities in the retention times and responses of compounds that elute near the boiling point of water. GC detectors that can be adversely affected by too much water include the electron capture detector and the mass spectrometer.

One technique that can be used to reduce water transfer to the column during P/WCC involves a flow-through

dryer constructed from Nafion tubing (4). The highly polar nature of the permeable Nafion allows water to diffuse out of the purge gas stream, but retains the majority of the nonpolar analytes in the stream. While simple, a Nafion dryer may not allow for the quantitative transfer of VOCs and can also lead to certain memory effects in the method (5).

In order to facilitate the use of P/WCC with GC/MS, and to provide an alternative to the Nafion approach, this paper describes a simple water trap that avoids memory effects as well as the losses of analytes that may occur in P&T and in P/WCC with a Nafion dryer. The trap makes use of the fact that the vapor pressure of water decreases significantly as temperature decreases. The trap (Figure 1) incorporates a short column packed with glass beads that can be maintained at a temperature such as -10°C during the bulk of the purge step. Extremely volatile analytes will pass through the trap where they can be focused on the column at WCC temperatures such as -90°C . A portion of the less volatile analytes and the bulk of the water will be collected on the trap. If the trap is warmed to $\sim 20^{\circ}\text{C}$ for the final 30–60 s of the purge step, essentially 100% of any trapped analytes can be purged from the trap and focused on the column. The small amount of water collected on the trap allows very high purging efficiencies. At the same time, the short duration of the period in which the water trap is warm minimizes the amount of water transferred to the column. The GC temperature program begins at the conclusion of the purge step.

Theory

When a total volume V_{g1} (mL) of gas is bubbled incrementally at temperature T_1 (K) through a sample volume V_{s1} (mL), a volatile analyte can be purged no faster than (6)

$$c_1/c_{1,0} = \exp[-(H/RT_1)V_{g1}/V_{s1}] \quad (1)$$

where $c_{1,0}$ is the initial concentration of the analyte in the sample, c_1 is the concentration remaining after passage of V_{g1} , H (atm $\cdot\text{m}^3/\text{mol}$) is the Henry's law constant of the analyte at T_1 , and R is the gas constant (8.2×10^{-5} m $^3\cdot\text{atm}/\text{mol}\cdot\text{K}$). If F (mL/min) is the flow rate at T_1 and the total pressure in the purge vessel, and t_1 (min) is the duration of the overall purge step, then $V_{g1} = Ft_1$. Table I summarizes the nomenclature.

The maximum possible fractional efficiency e_{p1} ($0 \leq e_{p1} < 1$) of the sample purging is given by

$$e_{p1} = (1 - c_1/c_{1,0}) \quad (2)$$

The value of e_{p1} will tend to approach 1.0 as H and V_{g1}/V_{s1} increase. Equation 1 gives the maximum purging rate and eq 2 gives an upper estimate of e_{p1} because bubbles with a finite lifetime in the purge vessel will never be able to become fully equilibrated with the liquid. However, available evidence for typical purging conditions suggests that eqs 1 and 2 provide very good approximations for all

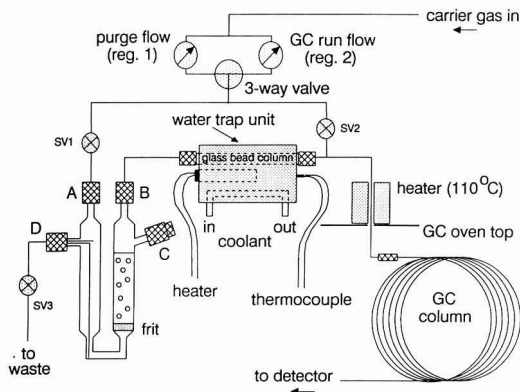


Figure 1. Schematic diagram of the apparatus used in P/WCC with incorporation of a water trap. Swagelok fittings are marked with cross-hatching.

Table I. Nomenclature

$c_{1,0}$	initial concentration of analyte in sample
c_1	concentration of analyte remaining in sample after passage of V_{g1}
$c_{2,0}$	concentration of analyte in trap at beginning of purging of warmed trap
c_2	concentration of analyte remaining in trap after passage of V_{g2}
e_{p1}	maximum possible fractional efficiency of the sample purging
e_{p2}	fractional efficiency of the purging of analytes in the water trap
E_{des}	desiccation efficiency (%) of the trap
$E_{overall}$	overall efficiency (%) for purging of analytes from a sample to the GC column
F	flow rate (mL/min) at T_1 and the total pressure in the purge vessel
H	Henry's law constant (atm·m ³ /mol) for the analyte at T_1
H_{water}	Henry's law constant (atm·m ³ /mol) for water at T_1 (4.2×10^{-7} atm·m ³ /mol at 20 °C and 1 atm total pressure)
p_1	vapor pressure (atm) of liquid water at the temperature of the warmed trap [0.0231 atm at $T_1 = 293$ K (20 °C)]
p_2	vapor pressure (atm) over ice at the trapping temperature [0.00257 atm at $T_2 = 263$ K (-10 °C)]
R	gas constant (8.2×10^{-5} m ³ ·atm/mol·K)
t_1	time (min) duration of the overall purge step
t_2	time (min) duration of purging of the warm trap
$t_1 - t_2$	time (min) duration that the trap is cold
T_1	temperature (K) in the purge vessel and in the warm trap
T_2	temperature (K) in the cold trap
V_{g1}	volume (mL) of gas bubbled at temperature T_1 (K) through sample (Ft_1)
V_{g2}	volume (mL) of gas passed at temperature T_1 (K) through warm water trap (Ft_2)
V_{s1}	volume (mL) of sample
V_{s2}	volume (mL) of liquid water in the trap
\bar{V}	molar volume (mL) of liquid water at T_1 (18 mL/mol)
W_{act}	volume of water that actually reaches the column
W_{pot}	volume of water that could have reached the column for a direct P/WCC purge at T_1 lasting t_1 minutes
$V_{w,co1}$	volume (μ L) of water actually transferred to the column

of the purgeable priority pollutants under typical purging conditions (3).

Let us assume that all of whatever analyte purged from a water sample according to eqs 1 and 2 is retained in a cold-zone water trap at temperature T_2 . If the trap is warmed rapidly from T_2 to T_1 , the continuing flow of purge gas from the purge vessel will begin to effect a repurging, and the trapped analyte will continue onto the column. If the total volume of gas purging the warmed trap is V_{g2} (mL) and if the volume of trapped liquid water is V_{s2} (mL),

then assuming that the purge gas leaving the purge vessel at this stage is essentially free of analyte leads to

$$c_2/c_{2,0} = \exp[-(H/RT_1)V_{g2}/V_{s2}] \quad (3)$$

and

$$e_{p2} = (1 - c_2/c_{2,0}) \quad (4)$$

where $c_{2,0}$ is the concentration of the analyte in V_{s2} at the beginning of purging of the warmed trap. If t_2 (min) is the time during which the warmed trap is purged, then $V_{g2} = Ft_2$. Since we have taken T_1 to describe the temperature of both purge steps, for any given analyte, the same value of H will describe both purge steps. Equations 3 and 4 assume a uniform liquid concentration in the warmed trap. Modeling the purging of the condensed water in this manner is reasonable since all of the water in the trap is likely to be condensed within a few millimeters, and the chromatographic efficiency of the packed bed in the trap is likely to correspond to a theoretical equilibrium plate height of at least 2 mm.

By application of the ideal gas law

$$V_{s2} = \frac{\bar{V}(t_1 - t_2)F(p_1 - p_2)}{10^6 RT_1} \quad (5)$$

where \bar{V} is the molar volume of liquid water (18 mL/mol), t_1 (min) is the duration of the overall purging, t_2 (min) is the length of time during which the trap is warm, $(t_1 - t_2)$ is the duration of time that the trap is cold, p_1 (atm) is the vapor pressure of liquid water at the temperature of the warmed trap [0.0231 atm at $T_1 = 293$ K (20 °C)], and p_2 is the vapor pressure over ice at the trapping temperature [0.00257 atm at $T_2 = 263$ K (-10 °C)]. The volume of water $V_{w,co1}$ (μ L) actually transferred to the column is given by

$$V_{w,co1} (\mu\text{L}) = \frac{\bar{V}F}{10^3 RT_1} [p_2(t_1 - t_2) + p_1 t_2] \quad (6)$$

Reducing T_2 will not allow $V_{w,co1}$ to be reduced below the limit given by eq 6 with $p_2 = 0$.

The desiccation efficiency of the trap is given by

$$E_{des} = (1 - W_{act}/W_{pot}) \times 100\% \quad (7)$$

where W_{act} is the amount of water that actually reaches the column, and W_{pot} is the amount that could have potentially reached the column for a direct P/WCC purge at T_1 lasting t_1 minutes. Therefore

$$E_{des} = \left[1 - \frac{p_2(t_1 - t_2) + p_1 t_2}{t_1 p_1} \right] \times 100\% \quad (8)$$

Although $V_{w,co1}$ will increase as t_1 increases, since $p_1 > p_2$, E_{des} will also increase. Figure 2 illustrates this behavior as a function of t_1 for $t_2 = 0.5$ min, $T_1 = 293$ K, and $T_2 = 263$ K. When $t_1 \gg t_2$, E_{des} approaches the asymptotic limit

$$E_{des} \approx (1 - p_2/p_1) \times 100\% \quad (9)$$

For $T_1 = 293$ K and $T_2 = 263$ K, this limit is 89% (Figure 2). Equations 5–8 all allow for the fact that the purge flow rate depends on the temperature, being equal to F at T_1 , and FT_2/T_1 at T_2 .

With a cold-zone water trap, the overall efficiency of P/WCC in transferring analytes from a sample to the GC column will be given by

$$E_{overall} \approx (e_{p1}e_{p2}) \times 100\% \quad (10)$$

Equation 10 is only an approximation. First, we assumed above that all of the analyte removed from the purge vessel is collected in the water trap. In fact, some will pass

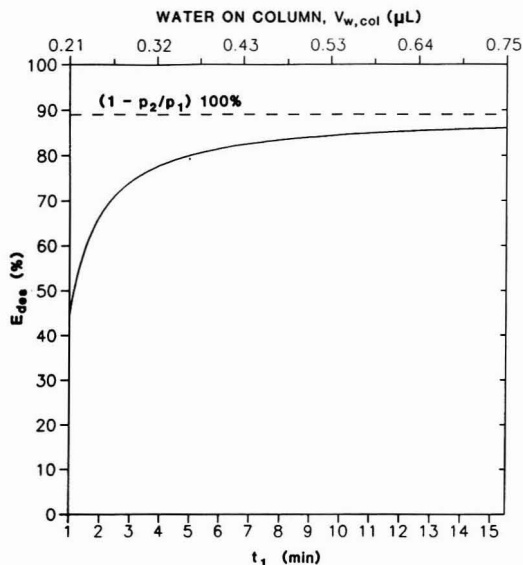


Figure 2. E_{des} as a function of t_1 for $t_2 = 0.5$ min, $F = 20$ mL/min, $T_1 = 293$ K, and $T_2 = 263$ K. When $t_1 \gg t_2$, E_{des} approaches the asymptotic limit $(1 - p_2/p_1) \times 100\%$. For the conditions of this figure, this limit equals 89%.

untrapped onto the column. This will tend to make e_{p2} underestimate the transfer efficiency of the region downstream of the purge vessel and make eq 10 underestimate $E_{overall}$. Second, we know that eq 3 assumes that the purge gas flowing through the warmed water trap is free of analyte. In actuality, that gas will always continue to remove some portion of analyte from the purge vessel. This second assumption will tend to cause eqs 3 and 4 to overestimate e_{p2} . However, this tendency will only be very slight as long as H for the analyte is significantly greater than the H for water itself. Indeed, even if all of the water in the purge gas is condensed into V_{g2} , all analytes that satisfy this criterion will exert a partial pressure that is much higher than that from the original sample, and so the purge gas for V_{g2} will in fact be *relatively* low in analyte. With $H_{water} = 4.2 \times 10^{-7}$ atm·m³/mol at 20 °C and 1 atm total pressure, all of the purgeable priority pollutants are characterized by H values that are much larger than this value (see Table I in ref 3).

On the basis of the above discussion, we conclude that eq 10 will provide a lower bound on $E_{overall}$ for volatile organic compounds. Importantly, for the types of conditions used with P/WCC, e_{p2} will almost always be extremely close to 1.0. For example, for $F = 20$ mL/min, $t_1 = 15$ min, $t_2 = 0.5$ min, $T_1 = 293$ K, and $T_2 = 263$ K, then eq 5 gives V_{s2} as only 0.0046 mL. Thus, even when H is extremely small, say 2×10^{-5} atm·m³/mol, eq 4 gives $e_{p2} = 0.97$. We conclude that eq 10 will provide a very good estimate of $E_{overall}$ in P/WCC, and moreover, that to a very good approximation we will usually have

$$E_{overall} \approx e_{p1} \times 100\% \quad (11)$$

Figures 3–5 give $E_{overall}$ vs t_1 calculated according to eq 10 with V_{s1} ranging from 2 to 10 mL, and for the same values of F , t_2 , T_1 , and T_2 discussed in the preceding paragraph. In all cases, the bottom x axes begin at $t_1 = 1$ min, since in P/WCC it seems likely that ~0.5 min represents (1) a lower bound for useful values of the period during which the water trap is cold ($t_1 - t_2$) and (2) a value for t_2 that can provide $e_{p2} \approx 1$ while still keeping $V_{w,col}$

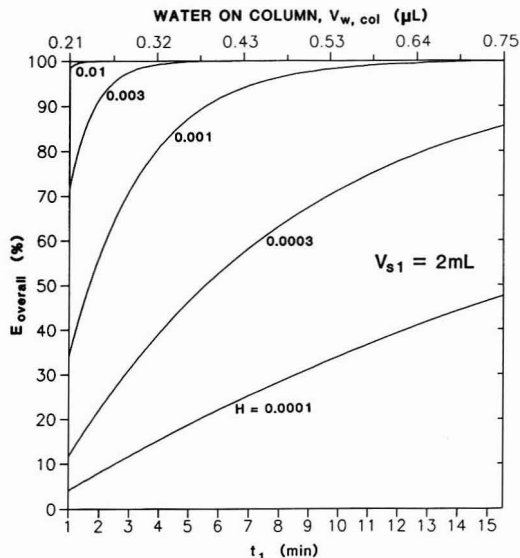


Figure 3. $E_{overall}$ as a function of t_1 for $V_{s1} = 2$ mL, $F = 20$ mL/min at T_1 , $t_2 = 0.5$ min, $F = 20$ mL/min, $T_1 = 293$ K, and $T_2 = 263$ K.

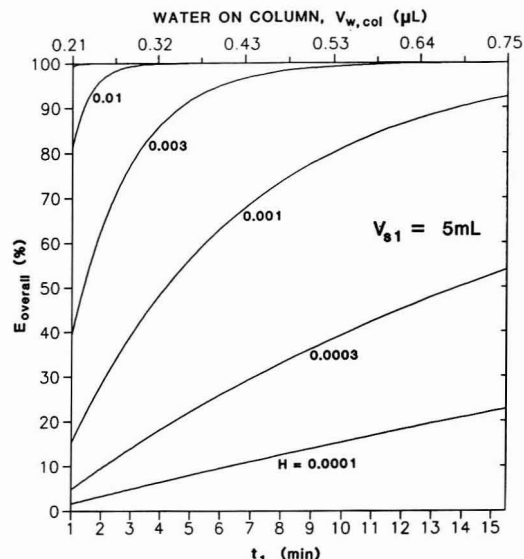


Figure 4. $E_{overall}$ as a function of t_1 for $V_{s1} = 5$ mL. Other conditions as in Figure 3.

small. Assuming $t_2 = 0.5$ min, the top x axes give $V_{w,col}$ as it depends on t_1 . When t_1 is small, a large fraction of $V_{w,col}$ is transferred to the column during the short t_2 time period. As a result, $V_{w,col}$ increases only slowly as t_1 increases upward from $t_1 \sim 2$ min.

H values for VOCs range from 0.2 atm·m³/mol for methyl bromide to 0.0001 atm·m³/mol for the chlorinated ethers (3). At $T_1 = 293$ K, and with $V_{s1} = 2$ mL, Figure 3 shows that $E_{overall}$ values approaching 30% are easily obtained even for H as small as 0.0001 atm·m³/mol. Figure 5 indicates that most VOCs of interest can be purged efficiently with $V_{w,col}$ values of <0.5 μ L even when $V_{s1} = 10$ mL. By comparison, assuming standard P&T values of 440 mL for V_{g1} and 5 mL for V_{s1} , eqs 1 and 2 indicate that conventional P&T with an 11-min purge will yield a

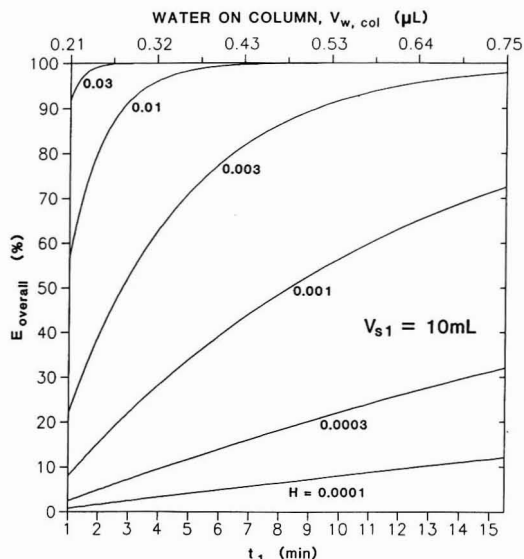


Figure 5. E_{overall} as a function of t_1 for $V_{s1} = 10$ mL. Other conditions as in Figure 3.

purging efficiency of 31% for $H = 0.0001$ atm·m³/mol.

Experimental Section

The P/WCC system in Figure 1 is a modified version of one described elsewhere (3). The differences involve (1) use of the water trap, (2) placement of the waste port (D) on the side of the purge vessel, and (3) addition of both a $1/16$ in. o.d. drain line and a $1/16$ in. stainless steel (SS) o.d. flush line through port D. Modification 2 prevents the portion of sample that might seep through the frit prior to the purge step from becoming isolated from the purge gas. Modification 3 allows the purge vessel to be both drained and flushed when pressurized.

The glass bead column inside the aluminum block water trap unit was constructed with a 6.5 cm long piece of $1/8$ in. o.d., 0.085 in. i.d. SS tubing. The 0.45–0.50-mm beads were held in place by a small amount of glass wool on each end. The $1/8$ -in. tube was connected to the $1/16$ -in. SS gas lines with Swagelok reducing unions. The aluminum block was wrapped with a small amount of fiberglass insulation to help it achieve -10 °C during the initial portion of the purge step. During that portion, liquid coolant (water containing 30% ethanol) at -10 °C was circulated through the block. To prevent the fittings on the glass bead column from becoming isolated cold spots, a small fan was aimed at the block at all times. When the 100-W cartridge heater in the block was activated to achieve ~ 20 °C during the t_2 (1 min) portion of the purge step, coolant flow to the block was halted, and any coolant remaining in the line was blown out by using a compressed air line connected to the upstream side of the coolant line through a snap valve. (As an convenient alternative to the water/ethanol mixture, cold nitrogen gas from a liquid nitrogen dewar could be used as the coolant.) For all analyses, the value of t_1 used was 7 min.

To achieve a purge flow F of 20 mL/min, a pressure of 30 psi was set on the purge flow gas regulator. During all phases of the purge step, SV1 was open, SV2 was closed, and the column was maintained at a WCC temperature of -90 °C. At the conclusion of each purge, SV2 was opened to provide carrier gas at the GC run pressure (5 psi). The GC temperature program used was ballistic to -30 °C

and then at 10 °C/min to 215 °C. Data acquisition was begun at -30 °C. The column used was a 30 m long, 0.32 mm i.d. DB-624 (1.8- μ m film thickness) fused-silica column from J&W Scientific (Folsom, CA). As described elsewhere (3), the inlet of the column was fitted with an "ice trap" and the exit end was interfaced to a Finnigan 4000 GC/MS equipped with conventional diffusion pumps. At the conclusion of each GC run, the three-way valve was rotated to select the purge pressure again, SV3 was opened, and the trap block was heated to 100 °C for 2 min. This provided a back-flush cleaning of the trap as well as a draining and flushing of the purge vessel through the two $1/16$ in. o.d. lines inserted through port D. As with the P&T method, P/WCC with the water trap can be automated through the use of two multipoint gas valves.

Results and Discussion

The water trap described above was tested by analyzing a 4 μ g/L standard solution containing three VOC internal standard (IS) compounds: 1,2-dichloro-1,1-difluoroethane (IS1), 2-bromo-1-chloropropane (IS2), and ethylbenzene- d_5 (IS3). IS1–IS3 eluted at 38, 93, and 110 °C, respectively, i.e., before, during, and after the elution of the water transferred to the column. A total of 34 replicate standards were run over several days without the water trap. Another 34 replicates were then run over several days with the water trap. Use of the water trap reduced $V_{w,col}$ to ~ 0.4 μ L.

For each analysis, the GC/MS areas for IS1 and IS2 were normalized to the area for IS3 (IS3 would be expected to be least affected by the eluting water). Without the water trap, the relative standard deviations (CVs) for the normalized areas for IS1 and IS2 were 17.0 and 49.3%, respectively. With the water trap, the two CVs were reduced substantially to just 11.1 and 11.8%, respectively. The retention times of the compounds also became much more reproducible. Without the water trap, the absolute retention time window for IS2 was 740 ± 30 s; with the water trap, the variation was reduced to only ± 2 s. The reduction of $V_{w,col}$ to ~ 0.4 μ L achieved with the water trap thus provided large improvements in response and retention time reproducibility. Therefore, use of the water trap allows the P/WCC method to be used very effectively with large purge gas volumes.

Acknowledgments

The assistance of Lorne M. Isabelle, Bruce A. Tiffany, and John M. E. Storey in a portion of this work is gratefully acknowledged.

Literature Cited

- U.S. EPA Test Methods for Organic Chemical Analysis of Municipal and Industrial Wastewater; EPA-600/4-82-057; Longbottom, J. E., Lichtenberg, J. J., Eds.; U.S. EPA: Washington, DC, 1982.
- Pankow, J. F. *HRC&CC, J. High Resolut. Chromatogr. Chromatogr. Commun.* 1987, 10, 409–410.
- Pankow, J. F.; Rosen, M. E. *Environ. Sci. Technol.* 1988, 22, 398–405.
- Cochran, J. W. *HRC&CC, J. High Resolut. Chromatogr. Chromatogr. Commun.* 1988, 11, 663–665.
- Rosen, M. E. Ph.D. Thesis, Oregon Graduate Center, Beaverton, OR, 1988.
- Pankow, J. F. *Anal. Chem.* 1986, 58, 1822–1826.

Received for review December 1, 1989. Revised manuscript received July 11, 1990. Accepted July 25, 1990. This work was made possible with federal funds from the U.S. Geological Survey (USGS) under Grant 14-08-0001-G1135. The contents do not necessarily reflect the views or policies of USGS, nor does mention of trade names constitute endorsement for use.

Solubilization of Polycyclic Aromatic Hydrocarbons in Micellar Nonionic Surfactant Solutions

David. A. Edwards, Richard G. Luthy,* and Zhongbao Liu

Department of Civil Engineering, Carnegie Mellon University, Pittsburgh, Pennsylvania 15213

■ Experimental data are presented on the enhanced apparent solubilities of naphthalene, phenanthrene, and pyrene resulting from solubilization in aqueous solutions of four commercial, nonionic surfactants: an alkyl polyoxyethylene (POE) type, two octylphenol POE types, and a nonylphenol POE type. Apparent solubilities of the polycyclic aromatic hydrocarbon (PAH) compounds in surfactant solutions were determined by radiolabeled techniques. Solubilization of each PAH compound commenced at the surfactant critical micelle concentration and was proportional to the concentration of surfactant in micelle form. The partitioning of organic compounds between surfactant micelles and aqueous solution is characterized by a mole fraction micelle-phase/aqueous-phase partition coefficient, K_m . Values of $\log K_m$ for PAH compounds in surfactant solutions of this study range from 4.57 to 6.53. $\log K_m$ appears to be a linear function of $\log K_{ow}$ for a given surfactant solution. A knowledge of partitioning in aqueous surfactant systems is a prerequisite to understanding mechanisms affecting the behavior of hydrophobic organic compounds in soil-water systems in which surfactants play a role in contaminant remediation or facilitated transport.

Introduction

Contamination of soil by toxic and/or hazardous organic pollutants is an environmental concern. Hydrophobic organic compounds, such as polycyclic aromatic hydrocarbons (PAHs), are of special interest because they are strongly sorbed to soil or sediments (1, 2). As a consequence, remediation of hydrophobic organic contamination in soil-water systems is often dependent on desorption of the contaminant from the soil surface and subsequent incorporation of the pollutant into the bulk aqueous phase. Once in the bulk aqueous phase, engineered treatment systems may be used to effect remediation. Surfactants may be beneficial for use in soil-washing or soil-flushing pump-and-treat technologies by assisting solubilization of sorbed hydrophobic contaminants (3-5). Surfactants may also impact microbial remediation of hydrophobic organic contaminants in soils by affecting the accessibility of the organic compound to microorganisms.

Implementation of surfactant treatment for soil remediation must account for a number of factors, including efficient surfactant recovery and reuse. Other factors that must be considered include the surfactant modification of hydrophobic organic compound soil/water partitioning, clay interactions with surfactant and injection water, and surfactant sorption, biodegradation, and effects on biota. These various issues are not addressed in this paper, the scope being limited to a single process among the many physical, chemical, and biological processes that may take place in the course of successful surfactant remediation of soil.

In addition to the potential benefit that may result from deployment of surfactants in remediation of contaminated soil and sediments, there is also interest in understanding the role of surfactants in facilitating the transport of hydrophobic organic compounds. The immense quantity of surfactants used in industrial and household applications

gives rise to concern for the effects of these compounds in the environment (6). Aggregates of surfactant molecules, or micelles, may act as organic colloids and increase the mobility of contaminants in the subsurface (7).

Presently, there is little understanding of the interaction of surfactants and hydrophobic organic compounds in soil or sediment systems. The purpose of this investigation is to explore the solubilization of PAH in nonionic surfactant solutions in order to determine mole fraction micelle-phase/aqueous-phase partition coefficients. These data can then be coupled with additional information from PAH solubilization experiments in soil-water systems in order to allow prediction of PAH compound partitioning between water, surfactant micelles, and soil.

Surfactant Monomers and Micelles

A surfactant molecule is amphiphilic, having two distinct structural moieties, one polar and the other nonpolar. The polar moiety of the molecule has an affinity for water and other polar substances, while the nonpolar moiety is hydrophobic. As a result of its amphiphilic nature, a surfactant molecule may dissolve in water as a monomer, adsorb at an interface, or be incorporated with other surfactant molecules as part of a micelle. At surfactant concentrations less than a compound-specific threshold value, surfactant molecules exist predominantly in monomeric form, with some fraction being adsorbed at system interfaces.

The surfactant concentration at which monomers begin to assemble in ordered, colloidal aggregates is termed the critical micelle concentration (CMC). The CMC represents a narrow concentration range over which the partial derivatives with respect to surfactant concentration of many solution properties, e.g., surface tension, display abrupt changes in value (8). In micelle-forming solutions, the CMC approximates monomeric solubility. At surfactant concentrations greater than the CMC, additional surfactant is incorporated into the bulk solution through micelle formation (9). The average number of surfactant molecules in a micelle is called the aggregation number.

Nonpolar surfactant moieties spontaneously associate with each other in the process of micellization to form organized, dynamic chemical structures having such geometrical configurations as spheres, oblate spheroids, or prolate spheroids (10). The hydrophobic portion of each molecule in the micelle is directed inward, toward the center of the aggregate, forming with the other hydrophobic moieties a liquid core, which has a fairly smooth boundary with the outlying hydrophilic chains and polar solvent (11, 12). The central region of the micelle thus constitutes a hydrophobic pseudophase that is distinct in its properties from the polar solvent (13). The hydrophilic portion of a micellar molecule of a nonionic surfactant, the type used in this study, is a hydrated, oxygen-containing chain directed outward toward the solvent (8). The surfactant concentration at which micelle formation starts is a function of surfactant chemistry, temperature, ionic strength, and the presence and type of organic additives (8). CMC values for a number of surfactant solutions at different temperatures are tabulated in the compilation

Solubilization of Polycyclic Aromatic Hydrocarbons

The apparent solubility of otherwise slightly soluble hydrophobic organic compounds may be dramatically enhanced in solutions of surfactants at concentrations greater than the CMC. The hydrophobic core of each micelle can accommodate a certain amount of lipophilic organic compound as a solubilize (8). The amount of organic compound that is solubilized depends on surfactant structure, aggregation number, micelle geometry, ionic strength and chemistry, temperature, solubilize chemistry, and solubilize size (15). Solubilization of hydrophobic substances commences at the CMC and in general is a linear function of surfactant concentration over a wide range of surfactant concentrations greater than the CMC (8). With highly hydrophobic compounds, e.g., DDT, a lesser degree of apparent solubility enhancement may also occur in monomeric solution (6). Surfactant solubilization results in an isotropic colloidal solution, which is stable in the sense that it has the lowest possible sum of free energies of its components (15).

Polycyclic aromatic hydrocarbons are examples of hydrophobic compounds that may be solubilized by surfactants. As early as 1934, researchers began experimenting with surfactants to enhance the apparent solubility of PAH compounds (16). An example of work regarding surfactant solubilization of PAH is that of Klevens (17), who reported solubilization of benzene and 12 different PAH compounds in potassium laurate solution.

PAH Partitioning between Micellar and Aqueous Pseudophases

A measure of the effectiveness of a particular surfactant in solubilizing a given solubilize is known as the molar solubilization ratio (MSR). The molar solubilization ratio is defined as the number of moles of organic compound solubilized per mole of surfactant added to solution (15). The increase in solubilize concentration per unit increase in micellar surfactant concentration is equivalent to the MSR. In the presence of excess hydrophobic organic compound, the MSR may be obtained from the slope of the curve that results when the solubilize concentration is plotted against surfactant concentration. The MSR for solubilization of PAH compounds may be calculated as follows:

$$\text{MSR} = (S_{\text{PAH,mic}} - S_{\text{PAH,cmc}}) / (C_{\text{surf}} - \text{CMC}) \quad (1)$$

where $S_{\text{PAH,cmc}}$ is the apparent solubility of a PAH compound in moles per liter at the CMC; $S_{\text{PAH,mic}}$ is the total apparent solubility of the PAH compound in moles per liter in micellar solution at a particular surfactant concentration greater than the CMC; and C_{surf} is the surfactant concentration at which $S_{\text{PAH,mic}}$ is evaluated.

An alternative approach in quantifying surfactant solubilization consists of characterizing the partitioning of the organic compound between micelles and monomeric solution with a mole fraction micelle-phase/aqueous-phase partition coefficient. The micelle-phase/aqueous-phase partition coefficient, K_m , is the ratio of the mole fraction of the compound in the micellar pseudophase, X_m , to the mole fraction of the compound in the aqueous pseudophase, X_a (18). The value of K_m is dependent on surfactant chemistry, solubilize chemistry, and temperature. K_m may be calculated from experimental measurements by using the following formula:

$$K_m = X_m / X_a \quad (2)$$

Table I. Nonionic Surfactants Employed in This Study

surfactant	symbol	av mol formula	av MW
Brij 30	C ₁₂ E ₄	C ₁₂ H ₂₆ O(CH ₂ CH ₂ O) ₄ H	363
Igepal CA-720	C ₈ PE ₁₂	C ₈ H ₁₇ C ₆ H ₄ O(CH ₂ CH ₂ O) ₁₂ H	735
Tergitol NP-10	C ₉ PE _{10.5}	C ₉ H ₁₉ C ₆ H ₄ O(CH ₂ CH ₂ O) _{10.5} H	683
Triton X-100	C ₈ PE _{9.5}	C ₈ H ₁₇ C ₆ H ₄ O(CH ₂ CH ₂ O) _{9.5} H	625

The mole fraction of PAH compound in the micellar pseudophase, X_m , may be calculated as

$$X_m = (S_{\text{PAH,mic}} - S_{\text{PAH,cmc}}) / (C_{\text{surf}} - \text{CMC} + S_{\text{PAH,mic}} - S_{\text{PAH,cmc}}) \quad (3)$$

or, in terms of the MSR, as

$$X_m = \text{MSR} / (1 + \text{MSR}) \quad (4)$$

The mole fraction of PAH in the aqueous pseudophase, X_a , is approximated for dilute solutions by

$$X_a = S_{\text{PAH,cmc}} V_w \quad (5)$$

where V_w is the molar volume of water, e.g., 0.01805 L/mol at 25 °C. An expression for K_m is thus

$$K_m = (S_{\text{PAH,mic}} - S_{\text{PAH,cmc}}) / [(C_{\text{surf}} - \text{CMC} + S_{\text{PAH,mic}} - S_{\text{PAH,cmc}})(S_{\text{PAH,cmc}} V_w)] \quad (6)$$

This paper presents experimental observations for batch-test surfactant solubilization of PAH using 12 surfactant-PAH combinations in aqueous solution. K_m values are derived for each combination from the data. The PAH compounds of this study consist of a two-ring compound, naphthalene; a three-ring compound, phenanthrene; and a four-ring compound, pyrene. The surfactants of this study are all polyoxyethylene (POE) nonionic compounds. Nonionic surfactants chosen for batch tests include one alkyl POE type, two octylphenol POE types, and one nonylphenol POE type. Together, these three groups represent more than 70% of the 1.72 billion pounds of U.S. nonionic surfactant production in 1986 (19). Nonionic surfactants may have specific advantages compared to anionic or cationic surfactants in regard to certain aspects of engineered remediation of contaminated soils because of differences in surfactant charge, CMC range, toxicity, and biodegradability. The selection of the surfactants employed in this investigation was guided by prior experimentation dealing with solubilization of PAH compounds in soil/water suspensions (20).

Experimental Procedures

The surfactants employed in batch tests of this study are described in Table I. The surfactants were used as received from supplier or distributor without further purification. It is assumed that the number distribution of oxyethylene groups per molecule of each type of surfactant was heterogeneous since this is the case with nearly all commercially available nonionic surfactants (14). The PAH compounds of this study had purities greater than 98% and were obtained from Aldrich Chemical Co. The formulas and selected properties of the PAH compounds are listed in Table II. ¹⁴C-labeled PAH compounds were acquired from Amersham Corp. with specific activity values of 4.5 mCi/mmol for naphthalene, 11.3 mCi/mmol for phenanthrene, and 56 mCi/mmol for pyrene.

Batch tests for solubilization of PAH in surfactant solution were performed at 25 °C for 12 distinct systems, with each system comprising one of the four surfactants of Table I and one of the three PAH compounds of Table II. Each surfactant-PAH system involved 8–10 batch tests with surfactant solutions having a range of concentrations above and below the CMC. Replicate measurements were performed for each test. An individual batch test sample

Table II. Formulas and Properties of Polycyclic Aromatic Hydrocarbons of This Study

compd	mol formula	MW	solubility, ^a mol/L	log K_{ow} ^b
naphthalene	C ₁₀ H ₈	128	2.5×10^{-4}	3.36
phenanthrene	C ₁₄ H ₁₀	178	7.2×10^{-6}	4.57
pyrene	C ₁₆ H ₁₀	202	6.8×10^{-7}	5.18

^aSolubilities as reported by Mackay and Shiu (21). ^blog K_{ow} values from Karickhoff et al. (22).

consisted of a 5-mL solution containing deionized water, PAH stock, and surfactant stock, all of which were in a glass vial having a capacity of 8 mL. The vial was sealed with an open-port screw cap, which was fitted with a Teflon-lined septum to prevent loss of PAH from solution.

An individual PAH stock solution consisted of a mixture of a ¹⁴C-labeled PAH compound, nonlabeled PAH compound, and methanol. Each ¹⁴C-labeled PAH compound was supplied as a solid and was extricated from its packaging with either 10 or 20 mL of methanol to prepare a ¹⁴C-labeled solution. The radiolabeled solution was kept refrigerated in a foil-wrapped glass vial equipped with a Teflon-lined septum to protect the PAH in the solution from loss.

The activity of the solution was determined before the experiments were conducted by counting the decay rate of several solution samples in a Beckman LS 500 TD liquid scintillation counter (LSC). A sample was prepared by expressing a measured volume of the solution (e.g., 10 μ L) into a scintillation vial containing 10 mL of Scintiverse II liquid scintillation cocktail obtained from Fisher Scientific. The LSC counted the decay events per minute (DPM) of the radiolabeled PAH by employing the *H*-number quench monitor and compensation technique. The average background decay rate of 40 DPM was subtracted from the measured DPM. The ¹⁴C-labeled solution activity was obtained by dividing the corrected DPM by the solution volume and then converting this value to the equivalent number of moles of PAH per liter of solution by using the conversion factor of 2.22×10^6 DPM/ μ Ci and the specific activity of the radiolabeled PAH compound.

With a knowledge of the radiolabeled solution activity, each PAH stock, consisting of a predetermined mass ratio of radiolabeled to nonlabeled PAH, was prepared in deionized water so as to ensure that the batch-test sample activity would be at least 1–2 orders of magnitude greater than the background decay rate, and that the PAH mass in each batch test would be 20–80 times the PAH mass required to attain aqueous solubility, in order that the progress of solubilization upon addition of surfactant could be observed over a surfactant concentration range several orders of magnitude in value. The mass ratio of total PAH to radiolabeled PAH in each PAH stock was on the order of 10^2 – 10^3 , but varied for the different PAH compounds.

Batch tests for a particular PAH compound and a given surfactant combination employed a duplicate series of 8–10 vials, each consisting of solutions of varying surfactant concentration. Two surfactant stocks, one with a dilution factor of 1000 and the other with a dilution factor of 100, were made up in deionized water for each surfactant. A measured volume of surfactant stock was expressed by syringe into each batch-test vial. The more dilute surfactant stock was used to make the four or five solutions in a given series that were to have the lower surfactant concentrations, and the less dilute stock was used to make the remaining solutions that were to have the higher surfactant concentrations. The volume of surfactant stock to be added was calculated beforehand such that the re-

sultant surfactant concentrations would span a range of several orders of magnitude: e.g., 10^{-5} , 10^{-4} , 10^{-3} , and 10^{-2} M. The appropriate volume of water was added so that after addition of PAH stock, the total solution volume per vial would be 5 mL. A uniform volume of PAH stock prepared as previously described was then added to each vial in the two series.

The prepared sample vials were placed in a water bath at 25 °C and reciprocated at 80 cycles/min for approximately 24 h. Individual sample solutions were then processed in the following manner. Sample solution was withdrawn by syringe and expressed through a Teflon membrane filter of 0.22- μ m pore diameter, and then the solution was discarded, this process being repeated three times consecutively in order to allow sorption saturation of all internal surfaces of the syringe, filter, and needle. This was found in control tests to be necessary so as to prevent experimental artifacts. Duplicate aliquots were then withdrawn from the sample with the same syringe and needle and expressed through the preconditioned filter in order to remove solid-phase PAH and to pass only dissolved PAH in the aqueous pseudophase, and solubilized PAH in the micellar pseudophase, into two prepared scintillation vials. The volume of sample in each aliquot was selected to be either 0.5, 1, or 2 mL, depending on the series of experiments, but within a given series the aliquot volume was uniform. DPM values were then measured in the LSC to at least the 95% confidence level and recorded for subsequent background correction and conversion to PAH concentration units. Background DPM rates were periodically measured in scintillation vials containing scintillation cocktail but no sample.

The influence of methanol, present in each vial at approximately 1% by volume, on CMC value and solubilization effectiveness was evaluated for pyrene, the least soluble of the PAH compounds used in these experiments, and for which the potential influence of methanol would be the most apparent. The tests were performed by adding pyrene stock solution to each vial and allowing the solvent to evaporate to dryness over a period of several hours. After this evaporation step, C₈PE₁₂ stock solution in various predetermined amounts was added to the vials along with sufficient deionized water to bring the total solution volume of each vial to 5 mL. The entire process was then repeated as before, with the exception that the methanol fraction of the added pyrene stock solution was not permitted to evaporate before being mixed with surfactant solution.

Surface tension experiments to evaluate the CMC values of the four commercial surfactants of this study were conducted in a temperature-regulated laboratory at 24–25 °C with a Fisher Tensiomat Model 21 Du Nouy ring tensiometer. Surfactant solutions of varying concentration were made with surfactant stock and deionized water and were allowed to equilibrate for approximately 2 h before measurements were made. All glassware was cleaned with chromic acid solution, and the ring was cleaned with acetone and heated to redness in a gas flame. Multiple testing of each surfactant solution was performed to ensure that consistent readings were obtained, and corrections were made for the dial reading and the ring geometry in order to arrive at surface tension values (23).

Results and Discussion

Approximately 1% methanol was used in each batch test. Methanol was employed as a means of extricating ¹⁴C-labeled PAH compound from its commercial packaging; methanol was also used in the preparation of high-concentration nonlabeled PAH solution, which was mixed

Table III. PAH Solubility and Mole Fraction Micelle-Phase/Aqueous-Phase Partition Coefficients

surfactant	PAH compd	PAH solubility, ^a mol/L		MSR	log K_m
		no surfactant	$C_{surf} = CMC$		
Brij 30	naphthalene	3×10^{-4}	3.4×10^{-4}	3.17×10^{-1}	4.59
	phenanthrene	9×10^{-6}	2.0×10^{-5}	1.52×10^{-1}	5.57
	pyrene	1×10^{-6}	1.1×10^{-6}	7.15×10^{-2}	6.53
Igepal CA-720	naphthalene	3×10^{-4}	3.2×10^{-4}	3.23×10^{-1}	4.63
	phenanthrene	1×10^{-5}	1.1×10^{-5}	1.04×10^{-1}	5.68
	pyrene	8×10^{-7}	2.1×10^{-6}	4.25×10^{-2}	6.01
Tergitol NP-10	naphthalene	3×10^{-4}	4.0×10^{-4}	3.68×10^{-1}	4.57
	phenanthrene	1×10^{-5}	1.5×10^{-5}	1.60×10^{-1}	5.72
	pyrene	8×10^{-7}	1.2×10^{-6}	5.76×10^{-2}	6.41
Triton X-100	naphthalene	3×10^{-4}	3.2×10^{-4}	3.38×10^{-1}	4.64
	phenanthrene	1×10^{-5}	1.3×10^{-5}	1.11×10^{-1}	5.70
	pyrene	1×10^{-6}	1.9×10^{-6}	3.52×10^{-2}	6.03

^a With 1% by volume methanol.

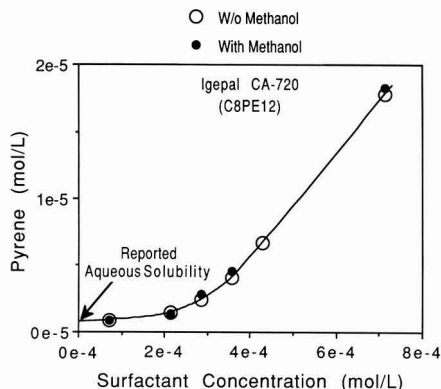


Figure 1. Solubilization of pyrene by C_9PE_{12} nonionic surfactant in the presence and absence of 1% by volume methanol. (Axis notation denotes base 10 exponentiation.)

with the radiolabeled solution to create the PAH stock. This allowed for dosing sufficiently high PAH concentrations such that batch-test solutions would have apparent PAH solubilities 20–80 times in excess of aqueous solubility as needed to measure the progress of solubilization. Methanol was a preferred solvent, as tests discussed below showed no effect on surfactant solubilization; most higher alcohols could not be utilized since they affect CMC values significantly (8). Although for batch tests for low-volatility PAH compounds it would have been possible to selectively evaporate methanol from PAH stock and still retain much of the PAH compound prior to addition of surfactant and water, this process would not be not feasible using higher volatility PAH compounds such as naphthalene because of loss to the atmosphere while methanol was being evaporated.

Table III provides measured values of apparent PAH solubility in solutions prepared with methanol but without surfactant. These values may be compared to reported aqueous solubilities given in Table I. Measured apparent PAH solubilities at zero surfactant concentration in the presence of 1% by volume methanol appear to be enhanced by ~20–30% relative to reported solubilities in pure water. This result is consistent with other experimental data for naphthalene solubility in the presence of 1% methanol (24).

The partitioning properties of PAH compounds are considered to be affected only slightly in the presence of a small amount of methanol (25). An assessment of whether 1% methanol in a batch test would measurably alter either the observed CMC or the slope of the solu-

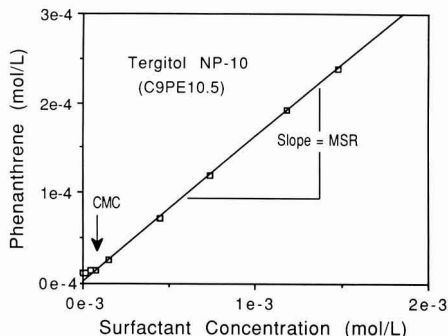


Figure 2. Solubilization of phenanthrene by $C_9PE_{10.5}$ nonionic surfactant. The slope of the solubilization curve is equal to the molar solubilization ratio. (Axis notation denotes base 10 exponentiation.)

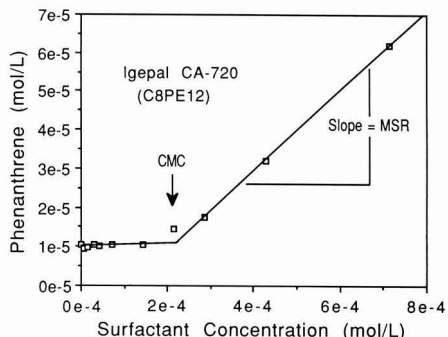


Figure 3. Solubilization of phenanthrene by C_9PE_{12} nonionic surfactant. The CMC is indicated by the intersection of the two linear regions of the solubilization relationship. (Axis notation denotes base 10 exponentiation.)

bilization curve is displayed in Figure 1 for a solution of pyrene and octylphenyl POE surfactant. It is apparent from this figure that the presence of methanol did not shift the CMC, nor did it change the slope of the solubilization curve. The molar solubilization ratio (MSR) remained constant.

Solubilization Relationships. PAH solubilization was plotted as a function of surfactant solution concentration for each data set. Plots of apparent phenanthrene solubility versus concentration of the surfactants $C_9PE_{10.5}$ and C_9PE_{12} are shown in Figures 2 and 3, respectively. In Figure 2, solubilization of phenanthrene by micellar $C_9PE_{10.5}$ is characterized by the MSR for that portion of the apparent solubility curve that correlates with $C_9PE_{10.5}$

Table IV. Critical Micelle Concentration Measurements for Commercial Nonionic Surfactants of This Study As Determined by Solubilization and Surface Tension Methods

surfactant	CMC, mol/L	
	solub tests	surf tension tests
Brij 30	2×10^{-5}	2.3×10^{-5}
Igepal CA-720	$(2-3) \times 10^{-4}$	2.3×10^{-4}
Tergitol NP-10	5×10^{-5}	5.4×10^{-5}
Triton X-100	2×10^{-5}	1.7×10^{-4}

concentrations in excess of the CMC. The value of the CMC for this surfactant is approximately 5×10^{-5} mol/L, denoted as in other tests by a sharp increase in the apparent solubility at this concentration and confirmed by independent surface tension measurements. It is evident that the relationship between the apparent phenanthrene solubility and the $C_9PE_{10.5}$ concentration above the CMC is linear. Figure 3 shows for C_9PE_{12} that there is only a very small increase in phenanthrene apparent solubility at surfactant concentrations less than the CMC, compared to increases in solubility at surfactant concentrations in excess of the CMC.

The slopes of all apparent PAH solubility curves of this study are linear at concentrations above the CMC, except for surfactant concentrations close to the CMC where there may be small curvature in the solubilization relationship due to surfactant inhomogeneities. The proportional dependence of PAH solubilization on micellar surfactant concentration results from the mass of surfactant that is added in excess of the mass of surfactant needed to attain the CMC, being manifest in bulk solution by the formation of micelles. This results in increased micelle volume, and the greater micelle volume present in bulk solution provides greater volume of hydrophobic micellar pseudophase available for PAH solubilization, with the extent of PAH partitioning per micelle being effectively constant.

When there is a diffuse rather than sharp inflection of the apparent solubility curve in the vicinity of the CMC of a commercial surfactant, it is believed that this is the result of either organic impurities in the surfactant solution or a polydisperse oxyethylene number distribution for the hydrophilic moieties of the surfactant molecules of the product (6, 14). The presence of polyoxyethylene chains of various lengths in a surfactant solution depresses to some extent the CMC in comparison to the CMC of specially prepared and purified homogeneous surfactants denoted by the same chemical formula (8, 14). An example of an indistinct curve inflection near the CMC is shown in Figure 3. In such a case, the CMC is obtained by taking the intersection of the projections from the linear portions of the apparent solubility curve above and below the CMC and confirming this estimate by surface tension measurements.

Critical Micelle Concentrations. Table IV shows CMC values estimated from solubilization data. Shown also for comparison are CMC values for the identical commercial surfactant products as determined by surface tension experiments in deionized water. Figures 4 and 5 show examples of determination of CMC values from surface tension experiments for solutions of $C_9PE_{10.5}$ and $C_{12}PE_4$, respectively, in deionized water. Data from these experiments allow determination of the CMC as the surfactant concentration denoted by the intersection of the two linear portions of a curve showing variation in surface tension as a function of the logarithm of C_{surf} . If the effect of hydrocarbon solubilizates on CMC values is slight, as indicated in ref 8, then the CMC values in deionized water

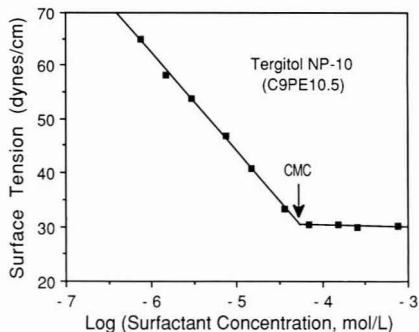


Figure 4. Determination of CMC by surface tension measurements for $C_9PE_{10.5}$ nonionic surfactant.

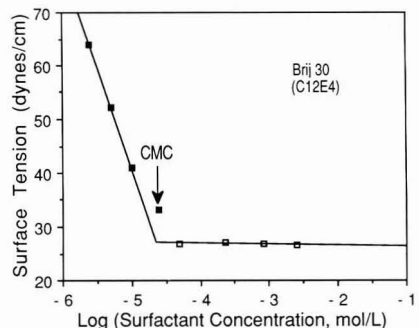


Figure 5. Determination of CMC by surface tension measurements for $C_{12}E_4$ nonionic surfactant.

should approximate CMC values in the presence of PAH. If, on the other hand, the amount and type of hydrocarbon solubilizate affects the CMC value of a surfactant, then there may be differences between CMC values in the presence of PAH solubilizates and CMC values in water. There may also be minor differences in CMC values for solutions with different solubilizates, as can be seen in Figures 1 and 3. In general, however, the CMC values obtained from the surface tension data for solutions of deionized water and surfactant show fairly close agreement to the CMC values inferred from the PAH solubilization data.

MSR and Micelle-Phase/Aqueous-Phase Partitioning. Determination of the slope of the linear portion of the apparent solubility curve at concentrations greater than the CMC for a given surfactant-PAH combination provides a direct numerical value for the MSR. The MSR reflects the capacity of 1 mol of a particular surfactant in micelle form to accommodate a given PAH solubilizate. Quantitatively, the MSR represents the average number of molecules of solubilizate per micelle divided by the aggregation number. The numerical value of the mole fraction micelle-phase/aqueous-phase partition coefficient, K_m , may be calculated from the MSR by using the following formula derived from eqs 1, 2, 4, and 5:

$$K_m = (55.4/S_{PAH,cmc})[MSR/(1 + MSR)] \quad (7)$$

Table III shows values of measured aqueous PAH solubility, $S_{PAH,cmc}$, MSR, and $\log K_m$ for the 12 surfactant-PAH combinations used in this study.

The parameter K_m represents organic compound partitioning between nonpolar and polar pseudophases. Thus, for a given surfactant, K_m values can be correlated with other hydrophobic-hydrophilic partitioning coefficients

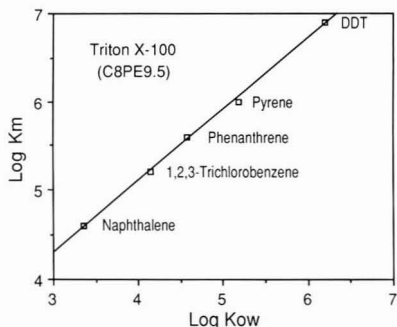


Figure 6. Correlation of $\log K_m$ and $\log K_{ow}$ for five hydrophobic compounds in $C_8PE_{9.5}$ nonionic surfactant solution. The values of $\log K_m$ for 1,2,3-trichlorobenzene and DDT are determined from solubility data of Kile and Chiou (6).

such as the octanol-water partition coefficient, K_{ow} . Figure 6 displays $\log K_m$ values plotted against $\log K_{ow}$ values for solubilization of five hydrophobic organic compounds in Triton X-100 at 25 °C. Three of the data points in Figure 6 represent the PAH compounds of this study with $\log K_{ow}$ values from Karickhoff et al. (22) and $\log K_m$ values as given in Table III. The other two data points are for solubilization of DDT and 1,2,3-trichlorobenzene. The $\log K_{ow}$ values for DDT and 1,2,3-trichlorobenzene are 6.19 (26) and 4.14 (27), respectively. The $\log K_m$ values for solubilization of these two compounds by Triton X-100 are computed from solubility data of Kile and Chiou (6). The solute solubility at the CMC is obtained by projecting the linear part of the pre-CMC portion of the apparent solubility curve to its intersection with the projection of the linear part of the post-CMC portion of the apparent solubility curve, a step that is necessary because of the heterogeneous OE number distribution of Triton X-100. The MSR value is obtained from the slope of the linear part of the post-CMC portion of the curve. The $\log K_m$ value for DDT in Triton X-100 is calculated as 6.87 by using a $S_{DDT,cmc}$ value of 9.35×10^{-8} mol/L and a MSR value of 1.28×10^{-2} . A $\log K_m$ value of 5.17 is obtained for 1,2,3-trichlorobenzene. Figure 6 shows that the relationship between $\log K_m$ and $\log K_{ow}$ in Triton X-100 solution is highly linear, and the data for the other surfactant solutions suggest similar linear relationships between $\log K_m$ and $\log K_{ow}$.

$\log K_m$ - $\log K_{ow}$ Correlation. The findings shown in Figure 6 are in accord with the results of Valsaraj and Thibodeaux (28), who demonstrated a linear relationship between $\log K_m$ and $\log K_{ow}$ for various hydrophobic organic compounds in micellar sodium dodecyl sulfate solution. This relationship is displayed in Figure 7 along with that for Triton X-100 solution. The slope obtained by plotting $\log K_m$ against $\log K_{ow}$ for the sodium dodecyl sulfate solution is nearly equivalent to the slope for the Triton X-100 solution, whereas the intercept is smaller. Such correlations may be dependent on the type of surfactant (34), as well as the units of expression of the partitioning relationship and whether there is an effect of solubility in the micelles due to high Laplace pressures in the micelles because of the curved interfaces (28).

An additional observation from this study is that the mole fraction of PAH in the micelle pseudophase in these solutions is negatively correlated with $\log K_{ow}$. The mole fraction of PAH in the micelle pseudophase is given by

$$X_m = K_m V_w S_{PAH,cmc} \quad (8)$$

A plot of the values of $K_m V_w S_{PAH,cmc}$ for solubilization of

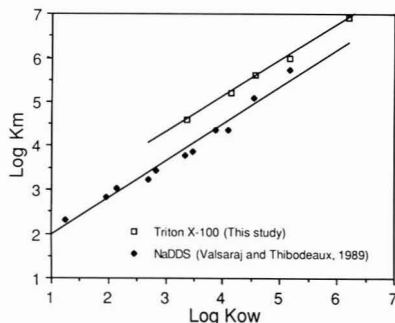


Figure 7. Comparison of $\log K_m$ - $\log K_{ow}$ correlations for hydrophobic solubilizates in octylphenol polyoxyethylene surfactant ($C_8PE_{9.5}$) and sodium dodecyl sulfate solutions.

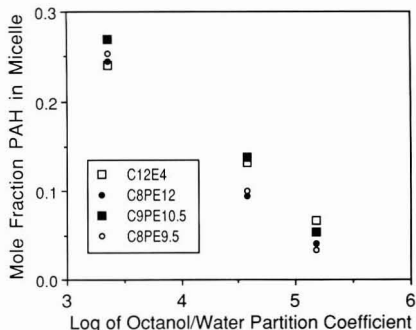


Figure 8. Correlation of mole fraction of naphthalene, phenanthrene, and pyrene in the micelle pseudophase with $\log K_{ow}$ in four nonionic surfactant solutions.

polycyclic aromatic hydrocarbons in the four nonionic surfactant solutions of this study is shown as a function of $\log K_{ow}$ in Figure 8. It appears for each of these particular surfactant solutions that $K_m V_w S_{PAH,cmc}$ is a nearly linear, monotonically decreasing function of $\log K_{ow}$, and that $K_m V_w S_{PAH,cmc}$ is only weakly dependent on surfactant composition. Although the more hydrophobic PAH compounds have smaller mole fractions in the micellar pseudophase, K_m , the ratio of the mole fraction in the micellar pseudophase to the mole fraction in the aqueous pseudophase, is larger with increasing value of solute K_{ow} , on account of a proportionally greater decrease in PAH solubility in monomeric solution with increasing solute hydrophobicity.

Characterization of partitioning in simple micelle-water systems as provided through K_m values is an essential prerequisite to proper modeling of hydrophobic organic compound partitioning in contaminated soils in which commercial surfactant or other amphiphile is present in micellar form. An initial approach to the use of K_m values in modeling subsurface contaminant transport in micellar surfactant solution in porous media has been presented by Valsaraj and Thibodeaux (28), although their approach does not explicitly consider the importance of sorption of surfactant to porous media.

The partitioning of organic hydrophobes in the presence of surfactants in soil-water systems may play a prominent role in certain aspects of abiotic remediation of contaminated soil (3, 4, 5, 29-32) and facilitated transport (7, 28), as well as possibly influence in situ bioremediation (32, 33). A better understanding of the physics and chemistry of surfactant-influenced hydrophobic organic compound partitioning in aqueous and soil-water systems will provide

improved mechanistic models for understanding these phenomena in environmental systems.

Conclusion

The apparent solubilities of naphthalene, phenanthrene, and pyrene were measured in solutions of nonionic polyoxyethylene surfactants. PAH solubility increased linearly with surfactant dose at bulk aqueous concentrations of surfactant in excess of the critical micelle concentration. The slope of such a relationship for a each solution of surfactant and PAH compound was used to determine the molar solubilization ratio, MSR, and the PAH mole fraction micelle-phase/aqueous-phase partition coefficient, K_m . The PAH compounds were solubilized in the range of ~ 0.04 – 0.4 mol of PAH/mol of micellar surfactant with K_m values in the range of $10^{4.6}$ – $10^{6.5}$. Values of $\log K_m$ for a particular surfactant–PAH system appear to be correlated with PAH octanol–water partition coefficients. These data can be used with additional information on surfactant and PAH sorption on soil to estimate PAH solubilization in soil–water–surfactant systems.

Acknowledgments

We express our appreciation to Annette M. Jacobson and Shonali Laha who provided useful comments.

Registry No. Brij 30, 9002-92-0; Igepal CA-720, 9036-19-5; Tergitol NP-10, 9016-45-9; Triton X-100, 9002-93-1; naphthalene, 91-20-3; phenanthrene, 85-01-8; pyrene, 129-00-0.

Literature Cited

- (1) Dzombak, D. A.; Luthy, R. G. *Soil Sci.* **1984**, *137*, 292.
- (2) Karickhoff, S. W. *J. Hydraul. Eng.* **1984**, *110*, 707.
- (3) Nash, J. H.; Traver, R. P. Field Evaluation of In-Situ Washing of Contaminated Soils with Water/Surfactants. *Proceedings of the 12th Annual Research Symposium*; EPA/600/9-86/022; Cincinnati, OH, 1986.
- (4) McDermott, J. B.; et al. Two Strategies for PCB Soil Remediation: Biodegradation and Sufactant Extraction. AICHe Meeting, New Orleans, LA, Spring 1988.
- (5) Rajput, V. S.; Pilapitiya, S.; Singley, M. E.; Higgins, A. J. Detoxification of Hazardous Waste Contaminated Soils and Residues by Washing and Biodegradation. In *Proceedings, International Conference on Physicochemical and Biological Detoxification of Hazardous Wastes*; Wu, Y. C., Ed.; Technomic: Lancaster, PA, 1989; pp 409–417.
- (6) Kile, D. E.; Chiou, C. T. *Environ. Sci. Technol.* **1989**, *23*, 832.
- (7) Huling, S. G. Facilitated Transport. EPA Superfund Ground Water Issue, EPA/540/4-89/003; Robert S. Kerr Environmental Laboratory, Ada, OK, 1989.
- (8) Rosen, M. J. *Surfactants and Interfacial Phenomena*, 2nd ed.; John Wiley and Sons: New York, 1989.
- (9) Martin, A. N.; Swarbrick, J.; Cammarata, A. *Physical Pharmacy*; Lea and Febiger: Philadelphia, PA, 1969.
- (10) Tanford, C. *The Hydrophobic Effect: Formation of Micelles and Biological Membranes*, 2nd ed.; John Wiley and Sons: New York, 1980.

- (11) Bendedouch, D.; Chen, S.-H.; Koehler, W. C. *J. Phys. Chem.* **1983**, *87*, 153.
- (12) Halle, B.; Carlstrom, G. *J. Phys. Chem.* **1981**, *85*, 2142.
- (13) Hunter, R. J. *Foundations of Colloid Science*; Clarendon Press: Oxford, 1987; Vol. 1.
- (14) Mukerjee, P.; Mysels, K. J. *Critical Micelle Concentrations of Aqueous Surfactant Systems*; NSRDS-NBS 36; U.S. Department of Commerce: Washington, DC, 1971.
- (15) Attwood, D.; Florence, A. T. *Surfactant Systems: Their Chemistry, Pharmacy and Biology*; Chapman and Hall: New York, 1983.
- (16) Sjoblom, L. In *Solvent Properties of Surfactant Solutions*; Shinoda, K., Ed.; Marcel Dekker, Inc.: New York, 1967; pp 189–262.
- (17) Klevens, H. B. *J. Phys. Colloid Chem.* **1950**, *54*, 283.
- (18) Hayase, K.; Hayano, S. *Bull. Chem. Soc. Jpn.* **1977**, *50*, 83.
- (19) Greek, B. F. *Chem. Eng. News* **1988**, *66*, (Jan 25), 21.
- (20) Liu, Z.; Laha, S.; Luthy, R. G. Surfactant Solubilization of Polycyclic Aromatic Hydrocarbons in Soil/Water Suspensions. *Water Sci. Technol.* **1991**, *23*, 475.
- (21) Mackay, D.; Shiu, W. Y. *J. Phys. Chem. Ref. Data* **1981**, *10*, 1175.
- (22) Karickhoff, S. W.; Brown, D. S.; Scott, T. A. *Water Res.* **1979**, *13*, 241.
- (23) Harkings, W. D. In *Physical Methods of Organic Chemistry*; Weissberger, A., Ed.; Interscience: New York, 1959; Vol. 1, Part 1 (Revised by A. E. Alexander).
- (24) Fu, J.-K. Ph.D Dissertation, Dept. of Civil Engineering, Carnegie Mellon University, 1985.
- (25) Jacobson, A. M. Ph.D Dissertation, Dept. of Chemical Engineering, Carnegie Mellon University, 1988.
- (26) Verschuere, K. *Handbook of Environmental Data on Organic Chemicals*, 2nd ed.; Van Nostrand Reinhold Co.: New York, 1983.
- (27) Chiou, C. T. *Environ. Sci. Technol.* **1985**, *19*, 57.
- (28) Valsaraj, K. T.; Thibodeaux, L. J. *Water Res.* **1989**, *23*, 183.
- (29) Ellis, W. D.; Payne, J. R.; McNabb, G. D. Treatment of Contaminated Soils with Aqueous Surfactants. Final Report EPA/600/2-85/129, NTIS PB86-122561, 1986.
- (30) Rickabaugh, J.; Clement, S.; Lewis, R. F. Surfactant Scrubbing of Hazardous Chemicals from Soil. *Proceedings, 41st Purdue Industrial Waste Conference*; Lewis Publishers: Ann Arbor, MI, 1986.
- (31) Vignon, B. W.; Rubin, A. J. *J. Water Pollut. Control Fed.* **1989**, *61*, 1233.
- (32) Laha, S.; Liu, Z.; Edwards, D.; Luthy, R. G. The Potential for Solubilizing Agents to Enhance the Remediation of Hydrophobic Organic Solutes in Soil–Water Suspensions. *Proceedings of the Second Annual IGT/GRI Symposium on Gas, Oil, Coal and Environmental Biotechnology*, New Orleans, LA, December 1989.
- (33) Rittman, B. E.; Johnson, N. M. *Water Sci. Technol.* **1989**, *21*, 209.
- (34) Valsaraj, K. T.; Thibodeaux, L. J. *Sep. Sci. Technol.* **1990**, *25*, 369.

Received for review May 14, 1990. Revised manuscript received August 2, 1990. Accepted August 3, 1990. This work was sponsored by the U.S. EPA Office of Exploratory Research under Grant 12-815325-01-0.

Nonequilibrium Sorption of Organic Chemicals: Elucidation of Rate-Limiting Processes

Mark L. Brusseau*

Department of Soil and Water Science, 429 Shantz Building 38, University of Arizona, Tucson, Arizona 85721

Ron E. Jessup and P. Suresh C. Rao

Soil Science Department, University of Florida, Gainesville, Florida 32611

■ The results of experiments designed to identify the process(es) responsible for nonequilibrium sorption of hydrophobic organic chemicals (HOCs) by natural sorbents are reported. The results of experiments performed with natural sorbents were compared to rate data obtained from systems wherein rate-limited sorption was caused by specific sorbate-sorbent interactions. This comparison showed that chemical nonequilibrium associated with specific sorbate-sorbent interactions does not significantly contribute to the rate-limited sorption of HOCs by natural sorbents. Transport-related nonequilibrium was also shown to not be a factor for the systems investigated. Hence, attempts were made to interpret the data in terms of two, sorption-related, diffusive mass-transfer conceptual models: retarded intraparticle diffusion and intraorganic matter diffusion. The analyses provide strong evidence that intraorganic matter diffusion was responsible for the nonequilibrium sorption exhibited by the systems investigated in this paper.

Introduction

Rate-limited or, nonequilibrium, sorption of organic chemicals by natural sorbents (i.e., soils, sediments, and aquifer materials) has been a topic of interest for quite some time. Perusal of the literature reveals that uncertainty exists in regard to the effects and relative importance of nonequilibrium sorption and its impact on the transport and fate of organic chemicals in surface (sediment/water) and subsurface (soil, aquifer) systems. Much of the confusion, we believe, can be attributed either directly or indirectly to inadequate knowledge of the mechanisms responsible for rate-limited sorption. Several different processes have been proposed as causing nonequilibrium sorption. However, past analyses have been based upon supposition or the fitting of models to data. The purpose of this paper is to report the results of experiments specifically designed to identify the mechanism(s) responsible for nonequilibrium sorption of hydrophobic organic chemicals (HOCs) by natural sorbents.

Conceptual Framework

Rate-Limiting Processes. Several processes have been proposed as being responsible for nonequilibrium sorption. To enhance forthcoming analyses and discussion, as well as to clarify terminology, these processes will be briefly reviewed. Rate-limiting processes have been grouped into two general classes: transport related and sorption related (1, 2). Transport-related nonequilibrium, often referred to as physical nonequilibrium, results from the existence of a heterogeneous flow domain. The influence of macroscopic heterogeneities (e.g., aggregates, macropores, stratified media) on solute transport has been well documented (see refs 1 and 3 for recent reviews). It should be noted that transport-related nonequilibrium affects both sorbing and nonsorbing solutes.

Sorption-related nonequilibrium may result from chemical nonequilibrium or from rate-limited diffusive mass

transfer. Chemical nonequilibrium (e.g., chemisorption) is caused by rate-limited interactions between the sorbate and sorbent. Specific sorbate-sorbent interactions may be relatively unimportant for the sorption of HOCs since their sorption is generally thought to be driven by a partitioning between the solution and organic matter components of the sorbent (4-7). Thus, chemical nonequilibrium may be ruled out as a probable nonequilibrium mechanism for HOCs (1, 8). This conclusion will be evaluated in light of experimental results in a forthcoming section. It must be stressed that, while chemical nonequilibrium may be unimportant for nonpolar organic chemicals, it may well be important for other organic chemicals such as pesticides (8, 9), which often have one or more polar functional groups.

Three different processes involving diffusive mass transfer can cause sorption-related nonequilibrium: film diffusion, retarded intraparticle diffusion, and intrasorbent diffusion. Film diffusion will not be considered further, as many researchers have shown that this mechanism is generally insignificant in comparison to other mechanisms (see ref 1 and references cited therein). Because much of the forthcoming results will be analyzed in terms of retarded intraparticle diffusion and intraorganic matter diffusion, these two are discussed in some detail in the following three sections.

Retarded Intraparticle Diffusion. Retarded intraparticle diffusion involves aqueous-phase diffusion of solute within pores of microporous particles (e.g., sand grains) mediated by retardation resulting from instantaneous sorption to pore walls. Such a mechanism was proposed for the rate-limited uptake/release of HOCs by sediments (10) and by aquifer materials (11). This model is based on the radial-diffusion models that have been developed in chemical engineering. An important assumption associated with this model is that most, if not all, sorption occurs inside the particles. For HOCs, whose sorption is generally controlled by organic matter, this means that most, if not all, organic matter must reside inside the particles.

Hindered diffusion is assumed to not be a factor in the usual conceptualization employed for the retarded intraparticle diffusion model. However, it has been suggested (1, 3, 12), based upon analyses of applications of the retarded intraparticle diffusion model to experimental observations, that this model cannot describe all aspects of the data without calling upon the concept of hindered diffusion. Hindered diffusion in fixed-pore systems, such as catalyst beads and zeolites, has received a great deal of attention. Equations of the following type

$$\log(D_0/D_p) = -0.5 - 1.98\lambda \quad (1)$$

where D_0 is the aqueous diffusion coefficient (L^2/T), D_p is the pore diffusion coefficient, and λ is the ratio of solute molecular diameter to pore diameter, have been reported by, among others, Satterfield et al. (13) and Chantong and Massoth (14). The values used for the regression coeffi-

cients in eq 1 are averages of those reported by the cited researchers. By use of eq 1 and a representative value of <1 nm for the molecular diameter of the solutes employed in this study, the pore diameter required to produce appreciable hinderance is estimated to be approximately 25 nm.

The pore size distribution of a sandy aquifer material was measured by mercury porosimetry and nitrogen desorption by Ball (11). The results revealed that 80% and greater than 90% of the internal pore volume comprised pores whose diameters exceeded 25 and 10 nm, respectively. If these results are at all representative of other sandy materials, it would appear that hinderance may not be important for many solutes of interest. This conclusion is supported by data that will be presented under Results and Discussion.

Intraorganic Matter Diffusion. Intrasorbent diffusion involves the diffusive mass transfer of sorbate within the matrix of the sorbent. Given organic matter as the predominant sorbent for HOCs, intrasorbent diffusion is usually considered to involve diffusion within the matrix of organic matter. Intraorganic matter diffusion was proposed as the rate-limiting mechanism for sorption of organic chemicals as early as 1966 by Hamaker et al. (15) and has since been proposed by several others (see refs 1 and 8 and references cited therein). While intraorganic matter diffusion is the most likely intrasorbent diffusion-related mechanism for HOCs, diffusion within, for example, matrices of expanding clay minerals may be important for other, polar, organic chemicals (cf. ref 16).

For the intraorganic matter diffusion model, the primary assumption is that sorbent organic matter is a polymeric-type substance within which sorbate can diffuse. The organic matter associated with natural sorbents has been reported to be a flexible, cross-linked, branched, amorphous (noncrystalline), polyelectrolytic polymeric substance (17-21). Direct confirmation of the "porous" nature of organic matter has been reported (19, 22). The conceptualization upon which the intraorganic matter diffusion model is based is consistent with the generally accepted view of the process by which HOCs are sorbed by natural sorbents (i.e., partitioning to sorbent organic matter).

Comparison of Intraorganic Matter Diffusion and Retarded Intraparticle Diffusion. Two major physical differences between organic matter and microporous particles and, hence, intraorganic matter diffusion and retarded intraparticle diffusion are readily apparent. First, the size of the "pores" associated with organic matter is similar to the size of the sorbate molecules, whereas for porous particles the pores are much larger than the diffusing molecule (except for the case of extreme hinderance). Second, while the pore networks for porous particles are fixed and comprised of rigid pores, the "pore network" associated with organic matter is dynamic and the "pores" are ephemeral rather than fixed. In spite of these differences, intraorganic matter diffusion has been considered as a form of retarded intraparticle diffusion (cf. ref 11). The application of theories developed for fixed-pore systems to diffusion in polymers is not appropriate, however, since junction and chain fluctuations render the use of λ rather questionable (23, 24). Hence, it is inaccurate to regard the free volume in organic matter as being a pore network in the conventional sense; rather the system should be considered as a flexible "mesh", a term utilized in polymer science (23, 25, 26). The importance of differentiating diffusion in polymers from that in fixed-pore systems has been recognized for quite some time (cf. ref 25). Accordingly, intraorganic matter diffusion should not

be interpreted in terms of fixed-pore models.

Theory

Modeling Nonequilibrium. A bicontinuum model based on first-order mass transfer will be used to analyze the results of our experiments. The various models available for simulating nonequilibrium sorption are reviewed elsewhere (1, 3, 27). With the first-order model, sorption is conceptualized to occur in two domains:

$$S_1 = FK_p C \quad (2)$$

$$dS_2/dt = k_1 S_1 - k_2 S_2 \quad (3)$$

where C is the solution-phase solute concentration (M/L^3), S_1 is the sorbed-phase concentration (M/M) in the "instantaneous" domain, S_2 is the sorbed-phase concentration (M/M) in the rate-limited domain, K_p is the equilibrium sorption constant (L^3/M), F is the fraction of sorbent for which sorption is instantaneous, t is time, and k_1 and k_2 are forward and reverse first-order rate constants ($1/T$), respectively. At equilibrium, eq 3 reduces to

$$k_1 S_1 = k_2 S_2 \quad S_2 = (1 - F)K_p C \quad (4)$$

Thus, for the ratio of rate constants we obtain

$$k_1/k_2 = (1 - F)/F \quad (5)$$

The following equations describe the transport of sorbing solutes during one-dimensional, steady water flow in a homogeneous porous medium:

$$\partial C^*/\partial p + (\beta R - 1) \partial C^*/\partial p + (1 - \beta)R \partial S^*/\partial p = (1/P) \partial^2 C^*/\partial X^2 - \partial C^*/\partial X \quad (6)$$

$$(1 - \beta)R \partial S^*/\partial p = \omega(C^* - S^*) \quad (7)$$

where

$$C^* = C/C_0 \quad (8a)$$

$$P = vL/D \quad (8b)$$

$$S^* = S_2/(1 - F)K_p \quad (8c)$$

$$R = 1 + (\rho/\theta)K_p \quad (8d)$$

$$p = vt/L \quad (8e)$$

$$\beta = [1 + F(\rho/\theta)K_p]/R \quad (8f)$$

$$X = x/L \quad (8g)$$

$$\omega = k_2(1 - \beta)RL/v \quad (8h)$$

and where C_0 is the solute concentration (M/L^3) of the influent solution, D is the dispersion coefficient (L^2/T), v is the average pore-water velocity (L/T), x is distance (L), L is column length (L), p is dimensionless time in pore volumes, ρ is bulk density (M/L^3), θ is volumetric soil water content, P is the Peclet number, which represents the dispersive-flux contribution to transport, R is the retardation factor, which represents the effect of sorption on transport, β is the fraction of instantaneous retardation, and ω is the Damkohler number, which is a ratio of hydrodynamic residence time to characteristic time for sorption. These last two terms specify the degree of nonequilibrium existent in the system, which decreases as either of the two increase in magnitude.

Interpretation of the First-Order Model in Terms of Diffusion-Based Models. The first-order mass-transfer model can be interpreted in terms of the two diffusion-based conceptual models by defining the rate constant (k_2) in terms of the appropriate diffusion coefficient of the solute and the shape factor, tortuosity, and

diffusion path length characterizing the sorbent. The following equation may be used to interpret k_2 in terms of retarded intraparticle diffusion (11):

$$k_2 = [15D_p/(R_{im}a^2)] = 15D_0/[(1 + (\rho/\theta_{im})K_p)\tau a^2] \quad (9)$$

where D_p is the pore diffusion coefficient (L^2/T), which can be related to the aqueous diffusion coefficient (D_0) through a tortuosity factor (τ), R_{im} is the retardation factor for sorption occurring inside the particle, θ_{im} is the volume fraction of internal porosity, and a is particle radius (L). The equation on the right-hand side is exact when all sorption occurs inside the particles, which is the usual assumption for the retarded intraparticle diffusion model.

Although the manner in which the first-order bicontinuum model can be interpreted in terms of intraorganic matter diffusion has been qualitatively discussed (1), no quantitative treatment has been presented to date. Such a treatment is presented below.

The two sorptive domains assumed by the bicontinuum model are represented by volume fractions V_1 and V_2 , which are the volumes of the respective domains per total sorbent mass (L^3/M). The macroscopic sorbed-phase concentrations, S_1 and S_2 , may be defined in terms of microscopic concentrations:

$$S_1 = s_1 V_1 \quad S_2 = s_2 V_2 \quad (10)$$

where s_i is the sorbate mass in region i per volume of region i . At equilibrium the following relationships are derived between F and V_i by using eqs 2 and 4:

$$F = V_1/(V_1 + V_2) \quad 1 - F = V_2/(V_1 + V_2) \quad (11)$$

The change in the sorbed-phase concentration of domain two is described by

$$V_2 ds_2/dt = k_t A (s_1 - s_2) \quad (12)$$

where k_t is a mass-transfer coefficient (L/T) and A is the cross-sectional area (L^2) through which mass transfer occurs.

In cases where it is difficult to explicitly define A and V , a mass-transfer constant (α , $1/T$) may be used. The mass-transfer constant is defined as

$$\alpha = k_t A / (V_1 + V_2) \quad (13)$$

Equation 12 may be rewritten in terms of the macroscopic sorbed-phase concentrations and rate constants by using eqs 10, 11, and 13:

$$dS_2/dt = \alpha[S_1/F - S_2/(1 - F)] = k_1 S_1 - k_2 S_2 \quad (14)$$

where

$$k_1 = \alpha/F = (k_t A/V_1) \quad (15a)$$

and

$$k_2 = \alpha/(1 - F) = (k_t A/V_2) \quad (15b)$$

For diffusion in polymeric materials, α can be related to the polymer diffusivity of the sorbate:

$$\alpha = cD_{py}/l^2 \quad (16)$$

where c is a shape factor, D_{py} is the diffusion coefficient (L^2/T^2) for the specific sorbate/polymer pair, and l is the characteristic diffusion length (L). Diffusion in polymers is dependent upon the physicochemical properties of the polymer, the diffusing molecule, and the solvating medium. For a given polymer and solvent, the diffusion coefficient decreases exponentially with increasing molecular weight (MW) or size of the diffusant (23, 28-33). This is especially true for systems where the size of the diffusant is similar

Table I. Properties of Soils and Columns

soil	particle size distribn, %			OC, %	ρ , g cm ⁻³	θ	L , cm
	silt	clay	sand				
Eustis	3.2	1.3	95.5	0.39	1.70	0.41	5.3
Lula	5.6	3.4	91.0	0.034	1.64	0.36	10.3
Tampa	2.3	0.6	97.1	0.13	1.64	0.42	10.6
Webster	40.9	29.5	29.6	3.41	1.50	0.55	2.8

to the size of the mesh, as would be the case for intraorganic matter diffusion. It is interesting to note that this dependency, given by $(MW)^{-n}$ where n ranges from 1.33 to 5 (30, 31, 33), is much stronger than that observed for aqueous diffusion coefficients, which is generally described by $(MW)^{-0.5}$. It should also be noted that the shape (e.g., branching; linear vs spherical) of the diffusing molecule also has a significant impact on diffusion in polymers (29, 34, 35).

Materials and Methods

Materials. The following analytical-grade chemicals (Fisher Scientific), were employed in the experiments: pentafluorobenzoic acid, benzene, toluene, *o*-xylene, *p*-xylene, trimethylbenzene, ethylbenzene, *n*-propylbenzene, *n*-butylbenzene, *n*-hexylbenzene, naphthalene, anthracene, chlorobenzene, 1,3-dichlorobenzene, 1,2,4-trichlorobenzene, 1,2,3,4-tetrachlorobenzene, tetrachloroethene, trichloroethene, 1,2-*trans*-dichloroethene, and quinoline. In addition, tritiated water was used as a nonsorbing tracer and ⁴⁵Ca (as ⁴⁵CaCl₂) was used to investigate isotopic cation exchange.

A sandy surface soil (Eustis fine sand) was used for all experiments except for those specifically noted. Other sorbents used were Lula and Tampa aquifer materials and Webster surface soil. Properties of these sorbents are reported in Table I.

Experimental Procedures. The apparatus and methods employed for the miscible-displacement studies were identical with those used by Brusseau et al. (27). The column was an Altex/Beckman preparative chromatography column (No. 252-18) made of precision-bore borosilicate glass, with an internal diameter of 2.5 cm. Two single-piston HPLC pumps (Gilson Medical Electronics, Model 302) were connected to the column, with a Rheodyne switching valve (Model 7060) placed in-line to facilitate switching between solutions that did or did not contain the solute of interest. The system was designed so that the solute contacted only stainless steel, glass, or Teflon. The flow rate used for all experiments was 3 mL/min ($v \approx 85$ cm/h), except where specifically noted. The lengths, bulk densities, and porosities of the columns are reported in Table I.

A flow-through, variable-wavelength UV detector (Gilson Holochrome) was used to continuously monitor concentrations of the organic solutes in the column effluent. Output was recorded on a strip-chart recorder (Fisher, Recordall Series 5000). The wavelength used for each experiment was determined by selecting for maximum UV absorbance. Effluent fractions were collected for tritiated water and ⁴⁵Ca. The activities of these two in the effluent fractions were measured by radioassay using liquid scintillation counting (Searle Delta 300).

The base solution for all experiments except that using hexylbenzene comprised HPLC-grade water with a matrix of 0.01 N CaCl₂. Saturated stock solutions for each solute were prepared by placing quantities in excess of their solubility limit in contact with the electrolyte solution and stirring for at least 48 h. Solutions were filtered sterilized

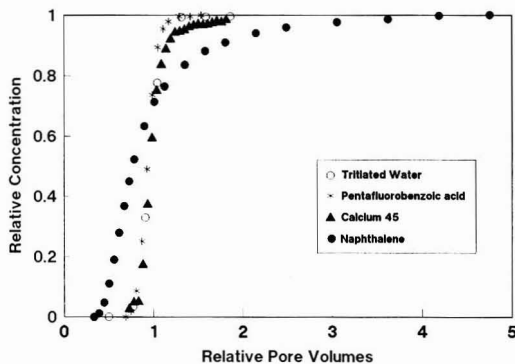


Figure 1. Breakthrough curves for tritiated water, pentafluorobenzoic acid, ^{45}Ca , and naphthalene.

with 0.45- μm filters prior to use. Aliquots of the stock solution were diluted with electrolyte solution until the desired concentration was achieved, which was generally 5–25% of the aqueous solubility. Because of the very hydrophobic nature of hexylbenzene, the experiment involving this solute was performed using a solution containing 30% volume fraction methanol. It has been shown that the relationship between k_2 and K_p exhibited by systems containing methanol fractions of less than approximately 70% does not deviate from the relationship exhibited by aqueous systems (36, 37). Hence, the use of methanol should not affect comparison of the results of the hexylbenzene experiment to the results of the other experiments.

Data Analysis. The results of the miscible displacement experiments employing the sorbing solutes were analyzed by use of a first-order bicontinuum model as discussed above. To run the model, knowledge of the following parameters is required: P , R , β , ω , and T_0 , the size of the input pulse in pore volumes. The value for P was obtained from the breakthrough curve (BTC) of a nonsorbing solute, tritiated water, using a nonlinear, least-squares optimization program (38) to solve the advective–dispersive local equilibrium transport model (39). The value for R , and thus K_p (see eq 8d), was obtained by moment analysis (27, 40). The size of the solute pulse, T_0 , is known from measurement. The two unknown parameters are thus β and ω . A nonlinear, least-squares optimization program (38) was used under flux-type boundary conditions to determine values for the two unknowns.

Values for k_2 and F were calculated by using the values of β and ω determined through optimization (see eqs 8f and 8h). Most of the analyses presented in this paper focus on the relationship between k_2 and K_p exhibited by the data. The k_2 and K_p values determined from the BTCs are therefore analyzed by the linear free energy relationship (LFER) approach, as utilized by Brusseau and Rao (8).

Results and Discussion

Evaluation of Transport-Related Nonequilibrium. Breakthrough curves obtained for tritiated water and pentafluorobenzoic acid (PFBA), both nonsorbing solutes, were symmetrical in shape and the Peclet number determined from optimization was independent of velocity. The BTC for ^{45}Ca was also symmetrical in shape, with only slight tailing (delayed approach to $C/C_0 = 1$). In contrast, the BTCs for the organic solutes were asymmetrical and exhibited significant tailing. The relative shapes of the BTCs are illustrated in Figure 1, where BTCs for tritiated

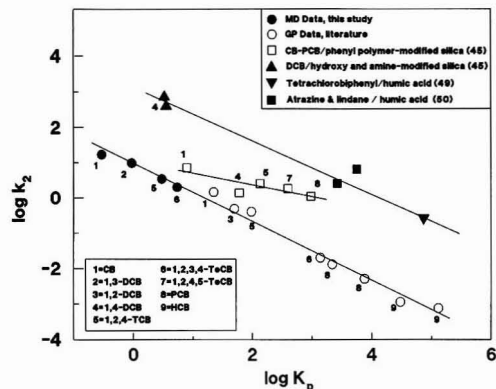


Figure 2. Comparison of rate data obtained for systems comprising reversed-phase packing material and humic acid to data obtained for natural sorbents. MD, miscible displacement; GP, gas purge; CB, chlorobenzene; DCB, dichlorobenzene; TCB, trichlorobenzene; TeCB, tetrachlorobenzene; PCB, pentachlorobenzene; HCB, hexachlorobenzene.

water, PFBA, ^{45}Ca , and naphthalene are plotted; note that relative pore volumes (p/R) are used for the abscissa to facilitate comparison. This behavior, where nonsorbing solutes exhibit symmetrical and velocity-invariant BTCs while sorbing solutes do not, is typical of systems wherein transport-related nonequilibrium is not a factor (1, 41).

As discussed earlier, hindered pore diffusion is not expected to be of importance for the systems employed in this study. This is supported by the results obtained for tritiated water and PFBA, where inspection of Figure 1 shows that the BTCs obtained for the two were identical. If hindrance were a factor, one might have expected differences between the two BTCs since PFBA is a much larger molecule. Given that the HOCs employed in this study are similar in size to PFBA, it is likely that hindrance is not a factor for them as well.

The logarithms of the values of k_2 and K_p determined for a series of chlorinated benzenes and Eustis soil are plotted in Figure 2. Similar data reported for chlorinated benzenes and sediments using the gas-purge technique were compiled from the literature (10, 27, 42, 43) and are also plotted in Figure 2. Transport-related nonequilibrium can be readily eliminated as a factor for the gas-purge data (27). Thus, the similarity between the data collected from miscible-displacement and gas-purge experiments provides further support to the contention that transport-related nonequilibrium was not a factor in our column experiments. The observed nonequilibrium would, therefore, appear to be caused by a sorption-related process.

To evaluate the role of sorbate–organic matter interactions in the observed sorption-related nonequilibrium, experiments were performed using a sample of Eustis soil that was treated with hydrogen peroxide to reduce the organic carbon content. For example, the nonequilibrium and retention exhibited by naphthalene was significantly reduced for the treated soil, in comparison to the untreated soil. This is consistent with earlier reports (41, 44) that the degree of nonequilibrium exhibited by HOCs was significantly diminished upon reducing the sorbent organic carbon content. Such behavior suggests that the nonequilibrium is sorption related, rather than transport related, and, in addition, that, in some manner, organic matter is involved. This would suggest that the process responsible for nonequilibrium could be chemical nonequilibrium, retarded intraparticle diffusion, or intraorganic matter diffusion.

Evaluation of Chemical Nonequilibrium. Experiments performed using reversed-phase liquid chromatography packing material and a series of chlorinated benzenes were recently reported (45, 46). Various organic modifiers were bonded to silica supports to evaluate potential mechanisms responsible for the rate-limited sorption of the HOCs by these synthetic sorbents. On the basis of the physical nature of reversed-phase packing materials, it is very unlikely that intraorganic matter diffusion would be a factor for such systems.

Retarded intraparticle diffusion was reported to be, at most, only a minor contributor to the observed nonequilibrium (45, 46). The pore size distribution of the porous silica particles employed in the experiments was 15–36 nm, which is in the lower range of that reported by Ball (11) for a sandy aquifer material. The relatively insignificant contribution of retarded intraparticle diffusion to the nonequilibrium exhibited by the porous particle systems of Szecody and Bales is in direct contrast to the proposal of Ball (11). The major difference between the systems employed by Szecody and Bales and the retarded intraparticle diffusion conceptual model is that most of the organic material and, hence, sorption is externally situated for the modified silicas. This highlights the central importance of the assumption employed in the retarded intraparticle diffusion model that all or most sorption occurs inside the particles. For systems where this is not the case, retarded intraparticle diffusion will be unimportant.

With intraorganic matter diffusion and retarded intraparticle diffusion eliminated, the rate-limiting mechanism for these data was suggested to involve constraints associated with π -bond formation (45, 46). Thus, while these packing materials should not be construed as being representative analogues for natural organic matter, the results obtained from these studies do provide valuable information on the impact of specific sorbate-sorbent interactions on the rate of sorption of HOCs.

Data for a series of chlorinated benzenes (monochloro-through pentachlorobenzene) and a phenyl polymer modified material (45) are shown in Figure 2. It should be noted that the carbon-referenced equilibrium constants associated with the phenyl polymer material were over an order of magnitude larger than those observed for natural sorbents, which suggests that the sorption mechanism involves greater energies of interaction in comparison to those involved for natural sorbents (45). Thus, it is possible that the rate constants obtained for these data are smaller than those representative of typical specific interactions between HOCs and natural sorbents.

Data for the retention of 1,4-dichlorobenzene on two polar-modified (amine and alcohol) silicas were also reported (45). The retention exhibited by these two surfaces was much more similar to that of natural sorbents. Interestingly, the rate constants for these data were significantly larger than those of the phenyl polymer data (see Figure 2). Inspection of Figure 2 reveals that the rate constants for the organic-modified silicas are 1–2 orders of magnitude larger than those obtained for the soils and sediments, which suggests that specific sorbate-sorbent interactions do not significantly contribute to the nonequilibrium observed for the natural sorbent systems.

Further insight into the impact of specific sorbate-sorbent interactions on the rate of sorption may be gained through analysis of experiments designed to evaluate the binding of HOCs by humic materials. It has been suggested that intraorganic matter diffusion would be of little significance for these systems, given the comparatively small dimensions of dissolved humic materials (47, 48).

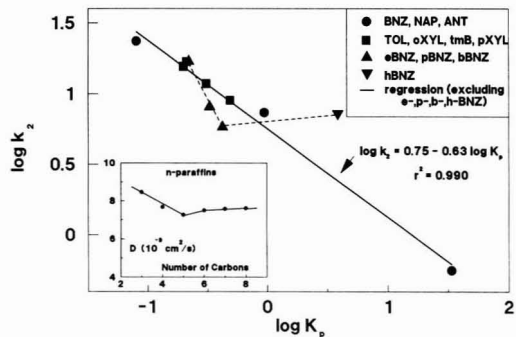


Figure 3. Data illustrating the impact of methyl group addition on sorption kinetics. BNZ, benzene; NAP, naphthalene; ANT, anthracene; eBNZ, ethylbenzene; pBNZ, *n*-propylbenzene; bBNZ, *n*-butylbenzene; hBNZ, *n*-hexylbenzene; TOL, toluene; oXYL, *o*-xylene; pXYL, *p*-xylene; tmB, trimethylbenzene. The data in the inset were obtained from van Amerongen (55).

Thus, rate constants obtained from these systems should be representative of the characteristic time of specific interactions (binding) between the sorbate and the sorbent.

Studies on the binding of 2,2',5,5'-tetrachlorobiphenyl (49) and atrazine (2-chloro-4-(ethylamino)-6-(isopropylamino)-*s*-triazine) and lindane (hexachlorocyclohexane) (50) by humic acid have been recently reported. Equilibrium and rate constants obtained from these results are plotted in Figure 2. The rate constants for the three humic acid data points are approximately 2 orders of magnitude higher than those obtained for the soils and sediments. These results, in addition to those of the HPLC packing materials, support the proposal of Brusseau and Rao (1, 8) that chemical nonequilibrium is not a major nonequilibrium mechanism for HOCs.

The analyses presented above provide strong evidence that the nonequilibrium sorption exhibited by the data reported in this paper was not caused by transport-related or chemical nonequilibrium. Hence, it would appear that either retarded intraparticle diffusion or intraorganic matter diffusion is the operative rate-limiting mechanism. The conclusion that a sorption-related diffusive mass-transfer mechanism is responsible for nonequilibrium sorption has been suggested by several researchers. However, it has not been possible to discriminate between these two mechanisms on the basis of the experiments reported to date. In the following sections data are reported that allow such a discrimination.

Influence of Molecular Structure. The effect of the molecular configuration of the sorbate on nonequilibrium sorption was probed with several alkylbenzenes. The base LFER, to which the alkylbenzene data will be compared, was established by using the unsubstituted series: benzene, naphthalene, and anthracene. The resultant LFER is shown in Figure 3. In terms of the retarded intraparticle diffusion model, the steep slope of the base LFER is explained by the presence of K_p in the denominator of eq 9 and the change in D_0 that occurs with the increase in molecular weight. In terms of the intraorganic matter diffusion model, the slope is explained through the strong dependency of the polymer diffusion coefficient, D_{py} , on molecular weight or size of the diffusing molecule (see eq 16). Interestingly, the magnitude of the slope exhibited by the data is similar to that observed for some polymer systems.

The impact of single or multiple additions of a single methyl group was evaluated by using toluene, *o*-xylene, *p*-xylene, and trimethylbenzene. Apparently, the addition

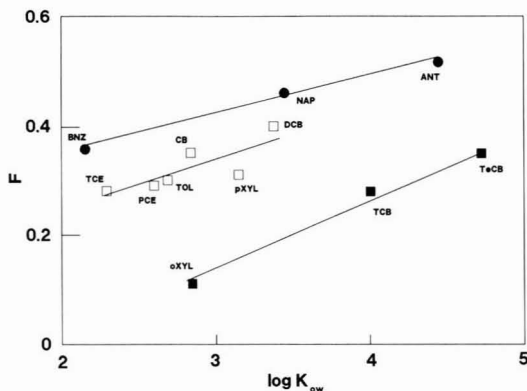


Figure 4. Data showing relationship between F , the fraction of instantaneous sorption, and the octanol/water partition coefficient (K_{ow}). See Figure 3 caption for acronym definitions.

of the functional group(s) does not result in behavior deviating from the LFER exhibited by the unsubstituted molecules (see Figure 3). The impact of adding a single, n -alkyl group was evaluated by using ethylbenzene, n -propylbenzene, n -butylbenzene, and n -hexylbenzene. Inspection of Figure 3 shows that the addition of an alkyl chain of three or more carbon units does alter the observed LFER.

The deviation of n -propyl-, n -butyl-, and n -hexylbenzene from the base LFER cannot be explained by the normal (i.e., no hindrance) retarded intraparticle diffusion model. Even though hindered diffusion is not likely to be of importance for this system, as discussed in prior sections, an attempt could be made to utilize this concept to explain the deviations. Hindrance is controlled by the size of the diffusing molecule (i.e., λ). Thus, it would be expected that molecules such as naphthalene and anthracene, considering their larger size and bulkiness, would exhibit greater deviations than those observed for propyl- and butylbenzene. In addition, the behavior of hexylbenzene relative to that of propyl- and butylbenzene cannot be explained by using the hindered diffusion concept since the diffusion of n -paraffins in zeolite, a fixed-pore system where hindrance is important, has been shown to be a strong function of the chain length (51–53).

The behavior exhibited in Figure 3 can be readily explained, however, by the intraorganic matter diffusion model. The presence of a three- or four-carbon chain (i.e., propylbenzene, butylbenzene) provides an increased opportunity for the molecule to become entangled with polymer chains, which results in an increased constraint on diffusion. However, the presence of additional carbons in the chain (i.e., hexylbenzene) has negligible effect because the diameter of the mesh required for diffusion of a linear molecule is the same, irrespective of length, up to some critical length (54–56). In other words, the energy required to activate a diffusion step for a linear alkyl chain is not significantly increased by addition of another carbon unit. Data illustrating this effect for diffusion of n -paraffins in polymeric materials were reported by van Amerongen (55) and are shown in the inset to Figure 3. Data exhibiting similar behavior have been reported by others (25, 57, 58).

The influence of molecular structure on the fraction of instantaneous sorption (F) is also of interest. Values for F are regressed against the log of the octanol/water partition coefficient (K_{ow}) in Figure 4. It appears that F increases with the log of K_{ow} . Since K_{ow} is directly related

to the molecular size of the solute, the results shown in Figure 4 suggest that F varies with molecular size. This behavior is consistent with the intraorganic matter diffusion model.

Recall from eq 11 that F represents the ratio of sorptive volume comprising the instantaneous sorption domain to total sorptive volume, which is the sum of instantaneous and rate-limited domains. Following the conceptualization inherent to the intraorganic matter diffusion model, the instantaneous sorption domain is considered to consist of the near-surface region of the organic matter while the rate-limited domain is considered to comprise the internal regions. The polymeric mesh characterizing the organic matter matrix may act as a molecular sieve, whereby larger sorbate molecules are excluded from portions of the free volume of the polymer because of size constraints (59, 60). As a result, the size of the rate-limited domain (V_2) may vary with sorbate size. A decrease in V_2 with increasing molecular size would cause F to increase (see eq 11), assuming that V_1 remains constant or varies more slowly with size.

Close inspection of Figure 4 reveals a second-order effect associated with the substitution pattern of the sorbate. First, F values for all substituted molecules fall below the line representing the unsubstituted sorbates (i.e., benzene, naphthalene, anthracene). Second, o -xylene, trichlorobenzene, and tetrachlorobenzene appear to be characterized by a separate line parallel to but lower than the lines representing the others. It is interesting to note that these three molecules are similar in that they are the only ones containing a functional group in the ortho position. One may speculate that, for two molecules of the same size, access to the volume representing the instantaneous sorption domain may be constrained to some degree for those that are substituted. In addition, molecules containing a functional group in the ortho position are the least "streamlined" and would, therefore, be constrained the most. Hence, with a smaller V_1 , F would be smaller for substituted molecules (see eq 11).

Comparison of ^{45}Ca and Quinoline to HOCs. Recall from Figure 1 that the BTC for ^{45}Ca exhibited little tailing in comparison to that exhibited by naphthalene. This suggests that the rate of sorption of ^{45}Ca is much faster than that of the HOCs. This is confirmed by inspection of Figure 5a, where the estimated rate constant for ^{45}Ca is compared to the LFER obtained for the HOCs.

In developing the retarded intraparticle diffusion model, it is assumed that the organic matter resides inside the porous particles, as discussed in a previous section. Organic matter is the predominant source of cation-exchange capacity for the Eustis soil, contributing approximately 70% of the total (41). The importance of organic matter as a source of cation-exchange capacity in soils has been well established (18, 20, 61). Since the sorption of ^{45}Ca is predominated by organic matter, just as it is for the HOCs, the effect of retardation on the diffusion of ^{45}Ca in the porous particles should be the same as that for the HOCs. This may be demonstrated by using eq 9. Inspection of eq 9 shows that, for a given porous medium, only D_0 and K_p are solute dependent (assuming no hindered diffusion). The contribution of organic matter to the sorption of ^{45}Ca can be estimated by multiplying the measured K_p by 70%. The resultant organic matter associated K_p is estimated to be 0.9 mL/g, which is very similar to the value measured for naphthalene (0.94). The D_0 value for ^{45}Ca is approximately a factor of 3 larger than that for naphthalene. Hence, by use of eq 9 it is seen that the k_2 value for ^{45}Ca should be, at most, a factor of 3 larger than the naph-

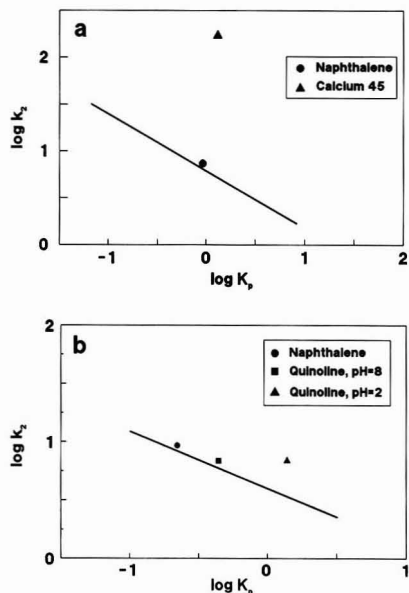


Figure 5. (a) Comparison of the rate-limited sorption of ^{45}Ca to that of the HOCs. Line represents LFER for all HOCs, excluding *n*-alkylbenzenes. (b) Comparison of the rate-limited sorption of quinoline in neutral and ionic forms to that of the nonionic HOCs. Line represents LFER for nonionic HOCs; note, Tampa aquifer material was used as the sorbent.

thalene value. Inspection of Figure 5a shows that the observed difference is much greater than that calculated with eq 9. Clearly, the data presented in Figure 5a cannot be explained by the retarded intraparticle diffusion model.

The fact that sorption of the HOCs is much more rate limited in comparison to that of ^{45}Ca can, however, be readily explained in terms of the intraorganic matter diffusion model. Cation exchange has been demonstrated to be an instantaneous physical process involving no chemical bond formation (62). Therefore, diffusion of the ion to/from the exchanger, rather than the actual exchange "reaction" itself, may be considered as the rate-limiting step for ion exchange (62, 63). Considering the nature and conformation of organic matter in water, it is likely that a relatively large proportion of free cation-exchange sites would be located near the sorbent/solution interface. Furthermore, on the basis of double-layer theory, it may be anticipated that the electroneutrality requirements for ion exchange can be satisfied by ions residing within the electrical field of the sorbent surface (cf. ref 64). As a result, the ion exchange of cations on organic matter substrates may be considered as essentially a film diffusion process. In other words, any rate-limited behavior exhibited in such systems may usually be attributed to film diffusion. This is supported by the work presented by Bunzl (65, 66), who investigated the kinetics of ion exchange of metal cations in humic acids and peat and concluded that the rate-limiting step was film diffusion. Thus, the mechanisms controlling rate-limited sorption of ^{45}Ca and the HOCs differ by the path length over which, and the medium through which, they must diffuse.

The behavior of an ionogenic compound, quinoline ($\text{p}K_a = 4.94$), was also evaluated. The data point obtained for an experiment performed with a system pH of 8, where quinoline exists in the neutral form, falls on the LFER established for the HOCs (see Figure 5b). This suggests that an ionogenic compound in its neutral form will exhibit

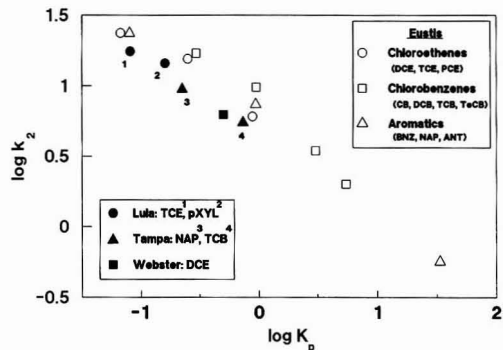


Figure 6. Comparison of data obtained with other sorbents to data obtained with Eustis soil. DCE, 1,2-*trans*-dichloroethene; TCE, trichloroethene; PCE, tetrachloroethene.

nonequilibrium sorption behavior similar to that of nonionic HOCs. A data point obtained for an experiment performed at a pH of 2, where quinoline exists in its charged state, is also plotted in Figure 5b. It is elevated above the LFER of the HOCs (and the neutral quinoline value). At lower pH's, where the ionized species will be present, it might be expected that the observed rate constant would be larger than that measured for the neutral species, since the k_2 measured in such a system would reflect contributions from ion exchange as well as intraorganic matter diffusion. While the results obtained for quinoline are readily explained in terms of the intraorganic matter diffusion model, they cannot be explained by using retarded intraparticle diffusion.

Experiments Using Other Sorbents and Velocities. Miscible displacement experiments were performed using three other sorbents (Lula, Tampa, Webster) in addition to the Eustis soil. The data obtained from these experiments are plotted in Figure 6, along with some of the data obtained for Eustis soil. While some difference appears to exist between the LFERs associated with Eustis and the other sorbents, which suggests that the nature of the sorbent may have an impact on the LFER, this difference does not appear to be of great significance for the sorbents employed in this study.

The data reported above were obtained from miscible displacement experiments using a pore-water velocity of approximately 85 cm/h. At this velocity, the experimental approach used herein, considering the resolution of the analytical and modeling procedures, should be able to discern the presence of rate-limited processes with characteristic times of reaction up to approximately 100 h. The potential existence of a rate-limited process with a larger characteristic time of reaction was investigated by performing experiments using slower velocities. For example, a BTC for TCE/Eustis was obtained with a velocity of 0.4 cm/h. Rate processes with characteristic times upwards of 100 days would be discernable at this velocity. The R value obtained for this slow velocity (2.34) was somewhat larger than the value obtained at the fast velocity (2.04).

The effect of long-term contact was further evaluated by using naphthalene and the Tampa soil. Naphthalene was displaced through the column until $C/C_0 = 1$ was reached. After a 40-day interruption, solution containing no naphthalene was then displaced through the column. The R value obtained for the elution curve was very similar to that obtained for the front, and to that obtained for a previously performed uninterrupted experiment. The elution curve did, however, exhibit more tailing (see Figure 7).

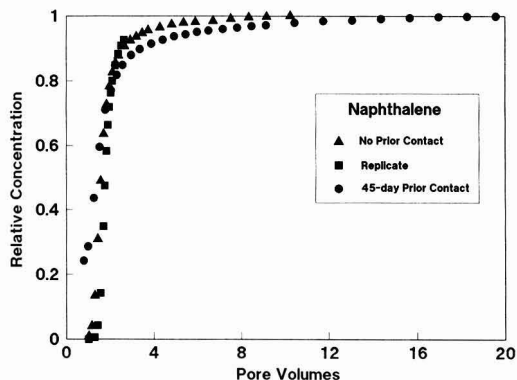


Figure 7. Comparison of long-term contact experiment to normal experiments for naphthalene and Tampa soil.

The results of these experiments suggest that there may be a relatively small additional degree of nonequilibrium that is not apparent at the faster velocity. This could very well involve the longer term migration of sorbate to highly hydrophobic regions of the organic matter.

Summary and Conclusions

A comparison of data obtained from systems wherein intraorganic matter diffusion was not a factor and whose rate-limited sorption was caused by specific sorbate-sorbent interactions to rate data collected for soils, sediments, and aquifer materials showed that the characteristic times of reaction associated with specific sorbate-sorbent interactions were much smaller than the time constants obtained for the natural sorbents. These results suggest that specific sorbate-sorbent interactions did not significantly contribute to the rate-limited sorption of the organic solutes, which supports the proposal that chemical nonequilibrium is not a major rate-limiting mechanism for nonionic, low-polarity organic chemicals. Transport-related nonequilibrium was also shown to not be a factor for the systems investigated. With chemical and transport-related nonequilibrium eliminated, the nonequilibrium sorption observed in the experiments appears to have been caused by a sorption-related, diffusion-limited mechanism. Two such mechanisms have been proposed, intraorganic matter diffusion and retarded intraparticle diffusion. At an operational level, a distinction between the two may not be necessary. However, such a distinction is essential to a mechanistic understanding of the sorption dynamics of organic chemicals.

Several sets of experimental results were presented that could not be explained by using the retarded intraparticle diffusion model. Conversely, they could be explained very well by using the intraorganic matter diffusion model. These results provide strong indirect evidence that the nonequilibrium sorption exhibited by the data reported in this paper was caused by intraorganic matter diffusion. In addition, the nonequilibrium sorption of an ionogenic compound in its neutral form was shown to be similar to that of nonionic HOCs. This observation is important given that many common groundwater contaminants are ionogenic.

The conceptualization upon which the intraorganic matter diffusion model is based is consistent with the generally accepted view of the process by which HOCs are sorbed by natural sorbents (i.e., partitioning to sorbent organic matter). However, the simplified view of partitioning into an organic phase generally ignores the specific

chemical and physical nature of organic matter. While this approach may be adequate in many cases for equilibrium sorption, it is not adequate when considering nonequilibrium sorption. For the latter case, the polymeric nature of organic matter, as well as the dynamics of diffusant-polymer interactions, must be considered.

A question of major interest, in a general sense, is how important the impact of nonequilibrium sorption is on the transport and fate of organic chemicals. The importance of nonequilibrium sorption is expected to be scale dependent (67). For example, the impact of rate-limited sorption is certainly apparent at the laboratory scale; however, the results of recent analyses suggest that nonequilibrium sorption does not significantly contribute to the nonideality observed for the transport of HOCs in groundwater under natural-gradient conditions (67, 68). Sorption nonequilibrium may, however, be of significance for transport under induced-gradient conditions, such as those associated with the "pump and treat" technique of remediating contaminated aquifers (67, 68). It is hoped that the research reported herein will contribute to the resolution of this question.

Registry No. Pentafluorobenzoic acid, 602-94-8; benzene, 71-43-2; toluene, 108-88-3; o-xylene, 95-47-6; p-xylene, 106-42-3; trimethylbenzene, 25551-13-7; ethylbenzene, 100-41-4; n-propylbenzene, 103-65-1; n-butylbenzene, 104-51-8; n-hexylbenzene, 1077-16-3; naphthalene, 91-20-3; anthracene, 120-12-7; chlorobenzene, 108-90-7; 1,3-dichlorobenzene, 541-73-1; 1,2,4-trichlorobenzene, 120-82-1; 1,2,3,4-tetrachlorobenzene, 634-66-2; tetrachloroethene, 127-18-4; trichloroethene, 79-01-6; 1,2-trans-dichloroethene, 156-60-5; quinoline, 91-22-5.

Literature Cited

- (1) Brusseau, M. L.; Rao, P. S. C. *CRC Crit. Rev. Environ. Control* **1989**, *19*, 33.
- (2) Brusseau, M. L.; Jessup, R. E.; Rao, P. S. C. *Water Resour. Res.* **1989**, *25*, 1971.
- (3) Brusseau, M. L.; Rao, P. S. C. *Geoderma* **1990**, *46*, 169.
- (4) Chiou, C. T.; Peters, L. J.; Freed, V. H. *Science* **1979**, *206*, 831.
- (5) Chiou, C. T.; Porter, P. E.; Schmedding, D. W. *Environ. Sci. Technol.* **1983**, *17*, 227.
- (6) Karickhoff, S. W. *Chemosphere* **1981**, *10*, 833.
- (7) Mackay, D. M.; Powers, B. *Chemosphere* **1987**, *16*, 745.
- (8) Brusseau, M. L.; Rao, P. S. C. *Chemosphere* **1989**, *18*, 1691.
- (9) Brusseau, M. L.; Rao, P. S. C. *Environ. Sci. Technol.*, submitted.
- (10) Wu, S.; Gschwend, P. M. *Environ. Sci. Technol.* **1986**, *20*, 717.
- (11) Ball, W. P. Ph.D. Dissertation, Stanford University, Stanford, CA, October 1989.
- (12) Steinberg, S. M.; Pignatello, J. J.; Sawhney, B. L. *Environ. Sci. Technol.* **1987**, *21*, 1201.
- (13) Satterfield, C. N.; Colton, C. K.; Pitcher, W. H. *AIChE J.* **1973**, *19*, 628.
- (14) Chantong, A.; Massoth, F. E. *AIChE J.* **1983**, *29*, 725.
- (15) Hamaker, J. W.; Goring, C. A. I.; Youngson, C. R. In *Organic Pesticides in the Environment*; Advances in Chemistry Series 60; American Chemical Society: Washington DC, 1966; pp 23-37.
- (16) McCloskey, W. B.; Bayer, D. E. *Soil Sci. Soc. Am. J.* **1987**, *51*, 605.
- (17) Choudhry, G. G. *Humic Substances*; Gordon and Bresch: New York, 1983.
- (18) Hayes, M. H. B.; Swift, R. S. In *The Chemistry of Soil Constituents*; Wiley: New York, 1978; Chapter 3, pp 179-320.
- (19) Schnitzer, M. In *Soil Organic Matter*; Schnitzer, M., Khan, S. U., Eds.; Elsevier: New York, 1978; Chapter 1, pp 1-64.
- (20) Stevenson, F. J. *Humus Chemistry, Genesis, Composition, Reactions*; Wiley: New York, 1982; pp 443.
- (21) Wershaw, R. L. *J. Contam. Hydrol.* **1986**, *1*, 29.

- (22) Degens, E. T.; Mopper, K. In *Chemical Oceanography*, 2nd ed.; Riley, J. P., Chester, R., Eds.; Academic Press: New York, 1976; Vol. 6, Chapter 31, pp 59-112.
- (23) Peppas, N. A.; Reinhart, C. T. *J. Membr. Sci.* **1983**, *15*, 275.
- (24) Peppas, N. A.; Moynihan, H. J. *J. Appl. Polym. Sci.* **1985**, *30*, 2589.
- (25) Barrer, R. M. *Kolloid Z.* **1951**, *120*, 12.
- (26) deGennes, P. G. *Scaling Concepts in Polymer Physics*; Cornell University Press: Ithaca, NY, 1979.
- (27) Brusseau, M. L.; Jessup, R. E.; Rao, P. S. C. *Environ. Sci. Technol.* **1990**, *74*, 727.
- (28) Park, G. S. *Trans. Faraday Soc.* **1950**, *46*, 684.
- (29) Park, G. S. *Trans. Faraday Soc.* **1951**, *47*, 1007.
- (30) Klein, J. *Nature* **1978**, *271*, 143.
- (31) Moisan, J. Y. In *Polymer Permeability*; Comyn, J., Ed.; Elsevier: London, 1985; Chapter 4, pp 119-176.
- (32) Rogers, C. E. In *Polymer Permeability*; Comyn, J., Ed.; Elsevier: London, 1985; Chapter 2, pp 11-73.
- (33) Baker, R. *Controlled Release of Biologically Active Agents*; Wiley: New York, 1987.
- (34) Rogers, C. E.; Fels, M.; Li, N. N. In *Recent Developments in Separation Science*; Li, N. N., Ed.; CRC Press: Cleveland, OH, 1972; Vol. II, pp 107-155.
- (35) Kulkarni, M. G.; Mashelkar, R. A. *Polymer* **1981**, *22*, 1665.
- (36) Brusseau, M. L. Ph.D. Dissertation, University of Florida, Gainesville, FL, August 1989.
- (37) Brusseau, M. L.; Rao, P. S. C.; Wood, A. L. *Nat. Meet.—Am. Chem. Soc., Div. Environ. Chem.* **1989**, *29*, 137.
- (38) Van Genuchten, M. Th. Research Report No. 119, USDA Salinity Laboratory, Riverside, CA, 1981.
- (39) Lapidus, L.; Amundson, N. R. *J. Phys. Chem.* **1952**, *56*, 984.
- (40) Valocchi, A. J. *Water Resour. Res.* **1985**, *21*, 808.
- (41) Nkedi-Kizza, P.; Brusseau, M. L.; Rao, P. S. C.; Hornsby, A. G. *Environ. Sci. Technol.* **1989**, *23*, 814.
- (42) Karickhoff, S. W.; Morris, K. R. *Environ. Toxicol. Chem.* **1985**, *4*, 469.
- (43) Oliver, B. G. *Chemosphere* **1985**, *14*, 1087.
- (44) Brusseau, M. L.; Rao, P. S. C.; Jessup, R. E.; Davidson, J. M. *J. Contam. Hydrol.* **1989**, *4*, 223.
- (45) Szecody, J. E. Ph.D. Dissertation, University of Arizona, Tucson, AZ, 1988.
- (46) Szecody, J. E.; Bales, R. C. *J. Contam. Hydrol.* **1989**, *4*, 181.
- (47) Carter, C. W.; Suffet, I. H. *Environ. Sci. Technol.* **1982**, *16*, 735.
- (48) McCarthy, J. F.; Jimenez, B. D. *Environ. Sci. Technol.* **1985**, *19*, 1072.
- (49) Hassett, J. P.; Milicic, E. *Environ. Sci. Technol.* **1985**, *19*, 638.
- (50) Narine, D. R.; Guy, R. D. *Soil Sci.* **1982**, *133*, 356.
- (51) Ruthven, D. M.; Derrah, R. I.; Loughlin, K. F. *Can. J. Chem.* **1973**, *51*, 3514.
- (52) Doetsch, I. H.; Ruthven, D. M.; Loughlin, K. F. *Can. J. Chem.* **1974**, *52*, 2717.
- (53) Vavlitis, A. P.; Ruthven, D. M.; Loughlin, K. F. *J. Colloid Interface Sci.* **1981**, *84*, 526.
- (54) Prager, S.; Long, F. A. *J. Am. Chem. Soc.* **1951**, *73*, 4072.
- (55) van Amerongen, G. *J. Rubber Chem. Technol.* **1964**, *37*, 1065.
- (56) deGennes, P. G. *Phys. Today* **1983**, *36*, 33.
- (57) Barrer, R. M.; Skirrow, G. *J. Polym. Sci.* **1948**, *3*, 549.
- (58) Aitken, A.; Barrer, R. M. *Trans. Faraday Soc.* **1955**, *51*, 116.
- (59) Determann, H. *Gel Chromatography: Gel Filtration, Gel Permeation, Molecular Sieves*; Springer-Verlag: New York, 1968.
- (60) Yau, W. W.; Kirkland, J. J.; Bly, D. D. *Modern Size-Exclusion Chromatography*; Wiley-Interscience: New York, 1979.
- (61) Thompson, M. L.; Zhang, H.; Kazemi, M.; Sandor, J. A. *Soil Sci.* **1989**, *148*, 250.
- (62) Helfferich, F. G. *Ion Exchange*; McGraw-Hill Book Co.: New York, 1962.
- (63) Sposito, G. *The Chemistry of Soils*; Oxford University Press: New York, 1989.
- (64) Sposito, G. *CRC Crit. Rev. Environ. Control* **1986**, *16*, 193.
- (65) Bunzl, K. *J. Soil Sci.* **1974**, *25*, 5170.
- (66) Bunzl, K.; Schmidt, W.; Sansoni, B. *J. Soil Sci.* **1976**, *27*, 32.
- (67) Brusseau, M. L.; Rao, P. S. C. In *Contaminant Transport in Groundwater*; Kobus, H. E., Kinzelbach, W., Eds.; Balkema: Rotterdam, 1989; pp 237-244.
- (68) Brusseau, M. L.; Larsen, T.; Christensen, T. H. *Water Resour. Res.*, submitted.

Received for review January 9, 1990. Revised manuscript received July 2, 1990. Accepted August 20, 1990. This work was supported, in part, by the Florida Dept. of Environmental Regulation, Contract WM-254, and Electric Power Research Institute, Contract RP2879-7. Approved, as a joint contribution, for publication as Arizona Agricultural Experimental Station Journal Series No. 7277 and Florida Agricultural Experimental Station Journal Series No. R-00834.

Hydrolysis of Phenyl Picolinate at the Mineral/Water Interface

Alba Torrents and Alan T. Stone*

Department of Geography and Environmental Engineering, The Johns Hopkins University, Baltimore, Maryland 21218

■ As part of a study of the effect of mineral surfaces on the chemical transformation of organic chemicals, hydrolysis of a pesticide-like compound, phenyl picolinate (PHP) was examined in aqueous suspensions of amorphous silica (SiO_2), γ -aluminum oxide (Al_2O_3), anatase (TiO_2), hematite (Fe_2O_3), and goethite (FeOOH) in the absence of light. TiO_2 and FeOOH caused a significant increase in PHP hydrolysis rate in comparison to homogeneous solution. As the oxide loading increased, a corresponding increase in the rate of hydrolysis was observed. SiO_2 , Al_2O_3 , and Fe_2O_3 exhibited no surface-catalyzed hydrolysis. Although the extent of PHP adsorption was small (less than 5% of total PHP), adsorption was necessary in order for surface-catalyzed hydrolysis to occur. Hydrolysis of the isomer phenyl isonicotinate was not promoted by any of the oxide surfaces examined. These results indicate that adsorption of PHP occurs through chelate formation with surface metal centers involving the heterocyclic nitrogen and the carbonyl oxygen. Surface chelate formation is not possible for phenyl isonicotinate. Surface chelate formation involving PHP activates the carbonyl carbon toward hydrolytic attack in a way similar to metal ion catalysis observed in homogeneous solution.

Introduction

Numerous previous studies have examined the role of adsorption in lowering organic pollutant concentration and retarding pollutant migration in soils, sediments, and aquifers (see ref 1). Adsorption at the mineral-water interface may also, however, affect the nature of chemical degradation reactions and their rates (2). Effects of mineral surfaces on redox (3), polymerization (3, 4), and hydrolysis (5) reactions of organic pollutants have been observed. Relatively little is known, however, about the nature and magnitude of these effects.

Rate constants for many hydrolysis reactions in homogeneous solution have been reviewed by Mabey and Mill (6). Application of this information to aquatic environments in contact with mineral surfaces is difficult, because of uncertainties concerning the effect of adsorption on hydrolysis. El-Amamy and Mill (7) examined hydrolysis reactions of several organic compounds exhibiting different reactivity characteristics in suspensions of montmorillonite and kaolinite. The observed surface catalytic effect was strongest on partially hydrated surfaces (11% moisture content) and diminished dramatically when additional water was added.

In order for surface-catalyzed reactions to occur, organic molecules must first adsorb. The nature and extent of adsorption determine the way in which the mineral-water interface influences hydrolysis. Solute-surface interactions can be divided into (i) specific adsorption, where solute molecules chemically interact with individual surface groups (8-10), and (ii) nonspecific adsorption, where solute molecules experience electrostatic forces and changes in solvent characteristics in the vicinity of the mineral-water interface. If adsorption involves only nonspecific electrostatic interactions with the surface, then the rate enhancement is related directly to the concentration gradient of reacting species in the interfacial region (11). If, however, specific adsorption takes place, the structure and properties of the adsorbed organic compound may change, altering its susceptibility toward hydrolysis.

Catalysis of carboxylic acid ester hydrolysis reactions by acids (6) and by metal ions (12-14) has been observed in homogeneous solutions. Coordination of the carbonyl oxygens by protons lowers the electron density of the carbonyl carbon, facilitating nucleophilic attack (15). Metal ions can catalyze hydrolysis in two ways. First, coordination of the carbonyl oxygen by metal ions can take place, polarizing the oxygen-carbon bond. This facilitates nucleophilic attack at the carbonyl carbon (16-18). Because the carbonyl group is a relatively weak ligand donor group, a second ligand donor group is often necessary (via chelate formation) for metal binding and catalysis to be significant. Second, metal ion-aquo complexes can hydrolyze to produce hydroxo complexes, which then behave as nucleophiles (19, 20). Although the nucleophilicity of metal-coordinated hydroxy groups is typically less than that of OH^- , their concentrations in neutral and acidic solution can exceed concentrations of OH^- by several orders of magnitude.

Mineral surfaces can catalyze hydrolysis reactions of carboxylic acid esters in three ways:

(i) Metals bound to mineral surfaces can coordinate the carbonyl group (and adjacent ligand donor groups) of the ester. Catalysis arises from polarization of the carbonyl oxygen-carbon bond, facilitating nucleophilic attack.

(ii) Hydroxo groups bound to mineral surfaces can act as nucleophiles, providing OH^- for addition to ester molecules.

(iii) Electrostatic forces and other forces operative in the interfacial region can cause accumulation of reactants (ester and nucleophile), facilitating reaction.

Mechanisms i and ii are analogous to mechanisms for metal ion catalysis outlined above. Mechanism iii is unique to surfaces and depends upon the nature of the mineral-water interface (surface charge density, ionic composition in the interfacial region, and so forth).

We embarked on the present study of phenyl picolinate (PHP) hydrolysis in order to explore situations where mechanism i or mechanism ii catalysis might be important. PHP is a neutral ester, not subject to electrostatic accumulation or depletion near charged surfaces. PHP and other picolinic acid esters are subject to metal ion catalysis of hydrolysis in homogeneous solutions (18). Although oxygen atoms comprising the ester linkage are weak ligand donor atoms, the nitrogen heteroatom in the vicinity of the carbonyl oxygen contributes to metal binding and encourages the formation of the chelate complex responsible for the catalytic effect. Analogous surface chelate complexes have been postulated for the adsorption of picolinic acid at the mineral-water interface (21, 22). PHP and other esters capable of forming surface chelate complexes are therefore candidates for mechanism i surface catalysis. Pesticides such as chlorpyrifos and diazinon (both thiophosphate esters with neighboring nitrogen heteroatoms) are among these potential candidates. Our work with the relatively simple PHP hydrolysis reaction should improve our understanding of the effect of the mineral-water interface on the hydrolysis of this broader class of pollutants.

Materials and Methods

All solutions and suspensions were prepared from 18 μm cm resistivity water (DDW, Millipore Corp.). All glassware

Table I. Hydrolysis Rates at Different Mineral Surfaces Normalized by the Amount of Surface Area

oxide	S, m ² /g	pH _{zpc}	site density, sites/nm ²	k _{het} ^a L/(s/m ²)	
				pH 5.00	pH 7.00
SiO ₂ (27) (Aerosol 200)	182.0	2.4		≤3.17 × 10 ⁻¹⁰	≤6.98 × 10 ⁻¹⁰
Al ₂ O ₃ (type C)	92.8	8.9	2-4	≤6.28 × 10 ⁻¹⁰	≤1.37 × 10 ⁻⁹
FeOOH(2) (goethite)	50.1	7.9	6-7	6.54 × 10 ⁻⁹	1.33 × 10 ⁻⁸
FeOOH(1) (goethite + amorphous)	212.0	8.7	3-4	1.08 × 10 ⁻⁸	2.75 × 10 ⁻⁸
TiO ₂ (type P25)	55.0	6.5	3	8.47 × 10 ⁻⁸	8.94 × 10 ⁻⁸

^a k_{het} = (k_{obs} - k_{hom})/a.S.

was cleaned in 5 N HNO₃ and rinsed several times with DDW prior to use. Inorganic reagents were analytical grade (Fisher Chemicals), and the organic reagents were used as received (purity >99% from Aldrich and American Tokio Kasei). PHP was synthesized by the method reported by Felton and Bruce (23) and characterized by NMR.

Particle Preparation and Characterization. γ-Aluminum oxide (Al₂O₃, type C), amorphous silica (SiO₂, Aerosil 200), and titanium oxide (TiO₂, primarily anatase, type P25) were obtained from Degussa Corp. and used without purification. Hematite (Fe₂O₃, type Puratronic) was purchased from Johnson Matthey Corp. and had been annealed. FeOOH(1) was synthesized in our laboratory by addition of FeCl₂ to a 0.1 M acetate-buffered solution (pH 5.4) followed by sparging with 1.0 atm O₂. FeOOH(2) was synthesized by following a modification of the method of Atkinson et al. (24) in which Fe(NO₃)₂ was slowly pumped into a 0.50 M KOH stock solution at 5 °C and then placed in a 70 °C constant-temperature oven for 24 h. Both oxides were dialyzed in cellulose tubing and freeze-dried before storage.

Transmission electron microscopy (TEM) revealed two distinct morphologies in the FeOOH(1) sample, goethite-like rods and fine needles, suggesting the occurrence of two distinct mineral phases. Most particles were 0.1 μm in length or shorter. Electron diffraction lines were indistinct, indicating a low degree of crystallinity. FeOOH(2) samples, in contrast, exhibited electron diffraction lines typical of goethite. Rod-shaped particles typical of goethite range from approximately 0.1 to 1.0 μm in length.

Surface Properties. The specific surface area (S, m²/g) was determined according to the BET method (25). The number of fluoride-binding surface sites (in units of mol/m²) was determined following the method of Sigg and Stumm (26). One gram of each oxide was added to 100 mL of 5.0 × 10⁻³ M NaF solution. The pH was adjusted to 4.7 with an acetate buffer. After an adsorption period of 3 h, the remaining free fluoride in the suspension was analyzed by use of a fluoride-specific ion electrode (Orion Corp.). Monolayer coverage (one F⁻ atom adsorbed on each exchangeable surface site) was assumed.

Acid-base titrations were performed in a 15-mL double-walled beaker. The beaker was connected to a 25 °C water bath and the suspension was purged with N₂ to eliminate CO₂. The suspensions were titrated by adding 5-100 μL of 0.1 M NaOH at intervals of 3 min. The pH_{zpc} (pH of zero proton condition) of each sample was determined by conducting titrations at different electrolyte (NaNO₃) concentrations. Characteristics of these oxides are summarized in Table I.

Hydrolysis Experiments. Hydrolysis experiments were conducted in 40-mL glass vials sealed with Teflon/silicon rubber septa. A predetermined amount of each oxide was suspended in 29 mL of buffered solution. Constant pH was maintained with 1.0 mM acetate, p-nitrophenol, or phosphate buffers. Oxide suspensions were

equilibrated in the reaction solution for 10-12 h before the addition of the organic ester. The ionic strength was adjusted to 0.05 M with NaCl, and a constant temperature of 25 °C was maintained by incubation in a constant-temperature bath.

Stock solutions were used immediately after preparation by mixing an excess of PHP or 2-benzoylpyridine (2-BP) in DDW, followed by filtration (0.2-μm Nuclepore Corp. filter). No organic solvents were used to increase solubility; this eliminated solvent effects on hydrolysis rates (7). Stock solution (1 mL) was introduced into each reaction vial. Suspensions were continuously stirred in a constant-temperature bath with Teflon-coated magnetic stir bars. Vials containing TiO₂ were wrapped with aluminum foil to prevent photochemical oxidation. The absence of oxidation in these and other oxide suspensions was demonstrated by stoichiometric conversion of PHP to the hydrolysis product phenol.

Reaction progress was monitored with a Waters HPLC system using methanol and 5 mM acetate as eluents with a UV detection at 270 nm. The ester and its hydrolysis products were separated with a μ-Bondapak-C₁₈ column (Waters Corp.). The oxides were removed from 1-mL samples either by centrifugation (15000 ppm, 7 min), for aluminum, silicon, and titanium oxides, or filtration (0.2-μm Nuclepore Corp. filters), for iron oxides, and analysis was performed on the supernatant.

Adsorption Experiments. Several adsorption experiments were performed to provide collaborative evidence about the surface chemical reaction. Picolinate and phenol, hydrolysis products, are not degraded in suspensions containing the oxides under study. To examine the adsorption of these hydrolysis products, stock solutions of each compound were added to oxide suspensions, equilibrated for 10-12 h, and then centrifuged to separate supernatant from oxide particles. Picolinate adsorption was determined by measuring loss of picolinate in the supernatant solution with (i) a Dohrmann TOC analyzer and (ii) a Shimadzu UV-160 spectrophotometer. The amount of picolinate adsorbed was high, approaching 100% near pH 5.0. Adsorption of phenol was examined by measuring loss of phenol from supernatant solution by using HPLC. No significant adsorption of phenol was observed with any of the oxide adsorbents.

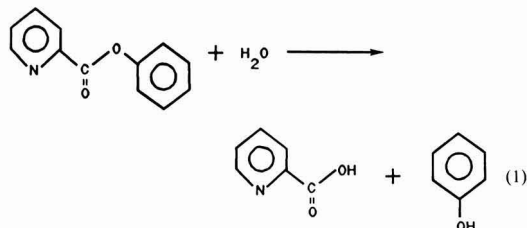
Determining the extent of PHP adsorption is complicated by the concurrent hydrolysis reaction. It was possible to estimate the maximum amount of PHP adsorption by a mass balance approach, which relied upon measurements of PHP and phenol concentrations in solution (see Results and Discussion). Based upon these calculations, less than 5% of PHP was adsorbed at any time during the hydrolysis experiments.

Adsorption of 2-BP was measured by the following procedure: (i) 30 mL of suspension was prepared and equilibrated for 10-12 h; (ii) supernatant and oxide were separated by centrifugation at 20000 rpm for 2 h; (iii) 2-BP (dissolved fraction) was measured directly in the super-

nant by HPLC; (iv) the surface of the collected oxide was rinsed three times with DDW and then resuspended in 3 mL of methanol; and (v) oxide particles were removed from the methanol solution by filtration and 2-BP (adsorbed fraction) was measured by HPLC.

Results and Discussion

Reaction stoichiometry for the hydrolysis of phenyl picolinate is as follows:



The pK_a of PHP is low (1.9, this study) and therefore the neutral species is predominant within the pH range of study. The pK_a 's of the carboxylic acid group and the nitrogen heteroatom of picolinic acid are 1.01 and 5.32 (29), respectively. Phenol is a neutral species within the pH range of study [pK_a 9.92 (30)].

In order to develop mass balance equations, the following variables are required: S , specific surface area (m^2/g); a , oxide loading (g/L); Γ_T , total available surface sites (mol/m^2); Γ_{free} , free surface sites (mol/m^2); $(i)_t$, total concentration (dissolved + adsorbed) of species i (mol/L of suspension); $[i]_{\text{aq}}$, dissolved concentration of species i (mol/L); Γ_i , amount of species i adsorbed (mol/m^2).

The following mass balance equations account for both the adsorption and hydrolysis of PHP:

$$(\text{phenol})_t = [\text{phenol}]_{\text{aq}} \quad (2)$$

$$(\text{PHP})_t = [\text{PHP}]_{\text{aq}} + aS\Gamma_{\text{PHP}} \quad (3)$$

$$(\text{PHP})_0 = (\text{PHP})_t + (\text{phenol})_t \quad (4)$$

$$\Gamma_{\text{PHP}} = (1/aS)[(\text{PHP})_0 - ([\text{phenol}]_{\text{aq}} + [\text{PHP}]_{\text{aq}})] \quad (5)$$

$(\text{PHP})_0$, the total concentration of PHP at the onset of reaction, is known, as well as $[\text{phenol}]_{\text{aq}}$ and $[\text{PHP}]_{\text{aq}}$ (from HPLC measurements of supernatant solution). As mentioned earlier, the amount of phenol adsorbed is insignificant and can be ignored in the mass balance equations. Thus, Γ_{PHP} can be calculated by using mass balance eq 5.

Measurements of Adsorption. According to equation 5, a decrease in the sum ($[\text{PHP}]_{\text{aq}} + [\text{phenol}]_{\text{aq}}$) indicates PHP adsorption. Figure 1 presents results from a hydrolysis experiment (in the presence of 10 g/L FeOOH(1)) where a measurable decrease was observed during a hydrolysis experiment. Although the amount of decrease was small [5% of $(\text{PHP})_0$], it was among the largest observed. In many other experiments, the decrease in ($[\text{PHP}]_{\text{aq}} + [\text{phenol}]_{\text{aq}}$) was too small to be detected. Clearly, the amount of PHP adsorbed at any given moment during hydrolysis experiments was a small fraction of the total concentration of PHP.

Hydrolysis of the PHP ester increases the uncertainty of adsorption determinations, because of the necessity of performing corrections for phenol production. A second, structurally similar compound has been identified, 2-benzoylpyridine, which does not undergo hydrolysis but

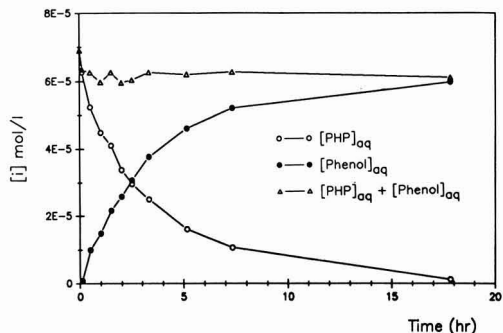
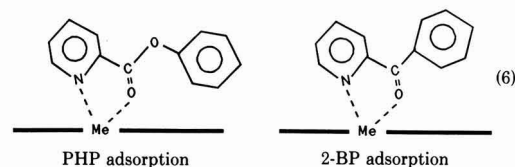


Figure 1. Hydrolysis of 6.90×10^{-5} M PHP in a suspension of 10 g/L FeOOH(1). *p*-Nitrophenol buffer (1×10^{-3} M) is added to maintain pH 7.0, and NaCl (0.05 M) is added to maintain constant ionic strength. A decrease in the quantity ($[\text{phenol}]_{\text{aq}} + [\text{PHP}]_{\text{aq}}$) is observed during the first hour of reaction, indicating that a small amount (5%) of PHP has adsorbed.

should coordinate surface-bound metals in a manner analogous to PHP:



Attempts were made to determine 2-BP adsorption on Al_2O_3 , TiO_2 , FeOOH(1), and FeOOH(2) by measuring loss from bulk solution, using a mass balance equation. The difference in dissolved concentrations before and after addition of oxide was too small to be detected. As described in the Experimental Section, 2-BP was also recovered from the oxide particles collected by centrifugation and analyzed by HPLC. When added in the same concentration range used for PHP (5.0×10^{-5} – 7.0×10^{-5} M), the extent of adsorption was between 3 and 5%. The pK_a of 2-BP is low (≤ 2.5), and therefore, the neutral species is predominant within the pH range of study. The amount of 2-BP adsorbed varied little between pH 4 and 8.

In order to test for adsorption of the hydrolysis products, adsorption of phenol and picolinate was examined. Phenol did not adsorb in detectable amounts while picolinic acid did adsorb, reaching a maximum extent of adsorption near 100% at pH 5. Over the range of PHP concentrations used in the hydrolysis experiments, the generation of picolinic acid did not influence the rate of the surface chemical reaction.

Overall Hydrolysis Kinetics. The following rate equation and its integrated form describe the observed decrease in the total concentration of PHP during hydrolysis:

$$-d[\text{PHP}]_{\text{aq}}/dt = k_{\text{obs}}[\text{PHP}]_{\text{aq}} \quad (7)$$

$$[\text{PHP}]_{\text{aq}} = [\text{PHP}]_0 \exp(-k_{\text{obs}}t) \quad (8)$$

Plots of $\log [\text{PHP}]_{\text{aq}}$ as a function of time were linear for all hydrolysis experiments; k_{obs} (units of s^{-1}) was calculated from the slope.

In pure aqueous solutions, hydrolysis arises from the combined effects of acid-catalyzed, neutral, and base-catalyzed pathways. At fixed pH, hydrolysis is characterized by the rate constant k_w (units of s^{-1}). Addition of a homogeneous catalyst (general-acid or -base catalyst at

$k_a (2.1 \times 10^{-3} \text{ M}^{-1} \text{ s}^{-1})$, $k_n (< 1 \times 10^{-6} \text{ s}^{-1})$, and $k_b (2.2 \cdot 5 \text{ M}^{-1} \text{ s}^{-1})$ were determined...

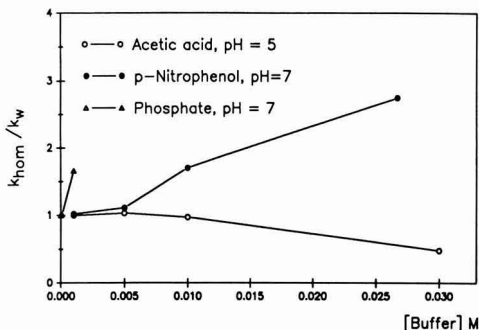


Figure 2. Effect of buffer concentration on PHP hydrolysis rate in particle-free solutions. k_{hom}/k_w represents the observed rate in the presence of buffer divided by the rate at the same pH without buffer.

concentration [B]) provides a competitive hydrolysis pathway characterized by the rate constant k_B (units of $\text{M}^{-1} \text{s}^{-1}$). Hydrolysis occurring in homogeneous solution can be represented by k_{hom} (equivalent to $k_w + k_B[B]$). Catalysis at the mineral-water interface is proportional to the specific surface area (S) and the oxide loading (a) and is characterized by the heterogeneous rate constant k_{het} (units of $\text{L m}^{-2} \text{s}^{-1}$). Thus, in the presence of both a homogeneous catalysis and a catalytic surface at constant pH, eq 7 becomes

$$\begin{aligned}
 -d[\text{PHP}]_{\text{aq}}/dt &= k_{\text{obs}}[\text{PHP}]_{\text{aq}} \\
 &= (k_w + k_B[B])[\text{PHP}]_{\text{aq}} + aSk_{\text{het}}[\text{PHP}]_{\text{aq}} \\
 &= (k_{\text{hom}} + aSk_{\text{het}})[\text{PHP}]_{\text{aq}} \quad (9)
 \end{aligned}$$

In this way, k_{obs} can be divided into a homogeneous (k_{hom}) and a heterogeneous (aSk_{het}) reaction term.

Hydrolysis in Particle-Free Solutions. In the absence of general-acid, general-base, or surface catalysis, the observed hydrolysis rate constant is given by the following equation:

$$k_{\text{obs}} = k_w = k_a[\text{H}^+] + k_n + k_b[\text{OH}^-] \quad (10)$$

Values of k_a ($1.6 \times 10^{-3} \text{ M}^{-1} \text{s}^{-1}$), k_n ($5.5 \times 10^{-7} \text{ M}^{-1} \text{s}^{-1}$), and k_b ($7.1 \times 10^{-8} \text{ M}^{-1} \text{s}^{-1}$) were determined from hydrolysis experiments performed between pH 2 and 10.

In addition to H_3O^+ , OH^- , and H_2O , other chemical species can act as acids or bases to promote hydrolysis (6). In order to test possible buffer effects, hydrolysis experiments were conducted in solutions where the nature and concentration of buffer species were varied. No effect on hydrolysis rates was observed by changing acetate concentration from 0 to $1.0 \times 10^{-2} \text{ M}$; however, at an acetate concentration of $3.0 \times 10^{-2} \text{ M}$, a 50% decrease in the hydrolysis rate was observed (Figure 2). *p*-Nitrophenol does not affect the hydrolysis rate at a concentration of less than 5 mM, while a rate increase was observed at higher concentrations. Phosphate causes a significant increase in rate even at concentrations lower than 1.0 mM. *p*-Nitrophenol and phosphate exert their catalytic effect through a nucleophilic displacement reaction. Both relative nucleophilicities (31) and concentrations must be considered in order to predict the magnitude of buffer-induced catalytic effects. Perdue and Wolfe (32) introduced the concept of "buffer catalysis factor" (BCF) to quantify the effect that buffers may have on hydrolysis rates. Figure 2 shows k_{hom}/k_w as a function of buffer concentration.

Hydrolysis by Mineral Surfaces. Experiments were performed to determine the effect of different mineral surfaces on the hydrolysis of PHP. Hydrolysis reactions were examined in either acetate or *p*-nitrophenol buffer

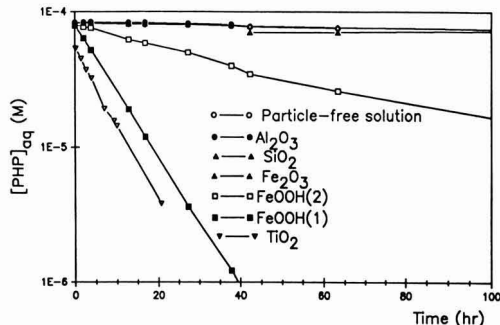


Figure 3. Effect of various mineral oxides on loss of PHP from solution via hydrolysis. All suspensions contained 10 g/L oxide, $1.0 \times 10^{-3} \text{ M}$ acetate buffer (pH 5.0), and $5.0 \times 10^{-2} \text{ M}$ NaCl.

solutions at a buffer concentration of $1.0 \times 10^{-3} \text{ M}$, where no significant buffer effect is expected.

Figure 3 shows the loss of PHP as a function of time at pH 5 as influenced by various oxides at a constant loading of 10 g/L. At constant pH, plots of $\log [\text{PHP}]_{\text{aq}}$ as a function of time were linear over the extent of the reaction followed (2-3 half-lives), indicating a first-order dependence on $[\text{PHP}]_{\text{aq}}$. This behavior was the same under different oxide loading and pH conditions. Figure 3 indicates that TiO_2 , $\text{FeOOH}(1)$, and $\text{FeOOH}(2)$ exerted a strong catalytic effect, while no significant catalytic effect was observed for SiO_2 , Al_2O_3 , or Fe_2O_3 . The absence of catalytic effect with Fe_2O_3 may result from the difficulty in wetting the particle surfaces. All other oxides used in the hydrolysis experiments wetted easily.

Buffers may influence overall rates of hydrolysis in oxide suspensions through either (i) general-acid or -base catalytic effects ($k_B[B]$, discussed earlier) or (ii) adsorption of the buffer at the mineral-water interface, which modifies the kinetics of surface chemical reaction (k_{het}). In order to explore these effects, hydrolysis reactions were performed in suspensions containing as much as $3.0 \times 10^{-2} \text{ M}$ acetate and *p*-nitrophenol buffers. Possible buffer adsorption was examined by measuring loss of the buffer from supernatant solution following centrifugation. For both buffers, no loss was detected. The effect of the two buffers on k_{obs} resembled observations from experiments in particle-free solution; high concentrations of acetate caused a slight decrease in k_{obs} , while high concentrations of *p*-nitrophenol caused an increase in k_{obs} .

The amount of available surface area is an important parameter for catalytic studies. Reactivities of different mineral surfaces can be evaluated by comparing the catalytic effect per unit surface area, given by k_{het} . As is shown in Table I, at both pH 5 and 7, the catalytic effect decreases in the order $\text{TiO}_2 > \text{FeOOH}(1) > \text{FeOOH}(2)$. Fe_2O_3 , Al_2O_3 , and SiO_2 have a negligible effect on hydrolysis rates. More extensive experiments examined the effects of pH (4.5 < pH < 7.5) and surface area loading (from 0 to $3.5 \times 10^3 \text{ m}^2/\text{L}$) on k_{obs} in the presence of TiO_2 , $\text{FeOOH}(1)$, and $\text{FeOOH}(2)$. As shown in Figure 4, the observed hydrolysis rate constant is directly proportional to surface area loading. Experiments were also performed where oxide particles were equilibrated with the reaction medium and then removed by centrifugation prior to PHP addition. No catalytic effect was observed, indicating that dissolved metal ions released by the particles had no effect on the hydrolysis reaction.

Effect of Ionic Strength. Increases in the concentration of the supporting electrolyte (e.g., NaCl) can influence the reaction in two ways. Electrolyte ions may

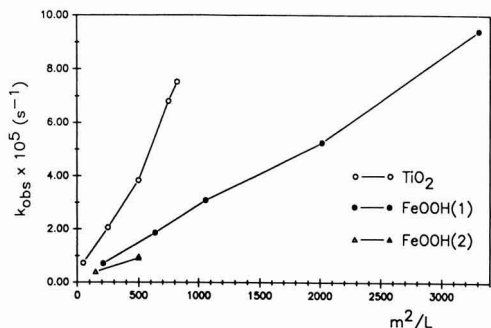


Figure 4. Effect of available surface area on PHP hydrolysis rates in TiO_2 , $\text{FeOOH}(1)$, and $\text{FeOOH}(2)$ suspensions. All suspensions contained 1.0×10^{-3} M *p*-nitrophenol buffer (pH 7.0) and 5.0×10^{-2} M NaCl.

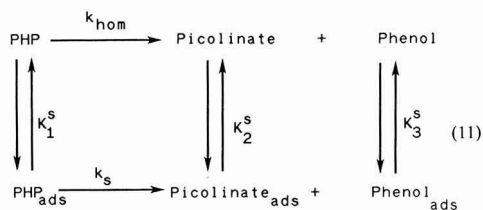
specifically adsorb via outer-sphere surface complexes. If the adsorption energy is sufficiently strong, adsorbed electrolyte ions will compete more successfully against PHP for available surface sites as the ionic strength is increased, lowering rates of interfacial reaction. Increasing ionic strength also increases the charge density in solution, which lowers the effective diffuse layer thickness of the electrical double layer ($1/\kappa$) (33). This, in turn, affects the potential distribution in the interfacial region and the relative importance of various electrostatic phenomena.

Increasing the NaCl concentration from 1.00×10^{-3} to 0.10 M had no significant effect on the hydrolysis rate at mineral surfaces. This suggests that the PHP-surface adsorption energy is significantly greater than the electrolyte-surface adsorption energy. (PHP may form an inner-sphere surface complex, while Na^+ and Cl^- may form outer-sphere complexes.) It also suggests that electrostatic phenomena are of little importance in surface-catalyzed PHP hydrolysis, which is reasonable owing to the neutral charge of the PHP molecule.

Hydrolysis of Phenyl Isonicotinate. PHP is capable of coordinating metal ions in solution via the carbonyl oxygen and heteroatom nitrogen ligand donor groups, forming a five-membered chelate ring. Analogous chelate formation with surface-bound metals should also be possible. In contrast, the isomer phenyl isonicotinate (PHI, $\text{p}K_a$ 2.1) has the same two ligand donor groups, but they are not properly situated for chelate ring formation. In order to gain insight into the mechanism of the surface chemical reaction, hydrolysis reactions of both PHP and PHI were examined in TiO_2 suspensions of similar composition. Between pH 4.5 and 7.5, no surface rate enhancement was observed for the isomer PHI. As was observed for PHP, less than 5% of added PHI was adsorbed under the experimental conditions examined.

Since both compounds are neutral, nonspecific adsorption arising from electrostatic interactions should be negligible. Outer-sphere surface complexes may exhibit a small difference in extent of adsorption between the two isomers. Inner-sphere complexes, in contrast, should exhibit large differences, because of favorable chelate formation involving PHP. Without the assistance of a nitrogen heteroatom in close proximity, it is quite unlikely that the carbonyl oxygen of the isomer PHI will be complexed to a surface-bound metal. Thus, PHP apparently forms an inner-sphere chelate, making it susceptible to surface catalysis, which is analogous to metal ion catalysis observed in solution.

Theoretical Treatment with Regard to Adsorption Phenomena. The system under study may be represented by the following scheme (34, 35):



where k_{hom} is equal to $(k_w + k_B[B])$. Adsorption measurements discussed earlier determined that substantial adsorption of picolinate takes place, while PHP and phenol adsorb to only a small extent. As a consequence, K_2^s is substantially larger than both K_1^s and K_3^s .

Rates of surface chemical reactions are proportional to the adsorption density of reactants. For this reason, eq 9 should be rewritten to express the rate of the surface contribution to reaction in terms of Γ_{PHP} , the PHP adsorption density:

$$-d[\text{PHP}]_{\text{aq}}/dt = k_{\text{obs}}[\text{PHP}]_{\text{aq}} = (k_{\text{hom}})[\text{PHP}]_{\text{aq}} + aS k_s \Gamma_{\text{PHP}} \quad (12)$$

k_s is the intrinsic rate constant (in units of s^{-1}) for hydrolysis of adsorbed PHP. k_{het} (eq 9) and k_s are related to one another through the dependence of Γ_{PHP} on $[\text{PHP}]_{\text{aq}}$. Assuming that PHP adsorption and desorption are fast relative to hydrolysis, Γ_{PHP} on $[\text{PHP}]_{\text{aq}}$ are in quasi-equilibrium with one another. For low surface coverage, a Langmuir isotherm predicts a linear relationship between Γ_{PHP} and $[\text{PHP}]_{\text{aq}}$:

$$\Gamma_{\text{PHP}} = K_1^s \Gamma_T [\text{PHP}]_{\text{aq}} \quad (13)$$

inserting into eq 12 yields

$$d[\text{PHP}]_{\text{aq}}/dt = -(k_{\text{hom}} + aS k_s K_1^s \Gamma_T) [\text{PHP}]_{\text{aq}} \quad (14)$$

According to this equation, if $[\text{PHP}]_{\text{aq}}$ is doubled, rates of both the homogeneous reaction and the heterogeneous reaction should also double. Experiments performed at increasing $[\text{PHP}]_{\text{aq}}$ confirm this relationship. Comparison with eq 9 reveals that k_{het} is equal to $k_s K_1^s \Gamma_T$. Integration of eq 14 yields

$$[\text{PHP}]_{\text{aq}} = [\text{PHP}]_0 \exp[-(k_{\text{hom}} + aS k_s K_1^s \Gamma_T)t] \quad (15)$$

Since a and S are known quantities and k_{hom} has been determined from experiments in particle-free solutions, eq 15 can be used to determine values of k_{het} . Since we were unable to measure the amount of PHP adsorbed (Γ_{PHP}), it is not possible to calculate either K_1^s (the equilibrium adsorption constant) or k_s (the hydrolysis rate constant for adsorbed PHP). For this reason, we can only discuss the combined effects of adsorption and surface reaction (k_{het}); surface hydrolysis rates corrected for different adsorption densities (k_s) cannot be discussed.

Figure 5 presents values of k_{het} as a function of pH in TiO_2 and $\text{FeOOH}(1)$ suspensions. Although k_{het} increases as the pH is increased in $\text{FeOOH}(1)$ suspensions, k_{het} is independent of pH in TiO_2 suspensions. These differences are probably caused by differences in the acid-base speciation of $\text{FeOOH}(1)$ and TiO_2 surfaces, which may influence the extent of PHP adsorption and the concentration of OH^- near the oxide surfaces.

Mechanism of Surface Catalysis. We propose that mechanism i is the most important in controlling the surface catalytic effect on the hydrolysis of PHP. Experimental results will now be discussed to support mechanism i.

Mechanism ii does not require specific adsorption of the ester, only that a portion of the ester resides in the in-

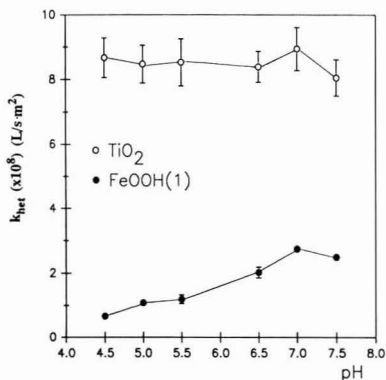


Figure 5. Effect of pH on k_{het} . k_{het} (equal to $\Gamma_T k_s K^3$) is higher in magnitude and less pH dependent for TiO_2 surfaces than for an equivalent area of $FeOOH(1)$. Suspensions were buffered with 1.0×10^{-3} M acetate or *p*-nitrophenol and contained 5.0×10^{-2} M NaCl. Each point was found by regressing k_{obs} against the surface area for five different oxide loadings.

terfacial region. For each molecule in the interfacial region, hydroxyl attack onto PHP and onto the isomer PHI should occur at approximately the same rate. (PHI may actually be faster, because of steric hindrance with PHP.) Since PHI does not experience surface catalysis, mechanism ii cannot be the dominant mechanism.

In order to evaluate the importance of mechanism ii, it is necessary to evaluate the nucleophilicities of different surface sites and the dependence of nucleophilicity on protonation level. It is difficult at this time to make statements about the relative nucleophilicities of different surface sites found on different minerals. To date such data have not been available. Our data exhibit no apparent relationship between the protonation level of the oxides examined and their catalytic reactivity. SiO_2 , which has only neutral and deprotonated groups, exhibited no catalytic activity. Although Al_2O_3 and $FeOOH$ are both protonated surfaces under the conditions examined ($pH < pH_{zpc}$), Al_2O_3 exhibits no catalytic activity, while $FeOOH$ exhibits strong catalytic activity. In homogeneous solution, as the nucleophilic group becomes protonated, nucleophilicity decreases dramatically (36). One would expect that the same trend should be observed for different protonation levels of the same mineral.

Both electrostatic and specific chemical interactions may be involved in the formation of surface complexes. If electrostatic forces are dominant, i.e., mechanism iii, a trend of decreasing surface catalytic effect with increasing electrolyte concentration should be observed. The effect of changing electrolyte concentration was, however, negligible. Clearly, competition for surface sites between PHP and electrolyte ions is not significant. Although OH^- concentrations at the surface may be affected by diffuse layer electrostatic interactions, this does not appear to be important. This observation, together with the fact that surface catalysis of comparable magnitude has been observed on positive, neutral, and negative TiO_2 and $FeOOH$ surfaces, indicates that surface charge and double-layer electrostatic interactions have a negligible effect on the reaction. To conclude, electrostatic interactions cannot account for the primary mechanism. This mechanism has been shown to apply in other situations where the ester carries a negative charge (11).

The fact that PHP is susceptible to surface catalysis, while PHI is not, indicates that the relative position of the two donor groups is important in the formation of a surface

complex. This is strong evidence that chelate formation involving both the nitrogen heteroatom and the carbonyl oxygen is important in the catalytic mechanism. Since chemical bonds are formed, chelate complexes (inner sphere) are stronger and will experience little competition with other more weakly adsorbing medium constituents (buffer ions, electrolyte ions, etc.). This agrees with the reported experimental results. At the same time, the nature of the underlying metal has more influence on the catalytic activity of an oxide than any other characteristic considered. This is additional strong evidence that the ester coordinates directly to the surface-bound metal.

Complex stability is clearly enhanced when a nitrogen donor group is present in the right position for chelate formation. The magnitude of this enhancement varies from one metal to another because of different affinities for nitrogen. Complex formation constants with ammonia provide a good indication of these differences (37). Stability constants for aluminum complexes with ammonia are substantially lower than stability constants for iron(III) with ammonia (38). [We have no information concerning stability of titanium(IV) complexes.] By analogy, stability constants for PHP chelation of surface-bound aluminum sites are likely to be considerable lower than for PHP chelation of surface-bound iron. This observation may explain the differences between the catalytic behavior of Al_2O_3 and $FeOOH$.

With these results, we propose that the coordination of the carbonyl group by a surface-bound metal through a chelate formation is responsible for the surface catalysis. The role of the metal center is to decrease electron density in the ester, thereby lowering the activation energy of hydrolysis.

Summary and Conclusions

Surface-catalyzed hydrolysis of phenyl picolinate has been observed in TiO_2 and $FeOOH$ aqueous suspensions, but not in SiO_2 or Al_2O_3 suspensions. Mechanism i, coordination of the carbonyl oxygen via a surface chelate, is responsible for the surface catalytic effect. This mechanism is analogous to metal ion catalysis of picolinate esters observed in particle-free solutions. The two ligand donor groups of PHP form a chelate with surface-bound metals, facilitating reaction. The nature and relative position of these donor groups is important; the isomer phenyl isonicotinate is unable to form a surface chelate and is not subject to surface catalysis. The lack of an ionic strength effect is collaborative evidence that inner-sphere PHP surface chelate formation precedes hydrolytic attack. The extent of PHP adsorption was too low to be measured. For this reason, differences in extent of adsorption among oxides could not be distinguished from differences in intrinsic rates of surface reaction. k_{het} , the overall surface-catalyzed hydrolysis rate constant, is a reflection of both adsorption and reaction.

Although PHP is not an important pollutant, it bears chemical and structural similarities to important classes of pesticides. By examining the adsorption and surface-catalyzed hydrolysis of such simple compounds as PHP, one can contribute to better understanding of more complex mineral surface-pesticide interactions and can assist in the development of models to predict consequences of pesticide use.

Acknowledgments

We would like to thank Gary Posner of the Department of Chemistry for his useful comments. Ellen M. Shulman-Roskes assisted with the synthesis of PHP. Jill Banfield and David Veblen assisted with electron mi-

croscopy. BET surface area measurements were provided by Micromeritics Instrument Corp.

Literature Cited

- (1) Jury, W. A.; Spencer, W. F.; Farmer, W. J. *J. Environ. Qual.* **1983**, *12*, 558.
- (2) Voudrias, E. A.; Reinhard, M. In *Geochemical Processes at Mineral Surfaces*; Davis, J. A., Hayes, K. F., Eds.; ACS Symposium Series 323; American Chemical Society: Washington, DC, 1986; Chapter 22.
- (3) Ulrich, H. J.; Stone, A. T. *Environ. Sci. Technol.* **1989**, *23*, 241.
- (4) Shindo, M.; Huang, P. M. *Soil Sci. Soc. Am. J.* **1984**, *48*, 927.
- (5) Mingelgrin, U.; Saltzman, S. *Clays Clay Miner.* **1979**, *27*, 72.
- (6) Mabey, W.; Mill, T. *J. Phys. Chem. Ref. Data* **1978**, *77*, 383.
- (7) El-Amamy, M. M.; Mill, T. *Clays Clay Miner.* **1984**, *32*, 67.
- (8) Kummert, R.; Stumm, W. *J. Colloid Interface Sci.* **1980**, *75*, 373.
- (9) Davis, J. A.; Leckie, J. O. *Environ. Sci. Technol.* **1978**, *12*, 1209.
- (10) Zachara, J. M.; Ainsworth, C. C.; Cowan, C. E.; Schmidt, R. L. *Environ. Sci. Technol.* **1990**, *24*, 118.
- (11) Stone, A. T. *J. Colloid Interface Sci.* **1989**, *127*, 429.
- (12) Johnson, G. L.; Angelici, R. J. *J. Am. Chem. Soc.* **1971**, *93*, 1106.
- (13) Angelici, R. J.; Leslie, D. B. *Inorg. Chem.* **1973**, *12*, 431.
- (14) Mortland, M. M.; Raman, K. V. *J. Agric. Food Chem.* **1967**, *15*, 163.
- (15) Hoffmann, M. R. *Environ. Sci. Technol.* **1980**, *14*, 1061.
- (16) Steffens, J. J.; Sampson, E. J.; Siewers, I. J.; Benkovic, S. J. *J. Am. Chem. Soc.* **1972**, *95*, 936.
- (17) Ketelaar, J. A. A.; Gersmann, H.; Beck, M. M. *Nature* **1956**, *177*, 392.
- (18) Fife, T. H.; Przystas, T. J. *J. Am. Chem. Soc.* **1985**, *107*, 1041.
- (19) Buckingham, D. A. In *Biological Aspects of Inorganic Chemistry*; Addison, A. W., Cullen, W. R., Dolphin, D., James, B. R., Eds.; Wiley: New York, 1977.
- (20) Buckingham, D. A.; Clark, C. R. *Aust. J. Chem.* **1982**, *35*, 431.
- (21) Davis, J. A.; James, R.; Leckie, J. U. *J. Colloid Interface Sci.* **1978**, *63*, 480.
- (22) Pope, C. G.; Matijevic, E.; Patel, R. C. *J. Colloid Interface Sci.* **1981**, *80*, 74.
- (23) Felton, M. A.; Bruce, T. C. *J. Am. Chem. Soc.* **1969**, *91*, 6721.
- (24) Atkinson, R. J.; Posner, A. M.; Quirk, J. P. *J. Phys. Chem.* **1967**, *71*, 550.
- (25) Brunauer, S.; Emmett, P. H.; Teller, E. *J. Am. Chem. Soc.* **1938**, *60*, 309.
- (26) Sigg, L.; Stumm, W. *Colloid Surf.* **1981**, *2*, 101.
- (27) Young, J. R. Ph.D. Thesis, California Institute of Technology, 1981.
- (28) Pelizzetti, E.; Minero, C.; Maurino, V.; Sclafani, A.; Hldaka, H.; Serpone, N. *Environ. Sci. Technol.* **1989**, *23*, 1380.
- (29) Green, R. W.; Tong, H. K. *J. Am. Chem. Soc.* **1956**, *78*, 4896.
- (30) Martell, A. E.; Smith, R. M. *Critical Stability Constants*; Plenum Press: New York, 1977; Vol. 3.
- (31) Swain, C. G.; Scott, C. R. *J. Am. Chem. Soc.* **1953**, *75*, 141.
- (32) Perdue, E. M.; Wolfe, N. L. *Environ. Sci. Technol.* **1983**, *17*, 635.
- (33) Stumm, W.; Morgan, J. J. *Aquatic Chemistry*; Wiley-Interscience: New York, 1981; p 617.
- (34) Spiro, M. *J. Chem. Soc., Faraday Trans. 1* **1977**, *73*, 1825.
- (35) Zepp, R. G.; Wolfe, N. L. In *Aquatic Surface Chemistry*; Stumm, W., Ed.; John Wiley & Sons: New York, 1987.
- (36) March, J. *Advanced Organic Chemistry: Reactions, Mechanisms, and Structure*, 2nd ed.; McGraw-Hill: New York, 1977.
- (37) Mulla, F.; Mariscano, F.; Nakani, B. S.; Hancock, R. D. *Inorg. Chem.* **1985**, *24*, 3076.
- (38) Evers, A.; Hancock, R. D.; Martell, A. E.; Motekaitis, R. J. *Inorg. Chem.* **1989**, *28*, 2189.

Received for review April 11, 1990. Revised manuscript received July 19, 1990. Accepted August 15, 1990. This work was supported by the Office of Exploratory Research of the U.S. Environmental Protection Agency (Grant R812944-01-0) and by the Water Resources Research Program of the U.S. Geological Survey (Grant 14-08-0001-G1647). The "Ministerio de Educación y Ciencia" of Spain provided fellowship support for A.T.

Application of the Master Analytical Scheme to the Determination of Volatile Organics in Wastewater Influent and Effluents

Larry C. Michael,* Edo D. Pellizzari, and Daniel L. Norwood†

Research Triangle Institute, P.O. Box 12194, Research Triangle Park, North Carolina 27709

■ Volatile organic compounds were isolated, identified, and quantitated in wastewater influents and effluents by using the EPA Master Analytical Scheme. These analyses were performed as part of a U.S. EPA assessment of water quality in the Great Lakes basin. In addition to 50 target compounds, up to 55 nontarget (unknown) compounds were identified and quantitated in 20 samples obtained from public-owned treatment works (POTWs). This analytical approach showed clear reductions between influents and effluents, in the number of compounds identified, the total concentration of halogenated and non-halogenated compounds, and the concentration of the largest component. Reductions in the number of target compounds detected in influents vs effluents were relatively small in proportion to reductions in the total amounts of halogenated and nonhalogenated compounds. Overall, reductions in nontarget compounds, before and after treatment, were comparable to reductions in target compounds in terms of both number and total concentration.

Introduction

Effluents from municipal wastewater treatment plants are commonly discharged into rivers, either directly or into smaller streams, which subsequently feed into rivers. The chemical composition of these effluents may be affected by many factors, including the industrial/municipal composition of the influent and the nature and performance of the treatment facility. Wastewater effluents contain a variety of pollutants that may ultimately affect the quality of the receiving surface water. Of these diverse pollutants some are present at very low concentrations ($\mu\text{g/L}$) but nevertheless pose a significant threat to water quality. In addition to their direct adverse influence on river water quality, low-level pollutants associated with municipal and industrial wastewaters may also deteriorate treatment efficiency through intrinsic toxicity to treatment plant biota. Overall, the influence of these micropollutants will be most acute during periods of low river volume, when the plant discharge(s) may represent a significant portion of the overall river composition.

A program was conducted by EPA's region V on the Great Lakes basin to acquire data needed to model the water quality impacts of specific organic pollutants. Chemical analysis of influent and effluent water samples from municipal wastewater treatment plants for specific organic pollutants was performed as part of this program. The organic analyses employed the Master Analytical Scheme (MAS) (1), a set of protocols developed to determine a broad spectrum of organic pollutants from a wide variety of chemical classes. The MAS volatile organics (VO) protocol is designed to measure purgeable organic compounds in wastewaters, as well as other types of water. The development and validation of the MAS protocol for volatile organics in water has been previously described (2, 3). The purpose of this study was to determine the

Table I. POTW Samples Analyzed for Volatile Organics by Using the Master Analytical Scheme Protocol

sample code		wastewater treatment	date
influent ^a	effluent ^b	plant collection location	collected
J11-I	J11-E	Jones Island ^c	08/19,20/85
J12-I	J12-E	Jones Island	08/19,20/85
J13-I	J13-E	Jones Island	08/19,20/85
J14-I	J14-E	Jones Island	08/19,20/85
A1-I	A1-E	Akron, OH	07/23,24/85
A2-I	A2-E	Akron, OH	07/23,24/85
G1-I	G1-E	Gary, IN	10/21,22/85
G2-I	G2-E	Gary, IN	10/21,22/85
W1-I	W1-E	Wyandotte ^d	12/15,16/85
W2-I	W2-E	Wyandotte	12/15,16/85

^aI, nonchlorinated influent. ^bE, chlorinated effluent. ^cMilwaukee, WI. ^dDetroit, MI.

relative levels of organic chemicals in influents and effluents at public-owned wastewater treatment works (POTWs) by using the MAS volatile organics protocol.

Experimental Procedures

The MAS VO protocol prescribed all aspects of sample handling and analysis, including sample collection, sample handling, analyte extraction and subsequent isolation of organics, and analysis of volatile organics by gas chromatography/mass spectrometry (1, 2).

Sample Collection and Handling. Volatile organic (VO) compounds were sampled according to the MAS protocols (1). Briefly, water samples were collected without headspace in 250-mL septum-sealed bottles containing National Institute of Science & Technology (NIST) deuterated internal standards (in crushable microcapsules) and magnetic stir bars. Sampling containers were supplied by Research Triangle Institute (RTI) to EPA's region V personnel, who collected the samples and returned them to RTI. Table I lists the samples collected and their origin. Upon receipt of each sample in the laboratory, chlorine was determined and stoichiometrically reduced with sodium thiosulfate. The microcapsules containing the NIST internal standards were crushed by rapid magnetic stirring. The samples were stored at 4 °C in the dark. Blanks (reagent water), controls (reagent water spiked with selected target analytes), and duplicate samples were also dosed with the internal standards and were maintained for quality control purposes.

Isolation of Volatile Components and Analysis. Prior to analysis of samples, system performance solutions (SPS) were analyzed on a Finnigan 4500 GC/MS/COMP to ensure that acceptable instrumental performance was maintained. The system performance solution comprised selected compounds listed in Table II. These compounds were introduced into the chromatographic system as a gas mixture to approximate the conditions encountered by sample components. Subsequently, relative molar response (RMR) factors were determined according to the VO MAS protocol (1) for the target analytes available in the RTI inventory vs deuterated internal standards and external standards. The external standards, 1-bromo-4-fluoro-

* Present address: Glaxo, Inc., 5 Moore Dr., Research Triangle Park, NC 27709.

Table II. System Performance Solution^a

test/function	components(s)	acceptance criteria	observed range
limit of detection (S/N) ^b	1,3,5-trimethylbenzene	S/N (<i>m/z</i> 51) >4:1	5.5-12
peak asymmetry (PAF) ^c	1-octanol	PAF (<i>m/z</i> 70 or 84) <250	140-240
	5-nonanone	PAF (<i>m/z</i> 57) <160	90-110
	acetophenone	PAF (<i>m/z</i> 120 or 105) <300	100-180
acidity/basicity ^d	acetophenone (A)		
	2,6-dimethylphenol (DMP)	DMP/A ratio 0.7-1.3	0.85-1.25
	2,6-dimethylaniline (DMA)	DMA/A ratio 0.7-1.3	0.4-0.5 ^h
separation number (SN) ^e	<i>n</i> -octane	SN ≥40	45-62
	<i>n</i> -decane		
chromatographic resolution (<i>R</i>) ^f	ethylbenzene	<i>R</i> ≥1	2.5->3
	<i>p</i> -xylene		
capillary capacity ^g	<i>n</i> -nonane	PAF >70	100->120
NIST internal standards	bromoethane- <i>d</i> ₅	recovery >40	>40
	chlorobenzene- <i>d</i> ₅		
	anisole-2,4,6- <i>d</i> ₃		
	naphthalene- <i>d</i> ₈		
external standards	1-bromo-4-fluorobenzene	N/A	N/A
	perfluorotoluene		

^a A comprehensive presentation of the application of the system performance solution is given in ref 1. ^b Signal-to-noise ratio for 10 ng of the specific component. ^c % peak asymmetry factor = $B/F \times 100$, where *B* is the width of the back half of the chromatographic peak and *F* is the width of the front half of the chromatographic peak—both at 10 above baseline. ^d Calculated as peak area ratio. ^e Separation number = $D/(W_1 + W_2) - 1$, where *D* is the distance between the apices; *W*₁, *W*₂ are the peak widths at half-height. ^f Calculated as valley = valley/peak height, where valley is the height of the interpeak valley above baseline; peak height is the height of the first peak of the doublet. ^g Calculated equivalent to peak asymmetry factor. ^h Not significant for nonpolar, volatile compounds.

benzene (BFB) and perfluorotoluene (PFT), were used to assess recovery of the internal standards and were used for quantitation only if recovery of all of the latter fell below 40%.

Volatile organic compounds were isolated from the water samples and analyzed as prescribed by the MAS protocol. Briefly, 200 mL of sample was transferred from the sample container into the purge flask, containing 60 g of anhydrous sodium sulfate, by means of a helium-pressurized sample delivery system. After the salt was dissolved, the sample was purged with helium for 20 min at 25 mL/min. During the purging, volatile organic sample components were partitioned into the gas stream and subsequently collected on a Tenax GC (Enka Research Institute, Arhem, The Netherlands) trap. After residual water vapor was removed from the trap with a 5-min "dry purge", the trapped compounds were desorbed from the Tenax trap for 8 min (15 mL/min He) at 200 °C, cryofocused in a liquid nitrogen cooled trap, and subsequently flash evaporated at 200 °C onto the capillary chromatography column. All samples, blanks, and controls were processed by this procedure.

Identification. The procedure for identifying chemicals is not delineated in the Master Analytical Scheme protocol. Compounds were divided into two groups: targets and unknowns. Targets were those compounds for which a relative molar response (RMR) factor had been previously determined. Unknowns were all other volatile organic compounds. Targets were identified by spectral matching of components eluting in specific retention time windows to INCOS (Finnaagin MAT) mass spectral library spectra or to published spectra. These retention windows were determined from the elution of target compounds in the calibration mixtures used previously to determine RMRs. Mass spectra for unknowns, detected above a predetermined threshold, were also compared with INCOS library or published spectra. Accuracy of identification of unknowns was reported as the FIT (i.e., the agreement of the intensity of an ion in the unknown with the intensity of the same ion in the library spectrum, integrated across all spectral ions).

Quantitation. Compounds isolated from water samples were quantified by using a spreadsheet program based on SYMPHONY (Lotus Development Corp.). This program

directly incorporated raw data files from the GC/MS data system into a master spreadsheet and calculated chemical concentrations by using the previously determined RMR factors.

Fifty compounds were targeted for measurement in each sample. Prior to sample analysis, a set of initial RMR values was compiled by repetitive analysis of a calibration mixture of target compounds and internal standards at known relative concentrations. Calculated RMR factors were then input directly to the spreadsheet for use in subsequent calculations.

RMR factors were also calculated for the internal standard compounds vs the external standard, PFT, from daily analysis of the system performance solution. These "daily" RMRs were regressed with the initial RMRs (for internal standards vs PFT) to yield a daily RMR correction factor. This correction factor consisted of a slope and *y* intercept which, when multiplied by the initial RMR database, resulted in an RMR factor that compensated for differences in instrument performance between the date the initial RMR database was created and the specific date of sample analysis (1). Blank samples were processed by using historical analyte recoveries (2). Mean background values (ng) were computed for all analytes detected above 1 µg/L in the blank samples. Control samples were processed by using this blank datum and assumed quantitative recoveries. Ultimately, target compounds identified in each sample were quantitated with the appropriate RMR, the RMR correction factor, the mean background value, the mean recovery and, finally, the sample volume to yield the concentration of that component in micrograms per liter. This mathematical process can be described by the equations

$$\mu\text{g(A)} = \frac{(\text{area}_A)(\text{MW}_A)(\mu\text{g(I.S.)})}{(\text{area}_{\text{I.S.}})(\text{MW}_{\text{I.S.}})(\text{RMR}_{A/\text{I.S.}})(\text{RMR corr. factor})} \quad (1)$$

$$\text{concn (ppb)} = \frac{(\mu\text{g(A)} - \mu\text{g(blank)})}{\text{recovery}_{(A)} \times \text{sample volume (L)}} \quad (2)$$

where *area*_A is the integrated peak area for analyte, A; *area*_{I.S.} is the integrated peak area for the internal standard;

Table III. Concentrations (ppb) of Target Compounds Quantitated in POTW Influent and Effluent Samples^a

compound ^c	mean rec ^d	POTW SITE ^{b,e,f}																			
		J1		J2		J3		J4		A1		A2		G1		G2		W1		W2	
		I	E	I	E	I	E	I	E	I	E	I	E	I	E	I	E	I	E	I	E
Aromatic Hydrocarbons																					
1,2,4-trimethylbenzene	94	7	<1	12	<1	10	<1	7	<1	<1	<1	2									
4-methylisopropylbenzene	100	6	<1	10		2	<1	12	<1	<1	29	<1	9	<1	8	<1	6	<1			
<i>p</i> -diethylbenzene	81	4		6	<1	5		7	<1	<1	<1		<1				<1				
<i>p</i> -diethylbenzene	81	4		6	<1	5		7	<1	<1	<1		<<1				<1				
<i>sec</i> -butylbenzene	113	<1		1		<1		1			5	<1	74	<1			<1				
naphthalene	74	1	<1	2	<1	2	<1	2	<1	<1			6	<1	5	<1	<1				
toluene	125	40	<1	66	<1	50	<1	73	1	7	<1	13	<1	5	<1	5	<1				
ethylbenzene	96	7		12		9		15	<1	8	12		2				2			6	
<i>p</i> -xylene	98	29	<1	40	<1	29	<1	39	<1	4	<1	8	<1	5	<1	91		10			
1,3,5-trimethylbenzene	181	7	<1	13	<1	9	<1	14	<1	<1	<1	2		<1	<1	<1	<1				
Halogenated Aromatic Hydrocarbons																					
1,4-dichlorobenzene	83	1	1	2	<1	2	<1	3	2	1	<1	3	<1	3	<1	3	<1	2	<1		1
Aliphatic and Alicyclic Hydrocarbons																					
1-octene	100							<1													
decane	89	11		21		12		15		3		9		3	<1	2		1			
undecane	50	9	<1	16	<1	10		12	<1	7	<1	14	<1	7	<1	6		10			
dipentene	96		<1		1	<1		3		2		2		5	<1						
nonane	75	4		9		5		6	<1	<1		<1		<1		<1		<1			
Halogenated Aliphatic Hydrocarbons																					
methylene chloride	154	17	49	27	34	14	17	33	39	16	45	31	28	2	14	1	13	3	3		2
chloroform	85	3	12	5		1	11	5	15	2	2	7	2	2	2	1	1	6	1		1
1,2-dichloropropane	128	<1	<1	<1	<1	<1	<1	12	<1									<1	<1		<1
tetrachloroethylene	118	2	5	3	3	3	5	4	6	3	<1	5	<1	2	2	<1	2	3	3		4
trichloroethylene	124		<1		<1	56	<1	59	<1	<1	<1	1	<1	25	<1	23	<1	7	<1		1
<i>trans</i> -1,2-dichloroethylene	100	41	<1	39		32	<1	97	<1	2	<1	4	<1	28	<1	34	<1	4			<1
bromochloromethane	100		<1		<1	<1		<1	2	<1	2		2								
1,2-dichloroethane	246					<1		1			2										
Miscellaneous Oxygen, Nitrogen, and Sulfur Compounds																					
carbon disulfide	100	8	<1	8	<1	<1	<1	19	<1	13	<1	21	<1	1	<1	3	<1	<1	<1		<1
diethyl ether	127					10	2	13	4												

^a Values reported as <1 ppb were greater than the limit of detection but less than the quantifiable limit (1 ppb). Absent values were nondetected compounds. ^b Identified in Table I. ^c Additional target compounds monitored but not detected above 1 µg/L in any sample included the following: *p*-ethyltoluene, 1,2,4-trichlorobenzene, benzyl chloride; *tert*-butylbenzene, 1-octene, 2-bromo-1-chloropropane, hexane, anisole, 1,3-dichlorobenzene, thiophene, 1,2-dibromoethane, bromomethane, phenyl ether, 2-methylfuran, benzyl ether, benzene, *o*-xylene, *o*-ethyltoluene, cyclohexane, heptane, octane, chlorobenzene, 1,2-dichlorobenzene, and dodecane. ^d Mean of five determinations; spiked at 1 ppb (nominal). ^e I, influent sample. ^f E, effluent sample. ^g Sample not analyzed.

MW_A is the molecular weight of analyte, A; MW_{IS} is the molecular weight of the internal standard; RMR/I.S. is the relative molar response of the analyte relative to that of the internal standard; and recovery_A is the fractional recovery of analyte A from control samples.

Recoveries of internal standards were calculated for each sample to determine the optimum internal standard ion(s) to be used for target quantitation. Sample components quantitated with internal standards recovered below 40% were footnoted as minimal values.

Nontarget compounds, "unknowns" (i.e., those compounds for which blank, recovery, and RMR values had not been determined), were quantified in a manner similar to that used for target compounds with the following exceptions: (1) a mean RMR for all internal standard ions was used; (2) no RMR correction factor was used; (3) a recovery of 100% was assigned; and (4) only compounds for which the mass spectrometer's INCOS computer had assigned a FIT of >0.900 were quantified. FIT is a semiquantitative measure of the agreement between the sample spectrum and the INCOS library spectrum, with 0.999 representing an exact spectral match. Quantitative values calculated for unknowns were not as accurate as those for the target compounds.

Results

Mean background values for all target compounds were

below the instrumental limit of detection except for methylene chloride, chloroform, and tetradecane. Methylene chloride and chloroform are ubiquitous compounds in reagent water and have been observed throughout development of the Master Analytical Scheme. Tetradecane is of unknown origin and cannot be accounted for on the basis of general hydrocarbon contamination as no other target hydrocarbons were detected. Mean recovery values (Table III) for target compounds ranged from 50 to 246%. The overall recovery for all targets was 105 ± 42%, with a median value of 100%.

Table III shows the concentrations of all target compounds found above 1 µg/L in all influent and effluent samples. Twenty-four additional compounds (see footnote, Table III) were monitored and occasionally detected but were present at levels too low to quantify accurately. No value is shown for compounds that were not detected. Nontarget compounds are listed in Table IV. Compound classes represented on this list include aliphatic and aromatic hydrocarbons, ketones, aldehydes, alcohols, carboxylic acids, and sulfur compounds, with aliphatic hydrocarbons being, by far, the most prevalent.

Figures 1-3 present an overall summary, by POTW site, of the number of target and unknown organics found, the total level of halogenated compounds, and the total level of nonhalogenated compounds. Plots for target and unknown compounds, in influents and effluents, are pres-

Table IV. Nontarget Compounds Identified in POTW Samples^a

1,1-biphenyl (2)	Aromatic Hydrocarbons	
1,2,3,4-tetramethylbenzene (2)	1-ethyl-3,5-dimethylbenzene	2-methylnaphthalene (2)
1,2,3,5-tetramethylbenzene (6)	1,3-dimethylnaphthalene	4-ethyl-1,2-dimethylbenzene (3)
1,2,4,5-tetramethylbenzene (6)	1,4-diethylbenzene	(1-methylethyl)benzene (5)
1,7-dimethylnaphthalene	2-ethylnaphthalene	ethenylbenzene, dimethyl derivative (5)
1-ethyl-2,3-dimethylbenzene (5)	2-ethyl-1,3-dimethylbenzene (2)	ethynylbenzene (4)
1-ethyl-2,4-dimethylbenzene	1-methylnaphthalene	diethylbenzene (4)
1-ethyl-2-methylbenzene (5)	1-methyl-2-(2-propenyl)benzene (3)	propylbenzene (6)
	1-(chloromethyl)-4-methylbenzene	
	Halogenated Aromatic Hydrocarbons	
none found		
	Miscellaneous Aromatics	
1,2-benzenedicarboxylic acid	2,7-dimethylbenzo[b]thiophene (2)	benzoic acid (3)
2,3,5-trimethylphenol	3,5-dimethylphenol	phenol (5)
2,4,6-trimethylphenol	benzaldehyde (2)	
	Aliphatic and Alicyclic Hydrocarbons	
1,1,2,2-tetramethylcyclopropane	2,2,3-trimethylhexane (2)	3-methyldodecane
2,5-dimethylheptane (3)	2,2,3-trimethylnonane (3)	undecane
2,6,11-trimethyldodecane (2)	2,2,3-trimethylpentane	(2-methylpropyl)cyclopentane
2,6-dimethylheptane (2)	2,2,4,6,6-pentamethylheptane (2)	butylcyclohexane (5)
2,6-dimethylnonane (2)	2-ethyl-2-methylheptane (3)	5,5-dimethyl-1-hexene (2)
17-pentatriacontane	3-methoxy-pentane	5-methyl-(E)-2-hexene
1-dodecane (4)	2,2-dimethylbicyclo[2.2.1]heptane	5-methyldecane (2)
1-ethyl-4-methylcyclohexane (4)	2,3,6-trimethylheptane	6-methyltridecane
2,3,7-trimethyloctane (6)	3-methylhexane	7-methyltridecane
2,3,8-trimethyldecane	(Z,E)-1,3,6-octatriene	propylcyclohexane (5)
2,3-dimethyl-2-hexane	4-methyldecane (2)	5,5-dimethylhexane
2,4,4-trimethyl-1-pentene (3)	decahydro-2-methylnaphthalene	5-ethyl-2-methylheptane (4)
2,4,6-trimethyloctane	2-methylnonane (4)	6-ethyl-2-methyldecane
2,4-dimethyldecane (2)	2-methylundecane (4)	6-methyl-(E)-4-decene
1,3,6-octatriene	2,2,5-trimethylheptane	ethylcyclohexane
2,6-dimethyloctane (2)	2,4,4-trimethyl-2-hexene	hexylcyclohexane (3)
2,6-dimethylundecane (6)	3,7-dimethylnonane (3)	methylcyclopentane (3)
2,7-dimethylnonane	2,2,4-trimethyl-1-pentene	pentane (9)
2-methyldecane	2,2,6-trimethyloctane (5)	1-methyl-4-(1-methylethyl)-1,4-cyclohexadiene
2-methylundecane (2)	propylcyclopentane (4)	2-methyl-4-(1-methylethyl)-7-oxabicyclo[2.2.1]heptane
2,2,3,4-tetramethylheptane (2)	3-methyldecane (5)	3-ethenyl-1,2-dimethyl-1,4-cyclohexadiene
2,2,3,4-tetramethylpentane (7)		
	Halogenated Aliphatic Hydrocarbons	
1,1-dichloroethane (4)	bromodichloromethane (1)	
	Miscellaneous Oxygen, Nitrogen, and Sulfur Compounds	
1,1-dichloro-1-nitroethane (3)	thiobismethane (3)	dimethyl disulfide (4)
1-butanol (2)	4,4-dimethyl-2-pentanone (2)	dodecamethylhexasiloxane (2)
2-butanone (4)	4-ethyl-1-octyn-3-ol (4)	methanethiol (2)
2-butoxyethanol (2)	4-methyl-2-pentanone (7)	<i>o</i> -decylhydroxylamine (7)
2-dodecanol	acetic acid	1,3,3-trimethylbicyclo[2.2.1]heptan-2-ol acetate
2,6-dimethyl-4-heptanone (2)	2-pentanone	1,7,7-trimethylbicyclo[2.2.1]heptan-2-one
2-butyl-1-octanol (7)	2-propanone (5)	2-methyl-5-(1-methylethyl)cyclohexanol acetate
2-ethylhexanol	2-propyl-1-heptanol (3)	5-methyl-2-(1-methylethyl)cyclohexanol
2-ethyl-1-hexanol	tetrahydrofuran (2)	5-methyl-2-(1-methylethyl)cyclohexanone
2-ethyl-4-methylpentanol	4,4-dimethyl-2-oxetanone	5-methyl-2-hexanone (4)
2-ethyl-4-methyl-1-pentanol (2)	decanal	dimethyl trisulfide
2,2,4,4-tetramethyl-3-pentanone	4-penten-2-ol	2-methyl-1-propanol

^a Parenthetical number indicates the number of samples in which the nontarget compound was identified.

ented in the same figure for a given parameter. Numbers of target compounds found, across all samples, were notably similar for both influents and effluents. Unlike target compounds, unknown compounds were not necessarily the same compounds in samples collected at different POTWs or between influent and effluent samples collected at the same treatment plant. Nevertheless, trends with unknowns were observed. Predictably, greater numbers and levels of compounds were measured in influents than in effluents. However, while differences in numbers of compounds detected between influent targets and effluent targets were, for most POTWS, very small (Figure 1), numbers of unknown VO compounds detected in influent samples exceeded those in corresponding effluents by factors ranging from 2 to 10 (Figure 1). This suggests a somewhat enhanced removal efficiency for nontargets over

targets. Although differences in numbers of target compounds found between influents and effluents were relatively small, differences in total amounts of halogenated (Figure 2) and nonhalogenated (Figure 3) targets between influent and effluent samples were generally quite large. It appears that, while the target compounds were not being eliminated by the treatment process, their cumulative amounts had been greatly reduced. For all sampling locations, halogenated target compounds accounted for the majority of the halogenated species (i.e., very few nontarget, halogenated compounds were identified). Furthermore, total halogenated target compound levels in influents generally exceeded corresponding effluent levels by a factor of 2–3 (Figure 2). However, while the total concentration of halogenated target compounds is appreciably lower in effluents than in influents, Table III clearly

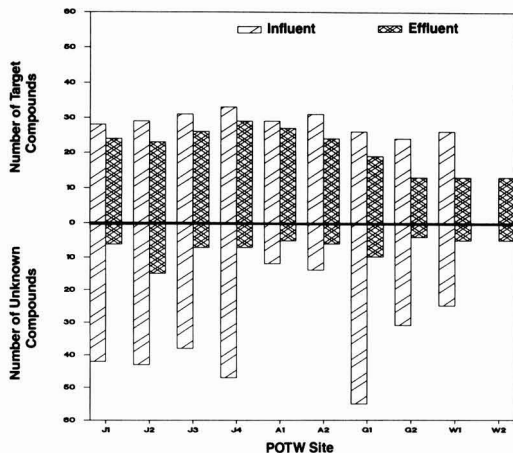


Figure 1. Number of target and nontarget volatile organic compounds found in influent and effluent POTW samples.

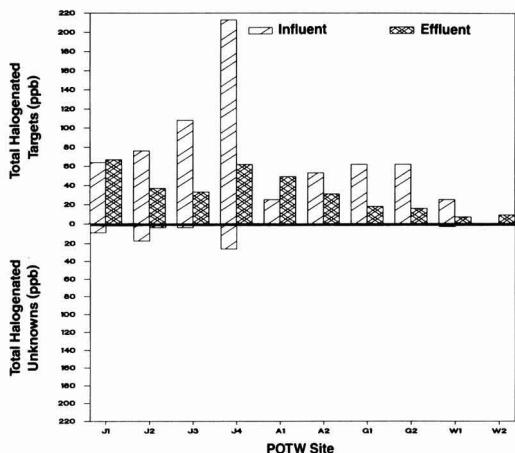


Figure 2. Total concentration of halogenated, target and nontarget volatile organic compounds found in influent and effluent POTW samples.

shows that methylene chloride and chloroform are enhanced in many cases after treatment. This observation may be indicative of in situ halogenation reactions resulting from the treatment process. Few, if any, halogenated nontarget compounds were detected in the wastewater effluent samples and in only 5 of the 10 influent samples (Figure 2). Conversely, comparable amounts of nonhalogenated target and nonhalogenated unknown compounds were found in most influent samples (Figure 3). Reductions in nonhalogenated compound levels as a result of wastewater treatment were, in general, more dramatic than reductions of halogenated compounds. This alludes to possible differences in actual treatment mechanisms acting upon halogenated and nonhalogenated species. Ratios of influent levels to effluent levels for both targets and unknowns at a given location ranged from 2 to >100, with effluent levels near or below the limit of detection for many locations.

Overall, toluene, *trans*-1,2-dichloroethylene, and methylene chloride predominated as the major compounds found in influent samples. Methylene chloride, chloroform, and tetrachloroethylene were the dominant targets found in effluents. Aliphatic hydrocarbons were the highest

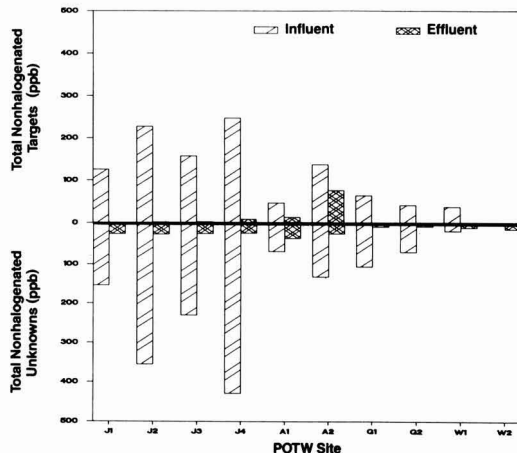


Figure 3. Total concentration of nonhalogenated, target and nontarget volatile organic compounds found in influent and effluent POTW samples.

concentration nontargets in influents and effluents, although methyl isobutyl ketone and an alkylsiloxane were present as major species in three influent and three effluent samples, respectively. It is highly likely that this siloxane was not a sample constituent but rather an artifact of the analytical system.

Summary and Conclusions

The results of the analysis of 19 samples (9 influent, 10 effluent) for volatile organic compounds using the Master Analytical Scheme protocol show that this approach can contribute to characterization of wastewater influents and assessment of treatment efficiency for POTWs and that VO analysis using the MAS can be applied to the chemical characterization of influents and effluents and also to assist in differentiation between POTWs. These results illustrate that characteristic differences in the 10 treatment facilities can be observed as a result of application of the MAS to volatile organic compounds.

Acknowledgments

We express sincere appreciation to RTI staff members S. Cooper and T. Pack for their assistance in sample workup and GC/MS/COMP analysis. Grateful acknowledgement is also expressed to Dr. A. W. Garrison and associated staff of the Athens Environmental Research Laboratory, U.S. EPA Athens, GA, for their assistance in sample acquisition and editing of the manuscript. Samples and background data were supplied by the Great Lakes National Program Office, U.S. EPA, under the direction of J. Giatina of that office. His assistance is greatly appreciated.

Literature Cited

- (1) Pellizzari, E. D.; Sheldon, L. S.; Bursley, J.; Michael, L. C.; Zweidinger, R. A. Master Analytical Scheme for Organic Compounds in Water. Final Report on U.S. EPA Contract No. 68-03-2704; U.S. Environmental Protection Agency, Washington, DC, 1985.
- (2) Michael, L. C.; Pellizzari, E. D.; Wiseman, R. W. *Environ. Sci. Technol.* **1988**, *22*, 565-570.
- (3) Michael, L. C.; Wiseman, R.; Sheldon, L. S.; Bursley, J. T.; Tomer, K. B.; Pellizzari, E. D.; Scott, T. A.; Coney, R.; Garrison, A. W.; Gebhart, J. E.; Ryan, J. F. Quality of Master Analytical Scheme Data: Purgeables and Volatile Organic Acids. In *Advances in the Identification and*

Analysis of Organic Pollutants in Water; Keith, L. H., Ed.; Ann Arbor Science: Ann Arbor, MI, 1981; Vol. 1, pp 87-114.

research described was funded by the U.S. Environmental Protection Agency (Contract 68-01-6904), it has not been subjected to the required peer and administrative review and does not necessarily reflect the views of the agency, and no official endorsement should be inferred.

Received for review December 13, 1989. Revised manuscript received July 16, 1990. Accepted July 31, 1990. Although the

Pesticide Occurrence and Distribution in Fog Collected near Monterey, California

Charlotte J. Schomburg,*[‡] Dwight E. Glotfelty,[†] and James N. Seiber

U.S. Department of Agriculture, Agricultural Research Service, Environmental Chemistry Laboratory, Beltsville Agricultural Research Center, Beltsville, Maryland 20705, and Department of Environmental Toxicology, University of California, Davis, California 95616

■ We analyzed pesticides in air and fog in several fog events sampled near Monterey, CA, to determine whether the uptake of pesticides in advected oceanic fog was different from uptake in fog forming under stagnant inversion conditions in California's Central Valley in the winter. Data for several pesticides common to both areas showed that the pesticide content and distribution were remarkably similar in the two locations. The conversion of organophosphorus insecticides to their corresponding oxons, and aqueous-phase enrichment factors, were also very similar. Evidence is presented to support the hypothesis that enhanced pesticide concentration in fogwater is caused by strongly sorptive nonfilterable particles and colloids in the fog liquid that are derived from atmospheric particles.

Introduction

The occurrence and distribution of pesticides in fog have been previously reported. Wintertime fog collected in the Central Valley of California was found to contain primarily organophosphorus insecticides used in winter dormant spraying of deciduous fruit and nut orchards. Concentrations in fogwater reached as high as 20-50 µg/L for parathion, diazinon, methidathion, and chlorpyrifos. Pesticide concentrations in the fogwater were higher than expected, considering the air pesticide concentration and Henry's law constants for the pesticides. Oxon transformation products were also found in these samples (1, 2).

Central Valley fog is the result of air stagnation and intense radiational cooling that occurs under high-pressure systems from December through February. The possibility exists that the high pesticide concentrations in this fog may result from the buildup of contaminants in the atmosphere under these stagnant conditions and therefore are unique to the Central Valley fog. By contrast, coastal fog, which forms along California's Pacific coast in late summer, usually results from the advection of oceanic air over land surfaces. One might expect that this fogwater would contain lower concentrations of pesticides in that there would be little opportunity for pollution buildup of the type found in the Central Valley. This coastal area is also a prime agricultural area where a variety of pesticides are used. We decided to analyze the pesticide content and distribution in these coastal fogs to determine whether the uptake and distribution was similar to that which occurs in Central Valley fog. To this end, simultaneous fogwater and interstitial air samples were collected during fog events near Monterey, CA, in September 1987. These samples

were analyzed for a variety of pesticides that are used on the agricultural crops in the area, as determined from pesticide use reports.

Methods

Sampling Locations. The coastal fog and air samples were collected from three locations along the Pacific coast near Monterey, CA, in September 1987. The first location was along Struve and Giberson Roads between State Highway 1 and the ocean, a distance slightly greater than 1.5 km. The roads were bounded by fields of lettuce, brussels sprouts, parsley, and squash, while large fields of broccoli, artichokes, and strawberries grow in the general vicinity. Two fog events were sampled at this location, one occurring on 9/16/87 and the other 9/20/87.

The second sampling location was Hecker Pass. This site was approximately 15 km from the coast at an altitude of approximately 300 m in the Coastal Range Mountains. The sampling site was a turnout along State Highway 152. There were no agricultural fields nearby, only forest land and a few residences. These samples were collected on 9/18/87.

The third sampling location was Aguajito Road, east of Monterey. This is a wooded area with a few homes along the road, and no agricultural fields nearby. The fog and air samples from this location were collected in two differing time periods to see if the fog pesticide content changed with time. These samples were collected on 9/19/87.

These coastal fog events would usually start to form after 3 a.m., be densest just before dawn, and be completely dissipated several hours after sunup. The water contents of these coastal fogs ranged from 0.05 mL/m³ for the later Aguajito Road sample to 0.21 mL/m³ for the Struve and Giberson Road sample on 9/20/87. Sampling locations, liquid water contents, filtered particle content, and pH values are listed in Table I.

Sampling. The liquid fog samples were collected by a high-volume fog sampler mounted on top of a pickup truck. The sampler is a scaled-up version of that reported by Jacob et al. (3). A 50-cm-diameter fan in the back draws air at the rate of 4400 m³/h across a screen consisting of four layers of 0.28-mm Teflon filaments wound around threaded rods. Fog droplets impact on the Teflon filaments, coalesce, and flow down the filaments into a Teflon-coated funnel. The fogwater then drains by gravity through a Teflon tube to a Teflon bottle inside the truck. Collection rate is approximately 1 L/h in fog with 400-m visibility. Collection efficiency is approximately 75%, with most of the loss due to reentrainment of coalesced water

U.S. Department of Agriculture.
University of California.

Table I. Coastal Fog Sampling Sites near Monterey, CA. Fog Events Sampled in September, 1987

location	date (time)	av liquid water content, mL/m ³	filtered fogwater particles, mg/L	pH	description
Struve and Giberson Rds.	9/16 (0539-0756)	0.16	74.4	6.6	agricultural area
Struve and Giberson Rds.	9/20 (0532-0927)	0.21	49.1	6.8	agricultural area
Hecker Pass	9/18 (0736-0946)	0.08	96.2	6.4	nonagricultural, mountain, wooded
Agujaito Rd.	9/19 (0650-0839)	0.12	184	5.4	nonagricultural, wooded
Agujaito Rd.	9/19 (0850-1011)	0.05	87.2	5.1	nonagricultural, wooded

drops from vibrating filament. The Teflon filaments, funnel, tubing, and collection bottle were thoroughly rinsed with water and then acetone before each fog collection.

Interstitial air was sampled at a rate of 45–50 m³/h with a high-volume dichotomous air sampler (4) that was mounted on top of the pickup truck next to the fog sampler. Fog droplets of ≥8 μm were removed from the incoming air through the large particle orifice. Small particles and vapors passed first through a glass fiber filter to trap particles and then through a bed (8.8-cm diameter, 2.6-cm depth) of XAD-4 resin (20/50 mesh, Rohm and Haas, Philadelphia, PA) to trap vapor-phase pesticides. The method of resin preparation is described elsewhere (5).

The fog sampler and the dichotomous air sampler were operated simultaneously by a small gasoline generator mounted in the back of the pickup truck. If a wind was blowing, the truck could be parked into the wind and remain stationary during sample collection. During periods of light and variable winds the truck was kept moving during collection to avoid contaminating the sample with generator exhaust. Blank samples of dichotomous glass fiber filters and XAD-4 resin were obtained by loading these materials into the dichotomous air sampler and turning the sampler pumps on for several seconds. These blanks were then treated just as samples.

Aliquots (20 mL) of fogwater were taken from each sample for pH determination. Aliquots (100 mL) were taken from the early Agujaito Road and Struve and Giberson Roads (9/20/87) fogwater samples for pesticide spiking. These two aliquots along with low-carbon water from the laboratory were each spiked with 10 μg of isofenphos. Isofenphos is an organophosphorus pesticide not expected to be found in fog or air samples from the coastal area. These spiked aliquots were treated as the other fogwater samples to check recovery and thion to oxon conversion during storage and sample workup.

Sample Workup. Fogwater samples were refrigerated until they could be extracted. The fogwater was first filtered through a double layer of weighed and baked glass fiber filters as described elsewhere (2). The fogwater and filters were then extracted by following procedures reported elsewhere (2, 6). Particle weights were determined on dried filters following extraction. Filters were then sent to an outside laboratory (Galbraith Laboratories, Inc., Knoxville, TN) for carbon, hydrogen, and nitrogen analysis of particles. Percent organic carbon content of the particles filtered from the fogwater could then be determined and used in pesticide partition coefficient calculations. Filter and glassware blanks, obtained from 100 mL of the same solvent used in the extraction procedure (dichloromethane), were carried through each step of the sample workup.

The XAD-4 resin used for air sampling was extracted three times with ethyl acetate (5). The dichotomous sampler glass fiber filters used to trap aerosol particles were extracted in a Soxhlet apparatus for 6 h with 1:1 hexane–acetone. (All solvents used were residue grade, Baxter, Burdick & Jackson Division, Muskegon, MI.)

All sample extracts were concentrated on a steambath by use of Kuderna–Danish evaporative concentrators with three-ball Snyder columns. In the final stages of the evaporation, the solvent was exchanged to benzene. Half of each extract was archived. The other half was fractionated into four fractions by normal-phase HPLC, using a hexane to methyl *tert*-butyl ether solvent gradient (5). The fractionation step effectively separated compounds by polarity and helped resolve peaks that otherwise would have coeluted during gas chromatograph (GC) analysis. Each of the fractions was concentrated and exchanged to benzene.

Gas Chromatographic Analysis. The pesticides were analyzed by gas chromatography using a Hewlett-Packard 5890A gas chromatograph equipped with a split inlet, 30 m × 0.32 mm i.d. DB 1+ bonded-phase capillary column with 0.25-μm film thickness (J&W Scientific, Folsom, CA), and a nitrogen–phosphorus detector. Gas flows at the detector were breathing air at 123 mL/min and, ultra-high-purity hydrogen at 5.3 mL/min. Helium was the carrier gas, at a flow rate of 2.3 cm³/min and linear gas velocity of 48 cm/s (all gases were obtained from Air Products and Chemicals, Inc, Allentown, PA). Initial column temperature was held at 160 °C for 1 min, then programmed upward at 5 °C/min to a final temperature of 210 °C, and held for 5–10 min. The detector temperature was 250 °C. The inlet temperature was 250 °C for the parent organophosphorus insecticides, 215 °C for oxons, and 230 °C for carbaryl analysis.

Confirmation was achieved by GC/mass spectrometry using a Hewlett-Packard 5970 mass-selective detector, a selective-ion-monitoring program, and similar chromatographic conditions as described above, or by quantitative agreement with a Tracor 222 gas chromatograph equipped with a packed column and a flame photometric detector. The Tracor GC column measured 1.8 m × 2 mm i.d. and was packed with 1.5% OV-17–1.95% OV-210 on 100/120 mesh Chromosorb W-HP (Supelco, Bellefonte, PA). This GC had a split inlet set at 190 °C, oven at 200 °C, and detector at 220 °C and was operated isothermally.

Results and Discussion

Pesticides. Pesticide concentrations measured in coastal fog are reported in Table II. The compounds found in the largest amounts and most easily identified in the coastal fog and air samples were diazinon, methyl parathion, malathion, methidathion, chlorpyrifos, and fonofos, all organophosphorus insecticides, and carbaryl, a carbamate insecticide. The organophosphorus compounds are known to be used extensively on agricultural crops in the area including broccoli, brussels sprouts, lettuce, melons, parsley, squash, strawberries, and artichokes. Carbaryl is commonly used on pastureland and by homeowners on lawns and gardens. The oxygen analogues or oxons of most of the organophosphorus insecticides were also identified in the coastal fog samples.

Pesticide concentrations were higher in the fogwater samples collected in the agricultural areas (Struve and Giberson Roads) (Table II) than in the nonagricultural

Table II. Pesticide and Oxon Concentrations ($\mu\text{g/L}$) Found in Coastal Fogwater Collected September 1987 near Monterey, CA

compound	sampling dates ^a				
	9/16 agr	9/18 non-agr ^b	9/19 early non-agr ^b	9/19 late non-agr ^{b,c}	9/20 agr ^c
diazinon	3.6	0.15	1.1	2.0	4.8
diazoxon	2.4	1.9	2.4	5.1	11
methyl parathion	0.046	0.19	<0.049	<0.10	0.43
methyl paraoxon	0.039	0.49	0.090	0.33	0.12
malathion	3.8	0.16	0.14	0.30	8.7
malaoxon	3.2	2.2	0.90	3.0	7.8
chlorpyrifos	0.036	<0.014	<0.014	0.012 tr	0.19
chlorpyrifos oxon	0.008	0.066	0.063	0.23	0.14
fonofos	0.030	<0.014	<0.014	<0.012	0.018
paraoxon	0.011	<0.012	0.034	0.35	0.015 tr
methidathion	0.036	<0.049	<0.040	<0.085	0.22
methidathion oxon	0.030	<0.056	<0.033	<0.012	0.028
carbaryl	0.069	4.0	2.7	2.4	0.098

^a9/16 and 9/20 at Struve and Giberson Rds., 9/18 at Hecker Pass, 9/19 at Aguajito Rd. ^b< indicates below the level of detection (LOD). ^ctr indicates trace, where LOD < tr < 3 × LOD.

Table III. Oxon to Thion Ratios for Several Organophosphorus Insecticides in Fogwater Collected near Monterey, CA in September 1987

parent pesticide	sampling date ^a				
	9/16 agr	9/18 non-agr	9/19 early non-agr	9/19 late non-agr	9/20 agr
diazinon	0.67	13	2.2	2.6	2.3
methyl parathion	0.85	2.6	>1.8	>3.3	0.28
malathion	0.84	14	6.4	10	0.90
chlorpyrifos	0.22	>4.7	>4.5	19	0.74
methidathion	0.83	>1.1			0.13

^a9/16 and 9/20 at Struve and Giberson Rds., 9/18 at Hecker Pass, 9/19 at Aguajito Rd.

areas at Hecker Pass and Aguajito Road. An exception to this is the carbaryl concentration, which was higher in the nonagricultural areas, perhaps due to the use of this compound by homeowners. The two compounds found in the highest concentrations, diazinon and malathion, were used on the widest variety of crops in the area.

Oxons. As with the parent compounds, the oxon concentrations were generally higher in the agricultural areas. However, in some fogwater samples the concentrations of the oxon exceeded the parent pesticide concentration. This is illustrated by the oxon to thion ratios given in Table III. The largest ratios were found in the nonagricultural areas, Hecker Pass and Aguajito Road. Diazoxon and malaoxon are especially prominent. The malaoxon concentration in the later Aguajito Road sample was 10 times the malathion concentration and chlorpyrifos oxon was almost 20 times the chlorpyrifos concentration.

Thion to oxon conversion appears to take place during atmospheric transport from agricultural areas to the nonagricultural areas. Laboratory-measured aqueous-phase conversion rates of organophosphorus insecticides in dilute peroxide solutions prove to be too slow to account for the oxon concentrations observed in fogwater to result from conversion within the fog droplet (7). The coastal fog events sampled generally lasted ~6 h. Most likely, thion to oxon conversion takes place in the vapor phase, followed by partitioning into the fog droplet (8). It is likely that the higher oxon levels in the later Aguajito Road

Table IV. Ranges of Concentrations, Oxon to Thion Ratios, and Enrichment Factors for Pesticides in Fogwater Collected near the Pacific Coast, September 1987, and in California's Central Valley, January 1986 (2)^a

compound	coastal	Central Valley
	Fogwater Concentration $\mu\text{g/L}$	
diazinon	0.15–4.8 (5)	0.31–18 (6)
methyl parathion	0.046–0.43 (2)	
parathion		2.7–39 (6)
malathion	0.14–8.7 (5)	
chlorpyrifos	0.036–0.19 (2)	0.39–7.7 (6)
methidathion	0.036–0.22 (2)	0.093–4.8 (6)
fonofos	0.018–0.030 (2)	
	Oxon to Thion Ratios	
diazinon	0.67–13 (5)	0.056–7.1 (6)
methyl parathion	0.28–2.6 (3)	
parathion		0.02–1.2 (6)
malathion	0.84–14 (5)	
chlorpyrifos	0.22–19 (3)	0.16–1.4 (5)
methidathion	0.13–0.83 (2)	0.79–2.2 (6)
	Enrichment Factors (EF)	
diazinon	30–50 (2)	6–160 (5)
parathion		4–29 (5)
malathion	6 (1)	
chlorpyrifos	19–25 (2)	7–74 (5)
methidathion		0.02–3 (5)
fonofos	3–5 (2)	

^aNumber of samples in range in parentheses.

sample were the result of the generation of photochemical oxidants from the increasing sunlight intensity.

The oxon to thion ratios of the coastal fogwater were similar to ratios found in the Central Valley fogwater (Table IV). This is an indication that the buildup of pollutants in the more stagnant Central Valley atmosphere is not the major reason for the conversion of thions to oxons. It is interesting to note that the highest oxon to thion ratios reported for the Central Valley fog events (2) were from the sample collected furthest from the pesticide application sites, as was the case with the coastal fogwater samples.

The conversion of isofenphos to isofenphos oxon in the spiked fogwater and laboratory water ranged from 0.18% to 1.4%, with the highest conversion taking place in the laboratory water. Isofenphos recovery from these spiked aliquots ranged from 100% to 118%. Isofenphos was not detectable in the nonspiked samples. The spiked laboratory water had been stored, refrigerated, 8 days before extraction. The spiked 9/20/87 fogwater had been stored 12 days and the spiked 9/19/87 fogwater had been stored 38 days refrigerated before extraction. These results indicate the storage and workup did not contribute to the thion to oxon conversion of isofenphos. Also, oxidant levels or other components in these fogwater samples were not affecting the conversion. Although the compounds identified in the fog samples were organophosphorus insecticides other than isofenphos, and the thion to oxon conversion rates may vary for different compounds, we feel the results of the spiking and recovery experiment indicate that the storage and sample workup did not contribute to the oxon levels found in the fog samples.

Comparison of Pesticide Concentrations in Coastal and Central Valley Fog. Some pesticides are applied both to vegetable crops grown near the coast and to dormant fruit orchards in the Central Valley. For pesticides common to both areas, concentrations found in the coastal fogwater were similar to the pesticide concentrations found in the Central Valley fog sampled in January 1986 (Table IV). Diazinon is one of the pesticides commonly used in

Table V. Water Solubilities and Air-Water Partitioning Constants (Henry's Law Constants) for Some Pesticides Found in Fog, Along with Pesticide Distribution among Phases of a Coastal Foggy Atmosphere Sampled September 20, 1987 near Monterey, CA

compound	water sol, mg/L	K_{aw}	distribn in foggy atmos				
			total, ng/m ³	air phase, %		water phase, %	
				vapor	part ^e	liquid	part. ^e
chlorpyrifos	0.3 (25 °C) ^c	1.7×10^{-4} (23 °C) ^a	1.4	94.3	2.8	2.2	0.7
fonofos	13 ^d	2.1×10^{-4} ^d	0.12	97.7	<LOD	2.3	<LOD
diazinon	40 (22 °C) ^c	4.6×10^{-6} (23 °C) ^b	1.2	26.4	9.9	62.4	1.3
diazoxon			2.0	4.1	8.0	87.8	0.10
parathion	12 (20 °C) ^c	3.5×10^{-6} (23 °C) ^a					
methyl parathion	25 (20 °C) ^c	2.5×10^{-6} (23 °C) ^a					
carbaryl	40 (30 °C) ^c	5.3×10^{-7} (20 °C) ^c					
malathion	145 (25 °C) ^c	2.0×10^{-7} (23 °C) ^a	1.7	11.2	7.1	81.4	0.3

^aData from Fendinger and Glotfelty (16). ^bData from Fendinger and Glotfelty (17). ^cData from Suntio et al. (18). ^dObtained or calculated from data in ref 19. ^eParticles.

both areas. Diazinon concentrations ranged from 0.31 to 18 µg/L in the 1986 Central Valley fog compared to 0.15–4.8 µg/L in the coastal fog. The pesticide concentrations in fogwater reflected the different pesticide usages in the two areas. For example, parathion is the most heavily used pesticide in the dormant spraying and is very prominent in the Central Valley fog, but it is not found in coastal fog. Conversely, malathion is very prominent in the coastal fog, but not in the Central Valley fog. This is because malathion is used extensively on vegetables in the coastal area whereas it is not used in the winter dormant spraying in the Central Valley.

Pesticide Distribution in the Foggy Atmosphere.

Pesticide distribution between liquid and vapor phases in a foggy atmosphere can be calculated from pesticide concentrations in fogwater and interstitial air samples that have been collected simultaneously. The observed distribution should be related to the dimensionless air-water distribution constant, a Henry's law constant (K_{aw}), calculated from the vapor pressure of a compound divided by solubility. Water solubility data and air-water distribution constants for some of the pesticides found in the fog are presented in Table V.

The distribution of several pesticides between liquid and vapor phases in the foggy atmosphere collected from an agricultural area within 1.5 km of the ocean is presented in Table V. Diazinon, diazoxon, and malathion favored the aqueous phase while chlorpyrifos and fonofos favored the vapor phase. This is consistent with their water solubilities and air-water distribution constants. Malathion and diazinon with the smallest air-water distribution constants would be expected to favor the aqueous phase. In addition, diazoxon, which would be expected to be more water soluble than its parent diazinon, clearly favors the aqueous phase in this foggy atmosphere.

Glotfelty et al. (2) reported on the distribution between liquid and vapor phases of a variety of pesticides in fog. They found that pesticide concentrations in the water phase were often much greater than would be expected from simple ideal solution equilibrium with the interstitial vapor concentration. They defined an aqueous-phase enrichment factor, EF, as the ratio K_{aw}/D , where D is the field-measured distribution coefficient. Enrichment factors calculated for coastal fog are presented in Table IV, along with ranges of EFs for Central Valley fog events sampled in January 1986.

It should be pointed out that the field-measured distribution coefficients are calculated from field-measured vapor-phase concentrations and dissolved water-phase concentrations. The vapor-phase pesticide concentrations are taken to be the sum of dichotomous glass fiber filter

plus resin pesticide concentrations. Recent work (9) has indicated air-phase particle concentrations may, in fact, be partly vapor-phase pesticides adsorbed to the glass fiber filter. Dissolved pesticide in the water phase is operationally defined as that material passing through a double layer of glass fiber filters. Also, temperature will affect EFs. K_{aw} values are usually based upon measurements made at 25 °C, while the coastal fog samples were collected near 13 °C. Since a 10 °C change in temperature produces a ~2-fold change in K_{aw} (10), a reduction of about a factor of 2 in reported EFs is probable.

The chlorpyrifos concentration in fogwater collected on 9/20/87 within 1.5 km of the ocean was 25 times the expected concentration with respect to K_{aw} and the measured air concentration of chlorpyrifos (Table IV). Enrichment was also evident for diazinon with 30–50 times the expected pesticide concentration in the fog droplets. There was enrichment of several other pesticides in the coastal fog, but not as high as for diazinon and chlorpyrifos. EF for malathion was 6 for one fog event and ranged from 3 to 5 for fonofos in two fog events. Enrichment factors tend to increase with increasing K_{aw} (Tables IV and V).

It is interesting to note that the enrichment of pesticides into coastal fog was very similar to that observed earlier in the Central Valley fog. Direct comparison can be made for two compounds, chlorpyrifos and diazinon (Table IV). Enrichment of these two compounds in fog collected within 1.5 km of the ocean was almost identical with their enrichment in the Central Valley fog. This suggests that the buildup of man-made pollutants under stagnation conditions in the Central Valley is not a key factor in the enrichment process, and that enhanced aqueous-phase concentration may be a general phenomenon in foggy atmospheres.

Sorption to Aqueous-Phase Particles. Shown in Table VI are the organic carbon based partition coefficients (K_{oc}) of several pesticides in filtered fogwater particles. This sorption is expressed as

$$K_{oc} = \frac{(\mu\text{g of pesticide/g of organic C of particles})}{(\mu\text{g of pesticide/mL of fogwater})} \quad (1)$$

Only very small amounts of pesticide were associated with the particles filtered from the fogwater. Organic carbon fractions of filtered fog particles ranged from 5.8% to 13.3%. Fog particle K_{oc} is analogous to the organic carbon based adsorption coefficient that has been used extensively to compare pesticide sorption to a variety of soils and sediments. Experimental values or values of soil K_{oc} determined from regression equations (11–14) are given for comparison in Table VI.

Table VI. Organic Carbon Based Partition Coefficients, K_{oc} , for Particles Filtered from Coastal Fogwater Collected near Monterey, CA in September 1987^a

compound	no. of filtered fog part. samples	filtered fog part. K_{oc} range, mL/g	soil K_{oc} , mL/g		sample date	K_{fp} , mL/g	K_{doc} , mL/g
			exptl	calcd			
chlorpyrifos	2	60000-76000	13600 ^b	8500 ^c	9/16/87 9/20/87	1.4×10^6 1.5×10^6	4.6×10^5 5.4×10^5
diazinon	5	1600-17000		570 ^c	9/16/87 9/20/87	4.7×10^4 1.8×10^5	6.6×10^5 1.1×10^6
carbaryl	1	540	230 ^b	570 ^c			
malathion	2	290-580	1797 ^d	280 ^c	9/20/87 9/16/87	3.3×10^5	1.1×10^5 1.0×10^6
fonofos					9/20/87		7.7×10^5

^a Experimental and calculated soil K_{oc} values are presented for comparison. Organic carbon based partition coefficients for filterable fog particles (K_{fp}) and nonfilterable or dissolved organic carbon (K_{doc}) calculated by using truly dissolved pesticide concentration in fogwater are also presented (truly dissolved pesticide concentration is defined in the text). For K_{doc} calculations, the average dissolved organic carbon value of 44 mg/L (2) was used. ^b Data from Kenaga and Goring (13). ^c Data from Kenaga (12). ^d Data from Rao and Davidson (14).

As can be seen, fog particle K_{oc} is quite large for chlorpyrifos and diazinon. Measured fog particle K_{oc} values for diazinon cover a wide range and are from 2-20 times greater than soil K_{oc} values. Similarly, fog particle K_{oc} values for chlorpyrifos are ~5 times greater than typical soil K_{oc} values. These results indicate that diazinon and chlorpyrifos both associate more strongly with organic carbon in particles in fogwater than with the organic carbon in soil. By contrast, fog particle K_{oc} for carbaryl and malathion are very similar to soil K_{oc} values. The relative affinity of these four compounds for organic carbon is in line with their respective solubilities (Table V).

The differences between fog particle K_{oc} and soil K_{oc} values reflect the different nature of the organic carbon associated with atmospheric particles and in soil. Atmospheric particles, which are either scavenged by or serve as nucleation particles for fog droplets, may derive part of their organic carbon from combustion sources (15). This sooty residue could thus have properties similar to activated carbon and will therefore be much more sorptive than organic matter originating from the biological humification of plant and animal residue in soil.

In attempting to better explain the enrichment of pesticides in fogwater beyond what is predicted from air-water distribution constants, we calculated partition coefficients, K_{doc} , which describe the partitioning of pesticides between dissolved organic carbon in the fog droplets and the fogwater. In this calculation, "dissolved organic carbon" would include any dissolved, fine-particle, and colloidal organic carbon that was not filtered from the fogwater by the double-layer glass fiber filters. We used pesticide concentrations in air for the coastal samples and air-water pesticide distribution constants K_{aw} (Table V) to calculate "truly dissolved" pesticide concentrations. Truly dissolved pesticide concentration is the ratio of concentration measured in the vapor phase to K_{aw} . This calculation results in the expected pesticide solubility in fogwater if it were pure water. The truly dissolved pesticide concentration was much smaller than measured fogwater concentrations. Subtracting truly dissolved pesticide concentration from the measured pesticide concentration of the fogwater resulted in a pesticide concentration assumed to be associated with the dissolved organic carbon in the fogwater. A dissolved organic carbon partition coefficient was calculated as

$$K_{doc} = \frac{(\mu\text{g of pesticide/g of dissolved organic C})}{(\mu\text{g of truly dissolved pesticide/mL of fogwater})} \quad (2)$$

Although dissolved organic carbon for the coastal fog samples was not measured, we expected it to be similar

to the average dissolved organic carbon value of 44 mg/L (range 38-55 mg/L) reported for the six 1986 Central Valley fog samples (2). The "truly dissolved" pesticide concentrations were used to recalculate the fog particle partition coefficients as shown in eq 3. These are reported as K_{fp} and are compared to several K_{doc} values in Table VI.

$$K_{fp} = \frac{(\mu\text{g of pesticide/g of organic C of particles})}{(\mu\text{g of truly dissolved pesticide/mL of fogwater})} \quad (3)$$

These partition coefficients, K_{fp} , are quite large compared to fog particle K_{oc} values calculated from the pesticide concentration measured by solvent extraction of the fogwater. For diazinon, K_{fp} is 10-30 times greater than fog particle K_{oc} . Similarly, K_{fp} for chlorpyrifos is 20 times greater than K_{oc} . It is most interesting that K_{doc} and K_{fp} values are very similar, usually within an order of magnitude with K_{doc} being greater. This suggests that the filterable and nonfilterable organic carbon in fogwater sorb pesticides in much the same way. This would indicate that they are possibly from the same source. These results strongly suggest that the enrichment of pesticides in fogwater can be attributed at least in part to the presence of dissolved or colloidal organic carbon in the fog droplets, as was suggested earlier (1, 2, 18).

Summary and Conclusions

A number of pesticides were detected in fog sampled along the Pacific coast near Monterey, CA. The pesticides were primarily those used on crops in the area, such as brussels sprouts, broccoli, lettuce, and strawberries. Apparently, the uptake of pesticides by fog occurs fairly rapidly, since concentrations of pesticides in fog droplets collected in an agricultural area within 1.5 km of the ocean were similar to the concentrations measured previously in the Central Valley fog.

The concentrations of toxic oxons of organophosphorus insecticides were high in coastal fogwater samples. Ratios of the oxon to parent increased with distance from the agricultural areas, indicating conversion was taking place during extended residence time in the atmosphere or fog. Ratios also increased after sunup, indicating that photochemical reactions might be important. From analysis of oxidant concentrations present in the fog (data not shown), it seems that homogeneous aqueous-phase oxidation within the fog droplets would be too slow to account for observed oxon levels.

We determined the distribution between fog droplets and the interstitial vapor phase for several insecticides in the coastal fog. We found that concentrations in the water

phase were greater than expected from air-water distribution constants and that aqueous-phase enrichment factors were very similar to those previously reported for Central Valley fog. We concluded that this phenomenon may occur widely in fog and probably does not result from air stagnation and buildup of contaminants that occurs during Central Valley fog events. The enrichment of the aqueous phase of fog is due in part to the sorption of pesticides by the dissolved and colloidal organic carbon in the fog droplets.

An organic carbon based partition coefficient, K_{oc} , was measured to determine pesticide distribution between the aqueous phase and the particle phase of the fog droplets. These partition coefficients were compared to K_{oc} values determined for soil adsorption of pesticides. Fog particle K_{oc} values for diazinon and chlorpyrifos were on the order of 10 times greater than soil K_{oc} values, while fog particle and soil K_{oc} values were similar for the more soluble malathion and carbaryl.

We hypothesize that the nonfilterable, dissolved organic carbon in fogwater exists in fine particles or colloidal form and, through pesticide sorption, may be responsible for the apparent enrichment of pesticides in fogwater. To test this hypothesis, we defined the truly dissolved pesticide as the ratio of concentration in air to K_{aw} . Using this truly dissolved pesticide, which was always much smaller than that measured by solvent extraction of filtered fog water, we calculated K_{doc} and K_{fp} for the dissolved organic carbon and filtered fog particle partitioning, respectively. We found that K_{fp} and K_{doc} were almost identical and very large, ranging from 10^5 to 10^6 for chlorpyrifos and diazinon. We conclude that our data support the hypothesis of the existence in fogwater of a colloidal phase, derived from atmospheric particles, that causes apparent pesticide enrichment.

Acknowledgments

We wish to thank the many reviewers for their helpful comments and suggestions. Also, we would like to acknowledge the loss of one of the authors during the time this manuscript was being prepared. Dr. Dwight E. Glotfelty died April 2, 1990. His expertise and original, innovative thinking in the areas of atmospheric chemistry and the environmental fate of pesticides will be greatly missed. His patience, encouragement, and friendship will be especially missed by those who have had the opportunity to work with him.

Literature Cited

- (1) Glotfelty, D. E.; Seiber, J. N.; Liljedahl, L. A. *Nature* **1987**, *325*, 602-605.
- (2) Glotfelty, D. E.; Majewski, M. S.; Seiber, J. N. *Environ. Sci. Technol.* **1990**, *24*, 353-357.
- (3) Jacob, D. J.; Waldman, J. M.; Hagi, M.; Hoffman, M. R.; Flagan, R. C. *Rev. Sci. Instrum.* **1985**, *56*, 1291-1293.
- (4) Solomon, P. A.; Moyer, J. L.; Fletcher, R. A. *Aerosol Sci. Technol.* **1983**, *2*, 455-464.
- (5) Wehner, T. A.; Woodrow, J. E.; Kim, Y.-H.; Seiber, J. N. In *Identification and Analysis of Organic Pollutants in Air*; Keith, L. A., Ed.; Butterworths: Boston, MA, 1984; Chapter 17.
- (6) Thompson, J. F.; Reid, S. L.; Kantor, E. J. *Arch. Environ. Contam. Toxicol.* **1977**, *6*, 143-157.
- (7) Draper, W. M.; Crosby, D. G. *J. Agric. Food Chem.* **1984**, *32*, 231-237.
- (8) Majewski, M. S.; Glotfelty, D. E.; Seiber, J. N. *Proceedings of the 36th ASMS Conference on Mass Spectrometry and Applied Topics*; San Francisco, CA, 1988; pp 577-578.
- (9) McChesney, M.; Seiber, J. N. Department of Environmental Toxicology, University of CA, Davis, 1989, unpublished.
- (10) Ligocki, M. P.; Leuenberger, C.; Pankow, J. F. *Atmos. Environ.* **1985**, *19*, 1609-1617.
- (11) Lyman, W. J. In *Handbook of Chemical Property Estimation Methods*; Lyman, W. J., Reehl, W. F., Rosenblatt, D. H., Eds.; McGraw-Hill: New York, 1982; Chapter 4.
- (12) Kenaga, E. E. *Ecotoxicol. Environ. Saf.* **1980**, *4*, 26-38.
- (13) Kenaga, E. E.; Goring, C. A. I. In *Aquatic Toxicology, ASTM STP 707*; Eaton, J. G., Parrish, P. R., Hendricks, A. C., Eds.; American Society for Testing and Materials, 1980; pp 78-115.
- (14) Rao, P. S. C.; Davidson, J. M. In *Environmental Impact of Nonpoint Source Pollution*; Overcash, M. R., Davidson, J. M., Eds.; Ann Arbor Science: Ann Arbor, MI, 1980; pp 23-67.
- (15) Capel, P. D.; Leuenberger, C.; Giger, W. *Environ. Sci. Technol.*, in press.
- (16) Fendinger, N. J.; Glotfelty, D. E. *Environ. Toxicol. Chem.*, in press.
- (17) Fendinger, N. J.; Glotfelty, D. E. *Environ. Sci. Technol.* **1988**, *22*, 1289-1293.
- (18) Suntio, L. R.; Shiu, W. Y.; Mackay, D.; Seiber, J. N.; Glotfelty, D. *Rev. Environ. Contam. Toxicol.* **1988**, *103*, 1-59.
- (19) Worthing, C. R.; Walker, S. *The Pesticide Manual*, 8th ed.; British Crop Protection Council: Thorton Heath, England, 1987.

Received for review March 12, 1990. Revised manuscript received July 20, 1990. Accepted August 1, 1990.

Detection of Poly(ethylene glycol) Residues from Nonionic Surfactants in Surface Water by ^1H and ^{13}C Nuclear Magnetic Resonance Spectrometry

J. A. Leenheer,* R. L. Wershaw, P. A. Brown, and T. I. Noyes

U.S. Geological Survey, Box 25046, MS 408, Denver Federal Center, Denver, Colorado 80225

■ Poly(ethylene glycol) (PEG) residues were detected in organic solute isolates from surface water by ^1H nuclear magnetic resonance spectrometry (NMR), ^{13}C NMR spectrometry, and colorimetric assay. PEG residues were separated from natural organic solutes in Clear Creek, CO, by a combination of methylation and chromatographic procedures. The isolated PEG residues, characterized by NMR spectrometry, were found to consist of neutral and acidic residues that also contained poly(propylene glycol) moieties. The ^1H NMR and the colorimetric assays for poly(ethylene glycol) residues were done on samples collected in the lower Mississippi River and tributaries between St. Louis, MO, and New Orleans, LA, in July–August and November–December 1987. Aqueous concentrations for poly(ethylene glycol) residues based on colorimetric assay ranged from undetectable to $\sim 28 \mu\text{g/L}$. Concentrations based on ^1H NMR spectrometry ranged from undetectable to $145 \mu\text{g/L}$.

Introduction

Approximately 3.8 billion kilograms of nonionic surfactants are used and disposed into the environment each year (1). About three-fourths of nonionic surfactants contain hydrophilic poly(ethylene glycol) (PEG) ethers (polyethoxylates) that are attached to hydrophobic fatty alcohol, alkylphenol moieties, or poly(propylene glycols). The alkylphenol polyethoxylates have slow degradation rates in the aquatic environment (2), and accumulations of alkylphenoxy carboxylic acids have been detected in sewage effluents and in river waters (3). Alkylphenols also accumulate in sewage sludges and have toxic effects on certain types of aquatic fauna (4). The linear alcohol polyethoxylates degrade more rapidly in the aquatic environment than do the alkylphenol polyethoxylates, but there are conflicting reports in the literature about the biodegradability of the polyethoxylate chain (5–9). Reported half-lives of the polyethoxylate chain in diverse aquatic systems varied from days to months.

The question of environmental persistence of PEG residues in nonionic surfactants in water is complicated by the lack of analytical methods that can readily be applied to detect trace concentrations. The more hydrophilic residues, such as the acidic metabolites, are not isolated efficiently from water by solvent extraction. PEG residues exist as a complex mixture of homologues of different molecular weights, and they do not have a chromophoric group that can be detected. Mass spectrometry of these residues often gives weak or nonexistent parent ions because of the labile nature of the ether oxygen bond during electron-impact ionization. However, alkylphenol polyethoxylate residues in sewage effluents and in surface water were determined successfully by using gas chromatography/mass spectrometry and methane chemical ionization, which did not destroy parent ions (10).

Nonionic surfactants of the polyethoxylate type and neutral PEG residues form solvent extractable, ion-pair complexes with cobalthiocyanate, which is the basis for a colorimetric method (11), and with potassium tetrakis-(4-fluorophenyl)borate, which is the basis for a titrimetric method (12). The response of the colorimetric method (11)

is dependent on polyethoxylate chain length, and chains containing less than six ethylene oxide units do not respond. Tobin et al. (9) developed a gas chromatographic method based on cleavage of the polyethoxylate chain, using hydrobromic acid, to form 1,2-dibromoethane, but their study was limited by inefficient extraction of hydrophilic polyethoxylate residues from water.

Proton NMR spectrometry has been used to determine chemical properties on nonionic surfactants, such as the degree of ethoxylation, the hydrophile-lipophile balance, and the solution of water by the polyethoxylate chain (13). Carbon-13 NMR spectrometry has been used to tentatively identify alkylphenol polyethoxylates in groundwater (14) and polyethoxylates in humic substances extracted from sewage sludges (15). The repeating proton and carbon units in the polyethoxylate chains are represented by a single peak in both ^1H and the ^{13}C NMR spectra; the presence of a single peak decreases the limit of detection when polyethoxylates are isolated in complex matrices that occur in water and sewage sludges.

The initial objective of this study was to characterize dissolved organic substances isolated from natural water samples (16) by ^1H and ^{13}C nuclear magnetic resonance spectrometry (NMR). The NMR spectra of organic solute isolates from Clear Creek in Wheat Ridge, CO, and from the lower Mississippi River contained sharp, well-resolved lines, which we tentatively assigned to PEG residues. This report deals with the confirmation of this tentative assignment by comparisons with NMR spectra of standards, and by colorimetric assay. The methods described here provide procedures for evaluating limits on quantitative analysis of PEG residues in complex mixtures of natural organic solutes isolated from water.

Experimental Methods

Isolation of Dissolved Organic Substances including Poly(ethylene glycol) Residues from Surface Water. Depth-integrated, representative water samples, 70–100 L in volume, were collected from the lower Mississippi River and its major tributaries at 15 sites in July–August 1987 and at 16 sites in November–December 1987. A total of 21 sites were sampled during the two sampling cruises. The Mississippi River study is part of an ongoing project by the U.S. Geological Survey to determine contaminants in water, sediment, and biota of the lower Mississippi River and to determine the transport of these contaminants in the various phases. Sampling and sample-processing procedures involving continuous-flow centrifugation and tangential-flow ultrafiltration used on board the ship were reported previously (17). The sample that permeated the 30 000 dalton porosity, cellulose membrane ultrafilter was acidified to pH 2, using hydrochloric acid, and passed at 2 L/min through a 10-L bed volume column containing Amberlit XAD-8 resin to adsorb the major portion (the fulvic acid fraction) of dissolved organic carbon (DOC).

The column was eluted on board the ship with 4 L of 75% acetonitrile/25% deionized water acidified to pH 2 with hydrochloric acid. The acetonitrile/water solvent combination efficiently eluted all classes of organic solutes adsorbed on the XAD-8 resin (18). Dissolved organic so-

lutes in the acetonitrile/water concentrate was isolated in the laboratory by vacuum evaporation of the acetonitrile, re-concentration and desalting of the organic solutes on an 800-mL bed volume column of XAD-8 resin, and elution with 2 L of 75% acetonitrile/25% water acidified to pH 2 with formic acid. The acetonitrile, water, and formic acid were removed by vacuum evaporation, and the residue was dissolved in deionized water and freeze-dried.

An alternate DOC isolation procedure was designed for smaller samples and potentially greater recoveries of fulvic acid because of the greater ratio of resin to water. In this alternate procedure, 10–20 L of filtered sample was acidified to pH 4 with HCl and vacuum evaporated to 100–200 mL before being passed through the 800-mL column of XAD-8 resin. Salts in the sample were eluted by using 400–500 mL of water acidified to pH 2 with formic acid, and the adsorbed organic solutes were eluted with 2 L of 75% acetonitrile/25% water acidified to pH 2 with formic acid. From this point on, the organic solutes were isolated as in the original procedure. This alternate isolation procedure was developed during January–February 1988, using five samples obtained from Clear Creek in Wheat Ridge, CO. These samples were filtered through 0.3 μm porosity, Balston glass-fiber cartridge filters before vacuum evaporation.

Synthesis and Characterization of Standards for Poly(ethylene glycol) Residues. A number of poly(ethylene glycol) (200-, 300-, 400-, and 1000-dalton average) and poly(propylene glycol) (425- and 725-dalton average) standards were obtained from Aldrich Chemical Co. The standards had a narrow range of polydispersity according to the manufacturer; the homologue molecular weight distribution ranged 5% above and below the mean.

The carboxylated PEG standards were synthesized from 200 and 400 dalton average PEG by a procedure developed by Steber and Wierich (5) that was scaled up 100-fold. Briefly, 700 mg of the PEG was oxidized by potassium dichromate in 2 N sulfuric acid reacting at 60 °C for 2 h. The carboxylated PEGs were then extracted into chloroform after addition of a saturated magnesium sulfate solution to the acid dichromate reaction mixture. After the chloroform was evaporated, the carboxylated PEGs were redissolved in water and adsorbed on BioRad AG-MP-1 anion-exchange resin in the hydroxide form. The resin column was eluted with water to remove unreacted PEG, and the carboxylated PEGs were eluted with 0.5 N sodium acetate solution. The water and sodium acetate were then removed from the carboxylated PEGs by adsorption chromatography on Amberlite XAD-8 resin by the method described previously for isolation of dissolved organic solutes from water.

All of the standards were characterized by ^1H and ^{13}C NMR spectrometry. By determining the ratio of end-group carbons (or protons) to internal units in the polymer chain, the molecular weight averages were found to be accurate; NMR spectrometry also determined the standards to be pure. The polymer chain was not detectably shortened by the oxidation process that produced the carboxylated standards, and dicarboxylated standards greatly predominated over monocarboxylated standards, as reported by Steber and Wierich (5).

Separation of Poly(ethylene glycol) Residues from Natural Organic Solutes. The separation procedure was developed using carboxylated PEG standards that were spiked 5% by weight into a fulvic acid previously isolated and characterized from the Suwannee River, GA (18). A flow chart of the separation procedure is shown in Figure 1.

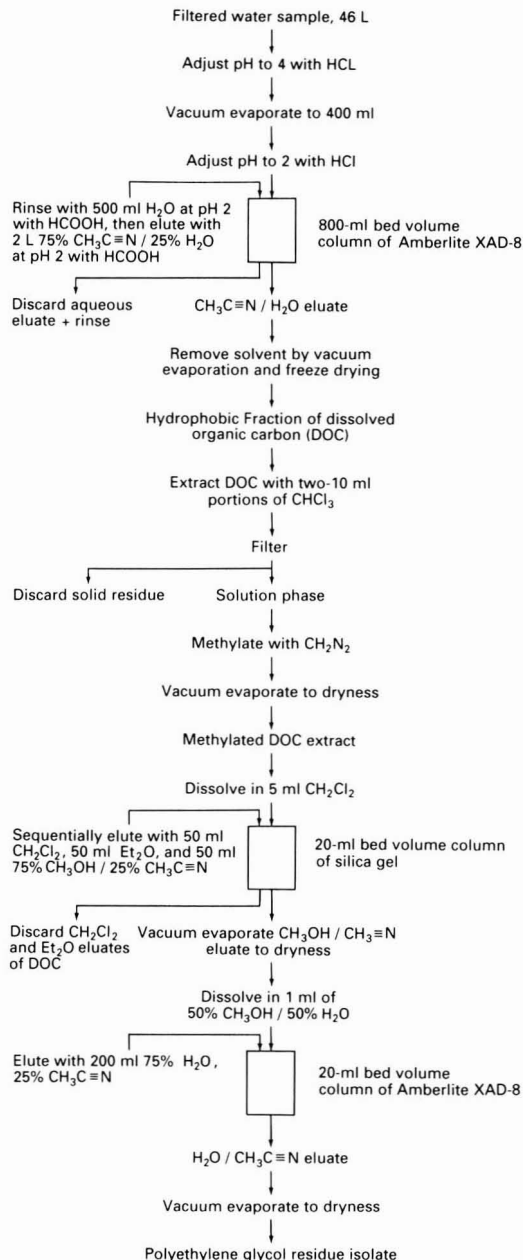


Figure 1. Flow chart of analytical procedure used to isolate PEG residues from water and associated solutes.

Neutral and acidic PEG residues containing two or more ethylene oxide units were extracted from 100 to 500 mg of freeze-dried fulvic acid (in the hydrogen form) with chloroform (5) during a 10-min treatment in an ultrasonic bath. The portion of the fulvic acid insoluble in chloroform was separated by filtration, and the soluble portion was methylated with gaseous diazomethane. The solution was evaporated to dryness and the residue was dissolved in 5 mL of methylene chloride, which was applied to a 20-mL bed volume column of silica gel. The column was sequentially eluted with 50-mL aliquots of methylene chloride, diethyl ether, and 25% acetonitrile/75% methanol.

The PEG residues have a high affinity for the silica gel and elute in the acetonitrile/methanol fraction. This fraction was evaporated to dryness and the residue was dissolved in 1 mL of 50% methanol in water. The residue concentrate was next applied to a 20-mL bed volume column of XAD-8 resin, and the poly(ethylene glycol) residues were eluted with 200 mL of 25% acetonitrile in water. Vacuum evaporation gave an isolated poly(ethylene glycol) fraction whose yield could be determined by mass measurement. The procedure was monitored by infrared spectrometric measurement of various residues obtained in the procedure. After development of the procedure with standards, it was applied to a 46-L sample obtained from Clear Creek in November 1989.

The principles upon which the separation procedure was based were the high affinity of PEG residues for silica gel relative to the less polar constituents of solvent-extracted fulvic acid and the hydrophilic nature of nature of PEG residues relative to less polar, methylated fulvic acid, which sorbed to XAD-8 resin. Both chromatographic separations of the normal-phase type on silica gel and reverse-phase type on XAD-8 resin were required to purify PEG residues from fulvic acid.

Nuclear Magnetic Resonance Spectrometry. For organic solutes isolated as free acids, 100 mg of the isolate was dissolved in 0.5 mL of deuterated dimethyl sulfoxide (DMSO- d_6). Sodium salts, formed by titrating the samples to pH 8 with sodium hydroxide, were dissolved in 0.5 mL of D_2O . Samples that contained large concentrations of PEG residues dissolved more readily in DMSO- d_6 than in D_2O . Solution in D_2O was facilitated by adding 20% deuterated acetonitrile by volume. Trifluoroacetic acid was added to the DMSO- d_6 to shift the exchangeable proton peak downfield so it would not interfere with the polyethoxylate peaks for 1H NMR spectra. The sample solution was placed in 5-mm glass tubes for 1H NMR assays.

A Varian FT-80A NMR spectrometer was used to measure the 1H NMR spectra. The 1H NMR spectra, obtained at 79.5 MHz, were generated by a pulse width of 3 s and a pulse delay of 5 s. The magnet was shimmed for each sample to obtain the best possible peak resolution, which is important in the integration of the peak caused by polyethoxylate protons. Only a few hundred transients were necessary on each sample to obtain a satisfactory signal-to-noise ratio.

The ^{13}C NMR spectra were measured on solutions of PEG isolates dissolved in DMSO- d_6 or D_2O /20% acetonitrile mixtures in 10-mm tubes on a Varian XL 300 spectrometer at 75.429 MHz. For the nonquantitative spectra, the transmitter was set for a 45° tip angle, and no pulse delay was used. The acquisition time was 0.2 s, and the sweep width was 30 000 Hz; continuous broad-band decoupling of protons by the WALTZ method was used. All of the spectra were recorded with a line broadening of 25 Hz. These conditions were chosen to obtain maximum signal-to-noise ratio for optimum structural group characterization. The quantitative spectra were measured by using inverse-gated decoupling in which the proton decoupler was on only during the acquisition of the free induction decay curve; an 8-s delay time was used.

Quantitation of Poly(ethylene glycol) Residues by 1H NMR Spectrometry. The fraction, due to the peak at 3.6 ppm, of the total integral curve (not including the H $_2O$ solvent peak) of the 1H NMR spectrum of isolated organic solutes was used to calculate the concentration of PEG residues in the sample. The equation used was

$$PEG (\mu\text{g/L}) = 0.48 \times FA (\mu\text{g/L}) \times f_{H(PEG)} \quad (1)$$

where PEG is the aqueous concentration of poly(ethylene glycol) residues, FA is the aqueous concentration of isolated fulvic acid, $f_{H(PEG)}$ is the decimal fraction of nonexchangeable protons attributed to PEG residues, and 0.48 is the ratio of FA/PEG nonexchangeable hydrogen percentages.

To determine the precision and limit of detection of the $f_{H(PEG)}$ measurement, fulvic acid, isolated from the Suwannee River, GA (18), was spiked with varying concentrations of 200 dalton average poly(ethylene glycol) to give $f_{H(PEG)}$ fractions between 0.005 and 0.15, which encompassed the range for the Mississippi River samples. "Cut and weigh" integration was compared with electronic integration for the best determination of $f_{H(PEG)}$.

To determine recovery of a PEG standard by the 1H NMR method of detection and quantitation, 1.2 mg of 400 dalton average PEG and 120 mg of Suwannee River fulvic acid were dissolved in 20 L of distilled water to which calcium chloride, magnesium sulfate, and sodium bicarbonate were added to approximate Mississippi River concentrations. This sample was vacuum evaporated to 300 mL, and the fulvic acid plus PEG were isolated on Amberlite XAD-8 resin as described previously. Total organic solute recovery (fulvic acid plus PEG) was assessed by determining dissolved organic carbon concentrations on sample solutions before and after processing. PEG recovery was determined by analyzing the 1H NMR spectrum of the isolate, and using eq 1 with the first factor adjusted to 0.375 because of the different composition of Suwannee River fulvic acid compared to Mississippi River fulvic acid. Suwannee River fulvic acid was used for the recovery and precision studies because its composition is accurately determined to where it can be regarded as a secondary standard (19).

Colorimetric Assays of Poly(ethylene glycol) Residues. The cobalthiocyanate method (11) was used to screen the organic isolates from samples collected from Clear Creek in Colorado and the Mississippi River for PEG residues. One hundred milligrams of sample was dissolved in 10 mL of water, 10 mL of cobalthiocyanate reagent was added, and 10 mL of methylene chloride was used to extract the blue cobalt-PEG complex. The method was calibrated by using a 1000 dalton average PEG standard that was spiked into a fulvic acid and salt matrix in water similar to that described in the previous section. The presence of fulvic acid and inorganic salts had no detectable effect on PEG quantitation compared to quantitation in distilled water. The pH of the aqueous phase during the extraction was 6.

The carboxylated PEG residues do not extract into chloroform at pH 6; therefore, the colorimetric method was tested by adjusting the aqueous phase to pH 2 with sulfuric acid and then adding 5 mL of a saturated $MgSO_4$ solution to 5 mL of sample solution to salt out the carboxylated PEG residues into methylene chloride. The colorimetric method then was calibrated by using the synthesized 400-dalton carboxylated PEG standard.

Results and Discussion

The first discovery of PEG residues in surface water was in the sample from Clear Creek collected in February 1988. The 1H NMR spectrum of this sample is shown in Figure 2. The large peak at 3.5 ppm tentatively was assigned to protons attached to carbons in polyethoxylate chains when compared with spectra of standard polyethoxylates dissolved in DMSO- d_6 . Confirmatory evidence for PEG residues was obtained from the ^{13}C NMR spectra also shown in Figure 2. The peak at 69.7 ppm (peak 5) cor-

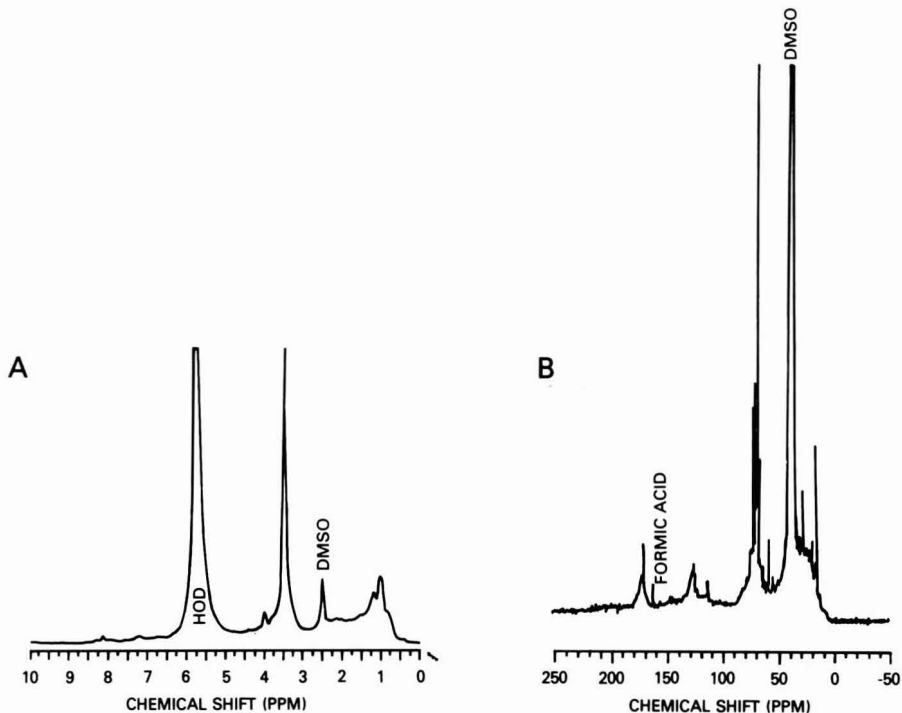


Figure 2. ^1H NMR (A) and nonquantitative ^{13}C NMR (B) spectra of organic solutes isolated from samples collected from Clear Creek, CO, in February 1988.

responded exactly to the chemical shift for carbon in the polyethoxylate in a 300-dalton average PEG standard.

To obtain more specific information on poly(ethylene glycol) residue composition, methane chemical ionization mass spectrometry (CI-MS) was attempted. Both the 200- and 400-dalton carboxylated standards were methylated, gas chromatographed, and detected by CI-MS. Only the 200 standard gave a normal homologue distribution of peaks after chromatography; the GC-MS of the 400-dalton standard appeared to be limited by volatility or molecular stability problems as the peaks were detected at a much reduced level of sensitivity. Molecular ions were not observed for the homologues detected for either standard. The predominate ion was at 117 mass units, which indicated that ether cleavage was as significant a problem for chemical ionization as for electron impact ionization.

The failure of CI-MS to give homologue-specific information led to the development of the separation procedure whereby PEG residues isolated from fulvic acid could be more specifically characterized by ^{13}C NMR. The large sample from Clear Creek taken in November 1989 yielded 60 mg of PEG residues after processing through the various separation procedures. The ^1H NMR spectrum of these residues is shown in Figure 3A and the ^{13}C NMR spectrum is shown in Figure 4A. Standard spectra of poly(propylene glycol) and neutral and acidic PEG residues are shown in Figure 3B-D for ^1H NMR and in Figure 4B-D for ^{13}C NMR. Numbered peak assignments from Figures 3 and 4 are included in structural elements in the computed average structure (from quantitative NMR data) of PEG residues shown in Figure 5; the chemical shifts of these peaks are listed in Table I.

An estimate of an average molecular size of PEG residues can be obtained by ratioing end-group polymer units to internal polymer units from the quantitative ^{13}C NMR

Table I. Chemical Shift Assignments^a (Proton and Carbon-13) for Structural Units in Poly(ethylene glycol) Residues Dissolved in D_2O

no. ^c	proton chem shift, ppm	carbon-13 chem shift, ppm
1	1.1	16.9
2	3.6	60.5
3	4.1	67.7
4	3.6	69.7
5	3.6	71.7
6	3.5	72.2 ^b
7	3.8	74.5 ^b
8		173.0

^aChemical shifts were adjusted to poly(ethylene glycol) data reported by Ribeiro and Dennis (22). ^bShift assignments are tentative; assignments of peaks 6 and 7 might be reversed. ^cPeak numbers in Figures 2 and 3 and structural unit numbers in Figure 4.

spectra (Figure 3A and B). The 725-dalton poly(propylene glycol) standard gave a computed weight of 710 daltons by this polymer ratioing method. The average weight of the poly(ethylene glycol) residue shown in Figure 5 was calculated to be about 2200 daltons by the polymer ratioing method after adjusting for the propylene oxide moieties. An average of 18 propylene oxide units and 25 ethylene oxide units was determined for this PEG residue. Both the presence of the propylene oxide units and the high molecular weight suggest the origin of the residue shown in Figure 5 is from block polymers formed by condensing ethylene oxide with propylene glycol. Block polymers are used as low-foam surfactants; one of their uses is in automatic dishwashing powders (20).

The ^{13}C NMR spectra provide key indicators of the type of PEG residue. Four of the peaks in the 60–75 ppm region

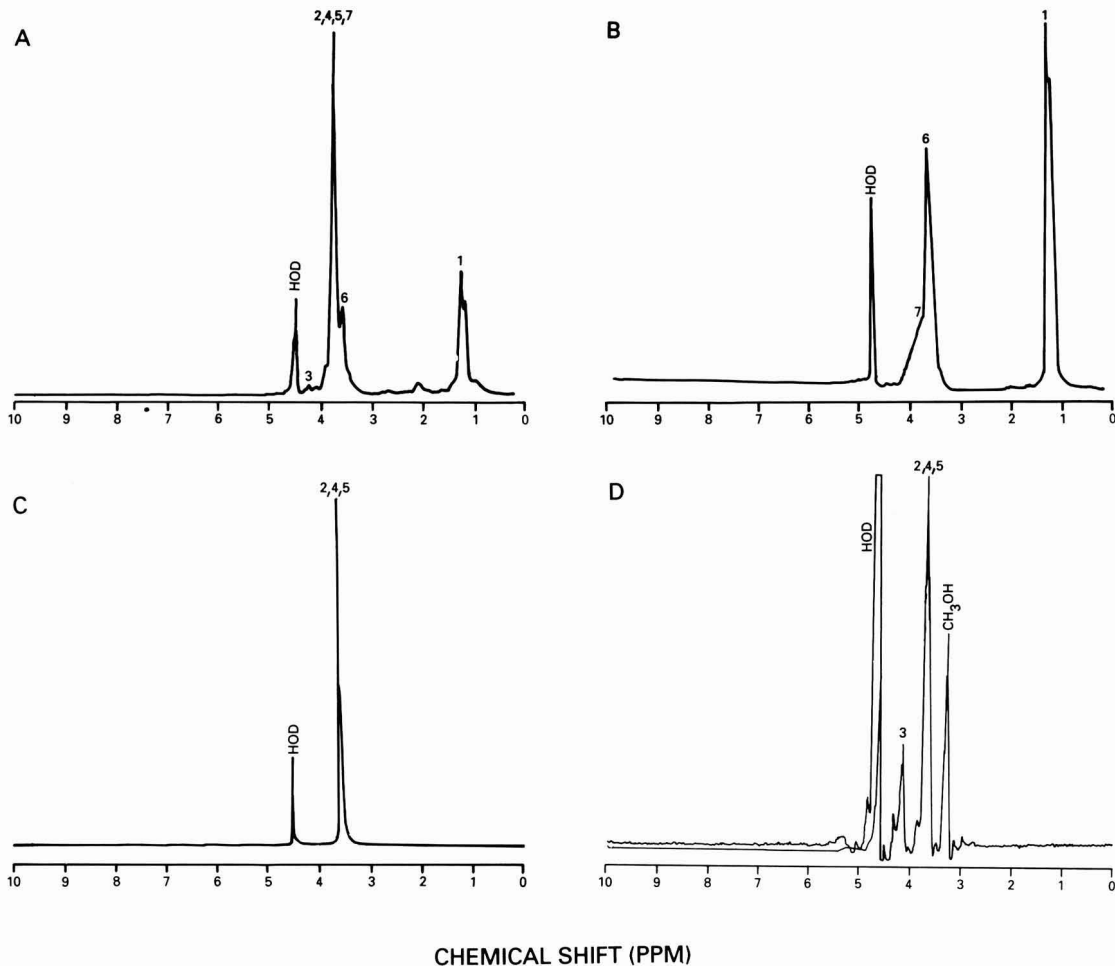


Figure 3. ^1H NMR spectra of (A) poly(ethylene glycol) residues isolated from Clear Creek, CO, in November 1989, (B) poly(propylene glycol) (425-dalton average), (C) poly(ethylene glycol) (300-dalton average), and (D) carboxylated poly(ethylene glycol) (200-dalton average). Spectra A and B were run with 75% $\text{D}_2\text{O}/20\%$ acetonitrile- d_3 as solvent. Spectra C and D were run with D_2O as solvent.

indicate neutral end groups at 60.5 ppm (carbon 2 of Figure 5), acidic end groups at 67.7 ppm (carbon 3 of Figure 5), internal polyethoxy units at 69.7 ppm (carbon 4 of Figure 5), and polypropoxy units at 74.5 ppm (carbon 7 of Figure 5). All of these peaks give a large response in the non-quantitative ^{13}C NMR spectra, which are much more sensitive than the quantitative spectra. These four indicator peaks can all be seen in the nonquantitative ^{13}C NMR spectrum of Figure 2B in which fulvic acid was present. The Clear Creek sample (February 1988) appears to contain lower molecular weight and more carboxylated residues (Figure 2B) than the November 1989 sample (Figure 4B).

The ^1H NMR and nonquantitative ^{13}C NMR spectra of organic solutes isolated from the sample collected from the Mississippi River at St. Louis, MO, are shown in Figure 6. Comparisons of the four indicator peaks in the ^{13}C NMR spectra indicate the PEG residues for the Mississippi River sample are more degraded (oxidized) and of lower molecular weight than are the residues observed in the Clear Creek samples.

The ^1H NMR spectrum of Figure 6 clearly shows the protons attached to poly(ethylene glycol) and poly(propylene glycol) units at 3.6 ppm. The quantitative determination of $f_{\text{H(PEG)}}$ in eq 1 was made after determining both the proton integrals of PEG and the background of fulvic acid; this background determination was possible with good precision because little variability was observed in ^1H NMR spectra of fulvic acids between different samples from the Mississippi River.

The factor $f_{\text{H(PEG)}}$ was linear with concentration between 0 and 0.15 for a six-point curve with poly(ethylene glycol) spiked into Suwannee River fulvic acid. The relative error (standard deviation/mean) of points from the curve was 6.5%. The minimum $f_{\text{H(PEG)}}$ that could be measured was 0.002. Electronic integration was slightly superior to "cut and weight" integration to determine $f_{\text{H(PEG)}}$. Assuming no variation in PEG residue properties, the two other factors from eq 1 that affect PEG residue determination in the fulvic acid isolates are the precision of fulvic acid concentration determination and the variability of fulvic acid exchangeable hydrogen content. The relative error of fulvic acid concentration was estimated to be 7% from combining dissolved organic carbon measurements with fulvic acid recovery data. The relative error of the non-exchangeable hydrogen determination was measured to be

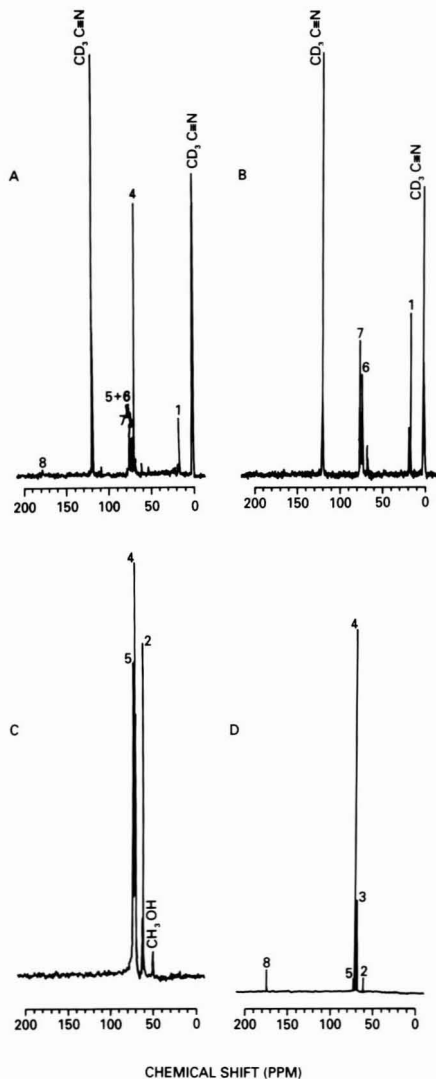


Figure 4. ^{13}C NMR spectra of (A) poly(ethylene glycol) residues isolated from Clear Creek, CO, in November 1989, (B) poly(propylene glycol) (725-dalton average), (C) poly(ethylene glycol) (300-dalton average), and (D) carboxylated poly(ethylene glycol) (200-dalton average). Spectra A and B were run with 75% D_2O /25% acetonitrile- d_3 as solvent. Spectra C and D were run with D_2O as solvent.

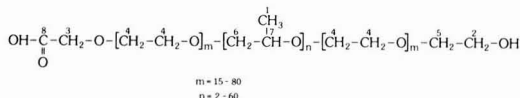


Figure 5. Average structure of poly(ethylene glycol) residues isolated from Clear Creek, CO, in November 1989 sampling.

4.6% by combining analysis of elemental data and titrimetric data of exchangeable hydrogen on 11 fulvic acid samples from the Mississippi River. The overall relative error obtained by adding these three factors in eq 1 is 18%. The limit of detection obtained by substituting the minimum $f_{\text{H(PEG)}}$ (0.002) into eq 1 at 3000 $\mu\text{g/L}$ fulvic acid is 2.9 $\mu\text{g/L}$. This relative error and limit of detection determinations just applies to the ^1H NMR measurement; an additional loss in precision and limit of detection will

be encountered during the organic solute isolation procedure.

The total organic solute recovery (fulvic acid + PEG) was 90% for the spiked recovery study, and the 400-dalton PEG standard recovery was 78% for this study. The lower recovery of the PEG compared to fulvic acid is not surprising in light of the known affinity of PEG for glass surfaces (21) that were available for sorption by the glassware used for sample processing. Carboxylated PEG residues, poly(propylene glycol) residues, and residues of varying homologue content and molecular weight likely give variable recoveries; but a comprehensive recovery study is beyond the scope of this paper, which is intended to report the initial detection and present limitations on quantitation of PEG residues in water.

The variations found in end-group composition, molecular weight, and especially poly(propylene glycol) content between the Mississippi River and Clear Creek samples indicate that PEG residue properties are not constant for PEG determination by eq 1. Overlap of poly(propylene glycol) protons with poly(ethylene glycol) protons (Table I) in the $f_{\text{H(PEG)}}$ measurement will result in an overestimate of polyethoxylate content and an underestimate of total polyethylene plus poly(propylene glycol) content.

Very short chain (two to three ethylene oxide units) residues were most likely not recovered by the fulvic acid isolation procedure on XAD-8 resin. Frontal chromatography of the most hydrophilic standard available (the carboxylated 200 dalton average PEG) was performed to determine a k' capacity factor; this standard gave a k' value of 8.2, which indicates the lower limit for quantitative recoveries of carboxylated PEG residues is near four ethylene oxide units for PEG residues in the Mississippi River where organic solutes with k' of 5.7 were quantitatively recovered. The alternative isolation procedure developed on the Clear Creek samples lowered the k' value to 1.1 to obtain greater recoveries of the short-chain PEG residues and hydrophilic fulvic acid.

The major limitation of the ^1H NMR spectrometric method is the lack of resolution between poly(ethylene glycol) and poly(propylene glycol) residues in the presence of fulvic acid. This problem may be solved by additional research combining a limited cleanup procedure with higher field ^1H NMR or nonquantitative ^{13}C NMR spectrometry calibrated for PEG residues. The present spectrometric method can be regarded as an estimate with allowance for the discussed limitations.

To confirm the presence of PEG residues in Clear Creek and the Mississippi River and its major tributaries, the colorimetric test using cobalthiocyanate was done on the same organic solute aliquots that were used to obtain the ^1H NMR spectra. A map of sample site locations along the Mississippi River and major tributaries is shown in Figure 7; results of the test are listed in Table II. For comparison, concentrations of PEG residues determined from ^1H NMR data also are listed in Table II.

The colorimetrically determined concentrations of PEG residues listed in Table II need to be regarded as minimum estimates of actual concentrations because short-chain and oxidized acidic residues do not respond to the cobalthiocyanate under the pH conditions used for the test. The sample obtained from Clear Creek in February 1988 contained 1200 $\mu\text{g/L}$ PEG by ^1H NMR spectrometric assay and 360 $\mu\text{g/L}$ by colorimetric assay. The average ratio of concentrations of PEG residues measured by ^1H NMR data to concentrations measured by colorimetric assays in samples from the Mississippi River and its major tributaries was 6.3:1.0, whereas the ratio in samples from Clear

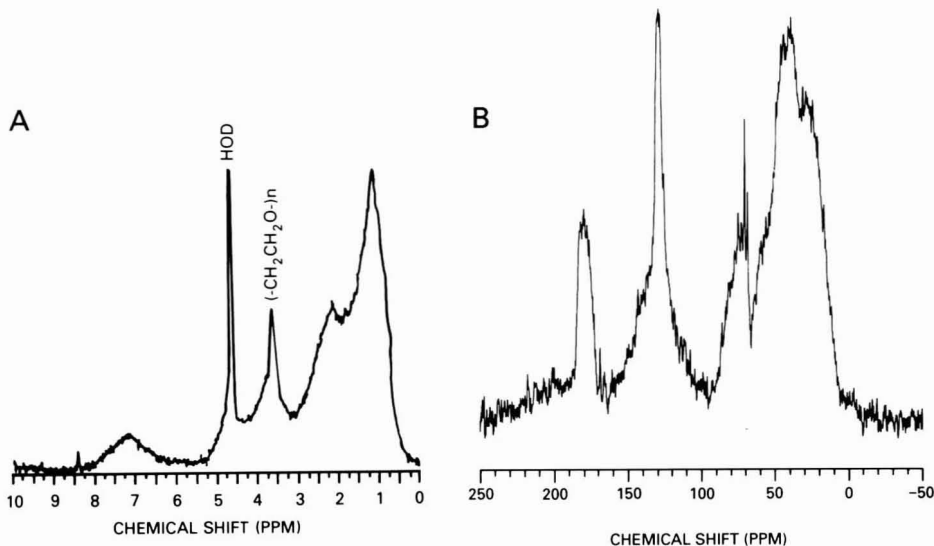


Figure 6. ^1H NMR (A) and nonquantitative ^{13}C NMR (B) spectra of organic solutes isolated from samples collected from the Mississippi River at St. Louis, MO, in July 1989.

Table II. Concentrations of Poly(ethylene glycol) Residues in Samples from the Mississippi River and Major Tributaries

sample site (number, Figure 7)	July–August 1987 sampling ^a		November–December 1987 sampling ^a	
	colorimetric detn, $\mu\text{g/L}$	^1H NMR detn, $\mu\text{g/L}$	colorimetric detn, $\mu\text{g/L}$	^1H NMR detn, $\mu\text{g/L}$
Illinois R. at Naples, IL (1)	8.9	33	NS	NS
Illinois R. below Meredosia, IL (2)	NS	NS	2.6	4
Mississippi R. near Winfield, MO (3)	3.1	30	2.2	34
Mississippi R. below Alton, IL (4)	6.8	50	NS	NS
Missouri R. at Hermann, MO (5)	28.3	145	NS	NS
Missouri R. at St. Charles, MO (6)	NS	NS	2.6	13
Mississippi R. at St. Louis, MO (7)	6.9	35	NA	65
Mississippi R. at Thebes, IL (8)	NS	NS	2.8	12
Ohio R. below Smithland Lock and Dam, IL–KY (9)	3.0	10	NS	NS
Ohio R. at Omsted, IL (10)	NA	9	4.3	9
Mississippi R. below Hickman, KY (11)	NA	NA	1.1	10
Mississippi R. at Fulton, TN (12)	NA	NA	2.5	6
Mississippi R. at Helena, AR (13)	4.1	20	2.4	9
White R. at Mile 11.5, AR (14)	3.5	14	2.2	4
Arkansas R. at Mile 55.9 AR (15)	NA	18	NS	NS
Mississippi R. above Arkansas City, AR (16)	6.1	37	2.1	15
Yazoo R. at mile 10, MS (17)	NS	NS	1.6	7
Mississippi R. below Vicksburg, MS (18)	1.5	13	2.2	6
Old River outflow channel near Knox Landing, LA (19)	5.4	12	0.3	ND
Mississippi R. at St. Francisville, LA (20)	1.3	19	ND	3
Mississippi R. below Belle Chasse, LA (21)	1.2	17	1.3	4

^aNA, not analyzed; ND, not detected; NS, no samples.

Creek was 3.3:1.0. The larger ratio for the samples from the Mississippi River and its major tributaries may be indicative of short-chain and acidic poly(ethylene glycol) residues, which were not detected by the colorimetric assay.

The cobalthiocyanate test also was applied to blank water extracts of the ultrafilters, to methylene chloride extracts of the ultrafilters, to blank eluates of the XAD-8 resin, and to a sample of deionized water that had been carried through the complete sampling and sample-processing procedure on board the ship. Negative colorimetric tests for PEG residues were obtained for all these blanks.

To estimate the concentration of acidic PEG polymers, the colorimetric test was done at pH 2 and pH 7 using a 400 dalton average neutral PEG, the acidic PEG residue synthesized from the 400-dalton PEG, and the organic solute isolate from the sample collected from the Missis-

sippi River below Alton, IL. The colorimetric response increased 18% at pH 2 compared to the response at pH 7 for the sample from the Mississippi River; whereas, the response of the neutral PEG was independent of pH, and the carboxylated standard had no response at pH 7. At pH 2, the carboxylated standard gave only 33% of the colorimetric response of an equal weight of the neutral PEG, so the increase for the Mississippi River sample would be about 54% instead of 18% if the acid PEG had an equivalent response to the neutral PEG. These colorimetric data confirm the presence of poly(ethylene glycol) residues in the Mississippi River samples, and they also indicate the presence of carboxylated residues.

Conclusions

The combination of ^1H NMR and ^{13}C NMR spectrom-

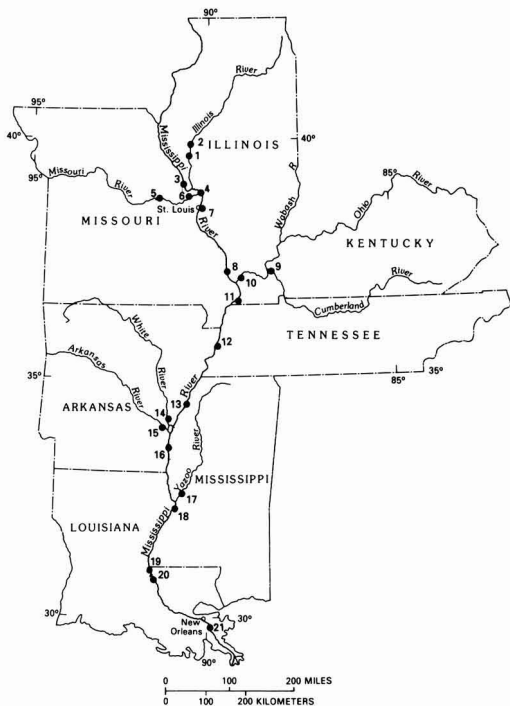


Figure 7. Location of sampling sites on the lower Mississippi River and major tributaries.

etry and colorimetric assays of organic solute isolates from various surface waters was able to detect, in microgram per liter concentrations, and identify, at the compound class level, PEG residues in surface water in the presence of natural organic solutes. The most specific technique was ^{13}C NMR spectrometry, which allows one to distinguish poly(ethylene glycols) from poly(propylene glycols) in the presence of natural organic solutes. Separation of the PEG residues from natural organic solutes by a combination of selective extraction, methylation, and chromatographic procedures enabled quantitative determination by ^{13}C NMR spectrometry of poly(ethylene glycols), poly(propylene glycols), neutral end groups, and acid end groups of PEG residues. However, the large sample size and extensive processing requirements of the quantitative ^{13}C NMR determination obviates its use for environmental monitoring of PEG residues in water. ^1H NMR spectrometry has adequate sensitivity for environmental monitoring, but it lacks the resolution to distinguish various end groups and poly(propylene glycol) content in PEG residues in the presence of fulvic acid.

The NMR and colorimetric assays of organic solutes isolated from Clear Creek and from the lower Mississippi River indicated that PEG residues are ubiquitous contaminants in these waters during both summer and winter. The ^1H NMR assay found 4–15 times the PEG residue concentrations in the lower Mississippi River than was determined by colorimetric assay of these samples. The concentrations of PEG residues found in Clear Creek, CO,

and in the lower Mississippi River make these residues one of the most abundant contaminant classes found in these surface waters.

Acknowledgments

We thank Tom Leiker for performing the GC/MS with methane CI detection of the carboxylated poly(ethylene glycol) standards. The assistance and advice of Wilfred Periera, Colleen Rostad, Larry Barber, and Jennifer Field regarding methodology for PEG residues are appreciated.

Literature Cited

- Greek, B. F., *Chem. Eng. News*, **1988**, *66* (Jan 25), 21–53.
- Baggi, G.; Beretta, L.; Gall, E.; Scolastico, C.; Treccani, V. In *The Oil Industry and Microbial Ecosystems*; Chater, K. W. A., Somerville, H. J., Eds.; Heyden: London, 1978; pp 129–136.
- Ahel, M.; Conrad, T.; Giger, W. *Environ. Sci. Technol.* **1987**, *21*, 697–703.
- McLeese, D. W.; Zitko, V.; Sergeant, D. B.; Burrige, L.; Metcalfe, C. D. *Chemosphere* **1981**, *10*, 723–730.
- Steber, J.; Wierich, P. *Appl. Environ. Microbiol.* **1985**, *49*, 530–537.
- Steber, J.; Wierich, P. *Water Res.* **1987**, *21*, 661–667.
- Larson, R. J.; Games, L. M. *Environ. Sci. Technol.* **1981**, *15*, 1488–1493.
- Vashon, R. D.; Schwab, B. S. *Environ. Sci. Technol.* **1982**, *16*, 433–436.
- Tobin, R. S.; Onuska, F. I.; Brownlee, B. G.; Anthony, D. H. J.; Comba, M. E. *Water Res.* **1976**, *10*, 529–535.
- Stephanou, E. *Int. J. Environ. Anal. Chem.* **1985**, *20*, 41–54.
- Milwidsky, B. M.; Gabriel, D. M. *Detergent Analysis*; Halstead Press: New York, 1982; pp 100–121.
- Tsubouchi, M.; Yamasaki, N.; Yanagisawa, K. *Anal. Chem.* **1985**, *57*, 783–784.
- Llenado, R. A.; Neubecker, T. A. *Anal. Chem.* **1983**, *55*, 93R–102R.
- Thurman, E. M.; Willoughby, T.; Barber, L. B., Jr.; Thorn, K. A. *Anal. Chem.* **1987**, *59*, 1798–1802.
- Bayer, E.; Albert, K.; Bergmann, W.; Jahns, K.; Eisener, W.; Peters, H. K. *Angew. Chem.* **1984**, *96*, 151–153.
- Leenheer, J. A. *Environ. Sci. Technol.* **1981**, *15*, 578–587.
- Leenheer, J. A.; Meade, R. H.; Taylor, H. E.; Pereira, W. E. *Water-Resour. Invest. Rep. (U.S. Geol. Surv.) No. 88-4220*, 1988, 501–512.
- Leenheer, J. A.; Brown, P. A.; Noyes, T., I. In *Aquatic Humic Substances: Influence on Fate and Treatment of Pollutants*; Suffet, I. H., MacCarthy, P., Eds.; Advances in Chemistry Series 219; American Chemical Society: Washington, DC, 1984; pp 25–39.
- Averett, R. C.; Leenheer, J. A.; McKnight, D. M.; Thorn, K. A., Eds. *Humic Substances in the Suwannee River, Georgia: Interactions, Properties, and Proposed Structures. Open-File Rep.—U.S. Geol. Surv.* **1989**, *No. 87-557*.
- Davidson, A. S.; Milwidsky, B. *Synthetic Detergents*, 7th ed.; Longman Scientific and Technical: New York, 1987; pp 34–46.
- Podoll, R. T.; Irwin, K. C.; Brendlinger, S. *Environ. Sci. Technol.* **1987**, *21*, 562–568.
- Ribeiro, A. A.; Dennis, E. A. *J. Phys. Chem.* **1977**, *81*, 957–963.

Received for review March 28, 1990. Revised manuscript received June 11, 1990. Accepted August 17, 1990. Use of trade names in this report is for identification purposes only and does not constitute endorsement by the U.S. Geological Survey.

Sorption and Microbial Degradation of Naphthalene in Soil-Water Suspensions under Denitrification Conditions

James R. Mihelcic* and Richard G. Luthy

Department of Civil and Environmental Engineering, Michigan Technological University, Houghton, Michigan 49931, and
Department of Civil Engineering, Carnegie Mellon University, Pittsburgh, Pennsylvania 15213

■ The microbial degradation of naphthalene under denitrification conditions in soil-water suspensions was dependent on solute partitioning between soil and water. Soil-associated naphthalene was in equilibrium with aqueous-phase solute, with the rate of naphthalene degradation being mixed order with respect to aqueous concentration. The rate of degradation was modeled by coupling Michaelis-Menten kinetics for aqueous-phase solute with an intraaggregate radial diffusion model for naphthalene sorption and desorption with soil. It was shown by modeling and confirmed by experiment, for the soil suspension particle sizes employed in these tests, that the naphthalene sorption-desorption process was reversible and rapid compared to the rate of microbial degradation. The maximum rate of microbial degradation was proportional to the soil-to-water ratio and independent of nitrate concentration for initial nitrate concentrations greater than several hundred micrograms per gram of soil. Nitrate reduction was described by utilizing the total mass removal of naphthalene and a stoichiometric conversion factor. A coupled solute desorption-degradation model is presented for microbial degradation of hydrophobic organic compounds that are desorbed from porous soil aggregates, assuming sorbed solute is inaccessible to microorganisms and that the rate of solute release from the solid is rapid compared to the rate of retarded intraaggregate diffusion.

Introduction

Knowledge of the transport and fate of pollutants that have been discharged into soil-water systems is important for understanding the effects of environmental contaminants in the subsurface environment. Mihelcic and Luthy (1, 2) have provided experimental evidence for the microbial degradation of low molecular weight polycyclic aromatic hydrocarbons (PAH) under denitrification conditions. In that work it was shown that acenaphthene and naphthalene were microbially degraded under nitrate-excess conditions, but not under anoxic nitrate-limiting conditions. The purpose of the results presented here is to develop and experimentally verify models that combine biological degradation and sorption-desorption reactions of naphthalene in batch soil-water suspensions under denitrification conditions, and the associated nitrate reduction.

Nitrate Reduction. A number of investigations have shown that the rate of denitrification in either wastewater or soil systems is dependent on the type of available organic material (3, 4). For this reason some researchers have incorporated into denitrification models various fractions of available organic carbon, each with a respective rate of decomposition (5-7). For soils, the fraction of organic carbon that is mineralizable under denitrification conditions, and not the total organic carbon content, has been strongly correlated to denitrification rates (8-12).

The effect of nitrate concentration on the denitrification rate in soils has been described as either a first-order (9,

13), zero-order (14), or mixed-order reaction (11, 15-18), while the effect of carbon substrate has been described by a first- or mixed-order reaction with respect to substrate concentration (11, 19). These assorted rate relationships resulted from studies that employed various concentrations of nitrate and different experimental protocols including column studies, completely mixed batch reactors, and unimixed flooded and unflooded soils.

Many of the investigations that have shown soil denitrification kinetics dependent on nitrate concentration were conducted under flooded soil conditions with standing water (20, 21). Tests that examined various situations indicated that flooded and unflooded soils exhibit first- and zero-order kinetics, respectively. The difference in the rate dependency was attributed to a diffusion-limiting reaction in the flooded soil system. It appears for batch soil denitrification tests with a soil suspension being agitated periodically that the rate of nitrate reduction will be zero order with respect to nitrate for aqueous-phase nitrate concentrations greater than several milligrams per liter, corresponding to appreciably greater than several micrograms of NO_3^- per gram of soil.

Organic Compound Mineralization. In general, the microbial degradation of an organic compound in soil and water systems can be described according to Monod kinetics. Limiting forms of the Monod rate equation are often employed to describe microbial degradation of organic compounds in soils and aquatic environments. For example, Paris et al. (22, 23) utilized Monod kinetics to describe the microbial removal rate of malathion, chlorpropham, and the butoxyethyl ester of 2,4-D in natural waters. The authors assumed that the bacteria concentration remained constant and that the low solubility of the hydrophobic organic compounds in water resulted in a first-order rate dependency. They showed, by varying the initial bacterial concentration by orders of magnitude, that there were proportional changes in a pseudo-first-order rate constant. Other researchers have incorporated bacterial growth kinetics for the modeling of soil and water systems in which microbial growth influenced the shape of the substrate disappearance curve (24-29). Microbial growth and other factors that affect the shape of the substrate disappearance curve have been reviewed elsewhere (30).

Solute Partitioning. As discussed elsewhere (2), the role of organic solute sorption on microbial degradation may be to decrease the total amount of solute available to microorganisms for degradation (31), as well as result in the entrapment of solute in soil micropores for long periods of time (32). In one study, the desorption rate from bentonite clay did not limit microbial degradation of *n*-decylamine (33). Sorption processes have been incorporated into a model that described substrate disappearance, assuming that the sorption kinetics were rapid compared to the rate of microbial degradation (34). In that model, solute sorption reduced the potential amount of degradable substrate by lowering the aqueous-phase concentration. Ogram et al. (31) demonstrated for the herbicide 2,4-D, in short-term tests with acclimated organisms, that

Michigan Technological University.
Carnegie Mellon University.

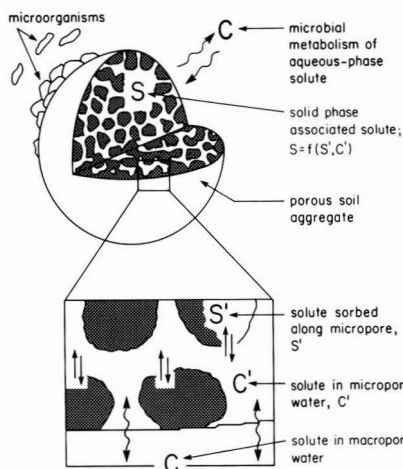


Figure 1. Conceptual drawing of the processes occurring during the microbial degradation of a hydrophobic organic compound in a soil-water suspension. Microorganisms are size excluded from the micropores, and local equilibrium exists between solute in micropore water and on micropore surfaces. Adapted from ref 47.

sorbed-phase solute was not amenable to microbial degradation.

Model Development

The following section explains the development of an approach to describe the microbially induced changes in naphthalene and nitrate concentrations in acclimated soil-water suspensions with temporal consideration of the potential effects of organic solute sorption and desorption on naphthalene degradation.

Microbial Degradation of Polycyclic Aromatic Hydrocarbons. The microbial degradation of naphthalene in a soil-water suspension is envisioned to occur through the processes illustrated in Figure 1. For a system maintained under gentle suspension with an acclimated microorganism population, the degradation of naphthalene will occur through the solute residing in the bulk aqueous phase. The rate of degradation is proportional to the substrate concentration in the bulk aqueous phase, C , and the active cell population. It is assumed that solid-associated solute, S , is inaccessible to the microorganisms. As the aqueous-phase solute concentration begins to decrease, a concentration gradient develops which allows sorbed solute, S' , to desorb and diffuse through pore water, C' , into the bulk phase. The solid is viewed as a porous aggregate with the solute desorption process being dependent upon retarded intraaggregate diffusion to the bulk aqueous phase with the release of solute into micropores being rapid relative to the rate of retarded intraaggregate diffusion. It is assumed that the bulk-phase concentration is uniform and there is sufficient turbulence so no outside boundary layer resistance between the bulk phase and the particle exists. This assumption is appropriate for the experiments conducted in this work with soil-water suspensions maintained under gentle agitation. It is also assumed that there is no mass-transfer resistance between a compound desorbing from the solid phase to a biofilm that may be on, or near, the particle surface, or mass-transfer resistance for the organic compound to diffuse to the microorganisms from the bulk aqueous phase. These processes can be described by coupling a microbial degradation kinetic expression with a solute-soil radial diffusion model (35) for the sorption and desorption of organic compounds

within porous spherical soil aggregates.

The change in aqueous-phase organic solute concentration with time as a result of sorption and desorption can be written as follows:

$$\frac{dC}{dt} = -\frac{V_s}{V} \frac{d\bar{S}}{dt} \quad (1)$$

where C is the aqueous concentration of naphthalene (mol/mL); \bar{S} is the average solute concentration in the solid integrated over the sphere (mol/cm³ total); V_s is the volume of the solid (cm³ total) and equals $V\rho/(1-n)\rho_s$, where ρ is the soil-to-water ratio (g of solid/cm³ of liquid) and ρ_s is the specific weight of the solid (g of solid/cm³ of solid); n is the intraaggregate porosity of the solid (cm³ of liquid/cm³ total); V is the volume of the liquid phase (cm³ of liquid); and t is time (min). The sorption-desorption process is dependent on the solute effective intraparticle diffusivity, which is defined as (35, 47)

$$D_{\text{eff}} = D_m n^2 / [(1-n)\rho_s K_p + n] \quad (2)$$

where D_m is the aqueous solute molecular diffusivity and K_p is a linear sorption partition coefficient (cm³ of liquid/g of solid). The time to approach equilibrium is proportional to the value of the sorption partition coefficient and square of the particle mean volumetric radius.

Michaelis-Menten kinetics are used to describe microbially induced substrate depletion from the aqueous phase; thus, the overall change in concentration of organic solute in the aqueous phase is provided by coupling the change due to sorption and desorption from the soil with the change resulting from microbial substrate depletion of aqueous-phase solute:

$$\frac{dC}{dt} = -\frac{V_s}{V} \frac{d\bar{S}}{dt} - \frac{K_{\text{max}} C}{K_s + C} \quad (3)$$

where K_{max} is the maximum rate of the reaction (mol/mL-min or mg/L-day) and is equal to $\mu_m B/Y$, where μ_m is the maximum growth rate, B the bacterial population, and Y the yield factor for conversion of substrate to biomass, and K_s is the half-saturation coefficient (mol/mL or mg/L).

If it is assumed that an acclimated microbial population is constant and proportional to the mass of soil in the system, then K'_{max} can be defined as the maximum rate, K_{max} , divided by ρ . The units of K'_{max} are mol/g-min (or mg/g-day). The assumption of a constant active microbial population and proportionality between microbial population and soil-to-water ratio is appropriate for the experiments performed in this study. These experiments employed small amounts of acclimated soil, the mass of naphthalene used for acclimation was typically greater than the mass employed in batch tests, and MPN counts of denitrifiers indicated no significant increase over a test duration.

As discussed later, for naphthalene and the particles used in the experimental portions of this work, the solute residing in the sorbed and aqueous phases may be assumed to be in equilibration over the course of the experiment. This assumption was justified because the solid was maintained in gentle suspension, and it was demonstrated that the process of microbial degradation occurred over time periods of days, whereas supplemental experiments with sterile controls showed that sorption and desorption occurred over a time period of approximately 1 h (36). Thus, the change in average sorbed-phase concentration with time can be related to the aqueous-phase concentration by a partition coefficient:

$$\frac{d\bar{S}}{dt} = K_p \rho_s (1 - n) \frac{dC}{dt} \quad (4)$$

Substitution of eq 4 into eq 3 and a reduction of terms yields

$$\frac{dC}{dt} = -\frac{K_{\max} C}{K_s + C} (1 + \rho K_p)^{-1} \quad (5)$$

Because of the rapidity with which naphthalene may attain sorption and desorption equilibrium with respect to degradation in the experiments performed in this study, K_{\max} and K_s were estimated from experimental data of aqueous-phase concentration versus time with a nonlinear parameter estimation program that utilizes principles of Bayes and Maximum Likelihood (37), applied to eq 5. An experimentally determined K_p (12 cm³/g) (2) and test-specific soil-to-water ratio were employed for parameter estimation.

The model described by eq 3 was used to verify the equilibrium assumption for estimating K_{\max} and K_s and evaluate the effect of sorption and desorption kinetics on the microbial degradation for unexplored conditions (36, 38). A radial diffusion model (39) was modified to include the microbial degradation terms included in eq 3 and is referred to as a coupled solute desorption-degradation model. This model combines a retarded radial diffusion mechanism for sorption and desorption from soil with microbial decay. The model permits input of physical, chemical, and biological parameters of the system.

Nitrate Reduction. The introduction of a degradable organic solute, such as naphthalene, into a soil environment contributes another source of available carbon in addition to mineralizable soil organic carbon. For the case of naphthalene in a soil-water suspension, one source of organic carbon substrate may dominate the loss of nitrate from a soil-water system. For experimental results presented previously (1, 2), these two substrate sources were of near-equal magnitudes. However, for the tests described here, which employed soil acclimated to naphthalene through a process in which there was sufficient nitrate present over a month or more followed by replacement of additional naphthalene, naphthalene was a much larger source of substrate than mineralizable soil organic carbon. This was a consequence of mineralizable soil organic carbon considered to be exhausted, since previous experiments had shown that it was depleted in approximately 3 weeks (2). Thus, for the case of tests conducted with sufficient naphthalene and an acclimated soil, mineralizable soil organic carbon was assumed to be negligible, assuming slow conversion of residual soil organic carbon to labile organic carbon. Nitrate reduction was modeled by relating it to the total aqueous- and sorbed-phase naphthalene utilization by a stoichiometric conversion factor of 48 mol of nitrate/5 mol of naphthalene (2). This conversion assumed that naphthalene is mineralized to only carbon dioxide and water and nitrate is reduced to nitrogen gas.

Materials and Methods

Experiments were conducted to determine the kinetics of microbial degradation of naphthalene including the effect of the initial nitrate concentration and soil-to-water ratio on the rate of naphthalene degradation. Tests with no headspace were conducted in 50-mL glass centrifuge tubes, sealed with Teflon-lined septum tops. This allowed direct aqueous sampling through the septum after solids separation. The samples contained 1–5 g of acclimated soil, and the aqueous phase contained mineral medium,

nitrate, and naphthalene. Blanks containing only mineral medium and naphthalene, and sterilized controls containing autoclaved soil (3 consecutive days for 1 h at 121 °C and steam pressure of 20 psi) with 200 mg/L HgCl₂, mineral medium, and naphthalene were used throughout to ensure no loss of naphthalene via abiotic processes. The soil used in this study was an undisturbed, subhumid grassland soil of the Barnes-Hamerly Association. The soil was air-dried, screened to pass a U.S. standard sieve no. 10, and placed in refrigerated storage. The mineral medium, prepared in deionized water, provided buffering capacity, nutrients, and sustaining electrolyte and had a pH of 6.8. The mineral medium was prepared such that after dilution with stock naphthalene solution the background electrolyte was 0.01 N CaCl₂ with the following salts (in mg/L): KH₂PO₄, 8.5; K₂HPO₄, 21.75; Na₂HP-O₄·7H₂O, 33.4; FeCl₃·6H₂O, 0.25; NH₄Cl, 1.7; and MgS-O₄·7H₂O, 22.5.

The samples were void of oxygen as verified by titrametric procedures. For the experiments described herein, acclimated soil was utilized in order to eliminate an acclimation period. This also supported the assumptions that the mineralizable soil organic carbon was negligible and the bacterial population remained constant over the duration of an experiment.

Preparation of Acclimated Soil. Acclimated soil was prepared by two methods. One technique entailed placement of a saturated naphthalene solution containing mineral medium and nitrate in a 1-L glass jar. This mixture was purged with helium gas for 1 h and 100 g of soil was added. The system was purged for another 0.5 h, after which the jar was sealed with minimal headspace. Aluminum foil was placed between the seal and the aqueous mixture. The slurry was mixed 3 h/day by a magnetic stirrer. Naphthalene and nitrate were analyzed periodically by briefly opening the seal and placing a helium purge in the sample while collecting approximately 15 mL of aqueous sample. This typically resulted in the sample being exposed for intervals less than 1 min. The soil was considered acclimated when naphthalene had attained nondetectable levels and nitrate had attained a value consistent with that predicted by consideration of the nitrate demand exerted by oxidation of naphthalene and the labile fraction of naturally occurring soil organic carbon. This process entailed the reduction of several hundred milligrams of nitrate per liter in the system. During acclimation it was observed that aqueous naphthalene concentrations remained constant for approximately 2 weeks, after which degradation occurred. This lag period was consistent with that observed in previous degradation tests with unacclimated soil. Acclimated soil was also obtained by reserving soil samples from prior tests in which naphthalene had attained nondetectable levels via microbial degradation.

Effect of Nitrate Concentration on the Degradation Rate. Experiments were conducted to assess whether naphthalene degradation was independent of nitrate concentration. Samples were prepared with initial nitrate concentrations of 35–135 mg/L NO₃⁻. All other initial experimental parameters were the same as in previous experiments conducted with 2 g of soil (2).

Effect of Soil-to-Water Ratio on the Degradation Rate. Experiments were performed with soil-to-water ratios of approximately 1, 2, and 5 g per 50 mL in order to examine the proportionality of the maximum rate, K_{\max} , with respect to the mass of acclimated soil. All other initial experimental parameters were the same as experiments discussed previously.

Enumeration of Denitrifying Organisms. The denitrifying cell population was enumerated by an MPN method (40) using two different bacterial growth media for comparison (40, 41). A comparison of the mass of naphthalene applied during acclimation and test conditions was conducted in order to test the assumption that any denitrifier growth during the test was small relative to the initial number present.

Soil Particle Size Characterization. The soil particles employed in this study were characterized by electron microscopy in order to confirm their porous aggregate nature and to assess whether the particle size distribution changed significantly over the duration of a test. Samples were prepared for electron microscopy by combining 2 g of soil and approximately 50 mL of 0.01 N CaCl₂ deionized water and shaking for 24 h.

Two replicate sample sets were employed for scanning electron microscopy (SEM). One set was agitated on a wrist-action shaker for 4 h. The other set was agitated 4 h daily for 1 month. The samples were prepared for SEM analysis by sampling the suspensions with a medicine dropper and combining two drops with 20 mL of deionized water and filtering through a 0.2- μ m Nuclepore filter (Millipore Corp.). The filter was mounted on an aluminum stub with an amorphous graphite suspension (SEEVAC). Particle size distribution was performed by a scanning electron microscope with LeMont Scientific software. Particles greater than 0.32 μ m were counted 100% of the time.

Sorption-Desorption Reversibility and Rate Tests. Tests were conducted to measure the reversibility and kinetics of naphthalene sorption and desorption. Batch sorption tests were run in 50-mL centrifuge tubes with various amounts of soil and aqueous medium containing naphthalene and electrolyte (2).

Batch desorption isotherms were obtained in a similar manner by combining 5, 10, 15, or 20 g of sterilized soil with an aqueous phase of naphthalene and 0.01 N CaCl₂. Samples were initially equilibrated for periods of 1, 3, or 36 days in three experiments. A successive desorption test (42) consisted of decanting the supernatant and replacing it with deionized water containing CaCl₂. Liquid volume was measured to 10⁻² mL since the calculation of solute mass desorbed included a correction for the pore water that had been entrained during the solids separation process. These samples were equilibrated on a wrist-action shaker for 8 h and centrifuged, and the aqueous phase was analyzed for desorbed naphthalene. This process was repeated to obtain successive desorption measurements until no significant desorption was observed from the soil particles.

A set of batch tests was performed to measure the rate of naphthalene sorption and desorption. Samples contained 1 or 3 g of sterilized soil per 50 mL, and blanks which contained no soil were run concurrently. Samples were shaken 4 h daily and centrifuged, and the supernatant was analyzed. This experimental setup could only monitor concentrations for time increments as short as several hours. In an effort to minimize the interval prior to the time of the first sampling point, the time increment for initial equilibration and subsequent centrifuging was abbreviated by equilibrating the first sample for 0.5 h, followed by centrifuging for 0.5 h, prior to analysis. After analysis, the soil samples were then employed for desorption tests by reserving the solids that contained naphthalene, adding solute-free aqueous phase, and resuspending.

Analytical Procedures. Organic solute analyses were performed with a HPLC equipped with an LC-PAH col-

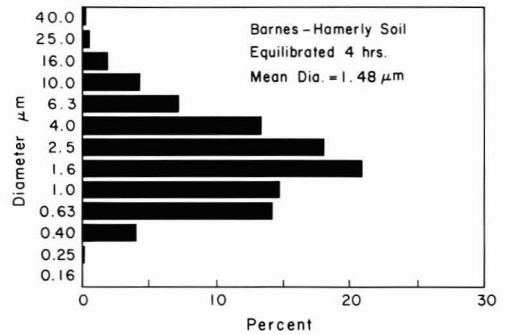


Figure 2. Particle size distribution obtained from scanning electron microscopy for a soil-water suspension equilibrated for 4 h.

umn (Supelco Inc.) and fluorescence detector. Shaking was performed with a wrist-action shaker and centrifuging at 875g with a clinical centrifuge. Aqueous nitrate, nitrite, and sulfate were analyzed with a Dionex IC 14 ion chromatograph (IC) equipped with an AS3 separator column and a 35350 anion fiber suppressor column. Prior to analysis by IC methods, organic constituents were removed by passing 15 mL of aqueous sample through a C₁₈ cartridge (Water Associates, Inc.).

Results

Soil Particle Characterization. Figure 2 shows a representative particle size distribution obtained by SEM for a sample agitated for 4 h. The abscissa shows the percent of total particles counted. The size range of the particles was 0.25–50 μ m with a geometric mean diameter of 1.5 μ m, which was verified by replicate tests. Graphical and statistical comparison of the cumulative particle size distributions from replicate results showed that the particle diameter was log-normally distributed and did not vary with either 4 h or 36 days of intermittent shaking (36).

The volumetric mean diameter was calculated from the number mean diameter (43):

$$\log(\bar{d}_p)_V = \log(\bar{d}_p)_N + 6.9(\log \sigma_g^2) \quad (6)$$

where $\bar{d}_p)_V$ is the volumetric mean diameter (μ m), $\bar{d}_p)_N$ is the number mean diameter (μ m), and σ_g is the geometric standard deviation. The volume mean diameter was determined to be 35 μ m. This value was used in the coupled solute desorption-degradation model.

The particle width-to-length ratio was determined by SEM analysis for the four samples employed for particle size determination. The width-to-length ratio ranged from 0.42 to 0.44, and thus, the particles were somewhat ellipsoidal rather than spherical; though for modeling purposes, the particles were assumed to be spherical aggregates. Electron micrographs showed that the particles had irregularly shaped interior voids.

Sorption-Desorption Reversibility and Rate Tests. Figure 3 shows sorption and desorption isotherm data for an experiment in which naphthalene was initially equilibrated for 3 days. Each point in the figure represents an individual sample. This figure shows that the sorption and desorption isotherms have similar slopes, as was evident in other experiments in which naphthalene was initially equilibrated for periods of 1 and 36 days. The results suggest that naphthalene sorption was reversible and solute desorption kinetics were at least as rapid as the 8-h time period allocated for desorption equilibrium.

These tests were conducted for initial sorption equilibrium periods as long as 36 days in order to assess naph-

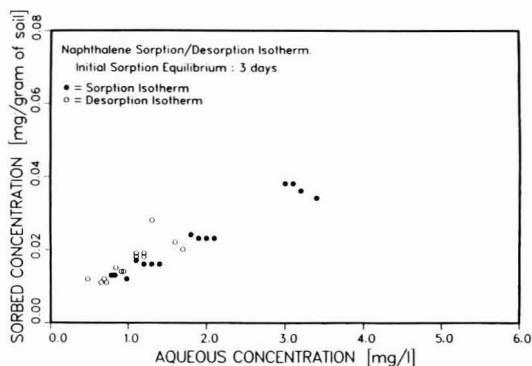


Figure 3. Naphthalene sorption and desorption isotherm data for an initial 3-day sorption equilibrium period.

thalene desorption for an equilibrium period comparable to the longest acclimation period observed in previous microbial degradation tests (1, 2). It was believed that the longer equilibrium period may have an effect on the extent to which naphthalene may be released from the soil. Karickhoff (44) suggested that the ease of solvent extracting sorbed PAH from soil decreased with increasing equilibration period. Karickhoff also reported results of organics release from sediments by sparging the system and trapping the organics on a chromatography column. Sorbed naphthalene was recovered (>90%) in minutes to a few hours, while hexachlorobenzene required 10–30 days for sorption equilibration times ranging from 5 to 58 days. Karickhoff concluded from this work, and the work of others, that intraparticle diffusion may have occurred, whereby a sorbate is slowly incorporated into a porous aggregated particle. The results shown in Figure 3 are consistent with Karickhoff's (45) observations with naphthalene. As explained below, the intraaggregate solute diffusion concept provides predictions consistent with the results of this study for naphthalene sorption and desorption.

Experimental data for naphthalene sorption and desorption kinetics are presented in Table I. Aqueous solute concentrations are presented for sorption periods ranging from 1.5 to 24 h for samples that contained 1 and 3 g of soil and desorption periods of 1–26 h. The values presented in Table I are the average of two to five samples, and the standard deviation is presented in parentheses. The samples with 3 g of soil contained a greater initial mass of naphthalene than samples with 1 g of soil, which accounts for the similarity in the aqueous-phase naphthalene concentration after sorption. The results show that the aqueous-phase concentration of naphthalene did not change with time after the first sampling point. For sorption the first sample was obtained at 90 min after sample preparation, while for the desorption tests the first sample was obtained 60 min after desorption was initiated. Thus, it appears that desorption equilibrium was attained in time periods less than 1 h.

Ninety percent sorption equilibrium of 1,4-dichlorobenzene ($\log K_{ow} = 3.4$) was attained in less than 100 min in another study for particles with a larger diameter than used in the tests reported here (47). In this study, naphthalene ($\log K_{ow} = 3.3$) attained close to 100% sorption equilibrium in less than or equal to 90 min. The experimental results presented in Table I, and studies of others (44, 45), appear to support the belief that naphthalene sorption onto soil is a reversible process and the rate of

Table I. Aqueous-Phase Naphthalene Concentrations for Sorption and Desorption in Soil-Water Suspensions with Different Equilibration Periods

equilb time, h	aq naphthalene concn, ^a mg/L	
	3 g of soil/50 mL	1 g of soil/50 mL
Sorption		
1.5	19.6 (0.20)	19.5 (0.85)
2.5	18.2 (0.40)	20.0 (1.6)
3.5	17.6 (0.60)	19.4 (0.20)
7.0	19.5 (0.05)	18.5 (0.20)
24	20.3 (2.4)	21.5 (1.7)
Desorption		
1.0	7.5 (0.050)	6.3 (0.30)
1.5	8.2 (0.20)	6.4 (0.20)
3.0	6.7 (0.30)	6.2 (0.05)
8.0	7.4 (2.3)	5.9 (0.30)
26	7.1 (1.7)	6.8 (0.62)

^a Mean values and standard deviations for two to five replicates.

desorption is relatively fast. This finding is important for modeling the rate of microbial degradation of naphthalene in a soil-water suspension.

Enumeration of Denitrifying Organisms. Five MPN tests with acclimated soil provided an initial average population of $1.2 \times 10^5 \pm 6 \times 10^4$ denitrifiers/g of soil with one growth medium (40) and 1.2×10^5 denitrifiers/g of soil with a second growth medium (41). Three measurements at the conclusion of naphthalene degradation tests showed $1.4 \times 10^5 \pm 9 \times 10^4$ denitrifiers/g of soil. Although no direct measurement was made of the growth of specific naphthalene degraders, comparison of the mass of naphthalene applied per gram of soil for acclimation and test systems provides further support that the naphthalene-degrading population did not change significantly over the course of an experiment. For experiments 1–3, the mass of naphthalene applied was similar during both acclimation and tests, while in experiments 4–6, the mass of naphthalene applied was up to 1 order of magnitude greater during acclimation than during the test. Thus, it is expected that at least in experiments 4–6 any growth in population of naphthalene-degrading organisms was small relative to the initial number.

Additional characterization of the microorganisms was conducted (48). The total bacteria population was $3.0 (\pm 0.6) \times 10^7$ cells/mL as estimated by an acridine orange direct count procedure, plus approximately 7×10^5 fungal spores/mL and occasional fungal- and actinomycete-like filaments. Most of the isolates were Gram positive.

Microbial Degradation of Naphthalene. Six individual tests with multiple samples were performed to examine the degradation of naphthalene. Three of the tests used acclimated soil obtained from a single large batch of soil that had been exposed to naphthalene, whereas the other three tests used acclimated soil obtained from samples reserved from prior degradation tests. Blanks and controls remained constant over the duration of the tests, indicating no abiotic loss of solute. Representative data in Figure 4 show that the microbial degradation of naphthalene followed mixed-order kinetics regardless of the procedure employed to obtain an acclimated microorganism population. In this figure, ND represents an analytical determination less than the detection limit of 0.01 mg/L (7.8×10^{-11} mol/mL). Each data point represents the determination from one or two individual samples, which were discarded after sample analyses.

The results of biokinetic parameter estimation for experimental data obtained from various tests conducted over a time period of 9 months are shown in Table II.

Table II. Experimentally Determined Biokinetic Coefficients and Initial Conditions for Modeling the Microbial Degradation of Naphthalene under Denitrification Conditions

expt	% mineralized ^d	soil, g	K_{max} , mg/L-day	K'_{max} ^e , $\times 10^3$ mg/g-day	K_s , mg/L	C_i ^f mg/L	N_i ^g mg/L
1 ^a	100	1.1104	0.20	9.00	0.33	2.0	134
2 ^a		5.2789	0.47	4.48	0.40	2.0	135
3 ^b	93	2.0000	0.75	18.8	1.0	3.1	35
4 ^c	55	2.0000	0.39	9.75	0.20	5.6	37
5 ^c	100	2.0000	0.35	8.75	0.36	4.0	50
6 ^c	100	5.2789	0.83	7.90	0.54	3.6	37

^a Experiments conducted from soil samples reserved from previous experiments that examined microbial degradation of naphthalene. ^b Experimental data from ref 2. ^c Experiments conducted from a single batch of acclimated soil. ^d Estimation of the percent of total naphthalene mineralized based on the stoichiometry of nitrate reduction and naphthalene mineralization (2). ^e K'_{max} is K_{max} normalized for the soil-to-water ratio (g of soil/mL of water). ^f C_i is the aqueous naphthalene concentration after a 1-day sorption equilibrium. ^g N_i is the initial nitrate concentration (mg of NO_3^- /L).

Shown are the maximum rates and half-saturation coefficients along with the initial experimental conditions. Comparison of the experimental data and coupled solute desorption-degradation model response is provided in Figure 4, parts a-c, which correspond to experiments 1, 3, and 6, respectively. The goodness of fit of the parameter estimate was judged by inspection of the model prediction versus experimental data, and by the summation of the standard deviation of the residuals between the measured and predicted responses, which were 0.36, 0.074, 0.016, 0.68, 0.51, and 0.29 for experiments 1-6, respectively.

The estimation of the parameters K_{max} and K_s employed all data having values above the detection level as well as the first nondetectable data point, which was taken as 0.01 mg/L. Sensitivity analysis was performed to examine the effect that decreasing the time of occurrence of the nondetectable data point would have on the estimation of the biokinetic parameters. This was performed by varying the time for the first measured nondetectable concentration to that time of the lowest detectable concentration.

The estimated values of K_{max} and K_s were not sensitive with respect to the time of observance of the first nondetectable concentration. For example, for data in experiment 6, the nondetectable point was changed from 19 to 17 days. This caused K_{max} to increase from 0.83 to 0.85 mg/L-day, while K_s remained at 0.54 mg/L. Likewise in experiment 3, the time of occurrence of the nondetectable point was changed from 18 to 17 and 16 days. This caused K_{max} to change from 0.75 to 0.74 mg/L-day, respectively, whereas K_s remained at 1.0 mg/L. This slight change in the estimated parameters did not affect the error residual in the parameter estimation program between the predicted model response and the experimental data. Experiments 1, 2, and 4 were expected to show similar insensitivity to the time of first observance of nondetectable naphthalene concentration since these results showed a similar set of experimental data in which measurable aqueous-phase solute concentration data spanned 2 orders of magnitude.

The microbial kinetic parameters for experiment 5 were estimated from five experimental data points, four of which had an aqueous concentration greater than 1 mg/L and one which was nondetectable. Sensitivity analysis on the parameters estimated for this experiment showed that as the time of nondetection was decreased from 23 to 22, 20, and 18 days, K_{max} decreased from 0.35 to 0.34, 0.32, and 0.32 mg/L-day, respectively, while K_s decreased from 0.36 to 0.24, 0.16, and 0.10 mg/L, respectively. Thus, in this instance there was a small difference in the range of the predicted biokinetic parameters from 0.32 to 0.35 mg/L-day for K_{max} and 0.10 to 0.36 mg/L for K_s . In summary, it was concluded that the parameters K_{max} and K_s were

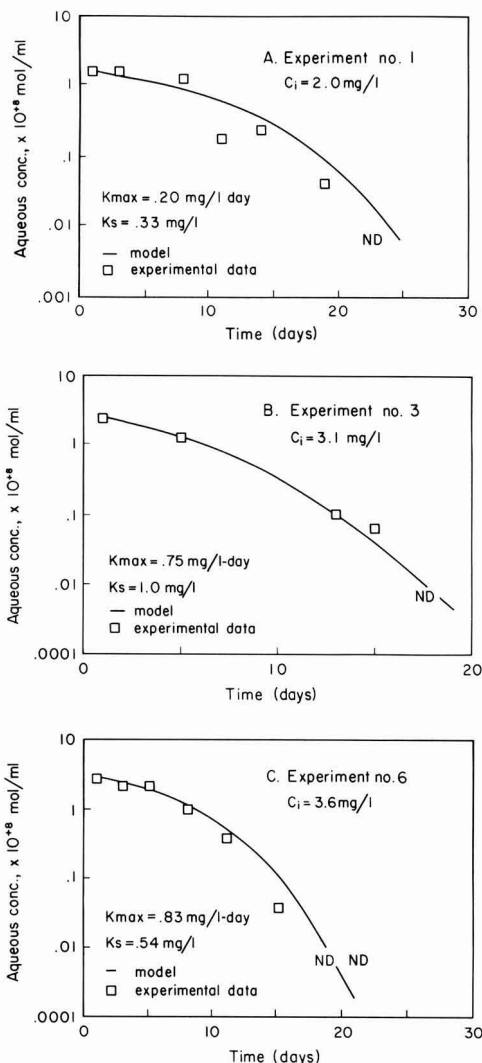


Figure 4. Experimental data and coupled solute desorption-degradation model response for microbial degradation of naphthalene in a soil-water suspension under denitrification conditions. Experiments 1, 3, and 6 correspond to panels A-C, respectively. ND corresponds to a nondetectable measurement.

insensitive to the time of measurement of the first nondetectable aqueous-phase naphthalene concentration, es-

Table III. Comparison of Desorption Equilibrium Assumption and Coupled Desorption-Degradation Model for Estimating Microbial Degradation of Naphthalene in a Soil-Water Suspension

time, day	calcd aqueous-phase naphthalene concn, $\times 10^8$ mol/mL	
	coupled desorption-degradation eq 3	desorption-equilibrium eq 5
1	1.6	1.6
4	1.2	1.1
8	0.70	0.66
12	0.29	0.28
16	0.070	0.066
20	0.010	0.0093

pecially for the situations in which the aqueous concentration data gave values encompassing ~ 2 orders of magnitude.

The results in Table II indicate that the degradation rate is independent of nitrate for aqueous-phase nitrate concentrations greater than several milligrams per liter. Initial nitrate concentration was varied by a factor of approximately 3.5, from 37 to 135 mg/L, for experiments 1 and 4-6, yet the maximum rate normalized to account for the amount of soil (K'_{\max}) remained relatively constant in the range (7.9-9.75) $\times 10^{-3}$ mg/g-day. Experiments 2 and 3 show values of K'_{\max} that are outside this range, but the values vary inversely with respect to nitrate. For this reason it was judged that the variation was not attributable to nitrate-dependent microbial kinetics. The half-saturation coefficient, K_s , remained constant over the range of tests except for experiment 3. This may have been a result of aged soil, as experiment 3 was conducted approximately 7 months prior to the other five experiments.

For all six tests, the average value of K_s was found to be 0.48 mg/L with a standard deviation of 0.28 mg/L. If the samples reserved from the large batch acclimation procedure are considered collectively, the average K_s was equal to 0.37 mg/L with a standard deviation of 0.17 mg/L. This average value agrees with the result from experiment 1, for which it was estimated that there was 100% mineralization of naphthalene.

The average value of K'_{\max} for all six samples was found to be 9.8×10^{-3} mg/g-day with a standard deviation of 4.8×10^{-3} mg/g-day. If the three samples prepared from the large batch of acclimated soil are considered separately, the average value of K'_{\max} was 8.8×10^{-3} mg/g-day with a standard deviation of 0.95×10^{-3} mg/g-day. This average value for similarly prepared experiments agrees with the result from experiment 1, for which it was estimated that there was 100% mineralization of naphthalene. As hypothesized, K_{\max} was found to be dependent on the initial amount of acclimated soil originally placed within the experimental system. This result agrees with the work of Paris et al. (23).

Table II also presents an estimate of the percent naphthalene mineralized, which is based on the stoichiometry of nitrate reduction to $N_2(g)$ and naphthalene mineralization to carbon dioxide and water only (2). It was estimated that the extent of naphthalene mineralization ranged from 55 to 100%.

Equilibrium Sorption-Desorption and Coupled Desorption-Degradation Model. Verification of the rapid desorption kinetic assumption inherent to eq 5 was performed by comparing the predicted results from the models expressed by eqs 3 and 5. This comparison is presented in Table III for parameters obtained from experiment 2 and shows that the solutions to both approaches are essentially identical. This is a result of the

rate of intraparticle diffusion being rapid compared to the kinetics of microbial degradation for the soil used in these tests. This was also demonstrated experimentally by comparison of desorption kinetic tests and biological degradation tests, where desorption was shown to occur over time periods of less than 1 h while degradation occurred over periods of 2-3 weeks. The model responses provided by the coupled solute desorption-degradation model in Figure 4 agree closely with the experimental data, as was the case for the other three experiments whose results are provided elsewhere (36).

These calculations use a mean volumetric particle radius of 17.5 μm , experimentally determined K_p of 12 cm^3/g (2), and n of 0.13 (47). The molecular diffusivity for naphthalene in water at 25 $^\circ\text{C}$ was estimated to be 7.24×10^{-6} cm^2/s by the Hayduk and Minhaus correlation (49) as recommended by Reid et al. (50). The experimental data in Table III clearly demonstrate that the rate of microbial degradation was not limited by sorption kinetics owing to the reversibility and rapidity of sorption and desorption for the soil-water suspensions employed in this investigation.

The results for experiments 4-6 were obtained from experiments initiated from a large batch of acclimated soil. The maximum rates in experiments 4 and 5, with 2 g of soil, were 0.39 and 0.35 mg/L-day, respectively, whereas the maximum rate in experiment 6 for a system with approximately 5.3 g of soil was 0.83 mg/L-day. It may be expected that the system with 5.3 g of soil would have a maximum rate of 2.6 times greater than the system with 2 g of soil, as it was hypothesized that the maximum rate would be a function of the initial active cell population. The estimated maximum rate was approximately 2.2 times greater in the system with 5.3 g of soil compared to the system with 2 g of soil. However, this does not imply that the time required to attain nondetectable aqueous-phase naphthalene concentration would be more than twice as rapid for tests with 5.3 g of soil. In comparison of experiment 6 with experiments 4 and 5, which had similar initial aqueous naphthalene concentrations after initial sorption equilibrium, it was observed that experiment 6 did not attain nondetectable levels 2.2 times faster than experiment 4 or 5. In fact, the rate was only slightly more rapid, as nondetectable levels were attained in 28 and 23 days, respectively, for experiments 4 and 5, and 19 days for experiment 6. The similarity in these results is a consequence of the mass of solute associated with the solid phase. Measured initial aqueous mass was approximately 2.2×10^{-6} , 1.6×10^{-6} , and 1.4×10^{-6} mol for experiments 4-6, respectively, while the estimated sorbed mass was 1.0×10^{-6} , 0.75×10^{-6} , and 1.8×10^{-6} mol, respectively. Thus, the test with 5.3 g of soil had a greater amount of naphthalene sorbed to the solid phase, and release of naphthalene to the aqueous phase prolonged the time to deplete naphthalene to nondetectable levels than may otherwise be anticipated for a system in which there was no reservoir of sorbed-phase solute.

Figure 5 illustrates this point in a different manner. Shown are model simulations of the total aqueous and sorbed naphthalene in a soil-water system as a function of the soil concentration. The initial total naphthalene in the system was 2.34×10^{-5} mol, and K_{\max} and K_s were set at 0.20 mg/L-day and 0.33 mg/L, respectively. All other model inputs were the same as used in modeling the experimental systems. Figure 5 shows that the system with less soil had less total naphthalene remaining after 30 days. Increased sorption lowers the aqueous-phase concentration and hence the mass removal rate. For example, initial

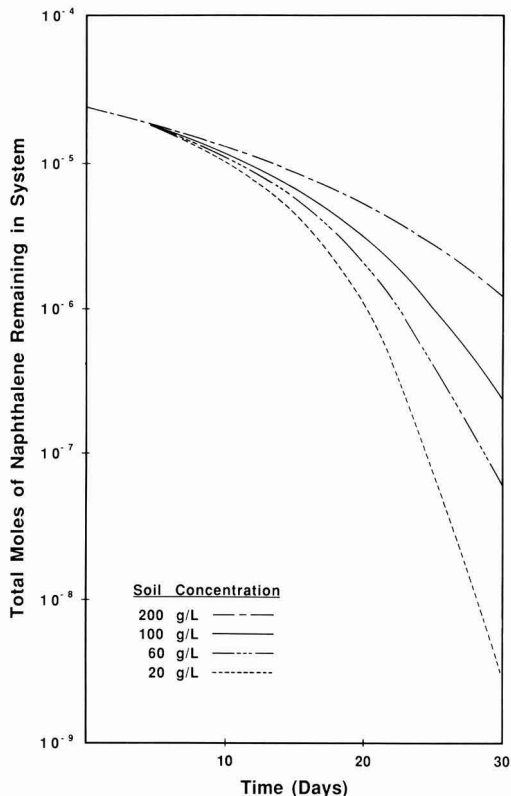


Figure 5. Coupled solute desorption–degradation model simulation for initial [naphthalene] = 2.34×10^{-5} mol, $K_{\max} = 0.20$ mg/L-day, $K_s = 0.20$ mg/L, and soil concentrations of 20, 60, 100, and 200 g/L. All other model inputs are the same as used during modeling the experimental system.

aqueous naphthalene concentration was approximately 1.9×10^{-8} , 1.4×10^{-8} , 1.1×10^{-8} , and 0.69×10^{-8} mol/mL for the system with 20, 60, 100, and 200 g/L solids, respectively. The soil acts as a reservoir for release of sorbed-phase naphthalene, prolonging the time for aqueous depletion.

Nitrate Reduction. The purpose of developing a nitrate reduction model was to estimate the nitrate reduction associated with degradation of PAH compounds under denitrification conditions. Under nitrate-excess conditions, the denitrification rate can be related to the substrate removal rate by a stoichiometric conversion factor (48 mol of nitrate/5 mol of naphthalene), assuming the denitrification end products are carbon dioxide, water, and nitrogen gas (2). This study measured the concentration of only nitrate and nitrite. Nitrite concentrations were typically below detection levels in all samples.

Though toward the end of experiment 6 the nitrate concentration approached nondetectable levels, these data were utilized in modeling because at the time when nitrate was nearing nondetectable levels, over 99% of the naphthalene had been degraded. Also, it is possible that denitrification intermediates were still available as electron acceptors. Parts A and B of Figure 6 compare the predicted and experimental nitrate concentration over time for experiments 5 and 6, respectively. Nitrate depletion was modeled relatively close to that observed in experiments. Additional study is needed to define the relationships between stoichiometric organic compound deg-

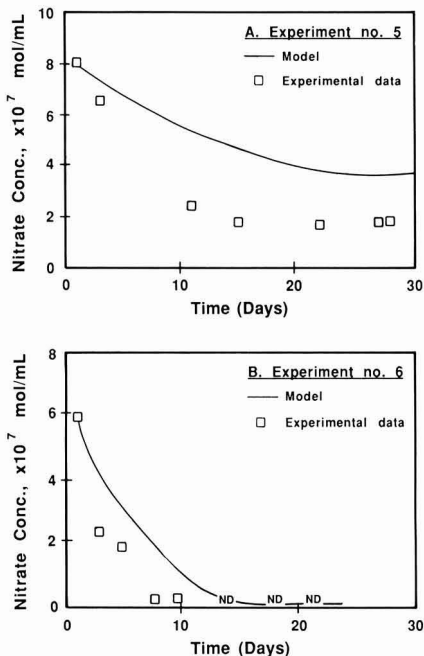


Figure 6. Experimental data and model response for nitrate reduction associated with the microbial degradation of naphthalene. Panels A and B correspond to experiments 5 and 6, respectively. ND refers to a nondetectable measurement.

radation and nitrate utilization.

Conclusions

The microbial degradation of naphthalene under denitrification conditions in batch soil–water suspensions was described by a kinetic model that included consideration of the sorbed-phase solute. This approach combined a retarded radial diffusion model to describe solute sorption and desorption with Michaelis–Menten kinetics to describe the rate of substrate depletion from the bulk aqueous phase, assuming the bacterial concentration was constant over the period of interest and sorbed solute was inaccessible to microorganisms. Experimental measurements showed and modeling confirmed that the process of naphthalene sorption–desorption was reversible and the kinetics were rapid compared to those of microbial degradation for the soil particle size employed in this investigation. The rate of naphthalene degradation was independent of nitrate concentration and proportional to the soil-to-water ratio in the range of 1–5 g/50 mL as employed in the batch microbial degradation experiments. Nitrate reduction was related to naphthalene degradation by a stoichiometric conversion factor that assumed end products of carbon dioxide, water, and nitrogen gas.

The concepts and assumptions embodied in the coupled desorption–degradation model are potentially very significant when the reactions and fate of hydrophobic organic compounds in soil–water systems are evaluated. This suggests the need for understanding the various interactions among the physical, chemical, and biological parameters of the soil–water system. Compound hydrophobicity, soil particle size, and rate of release of sorbate from the solid are expected to influence strongly the microbial degradation reactions. There is need for additional research on the extent to which hydrophobic solute solu-

bilization must occur before there may be significant microbial degradation. This has important implications for remediation of soil and groundwater systems contaminated by hydrophobic organic pollutants.

Acknowledgments

Characterization of the microorganism population was performed by the laboratory of William C. Ghiorse, Department of Microbiology, Cornell University. Beth Ebling assisted with analytical measurements.

Literature Cited

- (1) Mihelcic, J. R.; Luthy, R. G. *Appl. Environ. Microbiol.* **1988**, *54*, 1182-1187.
- (2) Mihelcic, J. R.; Luthy, R. G. *Appl. Environ. Microbiol.* **1988**, *54*, 1188-1198.
- (3) Jacobson, S. N.; Alexander, N. *Soil Biol. Biochem.* **1980**, *12*, 501-505.
- (4) Lewandowski, Z. *Water Res.* **1982**, *16*, 19-22.
- (5) Jenkinson, D. S.; Rayner, J. H. *Soil Sci.* **1977**, *123*, 298-305.
- (6) Reddy, K. R.; Khaleel, R.; Overcash, M. R. *J. Environ. Qual.* **1980**, *9*, 434-442.
- (7) Molina, J. A. E.; Clapp, C. E.; Shafer, M. J.; Chichester, F. W.; Larson, W. E. *Soil Sci. Soc. Am. J.* **1983**, *47*, 85-91.
- (8) Burford, J. R.; Bremner, J. M. *Soil Biol. Biochem.* **1975**, *7*, 389-394.
- (9) Stanford, G.; Vander Pol, R. A.; Dzienia, S. *Soil Sci. Soc. Am. Proc.* **1975**, *39*, 284-289.
- (10) Beauchamp, E. G.; Gale, C.; Yeomans, J. C. *Commun. Soil Sci. Plant Anal.* **1980**, *11*, 1221.
- (11) Reddy, K. R.; Rao, P. S. C.; Jessup, R. E. *Soil Sci. Soc. Am. J.* **1982**, *46*, 62-68.
- (12) Batonda, J.; Waring, S. A. *Rev. Rural Sci.* **1984**, *No. 5*, 231-239.
- (13) Stars, J. L.; Parlange, J. Y. *Soil Sci. Soc. Am. Proc.* **1975**, *39*, 875.
- (14) Stammers, W. N.; Robinson, J. B.; Whiteley, H. R. In *Dynamics of Lotic Ecosystems*; Fontaine, T. D., Bartell, S. M., Eds.; Ann Arbor Science: Ann Arbor, MI, 1983; pp 479-486.
- (15) Bowman, R. A.; Focht, D. D. *Soil Biol. Biochem.* **1974**, *6*, 297-301.
- (16) Kohl, D. H.; Vithaysthil, F.; Whitlow, P.; Shearer, G.; Chien, S. H. *Soil Sci. Soc. Am. Proc.* **1976**, *40*, 249-253.
- (17) Oren, A.; Blackburn, T. H. *Appl. Environ. Microbiol.* **1979**, *37*, 174-176.
- (18) Ryden, J. C. *J. Soil Sci.* **1983**, *34*, 355-365.
- (19) Rolston, D. E.; Rao, P. S. C.; Davidson, J. M.; Jessup, R. E. *Soil Sci.* **1984**, *137*, 270-279.
- (20) Reddy, K. R.; Patrick, W. H.; Phillips, R. E. *Soil Sci. Soc. Am. Proc.* **1978**, *42*, 268-272.
- (21) Phillips, R. E.; Reddy, K. R.; Patrick, W. H. *Soil Sci. Soc. Am. Proc.* **1978**, *42*, 272-278.
- (22) Paris, D. F.; Lewis, D. L.; Wolfe, N. L. *Environ. Sci. Technol.* **1975**, *9*, 135-138.
- (23) Paris, D. F.; Steen, W. C.; Baughman, G. L.; Barnett, J. T., Jr. *Appl. Environ. Microbiol.* **1981**, *41*, 603-609.
- (24) Robinson, J. A.; Tiedje, J. M. *Appl. Environ. Microbiol.* **1983**, *45*, 1453-1458.
- (25) Simkins, S.; Alexander, M. *Appl. Environ. Microbiol.* **1984**, *47*, 1299-1306.
- (26) Brunner, W.; Focht, D. D. *Appl. Environ. Microbiol.* **1984**, *47*, 167-172.
- (27) Focht, D. D.; Brunner, W. *Appl. Environ. Microbiol.* **1985**, *50*, 1058-1063.
- (28) Simkins, S.; Mukherjee, R.; Alexander, M. *Appl. Environ. Microbiol.* **1986**, *51*, 1153-1160.
- (29) Sufliata, J. M.; Smolnski, W. J.; Robinson, J. A. *Appl. Environ. Microbiol.* **1987**, *53*, 1064-1068.
- (30) Alexander, M. *Environ. Sci. Technol.* **1985**, *18*, 106-111.
- (31) Ogram, A. V. I.; Jessup, R. E.; Ou, L. T.; Rao, P. S. C. *Appl. Environ. Microbiol.* **1985**, *49*, 585-587.
- (32) Steinberg, S. M.; Pignatello, J. J.; Sawhney, B. L. *Environ. Sci. Technol.* **1987**, *21*, 1201-1208.
- (33) Wszolek, P. C.; Alexander, M. *J. Agric. Food Chem.* **1979**, *27*, 410-414.
- (34) Steen, W. F.; Paris, D. F.; Baughman, G. L. In *Contaminants and Sediments. Volume 1. Fate, and Transport Case Studies, Modeling, Toxicity*; Baker, R. A., Ed.; Ann Arbor Science: Ann Arbor, MI, 1980; pp 477-482.
- (35) Wu, S. C.; Gschwend, P. M. *Water Resour. Res.* **1988**, *24*, 1373-1383.
- (36) Mihelcic, J. R. Ph.D. Dissertation, Carnegie Mellon University, 1988.
- (37) McCroskey, P. S.; McRae, G. J. Chemical Engineering Department, Carnegie Mellon University, 1987.
- (38) Mihelcic, J. R.; Luthy, R. G. In *Conference on Physicochemical and Biological Detoxification on Hazardous Wastes*; Wu, Y. C., Ed.; Technomic Publishing Co., Inc.: Lancaster, PA, 1989; pp 708-721.
- (39) Wu, S. Ph.D. Dissertation, Massachusetts Institute of Technology, 1986.
- (40) Alexander, M. In *Methods of Soil Analysis, Part II: Chemical and Microbiological Properties*; Black, C. A., Ed.; American Society of Agronomy, Inc.: Madison, WI, 1965; pp 1467-1472, 1484-1486.
- (41) Argaman, Y.; Brenner, A. J.—*Water Pollut. Control Fed.* **1986**, *58*, 853-860.
- (42) DiToro, D. M.; Horzempa, L. M. *Environ. Sci. Technol.* **1982**, *16*, 594-602.
- (43) Seinfeld, J. H. *Atmospheric Chemistry of Physics of Air Pollution*; John Wiley and Sons: New York, 1986.
- (44) Karickhoff, S. W. In *Contaminants and Sediments. Volume 2. Fate and Transport Case Studies, Modeling, Toxicity*; Baker, R. A., Ed.; Ann Arbor Science: Ann Arbor, MI, 1980; pp 193-205.
- (45) Karickhoff, S. W. *J. Hydraul. Eng.* **1984**, *110*, 707-735.
- (46) Gschwend, P. M.; Wu, S. C. *Environ. Sci. Technol.* **1985**, *19*, 90-96.
- (47) Wu, S. C.; Gschwend, P. M. *Environ. Sci. Technol.* **1986**, *20*, 717-725.
- (48) Balkwill, D. L.; Ghiorse, W. C. *Appl. Environ. Microbiol.* **1985**, *50*, 580-588.
- (49) Hayduk, W.; Minhaus, B. S. *Can. J. Chem. Eng.* **1981**, *60*, 295.
- (50) Reid, R. C.; Prausnitz, J. M.; Poling, B. E. *The Properties of Gases and Liquids*, 4th ed.; McGraw-Hill Book Co.: New York, 1987; pp 577-631.

Received for review August 7, 1990. Accepted August 20, 1990. This investigation was supported by the U.S. Department of Energy, Coal Conversion Project Branch, Contract DE-AC18-84FC10619. Leland Paulson was the project manager.

Use of Colloid Filtration Theory in Modeling Movement of Bacteria through a Contaminated Sandy Aquifer

Ronald W. Harvey*

U.S. Geological Survey, Water Resources Division, Menlo Park, California 94025

Stephen P. Garabedian

U.S. Geological Survey, Water Resources Division, Marlborough, Massachusetts 01752

■ A filtration model commonly used to describe removal of colloids during packed-bed filtration in water treatment applications was modified for describing downgradient transport of bacteria in sandy, aquifer sediments. The modified model was applied to the results of a small-scale (7 m), natural-gradient tracer test and to observations of an indigenous bacterial population moving downgradient within a plume of organically contaminated groundwater in Cape Cod, MA. The model reasonably accounted for concentration histories of labeled bacteria appearing at samplers downgradient from the injection well in the tracer experiment and for the observed 0.25- μm increase in average cell length for an unlabeled, indigenous bacterial population, 0.6 km downgradient from the source of the plume. Several uncertainties were apparent in applying filtration theory to problems involving transport of bacteria in groundwater. However, adsorption (attachment) appeared to be a major control of the extent of bacterial movement downgradient, which could be described, in part, by filtration theory. Estimates of the collision efficiency factor, which represents the physicochemical factors that determine adsorption of the bacteria onto the grain surfaces, ranged from 5.4×10^{-3} to 9.7×10^{-3} .

Introduction

The recognition that water-supply well contamination by microbial pathogens is a major cause of waterborne disease outbreaks in the United States (1) and the increasing interest in the use of genetically altered (engineered) and "waste-adapted" bacteria for aquifer restoration are leading to efforts to model more accurately the transport of bacteria through porous media. The ability of bacteria that are capable of degrading highly refractory compounds to reach contaminant-affected areas is critical to the success of several proposed schemes involving in situ treatment of organically contaminated groundwater. Theoretical models that describe bacterial movement through porous media have been developed (2-4). However, few attempts have been made to model data resulting from controlled transport experiments involving bacteria in groundwater, and several aspects of bacterial migration through the subsurface are not well understood.

An important determinant of the extent of bacterial movement in sandy aquifers is the interaction between the bacteria and solid surfaces, which can involve a number of complex and interactive processes that are difficult to describe mathematically (5). In recent small-scale (2 m), forced-gradient tracer experiments, many of the labeled, indigenous bacteria that were reintroduced into sandy aquifer sediments became immobilized at particle surfaces (6). It was also observed that immobilization of bacteria-sized microspheres was inversely related to size, suggesting that sorption and not straining was the important control over the extent of transport. Matthess and Pekdeger (7) have suggested that filtration theory (8), which has been used to describe the removal of colloidal particles

during packed-bed filtration in water-treatment applications, may be employed in models of bacterial transport in groundwater. An important parameter in the filtration model is the so-called collision efficiency factor, α , which must be experimentally determined. Little information is available on the values of α for sorptive removal of microbes moving through aquifer sediments.

The objective of our study was to evaluate the advantages and limitations of using filtration theory in mathematical descriptions of bacteria transport through sandy aquifer sediments and to compare resulting estimates of α with other published values. The experimental work involved a small-scale (7 m), natural-gradient tracer test in which fluorochrome-labeled groundwater bacteria were reintroduced into a sandy, sewage-contaminated aquifer and their concentration histories at samplers downgradient compared with those of a conservative tracer (Br^-). Observed bacterial transport behavior was simulated with a filtration model that was modified to include advection, storage, physical dispersion, and reversible adsorption. The filtration model was also used to predict the effect of the aquifer sediments upon the size distribution of bacterial populations moving through it. This involved comparing predicted and observed changes in the size frequency distribution for a morphologically diverse, free-living (unattached) bacterial population moving downgradient along a 0.6-km-long transect through a plume of organically contaminated groundwater.

Methods

Injection Experiment. A small-scale, natural-gradient groundwater tracer experiment was run in October 1987 at U.S. Geological Survey well site F347 in a sandy aquifer on Cape Cod, MA, using Br^- and labeled bacteria. An earlier tracer test at this site involving bacteria-sized microspheres is described by Harvey et al. (6). Contaminated groundwater was collected with a stainless-steel submersible pump from a screened (250- μm slot width) PVC observation well that was located 100 m downgradient from an on-land, treated-sewage infiltration bed. A morphologically diverse population of bacteria was concentrated on-site from 600 L of contaminated groundwater to 8 L (final volume) by using a hollow-fiber, tangential-flow filtration device at a processing rate of 2 L/min (9). Recovery of bacteria was $\sim 33\%$. Recovered bacteria (0.2-1.4 μm , 0.6- μm average cell length) were stained with a DNA-specific fluorochrome, 4',6-diamidino-2-phenylindole (DAPI), using a previously described procedure (6). The stained bacteria were diluted with groundwater collected at the injection test site to a final volume of 90 L. The consequential dilution of the DAPI stain precluded staining other bacteria in the aquifer. Bromide was added to the injectate to a final concentration of 150 mg/L.

Bacteria and Br^- were added slowly (0.85 L/m) to the aquifer at 8.5 and 9.1 m below land surface (BLS) and monitored as they moved with the natural flow of

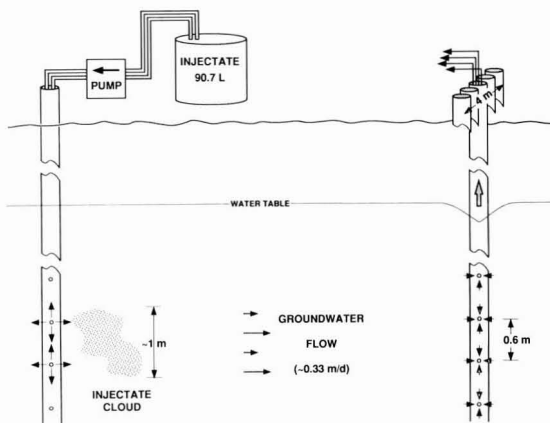


Figure 1. Schematic representation of the small-scale, natural-gradient tracer experiment with Br^- and labeled bacteria.

Table I. Transport Parameters for the Small-Scale Tracer Experiment

param ^a	9.1 m BLS	8.5 m BLS
A	0.51 m ²	
α_L	2.2 cm	2.2, 5.3 cm ^b
C_{max}/C_0	0.093	0.035
d	0.59 mm	
d_p	0.2–1.4 μm	
g	9.81 m/s ²	
k	1.38×10^{-16} g cm ² /s ² K	
μ	1.14×10^{-2} g/cm s	
η	$(1.0\text{--}3.5) \times 10^{-2}$	
RB	0.21	0.15
ρ	0.999 g/cm ³	
ρ_p	1.001 g/cm ³	
ρ_b	1.72 g/cm ³	
T	2.88×10^2 K	
θ	0.35	
V	9.1×10^{-2} m ³	
v	0.335 m/day	0.33, 0.25 m/day ^b
x	6.8 m	
K_d	0.061	
k_f	0.002	
k_r	0.4	

^a Estimates for d and θ were determined in a previous study [LeBlanc (11)]. ^b Estimates are for the faster and slower zones, respectively.

groundwater past a row of multilevel sampling devices (MLSD) set perpendicular to the direction of groundwater flow 6.8 m downgradient (Figure 1). Experimental parameters and conditions are listed in Table I. Groundwater samples (500 mL) were collected daily from sampling ports located in the path of injectate travel. Bromide was measured with a specific-ion electrode and confirmed by ion chromatography (Waters ICP-A column with borate-gluconate buffer at 1.2 mL/min at 25 °C). Preparations for enumeration of DAPI-stained bacteria were made with 100–200 mL of sample to obtain accurate counting statistics. The DAPI-stained bacteria in these samples were clearly visible by epifluorescence microscopy (340–380-nm excitation) after the month-long tracer test and after a 2-month, 12 °C test incubation in filter-sterilized Cape Cod groundwater. The bacteria were enumerated on black polycarbonate membrane filters (0.2- μm pore size, 25-mm diameter) by using a microscope that was fitted for epifluorescence (10). The possibility of growth of the DAPI-stained population during the tracer experiment was

investigated by monitoring abundance of DAPI-stained bacteria in a control suspension and in tracer test samples for a 30-day period after collection.

Contaminant Plume Study. The plume study involved modeling changes in the population of free-living bacteria during transport downgradient in a 640-m-long section of the contaminant plume. The plume of organically contaminated groundwater (~4 km in length) was formed by the on-land disposal of secondary sewage effluent from a sewage treatment plant at Otis Air Force Base, MA. The contaminant plume is characterized by elevated levels of specific conductivity (up to 400 μS), dissolved organic carbon (DOC; up to 4 mg/L), and temperature (up to 18 °C) relative to adjacent uncontaminated groundwater (<80 μS , <1 mg/L, and 10 °C, respectively) (11). Groundwater samples were taken from observation wells at 0, 0.38, and 0.64 km downgradient from the sewage-infiltration beds along a longitudinal transect through the core of the plume. Samples were immediately fixed with formaldehyde (2% w/v final concentration) and stored at 4 °C. Bacterial abundances were determined with acridine orange stain and epifluorescence microscopy (12). Bacterial size distributions were determined from scaled photomicrographs by a previous described procedure (13).

Formulation. A colloid filtration model was incorporated into a simple transport model to explain the movement, losses due to adsorption, and spreading of DAPI-stained bacteria in the small-scale injection test. A one-dimensional equation for the transport of bacteria, which contains terms for storage, reversible and irreversible adsorption, dispersion, and advection can be written as

$$\theta \frac{\partial c}{\partial t} + \rho_b \frac{\partial s}{\partial t} = D\theta \frac{\partial^2 c}{\partial x^2} - v\theta \left(\frac{\partial c}{\partial x} + k_p c \right) \quad (1)$$

where θ is the porosity; c the concentration of bacteria in solution; t the time after injection; ρ_b the sediment bulk density; s the concentration of reversibly adsorbed bacteria on the solid surface; D the dispersion coefficient, which is equivalent to the product of the longitudinal dispersivity (α_L) and the fluid velocity (v); x the spatial coordinate; and k_p the irreversible adsorption constant. The latter may be described by the colloid filtration model (8) used to explain the removal of colloidal-sized material during filtration in packed-bed systems:

$$k_p = \frac{3(1-\theta)}{2d} \alpha \eta \quad (2)$$

where d is the diameter of the porous media grains, α is the collision efficiency factor, and η is the single-collector efficiency.

The methods used to handle adsorption of bacteria during transport are analogous to the first-order reversible and two-site adsorption models commonly used in virus transport literature (14). Two different forms of the reversible adsorption term in eq 1 were used; the first assumes a linear isotherm and relatively fast adsorption with respect to advection, i.e.:

$$s = K_d c \quad (3)$$

If the adsorption constant (K_d) does not vary with time, the time variation of bacteria on the solid and in solution can be related directly:

$$\frac{\partial s}{\partial t} = K_d \frac{\partial c}{\partial t} \quad (4)$$

The other type of reversible adsorption term assumes a first-order kinetic reaction for the rates of adsorption and desorption:

$$\frac{\delta s}{\delta t} = k_f c - k_r s \quad (5)$$

where k_f and k_r are the forward and reverse adsorption rate constants, respectively.

Our approach in modeling transport of bacteria involved use of reported values for θ and ρ_p , estimation of α_L and v by calibrating model solutions to the observed breakthrough curves of the nonreactive solute (Br^-), and determination of the remaining parameters (K_d , k_f , k_r , $\alpha\eta$) by calibrating different solutions of eq 1 to observed bacteria breakthrough curves. The parameter pair ($\alpha\eta$) was treated differently because the effect of changing either parameter on the model output is identical. This is because the two parameters only appear in eq 2 together and, therefore, cannot be separately calibrated. The approach used here was to estimate η by use of a published equation (8), since the factors determining α are less well understood, and then use α as the calibration parameter.

The single-collector efficiency, η , is the rate at which particles strike a single porous media grain divided by the rate at which particles move toward the grain and represents the physical factors determining particle collision. If close-approach effects are neglected, its value can be estimated by the following (8):

$$\eta = \eta_D + \eta_1 + \eta_G = 0.9 \left[\frac{kT}{\mu d_p dv} \right]^{2/3} + 1.5(d_p/d)^2 + \frac{(\rho_p - \rho)gd_p^2}{18\mu v} \quad (6)$$

where η_D is the colloid collector collision caused by Brownian motion, η_1 the colloid collector collision caused by interception, η_G the colloid collector collision caused by settling, k the Boltzmann constant, T the solute temperature, μ the fluid viscosity, d_p the bacterial diameter, ρ the fluid density, ρ_p the bacterial density (specific gravity of bacterial biomass), and g the gravitational constant. Because each of the parameters in eq 6 can be independently measured, η was estimated for each size class of bacteria and the subsequent size-specific breakthrough curves were superposed to obtain a composite breakthrough curve for the entire bacterial population.

The collision efficiency factor, α , in eq 2 is the efficiency with which collisions between colloidal-sized particles and the stationary solid surfaces result in the immobilization of the bacteria and represents the physicochemical factors determining bacterial attachment to the solid surface. α was calibrated by assuming that the irreversible adsorption term in eq 1 was the only process that significantly and permanently reduced the total mass of bacteria in solution. In comparison, there is no loss of bromide from solution and α can be estimated by using the ratio of the relative masses of bacteria to bromide (RB) at the sampling well:

$$RB = \int_{t_0}^{t_f} \frac{C(t)}{C_0} dt / \int_{t_0}^{t_f} \frac{Br^-(t)}{Br_0^-} dt \quad (7)$$

where C_0 and Br_0^- are the bacterial and bromide concentrations, respectively, at point of injection and t_0 and t_f are the respective times at the beginning and end of breakthrough.

If it is assumed that the mass entered the system at one time (i.e., a pulse input), then α can be found by using a time moments analysis (15):

$$\alpha = \frac{d\{[1 - 2(\alpha_L/x_1) \ln(RB)]^2 - 1\}}{6(1-\theta)\eta\alpha_L} \quad (8)$$

where x_1 is the distance from the injection point to the MLSD. Equation 8 can be simplified when the dispersivity

is small with respect to the travel distance ($\alpha_L/x_1 < 0.01$):

$$\alpha = \frac{-d \ln(RB)}{1.5(1-\theta)\eta x_1} \quad (9)$$

Equations 8 and 9 can be used to estimate α from known parameters (d , θ , η , x_1), and the measured loss of relative mass, RB.

Solutions to eq 1, with appropriate boundary and initial conditions, were compared with breakthrough curves and used to explain the transport of bromide and bacteria. The two different reversible adsorption models produce different solutions to eq 1. The solution for the linear adsorption model (eq 3), with a pulse input above (or below) background concentration, is a well-known solution for relative concentration with a first-order decay term

$$\frac{C(t)}{C_0} = \frac{V_0}{A\theta[4\pi\alpha_L x']^{1/2}} \exp \left[\frac{-(x_1 - x')^2}{4\alpha_L x'} - k_p x' \right] \quad (10)$$

where V_0 is the initial injection volume, A the cross-sectional area of flow through the porous media, x' the spatial coordinate for the center of mass (vt/R), and R the retardation coefficient ($1 + \rho_p K_d/\theta$).

For bromide, there is no adsorption ($K_d = k_p = 0$) and $x' = vt$. Therefore, a simplified version of eq 10 (assuming α_L is small relative to x_1) was used to model its breakthrough curves. It is apparent from eq 10 that the peak bromide concentration occurs when the center of mass passes by the sampler (i.e., $x' = x_1$, $v \approx x_1/t_{peak}$), and the fluid velocity can be directly obtained from the known distance between injection and sampling points and the time to the peak bromide concentration. The dispersivity parameter (α_L) is obtained from the bromide curve by use of the following relation based on eq 10:

$$\alpha_L = \frac{x_1(\Delta t/t_{peak})^2}{16 \ln 2} \quad (11)$$

where Δt is the duration of breakthrough when $[Br](t) > 1/2[Br]_{max}$; $[Br]_{max}$ the peak bromide concentration, and t_{peak} the time to peak concentration. The area of the porous media through which the solutes or particles flow, A , can be found by calibration using the peak bromide concentration ($[Br]_{max}$) and eq 10, when $x' = x_1$:

$$A = \frac{V_0}{([Br]_{max}/[Br]_0)\theta(4\pi\alpha_L x_1)^{1/2}} \quad (12)$$

The solution for eq 1 with the kinetic adsorption term (eq 5) and a pulse input is found by using a modified form of a solution by Valocchi (15)

$$\frac{c(t)}{c_0} = L^{-1} \left[\frac{V_0}{\theta A x_1} \exp \left[\frac{x_1}{2\alpha_L} \left[1 - \left[1 + \frac{4\alpha_L}{x_1} \left[p + k_p x_1 + \frac{p\rho x_1 k_f}{\theta(vp + k_r x_1)} \right] \right]^{1/2} \right] \right] \right] \quad (13)$$

where L^{-1} indicates the inverse Laplace transform for the quantity inside the outermost bracket and p represents the Laplace domain parameter. The Laplace transform (eq 13) was numerically inverted by a method described by Crump (16) and available in the IMSL mathematics library. Equations 10 and 13 form the basis for the quantitative modeling of the bacterial breakthrough and explanation of the bacterial transport.

Results

Theoretical estimations of collector efficiency (η) and experimentally determined values of collision efficiency (α), which are the two key parameters in the filtration

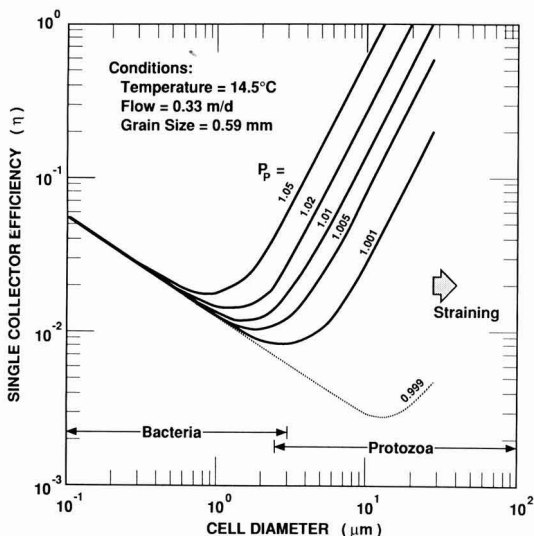


Figure 2. Theoretical estimates for the single-collector efficiency factor versus cell diameter for microorganisms traveling with the groundwater in the Cape Cod aquifer. Different curves represent different specific gravities of the biomass.

portion of the transport model, are given in Figure 2 and Table II, respectively. Collector efficiency, calculated by using eq 6 and measured physical parameters (Table I), was determined as a function of buoyant density (not measured in this study) and microbial size. At near-neutral buoyancy (1.001 g/cm³), diffusion was the primary determinant of collector efficiency for the bacterial size class (0.2–2 μm), but accounted for less than half of η for ~4–5-μm (diameter) protozoa that inhabit the aerobic portions of the contaminant plume; contributions of physical interception (η_i) were generally insignificant. The contribution of settling (η_c) to collector efficiency was generally significant for the larger microbial size classes (1 μm and larger), but was highly sensitive to small changes (e.g., 0.01 g/cm³) in buoyant density. A decrease in buoyant density from 1.05 to 1.001 g/cm³ corresponded to a shift in the optimal microbial size for transport (theoretically at the η function minimum) from ~0.8 to ~3 μm.

Table II. Estimates of the Collision Efficiency Factor (α) for Bacteria and Carboxylated, 0.23-μm (Diameter) Microspheres Being Transported through Sandy Sediments of the Cape Cod Aquifer

	depth, m BLS	distance, m	collision eff. factor ($\times 10^{-3}$)	
			bacteria	micro-spheres
injection test	9.1	6.8	8.1 ^a 5.4 ^b	26.4 ^a
	8.5	6.8	9.7 ^a 5.4, 8.5 ^b	ND ^d
contaminant plume		800	0.3 ^c	ND ^d

^a Estimated by using eq 9. Microsphere data from ref 9. ^b Determined by calibration (eq 10). Values at the 8.5-m depth are for the faster and slower zones, respectively. ^c Estimated by Reynolds (17) from the data of Harvey et al. (12). Estimate not corrected for bacterial growth. ^d ND, not determined.

Estimates of the collision efficiency factor, α , for bacteria in aquifer sediments are given for the two depths employed in the injection experiment and for the upgradient part of the contaminant plume (Table II). An estimate of α for carboxylated, bacteria-sized microspheres employed in an earlier experiment at the same site (6) is also listed for comparative purposes. It was found that estimated values of α were up to 30% higher for the shallower layer (8.5 m BLS) as compared with the deeper layer (9.1 m BLS) of aquifer sediment. Estimates of α for indigenous bacteria in the injection experiment are more than 20-fold higher than that estimated by Reynolds (17), who used previously reported bacterial distribution data for the contaminant plume (12). However, the estimates are ~3-fold lower than that calculated for the carboxylated microspheres.

The dimensionless concentration histories of Br⁻ and DAPI-stained bacteria at 6.8 m downgradient from point of injection are depicted in Figure 3 and 4 for the 9.1- and 8.5-m depths, respectively. Breakthrough of tracers at other sampled depths and at adjacent MLSD were not significant. For both depths, the patterns of breakthrough for stained bacteria and Br⁻ were similar. Breakthrough of Br⁻ (Figures 3A and 4A) and of stained bacteria (Figures 3B,C and 4B,C) exhibited single peaks and followed similar temporal patterns. However, substantial reversible behavior ("tailing") was observed for the stained bacteria at the 9.1-m depth, but not for Br⁻. Peak abundances in

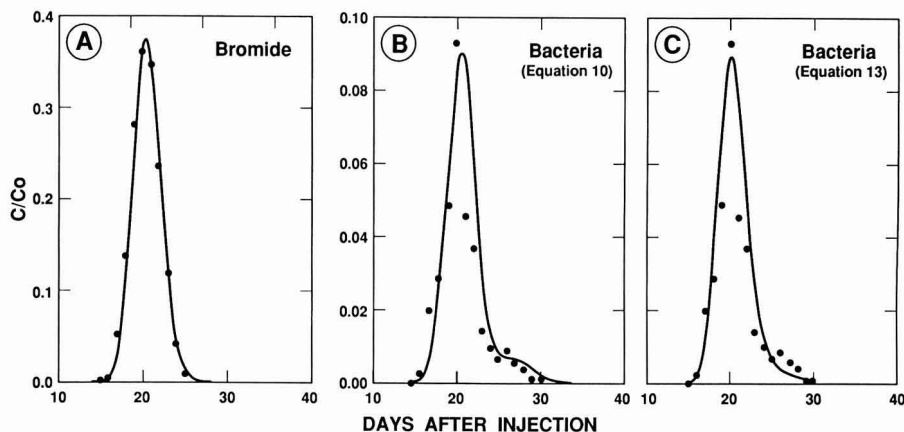


Figure 3. Observed dimensionless concentration histories (data points) and theoretical computer simulations (curves) for breakthrough at the 9.1-m depth (small-scale tracer experiment) of bromide (A) and stained bacteria (B and C). Retarded and unretarded (nonreactive) segments of the bacterial population are assumed in B and a uniformly reactive population with different constants describing sorption and desorption is assumed in C.

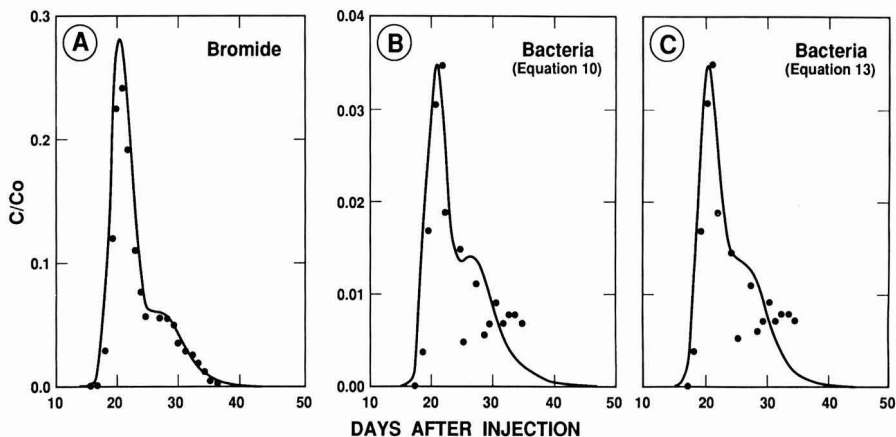


Figure 4. Observed dimensionless concentration histories (data points) and theoretical, two-zone computer simulations (curves) for breakthrough at the 8.5-m depth (small-scale tracer experiment) of bromide (A) and stained bacteria (B and C). Retarded and unretarded (nonreactive) segments of the bacterial population are assumed in B and a uniformly reactive population with different constants describing sorption and desorption is assumed in C.

stained bacteria and Br^- occurred within ~ 0.5 days of each other, but maximum dimensionless concentrations for stained bacteria were only 26 and 14% of that observed for Br^- at the 9.1- and 8.5-m depths, respectively. The ratios of relative masses of bacteria with respect to bromide (eq 7) were 21 and 15%, respectively.

A comparison of observed and predicted dimensionless concentration histories for bromide and stained bacteria is also shown in Figures 3 and 4. Dimensionless concentration histories for Br^- were simulated by use of the transport models described by eq 10, assuming no adsorption. Values and estimates for other parameters used are listed in Table I. Dimensionless concentration history for Br^- at the 9.1-m depth was simulated by assuming a single conductive zone. However, the physical heterogeneity that was apparent at the 8.5-m depth necessitated a two-zone (layer) application of the model for the shallower depth, as depicted in Figure 5. It was assumed that 25% of the sampled solute traveled through a less conductive (slower) zone in the aquifer, whereas the other 75% traveled through a more conductive zone. The final solution represents a superposition of individual solutions of eq 10 for the faster and slower zones.

At both depths, predicted dimensionless concentration histories for the stained bacteria from eqs 10 and 13 were reasonably close to what was observed in the small-scale experiments. However, the "tailing" in the observed concentration history of bacteria relative to Br^- was simulated in the model described by eq 10 by making the assumption that a small portion (7%) of the nonimmobilized, stained population interacted with surfaces of stationary particles in a reversible manner. The two-zone approach that was employed for Br^- to account for the physical heterogeneity at the 8.5-m depth was also used for the bacteria, although computer simulations for the latter portion of bacterial breakthrough were less accurate (Figure 4B). Simulations of bacterial breakthrough curves using eq 13, which assumes that all moving bacteria interact with surfaces, are shown in Figures 3C and 4C for the 9.1- and 8.5-m depths, respectively. Since little retardation was observed, little difference in accuracy was observed between the fast-adsorption (eq 10) and kinetic, nonequilibrium (eq 13) models in spite of the difference in approach.

Predicted and observed changes in the cell size frequency distribution for the indigenous bacterial population

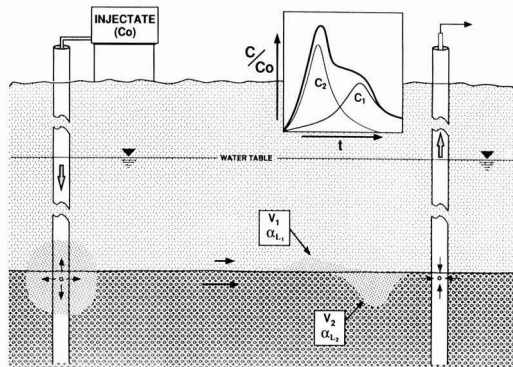


Figure 5. Schematic representation of the effect of adjacent zones of differing conductivities upon observed breakthrough of injectate transported through a layered aquifer.

being transported downgradient along a 680-m transect through the contaminant plume are depicted in Figure 6. Predicted changes that would be expected due to sorption were calculated by using eq 2 and were based upon the observed cell size distribution at the head of the plume (USGS well S314). The filtration model tended to underpredict the relative abundance of bacteria in the smallest size class ($0.2 \mu\text{m}$). There was also an overestimation of relative abundance in several of the larger size classes, particularly for the 1.2- and $1.4\text{-}\mu\text{m}$ classes. However, the predicted increase in the average cell size of the bacterial population with travel downgradient were within $0.06 \mu\text{m}$ of the observed value at 380 m downgradient (USGS well F347) and the same as the observed value at 640 m (USGS well F349).

Discussion

Model Parameters. Our approach and the one generally employed in laboratory studies involving colloid retention in porous media columns (18) was to first calculate collector efficiency (η) based upon physical measurements and then empirically determine the collision efficiency (α) based upon observed removal efficiencies and the theoretical value of η . The rationale is that η involves physical aspects of the filtration model that are better

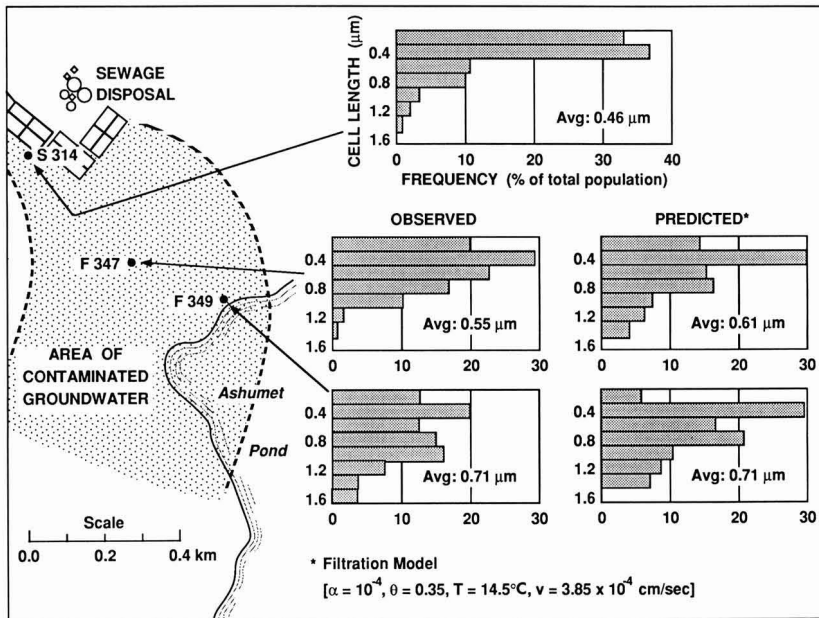


Figure 6. Observed and predicted changes in the size frequency distribution of the indigenous bacterial population that is being transported downgradient in the upper 640 m of the contaminant plume.

understood and more easily measured than are the chemical factors that affect α (18).

There are, however, several uncertainties in estimating collector efficiency for bacteria moving through aquifer sediments. One involves the effect of bacterial motility (locomotion by means of flagella), which can result in more rapid movement than that caused by random thermal (Brownian) motion (19). Chemotaxis (movement in response to chemical gradients) of motile bacteria toward or away from stationary surfaces further complicates estimates of η . Bacterial motility may not be a problem in our small-scale injection experiment, since the DAPI stain adversely affects bacterial activity (20). However, a substantial fraction (over half in some samples) of the free-living bacterial population in the contaminant plume appears to be motile. Therefore, more accurate estimates of the collector efficiency factors for indigenous bacteria in sandy aquifers may require inclusion of a term that accounts for the small-scale movement due to taxis. A simple expression describing the contribution of taxis is included in at least one theoretical model of microbial transport through porous media (2), but its validity in these applications has yet to be determined.

Another uncertainty involves the range of buoyant densities (ρ_p), which affects the magnitude of settling and the optimal size for transport (Figure 2). The more accurate measurements have involved centrifugation techniques based upon equilibrium sedimentation using density gradients created with colloidal silica (21). Unfortunately, such determinations involve pure cultures, typically fast-growing bacteria of clinical interest. Little information is available on the range of buoyant densities for indigenous bacterial populations in low-nutrient (oligotrophic) aquatic systems. However, it may be assumed that many bacteria in the Cape Cod aquifer are near-neutral buoyancy, judging from their slow sinking velocities. Although it is commonly assumed that the optimal diameter for transport through coarse, sandy sediment is $\sim 1 \mu\text{m}$, the optimal size for microbial transport through the Cape Cod

aquifer at near-neutral buoyancy (e.g., $\rho_p = 1.001$) may be $3\text{--}4 \mu\text{m}$ (Figure 2). This would not be the case for microbes with much higher specific gravities ($\rho > 1.1$), since the $3\text{--}4\text{-}\mu\text{m}$ class would predictably "settle out" onto grain surfaces.

Other uncertainties and complications in using eq 6 for microorganisms moving through sandy aquifers involve the effect of differences in both microbial and grain size morphology. The colloid-filtration model assumes spherical colloids and collectors. Deviation of individual sand grains from spherical morphology may result in some degree of error. Although there are a number of spherical (coccolidal) bacteria present in the Cape Cod aquifer, most appear to be rod shaped. There are also a number of spiral and filamentous forms (12). Morphological differences among microbes can result in different rates of attachment (22). However, the colloid filtration model has been successfully applied to sand-bed filtration where there is morphologic variation in both collector and colloid.

Collision efficiency factors for other in situ studies involving bacterial transport through sandy aquifer sediments are not available. The estimates in Table II ($5 \times 10^{-3} - 1 \times 10^{-2}$) compare favorably with an α value of 4.6×10^{-2} reported for laboratory experiments with *Pseudomonas aeruginosa* and glass surfaces at 10^{-3} M NaCl (23). However, propensity for attachment to surfaces can vary among bacterial species, with solution conditions, and with the nature of the solid surface (24). In a previous transport experiment with bacteria-sized microspheres, differences in the rate of immobilization were observed for microspheres having approximately the same diameter, but different surface characteristics (6). This suggests that the collision efficiency for bacteria may vary even among species of similar size and morphology. Since some aquatic bacteria may alter their propensity for attachment to solid surfaces in response to changes in nutrient conditions (25, 26), temporal changes in the apparent value of α would not be unreasonable for bacteria moving with contaminated groundwater. Consequently, comparison of labo-

ratory- and field-derived estimates of α values may be difficult to interpret.

The discrepancy between collision efficiency factors estimated from our injection test data and the value estimated earlier for the indigenous population in the contaminant plume (17) may be due to bacterial growth. Recent estimates of in situ growth rates for the unattached bacteria that are being transported through the most contaminated parts of the plume range up to 0.042 h^{-1} (16-h average doubling time) (27). However, growth was not observed for the DAPI-stained population in the injection test, due to the inhibitory effect of the DAPI stain or to differences in nutrient and environmental conditions between the groundwater at the injection site and the highly contaminated groundwater where the injectate population was collected. On the other hand, losses of bacteria during transport from nonsorptive processes such as straining, grazing by Protozoa, or lysis in response to unfavorable conditions, parasitism from bacteriophages, or *Bdellovibrio* may lead to an overestimation of collision efficiency. Losses of stained bacteria due to straining may not be significant, judging from the large median grain size of the aquifer sediments (0.59 mm) relative to the bacteria ($0.6 \mu\text{m}$). In general, straining becomes significant when the diameter of the suspended particles are $\geq 5\%$ of that of the media (28), although physical heterogeneity makes the application of this criterion less accurate. Also, the low level of dissolved oxygen ($<0.1 \text{ mg/L}$) may preclude the establishment of a substantial population of bacterivorous protozoa. Lysis did not appear to be much of a factor in the apparent attenuation of DAPI-stained bacteria in the injection experiments, since it was not significant during the subsequent month-long, 12°C sample incubations.

The differences in estimated values of collision efficiency for the two depths for which the injection test was run (8.5 and 9.1 m BLS) suggest that substantial changes in the apparent value of α may occur over relatively small distances in the aquifer. Spatial variability in the collision efficiency factor due to heterogeneity in the aquifer may necessitate a stochastic treatment of α in models of bacterial transport models. It should be recognized, however, that the colloid filtration model is very sensitive to the value of α and it is difficult to modify this parameter value without significantly changing the model output.

Filtration Theory in Modeling. Use of filtration theory appeared to give reasonable approximations of attenuation for the stained bacteria in the small-scale injection experiment (Figures 3B,C and 4B,C). However, the higher dimensionless concentrations of bacteria relative to Br^- during days 25–30 following injection at the 9.1-m depth suggest reversible adsorption behavior and the need for a model that allows for retardation of at least a portion of the bacterial population. Retardation was more extensive than that observed earlier in the forced-gradient experiment performed at another location in the aquifer (6). The role of physical heterogeneity in the observed differences in transport behavior of bacteria at different locations within the same aquifer complicates interpretation of data resulting from these field experiments.

Given the above cautionary statements, there is nonetheless a good fit to the breakthrough curves for both bromide and bacteria by the solute transport model that was modified to include irreversible and reversible adsorption. The successful employment of a solute transport model to simulate observed transport behavior of non-sorbing MS2 bacteriophage in columns of saturated sediment has been reported (29). However, adsorption ap-

pears to be a major mechanism controlling bacterial transport in our in situ experiments and accounted for removal of most (up to 85%) nongrowing bacteria within a 7-m travel distance. It is not clear from the data how the reversible component of bacterial adsorption should be represented in the overall model. Although the linear, instantaneous (fast relative to advection) adsorption model is appealing because of its simplicity, it is based upon the unverifiable assumption that only a small percentage (7%) of the bacterial population undergoes reversible adsorption. In contrast, the model involving kinetic limitation allows for the reversible adsorption of all unattached bacteria and has the same first-order form as the filtration portion of the model. A limitation in this approach is that the average characteristics that the rate constants represent are likely a continuum of different site types that may be poorly represented by a single average value. However, more accurate mathematical descriptions of sorption for a diverse bacterial population onto aquifer sediment surfaces is beyond the scope of this study, and more controlled experimentation needs to be done to delineate bacterial sorption and desorption behavior in the presence of aquifer sediments.

The relationship of bacterial size upon the likelihood of sorption during transport downgradient is suggested in Figure 6. The observed and predicted increase in average cell size with increasing distance downgradient suggests that transport favors larger bacteria ($>0.6 \mu\text{m}$). Several biological factors may also lead to changes in the size distribution, such as changes in nutrient levels or the abundance of bacterivorous protozoa. The effect of groundwater protozoa on average bacterial size in the contaminated groundwater is not well understood, but preliminary surveys suggest that protozoa may be less abundant in the anoxic core of the plume (N. Kinner, personal communication) where the samples used in this study were taken. Decreases in average cell size of bacterial populations in response to a severe carbon limitation (oligotrophic conditions) are well documented. Levels of dissolved organic carbon range from $\sim 4 \text{ mg/L}$ immediately downgradient to $\sim 1 \text{ mg/L}$ at 700 m downgradient. Therefore, the observation that bacteria were larger in nutrient-depleted groundwater at 380 and 640 m downgradient from the outfall as compared with those found in highly contaminated groundwater further upgradient is difficult to explain on the basis of nutrient conditions.

Increases in average diameter of a polydispersed population of carboxylated, bacteria-sized microspheres as a consequence of travel downgradient through the aquifer also have been observed (6). The relative breakthrough (C/C_0) of the largest [$1.35\text{-}\mu\text{m}$ (diameter)] carboxylated microspheres was observed to be over 10-fold higher than for the smallest [$0.23 \mu\text{m}$ (diameter)]. This may be predicted by using eqs 6 and 9, a specific gravity for the microspheres of 1.05, and a calculated α value of 2.6×10^{-2} (Table II). Therefore, an abiotic explanation for observed increases in average cell size of bacteria traveling downgradient through the contaminant plume seems reasonable. The predicted preference for transport of larger versus smaller bacteria may explain the relatively large size of free-living bacteria in uncontaminated groundwater at our site relative to "dwarf" bacterial populations often found in other nutrient-depleted aquatic environments such as the open ocean (30). The apparent effect of cell size upon immobilization occurring during transport downgradient has important implications in the proposed use of introduced, nonindigenous bacteria in aquifer cleanup. However, the size dependency of bacterial immobilization in

groundwater would also depend on the phenomenon of "filter ripening" (31) and average pore size. In aquifers where straining is an important determinant of bacterial transport, larger bacteria would be at a disadvantage.

In summary, there appear to be a number of advantages in using colloid filtration theory in modeling transport of bacteria through contaminated, sandy aquifers. The colloid filtration model is relatively simple, accounts for the abiotic mechanisms by which bacteria contact stationary solid surfaces, and can reasonably predict the effect of cell size upon the rate of immobilization. Some of the uncertainty in this application involves the buoyant densities of indigenous bacteria, the effect of bacterial motility on collector efficiency, and how to mathematically treat some of the physical differences between situations of groundwater flow through sandy aquifers and packed-bed filtration for which the model was developed. In addition, filtration theory does not account for differences in surface characteristics among bacteria or the effect of nonequilibrium adsorption or nonsorptive interactions of bacteria with particles. The effect of aquifer heterogeneity, growth, grazing by protozoa, lysis, and detachment from solid surfaces would necessitate the use of a more complex model for large-scale transport experiments with bacteria. However, our results suggest that filtration theory may be useful in a multicomponent description of immobilization in transport models involving bacteria in groundwater.

Acknowledgments

We are grateful to B. Howes and D. White (Woods Hole Oceanographic Institute) for assistance with the tracer test, to L. George for bromide analyses, and to D. Metge, J. Kuwabara (USGS), and R. Bales (University of Arizona) for review of this article.

Literature Cited

- (1) Keswick, B. H. In *Groundwater Pollution Microbiology*; Bitton, G., Gerba, C. P., Eds.; Wiley: New York, 1984; pp 59-64.
- (2) Corapcioglu, M. Y.; Haridas, A. *Adv. Water Res.* **1985**, *8*, 188-200.
- (3) Corapcioglu, M. Y.; Haridas, A. *J. Hydrol.* **1984**, *72*, 149-169.
- (4) Matthess, G.; Pekdeger, A.; Schroeter, J. *J. Contam. Hydrol.* **1988**, *2*, 171-188.
- (5) Harvey, R. W. In *Groundwater Contamination*; Abriola, L., Ed.; IAHS Press: Wallingford, UK, 1989; pp 75-82.
- (6) Harvey, R. W.; George, L. H.; Smith, R. L.; LeBlanc, D. R. *Environ. Sci. Technol.* **1989**, *23*, 51-56.

- (7) Matthess, G.; Pekdeger, A. *Sci. Total Environ.* **1981**, *21*, 149-159.
- (8) Yao, K. M.; Habibian, M. T.; O'Melia, C. R. *Environ. Sci. Technol.* **1971**, *11*, 1105-1112.
- (9) Kuwabara, J. S.; Harvey, R. W. *J. Environ. Qual.* **1990**, *19*, 626-629.
- (10) Harvey, R. W. *Limnol. Oceanogr.* **1987**, *32*, 993-995.
- (11) LeBlanc, D. R. In *Open-File Rep.—U.S. Geol. Surv.* **1984**, No. 84-475, 1-46.
- (12) Harvey, R. W.; Smith, R. L.; George, L. *Appl. Environ. Microbiol.* **1984**, *48*, 1197-1202.
- (13) Zehr, J. P.; Harvey, R. W.; Oremland, R. S.; Cloern, J. E.; George, L. H. *Limnol. Oceanogr.* **1987**, *32*, 781-793.
- (14) Yates, M. V.; Yates, S. R. *CRC Crit. Rev. Environ. Control* **1988**, *17*, 307-344.
- (15) Valocchi, A. J. *Water Resour. Res.* **1985**, *21*, 808-820.
- (16) Crump, K. S. *J. Assoc. Comput. Mach.* **1976**, *23*, 89-96.
- (17) Reynolds, M. D. Masters Dissertation, Massachusetts Institute of Technology, 1985.
- (18) Tobiasson, J. E.; O'Melia, C. R. *J.—Am. Water Works Assoc.* **1988**, *80*, 54-64.
- (19) Jenneman, G. E.; McInerney, M. J.; Knapp, R. M. *Appl. Environ. Microbiol.* **1985**, *50*, 383-391.
- (20) Parolin, C.; Montecucco, A.; Ciarrocchi, G.; Pedrali-Noy, G.; Valisena, S.; Palumbo, M.; Palu, G. *FEMS Microbiol. Lett.* **1990**, *68*, 341-346.
- (21) Kubitschek, H. E.; Baldwin, W. W.; Graetzer, R. *J. Bacteriol.* **1983**, *155*, 1027-1032.
- (22) Feldner, J.; Bredt, W.; Kahane, I. *J. Bacteriol.* **1983**, *153*, 1-5.
- (23) Martin, R. E. Ph.D. Dissertation, The Johns Hopkins University, 1990.
- (24) McEldowney, S.; Fletcher, M. *Appl. Environ. Microbiol.* **1986**, *52*, 460-465.
- (25) Fletcher, M.; Marshall, K. C. *Adv. Microbial Ecol.* **1982**, *6*, 199-240.
- (26) Kjelleberg, S.; Humphrey, B. A.; Marshall, K. C. *Appl. Environ. Microbiol.* **1982**, *43*, 1166-1172.
- (27) Harvey, R. W.; George, L. H. *Appl. Environ. Microbiol.* **1987**, *53*, 2992-2996.
- (28) McDowell-Boyer, L. M.; Hunt, J. R.; Sitar, N. *Water Resour. Res.* **1986**, *22*, 1901-1921.
- (29) Grondin, G. H.; Gerba, C. P. *Hydrol. Water Resour. Ariz. Southwest* **1986**, *16*, 11-15.
- (30) Watson, S. W.; Novitsky, T. J.; Quinby, H. L.; Valois, F. W. *Appl. Environ. Microbiol.* **1977**, *33*, 940-946.
- (31) Darby, J. L.; Desmond, F. L. *Environ. Sci. Technol.* **1990**, *24*, 1069-1079.

Received for review February 26, 1990. Revised manuscript received July 30, 1990. Accepted August 2, 1990.

ENVIRONMENTAL SCIENCE & TECHNOLOGY

ES&T



Editor, William H. Glaze
University of North Carolina,
Chapel Hill

Call TOLL FREE 800/227-5558
Outside U.S. 202/872-4363
Telex 440159 ACSP UI or
89 2582 ACSPUBS
TWX 710-822-0151

American Chemical Society
1155 Sixteenth Street NW
Washington, DC 20036 USA

For nonmember rates in Japan, contact
Maruzen, Co. Ltd.

**The premiere
research
publication in the
environmental
field.**

ES&T continues to give you the practical hard facts you need on environmental science . . . covering research, techniques, feasibility, products, and services.

Dealing with the chemical nature of water, air, and waste makes ES&T essential reading for environmental scientists both in the business and academic world.

Each monthly issue presents new knowledge and promotes scientific inquiry in such areas as the chemical nature of the environment and environmental changes through pollution or other modifications.

Also included are discussions on environmental analyses, governmental regulations, current environmental lab activities, and much more!



Name of American Chemical Society Publication

Author(s)

Ms No.

Ms Title

Received

This manuscript will be considered with the understanding you have submitted it on an exclusive basis. You will be notified of a decision as soon as possible.

[THIS FORM MAY BE REPRODUCED]

COPYRIGHT TRANSFER

The undersigned, with the consent of all authors, hereby transfers, to the extent that there is copyright to be transferred, the exclusive copyright interest in the above cited manuscript, including the printed version in any format (subsequently referred to as the "work"), to the American Chemical Society subject to the following (Note: if the manuscript is not accepted by ACS or if it is withdrawn prior to acceptance by ACS, this transfer will be null and void and the form will be returned.):

- A. The undersigned author and all coauthors retain the right to revise, adapt, prepare derivative works, present orally, or distribute the work provided that all such use is for the personal noncommercial benefit of the author(s) and is consistent with any prior contractual agreement between the undersigned and/or coauthors and their employer(s).
B. In all instances where the work is prepared as a "work made for hire" for an employer, the employer(s) of the author(s) retain(s) the right to revise, adapt, prepare derivative works, publish, reprint, reproduce, and distribute the work provided that all such use is for the promotion of its business enterprise and does not imply the endorsement of the American Chemical Society.
C. Whenever the American Chemical Society is approached by third parties for individual permission to use, reprint, or republish specified articles (except for classroom use, library reserve, or to reprint in a collective work) the undersigned author's or employer's permission will also be required.
D. No proprietary right other than copyright is claimed by the American Chemical Society.
E. For works prepared under U.S. Government contract or by employees of a foreign government or its instrumentalities, the American Chemical Society recognizes that government's prior nonexclusive, royalty-free license to publish, translate, reproduce, use, or dispose of the published form of the work, or allow others to do so for noncommercial government purposes. State contract number:

SIGN HERE FOR COPYRIGHT TRANSFER: I hereby certify that I am authorized to sign this document either in my own right or as an agent for my employer.

Print Authorized Name(s) and Title(s)

Original Signature(s) (in Ink)

Date

CERTIFICATION AS A WORK OF THE U.S. GOVERNMENT

This is to certify that ALL authors are or were bona fide officers or employees of the U.S. Government at the time the paper was prepared, and that the work is a "work of the U.S. Government" (prepared by an officer or employee of the U.S. Government as part of official duties), and, therefore, it is not subject to U.S. copyright. (This section should NOT be signed if the work was prepared under a government contract or coauthored by a non-U.S. Government employee.)

INDIVIDUAL AUTHOR OR AGENCY REPRESENTATIVE

Print Author's Name

Print Agency Representative's Name and Title

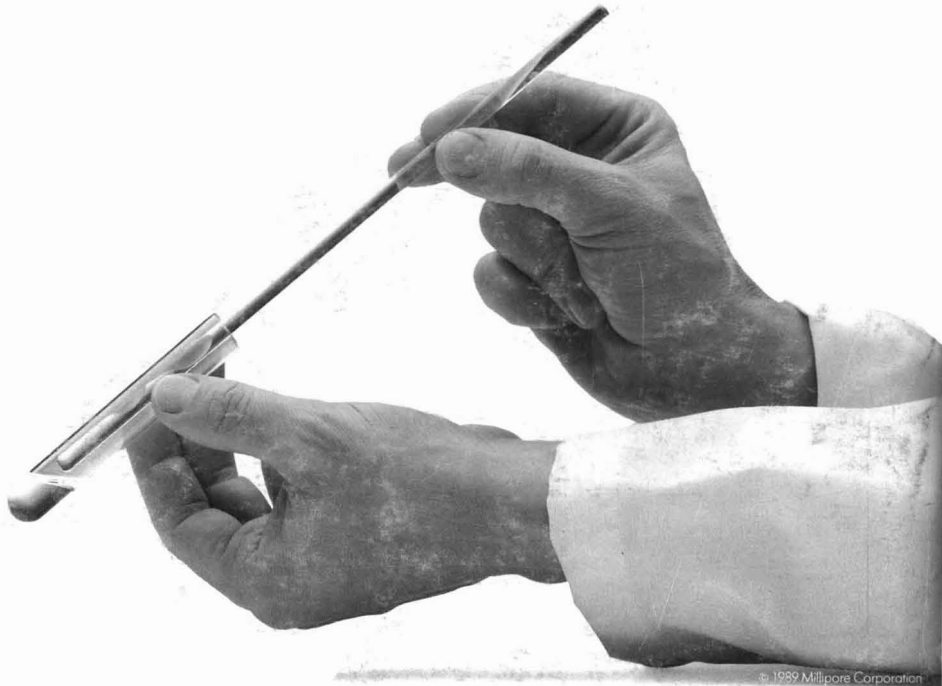
Original Signature of Author (in Ink)

Date

Original Signature of Agency Representative (in Ink)

FOREIGN COPYRIGHT RESERVED (NOTE: if your government permits copyright to be transferred, refer to section E and sign this form in the top section.)

[] If ALL authors are employees of a foreign government that reserves its own copyright as mandated by national law, DO NOT SIGN THIS FORM. Please check this box as your request for the FOREIGN GOVERNMENT COPYRIGHT FORM (Blue Form) which you will be required to sign. If you check this box, mail this form to: Copyright Administrator, Publications Division, American Chemical Society, 1155 Sixteenth Street, N.W., Washington, D.C. 20036, U.S.A. Otherwise, mail this form to the editor.



© 1989 Millipore Corporation

How gun cotton and a twist of the wrist made the world a safer place.

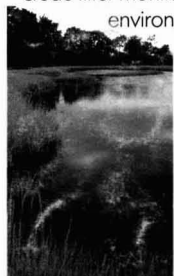
In 1855, a German scientist named Fick created quite a stir in the scientific community.

He took a glass rod, dipped it in some gun cotton (nitrocellulose), and literally started "stirring," or rolling the rod. Much to his delight, a thin "sac" formed on the surface of the rod. And the first membrane filter was created.

Fick was excited. Unfortunately, his colleagues weren't. Which explains why it took almost a century for his discovery to make an impact.

Today, refined offsprings of Fick's crude filter monitor workplace and environmental air quality, detect and treat diseases, uncover impurities in foods and drugs, and ensure water supplies are safe to drink.

Surprisingly, these and hundreds of other uses were advanced or



Millipore membranes have led to more rapid, accurate monitoring of coliform densities in water supplies.

developed by one company. Millipore.

But then, maybe it's not a surprise. Anyone who's worked in a lab has probably used a Millipore filter. In fact, over 100 million will be used this year.

For good reason, too. Over 120 contaminants



Millipore test kits can detect fine sand and metal particles to ensure airplane fuel reliability.

are regulated by the EPA, NIOSH and OSHA. Millipore has membranes to sample them all.

Their filters undergo as many as 25 individual tests.* (More than most people get during a routine physical.)

All this has helped Millipore learn a lot

about membranes.

But it's also given people the idea they're the only manufacturer of membranes.

"So," they conclude, "it doesn't matter what brand I buy. It's all Millipore."

Not so. To ensure you get accurate results—time after time—you've got to ask for Millipore by name.

Try it right now. Call 800-225-1380, or the nearest Millipore office, and ask for a free sample pack, featuring the new Isopore™ track-etched membrane.

After all, it's a lot easier than making your own.



Millipore originated many of the procedures which use membranes for pollution monitoring.



Consistent pore sizes allow Millipore filters to better detect and analyze gas line impurities.

* Depends upon application

MILLIPORE

CIRCLE 7 ON READER SERVICE CARD